TECHNISCHE UNIVERSITÄT WIEN

DISSERTATION

STRATEGIES TO CONTROL CELLULAR BEHAVIOR IN FIBRIN-BASED THREE-DIMENSIONAL MUSCULOSKELETAL TISSUE ENGINEERING APPROACHES

ausgeführt zum Zwecke der Erlangung des akademischen Grades eines Doktors der technischen Wissenschaften unter Leitung von

a.o.Univ.Prof. Dipl.-Ing. Dr.techn. Heinz Redl

Institut für Verfahrenstechnik, Umwelttechnik und Technische Biowissenschaften

(E166)

eingereicht an der Technischen Universität Wien

Fakultät für Technische Chemie

von

Mag. Philipp Heher

0403635

Praterstraße 30/2/17

A-1020 Wien

Wien, am 28. September 2018

EIDESSTAATLICHE ERKLÄRUNG

Hiermit erkläre ich an Eides statt, dass ich die vorliegende Dissertation "STRATEGIES TO CONTROL CELLULAR BEHAVIOR IN FIBRIN-BASED THREE-DIMENSIONAL MUSCULOSKELETAL TISSUE ENGINEERING APPROACHES" selbstständig verfasst und keine anderen als die angegebenen Quellen und Hilfsmittel verwendet habe.

Wien, am 28. September 2018

....

Philipp Heher

TABLE OF CONTENTS

ACKNOWLEDGEMENTS

KURZFASSUNG

Pathologische Zustände des muskuloskelettalen Systems sind die häufigste Ursache für chronische Langzeitschmerzen sowie körperliche Behinderung in der ersten Welt und betreffen Millionen Menschen global. Muskuloskelettale Erkrankungen repräsentieren eine Gruppe von mehr als 150 Krankheiten und Syndromen, deren Prävalenz durch globale Überalterung, erhöhte Fettleibigkeit und arbeitsbedingte physische Inaktivität weiter steigen wird. Laut der 2012 durchgeführten National Health Interview Umfrage wurden in diesem Jahr 126.6 Millionen US Amerikaner wegen einer muskuloskelettalen Erkrankung behandelt, wobei die jährlichen direkten und indirekten Kosten für das US Gesundheitssystem auf $213 Milliarden geschätzt wurden. Es besteht daher dringender Bedarf für eine Reduktion der immensen sozio-ökonomischen Belastung, welche durch akute und chronische Erkrankungen des muskuloskelettalen Systems für Gesundheitssysteme weltweit entsteht.

Heutige goldene Standards für die Behandlung von muskuloskelettalen Erkrankungen sind der Einsatz von autologen oder allogenen Transplantaten sowie von Prothesen, wie zum Beispiel Metallimplantate. Diese Prozeduren sind jedoch mit hoher Invasivität, Morbidität auf Seiten des Spenders, beträchtlichen immunologischen Risiken und der potenziell limitierten Anzahl an Spendergeweben verbunden. Außerdem sind heutige Standardtherapien, obwohl sie annehmbare Ergebnisse in der Rekonstruktion von Knochen, Bändern oder Sehnen erbracht haben, nicht passend für den Einsatz in weichen, dynamischen Geweben wie Skelettmuskel. Tatsächlich gibt es heute keine Methode für die Heilung von großen, traumatischen Muskeldefekten oder chronischen Muskelpathologien wie muskuläre Dystrophien oder Sarkopenie. In Hinblick auf die momentan limitierten Therapieoptionen hat sich das Forschungsgebiet des tissue engineering (Gewebezüchtung) daher zum Ziel gesetzt, alternative Strategien zu entwickeln. Der Ansatz von Skelettmuskel tissue engineering ist die Kultivierung von Muskelvorläuferzellen in einem passenden Biomaterial, bis ein funktionelles, biomimetisches Muskelkonstrukt entstanden ist, welches darauffolgend als Transplantat verwendet werden kann. Um die Funktionalität von *in vitro* gezüchtetem Muskelgewebe weiter zu steigern, hat sich das Forschungsgebiet kürzlich auf den Einsatz von fortgeschrittenen, dynamischen Zellkultursystemen fokussiert, welche die komplexe Struktur und Physiologie des Skelettmuskels besser rekapitulieren.

Kapitel I dieser Dissertation präsentiert ein neues dynamisches Kultursystem, das die schnelle Erzeugung von funktionellem Skelettmuskelgewebe durch Bioreaktor-basierte, automatisierte mechanische Stimulation erlaubt. Durch Imitation der biophysikalischen Stimuli, welche naturgemäß im Körper während der Muskelentwicklung und -regeneration auf Muskel einwirken, wird statische mechanische Belastung als potenter Auslöser für Muskelmaturation identifiziert. Außerdem stellt Kapitel I ein Reportersystem für Muskeldifferenzierung vor, welches für nicht invasive, longitudinale Probenanalyse in das dynamische Kultursystem implementiert werden kann um Zeit und Kosten zu sparen.

Skelettmuskel tissue engineering hat hauptsächlich natürliche Hydrogele als Biomaterialien verwendet, weil sie biokompatibel sind und ähnliche mechanische Eigenschaften wie natives Muskelgewebe aufweisen. Vor allem Fibrin, das Endprodukt der Blutgerinnung, wurde als ideales Biomaterial für die Züchtung von Skelettmuskel beschrieben. Fibrin Hydrogele weisen jedoch vergleichsweise schwache mechanische Eigenschaften auf, was die Entstehung von Muskelgewebe durch vorzeitigen Abbau des Materials behindern kann. Ein neues verstärktes natürliches Hydrogel, welches auf einem interpenetrierenden Polymernetzwerk von Fibrin und Hyaluronsäure basiert, wird in Kapitel II vorgestellt. Durch Einsatz dieser Doppelnetzwerk-Strategie wird gezeigt, dass der Einbau eines Hyaluronsäure-Polymernetzwerks in eine Fibrinmatrix ein neues Hydrogel mit verbesserten mechanischen und biologischen Eigenschaften ergibt.

Während die Verwendung von Fibrin als Zell- und Differenzierungsmatrix im Forschungsgebiet des tissue engineering einen neuen Zugang zu Geweberegeneration darstellt, werden Fibringele in der Klinik seit mehr als 100 Jahren als chirurgische Gewebekleber oder Hemostatika verwendet. Kapitel III präsentiert neue Anwendungsgebiete von Fibrin als vielfältige Abgabematrix für Zellen, Wachstumsfaktoren, Medikamente oder Gen Vektoren. Außerdem wird ein genereller Überblick über jüngste Fortschritte und künftige Trends im Feld des chirurgischen Klebens gegeben.

ABSTRACT

Pathological musculoskeletal conditions are the most common cause of severe long term pain and physical disability in 1st world countries, affecting hundreds of millions of people around the world. Musculoskeletal disorders are a group of more than 150 different diseases and syndromes, and global population aging in combination with rising obesity and work-related physical inactivity will further increase their prevalence. In the 2012 National Health Interview Survey, musculoskeletal medical conditions were reported by 126.6 million adults in the United States and the annual direct and indirect healthcare costs were estimated to be \$213 billion. There is thus an urgent need to address the immense socio-economic burden that acute and chronic disorders of the musculoskeletal system impose on healthcare systems worldwide.

Current gold standards for the treatment of musculoskeletal disorders are autologous or allogeneic grafting procedures or non-tissue prostheses such as metallic implants. However, most of these interventions are associated with high invasiveness, donor-site morbidity, considerable immunogenic risks and a potential shortage of graft donors. Furthermore, although they have yielded decent results in relation to bone, tendon or ligament reconstruction, these therapies are not suitable for soft dynamic tissues like skeletal muscle. In fact, there is no cure for large traumatic muscle defects or chronic muscle pathologies such as mucular dystrophies or sarcopenia. The field of tissue engineering has thus developed alternative strategies to address the shortcomings of current therapies. Skeletal muscle tissue engineering approaches employ the culture of muscle precursor cells in suitable biomaterial substrates until a functional, biomimetic muscle construct is generated which can subsequently be used as a transplant. More recently, the field has focused on more sophisticated, dynamic cell culture systems that account more precisely for the complex nature and physiology of skeletal muscle, with the aim of further increasing the functionality of *in vitro* engineered muscle tissue.

Chapter I of this thesis presents a novel dynamic culture system that allows for the rapid generation of functional skeletal muscle tissue through bioreactor-based, automated application of defined mechanical stimulation regimes. Mimicking the naturally occuring biophysical stimuli that act on muscle during development and regeneration with the bioreactor, static mechanical strain is identified as a potent trigger for muscle maturation. Furthermore, chapter I illustrates a reporter system for myogenic differentiation which can be employed in this dynamic culture model for noninvasive, longitudinal sampling in order to save costs and time.

Skeletal muscle tissue engineering has mainly employed natural hydrogels as scaffolds, as they are biocompatible and mimic the mechanical properties of native muscle tissue. Especially fibrin, the end product of blood coagulation, has been described as an ideal biomaterial for skeletal muscle engineering. However, fibrin hydrogels display comparably weak mechanical properties which may impede tissue formation through premature scaffold degradation. A new reinforced natural hydrogel, based on an interpenetrating polymer network of fibrin and hyaluronic acid, is presented in chapter II.

Using this double network strategy, the incorporation of a hyaluronic acid polymer network into a fibrin matrix is shown to yield a new hydrogel with improved mechanical as well as biological properties.

While the use of fibrin as a cell and differentiation matrix in tissue engineering is a more recent approach to tissue regeneration, fibrin gels have been used in clinics as surgical sealants, adhesives or hemostats for more than 100 years. Chapter III presents new strategies of how fibrin can be used as a versatile delivery vehicle for cells, growth factors, drugs or gene vectors. In addition, an overview of recent advances and future trends in the field of surgical sealing in general is given.

1. INTRODUCTION

The human musculoskeletal system is a complex organ system that gives the human body the ability to move through use of its skeletal and muscular components. It is primarily made of bones, cartilage, tendons, ligaments and skeletal muscles which together provide form, support, stability and locomotion to the body and also protect vital organs from damage through physical means. Pathological musculoskeletal conditions, also termed musculoskeletal disorders (MSDs), are the most common cause of severe long term pain and physical disability in 1st world countries, affecting hundreds of millions of people around the world [1, 2]. MSDs are a group of more than 150 different diseases and syndromes, and global population aging in combination with rising obesity and work-related physical inactivity will further increase their prevalence [3, 4]. In the 2012 National Health Interview Survey (NHIS), musculoskeletal medical conditions were reported by 126.6 million adults in the United States and the annual direct and indirect healthcare costs were estimated to be $213 billion [5]. Across the European Union member states, the total cost of lost productivity attributable to MSDs among people of working age is projected around 2% of gross domestic product (GDP) [6]. There is thus an urgent need to address the immense socio-economic burden that acute and chronic disorders of the musculoskeletal system impose on healthcare systems worldwide.

Current gold standards for the repair of musculoskeletal tissues entail intense surgical interventions for reparative or replacement therapy [7]. These therapies usually employ autologous or allogeneic grafting procedures or, in extreme cases, non-tissue prosthetics such as metallic strengthening devices or total joint replacements. However, most of these interventions are associated with high invasiveness, donor-site morbidity, considerable immunogenic risks and a potential shortage of graft donors. Consequently, there is an unmet clinical need for alternate musculoskeletal tissue-replacement solutions. The multidisciplinary field of tissue engineering and regenerative medicine (TERM) is actively investigating such strategies. The concept of tissue engineering (TE) evolved in the nineties as an approach to deliver cells on biodegradable polymers (with or without the presence of therapeutic biomolecules) into sites of injured tissue, either as transplants or to trigger endogenous regenerative processes. TERM has originally been described as "an interdisciplinary field that applies the principles of engineering and the life sciences toward the development of biological substitutes that restore, maintain or improve tissue function" [8]. Since then, the field of TE has expanded rapidly, resulting in the development of a vast amount of cellular and acellular strategies, and a myriad of scaffold materials [9], cell types [10] and delivery strategies [11] have been investigated over the last three decades. While significant advances in both musculoskeletal TE and clinical surgery have yielded promising combinational therapies in relation to bone, cartilage, ligament or tendon reconstruction [12], this is not quite the case for skeletal muscle.

At present, there is no adequate cure for acute muscle injuries such as traumatic volumetric muscle loss (VML) or chronic muscle pathologies like muscular dystrophies (MDs) or sarcopenia, the

irreversible age-related loss of muscle tissue. Although skeletal muscle possesses higher intrinsic regenerative capacity than other musculoskeletal tissues - especially cartilage, tendons or ligaments - the ability of muscle to heal is severely compromised when it is affected by a (congenital) chronic pathology. Moreover, volumetric traumatic defects usually result in loss of muscle function, muscle fiber atrophy and the formation of fibrous scar tissue or accumulation of fatty deposits. To this end, the gold standard in the treatment of VML is free functional muscle transfer (FFMT), where a flap of healthy, vascularized, innervated autologous muscle (usually lying in vicinity of the defect) is transferred to the site of injury [13]. FFMT is still considered the best option for restoring function in otherwise non-reconstructable muscles, however, a return to pre-injury levels of muscle strength and functionality usually does not occur. As an alternative approach, the field of skeletal muscle tissue engineering (SMTE) aims to replicate the structure and function of skeletal muscle tissue *in vitro* or *in vivo*, with the ultimate goal of implanting engineered muscle constructs as therapeutic devices instead of autologous transplants [14]. Classical SMTE strategies have employed the culture of muscle precursor cells on suitable biomaterial substrates until a functional, biomimetic muscle construct is generated which can subsequently be used as a transplant. More recently, SMTE has focused on more complex, dynamic culture systems that account more precisely for the complex nature and physiology of skeletal muscle [15, 16]. In doing so, the field has not just driven novel strategies to generate functional muscle tissue *in vitro* and *in vivo*, but also contributed to basic muscle research by providing powerful organotypic *in vitro* models to study muscle homeostasis, diseases or therapies on the molecular level [17].

2. THE STRUCTURE AND FUNCTION OF SKELETAL MUSCLE

Skeletal muscle is a highly dynamic and plastic tissue that comprises approximately 40% of the total body mass, making it the most abundant tissue in the human body [18]. It contains 50-75% of all body proteins and accounts for 30-50% of whole-body protein turnover [19]. Skeletal muscle is indispensable for multiple bodily functions. From a mechanical point of view, the main role of muscle is the conversion of chemical into mechanical energy to generate contractile force, which is central to locomotion, breathing or maintenance of posture. From a metabolic perspective, skeletal muscle is involved in the regulation of basal energy metabolism, thermogenesis or storage of important metabolites such as amino acids or carbohydrates. The latter is of great clinical significance as there is accumulating epidemiological evidence that physical activity plays an independent role in the prevention of frequent chronic diseases like type 2 diabetes [20], cardiovascular diseases (CVDs) [21], cancer [22, 23], dementia [24] or depression [25]. This has led to the recognition that skeletal muscle is an endocrine organ capable of acting on other tissues by secretion of metabolites, which is evident by the impairment of the body's ability to respond to stress and illness when muscle mass is reduced [26]. More recently, this concept has been greatly expanded by the notion that skeletal muscle produces and releases distinct cytokines or growth factors (termed myokines) in response to exercise which exert auto-, para- and endocrine effects [27, 28].

2.1. Skeletal muscle physiology

The human body contains more than 600 skeletal muscles which are connected to the skeletal system via tendons. In contrast to cardiac or smooth muscle, skeletal muscle lies under voluntary control through the somatic nervous system. In general, skeletal muscle is a highly organized composite structure consisting majorly of muscle fibers (myofibers) aligned in parallel, with interspersed blood vessels, nerves and connective tissue. Myofibers are elongated, cylindrical, multi-nucleated cells that arise from fusion of single muscle precursors (myoblasts) during muscle development and may contain hundreds of myonuclei [29]. Myofibers are the basic contractile units of skeletal muscle and display remarkable tissue plasticity, as they can undergo changes in fiber size (hypertrophy versus atrophy) as well as fiber type (slow-twitch versus fast-twitch fibers) [30]. The high degree of structural hierarchy in skeletal muscle can be observed from the whole muscle level down to the smallest intracellular contractile unit within the myofiber, the sarcomere (Fig. 1). Several myofibers are packed together in tight bundles within a fascicle, and several fascicles make up an entire muscle. At the same time, an individual myofiber is characterized by a precisely arranged intracellular contractile apparatus, containing a large number of thin longitudinal elements called myofibrils that themselves are made up by thousands of transversely aligned sarcomeres [31]. The sarcomeres in turn are mainly composed of the thin actin and the thick myosin filaments that mediate muscle contraction through

sliding past each other, which is referred to as the sliding filament model [32, 33]. Each sarcomere is defined as the segment between two Z lines which act as an anchoring point for the actin filaments. Even though actin and myosin are estimated to make up 70-80% of the total protein content of a single myofiber, a variety of other proteins are involved in preserving the mechanical and physiological integrity of the sarcomere [19, 34]. On one side, the giant protein titin (connectin) attaches to the Z line and to myosin, thereby stabilizing the thick filament, and further plays important roles in sarcomere assembly [35]. On the other side, nebulin is integrated in the Z line and binds and stabilizes the thin actin filaments together with alpha-actinin [36]. In addition, regulatory proteins such as the Ca^{2+}-dependent troponins or tropomyosin are associated with the actin filament and mediate the activation process that leads to myofilament sliding and, ultimately, force generation [19].
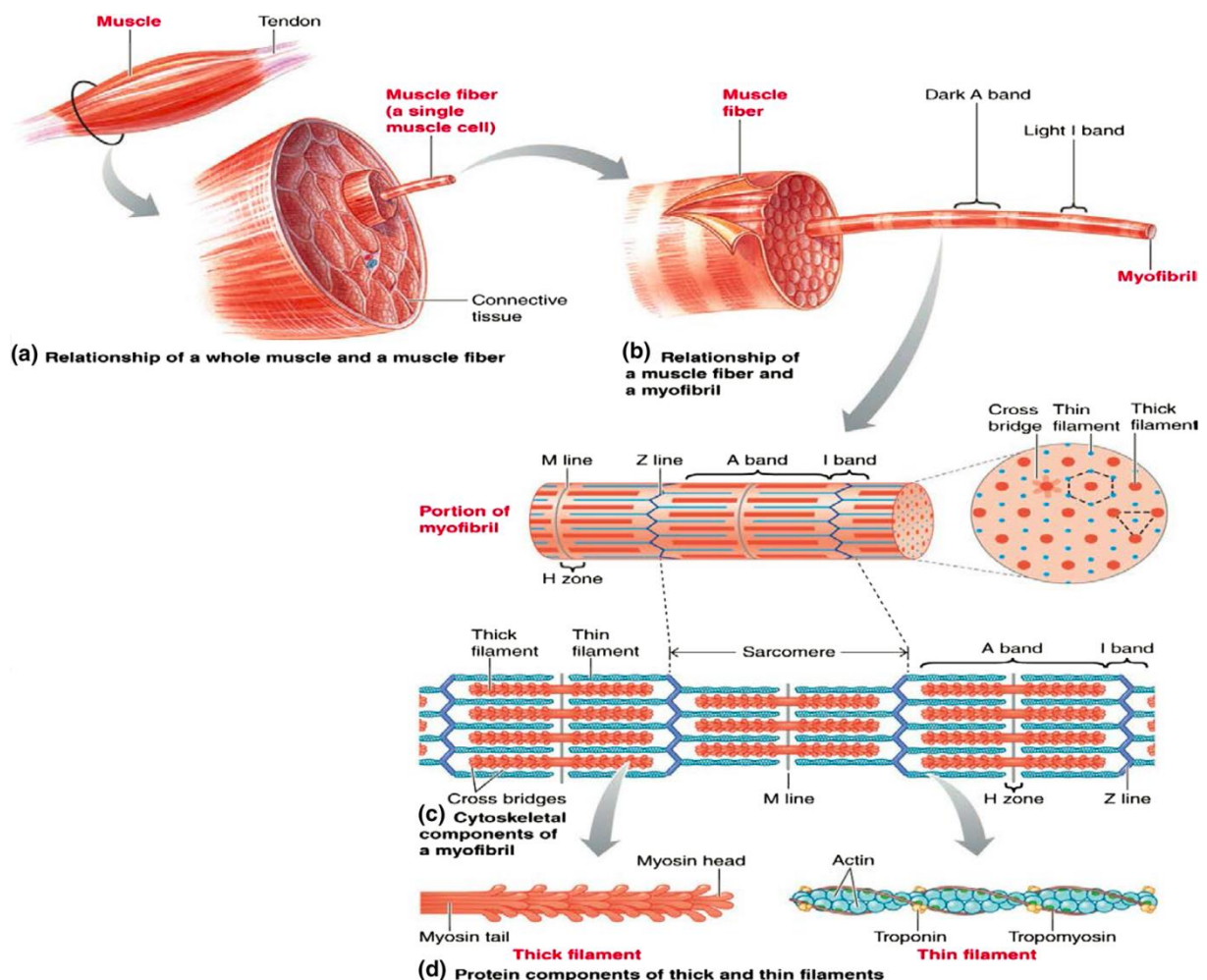
Fig. 1: *The structural hierarchy of skeletal muscle* (from [19]).

The distinct arrangement of areas with higher and lower protein density within the myofibril (that is, the entity of sarcomeric units) gives skeletal muscle a characteristic striated banding pattern under the microscope [15]. The two main bands are the dark A band and the lighter I band which alternate throughout the length of the myofibril. The Z lines appear as dark lines in the middle of each I band. A

lighter region, the H zone, lies in the middle of each A band and is again bisected by a darker line, the M line, which represents the middle between two Z lines.

Although skeletal muscle is a highly cellular tissue, extracellular matrix (ECM) proteins such as collagen or laminin play an important role in muscle physiology [37]. Layers of fibrous connective tissue can be found on different levels of muscle structural hierarchy and are categorized as epimysium (surrounding the whole muscle), perimysium (surrounding the fascicle) and endomysium (surrounding the myofiber). The skeletal muscle ECM not only forms a supportive framework that maintains muscle shape but also allows the myofibers to contract in synergy during movement. Importantly, blood vessels running along the fascicles can penetrate into the perimysium and form capillaries that connect to each individual myofiber. This is essential to ensure that the supply of O_2 and essential nutrients meets the high metabolic demands of active myofibers. At the same time, the axons of motor neurons follow the route of invading blood vessels and eventually terminate into the neuromuscular junctions (NMJ) necessary to transmit the synaptic signals for muscle contraction/relaxation from the peripheral nervous system (PNS) to the myofibers [14]. Central to this transmission are three distinct organelles in the sarcoplasm (cytoplasm) of the myofiber: the transverse tubular (also termed T tubule) system, the sarcoplasmic reticulum (the endoplasmic reticulum of the muscle cell) and the mitochondrial network (Fig. 2) [19].
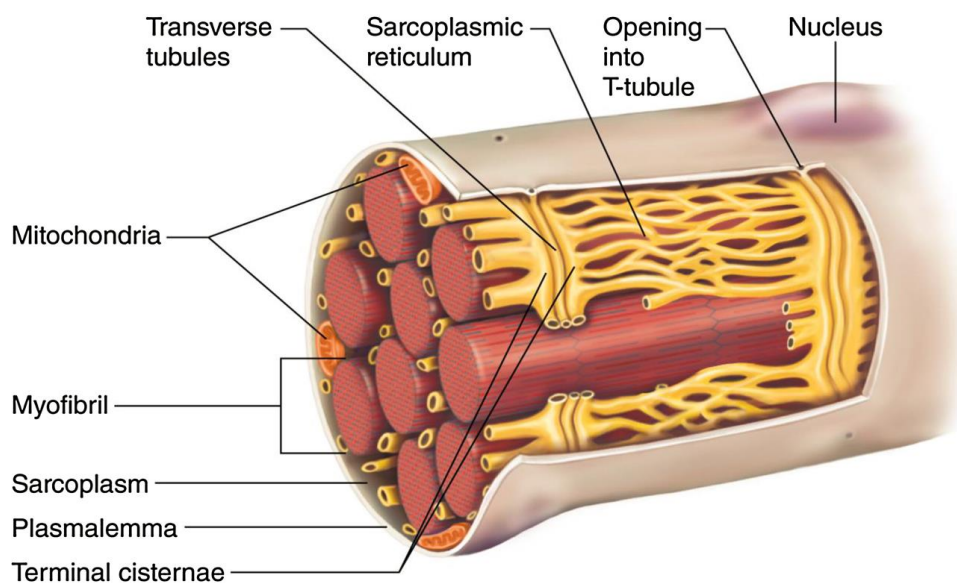
Fig. 2: *The T tubule and sarcoplasmic reticulum systems in the muscle fiber* (from [19]).

T tubules are invaginations of the sarcolemma (plasmalemma) whose main function is to conduct a nerve action potential to the interior of the myofiber. A three-dimensional (3D) network of T tubules forms the T tubular system which is in contact with the exterior and ensures that excitation can spread evenly throughout the myofiber [38]. Dysferlin, a Ca^{2+}-sensitive protein in the membrane of the T tubules, plays an important role in this process as it is a known regulator of vesicular fusion, receptor

trafficking and membrane repair [39, 40]. The T tubular system is in close contact with the sarcoplasmic reticulum which is responsible for the storage, release and (re-)uptake of Ca^{2+} in the myofiber. More precisely, Ca^{2+} is stored in the terminal cisternae, the ends of the sarcoplasmic reticulum, and two cisternae one both sides of a T tubule form a structure known as the triad [41]. The mitochondria in the sarcoplasm of the myofiber also form a 3D network (as opposed to other cell types where mitochondria rather function as isolated organelles) that provides the energy required for force generation when O_2 is available [42]. This network spans from the subsarcolemmal to the intermyofibrillar regions (and is thus exposed to different O_2 diffusion rates) and has distinct morphology, volume and enzymatic activity for different muscle fiber types [43]. The mitochondrial network is the main unit of muscle energy management and provides varying levels of adenosine triphosphate (ATP) through ATP or creatine phosphate (CP) buffering and shuttling [19].

Once a myofiber receives an action potential from a motor neuron in the NMJ (the motor neuron and the myofibers innervated by this neuron's axonal terminals are called a motor unit), a sequence of events is triggered that ultimately leads to muscle contraction. The coordinated molecular and cellular processes needed for the generation of force are described by the mechanism of excitation-contraction coupling (ECC) [44]. This mechanism has already been described in the 1950s and involves the rapid communication between electrical events in the sarcolemma of the myofiber [45]. In brief, the series of events starts with the release of the neurotransmitter acetylcholine (ACh) by a motor neuron into the synaptic cleft of the NMJ. This generates an action potential in the myofiber which propagates along the sarcolemma throughout the T tubular system to the triad. Changes in the membrane potential of the triad triggers Ca^{2+} release from the cisternae of the sarcoplasmic reticulum, leading to a rapid transient increase of free Ca^{2+} in the sarcoplasm. Ca^{2+} is necessary for sarcomeric contraction as it binds to the regulatory protein troponin C on the thin actin filament, which results in the displacement of the tropomyosin strands running along the actin filament [46]. This exposes a myosin-binding site on actin which is otherwise blocked by tropomyosin, initiates a tight interaction ("cross-bridging") between actin and myosin and enables the Ca^{2+}- and ATP-dependent "power stroke" of the myosin heads that mediate filament sliding and contraction (Fig. 3). Actin-myosin cross-bridges exist in two states, the weak-binding and strong-binding state. The generation of force begins when ATP is made available to an existing actin-myosin cross-bridge in the rigor state (strong-binding state). ATP binding to the myosin head detaches it from the actin filament (weak-binding state) and activates an adenosine triphosphatase (ATPase) in the head. Subsequent ATP hydrolysis results in the formation of adenosine diphosphate (ADP) and a phosphate ion (Pi) which remain bound to the myosin head. Importantly, ATP hydrolysis elicits a conformational change in the weakly bound myosin head, allowing it to swing over and interact with a new actin molecule. Release of Pi triggers the power stroke through a rotation of the myosin head which pushes the actin filament past it, followed by ADP release which restores the strong-binding rigor state of the actin-myosin cross-bridge [19].
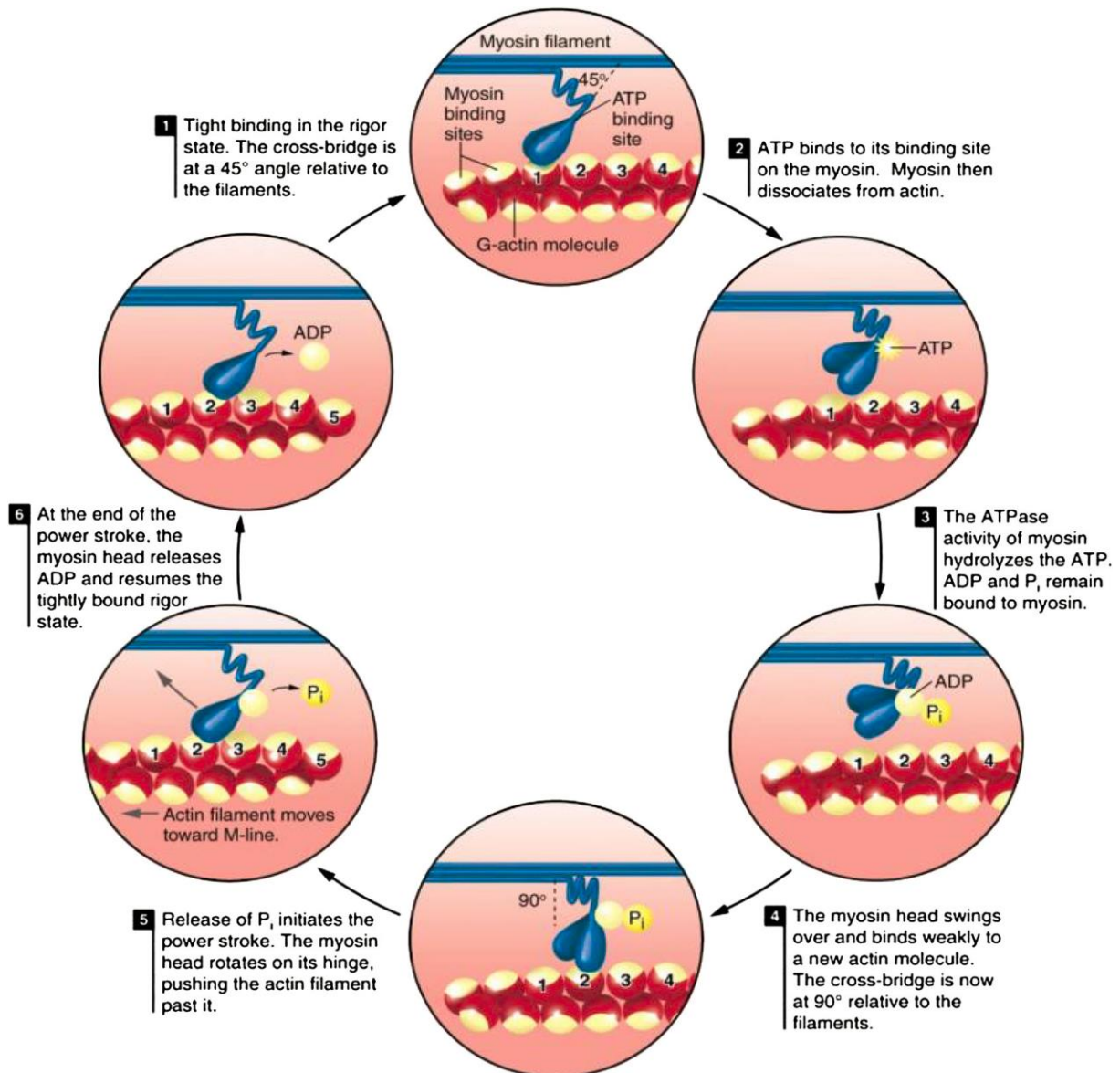
Fig. 3: *The actin-myosin cross-bridge and the mechanism of filament sliding by the myosin power stroke* (from [19]).

The actin-myosin cross-bridging cycle continues as long as sarcoplasmic Ca^{2+} and ATP concentrations are sufficiently high. Termination of muscle contraction (after the action potential from the motor neuron has faded) occurs when Ca^{2+} is actively sequestered back into the sarcoplasmic reticulum by the sarco(endo)plasmic reticulum Ca^{2+} ATPase (SERCA), which allows tropomyosin to block the binding sites for myosin on actin again [41].

Even though the general mechanism of force generation through actin-myosin cross-bridging is conserved throughout all muscles in the human body, there is still a remarkable plasticity on the myofiber level. The heterogeneity of human skeletal muscle is reflected by significant variability in the biochemical, mechanical and metabolic phenotypes of individual fibers [19]. Muscle can adapt to a variety of external stimuli, including the habitual level of contractile activity (for example endurance exercise training), the loading state (for example resistance exercise training), substrate availability

(for example nutrient supply) and other prevailing environmental conditions (for example thermal stress) [47]. This plasticity is common to all vertebrates, however, there is also large variation between individuals within a species [48]. During the last few decades, a variety of different criteria have been used to classify myofibers, including: (i) the color of the fiber (red vs. white) which correlates with myoglobin content, (ii) the contractile properties of the motor units in response to electrical stimulation, (iii) the speed of shortening during a single twitch (fast vs. slow), (iv) the degree of fatigability during sustained activation (fatigable vs. fatigue-resistant), (v) the predominance of certain metabolic or enzymatic pathways for energy provision (oxidative vs. glycolytic), or (vi) specific contractile protein isoform expression patterns, to name a few [19, 49]. To date, the predominantly used classification approach to distinguish myofiber types is the analysis of myosin heavy chain (MHC) isoform expression in the fiber. In humans, MHC is found in the forms of Type I, IIa and IIx, and myofibers can contain either one (pure fiber) or a combination (hybrid fiber) of these isoforms [50]. Thus, myofibers in human limb muscles are frequently classified as type I (slow, oxidative, fatigue-resistant), type IIa (fast, oxidative/glycolytic, fatigable) and type IIx (fast, glycolytic, rapidly fatigable) fibers. Furthermore, the existence of I/IIa and IIa/IIx hybrid fibers has been revealed [51, 52]. This has shifted the view on skeletal muscle as being a tissue composed of a defined subset of myofibers towards the recognition that myofiber (and muscle) plasticity is remarkably high, with physical activity being one of the primary regulators of fiber type alterations [53-56].

2.2. Mechanisms of skeletal muscle development and repair

Skeletal muscle development (myogenesis) and regeneration share common features as components of the regulatory pathways and transcription factors which are crucial for prenatal muscle development are redeployed for tissue reconstruction after traumatic muscle damage. Over the last decades, regenerative medicine has gained important insights into the complex biology of muscle homeostasis through the use of sophisticated experimental mouse models [57]. A central finding of this period was the observation that postnatal skeletal muscle possesses a subset of quiescent adult muscle stem cells (MuSCs), termed satellite cells (SCs), which reside in a niche on the surface of the myofiber. Upon injury, these cells become activated, proliferate and generate myoblasts which eventually differentiate and either fuse into existing myofibers or create myofibers *de novo* for regeneration [31]. Even though embryonic myogenesis parallels postnatal muscle regeneration, there are some important distinctions in the context of the involved cells, the niche conditions, the appropriate signals and the regulatory genes employed [58]. It is now generally accepted that SCs are closely related to the myogenic precursors of somitic origin [59], but how the uncommited character, or stemness, of the embryonic founder MuSCs is retained in SCs remains a matter of ongoing investigation.

2.2.1. Embryonic myogenesis

The embryonic development of skeletal muscle is a highly conserved process in all vertebrates and the underlying developmental and regulatory mechanisms have been the topic of several comprehensive reviews [58, 60-63]. Embryonic myogensis starts soon after gastrulation of the embryo, where embryonic polarity (essential for cell fate patterning) and the three germ layers ectoderm, endoderm and mesoderm are established [64]. The mesoderm can further be anatomically divided into lateral, intermediate and paraxial mesoderm, the latter giving rise to bilaterally paired blocks, termed somites, which develop along the anterior-posterior (head to tail) axis around the neural tube/notochord of the embryo [65]. The somites further undergo maturation into the ventral sclerotome (giving rise to the skeleton) and the dorsal dermomyotome (giving rise to the overlying skin and skeletal muscles of the trunk and limbs). Skeletal muscles of the body, with the exception of some head muscles, are derived from the dermomyotome. The lips of the dermomyotome will mature into the myotome, a primitive muscle structure containing committed muscle cells. As the embryo develops, the central part of the dermomyotome disintegrates and muscle progenitors intercalate into the primary myotome [60]. This population of progenitors already gives rise to a fraction of SCs that will later reside in postnatal skeletal muscle fibers [59]. At the same time, cells in the medial, lateral and central regions of the (dermo)myotome specify to progenitor lineages that later form distinct groups of anatomical muscles (Fig. 4A) [63]. For example, medial dermomyotome cells at the dorsal medial lip (DML) give rise to epaxial muscle progenitors that will later form the myotomal deep back muscles. Lateral dermomyotome cells at the ventral lateral lip (VLL) are the source of hypaxial progenitor lineages that form lateral trunk muscles or limb muscles [66, 67]. The latter are derived from a population of muscle progenitors with extensive migratory capacity, which delaminate from the VLL and migrate into the limb buds [68].
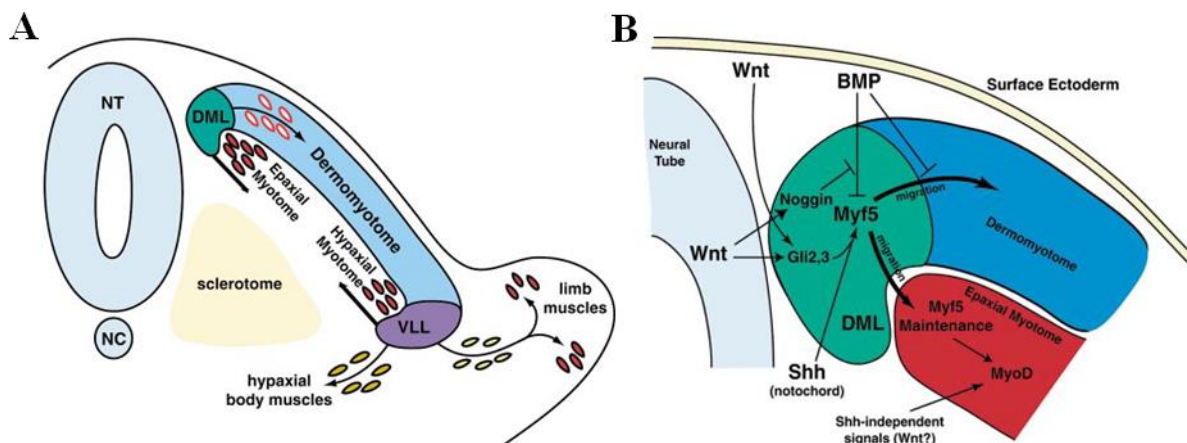
Fig. 4: *The fates of myogenic precursors during vertebrate embryonic development and instructive signals for their specification in the (dermo)myotome.* (A) Somite origins and fates of myogenic precursor cells in the dermomyotome. Cells of the DML migrate ventrolaterally, differentiate and form the epaxial myotome which will later give rise to epaxial deep back muscles. Cells from the VLL migrate dorsolaterally to form the hypaxial myotome and ventrally to form the ventral

body wall muscles. Furthermore, some myogenic precursor cells delaminate from the VLL, migrate and differentiate in the dorsal and ventral muscle-forming regions, where they give rise to the limb musculature. (B) Model for early myogenic specification in the dermomyotome. Myf5 expression in myogenic precursor cells of the DML is regulated through interactive Shh, Wnt, Noggin and BMP signaling. Wnt and Shh ligands trigger Gli-mediated Myf5 expression. Myogenic determination is negatively regulated by active BMP signaling which fosters Pax3 expression while delaying the induction of Myf5 and MyoD to expand the muscle progenitor pool before further myogenic commitment is initiated. The actions of BMP4 are antagonized by Wnt- and Shh-mediated activation of Noggin in the DML, which induces MyoD expression to commit the precursor cells to the myogenic lineage (adapted from [63]).

Cellular commitment in the somite is highly dependent on a variety of intrinsic and extrinsic factors and, initially, secreted morphogen gradients control the establishment and patterning of all subsequently developing somitic structures. These morphogens positively or negatively regulate the specification of muscle progenitors in the (dermo)myotome as well as the activation of the transcriptional network controlling embryonic myogenesis [60, 61, 63]. Central to this network are a family of basic helix-loop-helix (bHLH) transcription factors, called myogenic regulatory factors (MRFs), which are highly conserved in all vertebrates [69]. The MRFs myogenic differentiation 1 (MyoD), myogenic factor 5 (Myf5), myogenic factor 6 (Myf6 or MRF4) and myogenin (MyoG) are collectively expressed in the skeletal muscle lineage and their importance in myogenic specification is underscored by their ability to induce myoblast traits in non-muscle cell lines [63]. Other families of transcription factors are also implicated in the hierarchy that leads to the formation of skeletal muscle. For example, cells in the dermomyotome are marked by expression of the paired-homeobox (Pax) transcription factors Pax3 and Pax7, with the highest levels of Pax7 in the central domain and preferential Pax3 expression in the DML and VLL [70]. However, only Pax3, but not Pax7, is expressed in the long-range migrating cells which form the initial limb musculature. Mouse embryos carrying a Pax3 loss-of-function mutation do not develop the hypaxial domain of the somite and consequently no limb muscles, but the epaxial-derived muscles are less affected [71]. Pax3, together with Myf5, acts upstream of MyoD. No MyoD transcripts can be detected in Pax3-deficient mice and Pax3:Myf5:MRF4 triple-mutant mice are devoid of all body muscles, lacking MyoD expression and all other downstream myogenic factors [72]. Pax7, on the other hand, appears to be dispensable for embryonic muscle development. Ablation of the Pax3 lineage is embryonically lethal and prevents the emergence of Pax7-positive (Pax7^{+}) cells, while ablation of the Pax7 lineage affects later stages of myogenesis, causing smaller limb muscles with fewer myofibers at birth [73, 74]. This has led to the hypothesis that Pax3^{+} cells are "founder cells" that form a template of initial myofibers in the limb to which Pax7^{+} cells then contribute by forming secondary fibers and establishing the SC pool [58, 60, 75]. Notably, the sine oculis-related homeobox (Six) transcription factors Six1 and Six4 are currently considered the apex of the genetic regulatory cascade that directs dermomyotomal progenitors toward the myogenic lineage [60]. Six proteins bind to and translocate the eyes-absent homologues Eya1 and Eya2 to the nucleus, where they act as transcriptional co-activators of target genes such as Pax3, MyoD, MRF4 or MyoG [76]. The importance of Six transcription factors is underscored by their

regulatory role in Pax3 expression. Overexpression of Six1 and Eya2 in somite explants triggers Pax3 up-regulation, while Six1:Six4 or Eya1:Eya2 mouse mutants are devoid of Pax3 expression in the hypaxial dermomyotome and consequently do not form limb and trunk hypaxial muscles [77].

Myf5 is the first MRF expressed during embryonic development, being transiently expressed in the paraxial mesoderm and later, in concert with the other MRFs, during myotome formation [78, 79]. Initially, Myf5 expression in the dermomyotome is regulated by interactive wingless-Int (Wnt), Noggin, Sonic hedgehog (Shh) and bone morphogenetic protein (BMP) signals from surrounding tissues (Fig. 4B) [60, 63]. Members of the Wnt protein family such as Wnt1 and Wnt3 (secreted from the neural tube) or Wnt4, Wnt6 and Wnt7a (secreted from the surface ectoderm) are of particular importance for somite patterning and developmental myogenesis [80]. Mouse mutants deficient in Wnt1 or Wnt3 lack parts of the dermomyotome and show reduced expression of Myf5 and Pax3 [81], whereas Wnt6 and Wnt7a have been shown to preferentially induce MyoD expression in explant cultures of mouse presomitic mesoderm [82]. Along with Wnt signals, Shh signaling (from the notochord and the floor plate) is positively involved in the specification of muscle progenitors in the somite. Mammalian hedgehog proteins interact with the Patched receptor and trigger release of Smoothened which in turn regulates gene expression via glioma-associated oncogene-related (Gli) transcription factors [83]. Mice deficient in Shh or Smoothened display impaired sclerotome formation as well as reduced expression of Myf5 in the myotome [84, 85]. Gain-of-function studies in chicken embryos revealed that ectopic expression of Shh inhibits Pax3 expression in the dermomyotome, suggesting that Shh is essential for the maturation of dermomyotomal muscle progenitors into Myf5/MyoD expressing, committed myotomal cells that have down-regulated Pax3 and Pax7 [86, 87]. In contrast to Wnt and Shh, BMP signals negatively regulate the expression of certain myogenic genes. Especially BMP4 which is expressed in the lateral plate mesoderm retains sub-populations of muscle progenitors in an undifferentiated state by fostering Pax3 expression while delaying the induction of Myf5 and MyoD [88]. This suggests that BMP4 is responsible for the expansion of a muscle progenitor pool before further myogenic commitment is initiated. The actions of BMP4 are antagonized by Wnt and Shh signals in the DML of the dermomyotome through increased levels of Noggin [89, 90], which allows localized up-regulation of MyoD and has been proposed to initiate myotome formation.

The spatiotemporal provision of the extrinsic signals mentioned above commits dermomyotomal progenitors to the myogenic fate. In fact, three different "founder" stem/progenitor cell (FSC) populations arise [58]: i) The FSC1 population establishes the myotome ("primary muscle mass"), expresses Pax3 (and later Myf5/MRF4/MyoD) and originates primarily from the DML and VLL of the dermomyotome; ii) The FSC2 population is released from the central dermomyotome into the underlying myotome and expresses Pax3/Pax7 (and later MyoD/Myf5); and iii) The FSC3 population leaves the ventral dermomyotome to establish the skeletal muscles of the limbs and expresses Pax3, the tyrosine kinase receptor c-Met and the homeo-domain containing transcription factors Lbx1 and

Mox1 (and later Myf5/MyoD/MRF4). FSC1 is thought to be exhausted early in embryonic (primary) myogenesis, while FSC2 and FSC3 persist to contribute to the majority of SCs [91].

Eventually, the specification and myogenic determination yielding distinct FSC populations becomes manifest in up-regulation of Myf5 and MyoD. From this stage on, these proliferative MyoD$^+$ and/or Myf5$^+$ myogenic cells are referred to as myoblasts. However, cells that migrate from the somite to the limb buds have not yet activated these two MRFs and it is only when they reach the limb that they begin to express MyoD and Myf5 [92]. Both delamination and migration depend on the presence of c-Met and its ligand hepatocyte growth factor (HGF), also called scatter factor, produced by non-somitic mesodermal cells which thus delineate the migratory route for the myoblasts [93]. Pax3 is a transcriptional regulator of c-Met and mice deficient in c-Met, HGF or Pax3 do not develop limb muscles as myoblasts do not delaminate from the hypaxial dermomyotome [72, 94, 95]. Another homeo-domain containing transcription factor, Lbx1, is also implicated in the migration of cells from the somite. In Lbx1-deficient quail-chick chimaeras muscle progenitors do delaminate from the dermomyotome, but fail to migrate long range and stay in the vicinity of the somite where they may adopt other cell fates [96].

Once the myoblasts reach the limb, they have to proliferate extensively, a process that happens after the onset of Myf5 and MyoD expression in mice [61]. This is partially controlled by the homeobox transcription factor Msx1 which is present in migrating myoblasts at the forelimb level. Msx1 has been shown to keep cultured myoblasts dividing [97] and Msx1 overexpression in differentiated muscle cells induces them to re-enter the proliferative state [98]. Importantly, fibroblast growth factor (FGF) signaling provides a switch between myoblast proliferation and terminal differentiation into myofibers. The FGF family is heavily involved in limb myogenesis and it has been proposed that signaling through FGF receptors (FGFRs) differentially regulates myoblast proliferation [99], migration to the limb bud [100] and terminal differentiation [101]. For example, inhibition of FGFR4, but not FGFR1, leads to an arrest of myoblast differentiation through down-regulation of Myf5, MyoD and embryonic MHC (eMHC), resulting in the loss of limb musculature. Conversely, overexpression of FGF8 (a ligand for FGFR4) in somites promotes FGFR4 expression and myogenic differentiation [101].

Proliferating myoblasts withdraw from the cell cycle to become terminally differentiated myocytes which express the "late" MRFs MyoG and MRF4, and subsequently muscle specific genes such as MHC and muscle creatine kinase (MCK). The activation of the differentiation program also depends on the presence of transcription factors from the myocyte enhancer factor (MEF) family. MRFs can activate their own expression as well as that of MEF2 [102] and MEF2, although not having myogenic activity itself, can in turn potentiate the function of MRFs through transcriptional cooperation [103]. Terminally differentiating myoblasts will start to secrete fibronectin into the ECM which enables them to bind ECM components via fibronectin and the α5β1 integrin receptor. The importance of this interaction is highlighted by the finding that blocking of this receptor prevents myoblast fusion into

myofibers and thus functional muscle development [104]. Myoblast adherence to the ECM promotes cellular alignment followed by the cell elongation, which is mediated by different cell adhesion molecules (CAMs) and cadherins [105, 106]. By the time it expresses MyoG the myoblast becomes capable of fusion which involves a series of cell-cell recognition, adhesion, alignment and membrane fusion steps [107, 108]. Ultimately, this leads to the formation of a single multinucleated myofiber (also referred to as myotube) which starts to secrete the cytokine interleukin 4 (IL-4) that functions as a paracrine chemoattractant for the recruitment of other myoblasts to fuse into the exiting myofiber. As the myofiber matures, the transverse banding pattern becomes evident due to sarcomere assembly into myofibrils [107]. First primary fibers in mouse limbs appear around embryonic day (E) 11-14 and secondary fibers develop around the primary fibers at the time when muscle innervation starts, approximately at E14-16 [109].

Summarising, a complex network of extrinisic and intrinsic factors governs the series of events from somite patterning and muscle progenitor specification to terminal differentiation of committed muscle cells into multinucleated contractile myofibers. The Six and Pax transcription factors play a pivotal role upstream of the MRFs (Fig. 5) and differential expression of these factors in response to spatiotemporal provision of extrinsic stimuli specifies different muscle progenitor (FSC) populations that build up different muscles.
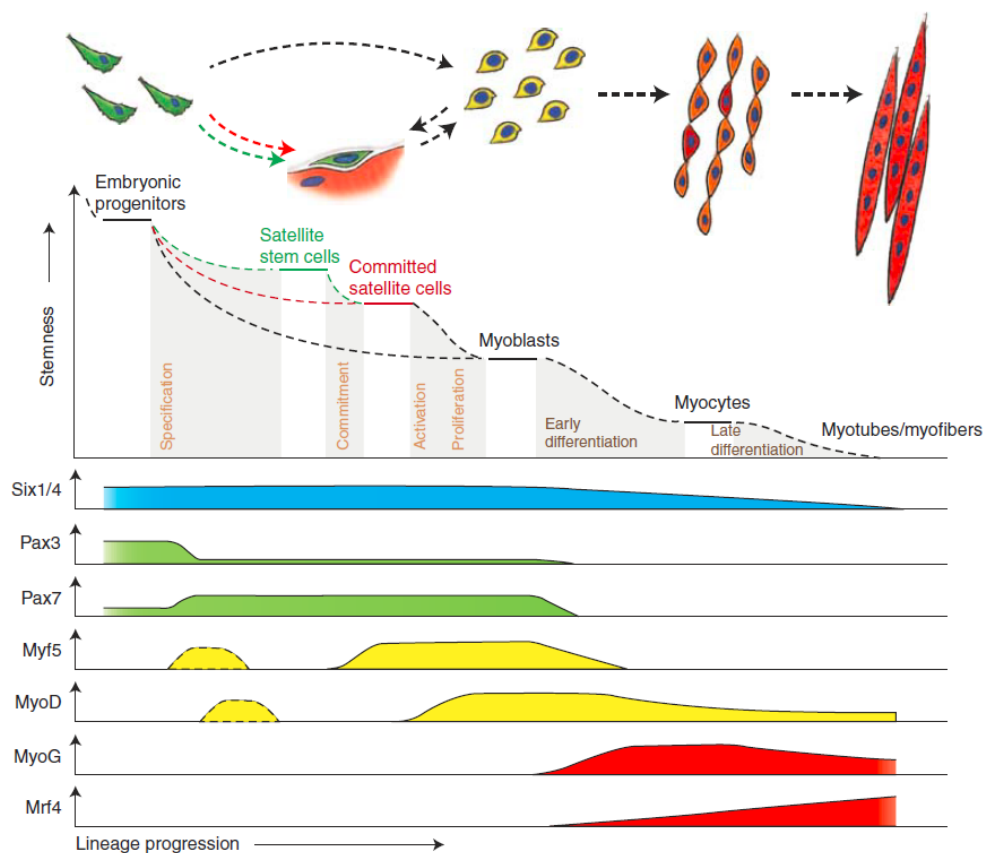
Fig. 5: *The hierarchy of transcription factors regulating the progression through the myogenic lineage, from muscle progenitor specification in the somite to terminal differentiation into contractile myofibers* (from [60]).

During the course of muscle development, a distinct sub-population of myoblasts fails to terminally differentiate, but remains associated with the surface of a developing myofiber as quiescent muscle SCs. After proliferation as Pax7^{+}/MyoD[+] myoblasts, most cells maintain MyoD but down-regulate Pax7 expression and commit to differentiation via activation of MyoG. Some myoblasts, however, maintain Pax7 but down-regulate MyoD and eventually withdraw from the cell cycle, regaining markers that characterize myogenic quiescence [31]. These SCs are the adult stem cell of the muscle and provide the basis for neonatal muscle growth and adult muscle repair/regeneration in response to injury or disease. Once activated, the SC goes through a similar transcriptional progression as the founder muscle progenitors in embryonic myogenesis (Fig. 5), but replenishes the SC pool through symmetric and asymmetric cell division for future rounds of muscle regeneration.

2.2.2. Skeletal muscle regeneration - the satellite cell

Unlike embryonic muscle development, muscle regeneration in higher vertebrates depends on the injured tissue retaining an ECM scaffolding serving as a template for the formation of new (regenerative) muscle fibers. In addition, tissue regeneration requires the recruitment of undifferentiated progenitor cells to the site of injury and, in skeletal muscle, this function is provided by SCs [60]. Ever since their discovery in 1961 [110, 111], the dynamics of SC biology in muscle homeostasis and the molecular markers that identify this cell population have been a topic of extensive research [112-116]. SCs reside in a distinct anatomic position between the surface of the myofiber sarcolemma and the basal lamina that surrounds the fiber, hence the name satellite cell (Fig. 6).
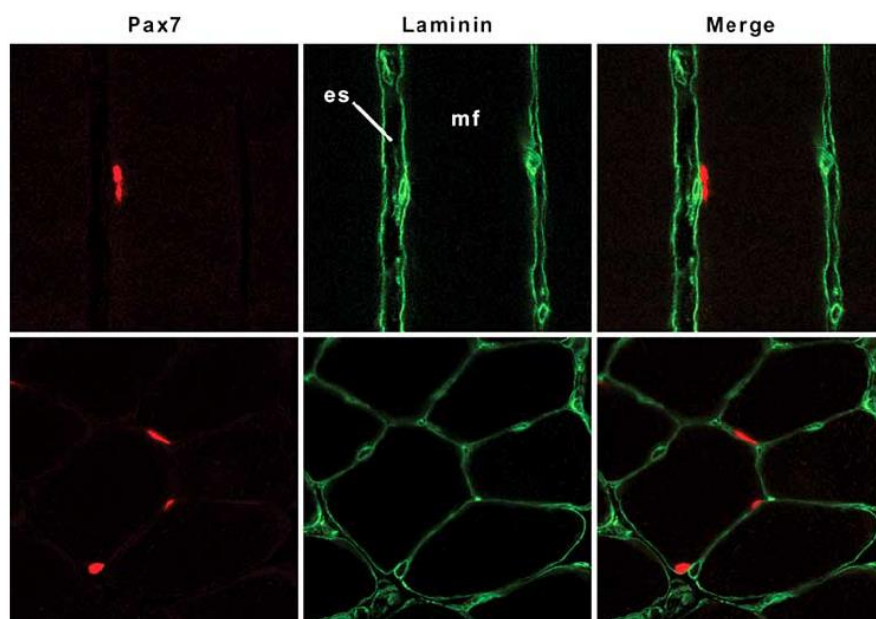
Fig. 6: *Satellite cells in rat skeletal muscle.* Quiescent satellite cells in adult rat soleus muscles can be recognized by the presence of Pax7 in nuclei (red) and their localization between the sarcolemma and the basal lamina (laminin stain, green). Upper panel: longitudinal section; lower panel: transverse section. mf: myofiber; es: extracellular space (from [117]).

Upon activation, SCs can generate myoblasts that then proliferate before they either fuse into an existing myofiber to become post-mitotic nuclei (myonuclei), or fuse with other myoblasts to form myotubes (immature myofibers). During early postnatal muscle growth, the main role of SCs is the addition of myonuclei to growing myofibers, whereas, in adult muscle, their role switches to providing myonuclei for homeostasis and hypertrophy, or in response to the more sporadic demands of myofiber repair and regeneration [116]. This is not just reflected by the difference in SC numbers observed in postnatal muscles (approx. 30% of total muscle nuclei) versus adult muscles (approx. 2-7%), but also by a progressive switch from SC proliferation in early muscle development to SC quiescence in fully formed adult muscle [114]. However, quiescent SCs retain the ability to extensively proliferate and differentiate in response to the needs for myonuclear turnover, myofiber hypertrophy or after muscle damage. This activation and proliferation of SCs is largely, if not entirely, responsible for the remarkable capacity for efficient muscle repair, with the generation of large numbers of new myotubes within as little as 3-4 days after severe acute muscle damage [118, 119].

Quiescent SCs express characteristic (although not unique) markers and the most widely used of these marker is Pax7 which has been shown to be essential for SC specification and survival [74, 120]. In contrast, Pax3 which is central in embryonic myogenesis is expressed only in quiescent SCs of a few specific muscle groups [121]. Myf5 is expressed in the large majority of SCs, however, lineage tracing experiments have demonstrated that about 10% of SCs have never expressed Myf5, hinting at the SC pool being a heterogeneous population of "commited" SCs (Pax7$^+$/Myf5$^+$) and "satellite stem cells" (Pax7$^+$/Myf5$^-$) [119, 122, 123]. Other quiescent SC markers include M-cadherin, Cluster of differentiation 34 (CD34), c-Met, caveolin-1, nestin or α7 and β1 integrins, and combinations of these markers have routinely been used to isolate and purify SC populations by cell sorting [124].

When muscle is damaged (or during early postnatal muscle growth), the SCs become activated and proliferate extensively. At this stage, the SC is often referred to as muscle precursor cell (mpc) or myoblast. The progression of activated SCs along the myogenic lineage parallels that of muscle progenitors in embryonic myogenesis and, again, is mainly controlled by the MRFs (Myf5, MyoD, MRF4 and MyoG; Fig. 5). Similarly to other adult stem cell types, SCs follow stochastic (symmetric) and asymmetric paradigms of self renewal, depending on the orientation of divisions with respect to the basal lamina (basal surface) and the sarcolemma of the fiber (apical surface) [125]. Upon activation, Pax7$^+$ SCs up-regulate Myf5 and MyoD and proliferate as Pax7$^+$/Myf5$^+$/MyoD$^+$ myoblasts. These SC-derived myoblasts divide symmetrically (parallel to the myofiber) and later adopt divergent fates. The majority of them will down-regulate Pax7, maintain MyoD expression and commit to terminal differentiation by up-regulation of MRF4 and MyoG, followed by fusion into the damaged myofiber. A small subset, however, will maintain Pax7 but down-regulate MyoD and withdraw from both cell cycle and immediate myogenic differentiation, returning to a state resembling quiescence [119]. Alternatively, apicobasal divisions (perpendicular to the myofiber) follow the asymmetric paradigm and give rise to two distinct fates: one daughter cell is pushed into the apical surface and

becomes Pax7$^+$/Myf5$^+$, while the other daughter cell remains adhered to the basal lamina and retains is stem cell identity (Pax7$^+$/Myf5$^-$) [123].The activated Pax7$^+$/Myf5$^+$ SC will then express MyoD and enter terminal myogenic differentiation. The intrinsic mechanisms responsible for the orientation of SC/myoblast divisions and subsequent myogenic commitment of the apical daughter cell are not fully understood. However, Delta1/Notch signaling and Wnt signaling (especially through Wnt7a) have been demonstrated to be extrinsic regulators of symmetrical and asymmetrical SC/myoblast division [126, 127].

The SC niche provides the specialized environment necessary to govern the balance between SC quiescence, activation and self renewal/differentiation. Apart from structural elements of the niche, growth factors, cytokines and neurotrophic factors also play a pivotal role in the regulation of SC activity. These function in auto- and paracrine ways and are produced and secreted by local cells such as the interstitial cells, microvasculature, NMJ, immune cells (mostly neutrophils and macrophages) or the (damaged) myofiber itself (Fig. 7) [113]. Growth factors are crucial in SC regulation and the sequence of their release and their concerted actions control both the up- and down-regulation of muscle specific genes. Among the stimulatory growth factor families promoting myogenic proliferation and differentiation HGF, FGF, vascular endothelial growth factor (VEGF), platelet-derived growth factor (PDGF), insulin-like growth factor (IGF) and stromal cell-derived factor (SDF) are the most prominently studied [128]. Furthermore, elevated levels of the cytokines granulocyte-colony stimulating factor (G-CSF) and interferon-γ (IFN-γ) can be detected in muscles after injury, suggesting a central role of the inflammatory response in SC activation and muscle repair [129, 130]. The major inhibitory growth factors are members of the transforming growth factor-β (TGF-β) superfamily [131]. These inlcude TGF-β1, Myostatin (Gdf8) and BMPs which all have potent inhibitory effects on both embryonic muscle development and postnatal muscle regeneration [132]. Some of these regulating factors reach muscle through systemic circulation, which underscores the importance of the microvasculature in maintaining muscle homeostasis. In humans, approx. 68% of SCs are located within 5µm from neighboring capillaries or vascular endothelial cells (ECs). In addition, there is a correlation between the number of capillaries per myofiber and the number of SCs [133]. Last but not least, structural components of the SC niche act as regulators of muscle repair, for example through controlling SC attachment. SCs bind the basal lamina (which is mainly composed of laminin-2 and type IV collagen) through integrin α7β1 and the sarcolemma of the myofiber through M-cadherin [113]. This linkage of the SC cytoskeleton to the surrounding ECM is integral for the transduction of strain-induced mechanical forces into chemical signals involved in myogenesis [134]. Furthermore, the basal lamina contains heparan sulfate proteoglycans (HSPGs), bound to laminin-2 and type IV collagen, which can capture growth factors, integrate them into the basal lamina and regulate their bioactivity [135, 136]. For example, HGF, FGF or members of the TGF-β superfamily (including Myostatin) are bound to HSPGs [137, 138] and *in vivo* studies in mice have shown that the presence of HSPGs is required for HGF and FGF signaling to function properly [139]. Upon injury,

SCs release matrix metalloproteinases (MMPs) and degrade the muscle (and niche) ECM, which allows them to migrate to the site of injury and also liberates the growth factors and cytokines "stored" in the ECM [140, 141]. The integrity of muscle ECM and the ability of SCs to bind to it is a crucial regulator of muscle homeostasis, which is demonstrated by the observation that knocking out laminin-2 in mice not only results in an almost complete absence of the basal lamina [142], but also a decrease in the total number of SCs [143].
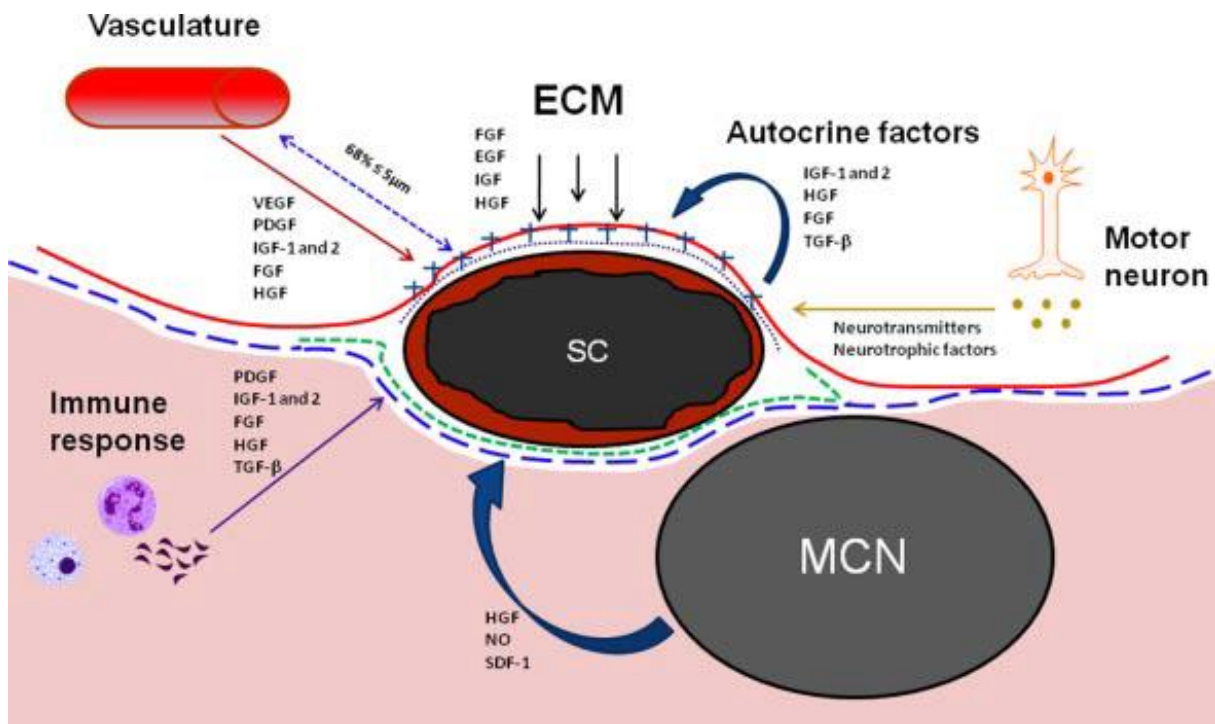
Fig. 7: *The SC niche and regulatory factors.* SCs are located within a specific niche between the sarcolemma (blue dashed line) and the basal lamina (red line). The basal side of the SC expresses integrins α7β1 (purple dotted line), linking the SC with laminin (blue crosses) in the basal lamina. The apical side of the SC expresses M-cadherins (green dashed line), which links the SC to the sarcolemma of the adjacent myofiber. The switch from SC quiescence to activation and proliferation is controlled by a plethora of (growth factor and cytokine) signals from surrounding cells such as the vascular endothelial cells, the motor neuron, invading immune cells or the myofiber. ECM: extracellular matrix; SC: satellite cell; MCN: Myonucleus (from [113]).

Whether a muscle injury is inflicted by a direct trauma or innate genetic defects, muscle regeneration is marked by three sequential but overlapping stages (Fig. 8): i) the destruction/inflammatory phase after myofiber necrosis or rupture, dominated by the invasion of macrophages, ii) the repair phase which involves phagocytosis of necrotic myofibers and the activation, differentiation and subsequent fusion of SC progeny (myoblasts) for repair and/or *de novo* generation of myofibers, and iii) the remodeling phase characterized by the maturation of new myofibers, remodeling of scar tissue and the restoration of muscle function [117, 144].
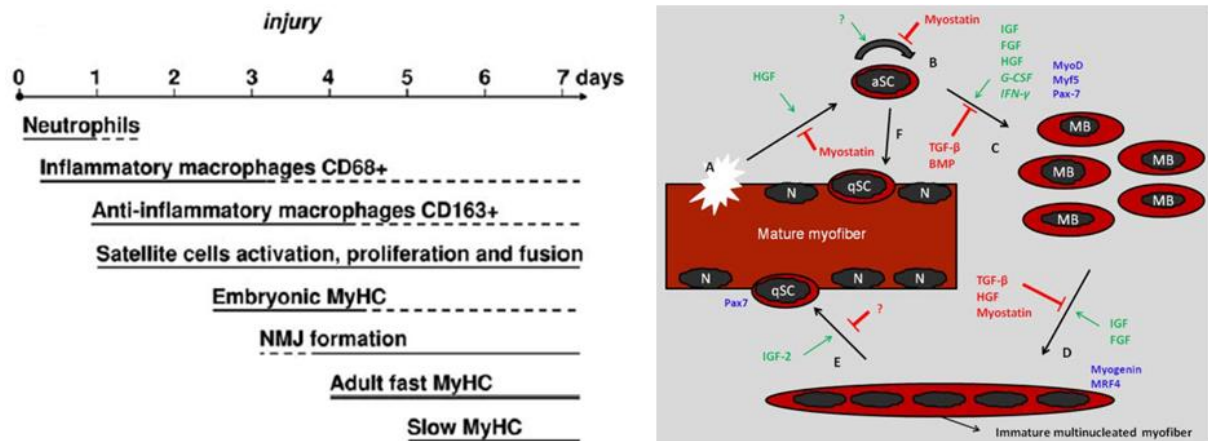
Fig. 8: *Stages of muscle regeneration.* Left: schematic representation of the temporal sequence of degenerative (inflammatory) and regenerative events following muscle injury (adapted from [117]). Right: following myotrauma (A), quiescent SCs are activated (by HGF) and enter the cell cycle for self renewal (B) and proliferation as Pax7$^+$/MyoD$^+$ myoblasts (C). Differentiating myoblasts up-regulate MyoG and MRF4 and either form new immature myotubes (D) or fuse to existing myofibers (not shown). Myofiber maturation entails movement of the initially central located myonuclei to the periphery of the fiber, into a subsarcolemmal position (E). After SC activation, a subset of SCs withdraws from the cell cycle and re-enters a state of quiescence (Pax7$^+$/MyoD$^-$) to replenish the SC pool (F) for future rounds of muscle regeneration. aSC: activated SC; qSC: quiescent SC; MB: myoblast; N: (myo)nucleus (from [113]).

The initial event of muscle degeneration is myofiber necrosis which is generally triggered by disruption of the myofiber sarcolemma, resulting in increased permeability. The loss of myofiber integrity after damage is reflected by increased serum levels of muscle proteins which are usually restricted to the sarcoplasm, such as the MCK [62]. Sarcolemmal breakdown or damage to the sarcoplasmic reticulum results in the loss of Ca^{2+} homeostasis and triggers calpain-dependent myofiber proteolysis. Calpains are Ca^{2+}-dependent proteases that can cleave myofibrillar and cytoskeletal proteins and are hence central for the process of myofiber autolysis [145]. Ca^{2+} influx and the entry of plasma proteins subsequently activates the complement system and induces chemotactic recruitment of leukocytes, initially neutrophils (detectable at significant levels already 1-6 hours after muscle damage [146]) and then macrophages [117]. Two distinct sub-populations of macrophages sequentially invade the injured muscle tissue [147]. Early invading M1 macrophages (CD68$^+$/CD163$^-$) reach their highest concentration 24 hours after injury and then rapidly decline. M1 macrophages have two important roles: they are responsible for the phagocytosis of necrotic muscle tissue and, at the same time, secrete pro-inflammatory cytokines such as tumor necrosis factor α (TNF-α) or IL-1β [148]. A second population of anti-inflammatory M2 macrophages (CD68$^-$/CD163$^+$), derived from pro-inflammatory M1 macrophages by a phenotype switch, reach their peak about 2-4 days after injury. M2 macrophages secrete anti-inflammatory cytokines such as IL-4 and IL-10, gradually terminate inflammation and release factors that stimulate the proliferation, growth and differentiation of myoblasts [149].

Following muscle damage, SCs become activated 2 days after injury and undergo rapid proliferation. Apart from the extrinsic signals in the niche discussed above (Fig. 7), other signals appear to also trigger SC activation. Generation of sphingosine-1-phosphate in the inner side of the SC plasma membrane as been shown to be essential for SC activation [150]. The production of nitric oxide (NO) by increased NO synthase (NOS) activity also seems to be important, possibly through activating SC MMPs which induce the release of HGF from the muscle ECM (especially the basal lamina) [151]. As mentioned above, Notch and Wnt signaling is involved in the switch from SC proliferation to myoblast differentiation, with Notch being prevalent during proliferation and Wnt (mostly Wnt7a) during differentiation [126, 152]. Defective Notch signaling leads to inhibition of SC proliferation and self renewal, while enhancement of Notch signaling has been shown to promote muscle regeneration in aged muscle [125, 153]. Altogether, these signals activate SCs which will then divide symmetrically and asymmetrically to generate large amounts of $Pax7^-/MyoD^+$ myoblasts while a sub-population of $Pax7^+/MyoD^-$ cells will replenish the SC pool (Fig. 8). Myoblasts then fuse into immature myofibers, a process that is positively regulated by IGF, FGF, HGF, G-CSF and IFN-γ and negatively regulated by factors of the TGF superfamily like Myostatin, TGF-β or BMPs.

The last stage of muscle regeneration is the maturation of newly formed or repaired myofibers and remodeling of the regenerated muscle. The subsequent growth of regenerated muscle may vary according to several factors, for example the type of injury, the involvement of vasculo-/angiogenesis and the reestablishment of NMJs and myotendinous connections. A crucial factor for successful muscle regeneration is the maintenance of the myofiber's basal lamina. Within an intact basal lamina SCs can proliferate and migrate to later fuse and form myofibers almost indistinguishable from pre-injury fibers within a short period of time [117]. This can be tracked by expression profiling of developmental muscle markers such as eMHC or histologically, as regenerated immature fibers can be recognized by the presence of centrally located myonuclei, a hallmark of muscle regeneration. An important aspect in myofiber maturation is nerve activity. Animals in rat soleus muscles have demonstrated that, until day 3 after injury, muscle regeneration in innervated vs. denervated muscles is almost undistinguishable, as both are composed of thin myofibers expressing eMHC. After 3 days, nerve terminals start to contact immature newly formed myofibers and 1-2 days afterwards innervation is fully functional in these fibers [154, 155]. Regenerating myofibers initially express MHCs typical for developing muscle, such as embryonic and neonatal MHCs, but soon start to express adult fast MHCs [118]. This switch in MHC isoforms is a default autonomous process independent of innervation [156], however, a second switch from fast to slow adult MHC which can be detected 5 days after injury in rat muscle is clearly dependent on slow motor neuron activity. This isoform switch does not occur in denervated muscle but can be induced by electrical stimulation of denervated regenerated muscle with a slow-type impulse pattern [157].

In addition to SCs, other non-muscle or muscle stem cells show myogenic potential and may be involved in muscle repair and regeneration [62, 113, 124]. A seminal study by Ferrari et al. [158]

demonstrated that multipotent hematopoietic stem cells (HSCs) from the bone marrow, when injected intramuscularly or intravenously (systemically), can contribute to muscle regeneration by providing new myonuclei, albeit with very low frequency. A circulating sub-population of HSCs, CD133^{+} (AC133^{+}) cells have also been shown to be competent for myogeneis and further can restore dystrophin expression in dystrophic mouse muscle after systemic injection, although again at very moderate levels [159]. These CD133^{+} cells can also be found in muscle (entering through circulation) and have thus also been termed muscle-derived stem cells (MDSCs) [160]. The heterogeneous muscle side population (SP) cells, a rare and poorly defined MDSC type, have the potential to give rise to both myocytes and SCs after intramuscular injection as well as to restore dystrophin expression in mice [161, 162]. MDSCs are an increasingly interesting alternative to SCs for muscle regeneration, as they have unique characteristics usually associated with non-committed progenitor cells such as high capacity for self renewal, proliferation and multipotency [163]. Another source of muscle stem cells is the infiltrating micro-vasculature: mesoangioblasts (MABs) are blood vessel-associated progenitors that express endothelial markers when isolated from the embryo and pericyte markers when isolated from postnatal tissues [124, 164]. Both MABs as well as their progeny, pericytes, are able to cross the vessel wall, fuse to the myofiber and contribute to muscle regeneration. More importantly, they have been systemically administered into dystrophic mice and dogs, where they ameliorated pathologic muscle morphology [165-167]. Furthermore, endothelial progenitor cells (EPCs) [168] and mesenchymal stem cells (MSCs) of various sources [168, 169] have been identified as capable of supporting myogenic differentiation. However, a shortcoming of MSC grafting is that they require at least transient (but forced) expression of myogenic specification/determination factors such as Pax3 or MyoD to enter the myogenic lineage [169, 170]. In this respect, a recently discovered sub-population of MSCs, multilineage-differentiating stess enduring (Muse) cells [171], might provide a feasible alternative. These cells were identified in mesenchymal tissues such as bone marrow, adipose tissue, dermis or connective tissue, have tri-lineage differentiation potential and are non-tumorigenic [171]. When grafted into immunodeficient mice, human Muse cells integrated into damaged muscles and contributed to both muscle fiber formation (as noted by the presence of dystrophin-positive human fibers) as well as to replenishment of the endogenous SC pool (identified by the presence of Pax7 positive human cells on the edge of fibers) [172]. However, even though clearly capable of participating in muscle regeneration, these cells have neither been tested for functional contribution in dystrophic animals nor have long-term outcomes been investigated so far.

Notably, long term functional muscle recovery in dystrophic animals after MSC engraftment has not been achieved. A general bottleneck of non-SC cellular muscle therapies is their requirement for more or less functional muscle homeostasis, provided by SCs. Although some cell types have been shown capable of partially repopulating the SC niche, it has been shown conclusively that muscle regeneration cannot be fully recovered by any of the aforementioned cell types without the presence of

SCs. This emphasizes the seminal observation that skeletal muscle fails to regenerate after genetic ablation of SCs [31, 173].

2.3. Acute and chronic skeletal muscle pathologies

Injuries of the musculoskeletal system are extremely common. In sports, for example, muscle injuries account for 10-55% of all sustained injuries with over 90% of these injuries being either contusions, lacerations or strains [174, 175]. These muscle injuries usually result in physical myotrauma without significant loss of muscle tissue, provided that only a fraction of muscle is affected [176]. This is due to the robust capacity of skeletal muscle for regeneration following injury that is relying on the SCs. In fact, this remarkable regenerative potential was first demonstrated in rats, where an entire muscle was completely removed, minced and placed back into its compartment, with the outcome that, after time, the muscle had regenerated enough to produce contractile force again [177]. However, the intrinsic regenerative potential of muscle following damage is dependent on the type and extent of injury and even in less severe injuries, the repair process may not be 100% efficient [144]. When traumatic events lead to VML, the regenerative myogenic potential will be drastically reduced, and if more than 20% of the affected muscle is lost, the natural repair process will fail to regenerate the defect. This results in an accumulation of scar tissue and denervation of the portion of muscle distal to the defect which subsequently completely loses its function [178-180]. Common causes for VML are traumatic injuries to the extremities from accidents in traffic (especially motor vehicle accidents), open fractures (in both civilian and military populations) or surgical loss of muscle, for example due to tumor ablation [181, 182]. Whatever the cause, VML is generally defined as an irrevocable injury sustained by skeletal muscle and characterized by a permanent loss of tissue structure and function [182]. The result is life-long disability which severely affects quality of life and in cases of extreme traumatic injury, amputation is the only viable treatment. Otherwise, current state-of-the-art treatments are limited to scar tissue debridement and placement of muscle flaps around the site of tissue defect (FFMT) [183]. However, FFMT, while restoring function, does not regenerate the lost muscle tissue and typically results in alterations of the anatomy and biomechanics for both recipient and the donor sites [184].

During the muscle repair process, muscle cells, blood vessels and nerves infiltrate the wound area. Concurrent with the formation of new muscle, the gap between the remaining functional myofibers is bridged by collagenous scar tissue to preserve the transduction of force along the muscle. In less severe injuries like sprains or contusions, this tissue scar also acts as a conduit to promote the formation of new myofibers. After VML, however, the rate at which fibroblasts deposit scar tissue exceeds that of regenerative myogenesis, thereby creating a dense cap that blocks regenerating myofibers from bridging the defect. As a consequence, the original muscle is split in two parts, with the distal part remaining denervated and losing its function (Fig. 9). Over time, this part of the muscle

will be lost due to atrophy [144]. Furthermore, volumetric muscle defects are also associated with irregularities during the muscle maturation and remodeling phase. These include (i) incomplete fusion of immature myofibers with the formation of forked myofibers, (ii) segmental necrosis followed by SC fusion with the viable myofiber stump, (iii) SC differentiation and fusion under the basal lamina of an existing myofiber with formation of a "satellite fiber", and (iv) the rare event of "orphan myofiber" formation outside the basal lamina from migrated SCs or stem cells from other sources [117, 144, 185].
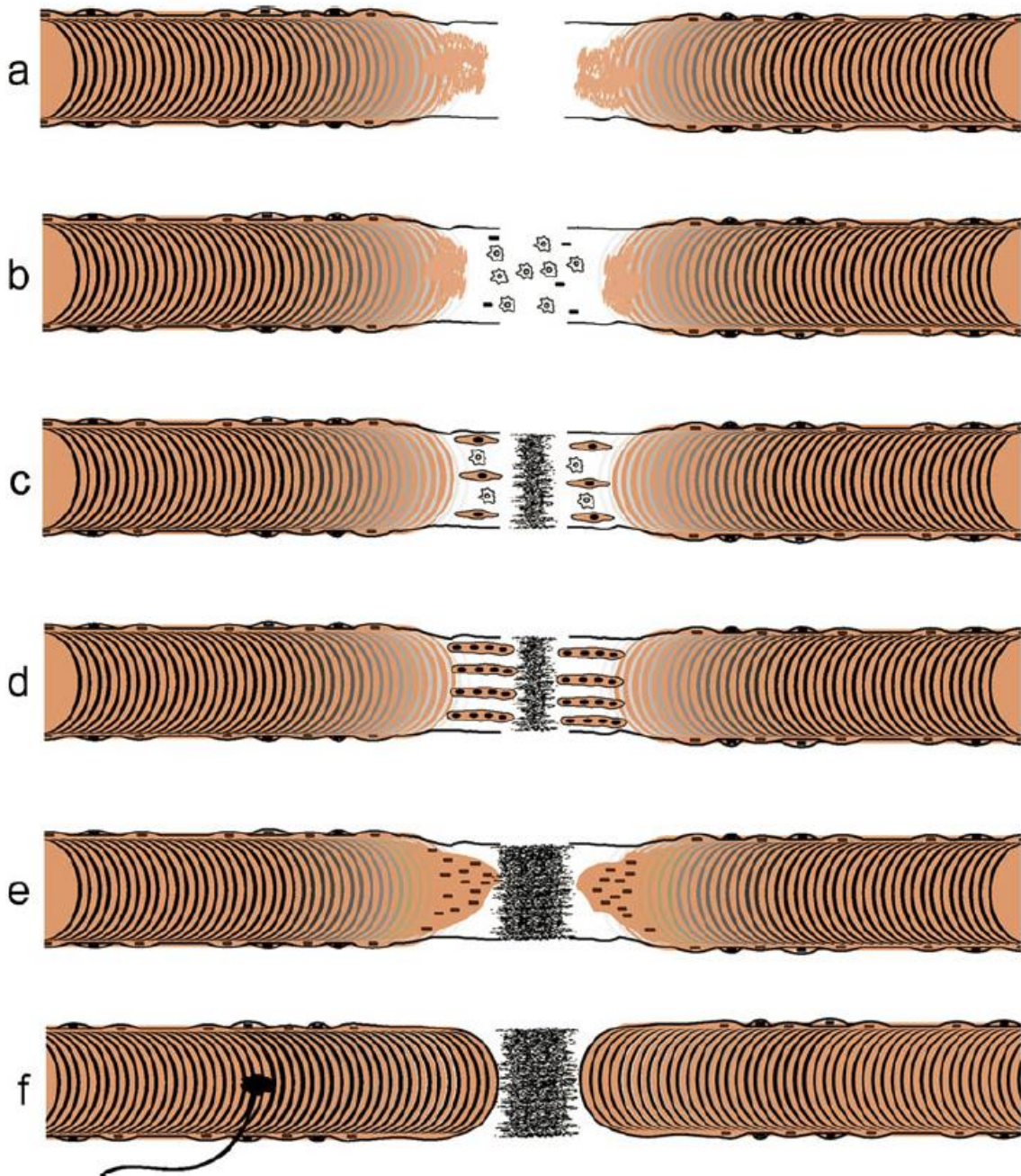

Fig. 9: *Repair of large muscle defects with volumetric loss.* Following a volumetric muscle injury (a), damaged and necrotic myofibers are degraded by invading inflammatory cells (neutrophils, macrophages) which remove cell debris and attract/activate SCs (b). SCs proliferate and differentiate into myoblasts, while fibroblasts start to deposit scar tissue (c).

31

Newly formed immature myotubes fuse with existing myofibers to restore function (d). In the case of VML, scar tissue formation proceeds more rapidly than myogenesis, leading to the formation of a dense cap that prevents the myofibers from bridging the wound (e). This splits the muscle into two parts and, consequently, the distal tissue (*right*) which does not contain any NMJs becomes denervated and subsequently atrophic (from [144]).

Apart from acute traumatic events such as VML, other (chronic) pathologic scenarios can result in permanent muscle loss. Aging presents such a scenario and one of its distinct features is the presence of muscle weakness and atrophy. The age-related, irreversible and permanent loss of muscle mass and force is termed sarcopenia [186]. Sarcopenia is the major cause of impaired physical function, which contributes to mobility disability, falls and hospitalization in the elderly. Lower muscle mass an strength are also associated with a decline in bone mineral density and a greater risk of osteoporotic fractures in older adults [187]. In humans, skeletal muscle mass decreases by almost 50% between ages 20 and 90 years, and muscle strength, which peaks about age 30 years, is lost at a rate of 15% per decade starting around age 50 years and subsequently accelerates to about 30% per decade at age 70 years [188].

In contrast to widely-used measurements of bone density that reflect bone strength and allow prediction of fracture risks, a precise definition of low muscle mass and strength has not been established. Sarcopenia is commonly considered analogous to osteoporosis, yet, unlike osteoporosis which can be diagnosed on widely accepted clinical criteria [189], sarcopenia is not recognized as a clinical condition [187]. There are, however, some distinct structural features observable in aged muscle on the single fiber level as well as that of a whole muscle. The most prominent changes are (i) decreased SC and myofiber numbers, (ii) reduced myofiber size and (iii) decreased expression of MHCIIa in conjunction with a shift to proportional increase in the MHCIIx isoform [190]. These "hallmarks" of aged muscle are the result of a changing muscle microenvironment over a lifespan and attributable to a combinatorial variety of intrinsic and local or systemic extrinsic factors [191]. In this respect, a prominent factor driving age-related loss of muscle strength are neurophysiological alterations that lead to gradually increasing functional impairments. These alterations include erroneous motor unit remodeling events, motor neuron death (causing motor unit loss) or sporadic myofiber atrophy and are not only linked to increasing muscle denervation in advanced age but also switches in MHC fiber isotypes [192]. While this is observed on the level of an entire muscle, accumulating dysregulation of factors and signaling pathways that control SC behavior also drive pathogenesis in sarcopenia. Alterations in the local presence of Notch, Wnt or TGF-β ligands have been shown to affect SC self renewal and differentiation. For example, aged muscles show decreased expression of the Notch ligand Delta1, crucial for SC activation and self renewal [153], or increased levels of circulating Wnt3a, which induces undesirable fibrogenic differentiation of SCs and also antagonizes Delta1/Notch signaling [152, 193]. Elevated levels of TGF-β superfamily members, most notably Myostatin (Gdf8) and Gdf11, have been shown to be involved in decreasing muscle mass and interfering muscle repair [194, 195]. Furthermore, changes in the hormonal balance affect the

regulation of muscle homeostasis, and declines in testosterone, vitamin C, insulin or oxytocin levels appear to play a role in the pathogenesis of sarcopenia [196]. One of the probably most direct pathological effects is caused by a gradual dysregulation of the inflammatory response after injuries in aged muscles. The exposure of SCs in an aged niche with a progressively altered cytokine composition has deleterious effects on muscle regeneration, and SC exhaustion has been linked to constantly elevated IL-6 and TNF-α levels [191, 197].

Some of the combinatorial deleterious effects of the (local or systemic) extrinsic factors mentioned above have been demonstrated in heterochronical animal grafting experiments. Aged muscles grafted into muscles of young animals exhibited an increase in muscle mass and force, while the opposite was true for young muscles grafted into old hosts [198, 199]. In addition, although conflicting results have been found, young animals might repair destructed and/or denervated muscle more efficiently than old ones [200, 201]. The influence of the microenvironment in muscle regeneration was further confirmed in parabiosis experiments. When young and old mice are conjoined and their circulatory systems shared, the muscles of aged mice in such heterochronic parabiotic pairs exhibit a more robust regenerative response to local injury than do aged mice in isochronic pairs [193, 202]. Conversely, the regeneration of young muscles is impaired when exposed to an aged circulation system [193]. Importantly, these studies suggest that some of the pathological features in sarcopenia are reversible.

Apart from those caused by dysregulation of extrinsic factors, there are some cell-intrinsic dysfunctions in SCs that arise from alterations in multiple signaling cascades (which partially seem to be caused by dysfunctional inflammatory response). These include the p38α/β mitogen-activated protein kinase (MAPK), the growth factor stimulated FGFR and the cytokine-stimulated Janus kinase/Signal Transducer and Activator of transcription (JAK/STAT) signaling axes [191]. De-regulated MAPK and JAK2/STAT3 can negatively regulate SCs self renewal by restricting cell cycle progression and promoting myogenic differentiation [203-206], while aberrant p38α/β MAPK activity may suppress Pax7 expression through repressive chromatin modifications [207]. Altogether, these accumulating intrinsic changes lead to a progressive depletion of the SC reservoir by disruption of the balance of SC asymmetric self renewal. In this respect, age-related changes in muscle ECM composition and integrity, especially the basal lamina, may as well play an important regulatory role [208, 209].

Many of the pathological circuits driving sarcopenia are, to some extent, affected by the individual's lifestyle. In particular, diet and physical (in)activity can strongly modulate onset and progression of muscle loss. The latter is especially potent and resistance training (strength training exercise with progressive overload where muscles exert force against an external load), a common therapeutic measure, can attenuate muscle loss in the elderly [210]. Resistance training has benefits beyond improvements in muscle strength, such as improved balance, functional mobility, fall prevention or gait speed [190]. In addition to exercise, an appropriate diet, especially the uptake of anti-oxidants, can

ameliorate the progression of muscle loss through preventing overwhelming levels of oxidative stress and mitochondrial dysfunction, two other pathophysiological hallmarks of sarcopenia [211].

Finally, progressive skeletal muscle atrophy can also be caused by genetic disorders affecting important muscle proteins. MDs are a clinically, genetically and biochemically heterogeneous group of over 30 disorders that are characterized by progressive muscle wasting and weakness that affects limb, axial and facial muscles to variable degrees [212]. In specific forms, other muscles, including respiratory muscles, cardiac and smooth muscles or swallowing muscles, can also be affected. In rare variants, MDs may also be associated with involvement of other tissues and organs, such as the brain, inner ear, eye or skin [213]. In general, MDs differ in prevalence, disease onset, rate of progression, the types of muscles affected and the pattern of inheritance. The underlying genetic causes are heterogeneous and classifications of MDs are based on the location or function of the primary proteins defect. The main protein classes involved in the pathophysiology of MDs are muscle ECM and external membrane proteins, muscle enzymes or proteins with putative enzymatic function, sarcolemma-associated proteins, nuclear membrane proteins and sarcomeric proteins [213]. Some of these proteins can be found in, or in close proximity to, the dystrophin-glycoprotein complex (DGC; also called dystroglycan complex), a large oligomeric complex of sarcolemmal proteins and glycoproteins which forms a critical link between the muscle cytoskeleton and the ECM [213-215]. The DGC plays an indispensible role in stabilizing the myofiber against the mechanical forces of muscle contraction by providing a shock-absorbing connection between cytoskeleton and ECM. Duchenne muscular dystrophy (DMD), an X-linked recessive disorder, is the most common childhood form of MD and caused by a mutation in the DMD gene [216]. DMD encodes the protein dystrophin which is part of the DGC, and its absence results in increased muscle fiber fragility and susceptibility to injury in response to mechanical load. This results in continuous cycles of muscle de- and regeneration, which has a direct effect on the SCs as they are constantly exposed to an activating environment in dystrophic muscles [217]. Thus, the SC pool will be prematurely exhausted, a phenomenon that is also accentuated by aging [218]. This ultimately leads to (often asymmetric) progressive muscle weakness, usually accompanied by muscle atrophy. Early symptoms of DMD include waddling gait, poor balance, scoliosis and calf deformations and, ultimately, a wheelchair becomes necessary due to walking problems, in most cases around the age of 12 years. Further disease progression leads to respiratory problems and, around age 15-20 years, permanent ventilation will be needed. Pneumonia compounded by cardiac involvement is the most frequent cause of death which usually happens in the late teens to early 20s [212]. Becker muscular dystrophy (BMD) is a less severe form of DMD, where mutations in the DMD gene lead to truncated, but partially functional dystrophin protein variants. Therefore, BMD has a broader phenotypic range compared to DMD. More severe cases may present muscle weakness in childhood, but loss of the ability to walk typically occurs after the age of 12 years, in less severely affected patients sometimes even as late as the 7th or 8th decade of life [219]. Apart from the dystrophinopathies (DMD and BMD), several other classes of MDs exist

such as limb-girdle muscular dystrophy (LGMD), facioscapulohumoral muscular dystrophy (FSHD), congenital muscular dystrophy (CMD), Emery-Dreifuss muscular dystrophy (EDMD), myotonic muscular dystrophy (DM), distal muscular dystrophy (DD) or oculopharyngeal muscular dystrophy (OPMD). These MDs differ in the mutations involved in pathogenesis, onset, disease progression and the types of muscles affected (Fig. 10). However, their complex pathophysiology is beyond the scope of this thesis and has been comprehensively reviewed elsewhere [212, 213, 220, 221].
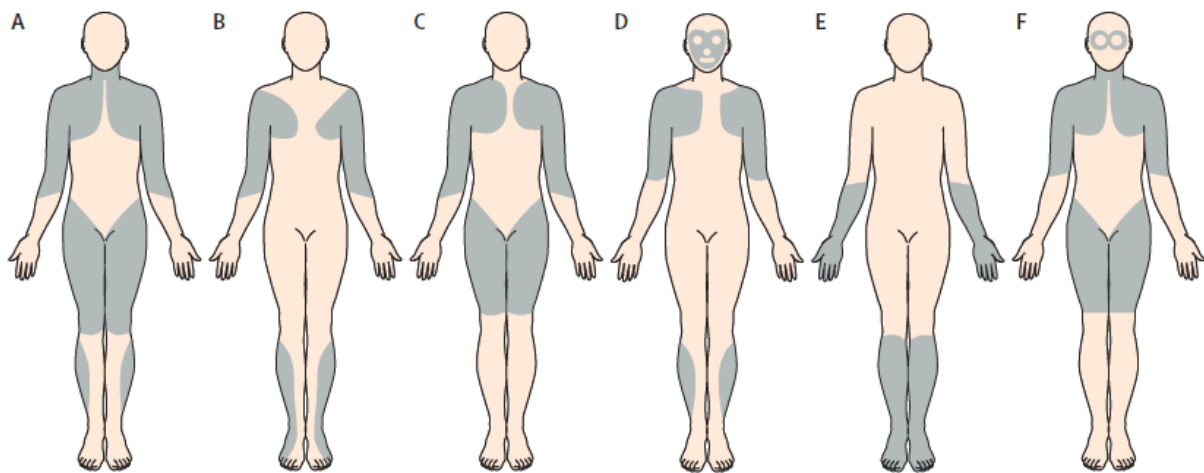
Fig. 10: *Patterns of distribution of muscle weakness in commonly observed MDs.* (A) DMD and BMD. (B) EDMD. (C) LGMD. (D) FSHD. (E) DD. (F) OPMD (from [213]).

As diverse as the genetic causes and symptoms of MDs may be, the one thing they all have in common is that currently they are incurable. Although the combination of clinical signs and an analysis of the possible mode of inheritance allows suspicion of specific forms of MD, the overlapping pathophysiological features between genetically distinct forms complicate specific diagnosis. Neither measurements of serum CK levels nor electromyography provide diagnostic tools stringent enough to pinpoint a specific form of MD. Most of the time, muscle biopsies have to be taken for histological assessment of muscle morphology and subsequent antibody-based biochemical analyses such as Western blot or immunofluorescence (IF) stainings allow identification of the primary protein defect to direct genetic testing. In this respect, the importance of early diagnosis has been unambiguously agreed on [213]. Given the heterogeneity of MDs and the bottlenecks in diagnosis, current treatment options are limited to symptomatic treatment. Depending on the type of MD, this may involve (i) administration of glucocorticoids, (ii) the introduction of non-invasive ventilation or mechanically assisted cough devices and, in later stages, tracheostomy, (iii) cardiac protection treatment such as administration of angiotensin-coverting-enzyme (ACE) inhibitors or β-blockers, routine echocardiography and, if applicable, pacemakers, and (iv) appropriate personalized physical exercises and dietary changes (especially Ca^{2+} and protein uptake as well as vitamin D supplementation) [213]. In general, early surgical intervention usually fails to restore muscle function and is therefore not

recommended. In addition, the period of bed-rest after surgery might actually be detrimental. However, selected surgical procedures in adolescents might be helpful in later stages of MDs. For example, the correction of contractures might delay inability to walk or the correction of scoliosis may increase the patient's ability to sit [212].

The socio-economic burden of chronic muscle pathologies to patients and health care systems worldwide is immense [222-224]. Thus, in recent decades, stem cell biology has focused on delivering healthy myogenic precursors into damaged muscles or genetically correcting dystrophic muscles *in situ*. The emergence of animal models recapitulating MDs, such as the *mdx* mouse or canine models, has prompted a great deal of research into the complex pathomechanisms as well as potential treatments [225]. With the notion that injected muscle precursors can deliver healthy dystrophin alleles via fusion into dystrophic *mdx* myofibers [226], first attempts of SC implantation therapy for DMD [227] or BMD [228] in humans have already been explored in the nineties. Since then, numerous trials in DMD patients were conducted using intramuscular injection of SCs and, to a minor extent, CD133^{+} cells [124]. These trials provided evidence for the safety of intramuscular SC injection, however, even though new dystrophin production was noted in many cases, long-term clinical benefits were generally not observed [229]. This is mainly due to the fact that cell injection into several locations of a muscle (or a few muscles) cannot elicit a general effect. In addition, injected cells distribute only locally, necessitating huge numbers of injections for the treatment of a complete muscle. Furthermore, immune reactions have been observed, even in immunohistocompatible animals [230], and rapid myoblast death *in situ* after injection is a common problem [231]. More recently, gene therapy approaches to replace or repair the mutated gene causing the MD have been developed, most of them targeting dystrophin [232]. A major problem herein is that dystrophin is the largest known human gene, comprised of 79 exons spanning approximately 2500 kilobases, giving rise to an mRNA transcript measuring 14 kilobases [233]. This makes cloning and subsequent delivery of the gene in conventional gene therapy vectors extremely difficult. Thus, the main strategies have focused on delivery and expression of dystrophin variants of reduced size [234] or exon skipping, where antisense oligonucleotides are used to target exons in the primary transcript which are subsequently spliced out (with their flanking introns) to restore the disrupted open reading frame [235]. However, although major advances in MD gene therapy have been made [236], the clinical success of the majority of therapeutic strategies has been rather limited. Money and time are strong limiting factors for all approaches, but especially for cell and gene therapy. The current stringency of legislative constraints will further delay clinical translation of novel strategies and will raise the cost to a point that, even in successful cases, will make it impossible to apply them [232]. Therefore, strategies that reduce costs and the development of safe and efficient delivery routes for cell and gene therapy alike will be required before potential treatments can be made available for larger numbers of patients.

3. SKELETAL MUSCLE TISSUE ENGINEERING (SMTE)

The limited clinical success of current treatments for VML or MD, such as autologous muscle transplantation or bolus injection of muscle precursor cells (to restore muscle function by delivery of therapeutic cells and/or healthy gene alleles), has prompted research on alternative strategies for muscle repair. The field of SMTE aims at providing new approaches for efficient delivery of cells and/or therapeutic biomolecules (growth factors, cytokines, drugs, gene vectors) on polymeric scaffold materials. To circumvent the shortcomings of current cell-based therapies, SMTE uses rationally designed degradable biomaterials as delivery matrices for muscle precursor cells. These biomaterials can act as temporary "niche-like" microenvironments capable of providing appropriate chemical and physical cues to the transplanted or host muscle cells. This offers several benefits over conventional bolus cell injection such as enhanced cell survival, improved functional maturation, higher protection from foreign body reactions and the recruitment of host vasculature and nerves into the defect site [237]. Furthermore, a scaffold can trigger tissue regeneration in the host on its own through its overall physicochemical properties or the incorporation of bioactive molecules. At present, acellular approaches employing designed instructive matrices are extensively studied and may obliterate the use of cells in some aspects of muscle regeneration in the future [16]. In addition, decellularized ECM scaffolds have been shown to contribute to functional muscle regeneration and are subject to clinical trials [238]. The combination of biomaterial-based cell and growth factor delivery from appropriately modified scaffolds has also been explored and provides a promising platform for topical muscle repair [239].

In general, there are two classical approaches to engineer skeletal muscle, *in vitro* or *in vivo* SMTE (Fig. 11A, B). *In vitro* SMTE attempts to generate mature and contractile skeletal muscle tissue by differentiating (allogeneic or autologous) myogenic precursor cells on or in biomaterial substrates until a functional tissue has developed that can be transplanted into the patient [15]. This commonly involves the use of patterned biomaterials and/or sophisticated bioreactor systems to generate aligned bundles of contractile myofibers. *In vivo* SMTE relies on transplantation of autologous myogenic precursor cells in combination with a biomaterial scaffold which creates a local niche at the defect site. Upon transplantation, the delivered cells can influence muscle regeneration by either integrating into the host muscle tissue or by providing paracrine signals that trigger endogenous regenerative processes [240]. This approach often bypasses extensive cell manipulation during *ex vivo* culture to preserve the functional properties of the cells which tend to change after prolonged periods of culture. Furthermore, this approach may also apply cells in combination with bioactive molecules that are incorporated into the biomaterial and released upon transplantation. Alternatively, the comparably novel strategy of *in situ* SMTE (Fig. 11C) employs biomaterials as guides to instruct the endogenous regeneration of injured muscle. Usually, this acellular approach involves precise biomaterial modifications which

enable spatiotemporal release of bioactive and chemotactic signals or the presence of specific surface cues such as cell adhesion motives or topological features on the micro- or nanoscale.
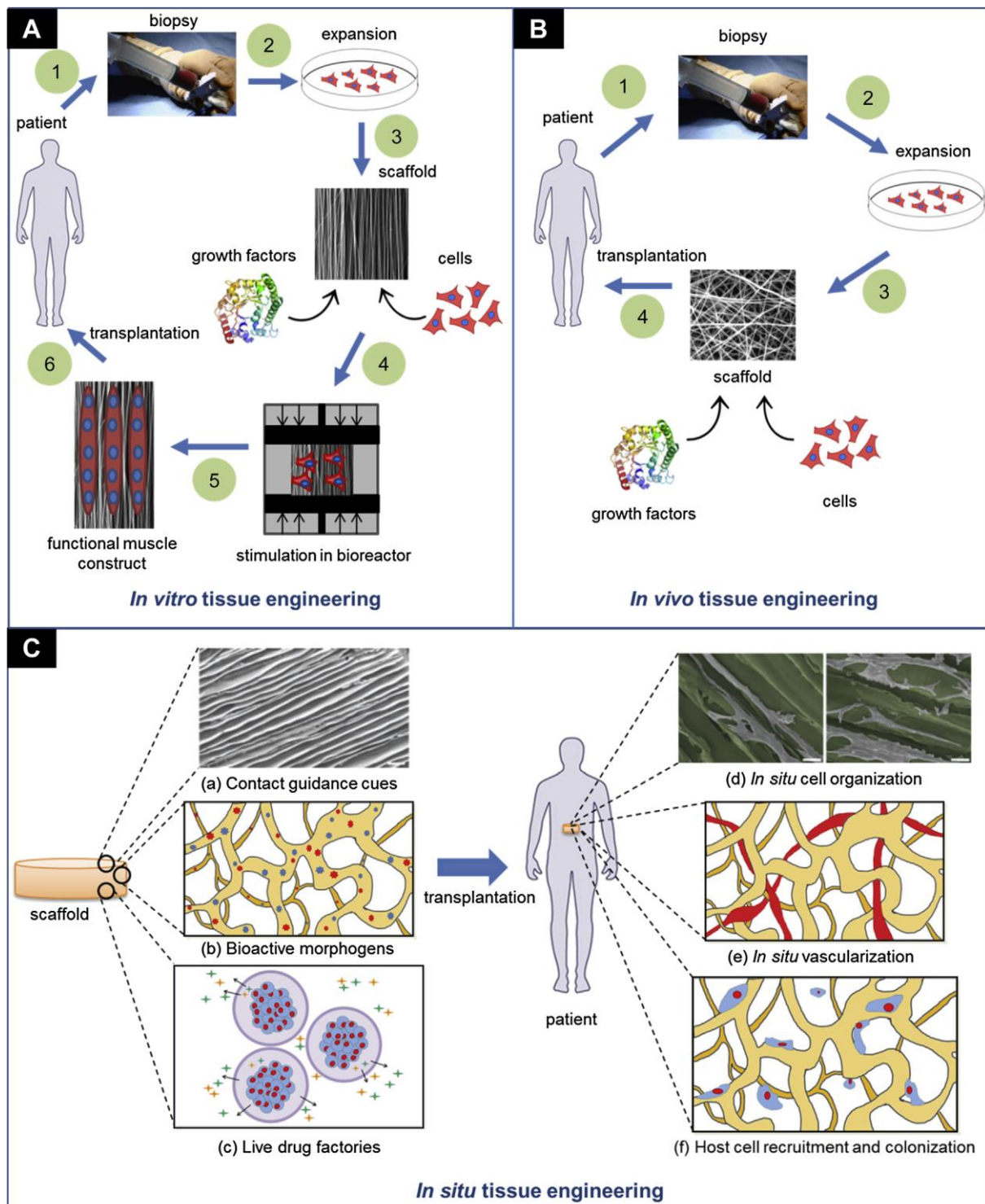
Fig. 11: *The three main SMTE approaches.*(A) *In vitro* TE involves the development of a functional tissue engineered muscle construct which consists of mature contractile myofibers. Bioreactors are often used in this approach to drive muscle maturation. (B) *In vivo* TE employs combinations of cells, scaffolds and growth factors that are transplanted into the patient without prolonged culture *ex vivo*. This combination provides a niche-like environment from which the cells can orchestrate the regenerative processes. (C) *In situ* TE uses instructive biomaterial matrices that act as guides to trigger endogenous

muscle repair. This is achieved by presenting cues that stimulate host cell recruitment and organization, while ensuring cell survival through the presence of a scaffold (from [16]).

The main challenge in the *in vitro* SMTE approach is the generation of large-scale muscle tissue with functional properties while maintaining high myofiber packing density and alignment. Upon transplantation, tissue engineered muscle tissue needs to generate sufficiently large contractile forces to be able to contribute to functional recovery of the host muscle. The maturation of engineered muscle up to the point of physiologically relevant contractile force generation has remained a key issue so far [241], however, the emergence of novel bioreactors and dynamic culture systems as well as the constantly improving understanding of relevant stimulation/maturation strategies are tackling this problem. Furthermore, volumetric tissue transplants may require pre-vascularization to maintain cellular viability, and co-cultures of myogenic and endothelial cells in biomaterial have been evaluated [242]. Significant advances in cell purification and stem cell culture, biomaterials science and nanofabrication or gene editing technology have greatly expanded the SMTE toolbox. Today, a variety of cell types, biomaterials and bioreactor-based maturation strategies exist and an overview over the most prominently used approaches shall be given in the following sections.

3.1. Cell types for skeletal muscle tissue engineering

The choice of an appropriate cell type and its inherent regenerative potential as well as an optimal delivery method are key determinants for the clinical outcome of a SMTE approach. Cell-based strategies can be utilized in either allogeneic or autologous settings and the route of administration into muscle tissue (on a scaffold, intramuscularly, intravenous or intra-arterial) has to be also considered [243]. SCs are widespread throughout adult muscle, accounting for 2-7% of total nuclei within a muscle fiber [114], and their natural role in muscle regeneration make them an attractive candidate for SMTE approaches. SCs can be isolated from muscle biopsies and enriched by fluorescence-activated cell sorting (FACS) [244] or magnetic-activated cell sorting (MACS) [245]. The regenerative potential of these cells is exceptional, as demonstrated by the ability of a single freshly isolated luciferase-expressing SC to engraft into mouse muscle, proliferate and participate in waves of massive proliferation and differentiation as a response to injury at later time points [246]. There is, however, a major hurdle to be overcome before SCs can be used in therapeutic interventions on a large scale. After isolation, *ex vivo* expansion of SCs for as little as 2 days results in a drastic reduction of their differentiation potential *in vivo* [244, 247], most likely due to removal of the SC from its niche. Therefore, classic SC culture formats need to be revisited and appropriate culture conditions including defined media formulations and, potentially, culture on pliant ECM matrices of defined ultrastructure to simulate a niche-like environment are being developed [135, 248, 249]. Traditionally, SCs have been isolated from skeletal muscle via two main routes, cellular outgrowth or whole tissue digestion

(Fig. 12) [250]. The outgrowth method involves mild enzymatic digestion of muscle ECM followed by myofiber separation through gentle trituration. This yields individual native myofibers with their SC attached and still in their niche. Myofiber plating activates SCs to proliferate and "outgrow" from the myofiber onto the cell culture dish, from where they can be harvested as population of myoblasts [251]. Alternatively, native muscle can be minced and fully digested, and a heterogeneous primary culture can subsequently be obtained by plating of the cell suspension after removal of debris and residual ECM [252]. After full digestion, the SC fraction (or other myogenic sub-populations) can also be enriched via FACS or MACS, as mentioned above.
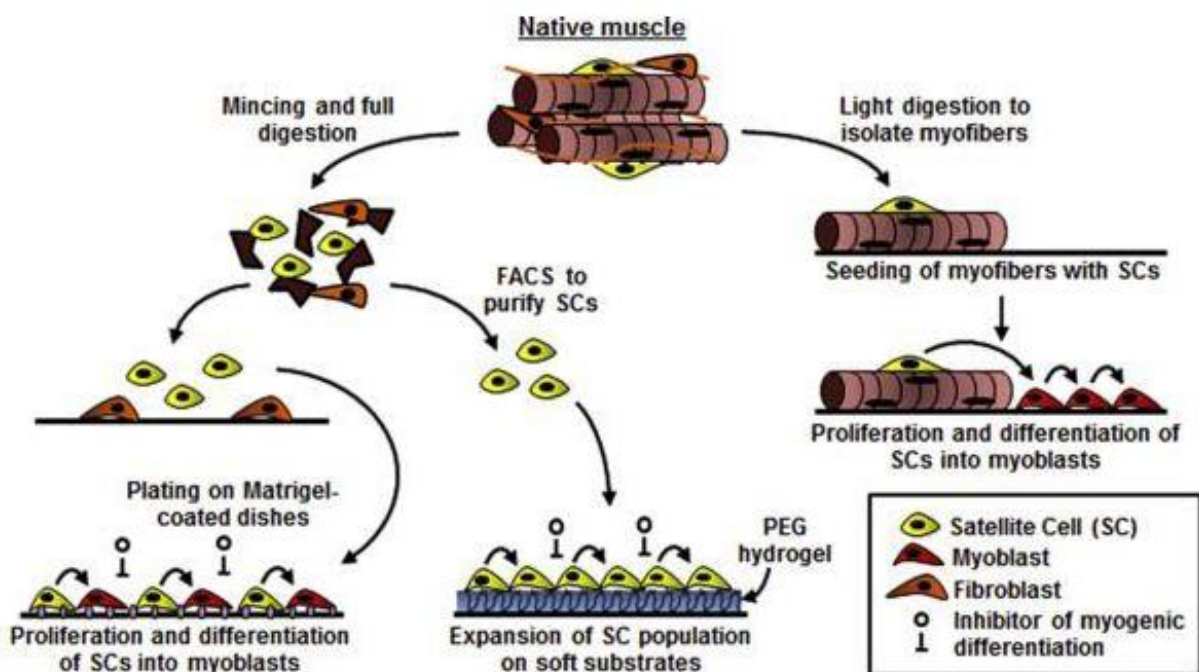
Fig. 12: *Methods to isolate and expand myogenic cells.* Starting from whole native muscle, the tissue can be mildly digested to isolate individual intact myofibers which yield activated SCs/myoblasts after plating (right). Alternatively, muscle can be fully digested to yield a suspension of heterologous primary cells (left). Additionally, the primary cell population from full muscle digestion can be subjected to cell sorting techniques like FACS or MACS to enrich for SCs. Subsequent cell culture often involves the use of pliant ECM matrices and defined media formulations to stimulate cell proliferation and control the switch to differentiation (from [250]).

The isolation and subsequent direct transplantation of single viable myofibers with attached SCs (with or without the presence of a scaffold) - without any transient cell culture - might be a promising SMTE approach, as the SCs never lose contact with their native niche and should therefore retain their regenerative potential.

For *in vivo* SMTE applications, delivery of freshly isolated SCs in hydrogels, even in small numbers (250 cells per gel), was demonstrated to elicit a superior regenerative response compared to delivery of SC-derived myoblasts (obtained after SC expansion *ex vivo*) [253]. However, the need for large cell numbers in order to elicit a robust long-term effect has nonetheless made myoblasts an attractive cell

source for clinical use [254]. Ever since the discovery that myoblast transplantation in *mdx* mice can restore dystrophin expression [226], a vast amount of studies has tested the efficiency of primary myoblast transplantation for dystrophic muscle regeneration [255-258]. Outside the context of MDs, myoblast delivery on/in a variety of scaffold biomaterials has also been extensively studied, demonstrating clinical relevance of this cell type for muscle repair [239, 259-262]. Most of these studies employed primary myoblasts, however, the availability of myoblast lines has greatly contributed to proof-of-concept studies in the field of *in vitro* SMTE. Myoblast lines such as murine C2C12 [263] or human C25 cells [264] can be expanded into vast amounts of cells and thus present an ideal cell source to fine-tune culture parameters (cell seeding density, type of biomaterial, scaffold properties, maturation strategies), especially in complex bioreactor-based culture systems, before primary cells are used. Importantly, a recent transcriptomics analysis has revealed that immortalization of C25 human myoblasts does neither interfere with their myogenic potential nor with any other major aspect of cell physiology (apart from the elicited protection against senescence) [265].

The inability of SCs to cross endothelial barriers and, thus, their inapplicability for systemic administration has prompted research looking into the potential of other MDSCs known to be involved in muscle repair for therapeutic delivery [266]. MABs and pericytes have been isolated from postnatal mouse, rat, dog and human tissue [124, 165, 232] and their feasibility for *in vivo* and *in vitro* SMTE approaches has been demonstrated [165, 166, 267]. Furthermore, muscle SP cells, a heterogeneous source of myogenic stem cells, have been shown to efficiently engraft into the host SC niche when transplanted into regenerating mouse muscles [268]. Muscle SP cells have also been isolated from human muscle [269], however, a thorough examination of their therapeutic potential remains elusive. $CD133^+$ ($AC133^+$) MDSCs, a circulating sub-population of HSCs, have been found to restore dystrophin expression after intramuscular injection in mice [159]. In addition, a comparison between the regenerative capacity of human $CD133^+$ MDSCs vs. SC-derived myoblasts by the same group showed superior muscle regeneration, more efficient repopulation of the SC niche and more extensive proliferation from the injection site after intramuscular administration of $CD133^+$ MDSCs into mouse muscle [270]. Concerning MSCs, a cell source prominently used in TERM, there is an ongoing debate whether these cells are actually able to differentiate into functional skeletal muscle *in vivo* [271]. There is evidence that MSCs may support myogenic repair [272], however, myogenic determination of these cells often requires transient but forced expression of MyoD or Pax3 [169, 170]. Although long-term benefits of MSC transplantation into injured muscles were not observed, they might still be beneficial for myogenic regeneration by providing paracrine signals [273]. Amniotic fluid stem cells (AFSCs) present an alternative multipotent cell source and have been shown to possess myogenic potential [274]. Tail vein transplantation of mouse AFSCs was shown to enhance muscle strength and the survival rate of affected animals in a mouse model of spinal muscular atrophy [275]. After cardiotoxin (CTX) injection into treated tibialis anterior (TA) muscles, only AFSC-treated muscles efficiently regenerated, in contrast to bone marrow-derived mesenchymal stem cells (BMMSCs)

which were used as controls. More recently, myogenic precursor cells derived from human embryonic stem cells (hESCs) or induced pluripotent stem cells (hiPSCs) are starting to produce clinically relevant outcomes. This is mainly due to vast improvements in cell culture strategies for efficient and directed myogenic specification of these cells in short periods of time [276-278]. Transplantation of hESC-derived skeletal myoblasts into regenerating muscles of nude mice resulted in long-term engraftment of these cells for up to 6 months, as confirmed by bioluminescence imaging [276]. Alternatively, embryoid body (EB) aggregation and subsequent myogenic differentiation of hESCs has been attempted, with similar outcomes compared to monolayer differentiation [277]. Importantly, teratoma formation was not observed in both of these studies. An important proof-of-principle study was performed by Tedesco et al. [279] who used genetically corrected hiPSCs derived from fibroblasts or myoblasts of LGMD patients, differentiated them into mesoangioblasts and tested cell transplantation in a humanized mouse model of LGMD. This led to functional amelioration of the dystrophic phenotype and restoration of depleted SCs, but, most importantly, it showed that "personalized" treatment with patient-specific iPSC-derived cells can be utilized for stem cell therapy. Initially, most the myogenic precursor cells mentioned above have been used in cell injections. More recently, they have been combined with biological scaffold materials (*in vivo* SMTE) to improve the efficiency of the given therapy, especially in respect to cell homing and survival (Fig. 13). However, some of these cell types have also proven useful for *in vitro* SMTE, where functional muscle tissue is generated by pre-differentiation of the cells on biocompatible scaffolds [15, 243].
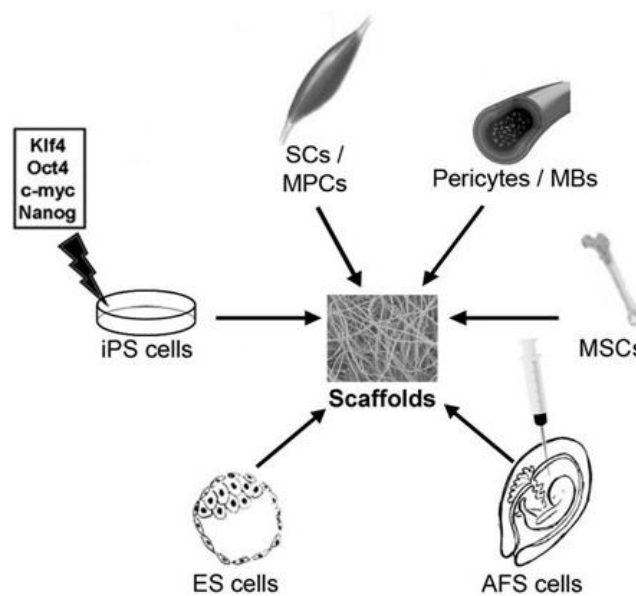

Fig. 13: *Possible sources of stem cell types for SMTE.* SCs: satellite cells; MPC: myogenic progenitor cells; MBs: mesoangioblasts; MSCs: mesenchymal stem cells; AFS cells: amniotic fluid stem cells; ES cells: embryonic stem cells; iPS cells: induced pluripotent stem cells (from [243]).

In conclusion, an appropriate cell type for SMTE and muscle stem cell therapy should meet the following criteria: (i) it ideally stems from a source that is easily accessible and allows generation of vast amounts of cells, (ii) it should grow as a homogeneous cell population in culture, (iii) it should be able to phenotypically withstand longer culture periods *in vitro* during expansion, (iv) it should be susceptible to transduction/transfection of vectors encoding therapeutic genes, (v) it should be applicable through systemic means such as intravenous or -arterial injection and still home to injured muscle efficiently, and (vi) it should have a myogenic differentiation potential that allows it to generate (or participate in the generation of) new myofibers *in situ* with full restoration of function [243].

3.2. Biomaterials for skeletal muscle tissue engineering

The evaluation of therapeutic cell sources suitable for muscle regeneration has been a topic of extensive research and the same can be stated about the development and characterization of feasible biomaterials for cell delivery. In the last two decades, significant advances in the rapidly growing field of biomaterials science have greatly expanded the SMTE toolbox which now offers a wide range of synthetic or natural scaffold biomatrices and numerous biofabrication methods to tune their structural and mechanical properties [16, 280, 281]. A general concept of TE is to generate biomaterials that mimic the native ECM and provide a supportive microenvironment for the delivered cells. ECM biomimicry of a biomaterial is an important aspect as it not only affects the cells within the material but also invading cells in the target host tissue. Therefore, a suitable biomaterial for tissue regeneration essentially has the same features than the target tissue's native ECM. Ideally, it (i) provides structural support for cells to grow, migrate and differentiate, (ii) has mechanical properties similar to those of the native tissue, (iii) provides bioactive cues for the cells to respond to (such as a certain topography or cell-adhesion motif pattern), (iv) has the capability to act as a reservoir for growth factors (either by biomaterial modification before transplantation or by sequestration of endogenous growth factors), and (v) provides a temporary cell matrix that supports remodeling by cells in response to tissue regeneration while gradually degrading in a non-toxic manner [282].

Current SMTE strategies employ three kinds of biomaterial classes: natural protein and polysaccharide hydrogels, synthetic polyesters or decellularized ECM of various sources (Table 1) [16, 283, 284]. Naturally derived hydrogels have been most commonly used as they are biocompatible, biodegradable, allow for spatially uniform cell seeding in 3D due to the abundance of cell adhesion sites, mimic the mechanical properties of native muscle tissue and may be applied in a minimally invasive manner. Hydrogels are highly hydrated insoluble polymer networks which promote nutrient diffusion and waste removal out of the gel through their equilibrium swelling while providing a structural framework for cell growth and migration through their insoluble polymer contents [285]. Collagen

SOURCE	MATERIAL	ADVANTAGES	DISADVANTAGES
Natural (Protein)	Collagen	Biocompatibility, biodegradability, somewhat tunable porosity/elasticity, injectability	Little control over 2D/3D topographical cues, poor mechanical properties, potential immunogenicity, variable qualities
Natural (Protein)	Fibrin	Biocompatibility, biodegradability, somewhat tunable porosity/elasticity, growth factor delivery, injectability, intrinsic angiogenic properties	Little control over 2D/3D topographical cues, poor mechanical properties, potential immunogenicity, variable qualities
Natural (Poly-saccharide)	Alginate	Biocompatibility, biodegradability, tunable porosity/elasticity, growth factor delivery, injectability	Little control over 2D/3D topographical cues, potential immunogenicity, variable qualities, necessity of modification with cell adhesion peptides (RGD)
Natural (Poly-saccharide)	Hyaluronan	Biocompatibility, biodegradability, somewhat tunable porosity/elasticity, injectability	Little control over 2D/3D topographical cues, weak mechanical properties, potential immunogenicity, variable qualities
Natural	Decellularized muscle ECM	Native structural and biochemical cues, structural integrity, matches host tissue mechanical properties potential injectability (of solubilized ECM) without loss of bioactivity	Need for effective removal of all cells, debris, chemical agents and detergents, not suitable for irregularly shaped defects unless applied as hydrogel, potential immunogenicity
Synthetic	PEG (PEO)	Biocompatibility, highly tunable elasticity, considerably cheaper than natural hydrogels, matrix uniformity, injectability, wide range of surface modifications	Necessity of modification with cell adhesion peptides (RGD) or ECM components (laminin, matrigel, fibronectin, fibrinogen), potential inflammatory response after degradation *in vivo*
Synthetic (Polyesters)	PLA, PGA, PCL, PLLA, PCLA, PLGA	Biocompatibility, precise control over physicochemical properties (tunable mechanical properties, degree of cross-linking or degradation rate), considerably cheaper than natural hydrogels, matrix uniformity, wide range of processing techniques (substrate patterning, electrospinning, etc.)	Processing may involve harsh reaction conditions (unsuitable for direct cell encapsulation or functionalization with growth factors), necessity of modification with cell adhesion peptides (RGD) or ECM components (laminin, matrigel, fibronectin, fibrinogen), no biomimicry with native ECM

Table 1: *Natural and synthetic scaffold materials commonly used in SMTE.* Natural protein- or polysaccharide-based hydrogels excel at biocompatibility, -degradability and the abundance of cell attachment motives, whereas synthetic polymers provide high mechanical stability and allow precise control over their overall physicochemical matrix properties (adapted from [16] and [286]).

[287-291], fibrin [259, 292-296], hyaluronan (hyaluronic acid) [253, 297] and alginate [239, 298, 299] hydrogels have been predominantly employed as scaffolds for SMTE [16, 283]. Collagen is the most abundant protein in the human body and the main component of natural ECM and has therefore been used in a multitude of TE applications [300]. Similarly, hyaluronan is an important component of the ECM and also plays a role as a signaling molecule in cell motility [301]. Fibrin, the end product of blood coagulation, has been commercialized as clinically approved hemostat, sealant and adhesive and, due to their versatility, fibrin hydrogels have been extensively used in a variety of TE strategies [302-304]. Alginate, a polysaccharide found in brown algae, has been shown to be a feasible and cheap hydrogel source due to its availability and has mainly been used as a particle-based delivery system for encapsulated therapeutic biomolecules (such as growth factors, drugs or gene vectors), rather than a cell and differentiation matrix for cells [305]. A general feature of natural hydrogels is their ability to carry and subsequently deliver bioactive factors upon transplantation, either through physical entrapment of the factor during hydrogel polymerization (especially for factors that have natural affinity for a given hydrogel) or by chemical conjugation of the factor to the gel [302, 306-308]. This has been utilized in both cellular and acellular approaches to modulate regenerative processes in the host muscle and combined delivery of cells and growth factors from hydrogels has yielded encouraging results [239, 291]. There are, however, shortcomings related to the use of hydrogels. Their weak mechanical properties potentially result in rapid degradation *in vivo*, possibly preceding the period of time needed for matrix remodeling during tissue regeneration. Uncontrolled material degradation may lead to donor cell anoikis - apoptosis induced from the loss of cellular attachment to a substrate [309]. Furthermore, protein-based scaffolds may elicit immune reactions and trigger the foreign body response [310]. In addition, the mechanical properties and topographical features of natural hydrogels cannot be reproducibly controlled on the micro- or nanoscale.

This has led to an extensive evaluation of synthetic materials in the context of their ability to support myogenic differentiation *in vitro* and muscle regeneration *in vivo* [16, 285, 311]. Synthetic materials offer precise control over the physicochemical properties of the respective matrix and a variety of microfabrication methods such as solvent casting, soft and photolithography or electrospinning exist to tailor such materials into defined structures like hydrogels with controllable degradation rate, polymer meshes, porous sponges or aligned threads [15, 312]. Poly(ethylene glycol) (PEG) is the most widely investigated synthetic polymer to make hydrogels and has unique properties like solubility in both water and organic solvents, non-toxicity and non-immunogenicity [313]. However, PEG lacks cell adhesion sites and therefore has to be functionalized to allow for proper cell binding. Among others, PEG/Arg-Gly-Asp (RGD) or PEG/fibrinogen hybrid gels have attracted widespread attention [314, 315], and especially the latter has been demonstrated to support muscle regeneration when used as a delivery vehicle for muscle precursor cells [316, 317]. PEG-based hydrogels have also shown to be feasible for growth factor delivery and thus provide a synthetic multi-modal delivery device [318, 319]. Other synthetic materials with varying biodegradability (ranging from weeks to years) have also

been introduced. These include polyester and their copolymers such as poly(lactic acid) (PLA), poly(glycolic acid) (PGA), poly(ε-caprolactone) (PCL), poly(l-lactic acid) (PLLA), poly(ε-caprolactone-co-lactide) (PCLA) or poly(lactic-co-glycolic acid) (PLGA) [320, 321], and state-of-the-art nanofabrication methods to tailor these materials into defined structures are available [15]. However, many of these methods involve harsh reaction conditions (for example the use of high voltage and/or toxic organic solvents), which makes these materials less amenable to direct encapsulation of cells. Polyesters can be functionalized with cell adhesion motives for proper cell attachment or drugs and growth factors to serve as instructive matrices *in situ* [322]. Even though the biocompatibility of polyester-based synthetic "designer matrices" is much lower compared to natural hydrogels, they have been shown to support myogenesis *in vitro* and muscle regeneration *in vivo* [323-328].

Both natural and synthetic materials have inherent shortcomings that decrease the clinical efficiency of muscle regenerative therapies. As mentioned earlier, natural ECM biomaterials may not be mechanically robust enough for long-term *in vivo* application, while synthetic polymers do usually not allow for high cell seeding densities (due to the lack of adhesion motives) and may cause chronic foreign body reactions if slowly or non-biodegradable. Therefore, hybrid materials combining the unmatched biocompatibility of natural materials and the mechanical and structural tunability of synthetic polymers have been developed [16, 320]. For example, combinations like PEG-fibrinogen [267] or PEG-laminin [329] hydrogels, PLLA-gelatin/fibronectin nanofibers [330], collagen hydrogels with incorporated parallel glass fibers [331] or electrospun PCL/collagen nanofiber meshes [332] have been identified as matrices that promote myogenic differentiation.

A somewhat alternative approach for muscle regeneration is the use of decellularized muscle ECM as scaffold biomaterial. This strategy addresses the difficulty in mimicking native tissues by using preformed scaffolds (with or without cells) while optimizing the material properties to stimulate cell survival, myogenic differentiation, vascularization and innervation *in situ*. Decellularized whole organs or acellular tissues are rich in proteins, growth factors and cytokines, with conserved chemical and architectural features of the tissue of origin, including the vascular bed [238, 333, 334]. Decellularized ECM has been shown to generally provide a pro-myogenic environment [334] and is capable of recruiting endogenous host (somatic and stem/progenitor) cells and modulating the innate immune response, which is paramount to wound healing [238]. Decellularized rodent muscles seeded with homologous myoblasts were found to promote functional myofiber formation *in vitro* [259] and *in vivo* [335]. Due to their sheer size, decellularized ECM scaffolds were also evaluated in the context of VML. This did not just employ decellularized muscle (which is inapplicable in humans due to donor site morbidity) [336] but also acellular tissue from other sources such as dermis, small intestinal submucosa or urinary bladder [238]. Interestingly, such acellular ECM matrices were found to effectively promote muscle regeneration without cell seeding prior to implantation, pointing once again at the pivotal role of the ECM in muscle development [337-340]. Two of the most criticized

disadvantages of decellularized ECM are the potential immunogenicity of acellular matrices derived from xenogeneic sources and their incapability for geometric adjustment to the usually highly irregular shape of volumetric muscle defects [341]. The use of injectable hydrogels derived from decellularized skeletal muscle ECM might offer a more flexible acellular SMTE approach [342]. Although this method destroys all existing architectural cues on the ECM (such as the vascular structures), the composition (proteins, growth factors, cytokines, etc.) of the hydrogel formulation is preserved and can still instruct endogenous regenerative processes. Importantly, a case study in a 19-year old soldier with VML demonstrated that an acellular ECM scaffold derived from porcine intestinal submucosa did not only increase muscle mass and performance, but also provided an immunologically safe treatment option [343].

3.3. Strategies for the *in vitro* generation and maturation of 3D tissue engineered skeletal muscle

Although *in vivo* and *in situ* SMTE approaches have yielded promising clinical results, the *in vitro* generation of volumetric functional skeletal muscle transplants (*in vitro* SMTE) has also been widely studied. Compared to the use of undifferentiated muscle progenitor cells (with or without the use of a scaffold) transplantation of biomimetic tissue engineered muscle may offer distinct advantages [241, 344]. Patient-specific tissue engineered muscle constructs using autologous cells can be precisely designed to mimic the native muscle architecture of the patient and their shape can be adjusted to fit the often irregular structural requirements of a specific defect. Further, the combination of skeletal muscle constructs and bioreactors allows for *in vitro* preconditioning (for example through application of mechanical or electrical stimulation) of the muscle to attain certain mechanical or metabolic characteristics, which will likely reduce mechanical overload at the injury site through the transplantation of already functional muscle tissue. In addition, appropriate cell/scaffold combinations enable the generation of functional myofibers while maintaining a niche-like microenvironment that protects the cells from the harsh conditions at the injury site, thus improving cell survival and transplant integration [344].

There are several key challenges in engineering 3D skeletal muscles *in vitro*. As the main goal of SMTE is to generate biomimetic tissue, the native structure and function of muscle needs to be precisely recapitulated, otherwise functional contribution to muscle repair *in vivo* upon transplantation will most likely not occur. Therefore, the major aims are (i) the reproducible fabrication of dense 3D skeletal muscle tissue with adequate dimensions and uniform cell (myofiber) alignment, (ii) the maximization of contractile force generation (which is directly related to the extent of muscle differentiation and maturation), including the optimization of cell-matrix interactions, and (iii) a cell-scaffold combination conductive for rapid vascularization and innervation to promote long-term survival and functional donor-host integration [241]. Taking into account all the structural and

functional peculiarities of native skeletal muscle, a myriad of cell-scaffold combinations and maturation strategies has been explored, all aiming at maximizing the two parameters cell alignment (for uniaxial force generation) and muscle differentiation/maturation (for maximal contractile force generation).

Initially, the main *in vitro* SMTE approach was "self assembly" of myoblast monolayers grown on protein-coated polydimethylsiloxane (PDMS) surfaces into 3D cylindrical tissue bundles. This idea was pioneered by Strohman et al. [345] who elegantly exploited the accumulation of contractile forces in differentiating muscle cells. Primary myoblasts were differentiated as monolayer on a flexible membrane pinned to a PDMS-coated cell culture dish at two opposing anchor points with silk sutures (which function as artificial tendons). Upon differentiation and fusion into myotubes, the muscle cells begin to contract and compact the membrane, resulting in detachment from the PDMS coating. Due to the fixation of the membrane at two points, the cells start to pull against these stationary anchors, which creates predictable lines of isometric strain. This "cell-mediated" passive internal strain promotes myotube alignment along the axis between the two posts, while the entire cell sheet rolls up into a cylindrical 3D structure. Self-assembly of myoblasts into scaffold-free "myooids" is still in use today and has been modified in many ways [346-348], for example through growth and differentiation of muscle cells on a fibrin layer on top of the PDMS membrane (Fig. 14A) [293].
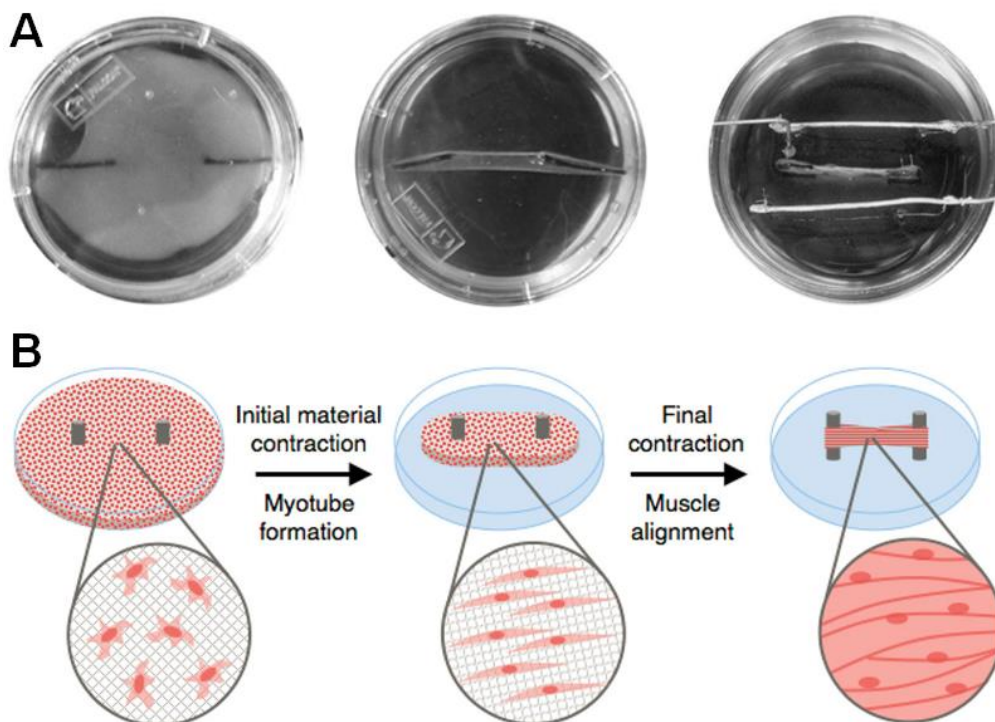
Fig. 14: *The two main strategies for the in vitro generation of 3D tissue engineered skeletal muscle.* (A) Self assembly of myoblast monolayers differentiated on flexible anchored hydrogel matrices into 3D "myooids". This method also allows the implementation of electrodes for electrical stimulation and subsequent measurement of twitch force through a force sensor (adapted from [293]). (B) Encapsulation of myoblasts in synthetic or natural 3D hydrogel scaffolds. Similar to the self

assembly method, anchoring of the ends of a cell-seeded 3D scaffold through stationary pins, felts, or meshes will induce myotube alignment as the cells differentiate and generate passive tension within the construct (from [286]).

The most commonly used *in vitro* SMTE strategy is the direct encapsulation of myoblasts in 3D scaffolds. In this approach, freshly isolated [294] or expanded [349] primary myoblasts or immortalized myoblast cell lines [350] are embedded into synthetic polymer scaffolds or natural hydrogels. In this regard, fibrin [293, 295, 351, 352] and collagen [287, 290, 349, 350] hydrogels have been extensively used, as they allow for high cell seeding densities and spatially uniform cell distribution due to the abundance of cell attachment sites. Cell/hydrogel mixtures can then be cast or molded into diverse 3D structures such as bundles, cylinders or sheets. Similar to the self assembly approach, the ends of such 3D constructs can be anchored to pins, felts or meshes to induce alignment via cell-mediated passive isometric tension within the scaffold. As a consequence of force generation by the muscle cells, the construct will compact over time, generating a bundle of aligned, densely packed myotubes (Fig. 14B). Notably, the contractile forces generated by such 3D skeletal muscle constructs are significantly higher than those generated by "myooids" [293, 294, 352]. This may be attributable to enhanced myoblast fusion and larger adult myofiber size resulting from the fact that cell encapsulation allows for much higher cell seeding and cell-cell interaction density compared to the (initial) 2D culture environment in self assembled "myooids" [344].

These two main *in vitro* approaches to generate contractile 3D skeletal muscle tissue have been in use for 30 years now, however, more recent research directed towards a further optimization and refinement of existing strategies has partially unraveled the immense complexity of engineering functional biomimetic skeletal muscle *in vitro*. This has not only led to a thorough recapitulation of appropriate scaffold biomaterials and their compositions and topographical features, but also entails the constant development of novel methodology to further drive myogenic maturation, such as stimulation of skeletal muscle constructs in bioreactors, or the exploration of strategies for *in vitro* or *in vivo* vascularization and innervation of engineered muscle.

3.3.1. Influence of matrix properties on myogenesis

The tremendous amount of synthetic and natural biomaterials available for SMTE has made it difficult to make a clear decision on what the most suitable scaffold material is. Regardless of the chosen material it is, however, very important to match the overall physicochemical properties of the selected matrix with those of native muscle. In this respect, natural hydrogels appear most suitable for SMTE as their high density of cell attachment sites allows spatially uniform 3D cell spreading. Furthermore, higher ultimate myofiber density can be obtained after cell-mediated hydrogel compaction compared to synthetic materials. The extent of cell adhesion (which enables control over the initial cell seeding density) in a matrix is an important regulator myogenesis [353] and, *in vitro*, RGD density, affinity

and nanoscale distribution have been demonstrated to modulate myoblast proliferation and differentiation [299, 354].

Importantly, the mechanical properties of a matrix have widespread implications on muscle function i*n vitro* and *in vivo* [286]. One of the most commonly used parameters for matrix elasticity (or stiffness) is the elastic modulus (Young's modulus; E_{mod}), usually assessed by mechanical (tensile or compression) and/or rheological testing. Native healthy skeletal muscle tissue possesses a Young's modulus of approximately 12 kPa and muscle diseases, injuries or aging have been shown to lead to an increase in muscle stiffness to a modulus of ≥18 kPa [204]. It is therefore evident that inappropriate mechanical cues affect the ability of muscle to regenerate *in vivo*, and that the sensitivity of muscle cells to their mechanical environment can be exploited by optimizing mechanical matrix properties to maximize the myogenic outcome *in vitro* [286]. Indeed, matrix elasticity has been shown to be a powerful stimulus even capable of directing stem cell lineage specification. In an interesting study, Engler et al. [355] differentiated naive human MSCs on collagen matrices of varying elasticity (Young's modulus) and observed that, without further supplementation of the cell culture medium with instructive signaling molecules, lineage specification was heavily influenced by the matrix properties. A very soft matrix (E = 0.1-1 kPa) promoted neurogenic differentiation, while a comparably stiff matrix (E = 25-40 kPa) was found to be osteoinductive. Intermediate matrix elasticity (E = 8-17 kPa) promoted myogenic differentiation of MSCs, and these outcomes were attributed to the similarity of the respective matrix elasticity/stiffness (soft, intermediate and stiff) to that of the respective tissue (nerve, muscle and bone). Similarly, myotubes have been reported to differentiate optimally (as assessed by the extent of sarcomeric striations) on substrates with skeletal muscle tissue-like stiffness (E = 12 kPa) [356]. In addition, when cultured on alginate scaffolds of varying stiffness (E = 1, 13 or 45 kPa, respectively), adhesion and proliferation of primary mouse myoblasts was found to be maximal on gels with a physiologically relevant Young's modulus (E = 13 kPa) [357].

There is a clear consensus on the importance of mimicking the mechanical properties of native muscle in terms of matrix elasticity/stiffness. However, other biophysical cues such as matrix porosity or distinct (micro)topographical features are equally important for the survival of transplanted cells *in vivo* or the functional maturation of engineered skeletal muscle *in vitro*. A careful consideration of these cues is especially critical for *in vitro* SMTE approaches, which aim at the generation of volumetric muscles consisting of aligned and densely packed contractile myofibers. Due to their requirements for nutrients and O_2, most cell types do not tolerate distances further than 200 µm from a blood vessel [358]. Consequently, an appropriate pore size and interconnectivity of a matrix is required for effective delivery of nutrients and removal of waste. A general notion is that 3D scaffolds with macropores (pore size 100-500 µm) are considered optimal for cell growth and migration in 3D scaffolds [359]. In the context of skeletal muscle, an evaluation of pore sizes in alginate scaffolds led to the finding that macropores of 400-500 µm significantly enhanced primary myoblast viability and migration compared to micropores (10-20 µm) or nanopores (<1 µm) [298]. Another important aspect

enabling control over cell behavior on or in scaffold biomaterials is contact guidance. Cells sense and respond to morphological characteristics of a matrix such as grooves, oriented pores or overall fiber arrangement by adopting the orientation of these topographical stimuli. Skeletal muscle is a naturally aligned tissue and, although cell alignment within 3D matrices is not required for the formation of contractile myofibers, it increases the efficiency of myoblast fusion since this process is hypothesized to mainly occur in a longitudinal end-to-end configuration [360, 361]. Therefore, the implementation of methodology to pre-align myoblasts to increase myofiber formation has become popular for *in vitro* SMTE approaches. To date, a variety of micro-/nanofabrication techniques like electrospinning, soft lithography, photolithography or unidirectional freeze-drying are routinely used to create a microenvironment that induces cell alignment [15, 312].

A commonly used approach to generate aligned matrices is electrospinning, where micro- or nanofibers are generated from a polymer solution by accelerating a charged polymer strand out of an outlet nozzle through a strong electrical field onto a collector unit [362]. Electrospun fibers mimic the anisotropic structural organization of muscle ECM and can thus provide potent contact guidance cues for tissue morphogenesis [363]. Electrospinning has been successfully used to fabricate aligned nanofibrous scaffolds that induce the alignment of myoblasts/-fibers and a variety of natural [296, 364-366] and synthetic [367-369] scaffold materials has been evaluated [370]. With the notion that electrospun synthetic fibers, although very stable and amenable to precise modulation on the nanoscale, display low elasticity and sparse cell attachment, attempts to combine electrospun synthetic and natural materials have also been made. As examples, composites like PCL/gelatin [371] or PCL/collagen [332] nanofibers, laminin coated polypropylene fibers [372] or matrigel coated polyesterurethane fibers [373] have been introduced. Alternatively to coating electrospun synthetic matrices, co-axial electrospinning of two different polymer solutions allows for the generation of fibers surrounded by the second polymer. A core-shell technique consisting of PCL nanofibers surrounded by collagen was introduced by Zhang et al. [374], who demonstrated that cell adhesion to such an electrospun composite was even further improved as compared to collagen coated PCL nanofibers. One of the drawbacks of electrospinning is that the pore size of the generated matrices is hardly controllable. Thus, electrospun 3D matrices usually consist of densely packed fibers which hampers cell infiltration [375, 376]. To circumvent this problem, co-spinning of sacrificial fibers into electrospun aligned 3D matrices has been proposed [377]. After the electrospinning process, these usually water-soluble fibers can be leached out, leaving behind interspaces for the cells to infiltrate and thereby increasing porosity without the need of fiber diameter increase. More recently, direct electrospinning of 3D aligned nanofibrous tubes was also accomplished and demonstrated to promote aligned myotube formation when seeded with myoblasts [378].

Another widely used strategy to induce alignment of myogenic cells on or in a matrix is surface micropatterning [15, 379]. This approach allows the introduction of defined topographical features such as parallel grooves, oriented pores or distinct adhesion peptide patterns into matrices by methods

such as abrasive grinding [380], photolithography [381, 382], soft lithography [383, 384] or unidirectional freeze drying [385]. Initially, micropatterned matrices (usually made from PDMS) were fabricated by rapid prototyping and either coated with adhesive proteins for cell attachment prior to cell seeding or directly used as a cell matrix. Alternatively, the micropatterned matrix can be used as a master template in solvent-casting procedures for the production of patterned matrices [386]. Cells can then be differentiated in such matrices into, for example, aligned myotubes which can later be transferred from a 2D setting onto biodegradable natural matrices for further processing into a 3D construct [387]. This transfer technique may also allow the generation of several 2D aligned myotube sheets which can then be stacked onto each other to generate multi-layered 3D muscle tissue [379]. Advances in scaffold fabrication methods now allow introduction of topographical features with a higher spatial resolution (down to the nano scale), which has not only been used to pattern solid materials [328], but also to pattern natural or synthetic hydrogels [351, 382, 384, 388]. In this respect, an interesting approach was introduced by Bian et al. [389], who used mesoscopic fibrin hydrogel molding to create reproducibly controllable complex muscle tissue structures. In this soft lithography technique, sub-millimeter PDMS posts are precisely manufactured to create appropriate pores and to vary the alignment of cells in a hydrogel across a large tissue area. Other rapid prototyping methods such as 3D cell-laden hydrogel printing (organ printing) may also be useful to generate precise hydrogel geometries while confining muscle cells in a desired 3D configuration [390]. In addition, unidirectional freeze drying has been reported as an alternative method to generate spatially oriented structures in 3D matrices [391]. The gradual formation of ice crystals induced by this process can be used to create highly porous hydrogel or sponge scaffolds with aligned pores and, by varying the freezing temperature, the average pore size can be adjusted [385, 392, 393]. The use of magnetic [394, 395] or electric fields [396] during hydrogel polymerization has been explored and, interestingly, electric fields were found to induce fibrin fibril alignment to a greater extent than magnetic fields [396]. Techniques that allow for control over scaffold topography in large scaffolds could be useful in the generation of volumetric skeletal muscle tissue as they can elicit cellular contact guidance while facilitating nutrient diffusion and cell migration due to their scalable porosity. The implementation of computer-aided design may further facilitate the fabrication of complex muscle tissue structures with high precision and reproducibility [397, 398]. Importantly, a variety of bioreactor-based 3D culture systems have been developed, where defined application of physiologically relevant biophysical stimuli (such as mechanical stretch, compression or electrical stimulation) can be used to simultaneously act as instructive biological cue on the embedded cells on one hand and as a contact guidance cue through patterning of the scaffold biomaterial on the other (these systems will be presented in greater detail below).

Summarizing, the choice of the biomaterial, adaption of its mechanical properties to the needs of muscle cells and the provision of defined contact guidance cues all affect the myogenic outcome in 3D *in vitro* SMTE approaches. However, apart from these biophysical stimuli, the biochemical

environment the cells encounter once encapsulated in a 3D matrix can also be fine-tuned. Biochemical cues like growth factors, signaling ligands or cytokines can be incorporated into a scaffold through covalent coupling, physical entrapment or ionic interactions [281]. This can be combined with the aforementioned scaffold fabrication techniques to yield patterned matrices capable of releasing and/or presenting these biochemical cues to the incorporated muscle cells in a spatiotemporal manner (Fig. 15) [286]. Furthermore, release of growth factors from a muscle cell-laden matrix after transplantation can instruct endogenous regenerative processes *in situ*, which provides a dual beneficial effect of the released factors acting both on the cells in the matrix as well as on endogenous muscle cells. As mentioned earlier, growth factors of the HGF, IGF, VEGF and FGF families are of particular importance for skeletal muscle regeneration as they regulate SC function, muscle hypertrophy and host muscle vascularization [113]. Release of IGF-1 from collagen-based engineered skeletal muscle was shown to elicit paracrine anabolic effects on muscle tissue *in vitro* [399], while sustained local VEGF release from injectable alginate hydrogels (without delivery of cells) successfully triggered angiogenesis in ischemic mouse hindlimb muscles, with a return of muscle perfusion to normal levels after 4 weeks [400].
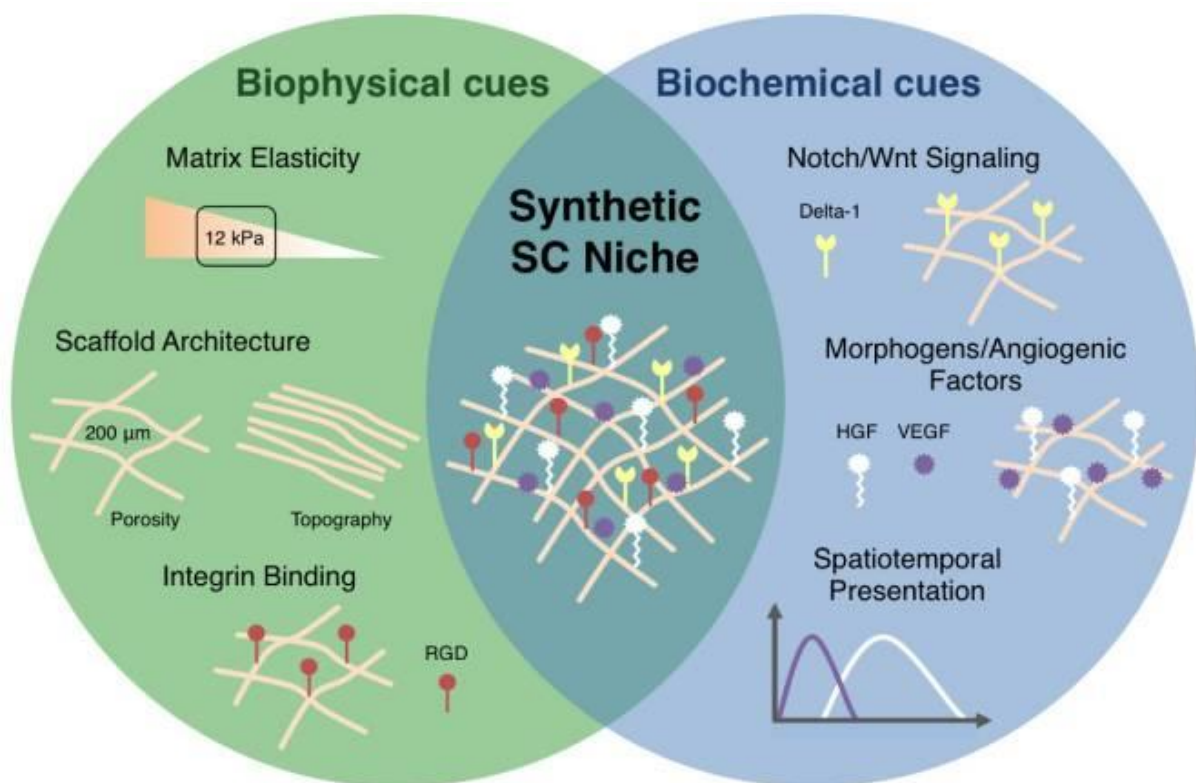
Fig. 15: *Design criteria for biomaterial-based SMTE approaches - towards engineering of a synthetic SC niche.* A variety of biophysical (matrix elasticity, porosity, topography, cell adhesion motif pattern) and biochemical (spatiotemporal presence of growth factors, cytokines or signaling ligands) cues affect muscle cell survival and fate. Fine-tuning of these cues allows for the generation of functional muscle constructs *in vitro* and can further improve cell survival and engraftment after transplantation *in vivo*, leading to more efficient regeneration of injured muscles (from [286]).

The synergistic presentation of multiple biochemical cues from the same matrix has also been explored. Based on the notion that a combination of multiple growth factors can more effectively influence the myogenic outcome compared to individual growth factor treatment [401], several acellular and cellular SMTE approaches using instructive hydrogel matrices have been reported [286]. For example, combined delivery of IGF-1 and VEGF incorporated into an injectable hydrogel scaffold was demonstrated to improve functional muscle regeneration following ischemic muscle injury, without the need for co-delivery of myoblasts [402]. Cellular approaches delivering primary muscle cells or SCs encapsulated in cell-instructive hydrogels containing growth factor combinations like HGF and FGF-2 [298] or IGF-1 and VEGF [239, 403] have also been shown to improve *in vivo* muscle regeneration after severe injury. Furthermore, covalent coupling of signaling ligands like the Notch ligand Delta1 to a hydrogel matrix may provide an additional therapeutic benefit, as direct and immediate exposure of SCs to Delta1 (which activates Notch signaling) within such a matrix was shown to maintain their engraftment potential during *ex vivo* expansion [404].

Rational and precise fine-tuning of the biophysical and biochemical matrix properties for muscle progenitor cells has yielded promising results with regard to engineering of a synthetic SC niche. Until recently, the major drawback of cellular *in vivo* SMTE approaches was that freshly isolated therapeutic SCs lose their stem cell potency (and, thus, their regenerative potential) over time during *ex vivo* expansion. A hallmark study by Gilbert et al. [248] identified substrate elasticity as a key regulator of SC self renewal in culture. Compared to SCs expanded on standard cell culture plastic (E ~ 10^6 kPa), SCs grown on pliant hydrogels made from PEG coated with laminin (E = 12 kPa) exhibited much higher engraftment rates and contributed more extensively to muscle regeneration after implantation into mice. This initial observation was further supported by Cosgrove et al. [204], who showed that SCs from aged animals can be rejuvenated when transiently cultured in a microenvironment simulating young muscle. Muscle aging is usually accompanied with an increase in muscle stiffness and a higher incidence of muscle cells expressing senescence markers due to elevated activity of the p38α/β MAPK pathway. The rejuvenating microenvironment consisted of a pliant PEG/laminin hydrogel matrix (E = 12 kPa) and p38α/β MAPK inhibitors. Subjecting primary muscle precursors from aged mice to this culture system rapidly expanded the residual functional SC population, which could then efficiently repair injured muscles in aged animals. Recently, Quarta et al. [249] reported a synthetic SC niche composed of an artificial myofiber made from collagen/laminin and a defined quiescence culture medium, which could effectively maintain self renewal of murine and human SCs for several days. Interestingly, SCs transiently cultured in the artificial niche contributed to muscle regeneration in mice more effectively than freshly isolated SCs, and with similar potency as SCs associated with their native myofiber, highlighting the importance of a niche-like environment *in vitro* for maintaining SC potency.

3.3.2. Bioreactors for muscle maturation

In general, tissue engineered skeletal muscle needs to be capable of generating sufficiently large forces in order to contribute to functional restoration of impaired host muscle upon transplantation. Myogenic differentiation, and thus force production, cannot only be enhanced by optimizing the physicochemical properties of the scaffold biomaterial to create a niche-like environment, but also by application of external biophysical stimuli, thereby optimizing the interactions that myofibers have with the surrounding 3D matrix [241]. In an attempt to create a more biomimetic cell culture environment compared to static conditions, various dynamic bioreactor-based tissue culture systems have been developed. Today, bioreactors are part of the standard TE toolbox, allowing for maintenance of a highly controlled environment for long-term tissue growth as well as for testing the response of growing tissues to defined external stimuli [405, 406]. Bioreactor design is particularly challenging in the context of striated (skeletal or cardiac) muscles which are naturally found in high stress environments and display a high degree of metabolic activity, complex cellular organization and electrochemical function. In the context of in vitro SMTE, bioreactors controlling flow and perfusion or applying defined regimes of mechanical (in the form of stretch or strain) or electrical (in the form of voltage) stimulation to engineered muscle constructs have predominantly been used [407].

Dynamic flow tissue culture bioreactors such as spinner flasks [408], rotating wall vessels [409] or perfusion systems [410] have been introduced to mimic the physiological delivery of O_2, nutrients or chemical signals via the blood flow, which provides significantly higher mass transfer rates compared to conventional static cultures. This is especially useful in 3D myogenic cell/scaffold culture systems, as elevated mass transfer reduces necrosis in the core of a muscle construct and thus allows for thicker tissues to be generated. In addition, microfluidic systems capable of precisely controlling perfusion and shear stress (through flow) in 3D muscle microtissues have been developed [411], which might enable the future use of such platforms for high-throughput drug screening [412].

While perfusion and flow bioreactors have more commonly been used in the context of cardiac or smooth muscle engineering, the majority of bioreactor-based in vitro SMTE strategies has focused on mechanical and/or electrical preconditioning of muscle cells [413]. Especially, bioreactors for the mechanical stimulation of muscle cells in the form of static (passive), progressive (ramp) or cyclic (intermittent) stretch to mimic growth [414] and physical exercise [415, 416], respectively, have been explored. These usually custom-made bioreactors are capable of applying physiologically relevant mechanical stimulation regimes to muscle tissue constructs by stretching the specimen along one (uniaxial), two (biaxial) or all planar tissue axes (multiaxial). However, since skeletal muscle naturally experiences mainly uniaxial strains, uniaxial mechanical stretching has been utilized most often for in vitro SMTE. The rationale behind this is that mechanical loading plays a central role in skeletal muscle development in vivo. Indeed, progressive passive tension of nascent skeletal muscles by bone growth (approximately 2 mm/week) during neonatal development not only influences muscle size,

length and myofibrillar organization, but also increases amino acid transport, total protein synthesis or SC activation and proliferation [417-423].

Almost 40 years ago, a pioneering study by Vandenburgh and Kaufman [424] laid the foundation for many of today's *in vitro* SMTE bioreactor systems. Reporting an *in vitro* model for stretch-induced skeletal muscle hypertrophy, they could show that embryonic chicken myotubes cultured on a flexible silicone membrane responded to longitudinal stretch with increased accumulation of total proteins, including myosin heavy chains. A decade after this report, follow-up studies by Vandenburgh et al. [290, 414, 425] demonstrated that embryonic avian myoblasts differentiated in a collagen hydrogel respond to a ramp pattern of cyclic stretch mimicking neonatal bone growth with increased rates of cell proliferation, myoblast fusion and protein turnover. Furthermore, mechanical stretch resulted in pronounced myotube alignment along the principle axis of strain, with significantly longer myotubes compared to static conditions. The horizontal cell stimulator used in this study was the first setup to mechanically stimulate 3D muscle constructs and basically provided the blueprint for future bioreactor systems. Since then, a multitude of systems has been introduced, capable of applying relevant cyclic, static or ramp strain regimes (or combinations thereof) to engineered 3D skeletal muscle tissue [262, 295, 350, 415, 416, 426-429]. The majority of mechanical stimulation bioreactors make use of a "floating anchor" to which a construct is attached on one end while the other end is attached to a fixed anchor (Fig. 16). Defined movements of the floating anchor through computer-controlled linear actuators or stepper motors allow for application of a defined strain (usually given in % scaffold length). For example, Okano and Matsuda [429] created ring-shaped collagen scaffolds with embedded C2C12 myoblasts and used a horizontal stationary post/movable hook setup within a custom-made culture flask (Fig. 16A). Cyclic mechanical stimulation resulted in the formation of highly dense muscle bundles, with alignment of both myotubes and collagen fibrils along the axis of strain. Du Moon et al. [416] subjected human muscle precursor cells seeded onto an acellular porcine bladder submucosa scaffold to cyclic strain in a linear motor-driven stimulator device. Strain was applied by tying one end of the construct to a stationary bar and the other end to a movable bar with sutures (Fig. 16B). Cyclic mechanical preconditioning produced aligned viable muscle tissue capable of generating contractile responses after 3 weeks of *in vitro* culture, and, upon transplantation into mouse muscle, the preconditioned muscle tissue generated significantly higher forces than statically cultured control tissues. In the first study to ever generate human bioartificial muscle (HBAM) *in vitro*, Powell at al. [350] casted cylindrical collagen/matrigel scaffolds seeded with human primary muscle cells in silicone molds containing end attachment sites (Fig. 16C). Subsequent preconditioning in a custom-made mechanical cell stimulator by using ramp strain (to mimic bone growth) followed by cyclic strain (to stimulate exercise-induced hypertrophy) increased muscle elasticity two- to three-fold, mean myotube diameter by 12% and myotube are by 40%. Furthermore, the system allowed for live monitoring of the internally and externally applied forces through implementation of a sensitive force transducer. Matsumoto et al. [295] reported a system similar to that of du Moon et al. [416] mentioned

above, as they also used sutures to tie a construct to a stationary and a movable bar (Fig. 16D). However, instead of an acellular scaffold, cylindrical fibrin scaffolds seeded with C2C12 myoblasts or human umbilical cord vein endothelial cells (HUVECs) were used. Static mechanical stimulation lead to both development of aligned myotubes as well as aligned vessel-like structures, suggesting that cellular alignment is a universal cellular response to uniaxial stretch. Auluck et al. [426] studied the effects of ramp or cyclic ramp strain on primary human muscle cells seeded in a collagen sponge (Gelfoam). One side of the cell-seeded sponges was attached to the inner aspect of specialized culture dishes with a locking device while the other side was attached to a cylindrical steel bar whose movement is controlled by an electromagnetic solenoid (Fig. 16E). Myotube formation was observed under all experimental conditions (strain regimes), however, progressive ramp strain resulted in elevated MMP-2 expression compared to cyclic ramp strain, demonstrating that the extent of ECM remodeling varies between different strain regimes. In addition, we have generated a bioreactor system ourselves, allowing for automated application of defined strain regimes (static, cyclic or ramp strain) onto ring-shaped myoblast-seeded fibrin scaffolds [430]. Using free-standing fibrin/cell constructs mounted onto a custom-made magnetic hook-spool system, static mechanical stimulation (which is conferred via moving magnets) led to rapid generation of aligned, mature myotubes with widespread sarcomeric patterning within 9 days of culture (see Chapter I).
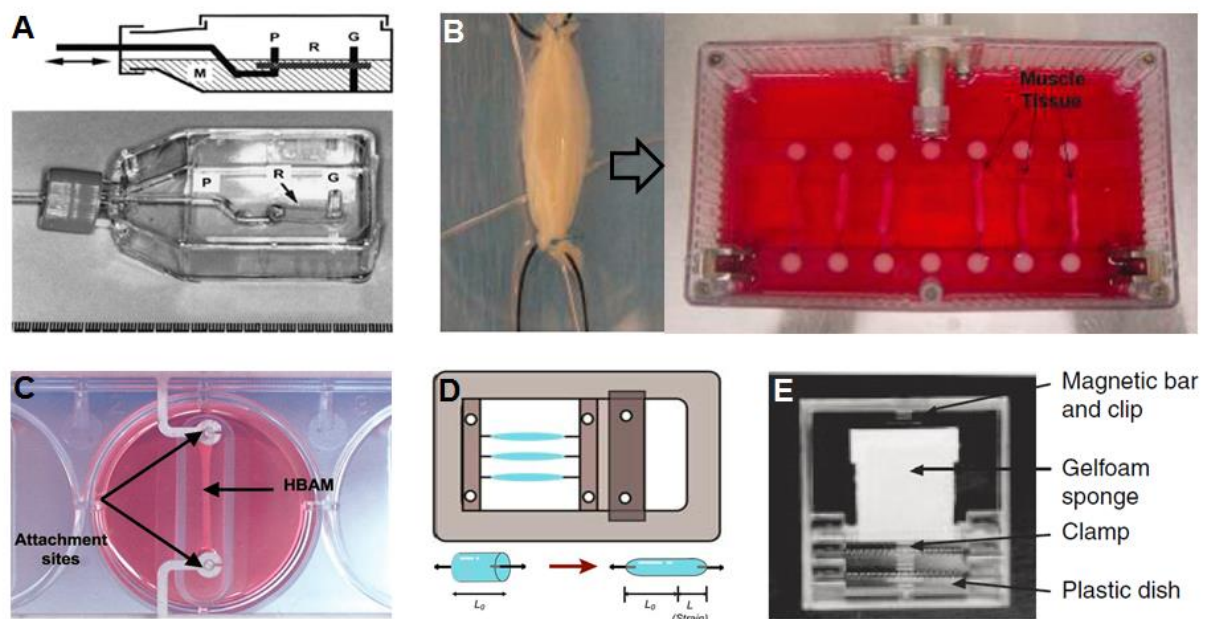
Fig. 16: *Bioreactor systems for mechanical stimulation of myogenic cells embedded in 3D scaffolds.* Depending on the type of scaffold and the desired mechanical stimulation regime, a variety of bioreactors for *in vitro* SMTE have been developed. (A) Ring-shaped cell/scaffold constructs (R) submerged in medium (M) that are attached to a glass (G) rod and a stepper motor-controlled piston (P) rod (adapted from [429]). (B) Decellularized porcine bladder seeded with human muscle cells tied to a stationary and a movable bar with sutures (adapted from [416]). (C) Cylindrical collagen/matrigel scaffolds seeded with human muscle cells (HBAM) in silicone molds containing movable end attachment sites with an implemented force transducer (from [350]). (D) Cylindrical fibrin scaffolds seeded with mouse muscle cells or HUVECs sutured to a stationary and a stepper motor-controlled movable bar (from [295]). (E) Collagen (Gelfoam) sponges seeded with human muscle cells

clamped at one end to the inner aspect of a specialized plastic cell culture dish while the other end is attached to a steel bar whose movements are controlled through an electromagnetic solenoid (from [426]).

Among others, these studies have shown the generally beneficial effects of mechanical stimulation on *in vitro* myogenesis. The most robust effects observed were cell/myotube alignment along the principle axis of strain, which is a prerequisite for uniaxial force generation of the engineered muscle tissue, and enhanced myoblast fusion and differentiation (in terms of myotube density, length, diameter and sarcomeric assembly), which determines muscle functionality. The latter is directly proportional with force production and, indeed, mechanically preconditioned engineered skeletal muscle tissue has been shown to contribute more efficiently to functional muscle repair in mouse models of VML than unstimulated (but differentiated) tissue, likely due to its capability to rapidly adapt to the mechanical requirements of the new environment upon transplantation [262, 415]. In addition, mechanical stimulation has been shown to enhance myogenic differentiation of non-muscle stem cells such as bone marrow- or adipose tissue-derived MSCs [431, 432].

While the majority of bioreactors uses similar setups to apply strain to nascent skeletal muscle tissue (for example by a motor-controlled floating anchor), the actual strain regimes reported are highly diverse [413]. The notion that cells can respond quite drastically to biophysical stimuli through mechanoresponsive signaling pathways has prompted research looking into the mechanisms guiding exercise-induced muscle hypertrophy [433, 434]. Static and cyclic stretch have been found to increase the secretion of auto- and paracrine factors, including IGF-1, HGF, adenosine monophosphate (AMP) or triphosphate, reactive oxygen species (ROS) or prostaglandins [151, 428, 433, 435, 436]. In muscle, these cytokines and growth factors can activate a variety of downstream effectors among which Phosphoinositide 3-kinase (PI3K), G protein-coupled receptor (GPCRs), MAPK, Ca^{2+} and AMP activated kinase (AMPK) signaling play important roles in skeletal muscle mechanotransduction [407, 433, 434, 437, 438]. PI3K seems to play a central role in stretch-induced muscle hypertrophy and is a known regulator of cell metabolism, thus affecting both cell proliferation and differentiation. IGF-1, and other growth factors/cytokines released upon mechanical stress, can activate PI3K in an auto- and paracrine manner [428] or can act via GPCRs to activate MAPK pathways [439]. The MAPK family can be sub-divided into extracellular regulated kinase (ERK), c-Jun NH2-terminal kinase (JNK, also known as stress-activated protein kinase) and p38 families, and increased ERK and JNK phosphorylation in skeletal muscle cells in response to mechanical stress has been reported [437]. G protein-coupled receptor activated phospholipase C (PLC) has also been shown to contribute to skeletal muscle mechanotransduction and further connects with Ras-Raf and Ca^{2+}-mediated signaling cascades [440]. PLC activation upon cyclic stretch [440] can subsequently trigger protein kinase C (PKC) which in turn can phosphorylate p53 (cell cycle arrest) or Raf (ERK activation) [441]. Given that PLC also mediates localized Ca^{2+} release from the sarcoplasmic reticulum by enzymatic cleavage of phosphytidylinositols, its stretch-induced activation could be a mechanism for Ca^{2+} influx amplification from the extracellular space [433]. Apart from the PLC pathway, intracellular Ca^{2+}

levels are also regulated by Ca^{2+} influx through stretch-activated channels (SACs) or active force generation [442, 443]. A role of the Ca^{2+}/calcineurin/cytoplasmic nuclear factor of activated T cells (NFAT) signaling axis in muscle hypertrophy has been established [444]. Calcineurin, also known as protein phosphatase 2B, is a Ca^{2+} and calmodulin (a Ca^{2+} binding protein) dependent phosphatase which can activate transcription factors of the NFAT and MEF2 families [444, 445] which, along with the MRFs, regulate the transcription of many muscle-specific genes (for example MHC isoforms) [446, 447].

Although the entity of mechanoresponsive signaling circuits and their complex interplay in response to biophysical stimuli in skeletal muscle is not yet fully understood, there is compelling evidence that exercise-related muscle hypertrophy is, at least partially, mediated by the IGF-PI3K-mammalian target of rapamycin (mTOR) axis [448]. mTOR signaling is mediated via two different mTOR complexes (mTORCs), mTORC1 which is sensitive to rapamycin and mTORC2 which is not inhibited by rapamycin. mTOR signaling can be induced by IGF binding to PI3K which, in turn, activates protein kinase B (PKB) via the 3 phosphoinositide-dependent protein kinase-1 (PDK1) [449]. Activated PKB can then phosphorylate and inhibit the activity of the tuberous sclerosis complex 1/2 (TSC1/2), triggering the activation of mTORC1 which signals downstream via the ribosomal protein S6 kinase (S6K, also known as p70S6K) [448]. Phosphorylation of p70S6K (specifically at Thr389) has been used as a read-out of mTORC1 activity and this rapamycin-sensitive branch of mTOR signaling has been shown to elicit the mechanically-induced changes in protein synthesis and skeletal muscle growth/mass [450-452]. Indeed, a pivotal study by Baar and Esser [453] demonstrated that high-resistance exercise in rats led to increased phosphorylation of p70S6K, which correlated with skeletal muscle mass. Bodine et al. [450] further reported that rapamycin prevents the mechanically-induced increase in p70S6K phosphorylation and efficiently blocks the hypertrophic response of muscle in response to mechanical loading. In addition, a negative regulation of otherwise elevated muscle protein synthesis after mechanical loading by rapamycin has been shown [454].

Much of what is known today about mechanotransduction in skeletal muscle homeostasis is derived from studies in animals or human patients. *In vivo*, skeletal muscle receives all kinds of mechanical stimuli, including passive tension or eccentric and concentric contraction. Therefore, *in vivo* studies looking into mechanoresponsive signaling pathways after exercise-induced mechanical muscle stimulation capture the response from all these stimuli. This is different from the application of defined mechanical loading regimes in the bioreactor-based dynamic *in vitro* culture systems. Therefore, *in vitro* SMTE has extensively evaluated different specific mechanical strains, for example cyclic vs. static vs. progressive stretching (or combinations thereof), and how these stimuli can enhance myogenic differentiation to maximize muscle maturation and contractility. With regard to mechanical strain regimes, it is noteworthy that not all stimulation regimes support *in vitro* myogenesis. In fact, contradictory data has been reported regarding the effects of mechanical stretch (promotion vs. inhibition) on various aspects of myogenic differentiation, including the expression of

important muscle genes (such as the MRFs) [455, 456] or muscle-specific proteins (for example MHC isoforms) [447, 457, 458] and, more general, the formation of myotubes [456, 458, 459]. A general notion from these studies is that specific parameters such as nature of stretch (cyclic vs. static), stretch amplitude, frequency and rest period play important roles in fine-tuning the balance between muscle cell proliferation and differentiation. Furthermore, a careful evaluation of the culture format and bioreactor type is necessary. In this respect, strain regimes promoting myogenic differentiation in 3D constructs might not do so in 2D monolayers and uniaxial stretching may elicit different cellular responses than bi- or equiaxial stretching. One of the probably most important aspects is to find appropriate biomimetic strain patterns that take into account the response of muscle cells over different developmental stages (SC/myoblast-myotube-mature myofiber). For example, cyclic mechanical stimulation has been found to promote SC/myoblast activation and proliferation while delaying the onset of myogenic differentiation [456, 460, 461]. At the same time, cyclic stretching can induce myofiber hypertrophy and maturation *in vitro* [350, 416, 427, 428], which correlates with functional recovery *in vivo* [262, 415, 462]. Currently, mechanical stimulation regimes consisting of an initial period of progressive stretch (to mimic bone growth) to trigger myoblast fusion into aligned myofibers followed by cyclic stretch (to mimic exercise) to induce myofiber hypertrophy and maturation seem to be the most promising approaches. So far, these stimulation patterns have elicited the most potent effects on myogenic differentiation, as shown by Candiani et al. [427] who found MHC protein levels to be increased 8-fold in preconditioned muscle cells compared to unstimulated controls. It is known that mechanical stretching plays a role in the regulation of slow and fast MHC isoform expression levels determining the slow- vs. fast-type myofiber composition which varies between different muscles [463, 464]. Therefore, a further elucidation of the involved mechanotransduction pathways might enable the use of specific mechanical stimulation regimes to engineer muscle tissue with a desired fiber type, with the goal of more closely matching the native muscle phenotype present at the injury site.

Similar to mechanical stimulation, culture formats enabling electrical stimulation of muscle cells in 2D and 3D settings have also been developed [413, 465]. Continuous contractile activity of skeletal muscle, initiated by the release of ACh from motor neurons in the NMJ, is of critical importance for the maintenance of muscle viability, mass and function. Bioreactors for electrical pulse stimulation (EPS) can simulate synaptic input and, thus, exercise and systems for endogenous stimulation usually apply graphite, steel or platinum electrodes parallel to cell monolayers or engineered 3D muscle tissue within a culture dish to reproducibly induce controlled field shock regimes [466-470]. Initially, electrical stimulation was performed on skeletal muscle cells in monolayer culture. Already in 1976, Brevet et al. [471] were the first to subject chick embryo skeletal muscle cells to electrical stimulation and observed a significant increase in total protein synthesis, especially for MHC proteins, compared to unstimulated controls. Almost two decades later, studies on the effects of chronic electrical stimulation on SCs isolated from newborn rat hind limbs revealed that electrical stimulation regimes

mimicking slow or fast twitch activation patterns greatly influence respective MHC isoform expression [472, 473]. Different burst (1, 4 or 100 s) and pulse (15, 40 or 100 Hz) frequencies were screened and the general notion was that stimulatory regimes that mimic aerobic exercise (more repetitive contraction, for example bursts every 1 or 4 s, and lower force contraction, for example pulse frequencies of 15 or 40 Hz) elicit slow fiber adaptation as assessed by analysis of slow MHCI isoform expression, while less frequent (bursts every 100 s) but more powerful contractions (100 Hz pulse frequency) elicit faster fiber formation (fast MHCII isoforms), mimicking resistance exercise [472]. In addition, this work demonstrated that simulation of slow twitches though electrical stimulation increased slow MHCI isoform expression to a greater extent in SCs derived from slow-twitch muscles than from fast-twitch muscles [473], suggesting that SCs possess a memory of the specific niche (in terms of the muscle fiber type) from which they were originally derived [413]. A follow-up study by Pette at al. [474] further showed that chronic low-frequency stimulation (CLFS) of regenerating rat fast-twitch muscles induces partial fast-to-slow fiber conversion, hinting at the potential of electrical stimulation to generate muscles with desired fiber type composition *in vitro*.
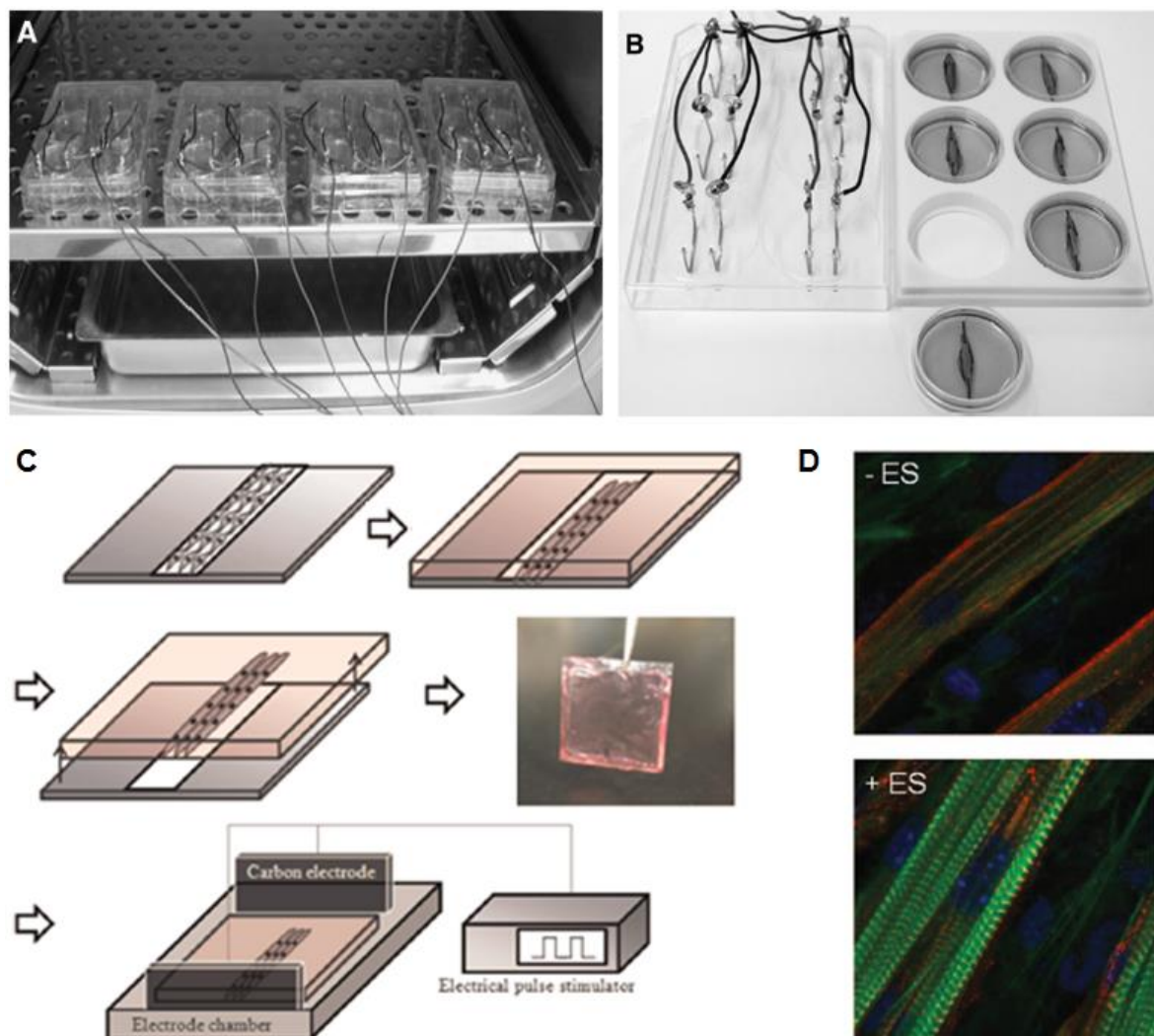

Fig. 17: *Bioreactors systems for electrical stimulation of myogenic cells in 2D and 3D culture formats.* (A) Parallelized array of electrodes for electrical stimulation of 2D monolayers, and (B) bioreactor for electrical stimulation of 3D skeletal muscle

constructs (adapted from [475]). (C) System for the transfer of line-patterned C2C12 myotubes from glass onto a fibrin hydrogel and subsequent electrical stimulation in a carbon electrode chamber connected to an electrical pulse stimulator (adapted from [468]). (D) Electrical stimulation of differentiating C2C12 myoblasts (+ES) increases sarcomere assembly and myotube contractility compared to unstimulated (-ES) controls. Blue: nuclei; red: sarcomeric α-actinin; green: F-actin (adapted from [476]).

While acute electrical stimulation has also been used to assess the contractility and maturity of engineered 3D skeletal muscle tissue through measuring single twitch or tetanic contractile forces [293, 347, 477], CLFS is increasingly implemented into *in vitro* SMTE approaches to trigger the exercise-induced functional maturation of muscle tissue (Fig. 17). A variety of studies have demonstrated the feasibility of electrical stimulation to enhance myogenic differentiation *in vitro*, enabling the generation of more mature adult muscle phenotypes with improved functional contractile properties [466-468, 470, 475, 476, 478-480]. Huang et al. [481] investigated the aforementioned hypothesis that SCs from fast and slow twitch muscles are different by engineering 3D muscle organoids from SCs isolated from fast TA or slow soleus rat muscles and subjected them to electrical stimulation. Time to peak twitch tension (TPT) and half relaxation time (1/2RT) were approximately 30% slower in soleus-derived engineered muscles. CLFS resulted in a 15% lower TPT and a 14% slower 1/2RT in TA-derived constructs, however, absolute force production was not altered. In soleus-derived organoids, CLFS yielded an 80% increase in total force production with no change in TPT or 1/2RT, confirming the theory that SCs derived from slow or fast twitch muscles have distinct memory for the respective muscle fiber type. Donnelly et al. [475] introduced a bioreactor system capable of applying defined electrical stimulation regimes (with regard to pulse amplitude, pulse frequency and work-to-rest ratio) to 2D myoblast monolayers or 3D muscle organoids (Fig. 17A, B). 2D cultures stimulated at high frequencies (100 Hz) responded with increased rates of protein synthesis, showing that appropriate electrical stimulation is an anabolic signal. Furthermore, an analysis of 3D skeletal muscle organoids (made from 90% C2C12 myoblasts and 10% 3T3 fibroblasts on fibrin) stimulated for 7 days with varying electric fields (1.25 vs. 2.5 vs. 5 V/mm) revealed increased force production and excitability at 2.5 V/mm as opposed to 5 V/mm, suggesting that moderate voltage stimulation is required to drive myogenic maturation in 3D engineered skeletal muscle tissue. Following up on the optimization of biomimetic electrical stimulation regimes, Khodabukus and Baar [479] investigated the effect of different pulse amplitude on the excitability of engineered 3D skeletal muscle organoids. By determining rheobase (the electrical field required to produce 50% peak twitch force at a given pulse width), which correlates inversely with excitability, they found that stimulation at a pulse amplitude of 4x rheobase resulted in the largest tetanic force, while stimulation at 6x rheobase or above led to reduced peak force and increased fatigability, likely due to electrochemical damage. Other studies also looked at the differences between the cellular responses to electrical stimulation in 2D vs. 3D myogenic culture systems or myoblast cell lines vs. primary muscle precursor cells [467, 470]. Interestingly, 3D skeletal muscle constructs made from primary mouse myoblasts responded

more drastically to electrical stimulation, with more widespread sarcomeric patterning and a transition from fast to slow MHC isoforms as opposed to 3D constructs made from C2C12 myoblasts.

Since electrical stimulation, although improving myogenic maturation and contractility, does not elicit myotube alignment, micropatterning techniques to generate parallel myotubes have been combined with electrical stimulation bioreactors. For example, Nagamine et al. [468] used glass substrates to pattern differentiating C2C12 myoblasts into parallel myotubes which were transferred onto fibrin hydrogels and subsequently electrically stimulated in a bioreactor (Fig. 17C). Similarly, Flaibani et al. [482] generated aligned myotubes from primary rat myoblasts on micropatterned PLLA membranes and subjected them to electrical stimulation, which resulted in improved myogenic differentiation and higher myotube density. In an interesting study, Liao et al. [480] validated a bioreactor system allowing for both mechanical and electrical stimulation. C2C12 myotubes on aligned electrospun PU fibers showed an increase in sarcomeric striations and myogenic differentiation marker expression when subjected to repeated stretching or electrical stimulation. Fast MHC isoform protein levels, however, were significantly higher after synchronized electromechanical stimulation compared to single treatment controls. The efficiency of this approach to drive myogenic functional maturation might be further enhanced by the use of electrically conductive electrospun nanofibers for a more homogenous distribution of electrical stimuli within the 3D construct [483].

These and many more studies have provided compelling evidence that electrical stimulation is a powerful stimulus to increase the contractility and excitability of 3D engineered skeletal muscle. EPS can manipulate intracellular Ca^{2+} transients and thereby created Ca^{2+} oscillations can not only accelerate *de novo* sarcomeric assembly (Fig. 17D) [476, 478], but can also elicit changes in MHC isoform expression determining muscle fiber type. While a thorough evaluation of appropriate biomimetic electrical stimulation regimes is still ongoing, especially in 3D engineered muscle tissue, a more recent study by Khodabukus et al. [466] identified CLFS of contraction durations between 60 and 600 s (with constant pulse frequency of 10 Hz) as an ideal regime to evoke similar metabolic adaptation of engineered skeletal muscle *in vitro* as occurring *in vivo* after aerobic exercise. Interestingly, in C2C12, electrical stimulation increased MHC expression for up to two weeks, but no further increase is found after that. This suggests that other factors such as the presence of other cells naturally found in muscle, defined media constituents or a combination of contraction types (for example isometric vs. concentric) will additionally be necessary for full force transmission, and, therefore, that most likely a combination of biochemical, mechanical and electrical stimuli will be necessary for complete muscle maturation [484].

3.3.3. Strategies for vascularization and innervation of tissue engineered muscle

Rapid integration of engineered skeletal muscle tissue with host vascular and nervous systems is a key prerequisite for the success of prefabricated constructs in repairing volumetric muscle defects.

Recently, both acellular [338, 485] and cellular [262, 415, 462] SMTE approaches have yielded promising therapeutic results in mouse models of VML, however, whether these strategies are applicable to human muscles which are several orders of magnitude bigger than mouse muscles remains elusive. Although the use of sophisticated bioreactor systems has expanded the *in vitro* SMTE toolbox by numerous methods to drive muscle functional maturation, the majority of studies so far has utilized avascular and -neural constructs. An inherent shortcoming of these approaches is that functional long-term contribution of such engineered contractile muscle tissues *in vivo* will require the presence or invasion of vascular structures to increase mass transport and prevent necrosis, and neuronal input to prevent muscle atrophy. Furthermore, the lack of a functional vascular bed strongly limits the generation of volumetric engineered muscle (which will be necessary to treat VML) [358], while the absence of innervation prevents functional muscle maturation [14].

Current methods for the vascularization of SMTE constructs can be divided into two categories, *in vitro* (pre)vascularization (the formation of vascular structures within the construct during cell culture prior to implantation) and *in vivo* vascularization (the stimulation of rapid ingrowth of host vasculature into the construct after implantation) [486, 487]. *In vitro* vascularization strategies have mainly relied on co-cultures of myogenic cells with vasculogenic cells such as ECs, EPCs or vascular smooth muscle cells (VSMCs) in 3D scaffolds. For example, van der Schaft et al. [488] subjected co-cultures of myoblasts and ECs in 3D collagen scaffolds to uniaxial passive tension and observed the formation of both aligned myotubes and vascular structures that seemed to form independently of each other. In addition, VEGF release from myoblasts in response to mechanical stimulation triggered vasculogenesis in a pracrine manner. Levenberg et al. [261] reported that 3D tri-culture of myoblasts, HUVECs and embryonic fibroblasts in highly porous PLLA/PLGA scaffolds yielded skeletal muscle constructs with pronounced vascular stuctures. Interestingly, the presence of fibroblasts increased the levels of VEGF expression within the construct compared to myoblast/HUVEC co-culture, thereby promoting a higher degree of endothelial vessel formation and stabilization. After transplantation, prevascularized constructs showed improved blood perfusion and survival of the skeletal muscle tissue. A follow-up study by the same group [489] also demonstrated that prolonged *in vitro* culture of such tri-culture muscle constructs to form well-developed vessels can further increase vessel density, which was found to support graft-host angiogenic collaboration, ultimately improving vascular integration and muscular maturation. Alternatively, a cell sheet technology-based approach using thermoresponsive polymer sheets to stack layers of myogenic and vasculogenic cells on top of each other has been shown to promote capillary formation *in vitro* and, when implanted subcutaneously into mice, anastomosis with the host vasculature *in vivo* enhanced myoblast survival [490].

The difficulty of culturing multiple cell types in one culture system, with the potential inherent inhibitory paracrine effects of myogenic cells on endothelial cells and *vice versa*, has led to the exploration of *in vivo* vascularization approaches. Although avascular SMTE constructs are limited in size, the maximization of functional muscle maturity (for example through pre-conditioning) prior to

transplantation is easier than in co-cultures. Upon transplantation, host vascularization of such constructs can restore the functional deterioration usually seen shortly after implantation but, over time, can further improve muscle maturation compared to preimplantation levels [352, 486]. However, without further modifications, the initial hypoxic response of avascular tissue engineered muscle *in vivo* limits this approach to small caliber grafts. Therefore, methods such as the delivery of functional muscle tissue on a matrix combined with sustained release of angiogenic factors from this matrix have been hypothesized to improve and accelerate host vascular integration. Sustained delivery of VEGF from cell-free alginate hydrogels has been shown to restore angiogenesis and perfusion levels [402] as well as skeletal muscle innervation [491] in ischemic mouse muscles. Combined delivery of angiogenic (VEGF) and myogenic (IGF-1) growth factors alone was found to improve functional muscle recovery *in vivo* [402], which could further be enhanced when a combination of VEGF, IGF-1 and myoblasts were delivered into muscle defects [239, 403]. Similarly, the delivery of myoblasts genetically engineered to transiently secrete VEGF upon grafting was shown to enhance neoangiogenesis in mouse muscle defects [492]. Alternatively, growth of 3D skeletal muscle constructs around arteriovenous loops can stimulate vascular invasion and subsequently enhance perfusion of the engineered tissue *in vivo* [493, 494]. More recently, an somewhat alternative approach was introduced by Shandalov et al. [327], who combined *in vitro* with *in vivo* vascularization to generate an engineered muscle flap. The aforementioned tri-culture construct (myoblasts, HUVECs and fibroblasts in PLLA/PLGA) was cultured *in vitro* until a small capillary net was formed and subsequently anastomosed with the capillaries sprouting from the recipient's femoral artery and vein *in vivo*. After a short period *in vivo*, the graft, now vascularized by invaded femoral vessels, was transferred as a muscle flap into a full-thickness abdominal wall defect. The implanted vascularized flap, bearing both host and human-derived blood vessels, became well integrated with the surrounding tissue and was capable of providing mechanical support to the abdominal wall. In the future, tissue engineered flaps based on this strategy may render the use of autologous FFMT unnecessary.

Muscle tissue functionality, which is inevitably linked to its contractile properties, is heavily influenced by (motor) neurons. *In vivo*, muscle denervation leads to a rapid loss of muscle mass and contractility [495]. Although myoblasts can differentiate and fuse into myofibers in the absence of innervation *in vitro*, they cannot fully mature in this aneural environment. Similar to the need for vascularization, functional maturation of tissue engineered skeletal muscle requires the presence of NMJs. Several studies have highlighted the importance of neuronal input on myogenic maturation through the use of *in vitro* co-cultures of muscle and neuronal cells in 2D and 3D settings [496-500]. Altogether, these studies showed that co-culture of myoblasts with motor neurons (usually derived from neural stem cells) promoted ACh receptor (AChR) clustering on the muscle cells [496, 499, 500], a hallmark of NMJ formation at the motor end plate, which significantly improved contractile force generation in engineered innervated muscles compared to "denervated" single myogenic cultures [497]. Furthermore, treatment of tissue engineered innervated skeletal muscle with the NMJ antagonist

curare blocked glutamic acid induced muscle contraction, indicating that the observed contractions were elicited by the motor neurons [498]. *In vivo* innervation of engineered skeletal muscle tissue has also been attempted, for example through implantation of myoblasts seeded in fibrin around the femoral vessels and transected femoral nerve in rats [501]. Indirect stimulation of the muscle tissue via the nerve elicited contraction and neurotized constructs showed contractile forces 5 times as high as non-neurotized controls. Furthermore, transplantation of a common peroneal nerve graft into denervated rat muscle was found to regenerate NMJs and partially recovered muscle function, although full restoration of contractility to pre-injury levels did not occur [502]. However, to date, in contrast to muscle vascularization, only few innervation approaches have been evaluated *in vivo*. It is therefore not clear whether co-cultures of myogenic and neuronal cells would add any therapeutic benefit compared to aneural muscle constructs which are a lot easier to generate. Thus, preconditioning of engineered skeletal muscle tissue with neuronal paracrine factors has been also explored, with the hypothesis that this may enhance myofiber maturation and expression of AChR clusters, which might facilitate *in vivo* innervation upon transplantation [486]. In particular, the supplementation of engineered skeletal muscle cultures with agrin, a factor known to be involved in AChR aggregation during synaptogenesis [503], has been demonstrated to increase the contractility of engineered muscle *in vitro* [504], likely due to increasing the density of AChR clustering [505], which also accelerated implant innervation *in vivo* [505].

4. FIBRIN - A VERSATILE SCAFFOLD FOR TISSUE ENGINEERING

The following sections are taken from a book chapter contribution to the book series "Tissue Engineering and Regeneration" (see below). This chapter provides a general and comprehensive description of the mechanisms of fibrinogenesis and -lysis as well as the broad application fields of fibrin sealants in clinics and TERM. Due to the length of this manuscript, only the parts relevant to this thesis were included here and partially adapted for the sake of brevity.

"From Hemostasis to Tissue Engineering - the manifold Applications of Fibrin Sealants in Regenerative Medicine"

Heher P.[1], Prüller J.[2], Fuchs C.[3], Redl H.[1]

[1] Ludwig Boltzmann Institute for Experimental and Clinical Traumatology/AUVA Research Center, Austrian Cluster for Tissue Regeneration, Vienna, Austria

[2] Randall Centre of Cell and Molecular Biophysics, King's College London, London, United Kingdom

[3] Department of Biochemical Engineering, City of Vienna Competence Team Bioreactors, UAS Technikum Wien, Vienna, Austria

The elastic hydrogel fibrin is the end product of the physiological blood coagulation cascade. Fibrin formation (fibrinogenesis) involves a cascade of enzymatic reactions that involve the activation of various coagulation factors (identified by the roman numerals FI to FXIII, with the lowercase appendix $_a$ indicating the activated form) which circulate as inactive zymogens that are activated upon proteolytic cleavage. Ultimately, this leads to the conversion of soluble fibrinogen monomers (FI) into an insoluble polymeric mesh-like fibrin network (FIa), often referred to as clot (thrombus), by the actions of the activated enzyme thrombin (FIIa). The process of blood clotting was first observed almost 2000 years ago by Galen of Pergamon (AD 129-199), a greek philosopher and physician, who identified fibrae (threads) in blood clots and circulating blood. These threads should later be described as fibrin fibers which form the structural basis of the blood clot. In the early 20th century, the german physiologist Paul Morawitz described the basics of blood coagulation as we know it today, identifying

several coagulation factors including fibrinogen, prothrombin or thrombokinase [506]. These findings laid the foundation for the "cascade" or "waterfall" models describing blood coagulation as a series of hierarchical enzymatic reactions that were later postulated and helped shape today's models of blood coagulation [507-509].

Today, blood coagulation in humans is well understood and the advances in protein purification methodology over the last decades have enabled clinicians to use purified formulations of fibrinogen and thrombin as two-component surgical sealants. These fibrin glues mimic the last step of blood coagulation (the formation of a stable fibrin clot) are now routinely used as clinically approved hemostats, adhesives or sealants in a variety of surgical procedures [304]. Furthermore, the exceptional biocompatibility and -degradability of fibrin sealants has led to their evaluation and widespread use as versatile delivery matrices for cells and/or bioactive therapeutic molecules (drugs, growth factors or gene vectors) in the field of TERM [302, 510].

4.1. The central role of fibrin in blood coagulation and wound healing

Blood coagulation is paramount to wound healing and a highly conserved mechanisms ubiquitous in all vertebrates [511, 512]. In general, blood clotting relies on the enzymatic conversion of soluble proteins into an insoluble fibrous structure, which eventually leads to hemostasis. This highly dynamic mechanism is, however, not only mediated by fibrin alone but the complex interplay of blood cells, plasma proteins and other factors released into the surrounding tissue upon a vascular injury [507]. Blood coagulation is triggered by damage to a blood vessel, leading to disruption of its endothelium. The resulting injury in combination with the exposure of blood to the sub-endothelial space triggers a cascade of enzymatic reactions mediated by the aforementioned coagulation factors. Most of these factors are serine proteases, however, there are a couple of exceptions, for example FV and FVIII are glycoproteins or FXIII is a transglutaminase (TG). The final step of this cascade, the formation of a stable fibrin clot, is mediated by the activated serine protease thrombin which catalyzes the conversion of soluble fibrinogen monomers into an insoluble fibrin meshwork. At the same time, thrombin cleaves and thereby activates FXIII which further stabilizes the fibrin clot through TG-mediated cross-linking of fibrin polymers.

In general, hemostasis is dependent on two simultaneous processes, primary and secondary hemostasis. Primary hemostasis involves the activation, adhesion and aggregation of blood platelets which form an initial platelet plug at the site of injury [513]. Platelet activation is triggered by the removal of the antithrombotic endothelium upon vessel injury, which exposes the platelets to the sub-endothelial matrix. The sub-endothelium is composed of various ECM proteins and especially the presence of collagen-bound von Willebrand Factor (vWF) renders the sub-endothelial matrix a highly thrombogenic environment which platelets are tethered to via interaction between their glycoprotein Ib (GPIb) receptor complex and vWF [514]. This interaction triggers two events: first, it results in

platelet aggregation leading to the initiation of platelet plug formation; second, it activates platelets to secrete factors that enhance platelet aggregation via a positive feedback loop as well as activating other platelets in a paracrine manner. Activated platelets switch the gene expression pattern of a set of integrins, including that of integrin $\alpha_{IIb}\beta_3$ (GPIIb-IIIa), which allows them to bind to the sub-endothelial ECM as well as to fibrinogen [515, 516]. Fibrinogen itself can then act as a mediator of platelet aggregation, as it is a divalent ligand that can be bound by integrin $\alpha_{IIb}\beta_3$ of two different platelets.

Secondary hemostasis refers to the process of fibrin formation through the concerted actions of blood coagulation factors and, ultimately, fibrinogen, thrombin and FXIIIa. During coagulation, the developing fibrin network is subsequently added to the initial platelet plug to form a blood clot. Traditionally, the blood coagulation cascade has been described as a "waterfall" model [508, 509] that is now well described and classified into an extrinsic and intrinsic pathway which eventually converge into the common pathway (Fig. 18) [507]. The extrinsic pathway, also known as tissue factor (TF) pathway, is triggered by damage to a blood vessel [517]. TF is the cellular receptor for FVII and expressed by adventitial cells like fibroblasts, smooth muscle cells or pericytes in the sub-endothelium. Under normal circumstances, TF does not interact with plasma coagulation factors such as FVII [518, 519], however, upon injury TF on these adventitial cells becomes exposed and, in the presence of Ca^{2+}, forms a complex with FVIIa which in turn activates FX. Subsequently, FXa and its co-factors FVa, phospholipid and Ca^{2+} can form the so-called prothrombinase complex that activates thrombin. Thrombin activation ultimately leads to the conversion of fibrinogen into fibrin and the simultaneous activation of FXIII which further increases the stability of the blood clot by intra- and intermolecular fibrin cross-linking [520]. The intrinsic pathway, also referred to as contact activation pathway, is believed to have less significance to the onset of hemostasis compared to the extrinsic pathway and is not triggered by vessel damage but by activation of FXII (Hageman factor) on a negatively charged surface. This triggers the sequential activation of FXI and FIX, the latter mediating FX activation along with its co-factors FVIIIa, phospholipid and Ca^{2+} [521, 522]. At the level of FX activation the extrinsic and intrinsic pathways converge, and all subsequent steps leading to the activation of thrombin and the formation of fibrin are part of the so-called common pathway.
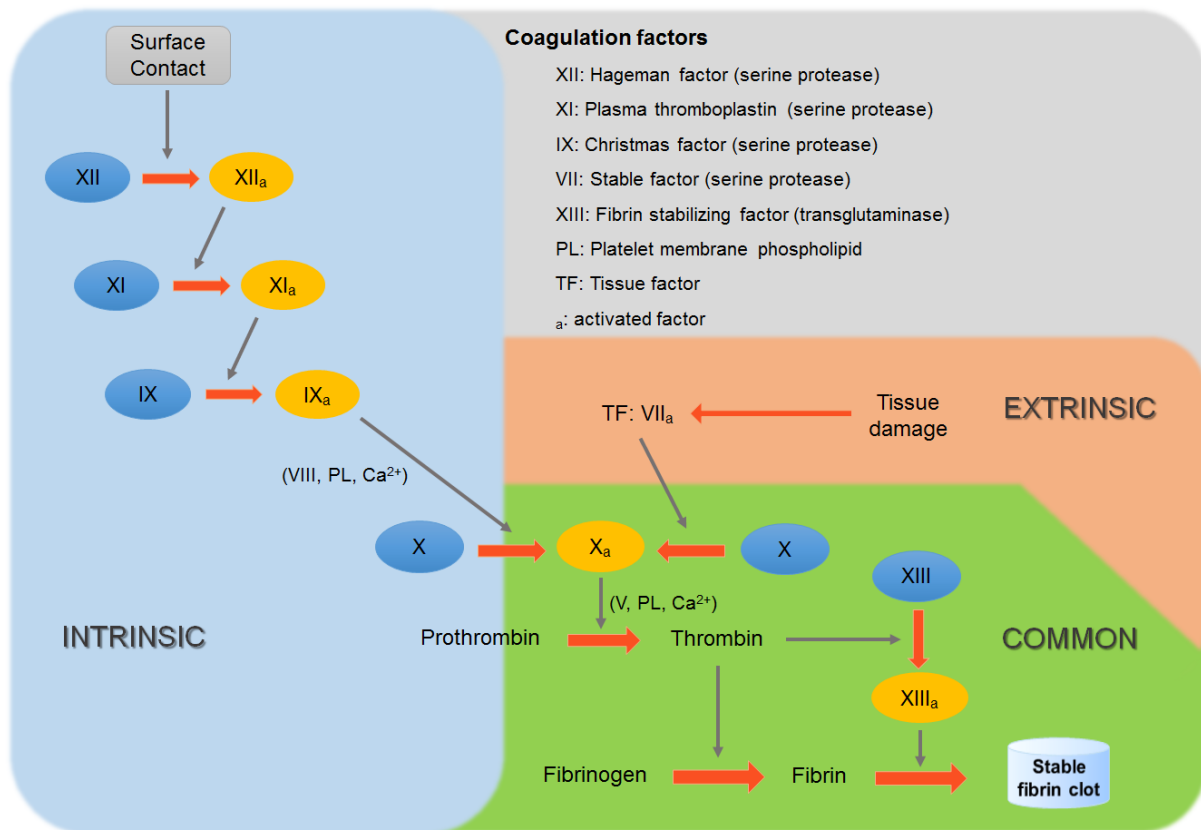
Fig. 18: *The blood coagulation cascade.* The "waterfall" model of coagulation describes blood clotting as a sequence of enzymatic reactions that convert inactive circulating plasma zymogens into active coagulation factors. The extrinsic (triggered by damage to a blood vessel) and intrinsic (triggered by surface contact) pathways converge at the level of FX activation. The prothrombinase complex consisting of FXa and its co-factors FVa, phospholipid and Ca^{2+} in turn activates thrombin. Thrombin plays a dual role in fibrinogenesis by converting soluble fibrinogen to insoluble fibrin and by activating FXIII which cross-links the nascent fibrin clot, ultimately resulting in the formation of a stable fibrin (blood) clot.

In summary, blood coagulation is a tightly regulated series of events involving the complex interplay of plasma clotting factors, blood cells, the ECM and other signals released from or present in surrounding tissues. With the notion that dysfunctions in blood clotting may lead to thrombosis or bleeding disorders, the regulation of the delicate balance between pro- and anticoagulant pathways, referred to as the hemostatic balance, is of great significance [523].

In the last decades, advances in the molecular and cellular biology of fibrinogen and fibrin have greatly expanded our knowledge of the manifold functions of fibrin(ogen) in wound healing [524, 525]. In general, every tissue disruption of an anatomic structure with consecutive loss of function can be classified as a wound and wound healing is a complex and highly dynamic process of cellular, humoral and molecular mechanisms which are initiated directly after wounding [526]. Hemostasis is the first of the 4 phases of acute wound healing and followed by the inflammation, proliferation/repair and remodeling phases. The formation of a provisional wound matrix by fibrin and blood platelets occurs immediately after injury and is usually completed within few hours. At the same time, hemostasis triggers the inflammatory response which can be divided into an early phase characterized

by neutrophil recruitment and a late phase marked by the appearance and transformation of monocytes. Subsequently, epithelial cells dissect the blood clot from the wound space in the process of reepithelialization to repave the surface of viable tissue for cellular infiltration. This allows for the actual wound healing to start (approx. 4 days after injury) with the formation of new granulation tissue (stroma) in the wound space. This phase is marked by the proliferation, migration and invasion of a variety of cell types into the wound matrix. For example, macrophages aid in debridement and matrix dissolution and also modulate inflammation, ECM secretion (fibroplasia) and wound angiogenesis, while fibroblasts deposit new ECM and endothelial cells are pivotal in wound neoangiogenesis. The physiological endpoint of mammalian wound repair is tissue remodeling accompanied by the formation of a scar, with the extent of scarring being directly proportional to the extent of inflammation during the process of wound healing [527].

Although the primary function of fibrin in wound healing is hemostasis, it also serves as a provisional matrix for the many different cell types involved in wound repair, making it one of the most important ECM proteins in the wound bed. In addition, the regulatory functions of fibrinogen and fibrin in later stages of wound healing are manifold and cover a wide range of signaling mechanisms [524, 525, 527, 528]: (i) coagulation is already part of the inflammatory response [529-531], (ii) fibrin, in conjunction with fibronectin and vitronectin, provides a temporary matrix for the recruitment and migration of cells from different tissues to the injured site [532-540], (iii) binding of cells involved in wound healing to fibrin partially modulates their phenotype and function [541-552], (iv) by-products of fibrinogenesis as well as fibrin degradation products (FDPs) serve as chemoattractants for immune cells and modulate angiogenesis [553-561], (v) fibrin directly or indirectly binds growth factors, cytokines or chemoattractants involved in wound healing, thereby acting as a natural reservoir that regulates their bioactivity [562-568], (vi) fibrin is directly pro-angiogenic [569-571], and (vii) the overall physicochemical properties of the fibrin matrix and its timely degradation partially regulate the wound healing process [572, 573].

Hemostasis might be the primary function of fibrin in wound healing, nevertheless, once a blood clot is present in the wound bed invading cells must deal with it. This involves the complex interplay of a variety of cell types and, even though other components of the ECM also fulfill pivotal roles in wound repair, the importance of instructive signals from the provisional fibrin matrix to modulate cell behavior during tissue regeneration has been unambiguously shown.

4.2. Mechanisms of fibrin formation and degradation

The formation of fibrin (fibrinogenesis) as well as its dissolution (fibrinolysis) are fundamental processes in tissue repair and regeneration. Any disruption of the vascular system must initially be plugged by a blood clot to ensure hemostasis before subsequent regeneration and restoration of vascular integrity can occur. However, under physiological conditions the blood clot is not a permanent structure. Once it has served its purpose fibrin needs to be degraded in a spatiotemporal

manner to prevent permanent occlusion of the blood vessel. Therefore, in the healthy human body, the molecular circuitry governing the formation and degradation of a blood clot are in a delicate balance, the hemostatic balance [574, 575]. Fibrin is central to this balance as it is both the primary product of blood coagulation as well as the ultimate substrate for fibrinolysis. The importance of the hemostatic balance is underscored by the fact that any acute perturbation may result in thrombosis or bleeding disorders, while more moderate but long-term disturbances may impair tissue remodeling and repair [576].

4.2.1. Fibrinogenesis

The main players in fibrinogenesis are the glycoprotein fibrinogen, the serine protease thrombin and the transglutaminase FXIII. The 340 kDa plasma glycoprotein fibrinogen is the monomeric form of fibrin. It is primarily produced by hepatocytes in the liver (and secondarily by thrombocytes) and circulates freely in the plasma at a concentration of 2-5 mg/mL with a half-live of around 7 days [577]. Fibrinogen is a dimeric molecule comprised of two sets of three polypeptide chains, termed Aα, Bβ and γ, which are linked by a total of 29 disulfide bonds [578]. Together these polypetides form an elongated, 45 nm long structure that consists of a central E domain (comprising the N-termini of all 6 chains) and two outer D domains which are formed by the Bβ and γ C-termini (the β_C and γ_C domains; Fig. 19) [579, 580]. In contrast to the β_C and γ_C domains, the globular Aα C-termini (α_C domains) are located in close proximity to the central E domain [581-583]. Two α-helical coiled-coil segments connect the outer D domains with the central E domain, where the Aα, Bβ and γ polypeptide chains are joined together by five symmetrical disulfide bridges [584-588]. Furthermore, additional disulfide bonds on either side of the coiled-coil region stabilize fibrinogen dimerization and structural integrity of the molecule [589]. The Aα chains are made of 610, the Bβ chains of 461 and the major γ chain form of 411 amino acid residues. Alternative splicing of the γ chain primary transcript leads to the formation of the minor γ chain variant γ' which contains a unique 20 amino acid sequence [590]. These γ' chains represent approx. 8% of the total fibrinogen γ chain population and are mainly found in heterodimeric γ/γ' fibrinogen molecules ("fibrinogen 2") which account for roughly 15% of plasma fibrinogen molecules [591]. Homodimeric γ'/γ' fibrinogen molecules circulate at comparably much lower concentrations, amounting for less than 1% of plasma fibrinogen molecules [592].
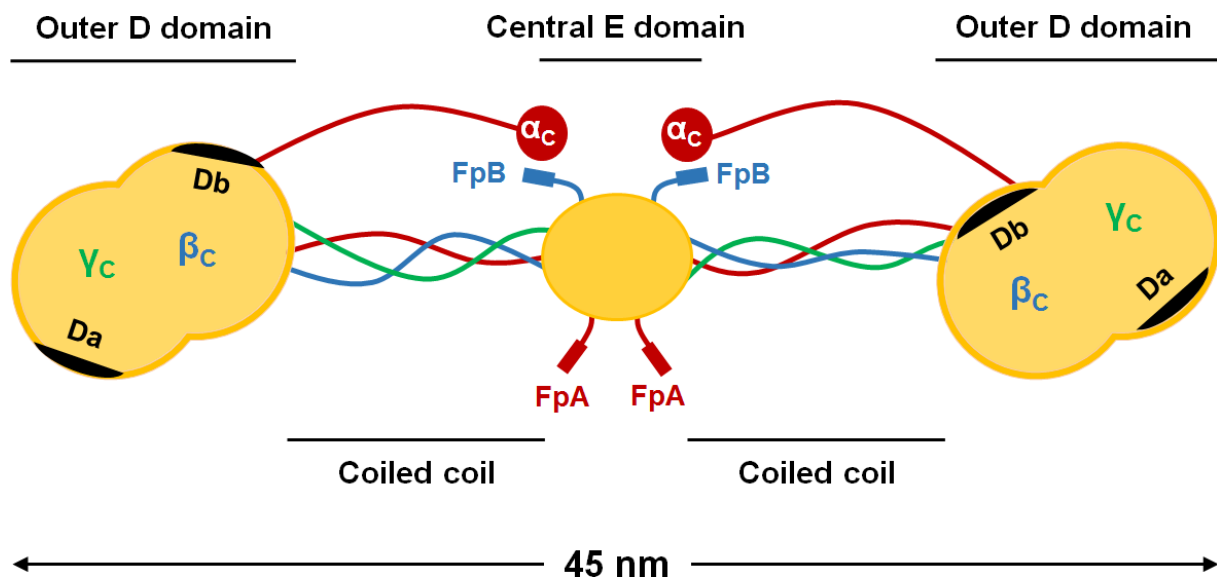
Fig. 19: *The structure of the fibrinogen monomer with its functional domains* (adapted from [579]).

Each fibrinogen molecule contains two RGD sequences on its Aα chains and two ala-gly-asp-val (AGDV) sequences on its γ chains, which both serve as primary recognition sites for cellular interaction via integrin receptors [534, 593-595]. In addition, the D domains contain several high- and low-affinity Ca^{2+} binding sites (on the γ chains and the Bβ chains, respectively) [578] which have been shown to play overlapping roles in the modulation of fibrinogenesis [596, 597] and -lysis [598]. Most notably, each Aα and Bβ chain contains an N-terminal fibrinopeptide (FpA and FpB, respecitvely), proteolytic cleavage of which by thrombin initiates fibrinogenesis (Fig. 19) [599].

The 39 kD serine protease thrombin (FIIa) catalyzes formation of fibrin by enzymatically cleaving fibrinogen to initiate polymerization. It is produced by hepatocytes and circulates in the plasma as the inactive zymogen prothrombin (FII) at a concentration of approximately 0.15 mg/mL [577]. During blood coagulation, thrombin is activated by the prothrombinase complex (consisting of FXa, FVa and phospholipid) which cleaves prothrombin in the presence of Ca^{2+}. Activated thrombin can subsequently cleave FpA and FpB on the Aα and Bβ chains, respectively, to induce the polymerization of fibrinogen monomers into fibrin protofibrils. In addition, thrombin cleaves and activates FXIII which cross-links the nascent fibrin polymer by introducing amide bonds between the α and γ or between to α or γ chains of adjacent fibrin monomers [600]. Furthermore, thrombin has been shown to act as a mitogen for smooth muscle cells and fibroblasts and therefore not only plays a role in fibrinogenesis, but also in wound healing [601-603].

The 326 kDa transglutaminase FXIII circulates in the plasma as an inactive zymogen (pFXIII) in the form of a noncovalently bound heterotetramer (A_2B_2) [604, 605]. This heterotetramer consists of two catalytic subunits (FXIII-A) and two carrier/inhibitory subunits (FXIII-B), and reaches a plasma concentration of up to 28 µg/mL [606]. The catalytic FXIII-A subunits are produced by cells of bone marrow origin, while the carrier/inhibitory FXIII-B subunits are produced by hepatocytes. In addition, there is a cellular FXIII form (cFXIII) that is present as FXIII-A_2 dimers in the cytoplasm of

thrombocytes, monocytes and macrophages [607]. The majority of pFXIII circulates bound to fibrinogen via its FXIII-B subunits. Importantly, fibrinogen does not only act as a carrier for circulating FXIII but also as a regulator of its activity [608]. Thrombin simultaneously initiates fibrinogenesis and FXIII cross-linking, the latter in association with the fibrin matrix, and the rate of FXIII activation is greatly enhanced by the presence of fibrin [609, 610]. Another regulatory mechanism is the Ca^{2+} concentration which controls FXIII activity not only by being a co-factor for the activation of thrombin (which in turn activates FXIII) but also by being a co-factor for the enzymatic conversion of FXIII into FXIIIa. Although FXIII activation can occur under forced, non-physiological Ca^{2+} concentrations (>50 mM) without the presence of thrombin [611, 612], this is accomplished much easier by the concerted actions of thrombin and Ca^{2+} [613].

Fibrinogenesis comprises a series of enzymatic and non-enzymatic reactions which all ultimately affect the properties and structure of the resulting fibrin polymer. In this respect, the molecular mechanisms governing fibrin formation and degradation not only determine the functionality of the blood clot, but also the development and outcome of various pathologies such as heart attack, ischemic stroke, trauma, cancer or coagulopathies [580]. In general, the sequence of the macromolecular assembly steps leading to the formation of a stable fibrin polymer can be broken down into the following stages (Fig.20) [600]:

1) Fibrinopeptide release
2) Interaction between polymerization sites and binding pockets ("knob-hole" interactions)
3) Fibrin oligomer and protofibril formation
4) Lateral aggregation and fibrin fiber formation
5) FXIIIa cross-linking (starting from the time of protofibril formation)
6) Fibrin branching and 3D network formation

Fibrinogenesis is initiated through thrombin-mediated cleavage of FpA and FpB from the N-termini of the Aα and Bβ chains of fibrinogen to yield a fibrin monomer (α β γ)₂ [599, 614]. This proteolytic cleavage leads to the exposure of two polymerization sites, E_A and E_B ("knobs" A and B), in the central E domain of the molecule. Each of these polymerization sites combines with a complimentary binding pocket, Da and Db ("hole" a and b), located in the D domain of an adjacent fibrin(ogen) molecule. Da is present in the C-terminus of the γ chain (the γ nodule) [615-617], while Db is located in the C-terminal β chain segment (the β nodule) of the D domain [615, 618]. Initially, E_A:Da interactions drive the aggregation of fibrin monomers in a half-staggered manner, with the central E domain of one molecule binding to the outer D domain of an adjacent molecule (Fig. 20). The subsequent longitudinal addition of fibrin monomers to the half-staggered fibrin dimer results in the formation of a double stranded oligomer, the twisted fibrin protofibril, in which the monomers align in an end-to-middle overlapping domain configuration [619-621]. In addition, interactions between two

neighboring D domains (D:D interactions) stabilize the end-to-end junctions between fibrin monomers and are indispensable for proper end-to-end alignment of fibrin monomers in assembling polymers [622, 623]. In contrast to E_A, less is known about the exact physiological role of E_B polymerization sites in fibrinogenesis. Interestingly, FpA is cleaved more rapidly than FpB in solution but, as polymerization proceeds, the rate of FpB release increases, suggesting that it is preferentially released from polymers [624]. This is concomitant with the observation that, in surface-attached fibrinogen, FpB can be cleaved at a faster rate than FpA [625], implying that the conformation of fibrinogen dictated the accessibility of the fibrinopeptides for thrombin. E_A:Da interactions have been shown to be about 6-fold stronger than E_B:Db interactions [626, 627]. Consequently, polymerization of fibrin monomers where only FpA has been cleaved (des-AA fibrin) results in much higher clot strength compared to des-BB fibrin (where only FpB has been cleaved) [628, 629]. Although this indicates that both E_A:Da and E_B:Db interactions are involved in fibrin protofibril formation, polymerization of des-AA fibrin yields thinner fibers compared those in fibrin formed after cleavage of both FpA and FpB [599]. This suggests that E_B:Db interactions are mainly involved in the lateral aggregation of protofibrils, although they are not exclusively required for it [579, 600].

The exact molecular mechanisms, particular structures and driving forces that govern lateral aggregation remain partially unknown, however, there are a couple of structures that have been shown to contribute to inter-protofibril lateral binding. These include E_B:Db interactions, the α_C domains [582, 630, 631], β_C domains [632], the coiled coil segments between the E and D domains [633] and N-glycosaminoglycans on the Bβ and γ chains [634]. The current model for fibrin fiber formation proposes intermolecular E_B:Db, α_C:α_C and β_C:β_C interactions to drive lateral aggregation after protofibril formation [632]. The α_C domains are connected to the fibrinogen monomer via a flexible, unstructured α_C connector and tethered non-covalently to the E domain [635]. Upon FpB cleavage, conformational changes in the E domain allow the α_C domains to dissociate from it [583, 636], making them available for intra- or intermolecular interaction with other α_C domains to promote lateral fibril aggregation. Although α_C domains are not essential for this process, they enhance it, as fibrin clots made from fibrinogen missing the α_C domains are made up of thinner fibers [637]. Additionally, the loss of electrostatic repulsion upon cleavage of the electronegative FpB may contribute to lateral aggregation independently of α_C:α_C or E_B:Db interactions. The latter, however, are hypothesized to induce rearrangements in the β_C domains of the D domain, which induces lateral intermolecular β_C:β_C interactions similar to the D:D end-to-end associations that drive protofibril formation.

Since the interactions governing initial lateral aggregation of fibrin protofibrils are weaker than the E_A:Da interactions that drive protofibril formation, protofibrils must reach a sufficient length - at least
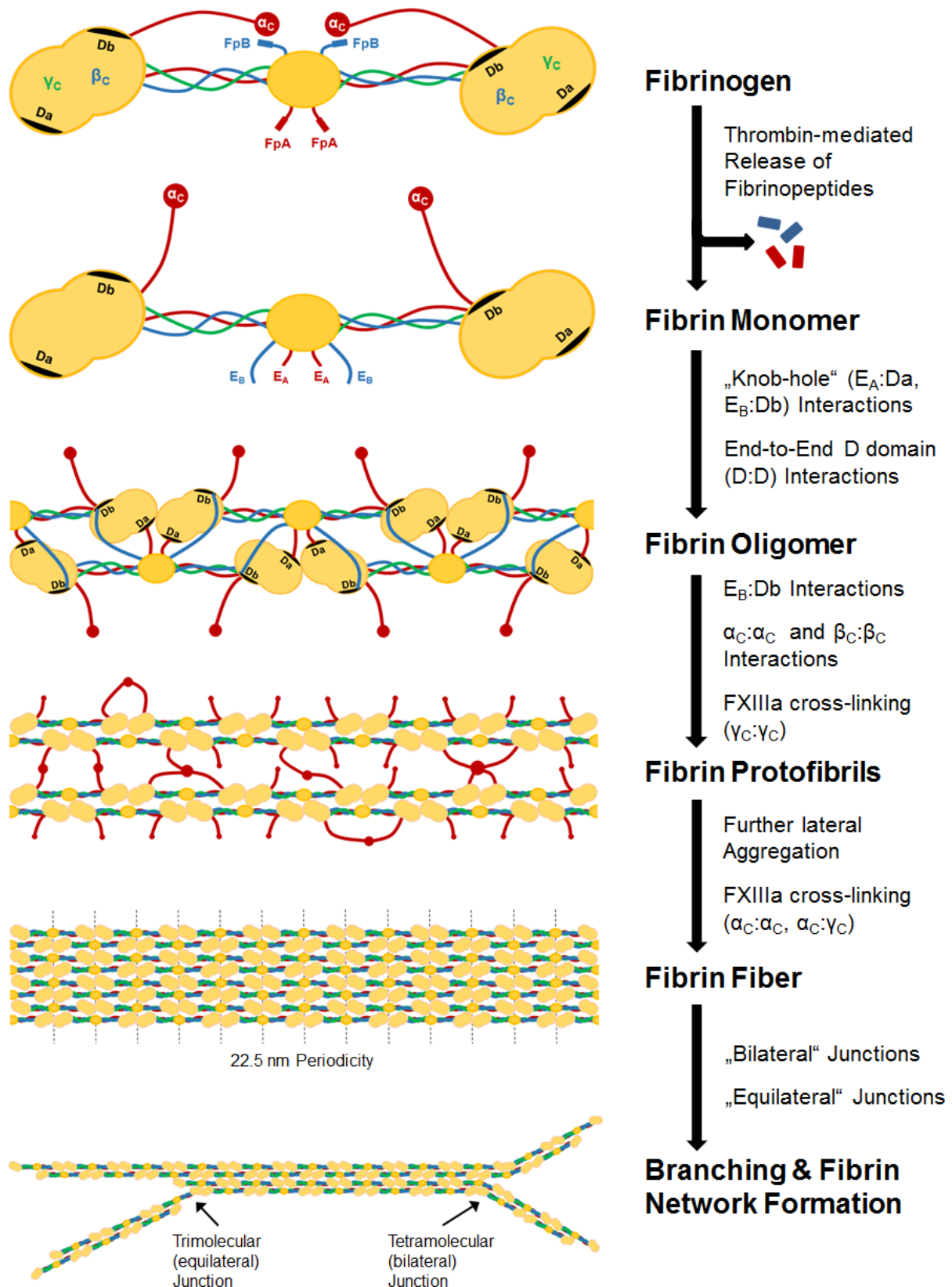
Fig. 20: *The thrombin-mediated initiation of fibrinogenesis* (adapted from [600]).

500 nm or 20-25 half-staggered fibrin monomers [638] - before lateral aggregation through cumulative intermolecular forces can occur [639, 640]. The specificity of intermolecular interactions during fibrin

fiber formation results in the fibers being paracrystalline structures, meaning that fibrin monomers are regularly arranged in longitudinal direction but less well ordered across a fiber. Consequently, fibrin fibers display repeats of 22.5 nm length (or one half of the length of a fibrin monomer), which can be visualized as a distinct band pattern by electron microscopy or X-ray diffraction (Fig. 20) [641, 642].

Upon initiation of fibrin polymerization the zymogen FXIII is transformed into its active form (FXIIIa) by the concerted actions of thrombin and Ca^{2+} [606, 608]. FXIIIa, a transglutaminase, stabilizes the nascent fibrin clot by introducing intermolecular covalent bonds between individual fibrin monomers, which improves the elastic properties of the fibrin network as well as its resistance to proteolytic degradation. Notably, this cross-linking reaction is essential for hemostasis, as FXIII deficiency results in severe bleeding disorders [643]. Correct timing of FXIII activation is crucial for efficient hemostasis and, in fact, FXIII is not activated until a critical mass of fibrin has polymerized - a delay that ensures that the developing hemostatic plug has sufficient supply of FXIIIa [644]. As mentioned earlier, thrombin plays a dual role in the synchronization of fibrinogenesis with FXIII activation, as it converts fibrinogen to fibrin while simultaneously initiating FXIII activation. This activation process is greatly accelerated by the presence of fibrin [609, 610] and involves the formation of a tight ternary complex between fibrin, FXIII and thrombin [578, 608]. Once activated, FXIIIa catalyzes the formation of several reciprocal, intermolecular ε-(γ-glutamyl)lysine covalent bonds between the side chains of ε-lysine (donor) and γ-glutamine (acceptor) residues [608]. The first FXIIIa-mediated cross-linking reaction is the formation of γ dimers by introduction of a covalent bond between the $γ_C$ domains of two adjacent γ chains [645-647]. Interestingly, the precise location of cross-linked γ chains is still controversial and whether they are positioned "transversely" between fibrin strands or "longitudinally" along each fibril remains a topic of debate [648, 649]. While "transverse" positioning between the D domains of opposing strands could explain the viscoelastic recovery behavior of fibrin after maximum stretching [650], more recent studies favor "longitudinal" cross-linking [651, 652]. The same intermolecular ε-(γ-glutamyl)lysine bonds are formed, although much more slowly, between the $α_C$ domains of two α chains [653, 654], thereby creating α chain oligomers or high molecular mass α chain polymers. Cross-linking also occurs between α and γ chains [655, 656] and intermolecular cross-linked α-γ-chain heterodimers have been identified in plasma fibrinogen molecules [657]. Fibrin clot stabilization through introduction of covalent bonds is a major consequence of FXIII activation, however, FXIIIa is also capable of linking other substrates to fibrin. These include modulators of fibrinolysis, other plasma glycoproteins, components of the ECM or growth factors [606, 644]. Thus, apart from stabilizing fibrin, FXIII also serves as a regulator of fibrinolysis, cell adhesion and wound healing.

For a 3D fibrin network to form, protofibril formation (elongation) and lateral aggregation (thickening) have to be accompanied by branching. Experimental evidence from structural studies points at two distinct mechanisms by which fiber branching may occur [658]. The first type of branch points develops when a double-stranded protofibril converges laterally with another protofibril to form

a four-stranded fibril (which may also diverge again into two separate protofibrils), thereby creating a "bilateral junction" (Fig. 20). This results in tetramolecular branch points and subsequent lateral convergence of additional fibrils may lead to multi-stranded versions of this structure [604, 639, 640, 659]. The second type, termed "equilateral junction", is formed by convergent interactions among three fibrin molecules that give rise to three double-stranded protofibrils [655, 660]. These trimolecular branch points form with greater frequency when fibrinopeptide cleavage is relatively slow [628] and, under such conditions, networks are more branched and less porous compared to those formed at higher thrombin activity [661]. Interestingly, as the number of branch points increases the fiber diameters decrease, suggesting that lateral aggregation and fiber branching compete [662]. Thus, conditions that favor lateral aggregation give clots with thick fibers and less branch points (coarse networks) while conditions that inhibit lateral aggregation yield clots made up of thinner fibers with more branch points (fine networks).

4.2.2. Fibrinolysis

Under physiological conditions, the blood clot is not a permanent structure. Once it has served the purpose of hemostasis it needs to be degraded to allow for tissue remodeling and to prevent permanent occlusion of the regenerated blood vessel. To preserve the hemostatic balance, the coagulation system is counteracted by the fibrinolytic system. Fibrin plays a central role in this balance as it is both the primary product of blood coagulation as well as the substrate for fibrinolysis. Similar to the blood coagulation cascade, the fibrinolytic processes are surface-related and involve a variety of circulating and tissue-related factors, such as fibrinolytic proteins (fibrinolysins), their inhibitors, activators and receptors [663].

In vivo, fibrinolysis is primarily driven by the so-called plasminogen (PLG) pathway (Fig. 21). Plasminogen, the zymogen of the main fibrinolysin plasmin, is a circulating 92 kDa single chain proenzyme that is primarily produced in the liver [664]. It contains 5 homologous 80 amino acid long triple loop structures called "kringles" [665]. The first (K1) and fourth (K4) of these kringles serve as Lys binding domains which mediate the interaction of PLG with fibrin, cell surface receptors and other regulators of PLG activity [666, 667]. Proteolytic cleavage of the circulating full-length form of PLG gives rise to its enzymatically active form, the serine protease plasmin [668]. The very substrate of fibrinolysis itself, fibrin, plays a crucial role in the regulation of PLG activation, as it binds and localizes both PLG as well as regulators of PLG activity, thereby facilitating their interactions. Each fibrinogen chain contains 104 Lys residues, with the C-terminal D domains containing several low-affinity and the α_C domains a set of high affinity binding sites for PLG [669]. Notably, intact fibrin(ogen) monomers initially demonstrate only weak affinity for the native full length PLG, as the majority of cryptic Lys binding sites only become exposed upon fibrinogenesis. Subsequent binding of PLG to C-terminal Lys residues in fibrin via its "kringles" leads to a series of conformational changes

in PLG that result in the exposure of two cleavage sites, one at Lys77 and the other at Arg561. Arg561 is now available for cleavage by PLG activators, while plasmin-mediated cleavage at Lys77 can further enhance the activity of PLG [670, 671]. Together, these mechanisms not only enable plasmin to regulate its own activity via a positive feedback loop, but also ensure that fibrinolysis is restricted to the fibrin clot only.

There are several PLG activators acting upstream of PLG, and PLG activation can be achieved by various mechanisms (Fig. 21). The two major endogenous PLG activators are tissue-type plasminogen activator (tPA) and urokinase-type plasminogen activator (uPA, also termed prourokinase). Both tPA and uPA are precursors of serine proteases that circulate in the plasma as single chain zymogens (sc-tPA and sc-uPA, respectively). The 72 kD glycoprotein tPA is synthesized and secreted primarily by vascular endothelial cells [672] and possesses two "kringles" homologous to those of PLG for fibrin binding [663]. Key in understanding the regulation of tPA activity is its co-localization with PLG on the surface of fibrin. The formation of localized ternary complexes between fibrin, PLG and tPA allows for tPA-mediated cleavage of PLG to yield plasmin. Similar to PLG activation, the presence of fibrin also serves as a regulator of tPA activity. While tPA is a weak activator of PLG in the absence of fibrin, its catalytic efficiency for PLG activation is enhanced 10^2- to 10^3-fold in the presence of fibrin [673, 674]. Similar to tPA, the 54 kDa glycoprotein sc-uPA also possesses a PLG-like "kringle" [675]. It is secreted by endothelial cells, macrophages, monocytes, the urinary epithelium and some cancer cells [663, 676]. However, in contrast to tPA, uPA does not require fibrin as a co-factor for PLG activation. Although uPA activity is fibrin-specific to some extent, it has much lower affinity for fibrin than tPA and is an efficient PLG activator in both the presence and absence of fibrin [677, 678]. Thus, uPA has been linked to both cell-mediated (in association with a specific uPA-receptor, uPAR or CD87) and intravascular fibrinolysis [679, 680]. Within a positive feedback loop, plasmin can cleave both sc-tPA and sc-uPA, transforming them from single-chain to more active, disulfide-linked two-chain (tc) polypeptides [663, 681, 682]. An alternative mechanism of PLG activation involves proteases that are traditionally classified within the intrinsic arm of the coagulation cascade (Fig. 18). These include kallikrein (which additionally can convert sc-uPA to tc-uPA), FXIa and FXIIa, which are all capable of activating PLG directly [683-685]. This fibrinolytic mechanism is initiated by activation of FXII and thus also termed FXII-dependent pathway.

Negative regulation of fibrinolysis is equally important for the preservation of the hemostatic balance. Inhibitory mechanisms are needed to prevent unregulated systemic plasmin or PLG activator activity to prevent excessive and uncontrolled degradation of plasma proteins. There are three major ways to negatively modulate fibrinolysis: (i) direct inhibition of plasmin, (ii) inhibition of PLG activators, or (iii) removal or blockage of binding sites for PLG/plasmin, tPA or uPA on fibrin. The majority of fibrinolysis inhibitors belongs to a family of serine protease inhibitors known as serpins [686]. All serpins form an irreversible covalent complex with the active site serine of the target serine protease, leading to neutralization of the enzyme. Proteolytic cleavage of the inhibitory serpin by the protease
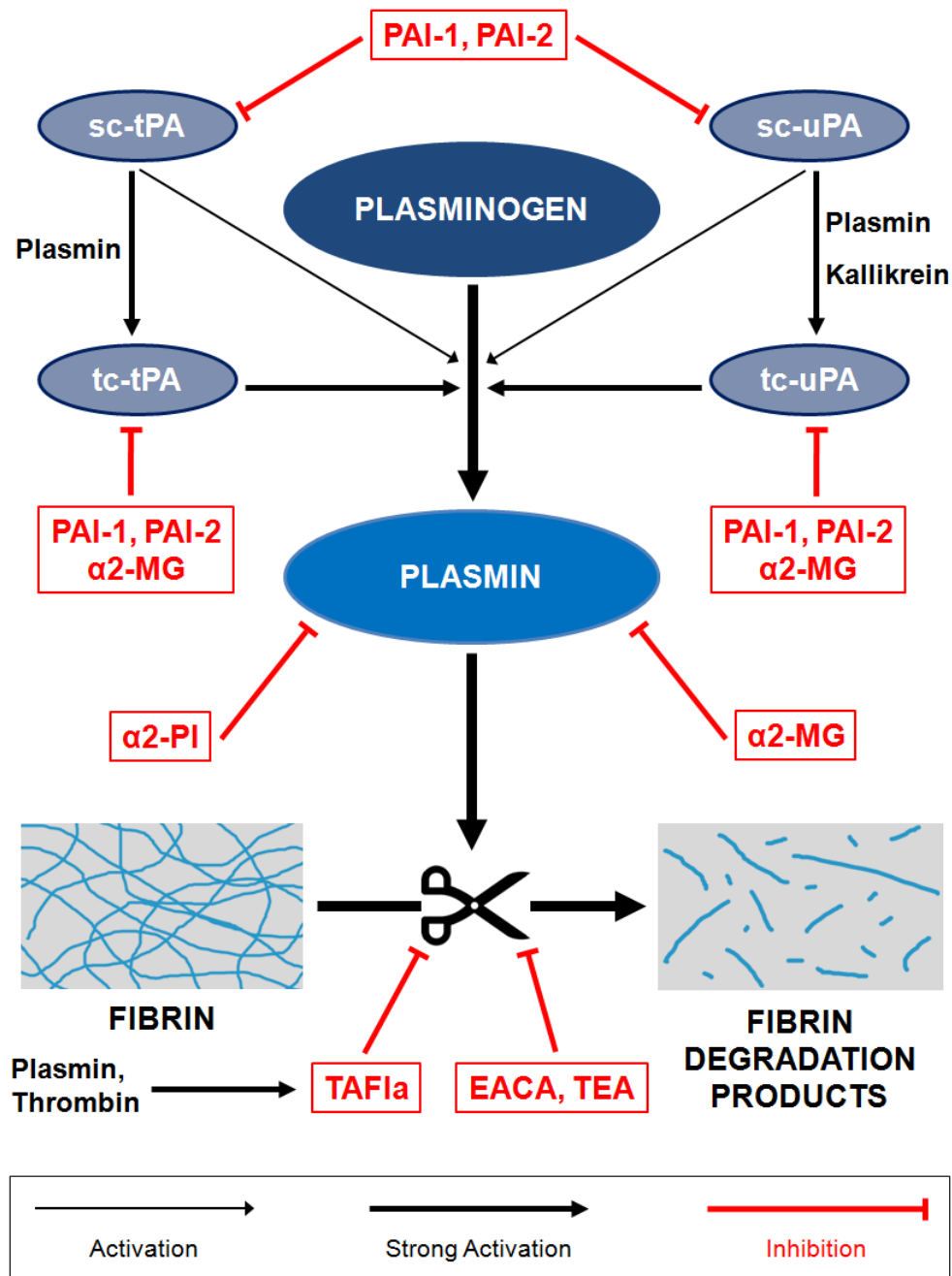
Fig. 21: *Mechanisms of PLG activation and regulation of fibrinolysis.* Proteolytic cleavage converts the PLG, the zymogen of the main fibrinolysin plasmin, into its active form. The serine protease plasmin can subsequently bind to and cleave fibrin. PLG/plasmin activation is mediated by the endogenous serine proteases tPA and uPA, which initially exist in single chain (sc) forms. Within a positive feedback loop, plasmin can convert sc-tPA and -uPA into their more active two-chain (tc) polypeptide forms. At the same time, plasmin can enhance its own activity by cleavage of PLG. Fibrinolysis is negatively regulated by inhibition of PLG activation (PAI-1, PAI-2, α_2-MG), direct inhibition of plasmin (α_2-PI, α_2-MG) or by removal/blockage of binding sites for PLG/plasmin or its activators on fibrin (TAFIa, EACA, TEA).

leads to inactivation of the complex which is then cleared from circulation. The three most important serpins in fibrinolysis are plasminogen activator inhibitor-1 (PAI-1), plasminogen activator inhibitor-2 (PAI-2) and α_2-plasmin inhibitor (α_2-PI or α_2-antiplasmin). Secreted by a variety of cell types including endothelial cells and platelets [687, 688], these serpins circulate in plasma at concentrations

in the same range as their target serine proteases and form inhibitory complexes with them with high affinity [671]. The single-chain glycoprotein α2-PI (70 kDa) is the primary inhibitor of plasmin, forming α2-PI-plasmin complexes with 1:1 stoichiometry by occupying plasmin's "kringle" domains [689]. The inhibition of free plasmin is a fast process in circulation or solution, however, when plasmin/PLG is bound to fibrin or cells, its Lys binding sites are blocked which protects it from α2-PI inhibition, allowing fibrinolysis to proceed [690, 691]. Alternatively, fibrinolysis can be inhibited by preventing the activation of PLG through tPA and uPA. Two well-characterized physiological inhibitors of tPA and uPA are the glycoproteins PAI-1 and PAI-2. PAI-1 (52 kDa), the most ubiquitous PAI, is present at high concentrations in plasma which explains the exceedingly short half-lives of tPA and uPA (4-8 minutes) in circulation [692]. PAI-1 is the most important and most rapidly acting inhibitor of tPA and uPA. It forms stable inhibitory equimolar complexes with both sc- and tc-tPA and with tc-uPA [693], while forming reversible complexes with sc-uPA [694]. PAI-2 exists in two forms: a non-glycosylated intracellular form (47 kDa) and a glycosylated secreted extracellular form (60 kDa) [695, 696]. Functionally, PAI-2 inhibits both tc-tPA and tc-uPA with comparable efficiency, but is less effective towards sc-tPA and does not inhibit sc-uPA [693, 697]. Binding of uPA to its cellular receptor uPAR decreases inhibition by both PAI-1 and PAI-2 to similar extents, however, both are still able to quite rapidly inhibit uPA [698].

Several additional proteins can act as plasmin inhibitors or PAIs. One of them is α_2-macroglobulin (α_2-MG), a large non-serpin glycoprotein (725 kDa) which circulates in plasma in vast quantities [663, 699]. It binds PLG activators and their inhibitory complexes as well as plasmin, although it inhibits plasmin activity with only about 10% of the efficiency exhibited by α2-PI [700]. Notably, cell-bound plasmin or PLG activators are protected from inhibition by α_2-MG [701]. Apart from α_2-MG, C_1-esterase inhibitor may serve as an inhibitor of tPA in plasma [702], while the protease nexin-1 may function as a non-circulating cell surface inhibitor of both PLG activators and plasmin [703]. Fibrinolysis can also be inhibited by preventing the interaction between PLG/plasmin or its activators and fibrin. A single-chain 35 kDa plasma metalloproteinase, the thrombin-activatable fibrinolysis inhibitor (TAFIa), also known as carboxypeptidase U (CPU), is a potent attenuator of fibrinolysis [704, 705]. TAFI (60 kDa) circulates in plasma as an inactive zymogen (TAFI or pro-CPU) and is activated by thrombin or, at high concentrations, plasmin as fibrin degradation progresses. Its activation by thrombin is accelerated by about 1250-fold in the presence of the endothelial cell membrane protein thrombomodulin [663]. Upon activation, TAFIa cleaves C-terminal Lys residues on fibrin which are critical for PLG or tPA binding and formation of the ternary complex that leads to plasmin generation. Mechanistic studies suggest that TAFIa acts predominantly through modifying the binding of PLG and plasmin to fibrin and to a lesser extent through modification of the binding of tPA to fibrin [706, 707]. This is also the mode of action of clinically used antifibrinolytics like ε-aminocaproic acid (EACA) or tranexamic acid (TEA). These lysine analogues, however, do not

decrease the amount of Lys binding sites on fibrin, but suppress fibrinolytic activity by competitively inhibiting the binding of PLG and plasmin to fibrin [708].

Plasmin-induced fibrinolysis of either fibrin(ogen) monomers or polymers involves a sequence of steps and yields diverse FDPs (Fig. 22). When plasma α2-PI levels are overwhelmed, for example when PLG activator concentrations/activity are high, plasmin may also degrade circulating fibrinogen monomers. Fibrinogen possesses distinct proteolytic cleavage sites for plasmin. Initially, the Aα chains are cleaved, followed by the Bβ chains and the coiled coil connector between the E and D domains [671]. More precisely, the α_C domain in fibrinogen presents an early target for plasmin cleavage [709]. In the next step, a peptide from the N-terminus of the β chain (the FpB) is removed [710]. The resulting 250 kDa molecule is termed fragment X and represents a clottable form of fibrinogen (Fig. 22A). Subsequently, fragment X is cleaved into fragment D (100 kDa) and fragment Y (155 kDa), which is mediated by cleavage of all three polypeptide chains (the coiled coil connector) between the E and D domains [711, 712]. A second cleavage in the connector region of fragment Y ultimately leads to another fragment D and fragment E which are the terminal degradation products and represent the major globular domains in fibrinogen [713-715].
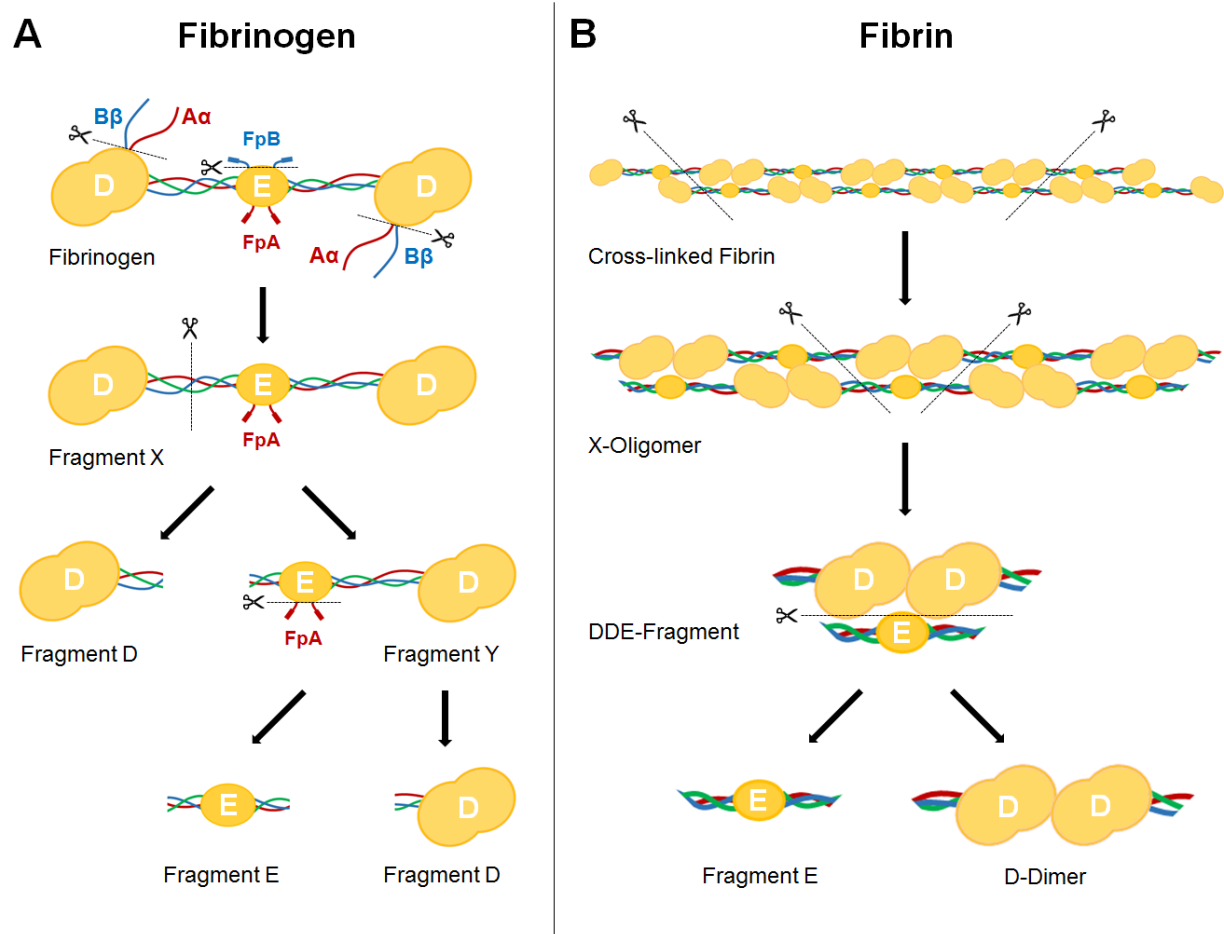

Fig. 22: *The plasmin-mediated degradation of fibrinogen and fibrin* (adapted from [576] and [663]).

The plasmin-mediated degradation of fibrin monomers as well as non-cross-linked fibrin polymers is identical to that of fibrinogen. Although the progression of proteolytic actions is similar to that of a fibrin(ogen) monomer (the C-termini of Aα and Bβ chains first, then the coiled coil connectors), cleavage of cross-linked fibrin initially results in the formation of more complex fragments designated as X-oligomers (Fig. 22B) [417, 716]. These oligomers consist of E and D domains in various combinations. Large X-oligomers are released at the beginning of fibrinolysis, whereas the fragments decrease in size as degradation proceeds. Eventually, cleavage of X-oligomers gives rise to DDE fragments, degradation of which results in the final FDPs D-dimer (two covalently bound D domains) and fragment E [576].

The exact mechanisms and progression of proteolytic events required for the full breakdown of a fibrin clot are not fully understood. However, there is evidence that efficient solubilization of a fibrin clot requires only approx. 25% of the total E-D connections to be cleaved while up to 50% of fibrin monomers can remain intact [717]. In addition, all three polypeptide chains within a fibrin monomer need to be cleaved through the same cross section in both adjacent monomers within a protofibril and in all protofibrils within a fiber. The fact that only a fraction of E-D connections needs to be broken down for full clot dissolution suggests that degradation of fibrin fibers is mainly achieved through clustering of PLG/plasmin molecules at certain points along the fiber, rather than uniformly at random positions. Recently, evidence for preferential transversal cleavage of fibers has been provided by atomic force microscopy studies of fibrin clots treated with plasmin [718].

It is noteworthy that plasmin also exerts non-fibrinoytic actions. Apart from fibrinogen and fibrin, plasmin may degrade a variety of ECM proteins. On one side, plasmin directly cleaves basement membrane proteins such as thrombospondin, laminin or fibronectin. On the other side, it facilitates the degradation of other ECM proteins such as collagen, vitronectin, elastin or aggrecan by activation of MMPs 1 and 3. These non-fibrin(ogen)-specific proteolytic actions indicate possible roles for plasmin in inflammation, wound healing and tissue remodeling, (tumor) cell invasion or prohormone activation *in vivo* [663]. Furthermore, several studies have demonstrated that plasmin also cleaves and inactivates a subset of coagulation factors *in vitro*, suggesting it is not only the primary fibrinolytic enzyme but may also have anti-coagulant properties [719-722]. Among these coagulation factors are FV, FVIII, FIX and FX, which makes plasmin a potential regulator of the intrinsic, extrinsic and common pathway of the blood coagulation cascade. However, since plasmin is one of the broad-spectrum serine proteases, the *in vitro* data do not necessarily imply the same role for PLG *in vivo*. In addition, its rapid thrombolytic activity makes it very difficult to detect a possible anti-coagulant role of plasmin *in vivo*. Even though animal studies are suggestive of an anti-coagulant effect of plasmin, further evidence is necessary to determine whether it could be used as a therapeutic agent to prevent thrombus formation [723].

4.3. Factors affecting fibrin clot structure and function

Altered or abnormal fibrin clot structure is a phenomenon linked to a variety of diseases such as stroke, coronary artery disease, thromboembolic disease, or ischemic heart disease [724]. Among the most prominent parameters affected by altered clot structure are clot stiffness, porosity/permeability, compaction rate, fiber diameter, degree of branching, clot absorbency and clot lysis time [725]. These factors represent the most prominent risk factors in thrombosis *in vivo*, but can also be exploited in fibrin-based tissue engineering approaches in order to create a matrix that can be adapted and optimized for a specific task and environment by modulation of those properties.

One of the simplest ways to alter the dynamics of fibrin polymerization and thus resulting fibrin gel properties is the variation of fibrinogen and thrombin concentrations or the modification of salt concentrations (especially Ca^{2+}) and ionic strength [726]. In this respect, the influence of fibrinogen concentration on fibrin stiffness/elasticity has been extensively studied. Even though various research groups produced different numbers regarding clot stiffness, mostly due to highly inhomogeneous test setups, a clear tendency can be observed, showing that increasing the concentration of fibrinogen results in enhanced clot stiffness (Fig. 23A). In these experiments, the stiffness of the viscoelastic fibrin polymer has generally been assessed by quantification of the E_{mod} [727, 728], the storage (shear) modulus (G') [662] or the tensile strength (TS) [729].
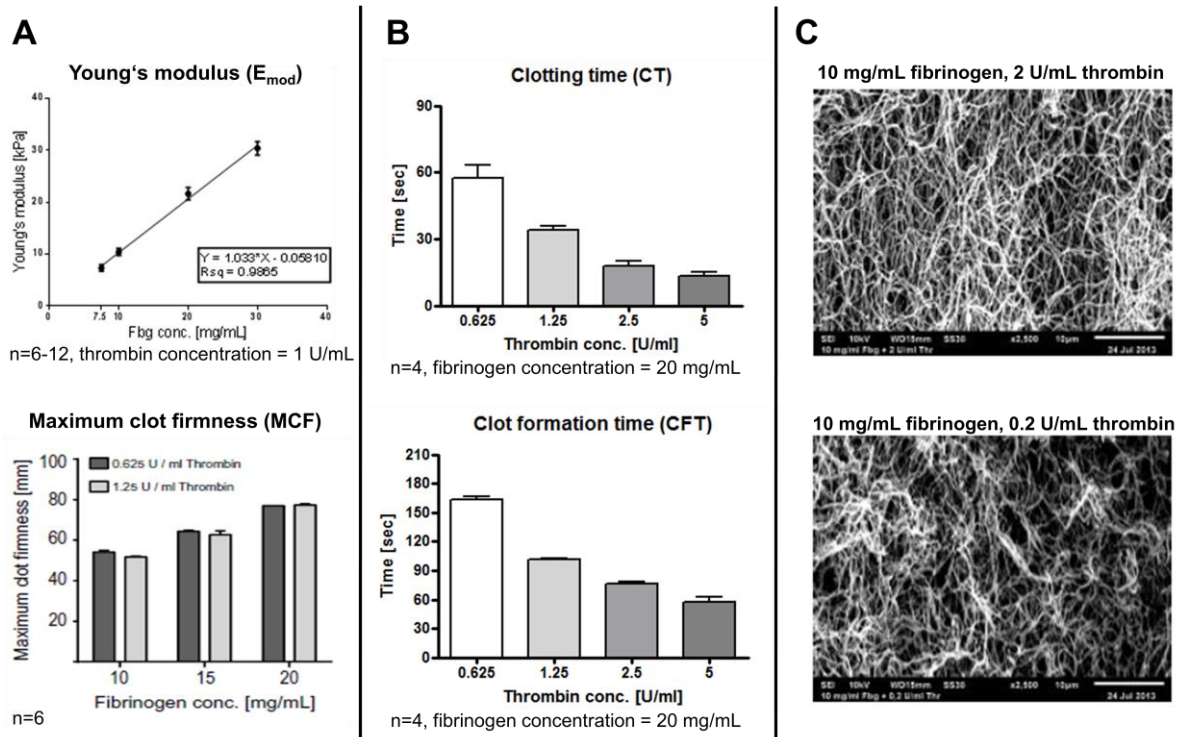
Fig. 23: *The influence of varying fibrinogen and thrombin concentrations on the dynamics of fibrin polymerization and the mechanical and structural properties of fibrin clots.* (A) Influence on varying fibrinogen concentrations on the Young's modulus and MCF of fibrin clots, as assessed by mechanical tensile testing (top; data shown as mean ± S.D) and ROTEM (bottom; data shown as mean + S.D.). At low concentrations (≤1.25 U/mL), thrombin does not influence clot MCF (bottom). (B) Influence on varying thrombin concentrations on the gelation rate (CT, top; CFT, bottom) of fibrin clots, as assessed by

ROTEM. Thrombin concentration and CT/CFT are directly proportional (data shown as mean + S.D.). (C) Scanning electron microscopy (SEM) images of fibrin polymerized at two different thrombin concentrations (2 vs. 0.2 U/mL) reveals differences in matrix porosity and fiber thickness (magnification 2500x, bar = 10 µm).

An interesting study by Duong et al. [730] analysed a stiffness index of a broad range of fibrin matrices prepared from fibrinogen (2-50 mg/mL) and thrombin (2-100 U/mL). This study evaluated a stiffness correlation for fibrin matrices by comparing different fibrinogen concentrations at constant thrombin concentrations and *vice versa*. In accordance with other studies and our own data (Fig. 23A), a positive correlation of the stiffness index with the concentration of fibrinogen in the matrix was shown. An increase of the thrombin concentration did also increase clot stiffness, but only at supraphysiological thrombin levels ($\geq$5 U/mL) and to a lesser extent than increasing fibrinogen concentrations.

Out of the different variables that can influence the structure of a fibrin clot at the time of gelation, thrombin concentration is the most important physiological influence. The addition of thrombin to fibrinogen *in vitro* induces a pattern of fibrin clot formation that closely resembles *in situ* clot formation, being composed of a lag phase followed by an increase in turbidity [731]. If fibrinogen concentrations are kept constant, the gelation rate - as assessed by measurement of clotting time (CT; the time needed for polymerization to begin) and clot formation time (CFT; the time needed for a clot of arbitrarily chosen stiffness to form) through rotational thromboelastometry (ROTEM) is directly proportional to the thrombin concentration (Fig. 23B). Notably, thrombin concentrations as low as < 0.1 U/mL already catalyze fibrin polymerization with thick, loosely cross-linked fibers, while an increase of thrombin concentration is accompanied by the formation of a less porous network composed of thinner and tighter cross-linked fibers (Fig. 23C). Fiber diameter is increased in loosely cross-linked gels, while fiber density and branching density are increased in tightly cross-linked gels [732, 733].

An additional factor influencing fiber diameter is the addition of Ca^{2+} ions to the fibrinogen/thrombin mixture. *In vivo*, Ca^{2+} is required for the assembly of the pro-coagulant complexes and, subsequently, the activation of thrombin. Addition of Ca^{2+} leads to the assembly of thicker fibrin fibers at a shorter CT than in its absence [734, 735]. Ca^{2+} is capable of releasing additional thrombin from fibrin mono- and polymers, therefore addition of Ca^{2+} would effectively increase the thrombin concentration in the fibrinogen/thrombin mixture [736]. This would explain the effect Ca^{2+} has on the CT, since simply increasing the thrombin concentration also decreases clotting time. The addition of 2.0 mM $CaCl_2$, representing physiological levels, was shown to already reduce the CT by 80% compared to controls, accompanied by a 400% acceleration of the rate (in µm/s) of fibrin formation [737].These effects were proven not to be dependent on ionic strength, as substitution of $CaCl_2$ with NaCl would not reproduce them. Additionally, apart from faster coagulation time, addition of Ca^{2+} also leads to increased resistance of the fibrin clot to lysis in a 30% urea solution [738]. Speculatively, this resistance is not due to changes in network structure, but rather to specific Ca^{2+} binding sites on fibrin, where bound

Ca^{2+} protects fibrin from proteolytic digestion [739] as well as thermal denaturation [740]. Apart from gelation time, addition of $CaCl_2$ has an effect on the porosity of forming fibrin clots, as an increase of $CaCl_2$ up to 20mM significantly increases their permeability coefficient [741]. The porosity of fibrin matrices is of significant importance, especially when they are used as 3D scaffolds for tissue engineering, as the diffusion of nutrients, waste or growth factors, as well as a certain degree of cell mobility has to be maintained throughout the scaffold. Porosity is not just modified by Ca^{2+} but also affected by fibrinogen and thrombin concentrations, as an increase in either parameter results in a decrease in total eluted volume in a flow assay [742]. Furthermore, an increase in fibrinogen concentration at constant thrombin concentration results in significantly smaller pore radii, which was confirmed by diffusion assays showing that fewer dextran particles of a given size were able to diffuse through the 3D matrix at increasing fibrinogen concentrations, independent from different thrombin concentrations [742].

Fibrin clot structure and mechanical properties as well as the clot's susceptibility to enzymatically catalyzed lysis play an important role in overall clot stability as they are directly linked to the rate of fibrinolysis. Under physiological conditions, a fibrin clot has to be able to withstand the pressure of blood flow by stretching without breaking and recoiling to the original shape [743]. As tPA and PLG act while they are bound to the surface of the fibrin clot, it is not surprising that pore size, permeability and fiber density play important roles in the regulation of fibrinolysis, especially in terms of the rate of clot lysis [744]. As expected, clots with a tight network, displaying small pores and high fiber density, are lysed slower than clots with a loosely cross-linked network [705]. Interestingly, although lysis of a clot composed of a thick fiber network progresses faster than that of a thin fibrin network, on the individual fiber level, thick fibers are lysed slower than thin fibers [733]. This underlines the importance of permeability and pore size, as these parameters do not come into effect at lysis studies on an individual fiber level, and could account for the observed differences between network and single fiber. Treatment of fibrin clots with aspirin not only reduces clot stiffness by up to 30% but also alters the network structure to allow increased permeability through the presence of thicker fibrin fibers, subsequently leading to a faster rate of clot lysis [745, 746]. Additionally, it has been shown that increased fiber thickness does not necessarily correlate with faster clot lysis, as clots with a thicker fiber network are subjected to a slower rate of lysis if the change in fiber diameter is not accompanied with an increase in permeability [747].

4.4. Fibrin-based interpenetrating polymer networks

Although the overall physicochemical properties of fibrin can be modulated by varying the concentrations of fibrinogen, thrombin and Ca^{2+}, or by varying the nature and degree of cross-linking, even stiff fibrin hydrogels display comparably weak mechanical properties. One approach to tackle this problem, especially *in vivo*, is the use of antifibrinolytic agents such as the serine protease

inhibitor aprotinin. However, the systemic administration of high concentrations of such compounds may harbour the risk of thrombosis or anaphylactic reactions and is therefore not considered a viable option [748].

The mechanical shortcomings of, especially, natural hydrogels have driven the development of novel strategies to improve their physicochemical properties. In this respect, interpenetrating polymer networks (IPNs) have emerged as innovative biomaterials for biomedical and pharmaceutical applications [749, 750]. Per definition, an IPN is "A polymer comprising two or more networks which are at least partially interlaced on a molecular scale but not covalently bonded to each other and cannot be separated until chemical bonds are broken. A mixture of two or more pre-formed polymer networks is not an IPN" [751]. Semi-IPNs differ from IPNs in that only one polymer system is cross-linked, while the polymer chains of the other system are just dispersed into the network without forming interpenetrating individual network structures. Consequently, in a semi-IPN, the constituent linear or branched polymers can be separated without the need of chemical bonds being broken [750]. In general, IPNs can be synthesized *in situ*, meaning that the constituents polymerize simultaneously (Fig. 24A), or sequentially, where one constituent network is polymerized first and the second added in a second reaction (Fig. 24B) [749].
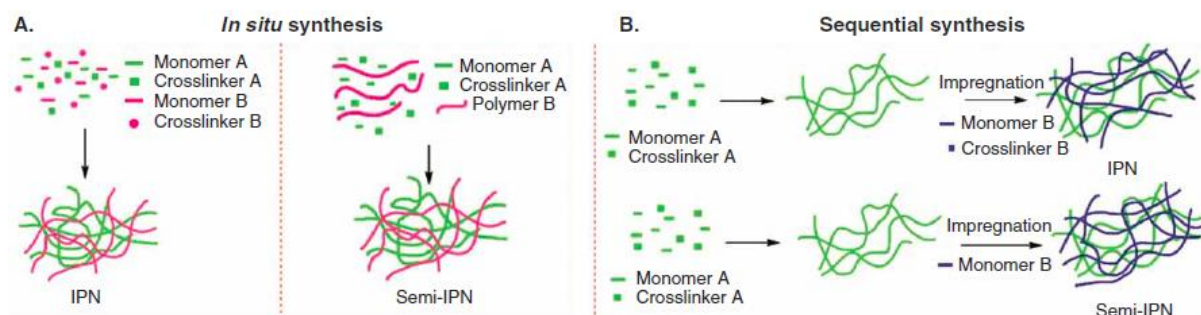

Fig. 24: *Strategies for the synthesis of IPNs and semi-IPNs* (adapted from [749]).

The beauty of the IPN approach for TE applications is that, in general, IPNs combine the properties of their individual polymeric constituents with usually synergistic effects. Initially, fibrin-based IPN hydrogels have been developed with the aim to improve the otherwise weak mechanical properties of pure fibrin formulations (for example rapid proteolysis *in vivo*, high swelling rate or extensive cell-mediated compaction). Among prominent examples are double networks based on fibrin and other synthetic or natural hydrogels such as collagen [752], hyaluronic acid [753], alginate [754], PEO [755, 756] or PVA [757]. While these studies have demonstrated that the respective IPNs display higher E_{mod} and/or TS, altered swelling characteristics and slower degradation rates than their single network counterparts, they have also found that combining the biochemical properties of two hydrogels can dramatically influence cellular behavior in/on them. In this respect, the presence of an additional hydrogel constituent cannot just improve the overall mechanical properties of the resulting IPN, but can also add biological features (for example certain cell attachment sites, bioactive ligands or specific

affinity for biomolecules) not present in the other constituent, and *vice versa*. Rowe and Stegemann [752] showed that VSMCs seeded in fibrin-collagen IPNs proliferated significantly faster than VSMCs seeded in single component controls. Lee and Kurisawa [753] reported similar data on the proliferation of fibroblasts seeded in fibrin-hyaluronic acid IPNs, with higher proliferation in the IPNs compared to pure fibrin or hyaluronic acid hydrogels. Furthermore, they demonstrated that the IPNs support angiogenic sprouting, which was found to be inversely proportional to material stiffness. In an interesting study, Shikanov et al. [754] encapsulated murine secondary follicles into fibrin-alginate IPNs to study *in vitro* follicle maturation. Initially, the IPNs provide a comparably stiff structural environment due to the presence of both polymer networks, however, cell-mediated fibrinolysis over time leads to a progressive decrease in the material modulus, up to a point where the material properties of the matrix are determined by alginate only. Exploiting these dynamic, cell-responsive mechanical properties of the fibrin-alginate IPN, the rate of meiotically competent oocytes was significantly higher after culture in the IPNs than in alginate alone. Combining the properties of a protein hydrogel and a synthetic polymer, Akpalo et al. [755] introduced a non-cytotoxic fibrin-PEO IPN with improved mechanical properties compared to fibrin alone. Recently, Gsib et al. [756] reported that such a mechanically reinforced fibrin-PEO IPN matrix can induce higher cell adhesion (across an array of cells from organ explants) and migration (skin and intestinal cells) than control hydrogels. Furthermore, no major inflammatory response was observed up to 12 weeks post implantation into nude mice.

Apart from the studies mentioned above, many more IPNs have been developed and a plethora of natural or synthetic materials and cross-linking strategies have been employed [750]. More recently, IPNs have also been tested for their ability to function as sophisticated drug delivery platforms. Specifically, IPN formulations in the form of microspheres or nanoparticles with tunable thermo- or pH-sensitive swelling behavior have been investigated as promising "smart" delivery systems capable of releasing an encapsulated drug in response to specific physiological stimuli. However, although a very interesting approach, the drug delivery potential of IPNs is beyond the scope of this thesis and has been comprehensively reviewed elsewhere [749, 758, 759].

4.5. Fibrin sealants in clinical practice

Commercial fibrin sealants, often referred to as fibrin glues, are two-component surgical sealant formulations comprised of a sealer protein and a hardener component. The sealer protein component contains, among other constituents, highly concentrated clottable fibrinogen and a certain amount of FXIII activity solubilized in an aqueous aprotinin solution. The hardener component contains highly concentrated thrombin solubilized in an aqueous $CaCl_2$ solution. The working principle of such fibrin sealants is that, upon combination and mixture of the two components (usually in a dual syringe

applicator), fibrinogen is rapidly converted into a stable cross-linked fibrin clot by thrombin and Ca^{2+}, mimicking the last step of blood coagulation but at much higher speed.

Today, fibrin sealants are among the most complex human plasma-derived products that are routinely used in surgical practice - both in terms of composition and range of clinical applications. In Europe, commercially available fibrin sealants have been available for over 40 years and have been extensively used as hemostats (to induce coagulation), sealants (to provide a sealing barrier to a leakage) and adhesives (to bond tissues together) [760, 761]. More recently, fibrin sealants have also been explored as a versatile delivery vehicle for the targeted delivery of therapeutic molecules (such as drugs, growth factors or gene vectors) and/or cells to specific tissues in the human body [302, 762].

The first use of fibrin as a hemostat dates back more than 100 years ago. In 1909, Bergel [763] successfully employed fibrin fleeces made from dried plasma as a source of fibrinogen to induce hemostasis. A significant improvement of this strategy was reported in the 1940s when two groups independently reported the feasibility of fibrinogen/thrombin mixtures in skin graft fixation [764, 765], which marked the first use of fibrin as an adhesive. However, the initial fibrin formulations showed poor consistency of performance due to their poor adhesive properties (most likely as a consequence of low fibrinogen concentrations), which prevented a more widespread use of fibrin sealants at that time. In was not before the early 1970s that fibrin re-entered the clinical stage, owing to advances in microsurgery, the availability of antifibrinolytics and, importantly, the emergence of efficient industrial plasma fractionation methods allowing for the production of concentrated fibrinogen and thrombin stocks. In 1972, a hallmark study by Matras et al.

[766] demonstrated that highly concentrated cryoprecipitates of fibrinogen/FXIII and thrombin can be employed as a sealant for peripheral nerve anastomosis in animals. This was also the first study reporting the addition of the protease inhibitor aprotinin to the sealer protein component to stabilize the fibrin clot by preventing premature fibrinolysis *in situ*. Three years later, Kuderna and Matras [767] used the same sealant formulation to successfully perform nerve anastomosis in humans. The fibrin formulation used in this study basically provided the blueprint for many of the commercial fibrin sealants available today and, based on the recipe of Kuderna and Matras, the first commercial fibrin sealant, TISSEEL© (Immuno AG, Vienna, Austria; now owned by Baxter Healthcare Corporation, Deerfield, United States), was introduced and approved in Europe in the 1970s. Other fibrin sealants like EVICEL© (Ethicon, Somerville, United States), Beriplast© (Behringwerke, Marburg, Germany) or Biocoll© (Centre de Transfusion Sanguine de Lille, Lille, France) would soon follow [768, 769], all similar to the initial TISSEEL© formulation. Due to safety concerns related to the use of bovine thrombin [770, 771] or the risk of viral transmission from pooled human plasma products, the Food and Drug Administration (FDA) initially revoked the license for clinical use of fibrin sealants in the United States [772]. This should delay the widespread use of fibrin sealants in the United States for another 20 years, as the FDA approved the two first commercial sealants TISSEEL© and Hemaseel APR© (Haemacure, Sarasota, United States) only in 1998 in response to the withdrawal

of bovine plasma protein usage, the implementation of extensive viral donor screening and the advances in automated viral reduction methods [773]. Since then, a variety of commercial fibrin sealants have been or are in the process of being licensed, including single-donor or pooled plasma products delivered either lyophilized or as frozen fluid formulations [774, 775].

The current version of TISSEEL© consists of two lyophilized components that are isolated from pooled human plasma (Table 2): the sealer protein component contains highly concentrated fibrinogen (usually >80 mg/mL) and FXIII (usually >10 U/mL) which needs to be reconstituted with an aqueous synthetic aprotinin solution (usually 3000 kallikrein inhibiting units (KIU)/mL); the hardener solution contains thrombin (usually 500 U/mL, a low thrombin fibrin sealant variant with 4 U/ml is also available) which needs to be reconstituted in an aqueous $CaCl_2$ solution (usually 40 mM). Alternatively, TISSEEL© is also available as a deep-frozen fluid formulation (in which both components are already solubilized) that is ready-to-use upon thawing.

	Active Component	Concentration	Origin	Excipients
Sealer Protein Solution	**Fibrinogen (clottable)**	80-120 mg/mL	Human plasma	Albumin (human)
	Factor XIII (activity)	10-50 IU/mL	Human plasma or human placenta	Histidine
				Nicotinamide
	Fibronectin (antigen)	5-20 mg/mL	Human plasma	Polysorbate 80
				Sodium citrate
	Aprotinin	3000 KIU/mL	Synthetic	H_2O
Thrombin Solution	**Thrombin (activity)**	4-500 IU/mL	Human plasma	Albumin (human)
				Sodium chloride
	Calcium chloride	40 mM	inorganic	H_2O

Table 2: *The formulation of TISSEEL© (Baxter Healthcare Corporation, Deerfield, United States), a commercially available fibrin sealant.*

Although the formulations of most commercially available fibrin sealants are similar, the contents of the sealer protein can vary depending on the fractionation method used, the clinical application of the sealant or local regulatory issues. Many fibrin sealants contain considerable amounts of the adhesive plasma glycoprotein fibronectin which is cross-linked into the fibrin clot by FXIIIa and not only contributes to clot stability, but also serves as an instructive cell attachment factor and opsonizing agent [776]. Due to its strong involvement in cell adhesion, migration, proliferation and differentiation, the presence of fibronectin can improve wound healing by promoting cellular infiltration into the fibrin clot at the wound site [777]. Other adhesive plasma glycoproteins such as vitronectin, laminin or thrombospondin may also be present in fibrin sealants as "contaminants" from plasma fractionation, however, whether they exert beneficial effects in wound healing (especially at the concentrations present) after sealant application remains elusive.

The ideal hemostat, sealant or adhesive is expected to fulfill certain performance criteria to be feasible and approved for clinical use. Safety, usability, cost-effectiveness and usability are among these criteria and, ideally, the sealant also promotes wound healing (or at least not interfere with it). Although many other natural, synthetic or composite hemostats, sealants and adhesives have been granted FDA approval for surgical application [778], fibrin sealants have been advocated by many clinicians as the material closest to the ideal operative sealant [779]. In particular, fibrin sealants excel at clinical versatility and biocompatibility, the latter being a problem associated with the use of synthetic sealants based on cyanoacrylate derivatives [780]. In fact, fibrin sealants are to this day the only commercially available product that is FDA approved as a hemostat, sealant and adhesive [304]. This has not only yielded a thorough clinical evaluation of fibrin in all three applications, but also prompted the development of specialized fibrin sealant applicators designed for linear, spray, endoscopic, laparoscopic or robotic techniques [577].

Traditionally, fibrin sealants were used as an adjunct to conventional means of achieving hemostasis, especially in tissues that are difficult to reach, too delicate to withstand suturing or too difficult to cauterize. Initially, trials carried out in cardiothoracic [781-783], hepatic [784], urologic [785] or intestinal surgery [786] accumulated evidence for the clinical efficiency of fibrin sealants to control perioperative bleeding in these settings. These studies laid the foundation for broad-label FDA approval of fibrin sealants as hemostats in general surgery. Other approved on-label indications nowadays include colon sealing at the time of colostomy closure, where fibrin is used as a sealant, or the attachment of skin grafts in burn wound grafting, where fibrin is used as an adhesive [304, 787] (Fig. 25).
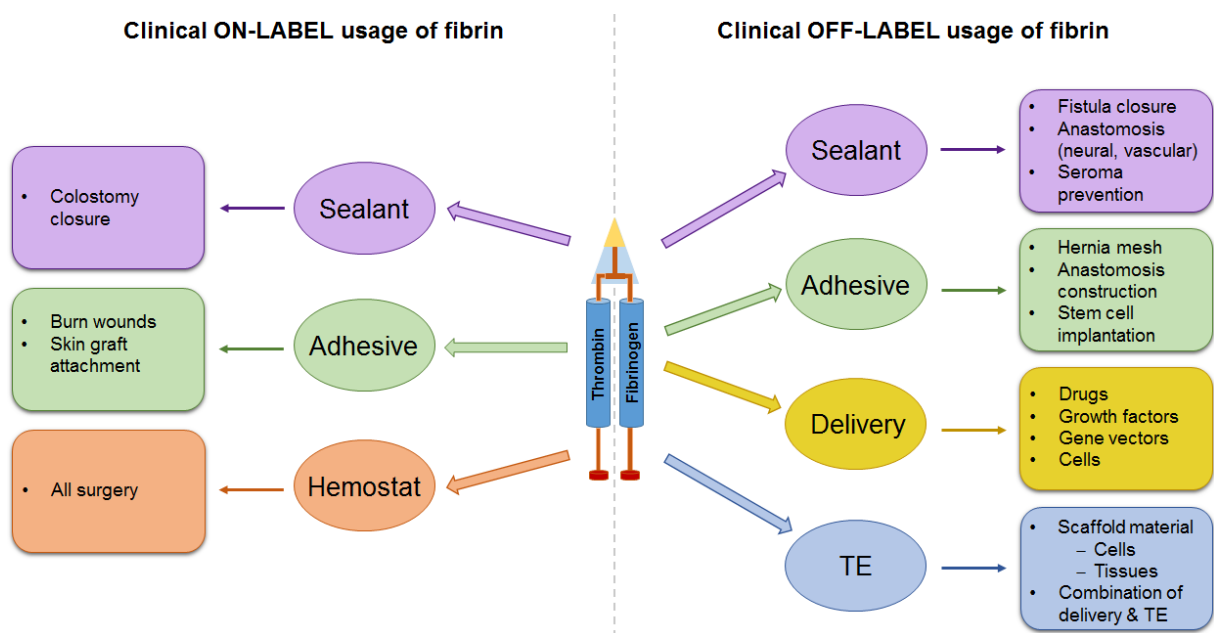
Fig. 25: *The clinical on- and off-label applications of fibrin sealants.* Fibrin sealants are the only commercially available product that is FDA approved as a hemostat, sealant and adhesive. While the on-label clinical applications have been well examined, several off-label indications have recently emerged. The most prominent novel application fields include fistula closure, hernia mesh fixation, stem cell implantation or drug/gene/growth factor delivery (adapted from [787]).

After four decades of research, the main clinical fields where the feasibility of fibrin sealants has been demonstrated are cardiovascular surgery, thoracic surgery, neurosurgery, plastic and reconstruction surgery, dental surgery, orthopedic surgery, hepatic surgery and gastrointestinal surgery [774, 775]. Two fibrin sealants, TISSEEL© and EVICEL© have broad-label approval for hemostasis and their clinical efficiency has been evaluated in numerous multicenter, randomized clinical trials [304]. These trials provided compelling evidence for the hemostatic potential of fibrin sealants in multiple surgical disciplines such as cardiac [783, 788], burn [789], pediatric [790], hepatic [791], orthopedic [792-794], dental [795, 796] and vascular surgery [797-801]. Apart from the liquid fibrin sealants, two fibrin-based hemostatic patches have recently been granted FDA approval: TachoSil© (Baxter Healthcare Corporation, Deerfield, United States), an equine collagen patch coated with fibrinogen and thrombin, and Evarrest© (Ethicon, Somerville, United States), a fibrinogen- and thrombin-coated oxidized cellulose patch. TachoSil© has been evaluated in clinical trials in cardiac [802], hepatic [803, 804] and renal [805] surgery and is now FDA approved as a hemostat in cardiac surgery. Evarrest© is currently approved as hemostat for soft tissue surgery after having been successfully evaluated in retroperitoneal, intra-abdominal, pelvic and non-cardiac thoracic surgical procedures [806-809]. Apart from hemostasis, fibrin is also approved as a sealant to prevent the leakage of bowel contents at the time of colostomy closure [304]. Furthermore, fibrin sealants have been granted FDA approval for use as adhesives in skin graft fixation procedures, for example to secure grafts at burn debridement sites or to attach skin flaps in face lift procedures. Several studies have demonstrated that the use of fibrin sealants in such procedures can reduce hemorrhage and wound contraction [810] and improves graft take, even at infected sites [811-813]. For this purpose, an approved low-thrombin concentration (4 instead of 500 U/mL) formulation of TISSEEL©, Artiss© (Baxter Healthcare Corporation, Deerfield, United States), has been shown to be especially efficient [814, 815], as the increased clotting time allows the surgeon to find the appropriate position of the graft before the sealant fully polymerizes.

In addition to the well-established (and FDA approved) usages in surgery, a variety of off-label usages for fibrin sealants have also been established. These include fistula closure [816, 817], hernia mesh fixation [818, 819], seroma prevention [820], dural closure [821], lung sealing after pulmonary resection [822], vascular or neuronal anastomosis [823, 824] or stem cell implantation [825, 826] (Fig. 25). More recently, a great deal of research has also focused on the use of fibrin as a scaffold biomaterial for cells or a delivery matrix for drugs and other therapeutic biomolecules in the field of TERM [510, 762, 827].

4.6. Fibrin as a versatile cell and delivery matrix in tissue engineering

A suitable biomaterial for TE applications is expected to be biocompatible, biodegradable, non-toxic and non-immunogenic. In the best case, the physicochemical properties of the material should be tunable to allow optimization of its mechanical and structural properties in order to maximize cell

adhesion, migration, proliferation or differentiation [828]. Fibrin meets all these requirements, as it is naturally involved in hemostasis and wound healing, where it interacts with a variety of soluble factors and acts as a (temporary) matrix for the many cell types involved in tissue repair. Several cell types can naturally bind to RGD sites on fibrin via specific integrin receptors, for example thrombocytes via integrin $\alpha_{IIb}\beta_3$ [516] or endothelial cells and fibroblasts via integrin $\alpha_V\beta_3$ [537, 829]. Importantly, fibrin also binds cell adhesive glycoproteins such as fibronectin [830], vitronectin [831] or thrombospondin [832], which can mediate cell binding and adhesion of cells not capable of binding fibrin directly. In the process of wound healing, fibrin acts as a local reservoir for different growth factors, cyto- and chemokines and enhances their bioactivity in a spatiotemporal manner: FGF-2 [565, 568], $VEGF_{165}$ [566], TGF-β1 [564], PDGF [563], IGF-1 [563] or IL-1β [567] can all be found in a native blood clot, with some of these factors having natural binding affinity for fibrin while others require binding to substances that bind fibrin (for example heparin).

4.6.1. Delivery of cells

Due to its intrinsic biological features, and the possibility to modulate the mechanical and structural properties of the matrix, fibrin has been extensively used as a delivery system for cells, drugs, growth factors and gene vectors - or combinations thereof (Fig. 26) [302, 303, 510, 762, 833-835]. Due to the abundance of adhesion motives, fibrin hydrogels can attain high cell seeding densities with uniform cellular distribution, while maintaining cell viability and promoting cellular proliferation, migration and differentiation. Therefore, the initial idea was that (stem) cells encapsulated into fibrin gels can be effectively used as regenerative tissue transplants. Indeed, the presence of fibrin as a scaffold protecting the cells from the initially harsh environment after transplantation was shown to lead to much higher cell engraftment efficiencies compared to local or systemic injection of cell suspensions [836]. This protective effect of the matrix results in higher cell survival, and both the encapsulated cells as well as invading cells from host tissues can then remodel the matrix, differentiate and gradually replace the scaffold with ECM proteins that they secrete themselves. During this process, host vascularization of the regenerating tissue is paramount to tissue maturation and functional maturation. In this respect, fibrin matrices have the advantage of triggering vascularization, as both fibrin as well as its degradation products have been shown to directly induce angiogenesis [555, 569-571].

The literature pertaining to fibrin-based cell delivery is vast and encompasses studies utilizing a wide range of (stem) cell types either encapsulated in or cultured on top of fibrin matrices. In this respect, one of the earliest instances was the use of fibrin meshes for autologous keratinocyte grafting in the tratment of chronic leg ulcers [837]. The feasibility of this approach was further underlined by subsequent studies in the field of cutaneous full-thickness wound repair employing fibrin to deliver keratinocytes [838, 839], fibroblasts [548, 840] or BMDMSCs [841]. At the same time, the use of

fibrin as a cell delivery matrix has spread out into multiple fields of TERM. Some prominent examples include fibrin-based delivery of osteoblasts for treatment of bone defects [842], chondrocytes for cartilage regeneration [843], preadipocytes for adipose tissue reformation after plastic surgery [844], urothelial cells for reconstruction of the urethra [845, 846], BMDMSCs for tendon repair [847], hepatocytes for liver regeneration [848], endothelial cells for *in vitro* [849] or *in vivo* [850] (pre)vascularization, myoblasts for cardiac [836] or skeletal [851] muscle repair or neural progenitor cells for spinal cord regeneration [852]. Fibrin has also been used to deliver MSC from various sources [853-857] and, more recently, ESC- and iPSC-derived progenitor cells [858, 859].
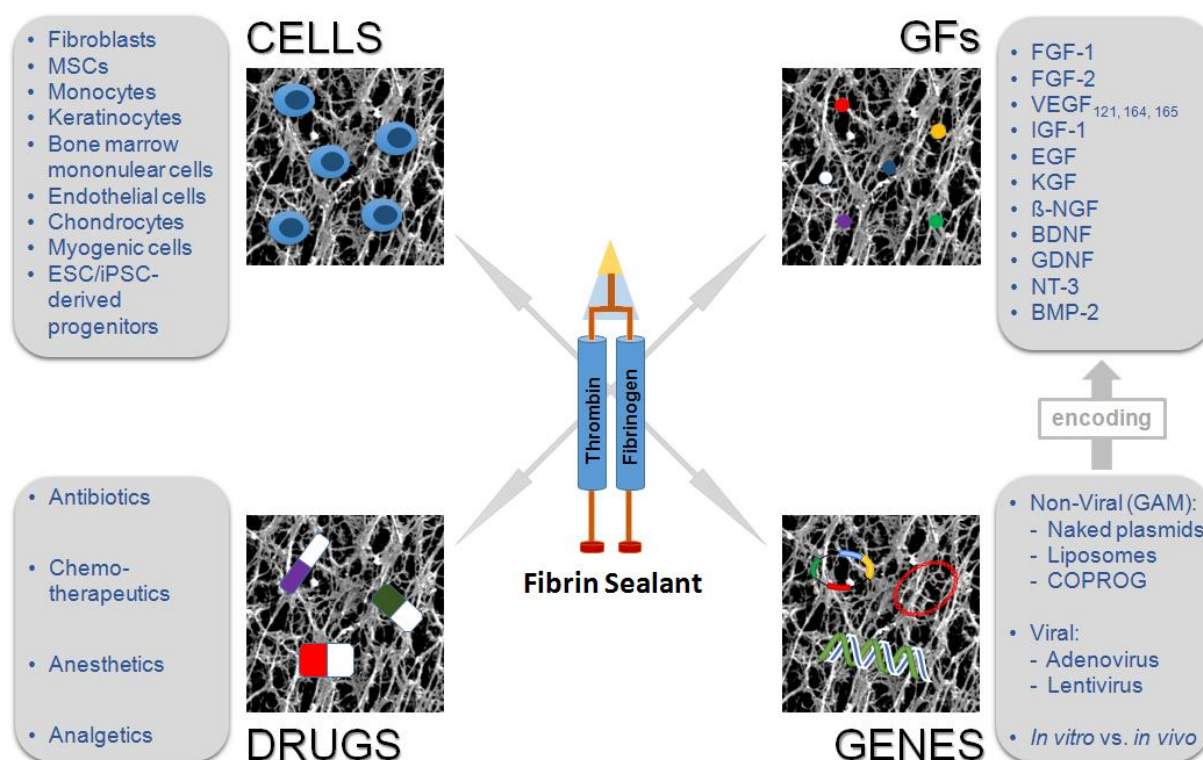

Fig. 26: *Fibrin, the versatile delivery matrix for TE applications.* Apart from being used as cell and differentiation matrix in TERM, fibrin hydrogels have been used for the local and sustained delivery of a variety of therapeutic biomolecules, such as growth factors, drugs or gene vectors (encoding specific growth factors). Given the promising therapeutic outcomes of each individual strategy, combined approaches (for example a combincation of cells and growth factors, or dual/sequential growth factor release) have also been studied to synergistically drive tissue regeneration (adapted from [302]).

These studies have not only proven the broad versatility of fibrin as a cell delivery vehicle, but have also resulted in a more thorough examination of the structural and mechanical properties of the matrix and their implications on cellular behavior. The adaptation of various cell types, including fibroblasts [840], keratinocytes [860, 861], chondrocytes [862], osteoblasts [863, 864] or MSCs [854, 865, 866], in response to changes in the overall physicochemical properties of fibrin has been addressed to optimize the matrix for a given cell type and application. The general notion from these studies is that the fibrinogen concentration (which correlates with matrix stiffness) has the biggest impact on the

cells, while the thrombin concentration (which correlates with gelation rate and modulates porosity) has a smaller but nevertheless considerable influence. Different cell types prefer different fibrin formulations and, in fact, the matrix properties have to be carefully optimized for each single cell or tissue type. For example, keratinocytes grow best on very soft fibrin matrices (1-3 mg/mL fibrinogen) [860], while fibroblast and MSC proliferation is highest in fibrin matrices of intermediate stiffness (5-17 and 18 mg/mL fibrinogen, respectively) [840, 854]. On the other hand, some cell types might prefer stiffer fibrin matrices, for example monocytes which require much higher fibrinogen concentrations (26-50 mg/mL) for optimal growth [867]. Fibrin matrix porosity and the degree of cross-linking also has implications on cellular behavior, as it affects cellular migration and nutrient diffusion. In general, moderate to low thrombin concentrations have been used (<10 U/mL) which not only increases the ease of handling (rapid polymerization might further lead to inhomogenous cell seeding in the hydrogel) but may also prevent detrimental effects of the matrix properties on cellular physiology [868, 869]. Summarizing, there is no matrix formulation that universally supports proliferation, migration and differentiation across all cell types. Thus, it is of utmost importance to fine-tune the structural and mechanical properties of the matrix for optimized cell viability, growth and functionality.

While many studies focused on the delivery of undifferentiated stem cells to sites of injury in the human body, fibrin has also emerged as a versatile cell differentiation matrix in TE. Applications of fibrin scaffolds range from the generation of functional tissue transplants for subsequent transplantation *in vivo* over developmental biological studies in 3D morpho- and organogenesis to pharmacological *in vitro* studies on biomimetic tissue constructs functioning as disease models or drug screening platforms. In this respect, a variety of engineered functional tissue constructs made from fibrin (or fibrin-based composites) in combination with one or several cell types have been vigorously investigated. Due to its natural involvement in wound repair and its intrinsic angiogenic properties, fibrin is considered an ideal biomaterial for vascular TE. Holnthoner et al. [849] introduced an autologous vascularization strategy based on the co-culture of endothelial cells with adipose-derived MSCs (ADMSCs) in fibrin. Using this *in vitro* model, a subsequent study showed that the ADMSCs exert paracrine effects on capillary network formation through secretion of pro-angiogenic factors [870]. With the notion that mechanical preconditioning increases vessel maturation [871], Tschoeke et al. [872] developed small-caliber vascular grafts using a fibrin-polylactide composite seeded with VSMCs which was subsequently lined with endothelial cells in a bioreactor. Dynamic mechanical preconditioning over 3 weeks resulted in the formation of a luminal evident endothelial lining and yielded grafts with supraphysiological burst pressures. A follow-up *in vivo* study by the same group [850] in a sheep carotid artery model showed a promising functional outcome for up to 6 months. Similarly, sophisticated bioreactor-based cardiomyogenic culture models for mechanical preconditiong of engineered heart tissue (EHT) in cardiac TE have been reported [873-875]. Fibrin has been shown to support myogenic differentiation and functional maturation *in vitro* [876] and has previoulsy been

used to deliver cardiomyogenic cells to infarcted areas of the heart to restore myocardial function [836, 877]. Hansen et al. [878] developed a minituarized high-throughput drug screening platform consisting of cardiomyocytes in fibrin/matrigel matrices which are anchored between flexible silicone posts to allow for contraction. The system was shown to enable long-term culture of the tissue constructs (over several weeks) and allows live monitoring the contractility of the miniature EHTs for pharmaceutical testing. More recently, the therapeutic potential of fibrin-based EHTs derived from iPSCs was also investigated. Weinberger et al. [879] used fibrin to deliver human iPSC-derived cardiomyoytes into large cardiac defects in guinea pigs and found an improvement of left ventricular fraction after 4 weeks. An interesting study by Menasché et al. [880] reported on the first transplantation of a fibrin scaffold containing hESC-derived cardiac progenitor cells into the infarct area of a 68-year-old patient during bypass surgery. At 3 months follow-up, an improvement of the left ventricular fraction was noted.

Fibrin has been used as a cell delivery matrix in skin TE for 30 years [837] and several intrinsic biological properties make it suitable for dermal application. Apart from its direct angioinductive properties [881], fibrin promotes keratinocyte proliferation and migration after incisional wounding [882] and enhances graft "take" of skin subsitutes, especially when applied as a thin layer (for example through spray application) over large wound areas [883]. The therapeutic efficiency of fibrin and keratinocytes in the treatment of skin defects is well established and led to the introduction of the commercially available autologous skin replacement product based on this strategy (BioSeed-S©; BioTissue Technologies AG, Freiburg, Germany). Furthermore, other studies have demonstrated the synergistic beneficial effects of combining fibrin-based keratinocyte delivery with dermal allografts for full-thickness wound healing [884, 885]. Based on the observation that epidermal regeneration is highly dependent on mutual fibroblast-keratinocyte interactions [886], improved clinical outcomes in terms of cutaneous wound repair *in vivo* have also been reported when such co-cultures and fibrin were used compared to individual delivery of each cell type alone [887, 888].

The field of nerve TE has partially focused on acellular strategies employing fibrin-based delivery of neurotrophic growth factors (which will be discussed later), however, fibrin has also been identified as a suitable matrix for neural differentiation of stem cells [889, 890]. In peripheral nerve repair, fibrin has been shown to prevent initial gapping at nerve repair sites [891] which might make it feasible as a nerve conduit biomaterial. Kalbermatten et al. [892] compared the efficiency of a fibrin versus poly-3-hydroxybutyrate as a conduit to bridge peripheral nerve lesions and found superior nerve regeneration distance and enhanced Schwann cell infiltration after one month when fibrin was used. A follow-up study [893] further demonstrated that the tubular fibrin conduit could effectively contribute to long-term nerve regeneration (compared to an autograft as control), as assessed by the total number of myelinated axons in the distal nerve stump and the weight of the connected soleus and gastrocnemius muscles after 3-4 months. Importantly, the addition of neurocompetent cells such as Schwann cells or MSC-derived neural cells to fibrin-based nerve conduits was found to increase the therapeutic

efficiency of this approach compared to acellular conduits [894]. This is supported by a more recent study by Schuh et al. [895] showing that MSC-derived pro-myelinating Schwann cells seeded onto electrospun fibrin/PLGA scaffolds form aligned Büngner-like structures *in vitro*, and the addition of aligned topological cues on the conduit could prove useful to induce guided axonal repair upon grafting *in vivo*.

Apart from cardiac or skeletal muscle, fibrin has been widely used as a scaffold material for therapeutic applications in other musculoskeletal tissues such as cartilage or bone. In cartilage TE, a variety of fibrin-based delivery strategies for the regeneration of fibrocartilage, elastic cartilage, craniofacial cartilage or articular cartilage have been reported [834, 896]. The majority of studies have used fibrin in combination with autologous chondrocytes [897-901] or MSCs [902, 903], and the general observation is that the addition of cells improves cartilage regeneration as compared to acellular strategies *in vivo*. However, mechanical failure of engineered neocartilage (especially at the interface with native cartilage) is still a mjor bottleneck of this approach. This has prompted research looking into the feasibility of fibrin-based composite systems to improve the mechanical properties of the regenerative cartilage transplants. For example, fibrin/PGA [904], fibrin/PLGA [905], fibrin/hyaluronic acid [906], fibrin/collagen [907], fibrin/alginate [908] or fibrin/PU [843] composites have been reported to support *in vitro* and *in vivo* neochondrogenesis. Similar approaches have been proposed for bone TE and, although there is still a debate whether fibrin has direct osteoinductive properties [909-913], the intrinsic pro-angiogenic properties of fibrin in combination with the immunomodulatory effects of MSCs have been demonstrated to promote bone healing by improving implant integration and tissue maturation in non-union fractures [914]. The fact that MSCs are considered a promising cell source for osteochondral repair has furthermore driven the development of specialized culture systems to streamline the expansion of these cells without a loss of osteogenic potential. In this respect, the use of fibrin microbeads (FMBs) for expansion of MSCs from different origins and species prior to subsequent osteogenic differentiation and implantation has proven very useful, both for *in vitro* [915, 916] and in vivo [917, 918] application. Similar to cartilage TE, several fibrin composites (mostly aiming at the biological functionalization of bioceramics or metallic implants) have been examined to address the problem of premature implant failure [919]. For example, the addition of fibrin to autologous bone grafts was reported to not only improve surgical handling and prevent graft displacement [920-922] but also accelerated neovascularization and growth stimulation of fibroblasts and osteoblasts [922] while considerably reducing the amount of bone graft resorption [923]. In addition, fibrin has been implictated to enhance the biological performance of bioceramics [924, 925]. Addition of fibrin to calcium $CaCO_3$ [926] or hydroxyapatite [927] scaffolds increases growth and osteogenic differentiation of MSCs. Notably, the addition of fibrin to calcium phosphate bone cements somewhat enables control over scaffold porosity [928] and the capacity of the material to support angiogenesis can be modulated by varying the fibrin to calcium phosphate ratio [929]. The combination of fibrin with bioinert metallic implants such as titanium alloys has also been

explored. For example, Kopf et al. [930] showed that pre-incubation of titanium with human whole blood greatly increased the attachment and subsequent osteogenic differentiation of primary human bone cells, while accelerating the rate of mineralization. In an interesting study, Kalia et al. [931] used a spray device to coat a titanium alloy with fibrin and MSCs prior to implantation into a sheep tibia defect. After 6 months, histological analysis indicated increased bone growth and bone contact to the implant surface compared to controls without fibrin and MSCs.

4.6.2. Delivery of therapeutic biomolecules

The observation that fibrin naturally binds and sequesters a subset of growth factors during blood coagulation and wound healing has led to the hypothesis that this natural affinity may be exploited for the sustained local release of therapeutic biomolecules. The concept of fibrin-based delivery is based on incorporating one or several pharmaceutically active substances (like growth factors, drugs or gene vectors) into a fibrin scaffold following application to the site of injury. In this respect, fibrin is an appealing delivery platform as it can be injected locally and can be functionalized during polymerization without the need of harsh reaction conditions by simply adding the substance of interest to one component of the fibrin formulation. Passive diffusion as well as plasmin-mediated fibrinolysis will then lead to release of the "cargo" from the matrix, thus delivering it locally at the site of application. However, only a subset of therapeutic biomolecules have natural affinity for fibrin, allowing for sustained release (at least over the course of days). Furthermore, rapid fibrinolysis after application might lead to a burst-like release profile, creating supraphysiological levels of the substance which will then be metabolized quickly. With the notion that sustained physiologically relevant dosage in required to elicit the greatest therapeutic effect [932, 933], a great deal of research has focused on strategies that enable control over the release kinetics of the substance of interest from the fibrin matrix, with the ultimate goal of spatiotemporally delivering bioactive compounds in a sustained manner at appropriate doses [302, 510, 762, 835, 896].

The simplest way of delivering a growth factor is simply dosing the fibrin formulation with it prior to administration to a specific site in the body. The binding affinity of the respective growth factor for fibrin (controlling diffusion) and the rate of fibrinolysis will determine the release profile, with slower, more sustained release for factors tethered to fibrin. Although non-fibrin-affinity growth factors such as FGF-1 (acidic FGF) or glial cell line-derived neurotrophic factor (GDNF) will mostly display burst-like release profiles, beneficial effects of fibrin-based delivery of these factors on wound angiogenesis [934] or dorsal root regeneration [935] have been shown. Apart from growth factor entrapment in fibrin, alternate methods for sustained release have been developed. These strategies aim at controlling release by modulating the binding affinity of a given therapeutic biomolecule to fibrin and include (i) the use of affinity-based systems where a substance of interest (that does not naturally bind fibrin) is tethered to fibrin through fibrin anchors (which bind the substance of interest as well as fibrin), (ii)

covalent cross-linking via bi-domain peptides that bind the substance of interest and can be cross-linked into fibrin, or (iii) the use of recombinant fusion proteins where the substance of interest is functionalized to gain binding affinity for fibrin. Several studies have demonstrated that growth factors with natural affinity for fibrin, for example FGF-2 (basic FGF) [565], $VEGF_{165}$ [566] or IL-1β [567], are primarily released upon cellular infiltration and subequent degradation of the fibrin matrix, resulting in sustained release over several days [936, 937]. Alternatively, to prevent burst release of growth factors that do not bind fibrin, heparin can be added to tether the respective growth factor to the fibrin matrix. Heparin binds fibrin [938] as well as many growth factors [933, 939, 940] and an advantage of this strategy is that the presence of free heaprin in the fibrin matrix will also sequester endogenous circulating growth factors *in situ*, thereby increasing their bioactivity as well [941]. In addition, the molar ratio of heparin to growth factor allows for modulation of the release kinetics. However, a significant amount of growth factors have low affinity for both heparin or fibrin, especially neurotrophic factors such as neurotrophin (NT)-3, nerve growth factor (NGF)-β or brain-derived neurotrophic factor (BDNF) [942], which has led to alternative strategies for their controlled and sustained release.

A pioneering study by Schense and Hubbell [943] reported an elegant way of covalently cross-linking growth factors into fibrin through the use of bi-domain peptides. Mimicking FXIIIa-mediated fibrin cross-linking, they introduced peptides containing an N-terminal FXIIIa substrate (derived from α2-PI) and a C-terminal bioactive domain of choice, for example a bioactive peptide, a heparin binding site or a growth factor. Such bi-domain peptides have been used to covalently incorporate RGD sites [943], laminin and N-cadherin peptides [944], VEGF121 [945] or ephrin B2 [946] into fibrin matrices through transglutaminase-mediated cross-linking. An affinity-based system has also been developed, where the bi-domain peptides are functionalized with a FXIIIa substrate and a C-terminal heparin binding domain (based on antithrombin III) [942, 947]. This system was used to effectively deliver neurotrophic factors (that have low affinity for heparin) for nerve regeneration by adjusting the ratio of heparin-binding peptide and added heparin, and reported outcomes range from enhance neurite extension to improved neural stem cell survival and functional neuronal differentiation [852, 948-950]. An elegant modification of the bi-domain peptide strategy was the incorporation of a plasmin α2 substrate sequence linker between the N-terminal FXIIIa substrate and the C-terminal growth factor binding domain [951]. This changes the release profile from diffusion- and fibrinolysis-dependent release to plasmin-sensitive release and the rationaly behind this approach was that proteolytic cleavage by endogenous plasmin provides *in situ* growth factor release on cellular demand (as the cells infiltrate the matrix and activate PLG). Therefore, such a system may provide variable rates of growth factor release dependent on the local cellular activity at the site of application. Indeed, NGF-β release with this approach enhanced neurote extension from chick embryonic dorsal root ganglia by 50% compared to unmodified NGF-β entrapment in fibrin [951]. Furthermore, such plasmin-sensitive bi-domain peptides have been successfully used to deliver keratinocyte growth factor (KGF) [952] to

stimulate cutaneous wound repair, and parathyroid hormone (PTH) 1-34 [953] or BMP-2 [954, 955] for bone regeneration. An alternative to bi-domain peptides is the generation of recombinant fusion proteins, where a growth factor is functionalized with a fibrin binding peptide. For example, Zhao et al. [956, 957] fused the "kringle" domains 1 and 4 of PLG to FGF-2 (termed K1FGF-2 and K4-FGF2, respectively) to fiúrther increase its binding affinity to fibrin. This led to higher retention of recombinant FGF-2 in the matrix while retaining its mitogenic properties and significantly accelerated neovascularization and wound healing compared to controls in a full-thickness incisional rat wound model.

Given the fact that tissue regeneration is a very complex process in which multiple growth factors, cell types and cytokines are involved, strategies for the orchestrated spatiotemporal release of multiple bioactive substances form the same fibrin matrix have also been explored. Multi growth factor release can be achieved by incorporation of several growth factors into fibrin [852, 958], however, sequential release of two or more growth factors requires different release kinetics for each factor. This can be achieved by exploiting the different natural affinities of growth factors for fibrin. For example, combined sequential release of FGF-2, $VEGF_{165}$ (both displaying high affinity for fibrin) and $VEGF_{121}$ (low affinity for fibrin) release was found to promote *in vivo* wound angiogenesis and vessel maturation to a much higher extent than single delivery of each factor (which still promoted angiogenesis) [937]. Alternatively, different release profiles can be achieved by the use of fibrin composite matrices, where the growth factors are tethered to different matrix components that have distinct degradation rates and binding affinities for the respective factor. Examples of such multimodal delivery systems for controlled, sequential growth factor release in wound healing include PEGylated fibrin for PDGF and TGF-β release [959], fibrin-coated PU-PDMS scaffolds for $VEGF_{165}$ and FGF-1 release [960] or growth factor-laden albumin microspheres embedded in fibrin for FGF-2 and granulocyte colony stimulating factor (G-CSF) release [961, 962].

With the notion that the administration of instructive fibrin matrices loaded with growth factors might not be enough to trigger tissue regeneration, a combination of cell and growth factor delivery (from the same matrix) has also been attempted. The rationale behind this approach is to not only synergistically drive tissue neoformation after injury through combined growth factor signaling and cell-mediated processes, but also to direct cell fate within the matrix. For example, combined delivery of dermal fibroblasts and FGF-2 was found to increase fibroblast proliferation *in vitro* [963], while co-delivery of PDGF and fibroblast improved wound coverage and cutaneous wound healing *in vivo* [964]. In nerve regeneration, delivery of ESC-derived neural progenitors with PDGF and NT-3 was reported to increase cell survival and neuronal differentiation after transplantation in a rat model of spinal cord injury [852]. In addition, co-delivery of TGF-3β and AFSCs from fibrin enhanced chondrogenesis *in vitro* and *in vivo* [965] and, similarly, the combination of osteoblasts and FGF-2 yielded enhanced ectopic bone formation in rats compared to fibrin-based osteoblast delivery alone [966].

Although fibrin-based growth factor delivery (with or without the addition of cells) has yielded promising pre-clinical results, the high cost and limited shelf life of growth factors still pesent major bottlenecks of this strategy. Furthermore, even sustained protein-based delivery usually requires high doses and repetitive administration, which might lead to undesired systemic side effects. Thus, strategies to use fibrin for the localized delivery of gene vectors encoding growth factors into target cells *in vitro* or *in vivo* have been developed and present a more recent approach to tissue regeneration. The general concept of fibrin-based gene delivery is to transfect or transduce either endogenous cells as they infiltrate the matrix or exogenous cells encapsulated in the matrix prior to implantation [967]. These cells can then produce and secrete the respective growth factor(s) *in situ*, inducing a localized regenerative response by auto- and paracrine mechanisms. In this respect, the feasibility of fibrin to effectively deliver viral or non-viral gene vectors in a variety of gene therapeutic tissue-specific strategies is now well established [302, 968-970]. Fibrin-based viral gene delivery has been most widely studied in the fields of cutaneous wound reapir and musculoskeletal regeneration, with Adenovirus (Ad), adeno-associated virus (AAV) and lentivirus (LV) being the gene vectors most predominantly used [968]. A variety of *in vitro* and *in vivo* studies looking into finding appropriate fibrin formulations for sustained delivery of Ad [827, 971, 972], AAV [973] or LV [974] vectors have found that low fibrinogen concentrations generally yield the highest infection efficiencies. Other studies have investigated specialized application methods such as spraying of viral gene vector-laden fibrin onto muscosal surfaces [975]. Interestingly, fibrin hydrogels were found to preserve viral bioactivity *in vivo* at higher levels compared to other commonly used natural hydrogels like collagen or alginate [972, 974]. Furthermore, strategies to cross-link viral particles into fibrin or to increase virus tropism for fibrin have been explored. Among these, the generation of recombinant viruses with a FXIIIa substrate fused to viral envelope proteins [976] or the immobilization of plasma membrane proteins into the fibrin matrix for enhanced viral retention [977] present promising novel approaches for more efficient gene transfer. The therapeutic potential of fibrin-based viral gene therapy for musculoskeletal repair has been shown by a variety of studies. Schek et al. [972] showed that intramuscular injection of fibrin containing Ad encoding BMP-7 led to ectopic bone formation in mice after 4 weeks. A follow-up study by the same group [978] demonstrated that adenoviral BMP-7 *ex vivo* gene therapy of fibroblasts and subsequent delivery of the cells in fibrin effectively induced bone formation in mice compared to *in vivo* BMP-7 gene therapy (administration of Ad encoding BMP-7 alone). Similarly, *ex vivo* infection of MSCs with Ad carrying BMP-2 and subsequent delivery of the cells in fibrin into rat cartilage defects led to the production of hyaline repair cartilage [979]. More recently, an inducible adenoviral BMP-2 vector has been engineered and, in combination with with MSCs, fibrin and a calcium phosphate ceramic, this tunable BMP-2 expression system gave promising results in a rat large bone defect model [980]. In (chronic) cutaneous wound healing, fibrin-based delivery of human fibroblasts transfected with Ad encoding KGF was found to promote wound healing and enhance reepithelialization in a humanized skin model [981]. In addition, delivery of Ad

encoding endothelial NOS (eNOS) in fibrin in a rabbit chronic ulcer model was shown to effectively trigger local endogenous eNOS expression, resulting in faster reepithelialization and wound closure compared to single treatment controls (fibrin or Ad encoding KGF alone) [982].

To address the risks associated with the use of viral vectors, such as vector integration or immuno responses to viral capsid proteins, non-viral gene therapy strategies have been introduced as a potentially cheaper and safer alternative. Given the inefficiency of naked DNA injections, the incorporation of plasmids into fibrin as a nucleic acid carrier has been reported to enable sustained vector retention through ionic interactions of the DNA with the matrix [983]. This has led to the concept of using fibrin as a gene activated matrix (GAM), where therapeutic plasmids are incorporated to slow down vector release, increase the chance of localized cell-vector interaction and, thus, enhance transfection efficiency [896]. Initially, this was hypothesized to provide a safe, transient gene delivery platform and, indeed, sustained plasmid DNA release for at least 19 days has been reported [984]. Analogous to viral gene delivery, the factors affecting the *in vitro* and *in vivo* transfection efficiencies of fibrin GAMs have been thoroughly investigated. Fibrinogen and plasmid concentrations, the mode of plasmid DNA condensation, such as lipo- and polyplexes or copolymer protected (COPROG) gene vectors, or the rate of fibrinolysis all greatly influence DNA release and cellular uptake [984-988]. In chronic wound healing, fibrin GAMs delivering VEGF plasmids have been shown to effectively trigger neoangiogenesis [989, 990] and the therapeutic effects of this approach can be further increased by the addition of lipofectamine [990]. Interestingly, the presence of fibrin was also found to drastically reduce the death of entrapped cells in response to high lipofectamine dosage [986]. The injection of fibrin containing a plasmid encoding pleiotrophin (PTN) into the ischemic myocardium of rats led to increased neovasculogenesis compared to naked plasmid injections [991]. Apart from wound angiogenesis, fibrin-based non viral gene therapy has probably been most widely studied in bone regeneration [992]. Although there is evidence that BMP-2 plasmid delivery accelerates fracture healing [993], the use of cationic polymers for DNA condensation was also found to decrease the therapeutic efficiency of this approach [988, 994]. This has led to the evaluation of physical means to enhance transfection efficiency, such as electroporation [995] or sonoporation [996], instead of using copolymers. In this respect, fibrin matrix-assisted sonoporation (MAS) has been shown effective in triggering *in vitro* and *in vivo* osteogenesis by increasing the BMP-2/7 transfection efficiency in fibrin-based GAM approaches [997, 998]. Finally, fibrin-based non viral *ex vivo* gene therapy approaches using transfected cells as the gene vector have also been addressed. For example, delivery of keratinocytes transfected with epidermal growth factor (EGF) in fibrin intofull-thickness wounds in mice led to a 180-fold increase in local EGF expression compared to controls [999]. The fibrin-based delivery of human preadipocytes transfected with VEGF through electroporation was found to increase vascularization in a chicken chorioallantoic membrane (CAM) angiogenesis model [1000]. Furthermore, combined delivery of MSCs and TGF-β1 plasmids in fibrin into full-thickness rabbit

articular cartilage defects was shown to efficiently induce the formation of well-integrated neocartilage 12 weeks after implantation of the matrix [1001].

The release of drugs from fibrin matrices is a somewhat different approach and one of the earliest instances of the use of fibrin as a delivery vehicle. Although systemic drug administration is generally a viable option, some cases (such as large-area burns or severe trauma) may require localized delivery in high pharmacological doses. The release kinetics of diverse antibiotics from fibrin have been analyzed [1002-1004], and the main challenge is to sustain drug release for adequate periods of time whithout compromising fibrin matrix integrity. Some antibiotics exert inhibitory effects on fibrinogenesis and fibrin clot rigidity [1002], however, in some cases this can be counteracted by increasing the degree of fibrin cross-linking through the use of high thrombin and/or FXIII concentrations in the formulation [1004]. Importantly, poorly water-soluble (lipophilic) antibiotics are retained significantly longer in fibrin, allowing for sustained release [1005]. Several studies have shown that fibrin hydrogels dosed with antibiotics exert prolonged bacteriostatic activity *in vitro* and *in vivo* [1003, 1005-1007], and fibrin-based delivery of streptomycin was even found highly effective in controlling multi-drug resistant *Staphylococcus aureus* infections in rats [1005]. To gain further control over the release profiles of especially hydrophilic antibiotics, pre-fabricated lyophilized fibrin/antibiotic matrices [1008, 1009] or composites such as fibrin coated drug particulates have been developed [1010-1012]. The release of chemotherapeutic agents from fibrin matrices has also been attempted. Examples include the fibrin-based delivery of enocitabine [1013], doxorubicin [1014], topotecan [1015] or carboplatin [1016, 1017]. Furthermore, an interesting study by Häfeli et al. [1018] demonstrated the feasibility of fibrin as a delivery vehicle for β-emitting radioisotopes for the treatment of brain tumors in rats. In addition, fibrin has been used to locally deliver anesthetics after plastic surgery, and patients receiving lidocaine-laden fibrin gels after subpectoral augmentation surgeries experienced less pain than those receiving only fibrin or lidocaine alone [1019].

5. AIM OF THE THESIS

This thesis was carried out within the frame of a European Union Framework Programme 7 project ("BIODESIGN") which was directed towards the development of new strategies for the rational design of ECM mimetic biomaterials. In addition, an integral goal of BIODESIGN was to evaluate such designed materials and link them to adequate and more predictive pre-clinical *in vitro* models in an attempt to reduce the use of animal models in musculoskeletal tissue engineering.

The main objectives of this thesis were:

1) Design of a fully-automated bioreactor system that allows application of tunable strain regimes to cells embedded in free-standing fibrin scaffolds.

A prototype of a closed bioreactor system that allows uniaxial application of strain onto ring-shaped (cell-seeded) free-standing fibrin scaffolds made by injection molding has previously been developed with our partner FHTW. Initially, this system only allowed for mechanical stimulation of one sample at a time. The initial goal was to develop a parallelized version of this prototyp to increase sample throughput (goal: simultaneous stimulation of 24-36 samples). At the same time, a new version of the custom-made graphical user interface (GUI) was programmed to gain control over adjustable strain regimes consisting of cyclic, static or ramp strain (and combinations thereof). The bioreactor system was then evaluated in the context of skeletal muscle formation, with the aim of generating a dynamic organotypic model of early skeletal muscle development. This was done using fibrin as a scaffold material and, initially, a mouse myoblast cell line (C2C12). Optimization parameters included the mechanical properties of the fibrin matrix, the cell culture protocol and an appropriate biomimetic strain regime. In the second stage of this project, a C2C12 line carrying a luminescent MCK reporter construct (*Metridia* luciferase under control of the MCK promoter; activation leads to secretion of luciferase which can then be sampled in the supernatant) was implemented into the dynamic culture system for non-invasive longitudinal monitoring of myogenic differentiation.

2) The Generation of a novel fibrin-based composite hydrogel to improve the mechanical properties of fibrin while maintaining biocompatibility.

This project aimed at the generation of an IPN consisting of fibrin and disulfide cross-linkable hyaluronan hydrogels, two major ECM components in the human body. The goal was to develop a method to combine the thrombin-mediated enzymatic cross-linking of fibrin with orthogonal disulfide cross-linking of hyaluronan *in situ*. In an ideal case, this reaction would perform stably in aqueous

solution under physiological conditions, which preserves the injectability of such an IPN formulation. The initial phase of the project involved screening and optimization of different concentrations of fibrinogen/thrombin and the hyaluronan derivatives (especially the molar ratios between the two) to fine-tune the kinetics of both reactions (that is, the formation of a fibrin and a hyaluronan network). Mechanical and structural characterization was performed with SEM, rheological measurements, mechanical testing (compression) and degradation studies. The second stage of the project was taking the fibrin-hyaluronan IPN into cell culture and evaluate cell-mediated matrix degradation kinetics. This further involved testing the effects of the novel formulation on the viability and proliferation of mesenchymal cells.

3) Providing comprehensive literature reviews on the versatility of fibrin sealants as versatile delivery platforms and on recent advances in the field of surgical sealing in general.

Although fibrin sealants have been in used in clinics for more than a century, research directed to refining current fibrin formulations as well as incorporating cells and/or bioactive molecules like drugs, growth factors or gene vectors to improve therapeutic efficiencies is still thriving. The third objective of this thesis was to present recent advances in fibrin-based delivery methodology for broad clinical use and novel developments in the area of surgical sealing in general in the form of two comprehensive reviews and a book chapter contribution.

CHAPTER I

**A dynamic 3D fibrin-based culture system
for the generation of highly aligned mature
skeletal muscle tissue through application
of mechanical strain via a bioreactor**

"A novel bioreactor for the generation of highly aligned 3D skeletal muscle-like constructs through orientation of fibrin via application of static strain"

Philipp Heher[1,2,3, #,*], Babette Maleiner[2,4,#], Johanna Prüller[1,2,4,#], Andreas Teuschl[2,4,5], Josef Kollmitzer[4,6], Xavier Monforte[2,4], Susanne Wolbank[1,2,3], Heinz Redl[1,2,3], Dominik Rünzler[2,4], and Christiane Fuchs[2,4,5]

[1] Trauma Care Consult, Vienna, Austria

[2] Austrian Cluster for Tissue Regeneration, Vienna, Austria

[3] Ludwig Boltzmann Institute for Experimental and Clinical Traumatology/AUVA Research Center, Vienna, Austria

[4] Department of Biochemical Engineering, UAS Technikum Wien, Vienna, Austria

[5] City of Vienna Competence Team Bioreactors, UAS Technikum Wien, Vienna, Austria

[6] Higher Technical Institute HTL –TGM, Department for Biomedical- and Health-Engineering,   Vienna, Austria

[#] These authors contributed equally to this work

[*] To whom correspondence should be addressed: Philipp Heher, Trauma Care Consult, Gonzagagasse 11/25, 1010 Vienna, Austria; Tel.: +43 680 2335821; Fax: +43 (0)5 9393-41982; E-mail: heherp@technikum-wien.at

ABSTRACT

The generation of functional biomimetic skeletal muscle constructs is still one of the fundamental challenges in skeletal muscle tissue engineering. With the notion that structure strongly dictates functional capabilities, a myriad of cell types, scaffold materials and stimulation strategies have been combined. To further optimize muscle engineered constructs, we have developed a novel bioreactor system (MagneTissue) for rapid engineering of skeletal muscle-like constructs with the aim toresemble native muscle in terms of structure, gene expression profile and maturity.

Myoblasts embedded in fibrin, a natural hydrogel that serves as extracellular matrix, are subjected to mechanical stimulation via magnetic force transmission. We identify static mechanical strain as a trigger for cellular alignment concomitant with theorientationof the scaffold into highly organized fibrin fibrils. This ultimately yields myotubes with a more mature phenotype in terms of sarcomeric patterning, diameter and length. On the molecular level, a faster progression of the myogenic gene expression program is evident as myogenic determination markers *MyoD* and *Myogenin* as well as the Ca^{2+} dependent contractile structural marker *TnnT1* are significantly upregulated when strain is applied.

The major advantage of the MagneTissue bioreactor system is that the generated tension is not exclusively relying on the strain generated by the cells themselves in response to scaffold anchoring but its ability to subject the constructs to individually adjustable strain protocols. In future work, this will allow applying mechanical stimulation with different strain regimes in the maturation process of tissue engineered constructs and elucidating the role of mechanotransduction in myogenesis.

STATEMENT OF SIGNIFICANCE

Mechanical stimulation of tissue engineered skeletal muscle constructs is a promising approach to increase tissue functionality. We have developed a novel bioreactor-based 3D culture system, giving the user the possibility to apply different strain regimes like static, cyclic or ramp strain to myogenic precursor cells embedded in a fibrin scaffold. Application of static mechanical strain leads to alignment along the axis of strain and concomitantly to highly aligned myotube formation. Additionally, the pattern of myogenic gene expression follows the temporal progression observed *in vivo* with a more thorough induction of the myogenic program when static strain is applied. Ultimately, the strain protocol used in this study results in a higher degree of muscle maturity demonstrated by enhanced sarcomeric patterning and increased myotube diameter and length. The introduced bioreactor system enables new possibilities in muscle tissue engineering as longer cultivation periods and different strain applications will yield tissue engineered muscle-like constructs with improved characteristics in regard to functionality and biomimicry.

1. INTRODUCTION

Skeletal muscle is the most abundant tissue type in the human body, accounting for roughly 40% of the total body mass [18]. Despite recent advances in the treatment of damaged skeletal muscle tissue clinical outcomes have been at best suboptimal [284, 1020]. In this respect, tissue engineering of transplantable functional skeletal muscle serves as an attractive alternative to replace and/or restore the damaged tissue. To achieve this goal, a variety of two- and three-dimensional skeletal muscle tissue engineering strategies have been developed, utilizing diverse scaffold materials and cell types [14, 241, 284]. Ever since Vandenburgh et al.'s pioneering work on myotube formation in collagen gels [290, 414], natural hydrogels have been extensively used as scaffold materials for skeletal muscle engineering due to their biocompatibility and –degradability [287, 293, 295, 351, 429, 488, 498]. Compared to non-biodegradable or synthetic materials, fibrin hydrogels offer superior properties for 3D skeletal muscle engineering [284], as they mimic the mechanical properties of native skeletal muscle tissue, with the possibility to modulate stiffness and pore size [580, 742, 1021]. Moreover, they allow for dense and spatially uniform cell distribution due to the high abundance of cell attachment sites - a crucial feature as the cell seeding density has been shown to directly affect myogenic differentiation and muscle structure [61, 353]. Besides, fibrin hydrogels have the advantage of binding growth factors that augment myogenesis, such as vascular endothelial growth factor (VEGF) [566], basic fibroblast growth factor-2 (bFGF-2) [565, 568] or, indirectly, insulin-like growth factor-1 (IGF-1) [562]. Altogether, these features render fibrin a very promising scaffold material for skeletal muscle engineering approaches.

From a developmental point of view, the functional capabilities of skeletal muscle tissue are strongly linked to its structure [1022]. In general, skeletal muscle is characterized by a highly ordered array of parallel muscle fibers. These initially originate from the fusion of myogenic precursor cells into multi-nucleated myotubes which later mature into muscle fibers comprised of many parallel myofibrils [14]. This maturation is accompanied by an increase in contractile force of the myofibril, which is actuated through relative movement of two interlocking macrostructures (myofilaments), the thin actin and thick myosin filaments [33]. As the main purpose of skeletal muscle tissue is to generate uniaxial force, engineered muscle constructs are expected to generate sufficiently large contractile forces to be able to restore the impaired host muscle function upon transplantation. Thus, two fundamental goals in skeletal muscle tissue engineering are parallel alignment of myotubes and a high degree of muscle maturity. With the notion that mechanotransduction plays a centralrole in myogenic differentiation [433], mechanical stimulation has been demonstrated to induce cellular alignment along the axis of strain [287, 414] and to stimulate muscle growth *in vitro* and *in vivo* [350, 1023]. While static mechanical stimulation is largely considered a trait related to induction of myogenic differentiation, inconsistent findings have been reported regarding the role of cyclic mechanical stimulation on signaling and myogenic marker expression, respectively [416, 456, 458, 1024].

For the generation of engineered biomimetic muscle constructs several strategies have been proposed. With regard to cellular alignment, micropatterned polymer surfaces offering precise control over scaffold nano- or microtopology have been used to promote guided myotube formation [331, 1025, 1026]. In terms of muscle maturity, electric stimulation has been demonstrated to enhance the contractile force of engineered muscle in two- and three-dimensional settings [467, 468, 477, 478]. In the past, diverse bioreactor systems enabling mechanical stimulation of cell-seeded scaffolds have been developed, serving as platforms that promote myotube alignment as well as muscle maturation. In an elegant approach, many of these systems make use of the contractile force that muscle cells generate upon differentiation: fixation of a scaffold between two anchor points creates predictable lines of isometric strain as the cells pull against the stationary posts. This cell-mediated internal tension has been shown to be sufficient to promote alignment along the principle axis of strain [287, 289, 293]. The majority of previously reported 3D skeletal muscle engineering approaches use scaffold anchoring as the primary source of strain to generate alignment, with the limitation that the extent and type of strain cannot be properly controlled.With the notion that provision of defined mechanical stimuli plays a central role in myogenesis, recent efforts in skeletal muscle engineering have focused on the development of bioreactors that allow for tunable mechanical stimulation [287, 295, 350, 415]. To generate biomimetic skeletal muscle constructs applying a physiologically relevant strain regime, we have designed a novel closed bioreactor system (MagneTissue) that allows for adjustable cyclic or static mechanical stimulation of cells embedded in a free standing ring-shaped fibrin matrix via strain transmission through magnetic force. With this system we sought to analyze the effect of a defined repetitive static stimulation protocol on cell alignment, morphology, myogenic differentiation and maturation of myotubes. Furthermore, we wanted to test whether application of static strain improves the myogenic outcome to a higher extent than scaffold anchoring. We demonstrate that, over a culture period of 9 days, static mechanical stimulation facilitates myoblast differentiation into a highly organized array of myotubes with widespread sarcomeric patterning and increased diameter compared to non-stimulated constructs. Moreover, we show that myogenic marker gene expression is enhanced when static strain is applied and generally follows a temporal physiological pattern, which demonstrates the high performance of the MagneTissue bioreactor system as a novel organotypic *in vitro* model for skeletal muscle tissue engineering.

2. MATERIALS AND METHODS

If not indicated otherwise, all chemicals and reagents were purchased from Sigma Aldrich (Vienna, Austria) and were of analytical grade. Primary antibodies for immunofluorescence stainings were anti-Myosin heavy chain (MHC) recognizing all MHC fast isoforms (Sigma Aldrich, Vienna, Austria) and

anti-Desmin (Cell Signaling, Cambridge, United Kingdom). Secondary antibodies labelled with Alexa Fluor 488 were purchased from Life Technologies (Lofer, Austria).

2.1. Cell culture

The mouse myoblast cell line C2C12 (American Type Culture Collection, Manassas, USA) was cultured in Dulbecco´s modified Eagle´s medium high Glucose (DMEM-HG; Life Technologies, Carlsbad, California), supplemented with 10% fetal calf serum (FCS; GE Healthcare, Buckinghamshire, United Kingdom), 1% penicillin/streptomycin (P/S; Lonza, Basel Switzerland) and 1% L-Glutamine (Lonza, Basel Switzerland). This medium will be referred to as growth medium (GM). Cells were grown on standard cell culture dishes (Starlab, Hamburg, Germany) in a humidified incubator at 37°C and 5% CO_2 and subcultured at 70-80% confluency to avoid induction of differentiation. Differentiation was induced by exchanging GM with DMEM-HG supplemented with 3% horse serum, 1% P/S and 1% L-Glutamine, referred to as differentiation medium (DM). Both GM and DM were supplemented with the fibrinolysis inhibitor aprotinin (Baxter, Deerfield, USA) at a final concentration of 100 KIU/mL for culture of cells in fibrin scaffolds.For 2D plastic control (cells cultured on standard cell culture dishes) and 2D fibrin control (cells cultured on top of a fibrin matrix; Fig. 30A and B, respectively) differentiation experiments, the same cell seeding densities ($5*10^5$ cells per well in a 6-well plate) were used. Furthermore, the same fibrin composition was used (20 mg/mL fibrinogen and 0.625 U/mL thrombin) for 2D culture and, subsequently, for the generation of the 3D fibrin constructs with embedded C2C12 mouse myoblasts.

2.2. Preparation and culture of fibrin rings

The clinically approved Tissucol Duo 500 5.0 ml Fibrin Sealant (Baxter, Illinois, USA) was used for preparation of the fibrin scaffolds. The scaffold molds (6 rings per mold) used to cast ring-shaped scaffolds (2 mm in diameter and 3 cm in length) were custom-made from either polyoxymethylene (POM) or stainless steel coated with Teflon (Fig. 27A). Fibrinogen was diluted to a concentration of 40 mg/mL with GM. Thrombin, diluted to 4 U/mL with 40 mmol/L $CaCl_2$, was homogeneously mixed with C2C12 cells in GM to a final concentration of 1.25 U/mL thrombin. 0.5 mL of the thrombin/cell suspension were mixed with 0.5 mL fibrinogen/GM solution and two scaffolds were cast immediately. The final concentrations for each scaffold were: 20 mg/mL fibrinogen, 0.625 U/mL thrombin and $3.2*10^6$ cells per scaffold (corresponding to $6.4*10^6$ cells/mL). After casting, the scaffolds were left to polymerize at 37°C and 5% CO_2 for 45 minutes. Fibrin rings of the unstrained or strained group were mounted onto a custom-made spool-hook system (Fig. 27B). All scaffolds were cultivated in 14 mL Snap-Cap Falcon tubes (BD Biosciences, Bedford, USA). Scaffolds were either kept floating in medium (control group; Fig. 27C) or were mounted onto the spool-hook system and stored in custom-made magnetic racks to keep them at 0% strain, representing the unstrained control group (Fig. 27D).

The same racks were used for the strain group until day 3 before they were applied to the MagneTissue bioreactor system for mechanical stimulation (Fig. 27E).
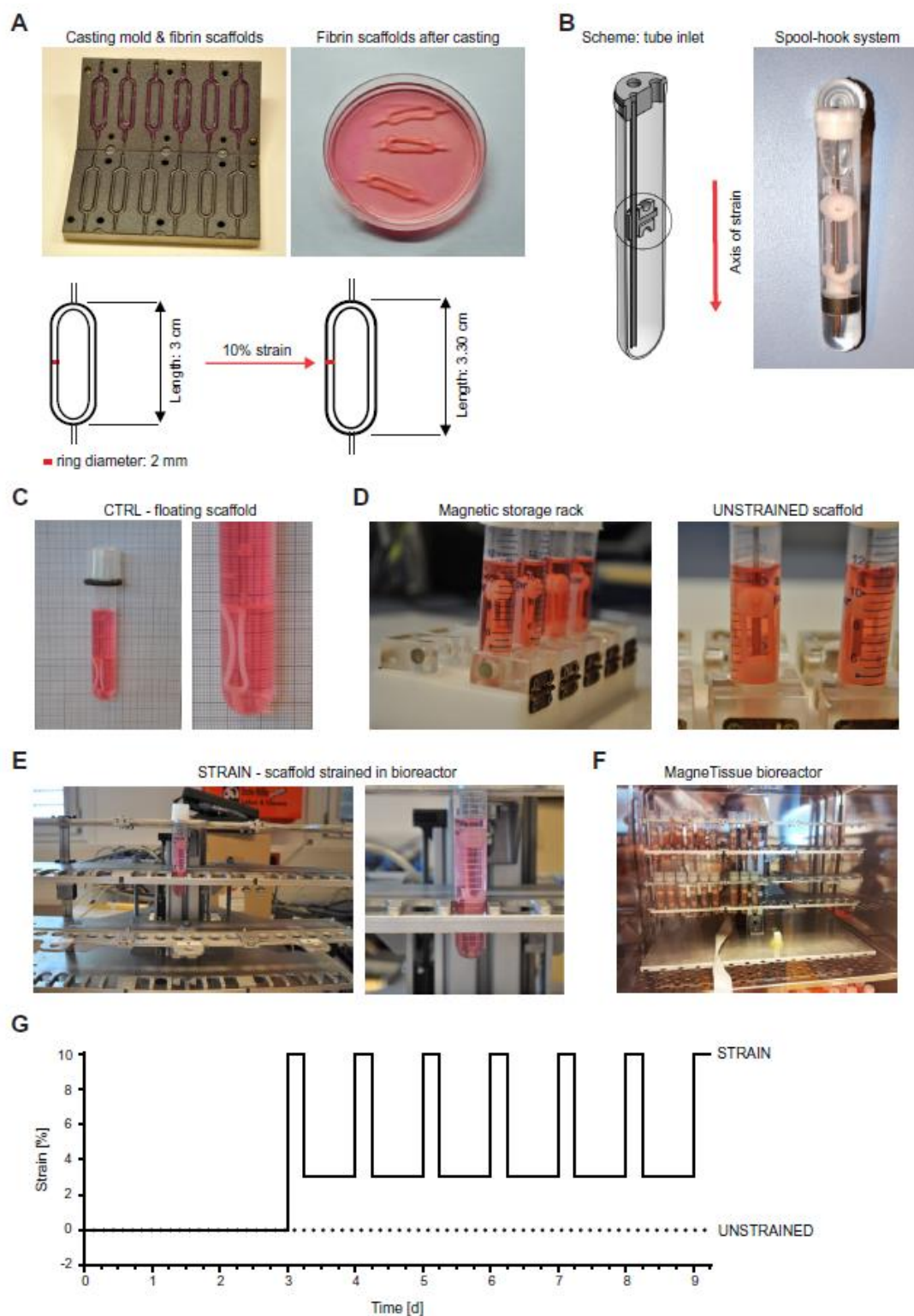

Fig. 27: *The MagneTissue bioreactor system.* A) Upper left: Teflon coated mold for scaffold preparation by injection. Upperhalf of the mold containing six freshly cast fibrin rings. Upper right: fibrin scaffolds released from the mold after polymerization. Below: Scheme displays proportions of the fibrin rings (3 cm in length and 2 mm in diameter) and the elongation during static mechanical stimulation. B) Left: custom-made tube inlet with the spool-hook system that fibrin rings are attached to. Right: scaffold mounted onto the spool-hook system before being stored in custom-made magnetic racks at

0% strain (UNSTRAINED group) or applied to the MagneTissue bioreactor for mechanical stimulation (STRAIN group). C) Representative image of controls (CTRL) -scaffolds embedded with C2C12 cells floating in medium. D) Left: custom-made magnetic rack for storage of unstrained samples over the whole culture period and for the strain group before applied to the bioreactor at day 3. Right: UNSTRAINED sample stored in magnetic rack receiving 0% strain. E) Representative image of STRAIN sample. At day 3 STRAIN samples are transferred from the magnetic rack to the bioreactor and subjected to the programmed strain protocol. F) Custom-made MagneTissue bioreactor system, where strain is applied via magnetic force transmission and parameters are controlled via custom-made software. G) The mechanical stimulation protocol: 3 days after construct preparation, 6 hours of static strain at 10% (exercise phase) followed by 18 hours at 3% (rest phase) are applied daily until the end of the culture period (day 9).

2.3. MagneTissue bioreactor system

The MagneTissue system is designed to fit into common cell incubators to guarantee a culture environment of 37°C and 5% CO_2. The bioreactor system has two superimposed rows holding the samples (Fig. 27E and F). Each row consists of a top sample holder plate which carries three tube cassettes for 6 samples each (36 samples in total) and a bottom plate containing permanent magnets which interact with the permanent magnets integrated into the hooks. By driving the bottom plate with a stepper motor the position of the hook is controlled contactless via magnetic force transmission. As a consequence, the relative movement of the bottom plate to the fixed top sample holder plate results in straining and/or relaxation of the fibrin samples. The mechanical part of the bioreactor system consists of a stepper motor which is mounted on an aluminum strut profile vertically to the bottom plate of the framework. The motor is integrated into a low profile linear axis (DryLin® SLN, igus GmbH, Cologne, Germany) in which it drives a ball-bearing spindle with a maximum driving torque of 0.1 Nm. To minimize torsion as a result of the applied movement a linear slide is mounted opposite to the motor linear axis. To control the movements of the stepper motor, controlled via the microcontroller ATmega16U2 (Atmel, San José, USA), an operator interface was programmed using MATLAB (The MathWorks GmbH, Ismaning, Germany). This software provides independent control of translational movements which can be set in mm up to resolutions of 10 μm. Furthermore, it allows the user to run cyclic motion patterns in number of cycles/min for the duration of an experiment. With the current set-up, movement speeds of 4 mm/sec can be realized. Hardware components for power supply and necessary modules for the motion control of the stepper motors are combined in a cubicle of electronic equipment.

2.4. Mechanical characterization of fibrin scaffolds

Tensile testswere performed using a Zwick BZ2.5/TN1S uniaxial material testing machine (Zwick GmbH & Co. KG, Ulm, Germany) with a 50 N load cell. Prior to testing, the scaffolds were equilibrated in 1x PBS for 24 hours and subsequently mounted on two spools – the same as used in the bioreactor system – for measurements. Samples were strained to failure at a rate of 20mm/min at room temperature and a relative humidity of 45–65%. Data was recorded after achieving a pre-load of 10 mN. To calculate the Young's modulus, the linear portion of the stress/strain curve was used.

Maximum clot firmness (MCF) was determined with rotational thromboelastometry (ROTEM) using a ROTEM© delta thromboelastometry system (TEM Innovations GmbH, Munich, Germany). Briefly, 300 µl of each fibrin formulation were used per measurement and the MCF was calculated live with the integrated ROTEM© delta software (build 1.6.0).

2.5. Mechanical stimulation of fibrin rings

At day 3 of culture mechanical stimulation in the MagneTissue bioreactor system was started by application of 10% static strain for 6 hours followed by an 18 hour rest phase at 3% static strain (Fig. 27G). This strain protocol was repeated for 6 days (including day 9). Furthermore, myogenic differentiation was induced by exchanging GM with DM supplemented with 100 KIU/mL aprotinin for 24 hours. From day 4 on, the media was partially changed every second day with GM supplemented with 100 KIU/mL aprotinin (5 mL new + 4 mL old medium).

2.6. Live/dead staining

At day 0, 3, 6 and 9 after scaffold preparation cell viability was assessed by staining the cells with CalceinAM and propidium iodide (PI). Whole fibrin rings were stained in serum free DMEM-HG medium containing 2.5 µg/mL CalceinAM and 1 µg/mL PI for 30 minutes at 37°C in the dark. The rings were analyzed with a Leica DMI6000B epifluorescence microscope (Leica Microsystems GmbH, Wetzlar, Germany).

2.7. Immunohistochemistry

Samples were fixed with 4% paraformaldehyde (PFA; Roth, Karlsruhe, Germany) for a maximum of 24 hours at 4°C. For immunofluorescence staining, the samples were permeabilized with Tris-Buffered Saline/0.1% (v/v) Triton X-100 (TBS/T), followed by a blocking step for 1 hour in PBS/T-1% (w/v) bovine serum albumin (BSA) at room temperature. Subsequently, the samples were incubated with the primary antibody at appropriate dilution in PBS/T-1% (w/v) BSA for 1 hour at 37°C (Desmin 1:100, MHC 1:400). After incubation with the primary antibody the samples were washed and incubated with the secondary antibody at appropriate dilution (1:400) in PBS/T-1% (w/v) BSA for 1 hour at 37°C. For nuclear visualization the samples were incubated with 4',6-Diamidino-2-phenylindole (DAPI) diluted 1:1000 in PBS for 10 minutes. All immunostained samples were analyzed on a Leica SP5 confocal microscope (Leica Microsystems GmbH, Wetzlar, Germany).

2.8. Scanning electron microscopy (SEM)

Samples were fixed with 2.5% formaldehyde for 2 hours at room temperature. After fixation, the fibrin rings were first cut into approximately 0.5 cm long pieces and then longitudinally for the characterization of the scaffold interior. Dehydration was performed using a graded ethanol series (40%, 50%, 60%, 70%, 80%, 90%, 100% for 15 minutes each) and sample incubation in a serial

dilution of hexamethyldisilazane (33%, 66%, 100% in ethanol absolute, for 1 hour each) was used for drying. Samples were mounted on aluminium stubs, sputter-coated with Pd-Au using a Polaron SC7620 sputter coater (Quorum Technologies Ltd., East Grinstead, United Kingdom) and examined with a JEOL JSM-6510 scanning electron microscope (JEOL GmbH, Eching/Munich, Germany).

2.9. Quantitative reverse transcription polymerase chain reaction (RT-qPCR)

At day 0, 3, 6 and 9 cells were harvested by digestion of fibrin rings in 1 mL of 100 U/mL nattokinase (Japan Bioscience Lab, California, USA) in PBS, pH 7.4 supplemented with 15 mmol/L ethylenediaminetetraacetic acid (EDTA) for 1 hour at 37°C under constant agitation, followed by total mRNA extraction using the peqGOLD total RNA Kit (VWR International GmbH, Erlangen, Germany). Per sample, 1 µg of mRNA was transcribed into cDNA with the DyNAmo cDNA Synthesis Kit (Life Technologies, Vienna, Austria). Quantitative PCR was performed with the KAPA Fast SYBR© Fast Universal Kit (VWR International GmbH, Erlangen, Germany) in a Stratagene© Mx3005P cycler (Agilent Technologies, Santa Clara, USA) in triplicates, using 10 ng of cDNA per reaction. Thermal cycle conditions were 5 minutes at 95°C, followed by 40 cycles of either 10 seconds at 95°C and 30 seconds at 60°C (*GAPDH*, *MyoD*, *TnnT1* and *Myf5*) or 30 seconds at 95°C and 1 minute at 60°C (*Myogenin*, *Desmin* and *Pax7*). Target cycle threshold (C_T) values normalized to the house keeping gene glyceraldehyde-3-phosphate dehydrogenase (GAPDH) were compared to corresponding values at each time point as well as day 0 for time dependent expression profiles using the comparative C_T ($\Delta\Delta C_T$) method. Primer sequences and primer concentrations used are listed in Table 3.

Target	Primer forward	Primer reverse	Primer conc. [nM]
GAPDH	AACTTTGGCATTGTGGAAGG	ACACATTGGGGGTAGGAACA	200
MyoD	ACTACAGTGGCGACTCAGAT	CCGCTGTAATCCATCATGCC	200
Myf5	TGACGGCATGCCTGAATGTA	GCTCGGATGGCTCTGTAGAC	200
TnnT1	AAACCCAGCCGTCCTGTG	CCTCCTCCTTTTTCCGCTGT	200
Myogenin	GGTCCCAACCCAGGAGATCAT	ACGTAAGGGAGTGCAGATTG	200
Desmin	AGAGGCTCAAGGCCAAACTAC	AGGGATTCGATTCTGCGCTC	200
Pax7	CGTAAGCAGGCAGGAGCTAA	ACTGTGCTGCCTCCATCTTG	400

Table 3: *Primer sequences and concentrations used for qPCR.*

2.10. Histological analysis

All histological analyses were performed with Fiji software [1027] from immunofluorescence confocal microscopy images taken at the end of the culture period (day 9). All samples were stained for MHC and nuclei were visualized with DAPI. Only MHC-positive cells containing three or more nuclei were rated as myotubes. The fusion index was calculated as the ratio of the number of nuclei in myotubes to the number of total nuclei in percent from images taken at 40x magnification. Myotube length and diameter measurements as well as myotube alignment analysis were performed with

images taken at 10x magnification. Myotube alignment was calculated as the angle between the long axis of a myotube and the axis of strain/mean orientation axis (defined as 0°), with the distribution of the respective percentage of myotubes shown in 15° angle deviation intervals. The width of an individual myotube was determined as the mean of 5 measurements taken at random positions perpendicular to the long axis at the respective position.Myotube length was determined only for myotubes containing 5 or more nuclei.

2.11. Statistical analysis

All data are presented as mean + standard deviation (SD) except for Figures 28A, 30G, 32B and C which are presented as box plots. For the relative expression of genes over time (Fig. 5) values are depicted as cubic spline curves. Normal distribution of data was tested with the D'Agostino & Pearson omnibus normality test. Comparisons between groups were calculated using One-way ANOVA with Tukey's multiple comparison test or Kruskal-Wallis test with Dunn's multiple comparison test and P-values ≤ 0.05 were considered as statistically significant. All calculations were performed using GraphPad Prism Software (GraphPad Software Inc., SanDiego, USA).

3. RESULTS

3.1. Preparation of fibrin rings and viability of 3D muscle constructs

Myogenic differentiation is highly affected by the mechanical properties of the biomaterial. Therefore, stiffness of different fibrin formulations was initially measured to find a fibrinogen concentration that yields scaffolds mimicking the stiffness of skeletal muscle which has been demonstrated to approximately range from 8 to 17 kPa [355]. Four different fibrinogen concentrations were used ranging from "soft" to "stiff" (10, 20, 30 and 40 mg/mL) and subjected to mechanical testing (Fig. 28A, left). Fibrinogen concentrations of 10 and 20 mg/mL displayed an averageYoung's modulus of 11.57 and 17.21 kPa, respectively, whereas higher concentrations (30 and 40 mg/mL) exceeded the modulus considered optimal for myogenesis (24.53 kPa and 31.27 kPa, respectively; Fig. 28A, middle). Although a fibrinogen concentration of 10 mg/mL seemed ideal, stiffer fibrin scaffolds (20 mg/mL fibrinogen) were used in this study, as the casting process was more reliable and the scaffolds more stable. Additionally,varying the thrombin concentration does not alter fibrin stiffness, as this is directly proportional to the fibrinogen concentration (Fig. 28A, right).

For the generation of 3D skeletal muscle constructs, we prepared ring-shaped fibrin scaffolds in which cells were homogenously distributed (representing day 0). For the following 2 days the scaffolds with embedded cells were either kept floating in media (control group, Fig. 27C) or assembled onto the spool-hook system and stored in a magnetic rack - representing the unstrained control group (Fig. 27D) and the strained group (Fig. 27E). This initial period was chosen as to allow cell adaption to their

new environment and propagate further proliferation, as cell density is a crucial factor for proper myoblast fusion and differentiation [353].
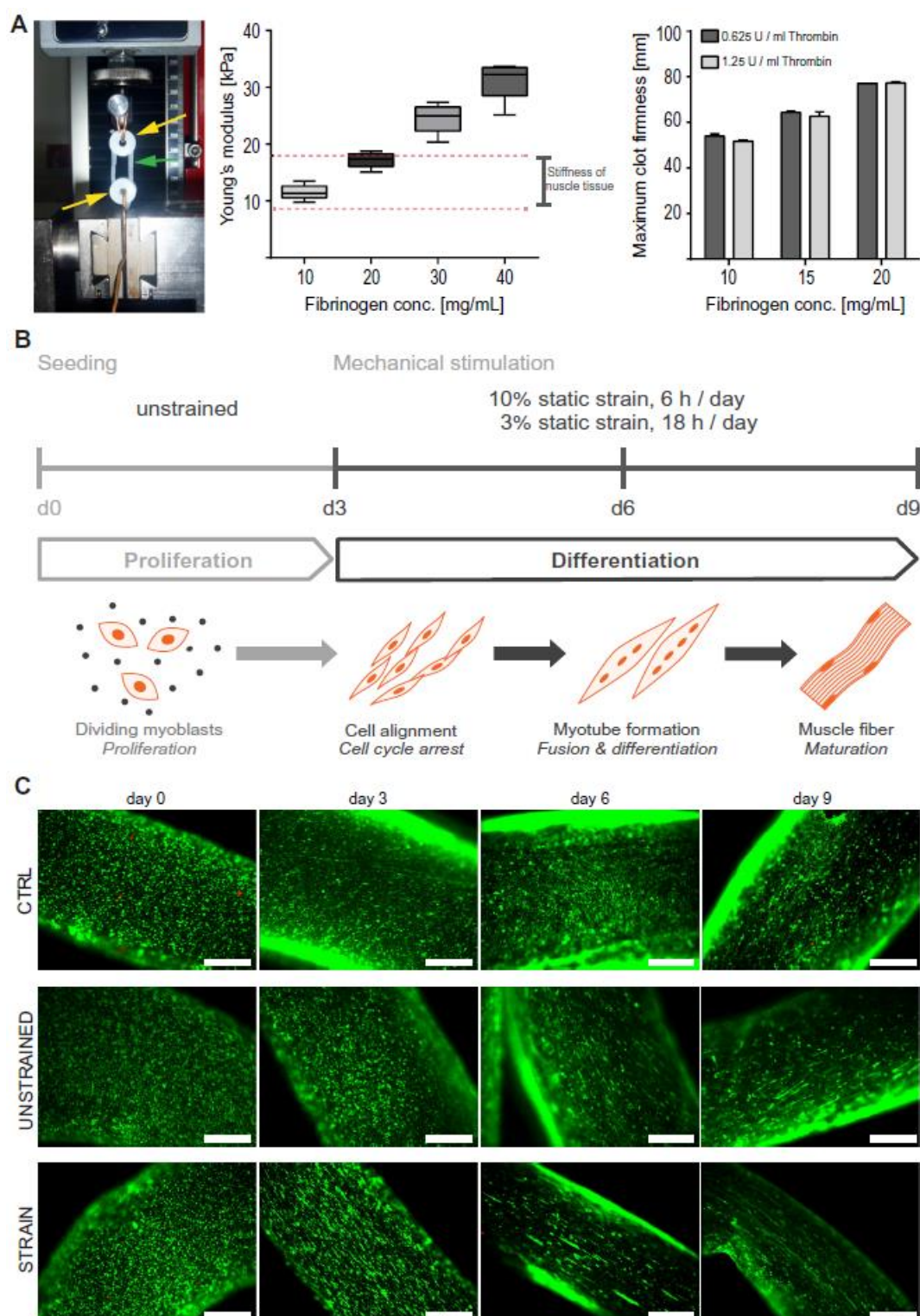

Fig. 28: *Scaffolds mimic the mechanical properties of native skeletal muscle and viability is not impaired in 3D cell-scaffold constructs.* A) Left: Representative image of mechanical test setup for fibrin scaffolds. Fibrin rings are mounted onto the same spools as used in the bioreactor. Yellow arrows – spools; green arrow – fibrin ring. Middle: Box plots depict the Young's modulus of scaffolds with increasing fibrinogen concentrations as indicated ($n = 5$). The Young's modulus within the red dashed lines marks the range of the stiffness of skeletal muscle as proposed in [355]. Right: Maximum clot firmness

of fibrinogen and thrombin concentrations as indicated was measured using ROTEM (n = 3; mean + S.D. (error bars)). B) Schematic representation of experimental design and working hypothesis. At day 0, ring-shaped fibrin scaffolds with embedded cells are cast and either assigned controls (floating in medium), unstrained samples (assembled on spool-hook system and kept at 0% strain) or strain samples (assembled on spool-hook system receiving static strain). The first two days, cells in scaffolds were allowed to recover from encapsulation and to proliferate. At day 3, the first round of 10% static strain for 6 hours was applied to the strain group followed by a rest phase of 18 hours at 3% strain. This stimulation protocol was repeated daily until inclusively day 9. During the culture period the cells started to align and withdrew from the cell cycle, followed by fusion and differentiation into myotubes. C) CalceinAM (green) / PI (red) staining was performed at day 0, 3, 6 and 9 in controls, unstrained and strained rings to assess viability and morphological changes over time. Scale bars represent 500 µm. CTRL = control, UNSTRAINED = unstrained rings, STRAIN = strained rings.

At day 3 differentiation was initiated and a daily static mechanical stimulation protocol consisting of 6 hours at 10% strain followed by 18 hours at 3% strain was performed for the strain group (Fig. 27E and G) until the end of the culture period (Fig. 28B). The rationale behind this protocol was to induce cell alignment in order to facilitate directed myotube formation in combination with a physiological mechanical stimulus to promote myogenic differentiation and maturation.

We assessed viability of the cells embedded in the fibrin rings by CalceinAM and PI staining (Fig. 28C). Over the culture period of 9 days viability was not impaired in any experimental group. Additionally, the macroscopic appearance of cells in the strained constructs at day 3 demonstrated a higher degree of alignment already after the first cycle of static stimulation, whereas in the control and unstrained group no such phenomena were observed. Alignment was even more prominent at day 6 and 9 in the strain group, compared to partial alignment of the cells in the unstrained and random orientation in the control group (Fig. 28C). Putative myotube formation could be observed from day 6 on in the strain group highlighted by the presence of elongated structures of CalceinAM-positive cells (Fig. 28C, lower panel). These data demonstrate that our experimental setup as well as the chosen composition of the biomaterialand the extent of static strain were appropriate as viability was not impaired and first morphological changes due to mechanical stimulation were observed.

3.2. Static strain induces fibrin fibril alignment and cellular orientation

To gain deeper insight into the effects of static mechanical stimulation in our system and how it affects fibrin and the incorporated cells, SEM analysis was performed at different time points. First, we analyzed the effect of a single round of stimulation of 6 hours at 10% strain. Fibrin fibrils of control and unstrained samples displayed random orientation whereas in strained samples fibril alignment along the axis of strain was highly increased (Fig. 29A, left). As expected, application of strain resulted in thorough cellular alignment compared to control samples where this effect was not observed. Unstrained samples, however, displayed altered cellular morphology compared to the controls, with partially aligned cells as a result of scaffold anchoring (Fig. 29A, right). On day 9, scaffold microstructure was similar to day 3, with random fibril orientation in the control and unstrained groups and preserved alignment in the strain group (Fig. 29B, left). In contrast to control

samples, both unstrained and strained samples showed a higher degree of cellular alignment (Fig. 29B, right).
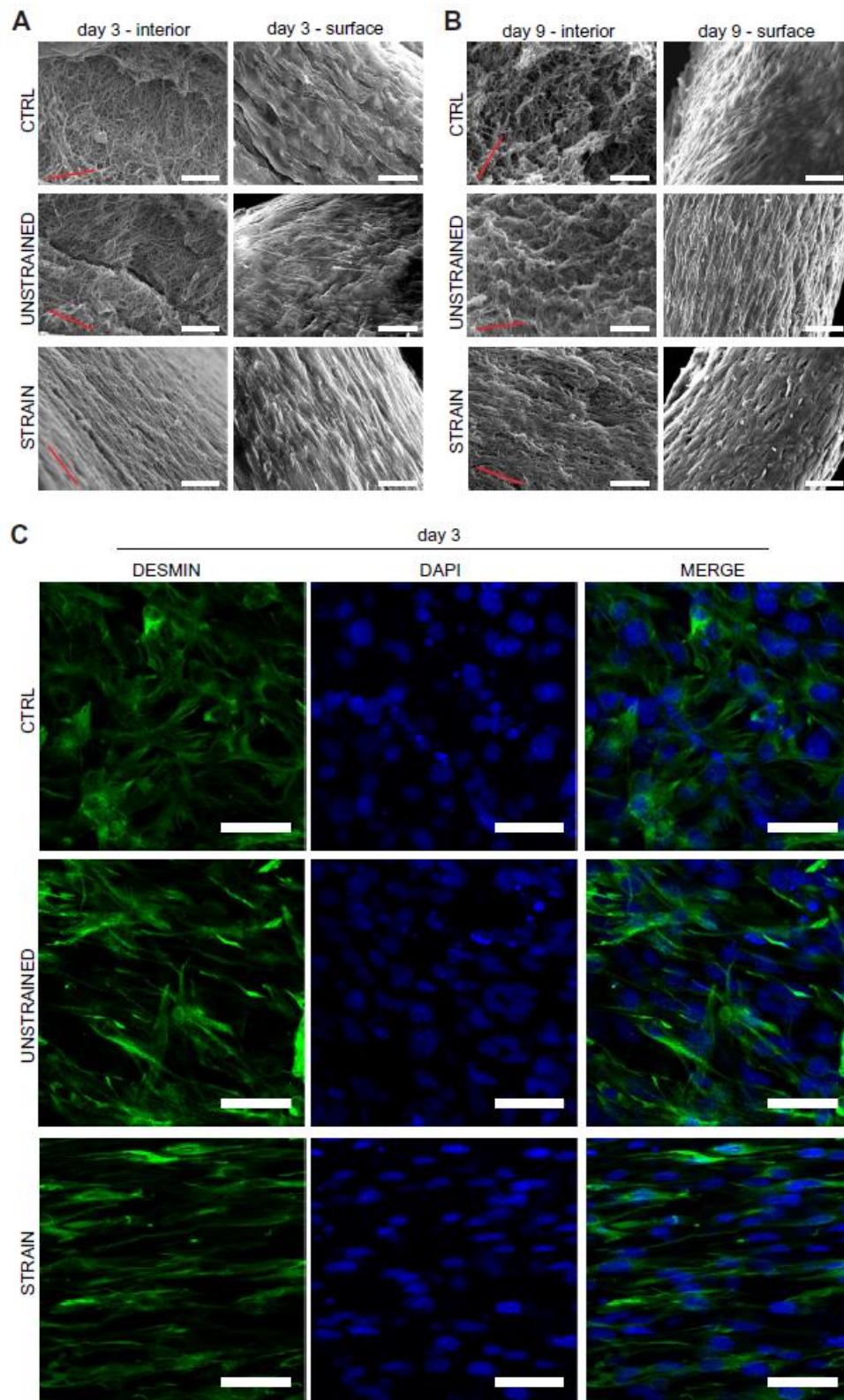

Fig. 29: *Mechanical strain leads to uniaxial fibrin fibril alignment and affects cell orientation.* A) To visualize changes in fibril alignment of the scaffolds after one round of mechanical stimulation (10% for 6 hours) at day 3, control, unstrained and strained samples were fixed and subjected to SEM analysis. Representative images of the interior (left) and surface (right) of

the scaffolds are shown. Red bars indicate mean orientation axis. B) Control, unstrained and strained rings were fixed after the last round of mechanical stimulation at day 9 and SEM imaging was performed. Representative images of the interior (left) and surface (right) of the scaffolds are shown. Red bars indicate mean orientation axis. C) Control, unstrained and strained fibrin rings after one round of 10% static strain for 6 hours at day 3. Scaffolds were fixed after mechanical stimulation was completed (STRAIN) along with the controls and the unstrained samples and subsequently stained for Desmin (green, left). A nuclear counterstain with DAPI (blue, middle) was performed. Scale bars represent 5 µm (A, B left panel) and 50 µm (A, B right panel; C), respectively. CTRL = control, UNSTRAINED = unstrained rings, STRAIN = strained rings.

Repeated cycles of static strain resulted in preservation of fibril alignment, as the interior and the surface of strained fibrin rings displayed overall uniaxial fibril and cell alignment at the end of the culture period. Scaffold anchoring (unstrained group) did not elicit changes in fibrin microstructure, nevertheless it promoted cellular alignment over time. In order to characterize if the observed strain-induced effect on the biomaterial was directly translated to the cells we performed immunofluorescence staining for the structural muscle marker Desmin [1028, 1029]. As expected, no noticeable changes in alignment were present in floating control samples, whereas unstrained samples displayed aligned cells to some extent. In contrast, one cycle of stimulation already had a thorough effect on the morphology and alignment of the cells. Static strain at 10% for 6 hours resulted in pronounced cell alignment, with elongated cells oriented in the direction of strain. Moreover, this effect was accompanied by the transition of nuclear morphology from a round to a stretched shape, a strong indicator for cellular polarity [1030] (Fig. 29C).

3.3. Repetitive static mechanical stimulation promotes myotube formation in a highly oriented manner

In order to substantiate the hypothesis that our repetitively applied static strain protocol enhances myogenic differentiation, myotube formation and alignment were analyzed after 6 days of stimulation. In general, mouse myoblasts differentiated on tissue culture dishes readily form multi-nucleated myotubes, however, with a high degree of myotube branching and random orientation (Fig. 30A). Myotube branching was not observed when myoblasts were differentiated on top of a fibrin substratum (20 mg/mL fibrinogen and 0.625 U/mL thrombin) for 6 days. In addition, a higher degree of sarcomeric patterning was evident compared to the 2D tissue culture plastic control (Fig. 30B). This effect is linked to the matrix properties as striations have been shown to primarily develop on substrates with a stiffness comparable to native muscle [356]. Looking at the situation in 3D, we observed that in all three experimental conditions myoblasts differentiated to MHC-positive myotubes until day 9. However, similar to the results obtained from the 2D differentiation experiments (Fig. 30A and B), myotubes from the control group were randomly oriented. In comparison, the unstrained samples exhibited a higher degree of myotube alignment with an increased fraction of elongated nuclei. The strain group demonstrated that the applied static mechanical stimulation protocol led to the

formation of highly aligned myotubes which appeared to be thicker compared to their control counterparts (Fig. 30C).
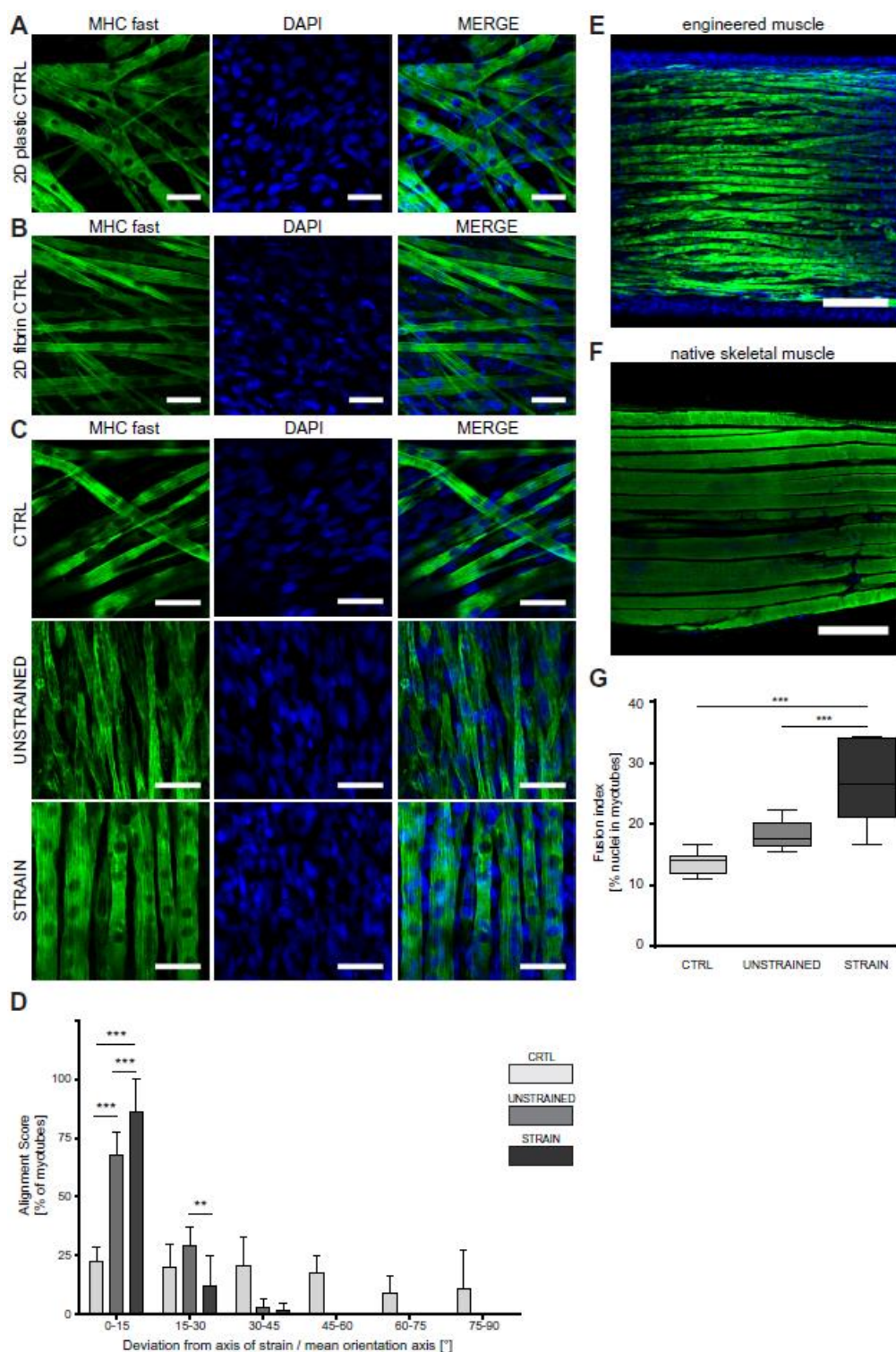

Fig. 30: *Application of strain promotes alignment of myotubes and augments myocyte fusion as well as muscle differentiation on the morphological level.* A) Cells grown on cell culture plastic serving as 2D controls were differentiated for 6 days and then stained for MHC fast (green, left) and a nuclear counterstain with DAPI (blue, middle) was performed. B) Cells were grown on top of a fibrin matrix with the same composition as in the 3D constructs and differentiated for 6 days. Myotubes were then stained for MHC fast (green, left) and a nuclear counterstain with DAPI (blue, middle) was performed. C) Control,

unstrained and strained fibrin rings after 7 rounds of static mechanical stimulation and 6 days of differentiation were fixed at day 9. Whole rings were stained for MHC fast (green, left) and a nuclear counterstain with DAPI (blue, middle) was performed. D) Alignment score giving the deviation of the long myotube axis from the axis of strain/mean orientation axis at day 9 calculated for control, unstrained and strained fibrin rings. Values are given in % (n = 9 of three independent experiments; mean + S.D. (error bars); **, p < 0.01; ***, p < 0.001; one-way ANOVA with Tukey's multiple comparison test). E) Strained fibrin rings at day 9 were stained for MHC fast (green) and DAPI for nuclear counterstain (blue). Overlay image is shown. F) Longitudinal section of a native mouse skeletal muscle (adductor femoris) stained for MHC fast (green) and DAPI for nuclear counterstain (blue). Overlay image is shown. G) The fusion index, representing the percentage of nuclei within myotubes relative to total nuclei, was analyzed at day 9 for all three experimental groups (n ≥ 7 of three independent experiments with more than 1000 nuclei analyzed per group; ***, p < 0.001; one-way ANOVA with Tukey's multiple comparison test). Scale bars represent 50 µm (A-C) and 250 µm (E-F), respectively. CTRL = control, UNSTRAINED = unstrained rings, STRAIN = strained rings.

Notably, sarcomeric patterning of myotubes in the strain group was more pronounced, indicating a higher degree of maturity (see also Fig. 32). To further characterize the qualitatively observed morphological findings the overall myotube alignment was quantified (Fig. 30D). More than 85% of all analyzed myotubes in the strain group were aligned in the direction of strain and the residual 15% showed a 15-30° deviation from the axis of strain. Approximately 70% of all myotubes analyzed in the unstrained group did not deviate more than 15° from the axis of strain, about 25% were 15-30° off and a very small percentage was 30-45° off. In comparison to these two groups the myotubes of the control group displayed deviations from the axis of strain/mean orientation axis at all angles, confirming random orientation (Fig. 30D).

Macroscopically, application of static mechanical strain for 6 days led to the generation of a construct consisting of a densely packed array of parallel myotubes reaching lengths of approximately 1mm (Fig. 30E), which mirrors essential characteristics of native muscle tissue (Fig. 30F). In order to quantify the efficiency of myotube formation the fusion index was determinedat the end of the culture period. The application of strain led to a significant increase in myocyte fusion compared to the control as well as to the unstrained group. The fusion index of controls was 15%, 20% in the unstrained group and reached 30% in the strain group, which roughly corresponds to a 2-fold and a 1.7-fold increase in myocyte fusion compared to the control and to the unstrained control, respectively (Fig. 30G).

3.4. Static strain significantly enhances expression of myogenic markers and highly improves muscle differentiation

With the notion that static strain appeared to strongly augment myogenic differentiation morphologically, we also tracked transcriptional levels of muscle specific marker genes over time with RT-qPCR to elucidate the performance of the bioreactor system in a more thorough manner. We chose to analyze a combination of early (*Pax7, Myf5, MyoD*), mid (*Myogenin*) and late stage-

specific/structural (*TnnT1, Desmin*) myogenic markers to observe the effects of static strain in the cascade of myogenic specification, differentiation and maturation.

Paired box homeodomain gene *Pax7* is an upstream transcriptional regulator of all four myogenic regulatory factors (MRFs) and essential for the activation of satellite cells and their commitment to the myogenic lineage by induction of *MyoD* [120, 1031]. *Pax7* has been shown to be highly expressed in activated satellite cells as well as, at low levels, proliferating myoblasts and is downregulated as the cells differentiate [121, 1032]. After the onset of differentiation (day 3), this downregulation was observed in all three treatment groups (Fig. 31A, right graph). Surprisingly, compared to the control, *Pax7* expression was slightly upregulated in the unstrained and, to a higher extent, in the strain group which received one cycle of static strain for 6 hours at 10% at day 3 before induction of differentiation (Fig. 31A, left graph). Although *Pax7* expression was expectedly downregulated during differentiation the strain group seemed to keep elevated *Pax7* levels compared to the control groups until day 9 (Fig. 31A, left graph). *Myf5*, *MyoD*, and *Myogenin* are basic helix loop helix transcription factors that belong to the MRFs [1033], with *Myf5* and *MyoD* required for myoblast determination and *Myogenin* essential for terminal differentiation into myotubes [1034]. The three MRFs peak in a temporal manner, with *Myf5*, although moderately expressed, being the first at day 3 (Fig. 31B, right graph) followed by both *MyoD* (Fig. 31C, right graph) and *Myogenin* (Fig. 31D, right graph) that peak at day 6. In comparison to the control and the unstrained group, application of static strain resulted in slightly higher expression of *Myf5* (Fig. 31B, left graph). *MyoD* on the other hand was influenced later than *Myf5* (Fig. 31C, right graph). By day 6, a gradual significant increase in *MyoD* expression could be observed in the unstrained (~1.5-fold) and the strain group, with the strain group displaying an approximately 1.8 – 2-fold induction compared to the control (Fig. 31C, left graph). This effect might be directly linked to the observed upregulation of both *Pax7* and *Myf5* – two transcription factors acting upstream of *MyoD* - at the onset of differentiation [1035]. *Myogenin* expression has been shown to be upregulated after the induction of *Myf5* and *MyoD* [1036] and did not differ on day 3 between the different experimental groups. However, after 3 days of differentiation (day 6) *Myogenin* expression was almost 1.6-fold increased in the strain group compared to the control group and 1.4-fold increased compared to the unstrained group. At day 9 the expression of the unstrained group and the strain group compared to the control remained elevated 1.7-fold and 2-fold, respectively (Fig. 31D, left graph), even though *Myogenin* expression in general peaked after 3 to 4 days of differentiation (Fig. 31D, right graph).

A very important aspect of skeletal muscle tissue engineering is the development of functional muscular ultrastructure. Thus, we analyzed the expression of two different structural marker genes, *Desmin* and *Troponin T1*(*TnnT1*). Desmin, a muscle-specific intermediate filament, is one of the earliest structural genes expressed in myogenesis and already expressed in satellite cells and proliferating myoblasts [1028]. Desmin filaments encircle the Z-disk, holding the actin filaments together and hence play a fundamental role in transmitting tension throughout the myofibril [1029].
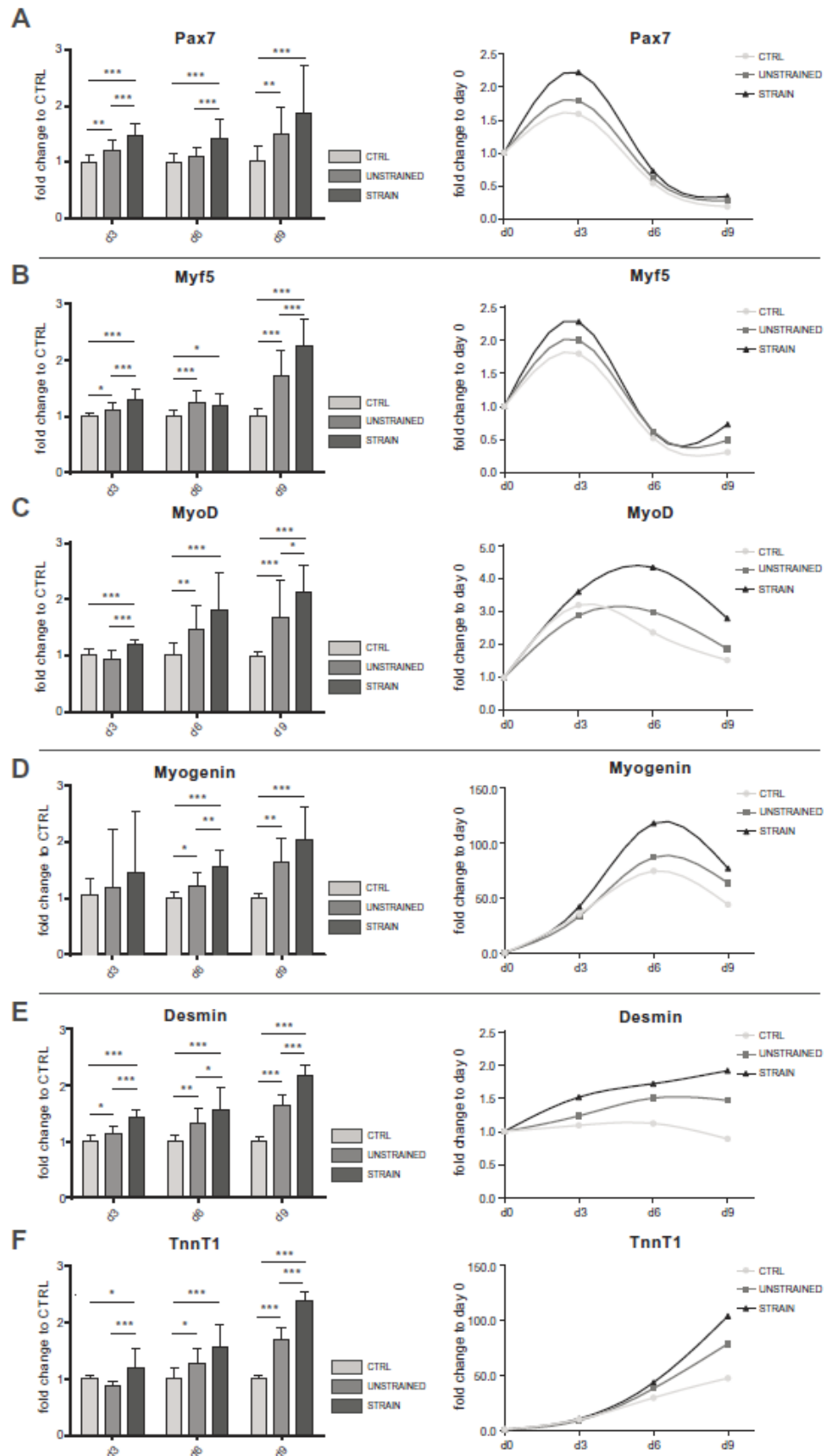
Fig. 31: *Mechanical strain enhances expression of early, mid and late stage-specific myogenic markers.* Total mRNA was isolated and RT-qPCR for a set of myogenic marker genes was performed. Bar graphs (left) depict fold change of expression levels normalized to controls at the indicated timepoints. Cubic spline curves (right) show relative expression over time, with fold induction normalized to day 0 within each group (n = 6 in triplicates of two independent experiments; mean + S.D. (error

bars); *, p < 0.05; **, p < 0.01; ***, p < 0.001). A) *Pax7* expression levels. One-way ANOVA with Tukey's multiple comparison test (day 3 and day 6) or Kruskal-Wallis test with Dunn's multiple comparison test (day 9). B) *Myf5* expression levels. One-way ANOVA with Tukey's multiple comparison test (day 3 and day 9) or Kruskal-Wallis test with Dunn's multiple comparison test (day 6). C) *MyoD* expression levels. One-way ANOVA with Tukey's Multiple comparison test (day 3 and day 9) or Kruskal-Wallis test with Dunn's multiple comparison test (day 6). D) *Myogenin* expression levels. Kruskal-Wallis test with Dunn's multiple comparison test. E) *Desmin* expression levels. One-way ANOVA with Tukey's multiple comparison test. F) *TnnT1* expression levels. One-way ANOVA with Tukey's multiple comparison test (day 3 and day 9) or Kruskal-Wallis test with Dunn's multiple comparison test (day 6). TnnT1 = Troponin T1; CTRL (light grey) = control, UNSTRAINED (middle gray) = unstrained rings, STRAIN (dark gray) = strained rings.

Desmin was significantly higher expressed in the strain group (at day 6 1.5-fold and more than 2-fold at day 9) compared to unstrained samples and controls (at day 6 1.3-fold and more than 1.5 fold on day 9; Fig. 31E, left graph). Overall, *Desmin* expression levels remained rather constant over time, with a moderate induction in the unstrained group and a more thorough induction when static strain was applied (Fig. 31E, right graph). *TnnT1* is the tropomyosin binding subunit of the troponin complex and as such plays an important role in Ca^{2+}-induced striated muscle contraction [1037, 1038]. Analysis of *TnnT1* therefore delivers an important read-out for the functionality and maturity of skeletal muscle tissue [1038]. On day 9, *TnnT1* expression was significantly enhanced in the strain group compared to the control (2.5-fold increase), while the unstrained group displayed an increase of almost 1.75-fold compared to the control (Fig. 31F, left graph). Over the culture period of 9 days, *TnnT1* relative expression levels increased in all three experimental groups (Fig. 31F, right graph).

In accordance with the results of the morphological analysis the qPCR data demonstrated that: i) myogenesis was not impeded in the 3D fibrin-cell scaffolds, as myotube formation could readily be observed in the controls and myogenic expression patterns progressed normally, with temporal regulation; ii) unstrained scaffolds (resembling anchored scaffolds) displayed a better performance morphologically as well as on the gene expression level compared to controls, due to contractile force generation in combination with scaffold polarity [293, 1026, 1039]; iii) with the application of static strain (10%) for 6 hours daily followed by a rest phase (3%) for 18 hours this effect could be markedly enhanced and led to significantly better alignment and higher expression levels of an essential set of myogenic markers in regard to induction of differentiation and myotube formation.

3.5. Application of static strain enhances muscle maturity

After we demonstrated an improvement in alignment and enhanced differentiation on the morphological and molecular level when strain was applied, we wanted to find out whether this induction was also linked to enhanced myotube maturity. Immunostaining for MHC and subsequent qualitative morphological analysis revealed a much higher occurrence of sarcomeric patterning in myotubes of the strain group (Fig. 32A), a structural feature directly linked to contractile force, indicating a higher degree of maturity. As myotubes appeared to be thicker when strain was applied (Fig. 30C, lower panel), myotube length and diameter were determined. In accordance with previously

published studies [350, 1040], unstrained constructs displayed enhanced myotube length and diameter compared to controls. However, this effect was further increased when strain was applied, as myotubes in the strain group were significantly thicker (~20%) and longer (~30%) than in unstrained samples, with myotubes reaching a maximum length of 1 mm (Fig. 32B and C).
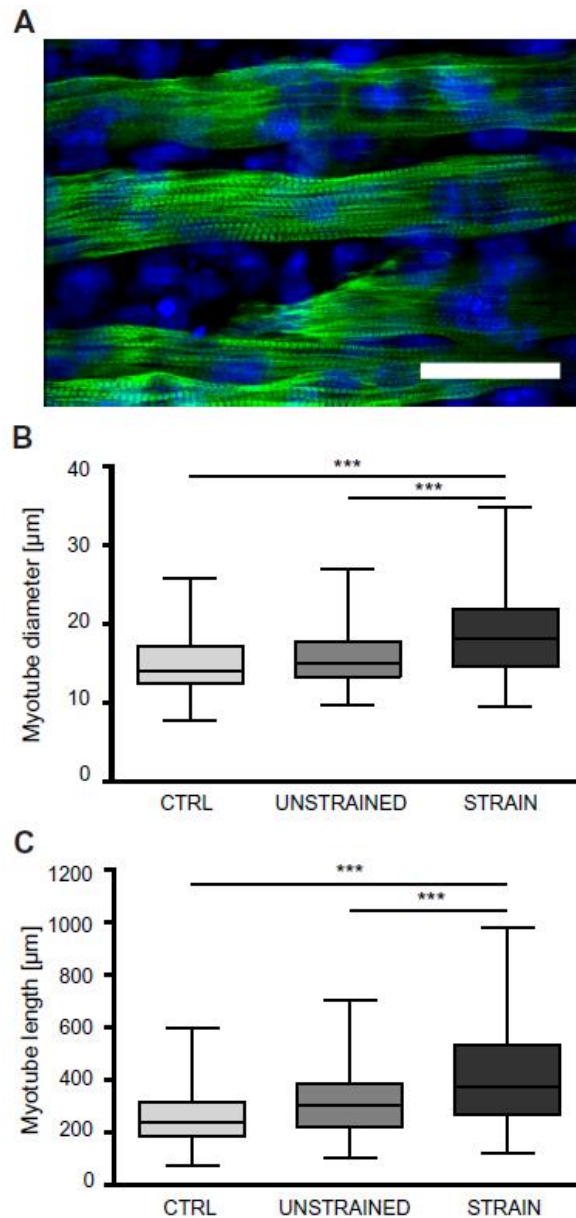

Fig. 32: *Static strain improves sarcomeric patterning and increases myotube length and diameter – three indicators for muscle maturity.* A) Representative immunofluorescence image of a strained sample at day 9 stained for MHC fast (green) and DAPI for nuclear counterstain (blue). Overlay image is shown. Scale bar represents 50 µm. B) Quantification of myotube diameter at day 9 (n ≥ 8 of three independent experiments with at least 146 myotubes per group analyzed; ***, p < 0.001; Kruskal-Wallis test with Dunn's multiple comparison test). **C)** Quantification of myotube length at day 9 (n ≥ 7 of three independent experiments with at least 202 myotubes per group analyzed; ***, p < 0.001; Kruskal-Wallis test with Dunn's multiple comparison test). CTRL = control, UNSTRAINED = unstrained rings, STRAIN = strained rings.

Altogether, these findings strongly support the hypothesis that static mechanical stimulation positively affects *in* vitro myogenesis on several levels: a higher degree of alignment promotes parallel myotube formation accompanied by enhanced gene expression levels of early, mid and late stage-specific marker genes which ultimately yields muscle constructs with a highly aligned array of myotubes displaying increased maturity.

4. DISCUSSION

Despite recent advances in the field of musculoskeletal tissue engineering, the *in* vitro generation of skeletal muscle constructs with structural and functional characteristics comparable to those *in* vivo is still a major challenge to overcome. Thus, scientists still seek feasible strategies to obtain mature, long, functional muscle fibers in volumetric constructs, with proper vascularization and innervation of the tissue. Proposed approaches to engineer muscle (-like) tissue range from scaffold anchoring [289, 293, 1039] or micropatterning of biomaterials for guided myotube formation [468, 1041, 1042] to electrical [467, 468, 475, 477, 478] or mechanical stimulation in bioreactorsin 2D [427, 458, 480, 1024, 1043] and 3D settings [287, 295, 350, 407, 414, 488, 1044, 1045]. However, while there is a clear consent in the field concerning the necessity for mechanical stimulation in 3D skeletal muscle tissue engineering, not all available systems offer programmable and individually adjustable control over strain parameters.Thus, software-controlled systems capable of applying tunable strain regimes (ramp, cyclic and static) are emerging as a very promising approach [287, 350, 415, 426, 1046].

With regard to the current limitations in skeletal muscle tissue engineering [407], we have established a custom-made closed bioreactor system (MagneTissue) which applies mechanical strain in a cyclic, static or ramp manner to cells embedded in a fibrin matrix via magnetic force transmission. Our results indicate that application of 10% static strain for 6 hours followed by a rest phase at 3% led to vastly improved alignment of both the biomaterial and the cells. As a consequence, myoblasts fused along the axis of strain in a highly ordered manner, resulting in a parallel array of myotubes with increased size and more pronounced sarcomeric patterning compared to controls. Additionally, our qPCR data verified static mechanical stimulation as an essential and potent regulator of early myogenesis, as structural genes important for muscle function and contractility were significantly upregulated when strain was applied, emphasizing the importance of mechanotransduction in muscle tissue engineering [433].

Choosing a biomaterial whose mechanical properties mimic those of skeletal muscle tissue is crucial for myogenic differentiation. Fibrin hydrogels are, to some extent, tunable in regard to stiffness, pore size, degradability and fibril diameter [579, 600, 742, 1021, 1039]. In contrast to other approaches using rather low fibrinogen to thrombin ratios [293, 295, 468, 1026], we chose a higher ratio (20 mg/mL fibrinogen, 0.625 U/mL thrombin) in our experimental setup for several reasons: i) the

stiffness is directly proportional to the fibrinogen concentration. The obtained constructs displayed a Young's modulus of about 17 kPa, which lies within the stiffness range proposed to be most suitable for myogenic differentiation [355, 356, 1047]; ii) the fibrinogen to thrombin ratio directly correlates with permeability and pore size as well as the ultimate tensile strength of the scaffold [1021]; iii) lower thrombin concentrations give slower clotting times, increasing the homogeneity of the fibrin meshwork, and have less detrimental effects on cell viability [1048].

After testing different mechanical stimulation protocols in preliminary experiments we found that a static strain period of 10% for 6 hours followed by 18 hours at 3% gave optimal results in terms of cell alignment, myoblast fusion, myogenic differentiation and myotube maturity. The rationale behind this stimulation protocol is to mimic *in vivo* muscle development during embryogenesis. Due to its attachment to bone, nascent muscle is subjected to strain as a consequence of bone growth, which is supposed to facilitate myofiber alignment and augment muscle maturation. This strain was calculated to be approximately 2–3% [414, 1049], therefore we used a stimulation of 3% as baseline strain for the constructs. Additionally, we added a daily strain period of 10% for 6 hours to provide a simulated isometric exercise stimulus. 6 hours of static stimulation have been demonstrated to lead to a thorough induction of signaling pathways related to myogenic differentiation (ERK, p38MAPK, AKT) on one hand and to the activation of a subset of key myogenic differentiation markers like *Myocyte Enhancer Factor 2C (MEF2C)*, *Myogenin* or *MHC* on the other [1043]. These data support our mechanical stimulation parameters of 3% and 10% alternating static strain per day as we could also show an improved myogenic outcome demonstrated by enhanced myogenic marker induction in response to strain (Fig. 30 and 31). A difference to other recently published approaches is that we do not apply cyclic strain to the constructs. The application of cyclic stimulation might also be a potent stimulus, however, previous reports indicate rather contradictory outcomes ranging from improved myogenic differentiationto enhanced proliferation and impaired muscle formation [416, 456, 458, 1024, 1044]. In preliminary studies we tested different mechanical stimulation protocols such as 1 hour of cyclic or static strain. We found that the primary response of the cells to cyclic stimulation was a delayed onset of myogenic differentiation (data not shown). On the contrary, 1 hour of static strain daily from day 3 on improved myogenesis but not to the same extent as with our current stimulation protocol. A combination of first cyclic then static strain (data not shown) could also not compete with the myogenic outcome achieved with 6 hours 10% static strain and 3% strain at rest phase.Thus, we hypothesize that, in early stages of muscle differentiation, uniaxial static strain is superior to cyclic strain as it more closely recapitulates the native situation in muscle development and growth [414, 1049]. Nevertheless, there is substantial evidence that cyclic strain might act as an upregulatory stimulus for muscle hypertrophy and maturation at later stages of myogenesis, when myotubes have already formed [350].

Our gene expression data demonstrate that myogenesis within the constructs follows a temporal sequence in accordance with the proposed induction pattern of myogenic markers during

differentiation [60]. However, we obtained interesting results regarding the expression of *Pax7*. C2C12 cells are a rhabdomyosarcoma-derived myoblast line and only weakly express *Pax7* [74]. Even though the precise role of *Pax7* is still under debate, induction of *Pax7* expression is largely considered a unique property of quiescent satellite cells re-entering the cell cycle [1050]. This process is stimulated by injury or exercise such as strain *in vivo,* as well as by culture in mitogen rich media *in vitro* [1051]. It is known that satellite cells undergo rapid proliferation concomitant with an upregulation of *Pax7* before initiation of differentiation (accompanied by upregulation of myogenin) [31]. Assuming that C2C12 myoblasts behave similar to satellite cells it can be speculated that culture of the cells embedded in fibrin could have a beneficial effect on proliferation compared to cell culture plastic. This might account for the global increase of *Pax7*expression between day 0 and day 3 of culture in all treatment groups. The increase in *MyoD* expression that is observed between day 0 and day 3 in all groups supports this theory, as proliferating satellite cells are characterized by co-expression of *MyoD* and *Pax7* [1052]. Additionally, it has been demonstrated that, even in immortalized cell lines such as C2C12, not all cells undergo myogenic differentiation as a subset remains in quiescence [1053]. This could explain the continuously elevated expression levels in the strain and unstrained groups, as the application of strain and/or endogenously generated cell-mediated strain could potentially cause partial activation of this quiescent sub-population. Considering the increased expression of *Pax7* after application of strain, it is not surprising that downstream targets *Myf5* and *MyoD*, who in turn regulate *Myogenin* expression, follow the same pattern of treatment group-specific increase in expression levels. However, in terms of expression of structural genes such as *TnnT1*, a marker for muscle contractility, another potential regulatory mechanism might be strain-induced opening of Ca^{2+} channels. It has previously been reported that mechanical stimulation increases intracellular Ca^{2+} concentrations in human lung fibroblasts [1054], human pulmonary microvascular endothelial cells [1055] and neonatal rat myocytes [1056] in a transient manner. The transient increase in intracellular Ca^{2+} levels shows a similar pattern as observed by Takayama et al. after electrical stimulation of C2C12-derived myotubes. Their study demonstrated that responsiveness to electrical stimulation was greater in myotubes displaying a higher degree of alignment and fusion, ultimately leading to an increase in myotube contractility [1057]. Connecting the higher responsiveness to intracellular Ca^{2+} levels when myotube alignment and fusion are increased to an increase in myotube contractility offers a feasible explanation for the strain-dependent upregulation of *TnnT1* expression in the strain and unstrained groups. This theory is additionally supported by the fact that, compared to day 3, the difference in *TnnT1* expression levels between the treatment groups is increased at day 6 and 9, when myotubes have already formed.

Overall, we found that static mechanical stimulation elicited a more thorough induction of the myogenic program, as the activation of myogenic determination factors at early stages of the culture protocol seems to propagate downstream, ultimately resulting in higher induction of structural and contractile marker gene expression.

Muscle tissue *in* vivo is naturally exposed to mechanical strain as a consequence of movement and exercise. This inherent susceptibilityof muscle to mechanical stimulation has been exploited in many skeletal muscle tissue engineering approaches using strain not just to generate alignment but also as a way to improve myogenic differentiation and maturation [287, 295, 350, 407, 1049, 1058].Thus, elucidating optimized patterns potentially consisting of both static and cyclic strain will be an important step to improve the performance of skeletal muscle engineering strategies. Besides, automated systems allowing for adjustable strain regimes will be valuable to study the role of mechanotransduction in myogenesis. In this respect, the MagneTissue bioreactor system offers a feasible platform to engineer skeletal muscle-like tissue as it utilizes mechanical stimulation of otherwise free-standing constructs to generate a combination of cell alignment and a myogenic differentiation stimulus that can be voluntarily controlled. Even the quite simple static stimulation protocol we used resulted in significantly improved myogenic differentiation on the morphological and molecular level compared to anchored constructs. As expected, scaffold anchoring (represented by the unstrained group in our setup) augmented the myogenic outcome but, nevertheless, better results were obtained when strain was applied. Additionally, strained constructs displayed longer myotubes, which has already been shown in one of the earliest myogenesis models established by Vandenburgh et al. in 1983, where a passive strain of 10-12% applied to avian skeletal myotubes was used [1040]. In another study by this group, human bioartifical muscles were stimulated with the use of a mechanical cell stimulator applying static and, subsequently, cyclic ramp strain, which resulted in a 12% (from 6.4 to 7.1 µm) increase in myofiber diameter [350]. With the use of the MagneTissue bioreactor system in a murine myogenic setting, myotube diameter was increased by roughly 20% from 15.7 µm in the unstrained group to almost 18.8 µm, reaching the fiber diameter range of adult murine skeletal muscle, which approximately spans from $10 - 100$ µm [1059].

The MagneTissue bioreactor system has been thoroughly evaluated in a 3D myogenic model, but is not just limited to muscle tissue engineering purposes. The versatile usage of different strain parameters, e.g. static, cyclic, ramp or a combination thereof, could be used to create *in vitro* muscle disease models related to sarcopenia, trauma and/or exercise-induced damage. Besides, other tissues in the human body such as tendons and ligaments are also highly influenced by mechanotransduction and may serve as additional application fields of the bioreactor. As future plans, we aim to develop vascularization strategies to facilitate nutrient and oxygen supply within the constructs. Another essential interest is to investigate the role of mechanotransduction and which mechanosensitive signaling pathways contribute to myogenic differentiation, which would help to gain greater insight into the spatiotemporal provision of distinct mechanical stimuli. Elucidating optimized strain patterns will be dependent on this knowledge and improve the performance of tissue engineered muscle by modulating these essential signaling pathways.

5. ACKNOWLEDGEMENTS

6. FUNDING

"A Noninvasive *In Vitro* Monitoring System Reporting Skeletal Muscle Differentiation"

Deniz Öztürk-Kaloglu, MSc[1,*], David Hercher, MSc[1], **Philipp Heher, MSc[1]**, Katja Posa-Markaryan, MSc[1], Simon Sperger, MSc[1], Alice Zimmermann, MSc[1], Susanne Wolbank, PhD[1], Heinz Redl, PhD[1], and Ara Hacobian, PhD[1]

[1] Ludwig Boltzmann Institute for Experimental and Clinical Traumatology, Vienna, Austria

[*] Address correspondence to: Deniz Öztürl-Kaloglu, MSc, Ludwig Boltzmann Institute for Experimental and Clinical Traumatology, Donaueschingenstraße 13, 1200 Vienna, Austria; E-mail: deniz.oeztuerk@trauma.lbg.ac.at

Published in *Tissue Engineering: Part C* on December 30th 2016

ABSTRACT

Monitoring of cell differentiation is a crucial aspect of cell-based therapeutic strategies depending on tissue maturation. In this study we have developed a non-invasive reporter system to trace murine skeletal muscle differentiation. Either a secreted bioluminescent reporter (Metridia luciferase) or a fluorescent reporter (green fluorescent protein [GFP]) was placed under the control of the truncated muscle creatine kinase (MCK) basal promoter enhanced by variable numbers of upstream MCK E-boxes. The engineered pE3MCK vector, coding a triple tandem of E-Boxes and the truncated MCK promoter, showed twentyfold higher levels of luciferase activation compared with a Cytomegalovirus (CMV) promoter. This newly developed reporter system allowed noninvasive monitoring of myogenic differentiation in a straining bioreactor. Additionally, binding sequences of endogenous microRNAs (miRNAs; seed sequences) that are known to be downregulated in myogenesis were ligated as complementary seed sequences into the reporter vector to reduce nonspecific signal background. The insertion of seed sequences improved the signal-to-noise ratio up to 25% compared with pE3MCK. Due to the highly specific, fast, and convenient expression analysis for cells undergoing myogenic differentiation, this reporter system provides a powerful tool for application in skeletal muscle tissue engineering.

1. INTRODUCTION

Tissue engineering of transplantable functional skeletal muscle tissue presents an attractive therapeutic approach for the treatment of muscle damage or disease. Skeletal muscle accounts for roughly 40% of the total body mass [18] and is indispensable for vital functions such as locomotion, breathing, temperature regulation, or tissue homeostasis. Consequently, damage or loss of muscle due to trauma or myopathies results in severe limitations of life quality. Despite recent advances in the field of skeletal muscle tissue engineering, the generation of volumetric muscle transplants still remains a major challenge [14]. The majority of skeletal muscle tissue engineering strategies utilize bioreactor systems for physiologically relevant mechanical [262, 287, 295, 350, 430] and/or electrical [467, 468, 477, 478] stimulation to increase myogenic differentiation and maturation. While there is a clear consensus in the field that mechanical/electrical stimulation benefits the myogenic outcome, defined stimulation regimes as well as standardized culture conditions to maximize muscle functionality and maturity *in vitro* remain elusive [284, 1060].

Current approaches to assess cell differentiation, morphology, and function *in vitro* involve standard methodology, such as reverse transcription quantitative polymerase chain reaction (RT-qPCR), immunostaining methods, or enzymatic assays [1041, 1061, 1062]. However, none of these methods allows for quantification in a nondestructive manner. In this respect, noninvasive reporter systems offer a valuable monitoring tool as they enable large-scale online tracking of myogenic differentiation and cell morphological changes over time.

Since the success of cellular therapies and bioreactor approaches depends strongly on the optimization of culture conditions, future skeletal muscle tissue engineering strategies will rely on nondestructive methodology for several reasons: (1) noninvasive assaying allows for sample reduction, which is especially valuable for muscle progenitor cell types that are not available in large quantities; (2) online assaying of the same sample over time may provide more relevant results; (3) noninvasive methods do not require time-consuming sample preparation.

The 82 kDa enzyme creatine kinase (CK) is a central regulator of cellular energy homeostasis. CK catalyzes the reversible ATP-dependent interconversion of creatine into phosphocreatine (PCr), building up a pool of rapidly diffusable PCr for spatiotemporal buffering of ATP levels [1063]. Thus, CK plays a pivotal role in tissues with high and fluctuating energy demands such as muscle. The muscle creatine kinase (MCK) isoenzyme is expressed in sarcomeric muscle, that is, in skeletal and cardiac muscle. It has generally been used as a myogenic differentiation marker as well as a marker for muscle integrity. The concentration of CK in blood has traditionally been considered an indirect marker of muscle damage, particularly for diagnosis of conditions such as myocardial infarction,muscular dystrophies (and muscle wasting), or cerebral diseases. However, there is an ongoing debate in the field on the reliability of serum CK levels in diagnostics [1064].

A variety of transgenic and tissue culture studies have demonstrated that MCK is expressed exclusively in differentiated skeletal and cardiac muscle [1065-1069]. Importantly, its truncated form, ranging from -80 to +7 bp relative to the transcriptional start site, is highly specific for skeletal muscle [1070, 1071]. The corresponding MCK enhancer contains a large number of conserved DNA patterns, referred to as E-boxes. These regulatory regions harbor a core consensus binding sequence for trans-acting myogenic transcription factors (TFs) as well as the consensus serum responsive factor-binding sequence $CC(A/T)_6GG$ [1072]. Furthermore, E-boxes contain an AT-rich site, which is known to bind ubiquitously expressed factors such as MEF-2 and MHox [1073]. We have developed a noninvasive reporter system to investigate the efficiency of murine skeletal muscle differentiation by placing either a secreted bioluminescent (Metridia luciferase) or a fluorescent (GFP) reporter protein under the control of a tissue-specific promoter. Depending on the differentiation status of the transfected cells, this system gets activated through the endogenous MCK promoter triggering reporter gene expression. In addition, to enhance the signal-to-noise ratio of the reporter, we have developed a further advanced reporter system carrying complementary microRNA (miRNA) targeting seed sequences (miRT) for regulatory myogenic miRNAs. The general strategy of this system is to integrate a subset of seed sequences into the 3' untranslated region (3'-UTR) of the designed constructs to decrease background signal of the reporter genes in undifferentiated cells. Previously performed miRNA expression profiling experiments demonstrated that particular miRNAs such as miR-222, miR-550, and miR-659 are down-regulated during myogenic differentiation (Table 4) [1074]. Their target genes are involved in the regulation of many biological processes including muscle development, kinase activity and regulation of cell signaling pathways [1074, 1075].

miRNA	Regulation	Mouse	Human
miR-222	↓	↓C2C12 diff. [1075, 1076]	↓pMyo diff. [1077]
miR-550	↓		↓pMyo diff. [1074]
miR-659	↓↓↓		↓pMyo diff. [1074]

Table 4: *miRNAs found to be downregulated during myogenic differentiation.* Arrows schematically indicate the extent of downregulation: ↓: fold change 1-3 fold, ↓↓↓: fold change 7-fold or higher [1074]. miRNA, microRNA.

Using a modular cloning approach, the aim of this study was to generate and evaluate four different modified versions of an MCK reporter plasmid containing a truncated MCK promoter. The effects of varying numbers of additional regulatory enhancer elements as well as the presence of miRNA seed sequences in the plasmids on reporter activity and specificity were studied in myogenic and non-myogenic cells. In conclusion, our results demonstrate that expression levels of the modified MCK promoter combined with E-Box elements were significantly higher than those reached with formerly used versions of other truncated MCK promoters. Furthermore, we show that the addition of miRNA

seed sequences targeting a subset of myogenic miRNAs increases the signal-to-noise ratio of the reporter system. Since the majority of current strategies for muscle repair utilizes cell-laden scaffolds, this framework can be a useful model for the noninvasive optimization of culture methods for myogenic differentiation in bioreactors.

2. MATERIALS AND METHODS

2.1. Construction of tissue-specific reporter vectors

The murine muscle creatine kinase (MCK) promoter was used to drive the expression of reporter genes. As shown in Figure 33, the MCK enhancer has been truncated to increase its activity and the sequences have been deposited in the GenBank databases (Accession No. AF188002) [1078]. The enhancer encodes a tandem of two E-box sequences described as left, right, or MEF1, which is known to be a higher affinity MyoD-binding site [1079]. The left site has been replaced with an additional copy of the MEF1 site, which has been named "2R" modification, as MyoD has not been detected within the left E-box (5'-AACACCTGCTGC) [1080]. Furthermore, another right E-Box sequence and modified S5 region (5'-GAGCGGTTA), which are shown above the wild type sequences in Figure 33, were constructed in 2R5S enhancer sequence to increase enhancer activity by reinforcing the MyoD-binding site [1081].

CCACTACGGGTCTAGGCTG**CCCATGTAAG**GAGGCAA**GGCCTGGGGA**CACC
                    ‾‾‾‾‾‾‾‾‾‾   ‾‾‾‾‾‾‾‾‾‾
                       CArG   AP2

                              Right E-BOX (2R)
                              ‾‾‾‾‾‾‾‾‾‾‾‾‾‾
                               -caacacct
CGAGATGCCTG**GTTATAATTAAC**CAGACATGTGGCTG**CCCCCCCCCCCCCC**
           ‾‾‾‾‾‾‾‾‾‾‾‾   ‾‾‾‾‾‾‾‾‾‾‾‾‾
             A/T rich   Left E-BOX

                      S5
                    ‾‾‾‾‾‾
                  gagcggtta
AACACCTGCTGCCTGAGCCTCAC------CCCCACCCCGGTGCCTGGGTC
‾‾‾‾‾‾‾‾‾‾‾‾
Right E-BOX- MEF 1

TTAGGCTCTGTACACCATGGAGGAGAAGCTCGC**TCTAAAAATAA**CCCTGT
                                  ‾‾‾‾‾‾‾‾‾‾‾
                                      MEF 2
CCCTGGTGGAT

Fig. 33: *Sequences of modified E-Box sites (77 bp) in MCK enhancer.* The sequence positions and alteration of 2R and S5 sequences are indicated. Core sequences are underlined in bold and the modified sequences indicated above, such as right E-

Box (2R), S5, and right E-Box-MEF1 [1078]. The AP2 (activating protein 2) [1082] as well as CArG [1083] consensus sequences are known to be recognition sites for transcription factors. MCK, muscle creatine kinase.

In this study, we constructed four different reporter vectors and for each vector enhancer elements were ligated upstream to the highly truncated basal promoter. These constructs were named: (1) ''E3MCK'' containing three 2R5S enhancer sequences, resulting in a total of six E-boxes and 3S5 sequences (6R-3S5) due to the absence of a Cytomegalovirus (CMV) enhancer (Fig. 34A); (2) ''E5MCK'' encoding fivefold 2R5S sequences resulting in a total of ten right E-boxes and five S5 sequences (10R-5S5) (Fig. 34C); (3) ''CE-E3MCK,'' which additionally has a CMV enhancer (Fig. 34B); (4) ''E3MCK-miRT'' containing E3MCK, including miRNA seed se-quences (Fig. 38). Myogenesis-associated miRNAs, such as miRNA-222, miRNA-550, and miRNA-659, were used as complementary target seed sequences (miRT). These seed sequences were ligated into the 3'-UTR downstream of the reporter gene to reduce the background activity and thus enhance the signal-to-noise ratio (Fig. 34).
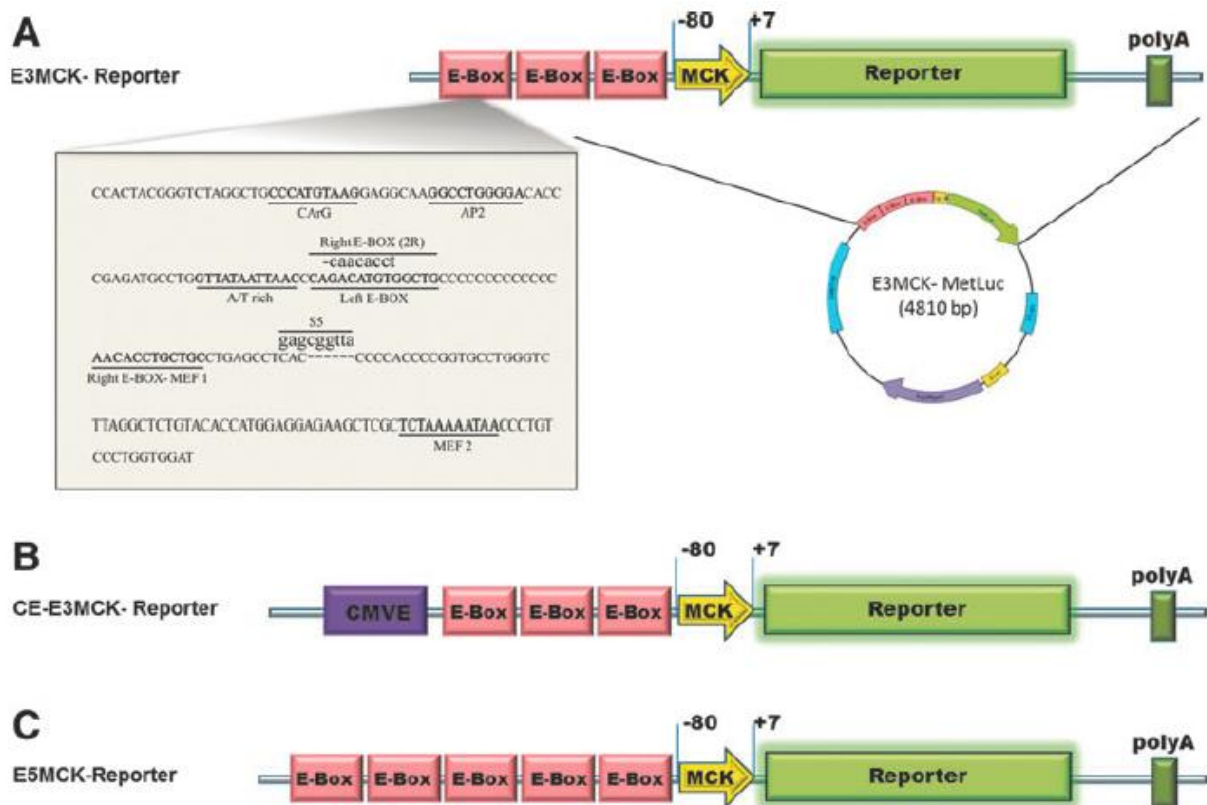

Fig. 34: *Schematic illustration of different MCK reporter vectors.* (A) E3MCK, (B) E3MCK (including CMV enhancer) and (C) E5MCK. All reporter vectors contain a highly truncated MCK promoter (positioned at -80 to +7) downstream of multiple tandem E-Boxes (MCK enhancers) and either fluorescence or bioluminescence reporters. MCK, Muscle Creatine Kinase; CMVE, Cytomegalovirus Enhancer; E-Box, Enhancer box; Poly A, Polyadenylation signal; Reporter: Green fluorescent protein (GFP) or Metridia Luciferase (MetLuc).

EcoRI and AgeI restriction enzymes were used to excise the cassette of the truncated MCK promoters from the plasmid pUC57-MCK (GenScript, Piscataway, NJ). The truncated promoter sequences were ligated into the pMetLuc2-Reporter vector (Clontech, Mountain View, CA) containing the secreted Metridia luciferase reporter gene. The CMV enhancer was amplified from the plasmid pMetLuc-control (Clontech) using the sense primer AGCTTTATTTAGGTGACACTATAGGGTAC and antisense primer CCTATAGTGTCACCTAAATAA. The GFP was created by *AgeI*/*NotI* digestion of pEGFP-N1 (Clontech) and was inserted into the *AgeI*/*NotI*-digested E3MCK and CE-E3MCK vectors, representing the fluorescent reporter plasmids (Fig. 33). All PCR reactions were performed using a Hot-Taq polymerase (VWR International GmbH, Erlangen, Germany) according to the manufacturer's instructions. All sequences were verified by control restriction digests and sequencing (data not shown).

2.2. Cell culture and myogenic/osteogenic differentiation

The mouse muscle myoblast precursor cell line C2C12 (No. ACC565, Germany) was cultured in Dulbecco's modified Eagle's medium high glucose (DMEM-HG; Lonza, Basel, Switzerland) containing 4.5 g/L d-glucose, supplemented with 2 mM l-glutamine (Sigma-Aldrich, Vienna, Austria), 100 U/ mL Penicillin/Streptomycin (P/S; Lonza), and 5% fetal calf serum (FCS; Lonza). This medium will be referred to as growth medium (GM). For myogenic differentiation of C2C12 cells, DMEM low glucose (DMEM-LG) supplemented with 1% FCS, 2 mM l-glutamine, and 100 U/mL P/S was used, referred to as differentiation medium (DM). Osteogenic differentiation was induced using DMEM-HG supplemented with 1% FCS, 2 mM l-glutamine, 100 U/mL P/S, and 300 ng/mL rhBMP2 (InductOS®, Wyeth, Madison, WI). NIH3T3 (mouse embryonic fibroblast), BICR10 (human buccal mucosa), and MG63 (human osteosarcoma) cells were purchased from ECACC (Salisbury, United Kingdom) and were cultured in DMEM-HG medium containing 10% FCS, 2 mM l-glutamine, and 100 U/mL P/S. HL-1 (mouse cardiac muscle) cells were incubated in Claycomb Medium (Sigma-Aldrich, St. Louis, MO) supplemented with 10% FCS, 2 mM l-glutamine, 0.1 nM norepinephrine, and 100 U/mL P/S.

2.3. Transfection

For transfection, cells were seeded into 24-well plates (Sigma-Aldrich, Darmstadt, Germany) at a density of 0.5 x 10^5/well 24 h before transfection (2.5 x 10^4/cm^2). Transfection was performed using 3 µL of PerFect DNA Transfection Reagent (VWR International GmbH) mixed with 1 µg of the respective reporter plasmid. The medium was changed 3 h after transfection. The transfected cells were incubated in DM for 6 days posttransfection before readout.

2.4. Myogenic differentiation on fibrin matrices

Differentiation experiments on fibrin hydrogels of different stiffness were performed using the TISSUCOL DUO 500 5.0 mL Fibrin Sealant Kit (Baxter, Westlake, TX). Myogenic differentiation of

C2C12 cells on standard cell culture plastic was compared with differentiation on fibrin matrices with varying fibrinogen concentrations. The 24-well plates (Starlab, Hamburg, Germany) were coated with 200 µL fibrin (final concentrations: 10 or 20 mg/mL fibrinogen, respectively, and 1 IU/mL thrombin) and left to polymerize for 45 min at 37°C, 5% CO_2. Fibrinogen was diluted with DMEM-HG, and thrombin with 40 mM $CaCl_2$. 5 x 10^5 C2C12 cells were seeded per well and myogenic differentiation was induced by exchanging the GM with DM 4 h postseeding. For osteogenic differentiation as a control, C2C12 cells were induced using 300 ng/mL of rhBMP2 and cultured in DM.

2.5. Mechanical stimulation of skeletal muscle-like constructs

Mechanical stimulation of E3-MCK-MetLuc C2C12 cells was performed as recently described [430]. Briefly, the cells were embedded into ring-shaped fibrin scaffolds (final concentrations: 20 mg/mL fibrinogen, 0.625 IU/mL thrombin, 3.2 x 10^6 cells per scaffold), which were mounted onto a custom-made spool-hook system and subsequently transferred into a bio-reactor system that allows for uniaxial mechanical stimulation through magnetic force transmission. At day 3 of culture, myogenic differentiation was induced by exchanging GM with DM and mechanical stimulation was started by application of 10% static strain for 6 h followed by 3% static strain for 18 h (rest phase). This daily stimulation pattern was repeated for 6 days (including day 9).

2.6. DNA quantitation assay (CyQUANT)

DNA content was measured using the CyQUANT Cell Proliferation Assay Kit (Invitrogen, Carlsbad, CA) following the manufacturer's instructions. Briefly, harvested cell pellets were incubated with 200 µL of CyQUANT GR dye/cell lysis buffer for 5 min protected from light at room temperature and fluorescence (excitation 485 nm, emission 520 nm) was detected on a fluorescence Polar Star plate reader (BMG Labtech, Ortenberg, Germany).

2.7. Secreted Metridia luciferase assay

For bioluminescence quantification and comparison of expressed signal intensities induced by different combinations of enhancer elements, cells were transfected with the reporter plasmids as described above and incubated for 5 days. The medium was changed 24 h before supernatant sampling (50 µL samples) to assess 24-h luciferase expression on day 6 posttransfection. To collect the supernatant for Metridia luciferase assaying of the skeletal muscle-like constructs, the samples were taken out of the bioreactor system and incubated in 1 mL of DM for 24 h at the end of the culture period. Each sample was assayed for secreted luciferase activity using coelenterazine as substrate and the appropriate assay buffer (NanoLight Technology, Pinetop, AZ) and all measurements were performed on a Polar Star Omega Luminometer (BMG Labtech) with Omega software (OMEGA Software GmbH, Obersulm, Germany). Quantification of reporter activity relative to a CMV promoter

was calculated by normalization of MetLuc activity to a negative control (osteogenic differentiation of C2C12) and to the basal MetLuc activity driven by a CMV promoter upon myogenic differentiation.

2.8. Quantitative reverse transcription-polymerase chain reaction

At day 6 posttransfection, C2C12 cells were harvested and total RNA was isolated using the TriFast reagent (VWR International GmbH) according to the manufacturer's instructions. RNA integrity was analyzed with gel electrophoresis and quantity was measured using a Hitachi U-5100 photometer (Metrohm Inula GmBH, Vienna, Austria). Two micrograms of RNA were subjected to DNaseI (Promega, Mannheim, Germany) digestion and subsequent complementary DNA (cDNA)-Synthesis was performed using the EasyScript^{TM} cDNA Synthesis Kit (ABM Good, Richmond, Canada). qPCR was performed with the CFX96 Real-Time System (Bio-Rad, München, Germany) using 10 µL KAPA SYBR$^{©}$ Fast Universal qPCR 2x· master mix (VWR International GmbH), NH_4^+-Buffer (Taq-Buffer; Life Technologies, Carlsbad, CA), 40 ng cDNA, and either 250 or 400 nM Primers. qPCR for hypoxanthine phosphoribosyl transferase (HPRT), myogenin (MYG), and osteocalcin (OC) was carried out with the following primers: qMYGs (GGTCCCAACCCAGGAGATCAT) and qMYGas (ACGTAAGGGAGTGCAGATTG) for MYG, qOCs (GTCTGACAAAGCCTTCATGTC) and qOCas (CTGTTCACTACCTTATTGCCCT) for OC, and qHPRTs (AGTCCCAGCGTCGTGATTAG) and qHPRT as (TGGCCTCCCATCTCCTTCAT) for HPRT as housekeeping gene.

2.9. Fluorescence microscopy

Fluorescence microscopy was performed on day 6 post-transfection for E3MCK-GFP, E3MCK-miRT-222-GFP, and E3MCK-miRT-550-GFP transfected cells, using a Zeiss Axio Observer Vert.A1 microscope (Zeiss, Oberkochen, Germany) and Axio Imager software.

2.10. Statistical analysis

All data are presented as mean ± standard deviation (SD; box and whiskers) or mean ± SD (bar diagrams). n indicates number of samples in one independent experiment. For the evaluation of multiple groups we used one-way analysis of variance followed by Tukey's *post hoc* analysis. For the analysis of two experimental groups, unpaired t-test was used. Statistical analysis was performed using GraphPad Prism 5 software (GraphPad Software). Differences were considered significant at ***$p <$ 0.001, **$p < 0.01$, and *$p < 0.05$.

3. RESULTS

3.1. Successful construction of skeletal muscle-specific reporter systems was verified by sequencing and cellular morphology

As represented in Figure 34, three different skeletal muscle reporter vectors with MCK promoters and enhancer elements were constructed in reporter plasmids in a combination with either GFP or secreted luciferase. C2C12 cells, a mouse myoblast precursor cell line, were used to assess the levels of luciferase expression after transfection. Differentiation of C2C12 cells into the myogenic or osteogenic lineage was confirmed by morphological analysis and RT-qPCR after 6 days of differentiation.

3.2. Reporter gene expression of all constructed vectors is triggered upon myogenic differentiation

The E3MCK-MetLuc reporter vector gave approximately twenty-fourfold increased expression levels upon myogenic differentiation in C2C12 cells. In contrast, the CMV-enhanced CE-E3MCK-MetLuc reporter exhibited less bioluminescence signal (about sixfold increase compared with a negative control). Finally, E5MCK-MetLuc exhibited eighteen-fold higher signal intensity and thereby no significant improvement in comparison to E3MCK-MetLuc (Fig. 35). In addition, osteogenic differentiation of C2C12 cells transfected with the plasmids indicated above resulted in signal intensity comparable to negative control background levels (Fig. 36).
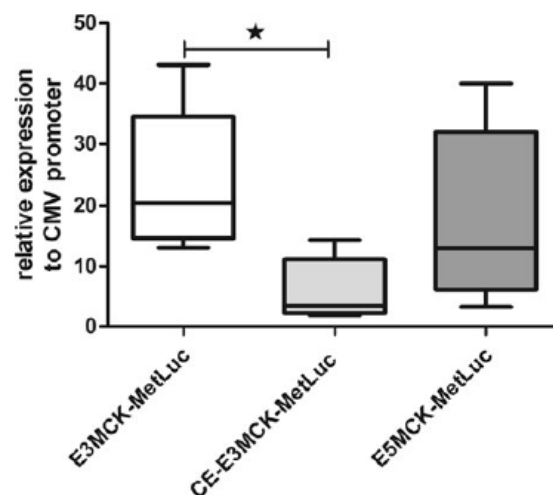

Fig. 35: *Comparison of E3MCK-MetLuc, CMV-enhanced CE-E3MCK-MetLuc and E5MCK-MetLuc bioluminescence readouts.* Supernatants of C2C12 cell lines were incubated for 24 h 6 days posttransfection under myogenic and osteogenic conditions. Significant luciferase expression was detected in cells transfected with indicated reporter plasmids. $n \geq 5$ of six independent experiments; values represent mean ± standard deviation; *$p < 0.05$; one-way ANOVA with Tukey's multiple comparison test. ANOVA, analysis of variance.

We also tested the reporter systems in nonmyogenic cell lines and in cardiomyocytes to determine lineage specificity. Luciferase expression driven by the promoter is highly up-regulated in C2C12 upon myogenic differentiation, but not in nonskeletal muscle cell lines (C2C12 after osteogenic differentiation, human osteosarcoma cells, mouse fibroblasts, human keratinocytes, and mouse cardiomyocytes, respectively) as quantified by bioluminescence assaying (Fig. 36).
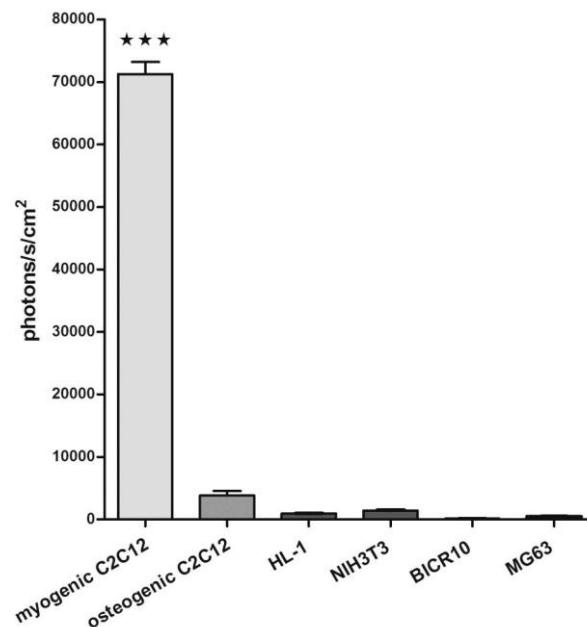

Fig. 36: *Comparison of E3MCK-MetLuc transfected cell lines.* This promoter showed significantly higher levels (twentyfold increase) of luciferase expression in C2C12 (after 5 days of myogenic differentiation) compared with control cell lines. The promoter was essentially inactive in nonskeletal muscle cell lines (C2C12 after osteogenic differentiation, mouse cardiomyocytes [HL-1], mouse fibroblasts [NIH3T3], human keratinocytes [BICR10], and human osteosarcoma cells [MG63], respectively). $n \geq 5$ of six independent experiments; values represent mean + standard deviation; ***$p < 0.001$; one-way ANOVA with Tukey's multiple comparison test.

3.3. Introducing myogenesis-associated miRNA seed sequences to the MCK-specific reporter system reduces background activity

Although the MCK-specific reporter system showed a high signal-to-noise ratio, further reduction of background activity was aimed for by introducing complementary seed sequences. Several miRNAs associated with the regulation of myogenic differentiation are known to be downregulated during myogenesis [1074]. These sequences were inserted into the 3'-UTR of the E3MCK construct to further enhance the signal-to-noise ratio of the reporter system due to decreased baseline signals (see Materials and Methods section for relative value calculation). Adding a triple combination of seed sequences (Fig. 37) to the plasmid (E3MCK-miRTtriple-MetLuc) gave bioluminescence activity comparable to the E3MCK-MetLuc plasmid containing no seed sequences. Insertion of a single seed sequence such as miRT-222 or mirT-550 resulted in the strongest signals. However, at the same time,

ligation of a miRT-659 seed sequence into the E3MCK-MetLuc plasmid did not improve the signal-to-noise ratio at all (Fig. 38).
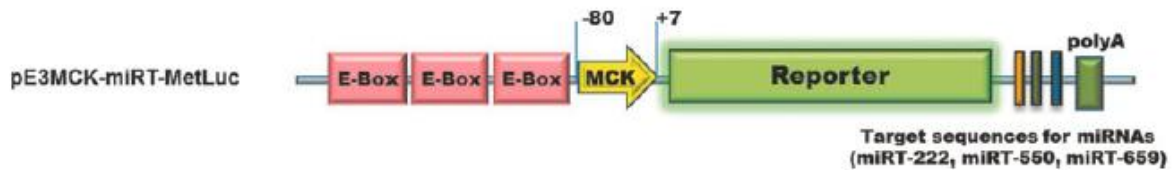

Fig. 37: *Schematic illustration of a MCK promoter-specific vector encoding additional seed sequences.* These target sequences, complementary to miRNAs (miR-222, miR-550, and miR-659), were ligated separately or in combination (E3MCK-miRT-triple-MetLuc). miRNAs, microRNAs.
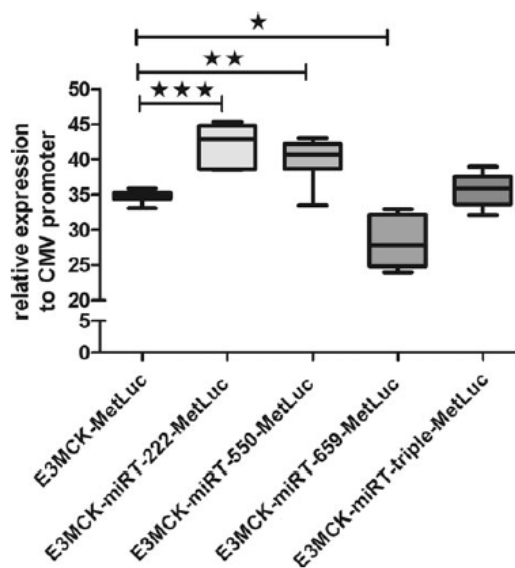

Fig. 38: *Activity of the reporter system combined with up to three different seed sequences for miRNAs (miR-222, miR-550, and miR-659), representing luciferase expression normalized to osteogenically differentiated negative controls.* After C2C12 differentiation for 6 days, the E3MCK-miRT-222-MetLuc and E3MCK-miRT-550-MetLuc reporter plasmids showed significantly higher luciferase activity compared with E3MCK-MetLuc. The E3MCK-miRT-659 promoter gave the lowest bioluminescence readouts, whereas a triple combination of seed sequences (E3MCK-miRT-triple-MetLuc) showed no significant effect on background reduction. $n \geq 6$ of six independent experiments; values represent mean $\pm$ standard deviation; ***$p < 0.001$, **$p < 0.01$, and *$p < 0.05$; one-way ANOVA with Tukey's multiple comparison test.

To directly assess the activity of the constructs combined with the GFP reporter, fluorescence microscopy was performed. The E3MCK-GFP and E3MCK-miRT-550-GFP plasmids demonstrated strong fluorescence intensity in C2C12 cells upon myogenic differentiation confirmed by a multinuclear myotube phenotype 6 days after transient transfection. In contrast, low background signal was detected in the control group with C2C12 cells differentiated along the osteogenic lineage (Fig. 39A). In addition, RT-qPCR control experiments demonstrated that OC was virtually not expressed after myogenic differentiation, whereas MYG expression was absent after osteogenic differentiation (Fig. 39B), which correlated with fluorescence microscopy results.
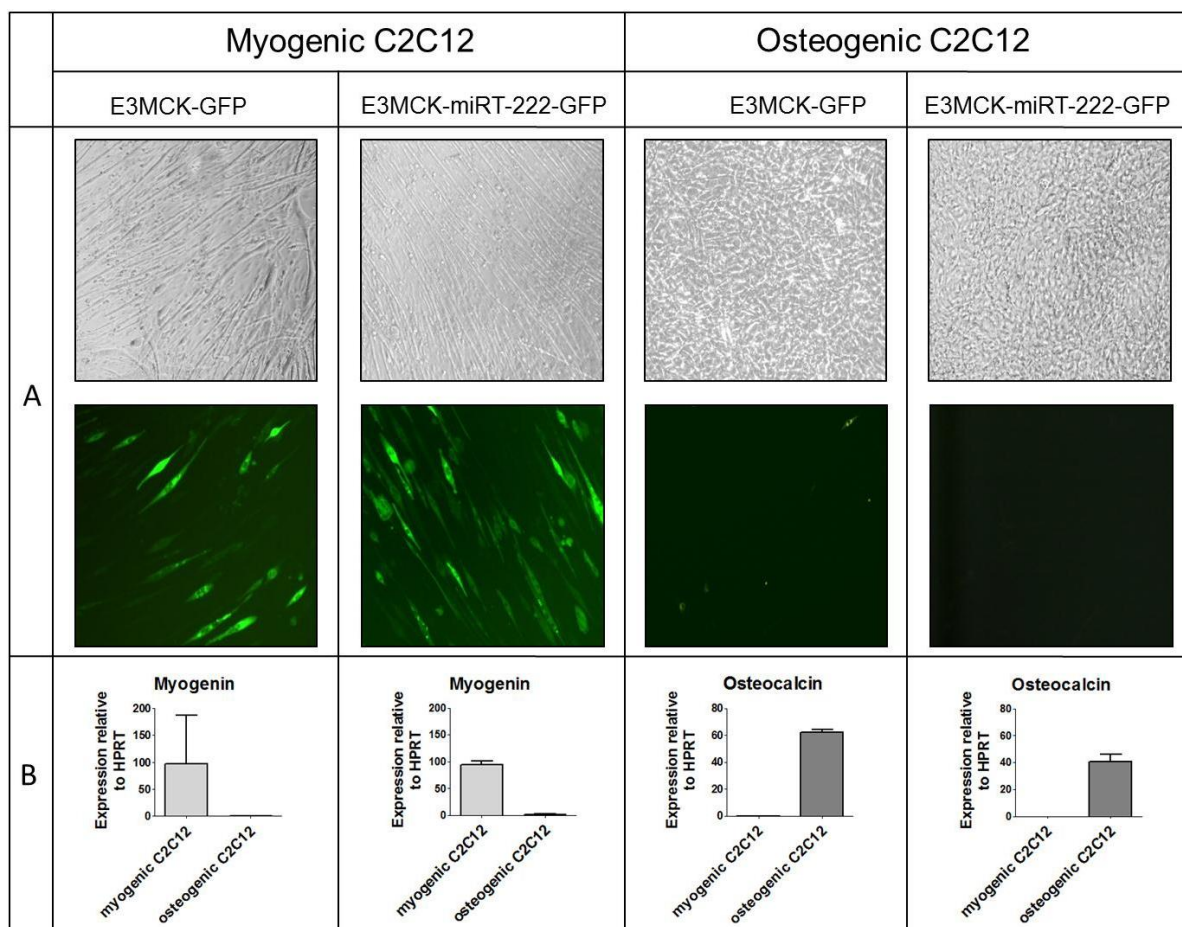
Fig. 39: (A) Morphological changes of C2C12 cells during terminal differentiation for 6 days posttransfection with reporter plasmids and GFP activation in C2C12 cells undergoing myogenic and osteogenic differentiation. The specific and strong activation of reporter expression and MCK promoter activation is traceable during myogenic differentiation, whereas only low background signals are detectable in osteogenic differentiation after transfection with E3MCK-GFP. It seems likely that background signals are optically reduced due to insertion of miR-222 seed sequences into the 3'-UTR of the E3MCK-GFP construct in comparison with the same plasmid (E3MCK-MetLuc) containing no seed sequences. Scale bars represent 200 µm. (B) Myogenin and Osteocalcin expression levels in E3MCK-GFP and E3MCK-miRT-222-GFP transfected cells as determined by RT-qPCR. Readouts are depicted as fold changes of the indicated target gene normalized to HPRT. $n = 3$; values represent mean + standard deviation. 3'-UTR, 3' untranslated region; HPRT, hypoxanthine phosphoribosyl transferase; RT-qPCR, reverse transcription quantitative polymerase chain reaction.

3.4. The E3MCK-MetLuc reporter system provides a sensitive and reliable screening and optimization tool for tissue engineering applications

Muscle precursor/stem cells are known to sensitively respond to matrix stiffness, with pliant matrices (suggested Young's modulus of 8–17 kPa) giving a higher degree of myogenic differentiation and maturation [355]. We wanted to investigate whether the E3MCK-MetLuc reporter system is sensitive enough to detect even moderate differences in MCK expression as readout for the degree of myogenic differentiation. Therefore, myogenic differentiation of C2C12 cells on two pliant fibrin matrices of different stiffness was compared with differentiation on standard cell culture plastic. Both fibrin

144

matrices triggered significantly higher luciferase expression upon myogenic differentiation after 7 days relative to the control, with the stiffer (20 mg/ mL fibrinogen) fibrin matrix giving better results than the softer (10 mg/mL) fibrin matrix (Fig. 40A). These results indicate that the reporter system is able to reflect moderate differences in myogenic differentiation as, although not significantly different in signal, both fibrin matrices are considered myogenic in terms of their stiffness.

Since mechanical stimulation of muscle precursor cells has been shown to be a feasible approach to achieve uniaxial cellular alignment as well as improved myogenic differentiation, we also tested whether the E3MCK-MetLuc reporter will give reproducible readouts in this setting. We have recently reported a bioreactor system that allows for uniaxial mechanical stimulation of cells embedded in fibrin matrices [430]. In this system, differentiation of C2C12 cells transfected with the E3MCK-MetLuc plasmid was monitored over 6 days. Application of static mechanical stimulation led to an approximately 1.7-fold increase of MCK expression signal compared with unstrained control samples at the end of the culture period (Fig. 40B). These results are in accordance with previous reports showing increased expression levels of early, mid, and late stage-specific myogenic markers after mechanical stimulation and once more underscore the versatility of this reporter system.
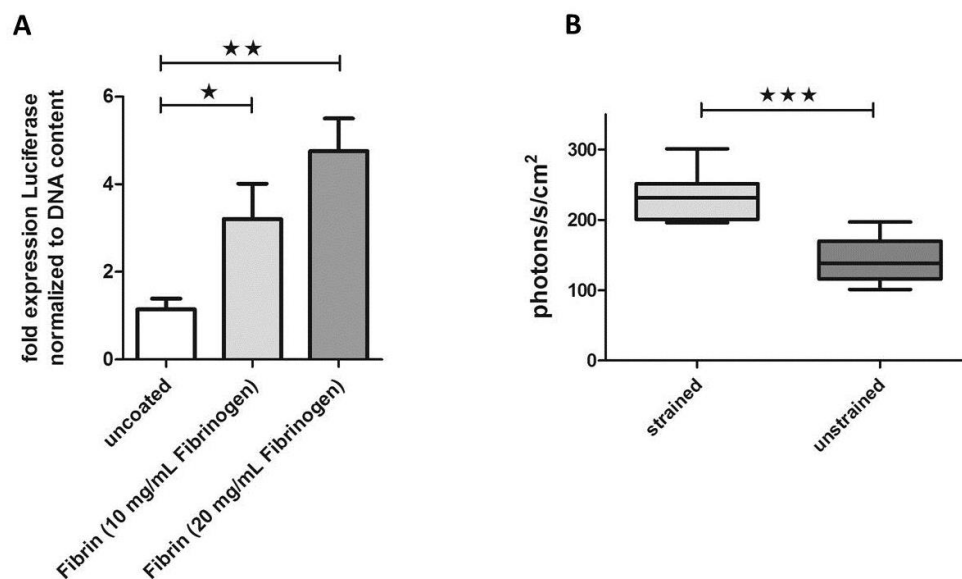

Fig. 40: *Tissue engineering application of reporter system.* (A) Secreted luciferase activation (E3MCK-MetLuc) upon myogenic differentiation of C2C12 cells relative to osteogenic differentiation, representing luciferase expression normalized to DNA content. Cells were cultivated on uncoated (plastic) and fibrin-coated (10 and 20 mg/mL fibrinogen) cell culture plates. $n \geq 3$ of three independent experiments; values represent mean + standard deviation; **$p < 0.01$ and *$p < 0.05$; one-way ANOVA with Tukey's multiple comparison test. (B) Application of strain stimulates myogenic differentiation of C2C12. Mechanical stimulation led to a significant increase in MCK expression in the strain group (approximately 1.7-fold higher) compared with unstrained controls after 6 days. $n = 4$ of two independent experiments; ***$p < 0.001$; one-way ANOVA with Tukey's multiple comparison test.

4. DISCUSSION

We successfully constructed a novel nonviral reporter system for monitoring of myogenic differentiation. Three enhancer elements were placed in tandem proximal to a truncated murine MCK promoter. In addition, miRNA seed sequences were added to the 3'-UTR of the constructs, both modifications resulted in reduced background signal activity, whereas strong fluorescence/bioluminescence signal was obtained in skeletal muscle cells, but not in nonmyogenic cell lines (Table 5).

Construct	Modification of reporter vector	Skeletal muscle specificity	Outcome/phenotype
E3MCK	Threefold tandem of 2R5S E-box elements	+++++	Twenty-fourfold higher promoter activation than CMV promoter
E5MCK	Fivefold tandem of 2R5S E-box elements	++++	Eighteenfold higher promoter activation than CMV promoter
CE-E3MCK	Threefold tandem of 2R5S E-box elements and CMV enhancer	++	Sixfold higher promoter activity compared with CMV promoter
E3MCK-miRT-222	Threefold tandem of 2R5S E-box elements and miRNA-222 seed sequence in the 3′-UTR region	+++++	Twenty-five percent reduced background activity compared with E3MCK
E3MCK-miRT-550	Threefold tandem of 2R5S E-box elements and miRNA-550 seed sequence in the 3′-UTR region	+++++	Nineteen percent reduced background signal compared with E3MCK
E3MCK-miRT-659	Threefold tandem of 2R5S E-box elements and miRNA-659 seed sequence in the 3′-UTR region	+++++	There is no enhancement on signal-to-noise ratio
E3MCK-miRT-triple	Threefold tandem of 2R5S E-box elements and miRNA-222-550-659 seed sequences in the 3′-UTR region	+++++	No effect on diminishing of background signal

Table 5: *Representation of modified constructs and their functions.* Plus signs indicate the estimated cell specificity, ranging from high specificity (+++++) to low specificity (+). 3'-UTR, 3' untranslated region; CMV, *Cytomegalovirus*.

4.1. Secreted reporter gene assay and specificity of the reporter system

We have demonstrated the practicability of a secreted bioluminescent reporter gene assay (Metridia luciferase), which has been previously reported to be a suitable tool for monitoring of various biological processes *in vitro* and *in vivo* [1084, 1085]. Our reporter system, composed of a bioluminescent reporter gene under the control of a modified truncated MCK promoter, enables noninvasive tracking of skeletal muscle cell differentiation *in vitro*. Substitution of the bioluminescent with a fluorescent reporter additionally provides a feasible tool for cell morphological analysis during myogenic differentiation. The vector is valuable for the optimization of culture conditions for specific lineage differentiation as well as time-lapse monitoring of myogenesis in three-dimensional (3D) *in vitro* skeletal muscle tissue engineering approaches.

With regard to specificity, several studies have reported that MCK is expressed at high levels only in skeletal and cardiac muscle [1086]. Also, Wang et al. demonstrated that even truncated MCK regulatory cassettes consisting of E-Boxes and the proximal promoter are active in skeletal muscle, but

inactive in other cell types such as liver cells [1081]. Our findings are consistent with this research; however, we aimed at the generation of a skeletal muscle-specific reporter system that displays higher reporter signal intensity than previous systems. Therefore, this study led us to further investigate how a modular approach can be used to modify the truncated MCK promoter in such a way that the reporter system is virtually off in cardiac muscle, thus maintaining specificity, while maximizing the signal.

We have successfully shown that all versions of altered Metridia luciferase MCK reporter systems, E3MCK, CE-E3MCK, and E5MCK (Fig. 34), gave stronger relative bioluminescence readouts compared with plasmids with the constitutively active CMV promoter. Since E3MCK displayed the highest signal intensity (Fig. 35), we chose to use this vector for subsequent evaluation and further modification. Myogenic differentiation of C2C12 cells transfected with E3MCK expectedly triggered strong reporter activity compared with nonskeletal muscle cells. In simple terms, strong luciferase expression was observed only in skeletal muscle, but the expression was almost absent in cardiac muscle cells (HL-1) as well as bone- (MG63, C2C12 after osteogenic differentiation), connective tissue- (NIH3T3), or skin (BICR10)-derived cell lines (Fig. 36). The high specificity and strong signal of the modified E3MCK reporter system for skeletal muscle is a direct result of the truncated MCK promoter *per se* being highly specific for skeletal muscle [18, 1086]. However, the addition of multimerized E-boxes very likely further increases specificity and signal intensity alike. MyoD1 and MYG, two key regulatory TFs in myogenic differentiation, are likely to stimulate MCK expression through interaction with enhancer elements [1086]. In fact, MyoD1 has been shown to have identical binding affinity for the MCK promoter as MEF1 [1080]. Since both TFs are only expressed in skeletal, but not cardiac muscle, the addition of multiple E-boxes is expected to increase reporter signal intensity through binding of endogenous MyoD1 and/or MYG with simultaneous restriction of reporter activity to skeletal muscle cells. Interestingly, there seems to be a cut-off for this endogenous MCK reporter activation, as addition of more than three E-boxes (e.g., in E5MCK) did not further increase signal intensity (Fig. 35).

4.2. Reporter gene activity driven from the improved MCK promoter obviates the use of constitutively active promoters

The tissue-specific MCK vector containing a triple tandem of 2R5S E-box elements and Metridia luciferase as a reporter gene (E3MCK) showed the highest levels of bio-luminescence activity compared with CMV promoter-driven expression (Fig. 35). As stated above, this suggests that any addition of MCK enhancers harboring multimerized MEF1 sites and MCK enhancer elements increases skeletal muscle-specific gene expression.

In addition, we incorporated a CMV enhancer in one of the reporter constructs (CM-E3MCK). The CMV enhancer is commonly used in gene transfer vectors due to its high levels of gene expression in a large variety of tissues. It contains also consensus sequences that are recognized by TFs associated

with myogenic differentiation [1087]. Interestingly, our designed E3MCK reporter plasmid with a CMV enhancer was less active than the constructs lacking the CMV enhancer (E3MCK and E5MCK; Fig. 35). This was somewhat surprising as there is evidence that the CMV enhancer increases the capacity of expression due to high-affinity binding of TFs to consensus sequences within different cell types [1084, 1088]. However, the observed reduction in reporter activity may be explained by the existence of shared consensus sequences in the CMV and MCK enhancer, resulting in competitive binding of regulatory TFs. Another explanation for the inferior performance of the CE-E3MCK construct could also be unspecific binding of other TFs to the CMV enhancer sequence. These interactions may either negatively regulate expression directly or by blocking the binding sites for myogenic TFs in the MCK enhancer sequences [1087].

4.3. Introduction of myogenic differentiation-associated miRNA seed sequences reduces background activity

Even though the E3MCK reporter system already gave decent signal intensity and specificity, we tried to further optimize the reporter plasmid to obtain minimal background signal. Several studies have previously shown that miRNA activity can be efficiently reduced by expressing complementary target sequences [1074, 1075]. To increase the signal-to-noise ratio (by reducing reporter background signal) of the reporter system, we hypothesized that this regulatory mechanism can be exploited to further reduce the effects of the leakiness of the E3MCK reporter system. Therefore, we explored the effects of three different miRNA seed sequences on reporter signal intensity upon incorporation into the E3MCK plasmid (Fig. 37). As shown in Figures 38 and 39, introduction of miRNA sequences into the E3MCK-MetLuc and E3MCK-GFP reporter plasmids not only resulted in stronger bioluminescence and fluorescence signals upon myogenic differentiation, but also reduced the background signal in osteogenically differentiated controls (Fig. 39A). Triple combination of indicated miRTs into main reporter construct (E3MCK) showed similar relative bioluminescence readouts. Interestingly, insertion of only mirT-659 seed sequences reduced relative luciferase expression due to increased osteogenic background signal. Our findings suggest that miRT-659 target genes might be involved in the regulation of transcription during osteogenesis in control cells. In fact, impact of miRT-550 and miRT-659 sequences on osteogenic differentiation is still unknown and should be investigated to get insight into the biological process. Conversely, miRT-222 and miRT-550 showed higher bioluminescence and fluorescence activity. This advanced reporter system combined with miRNA seed sequences might be a useful add-on to improve the signal-to-noise ratio in *in vivo* experiments.

4.4. Reliable noninvasive reporter systems present a feasible monitoring tool for skeletal muscle tissue engineering

We could demonstrate the feasibility of the reporter system in two-dimensional and 3D *in vitro* skeletal muscle engineering approaches. With the notion that secreted bioluminescent assays have

been shown to be more sensitive than cytosolic luciferase- or fluorescence-based reporter assays [1089], we chose to evaluate Metridia luciferase reporter activity by varying conditions that are known to affect myogenic differentiation, namely substrate stiffness and mechanical stimulation. Using C2C12 cells transfected with E3MCK, we could demonstrate that the reporter system was able to reflect gradual changes in myogenic differentiation upon culture on fibrin matrices of different stiffness (Fig. 40A). Pliant matrices are known to promote *in vitro* myogenesis [355] and we observed an approximately threefold (10 mg/mL fibrinogen) and fivefold (20 mg/mL fibrinogen) increase in reporter activity after myogenic differentiation on fibrin compared with cell culture plastic. Furthermore, we could reproduce the well-established beneficial effects of mechanical stimulation on myogenic differentiation [430] in a bioreactor-based 3D bioartificial muscle model using our reporter system, with an approximately 1.7-fold increase in reporter activity when static mechanical stimulation was applied (Fig. 40B).

Nondestructive assaying methods become increasingly important in tissue engineering as they reduce sample numbers and allow for time- and cost-efficient monitoring of the same sample set over time. Our tissue-specific reporter system provides a nondestructive analysis tool that is suitable for analysis and optimization of bioreactor-based culture systems as well as *in vitro*/*vivo* live cell monitoring.

5. ACKNOWLEDGEMENTS

6. DISCLOSURE STATEMENT

No competing financial interests exist.

CHAPTER II

Generation of a fibrin-hyaluronan interpenetrating polymer network to improve the mechanical and biological properties of fibrin hydrogels

"Hyaluronic acid-fibrin interpenetrating double network hydrogel prepared *in situ* by orthogonal disulfide cross-linking reaction for biomedical applications"

Yu Zhang[1,†], **Philipp Heher**[2,3,†], Jöns Hilborn[1], Heinz Redl[2,3,*], and Dmitri A. Ossipov[1,*]

[1] Science for Life Laboratory, Division of Polymer Chemistry, Department of Chemistry-Ångström, Uppsala University, SE 751 21, Uppsala, Sweden

[2] Austrian Cluster for Tissue Regeneration, Ludwig Boltzmann Institute for Experimental and Clinical Traumatology, Donaueschingenstrasse 13, A-1200, Vienna, Austria

[3] Trauma Care Consult GmbH, Gonzagagasse 11/25, A-1010, Vienna, Austria

[†] these authors contributed equeally to this work

[*] corresponding authors: Dmitri A. Ossipov: Lägerhyddsvägen 1, Box 538, 751 21 Uppsala, Sweden. Tel.: +46 18 471 7335; Fax: +46 18 471 3477. E-mail address: dmitri.ossipov@kemi.uu.se; Heinz Redl: Donaueschingenstrasse 13, 1200 Vienna, Austria. Tel.: +43 5 9393 41961. Fax: +43 5 9393 41982. E-mail address: office@trauma.lbg.ac.at

ABSTRACT

To strengthen the mechanical properties of a fibrin gel and improve its applicability as a scaffold for tissue engineering (TE) applications, a strategy for the *in situ* preparation of the interpenetrating network (IPN) of fibrin and hyaluronic acid (HA) was developed on the basis of simultaneous and orthogonal fibrinogenesis and disulfide cross-linking. The synthetic pathway included the preparation of mutually reactive HA derivatives bearing thiol and 2-dithiopyridyl groups. Combining thiol-derivatized HA with thrombin and 2-dithiopyridyl-modified HA with fibrinogen and then mixing the obtained liquid formulations afforded IPNs with fibrin-resembling fibrillar architectures at different ratios between fibrin and HA networks. The formation of two networks was confirmed by conducting reference experiments with the compositions lacking one of the four components. The composition of 2% (w/v) fibrin and 1% (w/v) HA showed the highest storage modulus (G′), as compared with the single network counterparts. The degradation of fibrin in IPN hydrogels was slower than that in pure fibrin gels both during incubation of the hydrogels in a fibrin-cleaving nattokinase solution and during the culturing of cells after their encapsulation in the hydrogels. Together with the persistence of HA network, it permitted longer cell culturing time in the IPN. Moreover, the proliferation and spreading of MG63 cells that express the hyaluronan receptor CD44 in IPN hydrogel was increased, as compared with its single network analogues. These results are promising for tunable ECM-based materials for TE and regenerative medicine.

STATEMENT OF SIGNIFICANCE

The present work is devoted to *in situ* fabrication of injectable extracellular matrix hydrogels through simultaneous generation of networks of fibrin and hyaluronic acid (HA) that interpenetrate each other. This is accomplished by combination of enzymatic fibrin cross-linking with orthogonal disulfide cross-linking of HA. High hydrophilicity of HA prevents compaction of the fibrin network, while fibrin provides an adhesive environment for *in situ* encapsulated cells. The interpenetrating network hydrogel shows an increased stiffness along with a lower degradation rate of fibrin in comparison to the single fibrin network. As a result, the cells have sufficient time for the remodelling of the scaffold. This new approach can be applied for modular construction of *in vitro* tissue models and tissue engineering scaffolds *in vivo*.

1. INTRODUCTION

The general idea of tissue engineering (TE) is based on the three-dimensional (3D) culturing of cells in suitable resorbable scaffolds followed by the implantation of the cell-seeded scaffolds *in vivo*. Hydrogels are 3D networks composed of cross-linked hydrophilic polymer chains. Hydrogels have been used as TE scaffolds and in cell therapy because they provide the cells with highly hydrated tissue-like environment [1090]. 3D encapsulation of cells in hydrogels is conducted *in situ*, i.e. during the polymer chains cross-linking; this affords a network to which the cells become entrapped and possibly attached. Ideally, hydrogels should mimic extracellular matrix (ECM) by providing a complex natural cocktail of tissue-specific signals. This is often achieved by supplying the cells with growth factors that have a very well-defined role in tissue development. Particularly, the stimulation of cellular growth and the proliferation and differentiation in hydrogel matrices were often relied on the simultaneous *in situ* encapsulation of the cells and growth factors. Among many factors that have to be considered in hydrogel design for TE, mechanical properties and the rate of scaffold degradation are important for providing adequate mechanical support for the cells during culture and space for scaffold remodelling. Moreover, in the case of load-bearing tissue, the scaffold must provide sufficient temporary support after implantation *in vivo* to withstand *in vivo* stress and loading [1091]. Natural macromolecules such as collagen, fibrin and hyaluronic acid (HA) have widely been used to generate hydrogels with 3D encapsulated cells as they possess many favourable properties for biomedical applications [1092].

Fibrin is formed during the physiological coagulation cascade after thrombin-mediated cleavage of fibrinogen in the presence of Ca^{2+}. Fibrinogen is an approximately 45-nm-long plasma protein composed of two sets of three polypeptide chains, Aα, Bβ and γ, which are joined together by six disulfide bridges. Upon activation by the serine protease thrombin, fibrinogen monomers have a great tendency to self-associate in a half-staggered manner to form insoluble fibrin, a 3D porous network structure. Furthermore, the activated blood coagulation factor XIIIa belonging to a family of transglutaminases rapidly cross-links γ chains in the nascent fibrin polymer by introducing intermolecular (γ-glutamyl)-lysine chemical cross-links between the lysine of one γ-chain and the glutamine of the other γ-chain. Fibrin sealants have been clinically used as a haemostatic agent in cardiac, liver and spleen surgery [775]. Due to their ability to support cell proliferation and differentiation, fibrin hydrogels have also been used in the last decade in a variety of TE applications, including engineering of cardiovascular, ocular, muscle and bone tissues [834]. However, fibrin has three major disadvantages: (1) compaction upon gel formation, (2) low mechanical strength, and (3) rapid degradation precluding proper tissue regeneration [578, 579, 834, 854, 876]. To improve the poor mechanical properties of fibrin, the combination of fibrin with other materials was suggested to obtain constructs with improved mechanical strength [752, 757, 1093, 1094].

HA is a non-sulfated glycosaminoglycan that is widely distributed in the ECM of connective tissues. It plays an important role in the regulation of cell adhesion and the morphogenesis and modulation of inflammation. Because of its high hydrophilicity, biocompability and unique viscoelastic properties, HA has been used in a number of clinical applications, including eye surgery to facilitate healing and regeneration of the surgical wounds (a surgical aid) [1095] and ear and sinus surgery [1092]. HA hydrogels are also promising materials in cell culture and drug delivery [1096-1099]. HA was chemically converted into mutually reactive derivatives that could form hydrogels upon simple mixing in an aqueous medium [1097]. Moreover, two orthogonal chemoselective cross-linking reactions were envisioned to form an interpenetrating network (IPN) of HA and fibrin to reinforce fibrin for TE applications [753, 1094]. Despite of these few examples of combination of HA and fibrin, little is known about which chemoselective chemistries can be tolerated without compromising the formation of fibrillar structure of fibrin and afford ECM resembling IPNs with improved mechanical properties and lasting for sufficient time for inducing cell proliferation and differentiation.

In this study, we investigated the use of disulfide cross-linked HA hydrogel in preparation of fibrin/HA IPN gels as an injectable and biodegradable scaffold for cell proliferation and differentiation. We first investigated if the obtained hydrogel was composed of two chemical networks of HA and fibrin. Mechanical properties of these new IPN gels were compared with those of single network counterparts as well as with the formulations wherein the conditions for one of the cross-linking reactions were compromised. Fluorescence spectroscopy was utilized for quantification of enzymatic degradation of hydrogels prepared from fluorescently labelled fibrinogen. Finally, viability, spreading and proliferation of cells encapsulated in IPN gels were studied in comparison with the single network analogues. Hydrogels degradation mediated by the cells laden in IPN hydrogels was also performed.

2. MATERIALS AND METHODS

2.1 Materials

HA sodium salt (MW 150 kDa) was purchased from Lifecore Biomedical, USA. 1-Ethyl-3-(3-dimethylaminopropyl) carbodiimide (EDC), N-hydroxybenzotriazole (HOBt), 2,2′-dithiodiethanol DL-dithiothreitol (DTT) and pyridyl disulfide were purchased from Sigma-Aldrich Chemical Co., Sweden. Hydrogels for rheological measurements were prepared with Tissucol (Baxter, Austria) 1.0 mL kit (fibrinogen, aprotinin, thrombin and $CaCl_2$ solution). For degradation studies, hydrogels were prepared from Tissucol Duo 500 (Baxter, Austria) 5.0 mL kit (fibrinogen and thrombin). Alexa-488-labelled fibrinogen was purchased from Life Technologies, Sweden. All solvents were of analytical quality. ^{1}H-NMR spectra of HA derivatives were recorded in D_2O with a JEOL JNM-ECP Series FT NMR spectrometer (400 MHz).

2.2. Synthesis of HA-hy-SSPy

HA was dually functionalized with hydrazide and thiol groups in one pot, as previously reported [1100]. In detail, 400 mg of HA sodium salt (MW 150 kDa, 1 mmol of disaccharide repeat units) was dissolved in 50 mL of distilled water. Two homodifunctional linkers, 1-(3-((hydrazinecarbonyl)oxy propyl) 2-(2-(methylthio)ethyl) hydrazine-1,2-dicarboxylate (**1** in Scheme 1A, 0.15 molar equivalent of HA repeat units) and 3,3'-disulfanediyldi(propanehydrazide) (**2** in Scheme 1A, 0.15 molar equivalent of HA repeat units) were added into HA solution followed by the addition of HOBt (1 molar equivalent per HA repeat unit), and the pH was adjusted to 4.7. EDC was added into the mixture at 0.3 molar equivalent per HA repeat unit. After the overnight reaction, the pH of the mixture was increased to 8 and DTT was added with 10:1 molar ratio to the sum amount of the linkers. After the next overnight treatment, the pH of the mixture was lowered to 3.5 and the mixture was thrice dialyzed against acidified water (pH = 3.5) and finally lyophilized. The obtained HA-hy-SH was analysed by ^{1}H-NMR to find the degree of modification with hydrazide (-hy: 10%) and thiol (-SH: 10%) groups.

Thiol groups in the resulting HA-hy-SH derivative were converted into 2-dithiopyridyl (-SSPy) groups by treatment with dipyridyl disulfide. Briefly, 300 mg of HA-hy-SH (0.75 mmol of HA repeat units, 0.075 mmol of -SH) was dissolved in 40 mL distilled water and pH was adjusted to 8.5. DTT at 10 molar equivalents per thiol group corresponding to 115.7 mg was added before addition of 247.8 mg (1.125 mmol) of dipyridyl disulfide in 30 mL methanol. After overnight reaction at room temperature, the mixture was thrice dialyzed using the above-described process and finally lyophilized to obtain HA-hy-SSPy derivative. ^{1}H-NMR confirmed quantitative conversion of thiol groups (10%) into -SSPy groups.

2.3. Synthesis of HA-SH

HA-SH was synthesized from native HA using only homodifunctional linker **2** (Scheme 1B) under the conditions described for the synthesis of HA-hy-SH derivative. The degree of thiol modification was 10%.
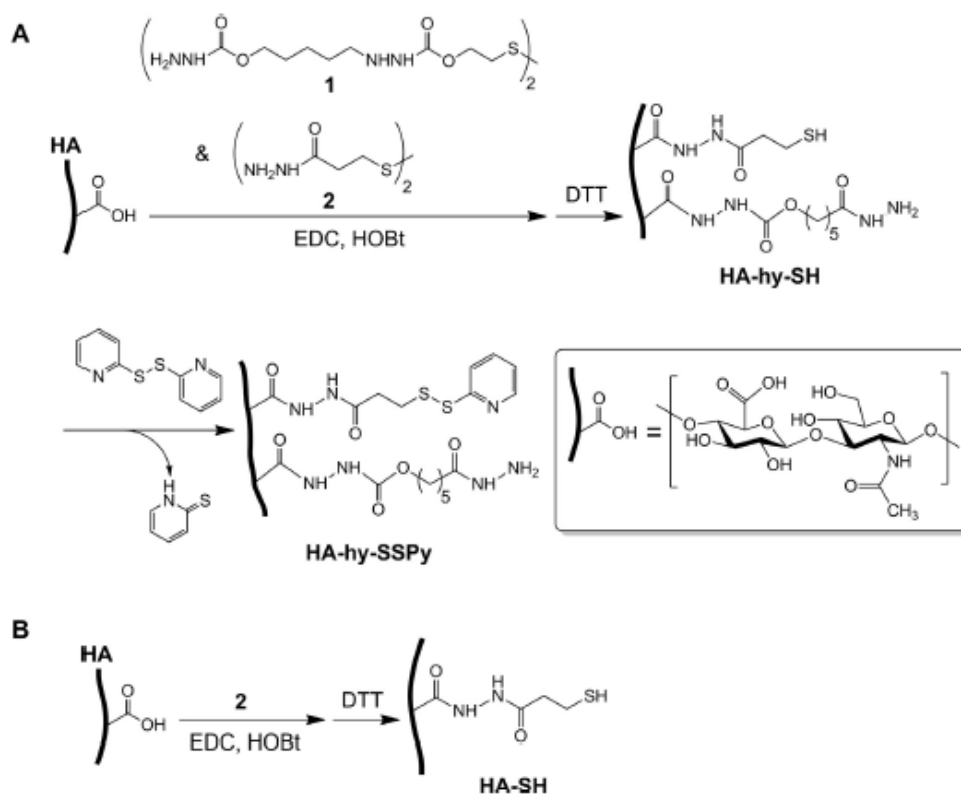
Scheme 1: *Synthesis of (A) HA-hy-SSPy and (B) HA-SH derivatives.*

2.4. Preparation of hydrogels

2.4.1. Preparation of stock solutions

Fibrinogen was dissolved in aprotinin solution (3000 KIU/mL) at 10% concentration. The obtained solution was further diluted to 8% (w/v) with aprotinin solution. Thrombin was dissolved in 40 mM CaCl$_2$ solution at 4 IU/mL concentration. Hyaluronan derivatives, HA-hy-SSPy and HA-SH were separately dissolved in serum free Dulbecco's Modified Eagle's medium at 2 % (w/v) concentration and neutralized with 2 M NaOH prior to use.

2.4.2. Preparation of IPNs

Fibrin&HA IPN hydrogels of 300 μL were prepared by mixing equal volumes (75 μL each) of fibrinogen, thrombin, HA-SH and HA-hy-SSPy. In particular, fibrinogen solution was mixed with HA-hy-SSPy solution to afford mixture A. Thrombin was mixed with HA-SH in a separate Eppendorf tube to afford mixture B. The hydrogel was subsequently made in a 2 mL syringe (with cut off head) used as a mould by first applying the mixture A and then adding the mixture B upon stirring with a pipette tip. The combined A + B mixture was further mixed and allowed to set at room temperature for 12 h. This procedure afforded an IPN with 2% of fibrin and 1% of HA. IPNs with lower concentration of fibrin (1%) and HA (0.5%) were prepared starting with diluted fibrinogen (4%) and HA derivatives (1%) solutions. The dilutions were performed with a serum free cell culture medium.

2.4.3. Preparation of fibrin gels

By mixing equal volumes (150 μL each) of fibrinogen (4% and 2% respectively) and 2 IU/mL thrombin, 2% and 1% fibrin hydrogels of 300 μL were prepared. Diluted solutions of fibrinogen and thrombin were prepared from the corresponding stock solutions and serum-free cell culture medium.

2.4.4. Preparation of control gels

Control single HA network hydrogel containing 1% fibrinogen was prepared analogously to IPNs but without thrombin. In this case, thrombin solution was replaced with 75 μL of serum free cell culture medium. Another control single network fibrin hydrogel containing 1% HA was prepared analogously to IPNs but by replacing the HA-SH solution with 75 μL of the HA-hy-SSPy solution.

For monitoring the degradation of hydrogels by fluorescence spectroscopy, fibrin and fibrin&HA IPN hydrogels were prepared as described above, the only exception being that Alexa Fluor© 488-labelled fibrinogen was used together with the non-labelled fibrinogen. Specifically, 67.5 μL of unlabeled fibrinogen was mixed with 7.5 μL of the fluorescent fibrinogen dissolved in the aprotinin solution at 10 mg/mL concentration.

2.5. Rheology studies

Mechanical properties of hydrogels were studied by rheology after preparation as well as after swelling the hydrogels in PBS for 24 h. Rheological measurements of hydrogels were performed on AR2000 rheometer (TA Instrument) using an aluminium plate geometry of 8 mm diameter and plate sample stage. The measurements were taken at 25 °C in the dynamic oscillatory mode with a constant strain of 1% and frequency ranging from 0.1 to 10 Hz. After setting for 24 h, the hydrogels were removed from syringes and weighed. After weighing, hydrogels were placed on a plate sample stage immediately to perform the measurements with normal force around 0.02 N. After measurements, hydrogels were soaked in 5 mL of PBS for 24 h.

2.6. SEM studies

Scanning electron microscopy (SEM) images of hydrogels were taken using Zeiss 1550 with AZtec EDS. Hydrogels were fixed in the 2% glutaraldehyde solution, dehydrated with graded ethanol, and air-dried to remove ethanol in the hood overnight. Specimens were then sequentially struck to sample stubs with double-stick conductive tape sputtered with gold before the morphology was determined.

2.7. Enzymatic degradation of hydrogels with nattokinase

Three 2% (w/v) fibrin gels and three IPNs (2% of fibrin and 1% HA) were prepared using Alexa Fluor© 488-labelled fibrinogen as described above. The hydrogels were set at room temperature overnight and then incubated in 3 mL of PBS containing 0.1 IU of nattokinase at 37 °C. The media

was replaced with fresh nattokinase solution every day. The collected degradation media at each time point was examined by fluorescence spectroscopy. All measurements were performed in triplicates.

2.8. Cell culture

The human osteosarcoma cell line MG63 (American Type Culture Collection, USA) was cultured in Dulbecco's modified Eagle's medium high glucose (DMEM-HG; Life Technologies, USA) supplemented with 10% foetal calf serum (GE Healthcare, United Kingdom), 1% penicillin/streptomycin (Lonza, Switzerland) and 1% L-glutamine (Lonza, Switzerland). This medium is referred to as growth medium (GM). Cells were grown on standard cell culture dishes (Starlab, Germany) in a humidified incubator at 37 °C and 5% CO2 and subcultured at 80%–90% confluence. For proliferation study, GM was supplemented with the fibrinolysis inhibitor aprotinin (Baxter, USA) at a final concentration of 100 KIU/mL.

2.9. Cell-mediated hydrogel degradation

Fibrin-HA IPNs and fibrin hydrogels were prepared as described above. Briefly, 5×10^5 MG63 cells were added to mixture B (HA-SH and thrombin) for IPN preparation or to the thrombin solution for fibrin gel preparation. In both cases, Alexa Fluor$^©$ 488-labelled fibrinogen (Life Technologies, USA) was added for fluorescence monitoring of the hydrogel degradation. Hydrogels with a volume of 200 µL were prepared in 2 mL syringes (B. Braun GmbH, Austria) with cut off head and left to polymerize at 37 °C, 5% CO2 for 45–60 min. Final concentrations were 1% fibrin, 0.5% HA, 1 IU/mL thrombin and 25 µg/mL Alexa Fluor$^©$ 488-labelled fibrinogen.

For fluorescence monitoring of fibrinolysis, fibrin hydrogels were dissolved in 100 IU/mL nattokinase (Japan Bioscience Labs, USA) in PBS, pH 7.4 supplemented with 15 mM ethylenediaminetetraacetic acid (EDTA; Sigma Aldrich, Austria). Fibrin-HA IPN hydrogels were dissolved in a 1+1 mixture of 200 IU/mL nattokinase and 100 mM N-acetyl-L-cysteine (Sigma Aldrich, Austria). Hydrogel degradation at different time points (day 0, day 3 and day 6) was performed at 37 °C for 30–45 min under constant agitation. Fibrinolysis was quantified with a GloMax$^©$ Multi + Detection System plate reader (Promega, USA) and calculated as the ratio between the total fluorescence of a dissolved hydrogel at the respective time point and the total fluorescence of a dissolved hydrogel at day 0. All measurements were performed in triplicates and fluorescence was acquired as the average signal from five consecutive reads.

2.10. Proliferation assay by DNA quantitation

In fibrin, HA and fibrin-HA IPN hydrogels of 150 µL volume, 3×10^5 MG63 cells were encapsulated. Final concentrations were 1.5 % fibrin, 0.75% HA and 1 IU/mL thrombin. For proliferation analysis, hydrogels were dissolved as described above and the cells were harvested by centrifugation at 1200 rpm for 5 min. The pellet was thoroughly resuspended in DMEM-HG supplemented with 5 µg/mL

HOECHST 33342 (Life technologies, USA), and the cell suspension was subsequently incubated in the dark at 37 °C for 60 min. Fluorescence measurements were performed in triplicates on a GloMax© Multi + Detection System plate reader, and fluorescence was acquired as the average signal from five consecutive reads.

2.11. Live/dead staining assay

At days 0, 2, and 5 after scaffold preparation, cells viability was assessed by staining the cells with Calcein AM and propidium iodide (PI; both from Sigma Aldrich, Austria). Whole scaffolds were stained in serum free DMEM-HG containing 2.5 µg/mL Calcein AM and 1 µg/mL PI for 30 min at 37°C in the dark. The cells were analysed with a Leica DMI6000B epifluorescence microscope (Leica Microsystems GmbH, Germany).

2.12. Statistical analysis

All data are presented as mean ± standard deviation (S.D.). Normal distribution of data was tested with the D'Agostino & Pearson omnibus normality test. Comparisons between experimental groups were calculated using One-way ANOVA (Analysis Of Variance) with Tukey's multiple comparison test and P-values ≤ 0.05 were considered statistically significant. All calculations were performed using GraphPad Prism Software (GraphPad Software Inc., San Diego, USA).

3. RESULTS AND DISCUSSION

3.1. Synthesis of HA-hy-SSPy derivative

Thiol-disulfide exchange reaction was chosen to provide a disulfide cross-linked HA network because it was proven to be cytocompatible for several cell types *in vitro* [1100]. We first considered forming a disulfide network by mixing the aqueous solutions of thiolated HA (HA-SH) and HA modified with 2-dithiopyridyl groups (HA-SSPy) [1101]. However, the kinetic of gelation of this system was too fast (less than 30 s) when the degrees of modification of HA derivatives with the functional groups was about 10% or even less. This precluded proper mixing of HA components with fibrin forming components. On the other hand, we anticipated dual functionalization of one of the HA components with hydrazide groups for possible orthogonal labelling of it with an imaging agent. Thus, dual functionalization of HA with both 2-dithiopyridyl (-SSPy) and hydrazide (-hy) groups was performed, providing the HA-hy-SSPy derivative (Scheme 1A) that later showed slower rates of disulfide cross-linking acceptable for the formation of IPN networks with fibrin. The complementary reactive HA-SH derivative was obtained according to previously reported procedure (Scheme 1B) [1102]. In particular, carboxylate groups of native HA (Scheme 1A) were activated with EDC and HOBt and then coupled to hydrazide groups of the linkers **1** and **2** through amide bonds. One pot treatment of the reaction

mixture with a reducing agent DTT allowed cleavage of disulfide bonds in the HA-coupled linkers leaving the free hydrazide groups and thiol groups attached to HA as we previously reported [1100]. The free thiol groups in the obtained HA-hy-SH derivative were consequently converted to 2-dithiopyridyl groups via the disulfide bond exchange reaction between HA-hy-SH and dipyridyl disulfide as depicted in Scheme 1A.

Dual modification of HA with 2-dithiopyridyl (-SSPy) and hydrazide (-hy) groups was confirmed by ^{1}H-NMR (Figure 41). Particularly, proton peaks at 7.39, 7.63, 7.18 and 8.25 ppm corresponding to four aromatic protons of 2-pyridyl substituent were observed together with peaks at 2.70 and 2.89 ppm corresponding to the methylene protons of the –C(O)CH_2CH_2-SS– side chains bridging HA backbone with the –SSPy functional group. On the other hand, α, β, γ, δ and ε-methylene protons of the hydrazide-terminated side chains (see Figure 41 for abbreviations) were detected at 2.3, 1.65, 1.38 and 4.15 ppm, respectively, as we previously reported for the synthesis of HA that was functionalized similarly with only hydrazide groups [1103].
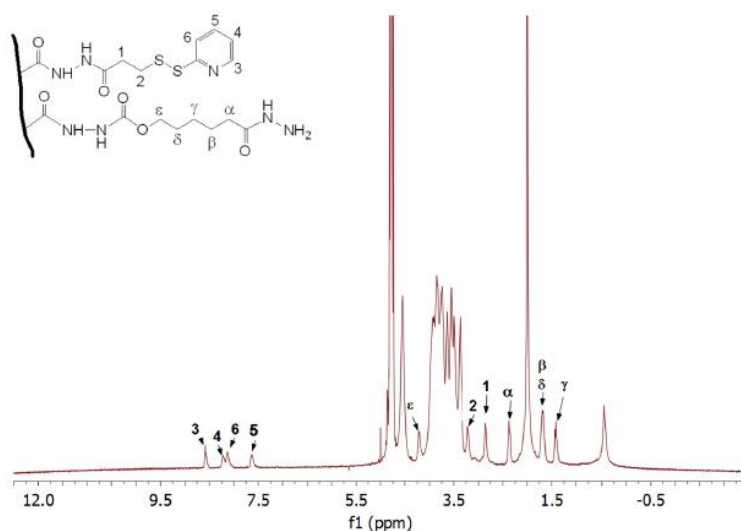

Fig. 41: *^{1}H-NMR spectrum of HA derivative dually functionalized with hydrazide and 2-dithiopyridyl groups (Ha-hy-SSPy).*

3.2. Formation of IPN gels

Due to the hydrophilicity of HA, we assumed that its combination with fibrin should keep water within the hybrid fibrin-HA matrix. We also surmised that HA should not be just a solute but constitute a part of the matrix. There are two ways to achieve this: (*i*) through chemical incorporation of HA into the fibrin network or (*ii*) by generation of two IPNs, one composed of fibrin and another composed of HA. However, in the latter case, the two cross-linking reactions should be chemically orthogonal to each other. We hypothesized that the formation of a disulfide network between thiolated HA (HA-SH) and HA modified with reactive 2-dithiopyridyl group (-SSPy) should be chemoselective towards enzymatically catalyzed steps of fibrin formation. To trace the HA network, one of the derivatives was also equipped with hydrazide (-hy) groups. Synthesis and structures of the HA

network forming derivatives, HA-SH and HA-hy-SSPy, are shown in Scheme 1. Since both fibrin and HA networks are formed after the mixing of two essential components (fibrinogen and thrombin for fibrin network; HA-SH and HA-hy-SSPy derivatives for disulfide cross-linked HA network), we anticipated simultaneous formation of the two networks via the pairwise combination of HA-hy-SSPy with fibrinogen and HA-SH with thrombin, followed by the mixing of the two combined solutions (Scheme 2). This platform of formation of IPN hydrogel that is triggered by a single mixing event was recently applied by us in the fabrication of hydrazone and disulfide IPNs [1104].
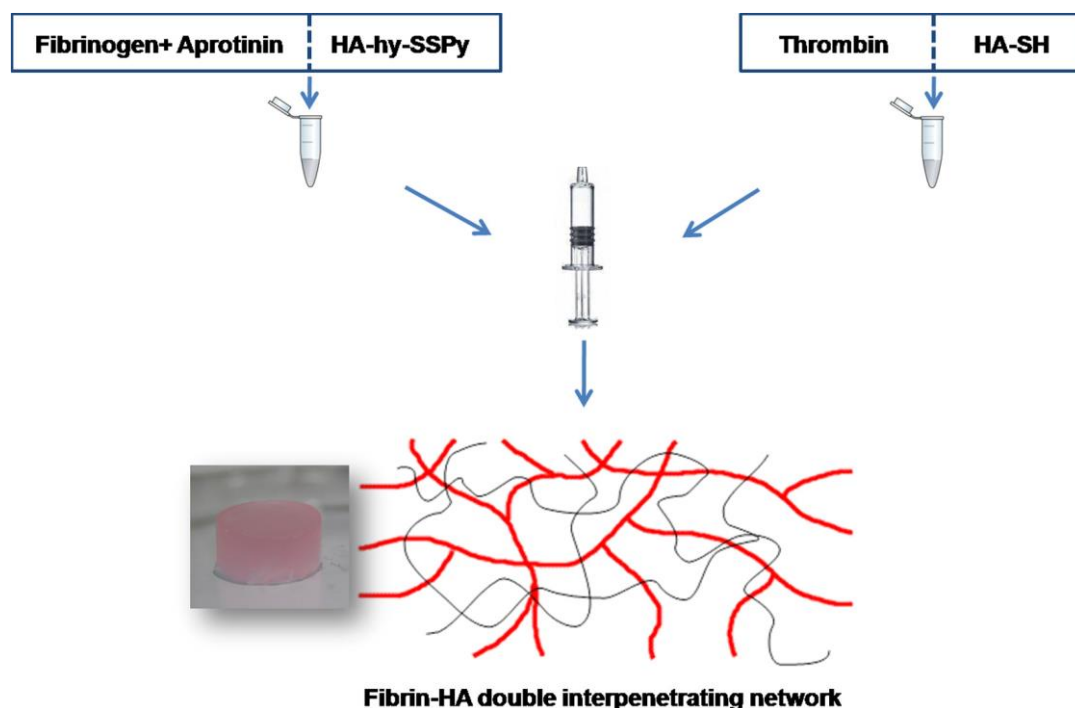
Scheme 2: *In situ formation of double IPN by the simultaneous and independent fibrin fibrils formation (depicted in red) and HA disulfide cross-links (depicted in black).*

Figure 42a shows the image of an IPN hydrogel formed with 2% fibrin and 1% HA in comparison with pure 2% fibrin (Figure 42b) or 1% fibrin (Figure 42c) hydrogels. The IPN hydrogel retained its shape after transporting from a syringe mould. Although pure 2% fibrin retained the cylindrical shape, it expelled small amounts of cell culture medium. In contrast, 1% fibrin gel lost around 70% of the medium and the mass of 1% fibrin gel was only 89.2 ± 23 mg (Table 6), indicating considerable shrinkage of the hydrogel. This result proved that HA assisted with maintaining water in IPN hydrogel, which is very important in the application of hydrogels as TE scaffolds [1105].
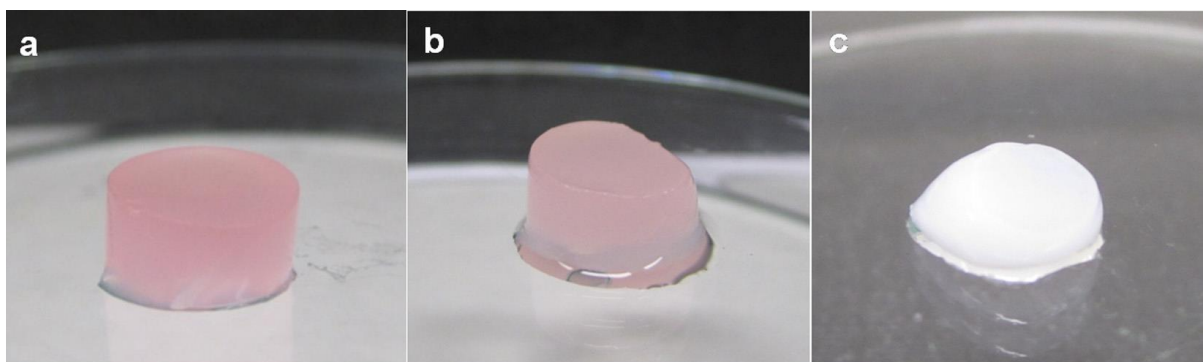
Fig. 42: *Images of a) 2% fibrin-1% HA IPN hydrogel, b) 2% fibrin hydrogel and c) 1% fibrin clot.*

Hydrogel type	Before swelling		After swelling	
	Mass, mg	G', Pa	Mass, mg	G', Pa
1%Fibrin	89.2 ± 23.0	not measured	71.3 ± 11.7	not measured
1.5%Fibrin	177.7 ± 5.0	503 ± 82	138.6 ± 4.1	839 ± 141
2%Fibrin	273.4 ± 33.0	1628 ± 250	189.8 ± 24.0	1304 ± 242
1%Fibrin-1% non-crosslinked HA	40.5 ± 6.9	not measured	28.8 ± 2.9	not measured
0.5%HA	266.0 ± 15.0	232 ± 22	174.1 ± 12.9	150 ± 6
0.75%HA	267.2 ± 7.5	328 ± 7	248.2 ± 14.4	335 ± 8
1%HA	241.6 ± 25.0	554 ± 118	233.2 ± 17.6	578 ± 62
1%Fibrinogen-1% HA	274.3 ± 18.6	1275 ± 110	271.6 ± 21.6	1331 ± 64
1%Fibrin-0.5%HA	284.6 ± 25.0	819 ± 65	259.3 ± 13.7	748 ± 85
1%Fibrin-1%HA	277.5 ± 21.5	1460 ± 117	276.6 ± 16.4	1507 ± 86
1.5%Fibrin-0.75% HA	232.0 ± 6.4	642 ± 10	230.8 ± 8.2	714 ± 49
2%Fibrin-0.5%HA	277.2 ± 21.5	1362 ± 169	261.0 ± 25.6	1418 ± 116
2%Fibrin-1%HA	265.4 ± 12.5	2306 ± 390	276.1 ± 14.0	2470 ± 527

Table 6: *Mechanical properties of IPN, fibrin and HA hydrogel.*

3.3. Conversion of fibrinogen to fibrin and disulfide cross-linking of HA can be simultaneously performed

As mentioned before, fibrinogen can polymerize into a fibrin gel after thrombin-mediated cleavage in the presence of Ca^{2+} ions. However, because polypeptide chains in fibrinogen are linked together via disulfide bonds, it was necessary to confirm whether fibrin can be formed in the presence of thiol and dithiopyridyl-modified HA derivatives. Moreover, enzymatic activity of transglutaminases relies on cysteine containing catalytic sites [1106] that might also interfere with the 2-dithiopyridyl functionality of HA. It is evident from Figure 43 that IPN hydrogel and its single network analogues (HA and fibrin hydrogels) have different morphologies. The image of IPN (Figure 43a) showed clear fibrillar network as expected, which proves that the conversion of fibrinogen to fibrin can occur even in the presence of mutually reactive HA derivatives (HA-SH and HA-hy-SSPy). This can be explained by the very fast reaction of HA-SH with HA-hy-SSPy forming a disulfide HA network via thiol-disulfide exchange reaction. As a result, HA-SH does not interfere with the thrombin-mediated removal of fibrinopeptides A and B from fibrinogen and subsequent polymerization of fibrin

monomers into a fibrin fibrillar network. However, this evidence is not enough to claim that chemical cross-linking of fibrin macromolecules can still occur in the IPN system similarly to that of pure fibrin. The morphology of the hydrogel formed with HA-SH, HA-hy-SSPy and fibrinogen was similar (Figure 43b) to the morphology of pure HA gel (Figure 43d) and was characterized by the appearance of polymer sheets rather than fibrils. It demonstrates that the presence of fibrinogen in the HA cross-linking mixture is not enough for the formation of an IPN. On the other hand, it proved that the HA disulfide network can be formed in the presence of fibrinogen. The fibrillar network of pure fibrin (Figure 43c) was denser compared with that of the IPN, which indicates some steric interference that HA network should impose during fibrillogenesis.
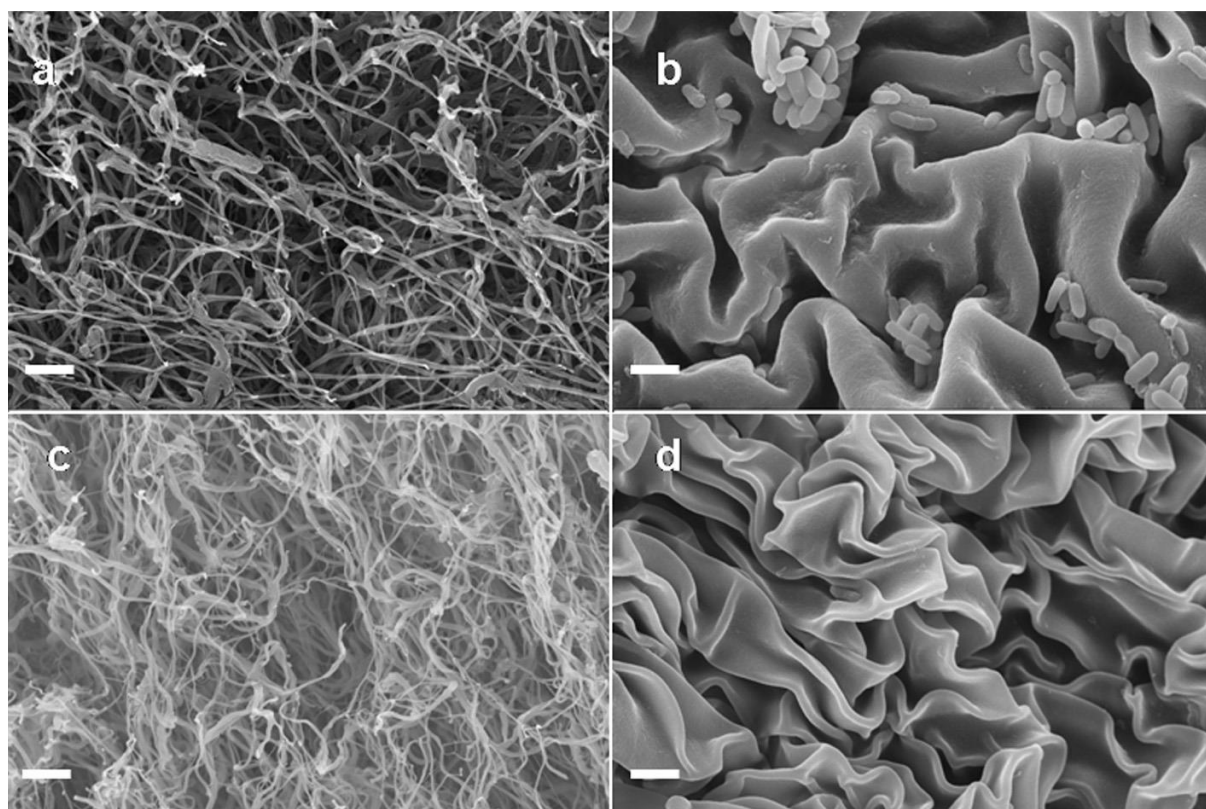

Fig. 43: *SEM images of a) 2% fibrin-1% HA IPN hydrogel; b) 1% fibrinogen-1% HA hydrogel; c) 2% pure fibrin gel; and d) 1% HA hydrogel.* Scale bars represent 1 µm.

3.4. Mechanical properties of double interpenetrating network and its single network counterparts

We examined mechanical properties of different hydrogels to assess whether the combination of two cross-linking processes can yield IPN hydrogel with improved total stiffness. The results are presented in Table 6. IPN hydrogels with concentration of fibrin 2% and 1% showed an increased storage module (G′) as compared with the corresponding pure fibrin gels. The improvement of stiffness was especially noticeable for 1% fibrin gel, which expelled most of the water after 24 h of setting and therefore could not be measured because of shrinkage. However, when supported with the HA

network, the resulting IPN with 1% fibrin maintained its shape; this can be seen by examining the masses of the hydrogels after setting. As expected, the G′ of the resulting IPN hydrogel increased with the concentration of HA from 0.5% to 1%. The same effect was also observed upon the increase of fibrin concentration from 1% to 2%. It is noteworthy that the formation of chemically cross-linked HA network is absolutely essential for the stabilization of the combined fibrin-HA hydrogel. In the formulation including only one type of HA derivative (HA-hy-SSPy), the resulting hydrogel repelled water similarly to pure fibrin gel. Examination of the data in Table 6 shows that the disulfide cross-linking of HA does interfere with the formation of fibrin and therefore cannot be considered as completely independent. For example, the combination of 0.5% HA with 2% of fibrin exhibited an elastic modulus of 1362 ± 169 Pa, which was lower that for the pure 2% fibrin (G′ = 1628 ± 250 Pa).

3.5. Enzymatic degradation of IPN and pure fibrin

Rheology measurements proved that disulfide cross-linked HA supported the fibrin network in the IPN hydrogel, which was generally mechanically stiffer than pure fibrin gels. This observation indicated that the IPN hydrogel is expected to degrade *in vivo* at a slower rate than pure fibrin. The time of scaffold resorption should match the time necessary for tissue regeneration, which normally occurs within several weeks. Therefore, the stability of the scaffold within this time is an essential characteristic in TE applications. It concerns both using hydrogels as scaffolds for cell transplantation as well as using hydrogels as delivery vehicles for growth factors (acellular approach). To assess the stability of new IPN hydrogels, they were incubated in PBS containing nattokinase, an enzyme exhibiting a strong fibrinolytic activity [1107]. The results were compared with the enzymatic degradation of pure fibrin gels. During the preparation of IPN and pure fibrin hydrogels, fluorescently labelled fibrinogen was used together with conventional fibrinogen to quantify fibrin degradation over time by fluorescence spectroscopy. This method also allows for non-invasive longitudinal fluorescence imaging *in vivo*. Pure fibrin gels were completely degraded in three days upon incubation in nattokinase solution (Figure 44). Under the same conditions, the initially opaque IPN hydrogels did not dissolve but became more transparent. Interestingly, the opacity remained in the interior of the hydrogel, while the periphery of the hydrogel turned transparent. It indicated that the partial degradation of only the fibrin part of the double network occurred, and this process was controlled by the diffusion of the enzyme. Note that pure HA hydrogels are transparent. Since nattokinase specifically digests fibrin, the HA disulfide network was therefore left intact.

Quantitative florescence measurements of the liquid degradation media confirmed that pure fibrin gel degraded in three days, whereas the major part of fibrin in IPN hydrogels degraded in five days. Hyaluronidase was subsequently added to the remaining HA network to get all macromolecules completely degraded into the form of soluble fragments. This allowed the measurement of the total fluorescence and calculation of the hydrogel degradation profiles (Figure 45). It was evident that at the beginning of incubation, IPN degraded slightly faster than fibrin. However, after the second day of

incubation, almost 80% of fibrin was degraded, whereas the IPN degraded to an extent of 63%. While pure fibrin completely degraded, 15% of fibrin still remained in the IPN hydrogel. The complete degradation of the remaining amount of fibrin in the IPN occurred within the next two days. Clearly, *in vitro* studies demonstrated that the degradability of fibrin can be diminished when it is supported by an interpenetrating HA network. However, note that the *in vitro* degradation in PBS solution cannot perfectly mimic the degradation of the hydrogels *in vivo*.
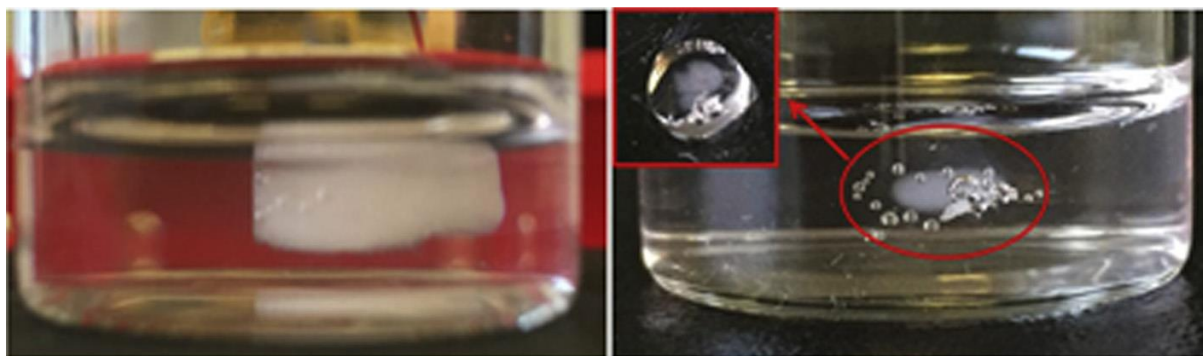

Fig. 44: *Photography images of fibrin and IPN hydrogels taken after three days of incubation in 3 mL PBS containing 0.1 unit of nattokinase.*
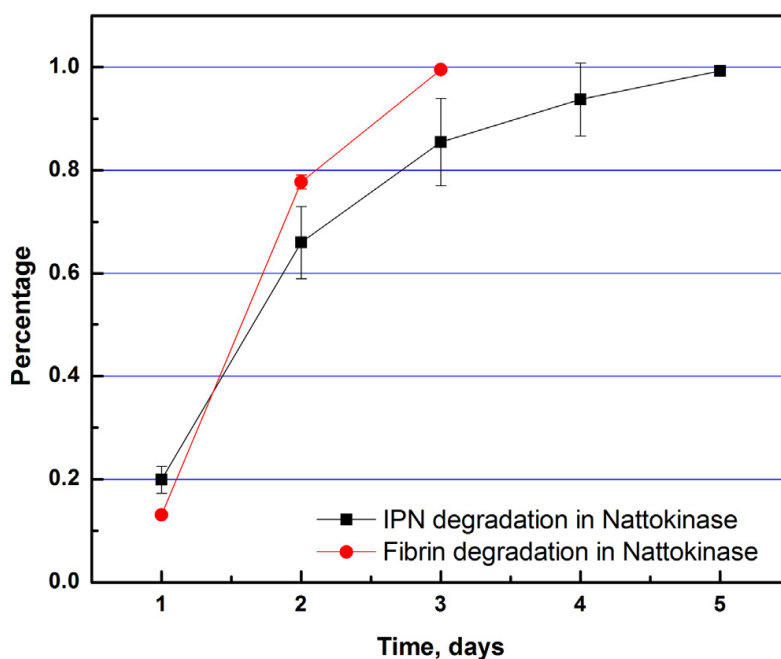

Fig. 45: *Degradation profiles of IPN hydrogel (black curve) and pure fibrin hydrogel (red curve) in nattokinase solution (0.033 U/mL).*

We assumed that the degradation profiles of cell-seeded scaffolds might be different. Therefore, we analysed cell-mediated *in vitro* scaffold degradation to confirm the results of the enzymatic degradation and to demonstrate the feasibility of the IPN hydrogels for three dimensional cell culture and cell therapy. Again, the presence of the reinforcing HA network in the IPN led to slower

degradation of fibrin as compared with pure fibrin formulations although to a rather moderate extent. More notably, fibrin gels were strongly compacted by the cells within only 3 days, whereas IPN hydrogels retained their shape over the culture period of 6 days (Figure 46). Analogously to the degradation in the nattokinase solution, IPNs turned from opaque to transparent during the cells mediated degradation. This result was indirect evidence that the cells were alive in the IPN hydrogel and re-modelled the construct through the fibrin degradation. Contrary, IPN hydrogels with no encapsulated cells remained opaque (data not shown). Note that culturing the cells in the IPN hydrogel does not result in the complete scaffold degradation as it occurs in pure fibrin-based material. Consequently, it can be performed for a longer time that is sufficient for the cells to deposit their own tissue-specific ECM. Considering these results, we assume that *in vivo*, the difference in degradation of both acellular and cell-laden hydrogels might be more pronounced, which will be tested in future projects.
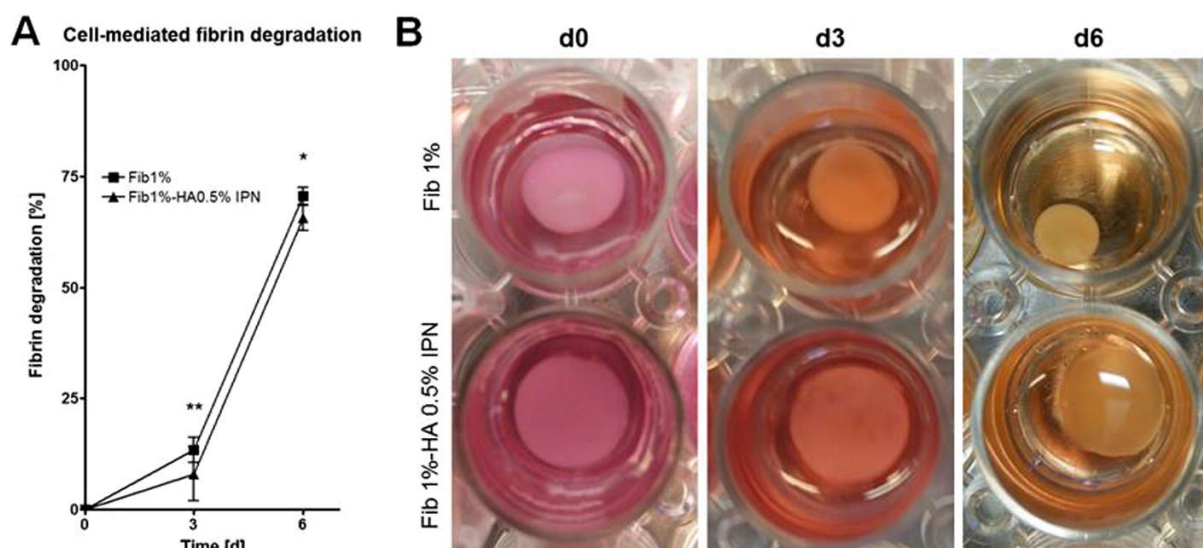

Fig. 46: *Cell-mediated degradation of fibrin and IPN hydrogels.* (A) Degradation profiles over 6 days, with slower progression of fibrinolysis in the IPNs (n = 3; mean ± S.D.; *p < 0.5, **p < 0.01; One-way ANOVA with Tukey's multiple comparison test). (B) Fibrin hydrogels are compacted by the cells over time, while the presence of HA in the IPNs counteracts this effect. Note the transition of the IPN from opaque to transparent due to fibrin degradation.

3.6. 3D cell encapsulation in IPN and in pure fibrin hydrogel

Fibrin has been used as a scaffold material for TE because it not only supports cell proliferation and differentiation but also displays a high degree of cytocompatibility due to the abundance of a variety of cell binding sites [866]. In addition, many different growth factors such as vascular endothelial growth factor and fibroblast growth factor-2 (bFGF) have been demonstrated to bind to fibrinogen [579]. On the other hand, HA is known by its anti-adhesive properties. However, HA contains several binding sites for the polymorphic glycoprotein CD44 that is expressed on the surface of many cells and tissues [1108]. CD44-HA interactions have been identified as the major mediator of melanoma cell proliferation [1109] and facilitated the migration of mesenchymal stem cell [1110]. A combination

166

of fibrin with an HA network is therefore expected to improve cell attachment to the HA network to promote proliferation and differentiation. Moreover, the fibrillar structure of the IPN should also improve oxygen and nutrient diffusion through the double network.

To investigate whether the combination of fibrin and HA in the IPN would further improve cellular attachment and proliferation in response to the availability of CD44 binding sites, MG63 human osteosarcoma cells were encapsulated within fibrin and HA and IPN hydrogels and cell viability and proliferation were tested (Figure 47). As expected, the addition of an HA network to fibrin in the IPN resulted in significantly improved cell proliferation, most likely due to the addition of CD44 binding sites to the fibrin hydrogel. This result should also be considered for the assessment of cell-mediated fibrin degradation in the IPN shown above. Degradation of fibrin should be facilitated by the higher number of cells but was effectively counterbalanced by the HA network. Furthermore, within 2 days, cells exhibited spread morphology when encapsulated within the IPN, a clear sign for improved cellular attachment to the hydrogel. Cell viability was not impaired in either of the tested hydrogel formulations. However, fibrin and HA hydrogels did not allow for cell spreading to the same extent as IPNs, as the morphology of the cells was predominantly round, which is often observed when cells are encapsulated into a stabilized hydrogel.
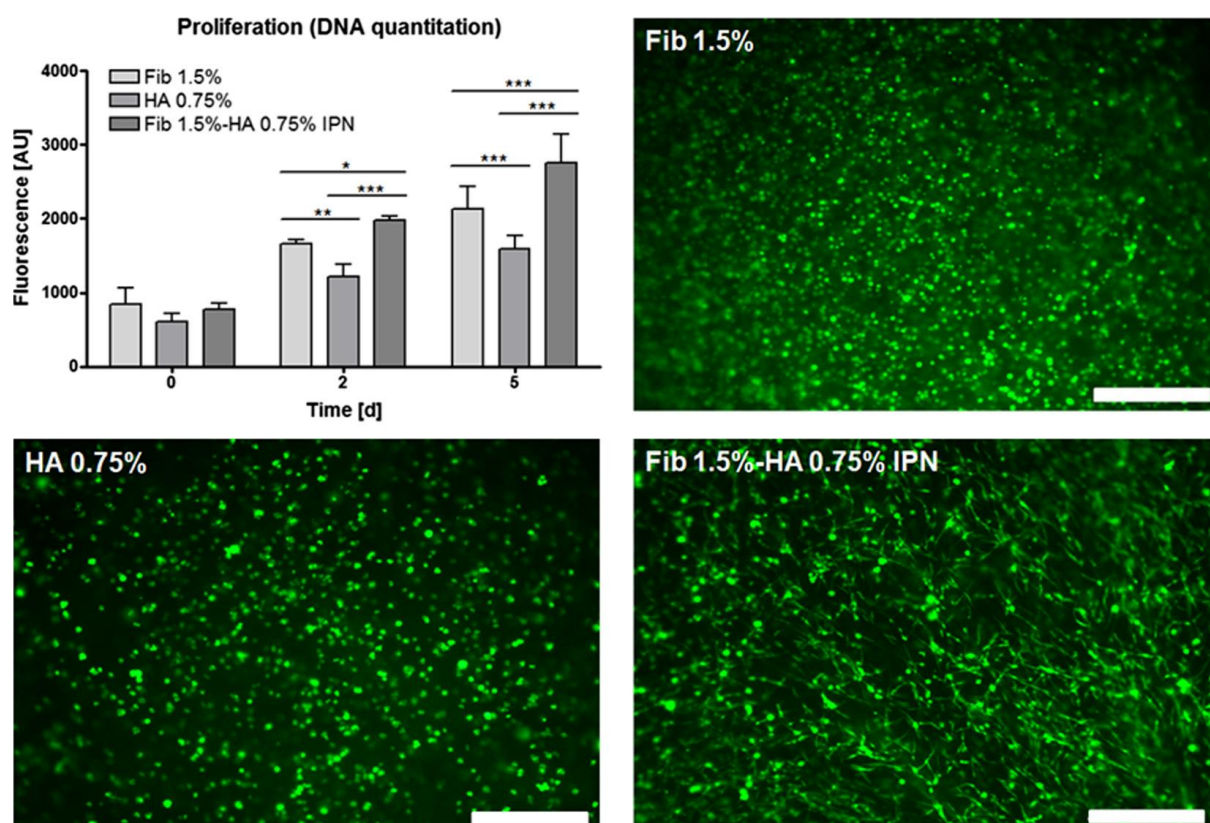

Fig. 47: *Fibrin-HA IPN hydrogels support cell viability and proliferation.* Upper left: the combination of fibrin and HA results in increased proliferation of MG63 cells compared to both materials alone within 2 days (n = 3; mean ± S.D.; *p < 0.5, **p < 0.01, ***p < 0.001; One-way ANOVA with Tukey's multiple comparison test). Upper right, bottom: live (green)/dead (red) staining of cells 2 days after encapsulation. The cells in the IPN display a spread phenotype, pointing at improved cell attachment, compared with the round cellular morphology in fibrin and HA hydrogels (bars represent 500 µm).

4. CONCLUSION

Hydrogels based on IPNs comprising the fibrin network and disulfide cross-linked HA network are formed *in situ*, i.e. due to the one-step mixing of two solutions containing mutually reactive fibrin and HA macromolecular precursors. It was proven that both types of networks can be formed, despite the fact that the two cross-linking processes are not completely independent of each other and that they influence the structure (strength) of the single networks, as compared with the conditions of their formation alone. Regardless of that, an increased stiffness of IPN hydrogel was observed in comparison to that of the pure fibrin gel, which might be due to entanglements between fibrin and HA networks. The IPN hydrogel comprising two networks also has a lower degradation rate compared with the pure fibrin gel *in vitro*. This indicates that the new IPN hydrogel may be more resident *in vivo* as a scaffold for tissue regeneration. This hydrogel also provides a more stable environment for 3D cell culturing, allowing superior cell adhesion and proliferation.

5. DISCLOSURES

No potential conflicts of interests exist.

6. ACKNOWLEDGEMEMTS

CHAPTER III

**Next-generation surgical sealants
and the manifold applications of
fibrin gels for (combined) cell, drug,
growth factor or gene vector delivery**

"An Overview of Surgical Sealant Devices: Current Approaches and Future Trends"

Heher P.[1], Ferguson J.[1], Redl H.[1,*], and Slezak P.[1]

[1] Ludwig Boltzmann Institute for Experimental and Clinical Traumatology/AUVA Research Center, Austrian Cluster for Tissue Regeneration, Vienna, Austria

* Corresponding Author: office@trauma.lbg.ac.at

ABSTRACT/SUMMARY

Introduction: Wound leakage is a common complication after surgical incision or resection. In the past, a variety of clinically approved surgical sealant devices have been used as an adjunct or alternative to conventional means of tissue sealing. However, there is still an unmet need for a sealant that can be universally applied over a wide range of clinical applications. This has further driven the emergence of both novel liquid surgical sealant devices and active hemostatic sealant patches to deal with the increasing complexity of surgical interventions in the field of hemorrhage control and wound leakage.

Areas covered: Emphasizing the literature from the past 5 years, this review covers the current offering of natural, synthetic or composite surgical sealant devices in liquid or patch form, their appropriate clinical indications as well as emerging technologies, strategies and products.

Expert commentary: Recent years have been marked by dramatic and continuous progress towards the development of novel surgical sealant devices and their rigorous clinical testing. In addition, next-generation sealant formulations such as active hemostatic sealant patches and bio-inspired or nanoparticle-based sealant concepts have been developed and are constantly being evaluated and refined.

KEY ISSUES

- Wound leakage, in the form of either bleeding or the release of other body fluids (e.g., blood, bowel contents, cerebrospinal fluid) or gases from a tissue (e.g., air), is a common complication after surgical incision or resection and can be lethal.

- Surgical sealant devices are surgical closure and securement products based on natural or synthetic compounds that can be used as an adjunct or alternative to conventional means of tissue sealing (such as suturing or stapling).

- At present, there is no surgical sealant device that can be universally used over a wide range of clinical applications, and each field of application needs to be carefully addressed through vigorous clinical testing.

- The characteristics of an ideal surgical sealant are non-toxicity, biocompatibility, biodegradability, strong tissue adhesion in wet environments, appropriate mechanical properties (especially related to elasticity, tissue compliance and degradation profile), hemostatic capacity, ease of use and low-cost.

- Surgical sealants based on natural compounds such as fibrin or collagen/gelatin excel at biocompatibility and their ability to actively support hemostasis and natural wound healing. On the other hand, synthetic surgical sealants allow precise control over their mechanical properties, can be modified with a variety of functional groups for crosslinking and can be designed to achieve comparably high adhesion strengths.

- Next-generation active hemostatic sealant patches have recently been introduced as an easy-to-use alternative to liquid sealants

- Novel surgical sealants inspired by nature and/or based on nanotechnological advances are a rapidly growing area of research and future sealant formulations may be modified to gain antibacterial properties or to elicit analgesic effects.

1. INTRODUCTION

Wound leakage, in the form of either bleeding or the release of other body fluids or gases from a tissue, is a common complication in general surgery. The need to effectively manage hemostasis and tissue sealing during surgery has greatly affected the development of modern surgical techniques over the last decades. In particular, surgical procedures that harbor a high risk of postoperative bleeding or leaking have been addressed by both the clinical and basic research community. These procedures still harbor a risk of severe complications and many adverse events are considered preventable [1111, 1112]. Classical approaches for reconnecting or sealing tissues have employed sutures, staples or wires. Although viable in general surgery, these methods can hardly be applied in a minimally invasive manner, may elicit further tissue damage, require extensive handling (especially suturing), increase the risk of infection and sometimes may not provide complete and immediate tissue sealing [1113]. These limitations have led to the development of surgical sealants as an alternative method for wound closure. Surgical sealant devices are a sub-group of surgical closure and securement products which include not only staples, sutures or tapes, but also hemostats, sealants or glues/adhesives. The general purpose of a surgical sealant device (tissue sealant) is to quickly adhere to a tissue to create a temporary barrier that can prevent the leakage of fluids (e.g., blood, bowel contents, cerebrospinal fluid) and/or gases (e.g., air) from a tissue opening after surgical incision or resection. In doing so, an appropriate sealant must be capable of adhering to the respective tissue and remain in place under the forces acting upon it for a duration sufficiently long enough to allow for wound healing [1114]. Surgical sealants can be used as adjuncts to conventional means of tissue sealing (such as suturing or stapling), however, they may also provide a feasible alternative for sutureless wound closure when used autonomously. Over the last two decades, the general trend towards quicker, simpler and minimally invasive surgical interventions along with advances in the field of biomaterial science has led to the development of a variety of surgical sealants. To date, several sealants based on crosslinkable natural or synthetic polymers (or a combination of both in composites) are routinely used in clinics [1115], especially in procedures on tissues that are difficult to reach, too difficult to cauterize or too delicate to withstand suturing. Although several surgical sealants are commercially available there is still an unmet need for a sealant that combines high adhesion strength with good biocompatibility and elasticity in a wet environment. The latter is especially important in tissues that undergo continuous contraction and expansion, such as the heart, skin, lungs or blood vessels. Notably, there is no surgical sealant that can be universally used across a wide range of surgical settings to date, as it is extremely challenging to achieve sufficient adhesion while preserving tissue biocompatibility, sealing efficiency and biodegradability.

According to the 2016 MedMarket Diligence LLC global report on surgical sealants, glues and hemostats [1116], the global market for these surgical materials is expected to grow from $5.7 billion in 2016 to $9.3 billion by 2022. This forecast not only underscores the increasing routine use of

surgical sealants in a growing number of clinical fields, but also outlines that many unmet needs may still remain in the pursuit of developing and implementing the ideal surgical sealant. This special report aims at providing an overview of commonly used natural, synthetic and composite elastic surgical sealants and their main clinical applications. Novel aspects in the development of hemostatic sealant patches/pads as an alternative to liquid sealants are also included. In addition, current limitations and recent advances will be briefly discussed, highlighting the scientific progress that has recently been made in the areas of both surgical sealant development as well as clinical application.

2. SURGICAL SEALANT DEVICES AND THEIR MAIN CLINICAL APPLICATIONS

Wound closure is a key step in various surgical procedures and each procedure carries specific risk factors. Therefore, it is of utmost importance to select a surgical sealant that best matches the requirements of a given surgical intervention. Although a variety of surgical sealants have been clinically approved, there are still extensive research efforts being made to engineer biocompatible, - degradable and flexible sealants capable of generating leak-free closures in soft tissues [1117-1120]. Currently, surgical sealants are classified into two major groups: natural sealants are based on natural compounds such as proteins or polysaccharides, while the majority of synthetic sealants are based on materials like cyanoacrylate, polyethylene glycol (PEG) or polyurethane (PU) [1113, 1115]. Surgical sealants based on natural polymers possess several advantages over synthetic sealants, including superior biocompatibility, *in vivo* degradability and their ability to instruct and support endogenous reparative processes. On the other hand, synthetic surgical sealants offer more precise control over gel time, swelling behavior, sealant mechanical properties and degradation rate, while being amenable to functional customizations that increase adhesion to the target tissue.

2.1. Sealants of natural origin

Fibrin sealants are one of the most commonly used biological sealant systems in modern surgery. The working principle of these sealants is to mimic the last stage of the blood coagulation cascade, the thrombin mediated conversion of fibrinogen into a crosslinked fibrin clot. Fibrin sealants are usually supplied as deep frozen or lyophilized two-component formulations consisting of highly concentrated solutions of fibrinogen/factor XIII and thrombin, which, upon mixing, form a stable fibrin hydrogel. Fibrin sealants are commercially available under many different brand names, such as Tisseel® (Baxter Healthcare, Deerfield, USA), Evicel® (Ethicon, Somerville, USA), Hemaseel APRTM (Haemacure, Montreal Canada) or Beriplast P® (CSL Behring, King of Prussia, USA), among others. Tisseel® gained Food and Drug Administration (FDA) approval in the USA in 1998 and, to this day, fibrin sealant remains the only material that is approved as a surgical sealant, hemostat and adhesive

[304]. Fibrin sealants have predominantly been used to control hemorrhage in peri- and postoperative settings (especially in cardiovascular and neurosurgery) and today have broad label FDA approval as hemostats and as sealants for colon sealing at the time of colostomy closure [304, 774]. A commercially available fibrin sealant with a low-thrombin formulation, Artiss® (Baxter Healthcare, Deerfield, USA), has been granted FDA approval as an adhesive for autologous skin grafting and face-lift procedures. Furthermore, composite surgical sealants based on fibrin and collagen are commercially available. For example, CoStasis® (Cohesion Technologies, Palo Alto, USA), now marketed as Vitagel™ (Angiotech Pharmaceuticals Inc., Vancouver, Canada), is such a formulation, containing bovine collagen, bovine thrombin and autologous plasma [1121]. In addition, surgical sealants based on gelatin, the irreversibly hydrolized form of collagen, have been introduced, such as chemically crosslinked gelatin-resorcinol-formaldehyde (GRF) or gelatin-resorcinol-formaldehyde-glutaraldehyde (GRFG) surgical sealants (MicroVal, Saint-Just-Malmont, France) [1122, 1123]. However, due to the toxicity of formaldehyde and glutaraldehyde, these early formulations of gelatin-based sealants have never gained FDA approval. Therefore, other crosslinking chemistries such as enzymatic crosslinking using a microbial transglutaminase (mTG) [1124] or photo-polymerization [1125] of gelatin have been explored to increase safety and are currently under preclinical investigation [1126, 1127]. Furthermore, several albumin-based surgical sealants based on similar polymerization reactions have been developed. For example, BioGlue® (Cryolife, Kennesaw, USA), a two-component sealant based on bovine serum albumin (BSA) and glutaraldehyde has FDA approval as adjunct to suturing or stapling in vascular and cardiac surgery [1128]. Again, the potential cytotoxicity of glutaraldehyde has led to the emergence of other albumin-based sealants employing alternate crosslinking agents. PreveLeak™ (Baxter Healthcare, Deerfield, USA), a sealant based on BSA and polyaldehyde [1129, 1130], and ProGel™ (Davol Inc., Woburn, USA), a composite sealant containing human serum albumin and a N-hydroxysuccinimide(NHS)-PEG crosslinker [1131], have both gained FDA approval and the latter is currently the only surgical sealant approved for sealing air leaks in thoracic surgery [1132].

Alternatively to protein-based sealants, a variety of polysaccharide-based sealants has been developed. In nature, polysaccharides often function as mediators of adhesion and surgical sealants based on crosslinked polysaccharides such as chitosan or dextran have been developed in an attempt to improve sealant adhesion beyond the capabilities of protein-based sealants [1113, 1133]. Chitosan is a non-toxic, biocompatible and biodegradable polysaccharide derived from chitin and has gained attention for biomedical use due to its intrinsic antioxidant and bacteriostatic properties [1134]. A photo-crosslinkable sealant based on chitosan and 4-acidobenzoic acid, (Az)-chitosan, has been developed and proposed for peripheral nerve anastomosis [1135]. The preparation of thin crosslinked chitosan adhesive films which are based on FDA approved materials and photonics has also been reported [1136]. Marketed under the brand name SurgiLux®, which now has FDA approval, the efficiency and safety of this chitosan-based sealant has been demonstrated in a variety of tissues. Furthermore, a

commercially available chitosan powder formulation, Celox™ (SAM Medical Products, Newport, USA), has been approved by the FDA as a hemostat [1137]. Similar to chitosan, the complex branched polysaccharide dextran is biocompatible, biodegradable and non-toxic. However, in contrast to chitosan, dextran does not contain reactive amino groups and therefore has to be modified by the introduction of functional groups for crosslinking such as aldehydes [1138], methacrylates [1139], or by preparing enzyme-crosslinkable dextran conjugates [1140]. ActaMax™ (Actamax Surgical Materials LLC, Wilmington, USA), a tissue sealant based on aldehyde-functionalized dextran combined with a PEG crosslinker [1141, 1142], is commercially available and has recently been granted FDA approval to start a pivotal clinical trial to evaluate its safety and efficacy as an adhesion barrier in abdominopelvic surgery. In addition, surgical sealants based on other polysaccharides such as chondroitin sulfate or alginate are currently in the experimental stages and have been comprehensively reviewed elsewhere [1115, 1133].

2.2. Sealants of synthetic origin

The safety concerns (immune reactions, viral transmission, potential cytotoxicity elicited by residual chemical crosslinkers, etc.) and performance issues associated with the use of some natural-based surgical sealants has driven the development of synthetic sealants. Elastic sealants based on synthetic polymers have attracted significant attention as wound closure techniques due to their structural and mechanical tunability and their comparably high adhesive strength. The most commonly used synthetic surgical sealants are based on alkyl-2-cyanoacrylates which are usually formulated as single-component devices. Solidification does not require a catalyst, as cyanoacrylate sealant polymerization can be initiated at room temperature by small amounts of water. Most commercially available cyanoacrylate sealants are based on n-butyl- or n-octyl-cyanoacrylates. For example, Glubran 2® (GEM SRL, Viareggio, Italy) and Trufill® (Cordis, Fremont, USA) have been granted FDA approval for endovascular use [1143, 1144], while Histoacryl® (B. Braun AG, Melsungen, Germany), Dermabond Advanced® (Johnson & Johnson, Somerville, USA) and Indermil™ (Covidien, Dublin, Ireland) are approved as alternative to sutures in topical skin wound closure [1145]. Cyanoacrylates are particularly effective in moist environments, display high bonding strength and their degradation rate (which correlates inversely with the length of the alkyl side chain) and overall mechanical properties can be modulated [1146]. However, a limitation of these sealants is the potential occurrence of medical complications due to the formation of toxic degradation products or through prolonged persistence of less biodegradable cyanoacrylate sealants [1147]. This has led to the development of alternate synthetic sealants and PEG-based devices present another class of frequently used synthetic surgical sealants. PEG is soluble in aqueous solutions and commercialized over a wide range of molecular weights with multiple end groups available for functionalization. In the last two decades, several commercially available two-component PEG-based sealants have been granted FDA approval as adjuncts to conventional suturing/stapling, for example DuraSeal™ (Covidien, Dublin, Ireland),

Sealant class	Product name(s)	Main Applications	Advantages	Disadvantages	References
Natural origin					
Fibrin	Tisseel®, Evicel®, Hemaseel APR™, Beriplast P®, Vitagel™ (fibrin-collagen composite)	Hemostasis (general surgery), colon sealing (adjunct to sutures), burn wound skin graft attachment	Biocompatibility, biodegradability, rapid curing possible, intrinsic properties supportive for wound healing	Poor adhesion, risk of disease/infection transmission or allergic reaction, comparably long preparation time, price	[304], [774], [1121], [1170,1171], [1173], [1189, 1190], [1194], [1205, 1206]
Gelatin	GRF, GRFG	Hemostasis (general surgery), vascular/cardiac surgery (aortic dissection)	Biocompatibility, biodegradability, high adhesive strength, tunability of overall physicochemical properties	Safety concerns (formaldehyde, glutaraldehyde), high swelling ratio	[1117], [1120], [1122-1127], [1172]
Albumin	BioGlue®, PreveLeak™, ProGel™	Hemostasis (vascular/cardiac surgery), lung sealing	Fast polymerization, high adhesive strength, prolonged persistence at site of application	Safety concerns (glutaraldehyde), prolonged persistence at site of application, rigidity, price	[1128-1132], [1207]
Chitosan	(Az)-chitosan, SurgiLux®, Celox™	Peripheral nerve anastomosis, hemostasis	Abundance, biocompatibility, antioxidant and bacteriostatic properties, cost-efficiency, adhesive strength	Not soluble in water unless modified, possible tissue damage through thermal irradiation (photo-crosslinking)	[1134-1137], [1175, 1176], [1178]
Dextran	ActaMax™	Gynecologic abdominopelvic surgery	Abundance, biocompatibility, adhesive strength, price	Need for functionalization prior to cross-linking, high swelling ratio	[1138-1142], [1178]
Synthetic origin					
Cyanoacrylate	Glubran 2®, Trufill®, Histoacryl®, Dermabond Advanced®, Indermil™	Endovascular (arteriovenous malformations), topical skin wound closure	High bonding strength, efficiency on moist surfaces, tunability of overall physicochemical properties, ease of use, price	Potential toxicity of degradation products or complications through prolonged persistence in the body, exothermic polymerization, limited to topical use	[1143-1147]
PEG	DuraSeal™, CoSeal®, FocalSeal®, Adherus®	Adjunct to sutures in dural (cranial and spine surgery), lung or vascular sealing	Rapid curing possible, biocompatibility, hydrophilicity, tunability of overall physicochemical properties	High swelling ratio, rapid degradation unless used as composite formulation, possible allergic reaction, price	[1148-1152], [1174], [1189], [1202]
PU	TissuGlu®	Abdominoplasty	Wettability, tunability of overall physicochemical properties	Potential formation of non-biocompatible degradation products, long setting time	[1153-1156]

Table 7: *Commercially available FDA approved natural and synthetic surgical sealants* (GRF: gelatin-resorcinol-formaldehyde; GRFG: gelatin-resorcinol-formaldehyde-glutaraldehyde; PEG: polyethylene glycol; PU: polyurethane).

CoSeal® (Baxter Healthcare, Deerfield, USA), FocalSeal® (used to be produced by Genzyme Biosurgery, Cambridge, USA, but is currently discontinued) or, more recently, Adherus® (Hyperbranch Medical Technology Inc., Durham, USA). These sealants are also amenable to spray application and indications include dural sealing to prevent cerebrospinal fluid leakage after cranial and spinal surgery (DuraSeal™, FocalSeal®, Adherus®), lung sealing (FocalSeal®) or vascular sealing of blood vessel anastomoses (CoSeal®, Adherus®) [1148-1152]. Furthermore, surgical sealants based on PU have been introduced due to their high elasticity, good wettability and strong bonding to tissues. Urethane, in its prepolymer form, can react with amino groups of proteins in the target tissue to create urea linkages, which promotes excessive adhesion strength [1153]. Usually, PU solidification is initiated by contact with aqueous solutions, but the observed long setting times (in the order of tens of minutes) are one drawback of this surgical sealant class. Therefore, novel formulations and crosslinking strategies have been examined to increase the gelation rate and biocompatibility/biodegradability of PU derivatives [1154]. A commercially available PU-based sealant, TissuGlu® (Cohera Medical Inc., Raleigh, USA), has recently been granted FDA approval as adhesive for abdominoplasty, based on clinical evidence for its efficiency to prevent seroma formation and to reduce post-surgery wound drainage [1155, 1156]. Other synthetic sealants are currently in experimental stages, and promising advances have been made with regard to polyester-, polyvinyl alcohol(PVA)- or dendrimer-based formulations, however, these sealants are beyond the scope of this special report and have been reviewed elsewhere [1115, 1157]. A list of currently FDA approved

natural and synthetic surgical sealants, their main clinical applications, advantages and disadvantages is provided in Table 7.

2.3. Active hemostatic sealant patches

Active hemostatic sealant patches (or pads) have recently emerged as an alternative to the well-established liquid surgical sealants and provide a versatile sealant option across several surgical settings [1119]. The first sponge- or fleece-like hemostatic matrices were based on gelatin [1158] or oxidized cellulose [1159] and introduced already in the 1940s. These topical hemostats provided a passive, low-cost and easy-to-use approach to hemorrhage control and have been commercialized as Gelfoam® (Pfizer Inc., New York, USA), a gelatin-based sponge, or Surgicel® (Ethicon, Somerville, USA) which is based on oxidized regenerated cellulose. However, the complexity of modern surgical procedures has driven the development of novel, advanced sealant patches that combine hemostasis with active sealing properties. These patches consist of a sheet- or foam-like backing and a functionalized self-binding surface, for example Tachosil® (Takeda Pharmaceutical, Osakashi, Japan; previously marketed as TachoComb®), a first-generation commercially available advanced sealant patch consisting of an equine collagen foam coated with human fibrinogen and thrombin on its active side [1160]. The mechanism of action is activated after manual compression of the patch onto a leakage. This rapidly establishes a physical barrier and activates fibrin formation through solubilization after contact with body liquids, which results in adhesion to the site of application and hemostasis. Tachosil® gained FDA approval in 2010 and is indicated as an adjunct to hemostasis in cardiovascular and hepatic surgery. The need for more efficient (=more adhesive) sealant patches has recently driven the development of second-generation composite sealant patches [1161-1164]. Evarrest® (Ethicon, Somerville, USA), based on human fibrinogen and thrombin on a cellulose/polyglactin 910 patch, and Hemopatch® (Baxter Healthcare, Vienna, Austria), a NHS-PEG coated collagen patch, represent such novel, commercially available advanced sealant patches. Evarrest® and Hemopatch® have been granted FDA approval as adjunct to hemostasis in various surgical fields [1119, 1162, 1163, 1165]. Veriset™ (MedTronic, Minneapolis, USA), a cellulose-based patch with PEG-trilysine coating, is currently being evaluated in clinical trials [1164, 1166]. A fully synthetic sealant patch, TissuePatch™ (TissueMed Ltd., Leeds, UK), has recently been approved in China as sealant device in thoracic surgery. TissuePatch™ is composed of a poly(lactide-co-glycolide) (PLGA) backing coated with the company's TissueBond™ adhesive, a copolymer of vinyl pyrrolidone (PVP) and NHS-functionalized acrylic acid (PAA), and is currently being tested in several surgical fields [1167-1169]. An overview of commonly used first- and second-generation sealant patches and their composition is presented in Table 8.

Patch composition	Product Name	Date of Approval	Main Applications	References
Natural origin				
Human fibrinogen/thrombin on equine collagen sponge	TachoSil®, TachoComb®	2004 (EMA), 2010 (FDA)	Adjunct to hemostasis in cardiovascular and hepatic surgery	[1160], [1204]
Composite				
Human fibrinogen/thrombin on composite patch made of oxidized regenerated cellulose and polyglactin 910	Evarrest®	2012 (FDA)	Adjunct to hemostasis in general surgery	[1162]
PEG-trilysine on oxidized regenerated cellulose	Veriset™	-	Intended for use as an adjunct to hemostasis in vascular surgery	[1164], [1166], [1193]
NHS-PEG on collagen fleece	Hemopatch®	2013 (EU) as hemostat 2016 (EU) for dural sealing	Adjunct to hemostasis in general surgery	[1119], [1163], [1165], [1193]
Synthetic origin				
TissueBond™ (copolymer of PVP and partially NHS-functionalized PAA) on a PLGA backing	TissuePatch™	2016 (CFDA)	Adjunct to hemostasis in head and neck surgery	[1167-1169]

Table 8: *Commercially available natural and synthetic topical active sealant patches* (PEG: polyethylene glycol; NHS: N-hydroxysuccinimide; PLGA: poly(lactide-co-glycolide); PVP: vinyl pyrrolidone, PAA: acrylic acid; FDA: Food and Drug Administration; EMA: European Medicines Agency; CFDA: China Food and Drug Administration).

2.4. Surgical sealant applicators

Application devices for surgical sealants are constantly refined and adjusted to newly introduced products and/or applications. Dual-syringe applicators, for example the Tisseel® Duploject System (Baxter Healthcare, Deerfield, USA) or Evicel® (Ethicon, Somerville, USA) dripping or gas-assisted applicators, have been complemented with other application devices such as mechanical ratchet systems or pressurized air-assisted spray applicators [1170]. While air assisted systems provide a convenient and fast way to apply larger volumes of sealant, both in open and endoscopic surgery, they bear the theoretical risk of inducing air embolism in the case of misapplication (for example through use at pressures higher than recommended or use in very close proximity to actively bleeding vessels) [1171]. Alternatively, airless applicator devices (Evicel® Airless Spray Accessory; Ethicon, Somerville, USA) for open or endoscopic use (e.g., Tisseel® Duplocath; Baxter Healthcare, Deerfield, USA) have been introduced, minimizing technical prerequisites and embolism risk. However, the spraying effect may be less pronounced in such applicators. Sealant application is also commonly performed via endoscopic applicators (e.g., Tisseel® Duplospray; Baxter Healthcare, Deerfield, USA) through trocars in endoscopic surgery or in minimally invasive surgery (MIS). Gas-assisted, endoscopic applicator devices are commonly designed to use CO_2 gas primarily over pressurized air and feature reduced gas flow rates. For example, the Tisseel® Duplospray MIS regulator allows for a flow rate of approximately 2 L/min as opposed to open gas spray systems that may use flow rates of up to 20 L/min.

In cases where a precise and defined sealant application is required, for example in hernia mesh fixation, a new micro dosing applicator, Talent IH™ (Primequal SA, Geneva, Switzerland), has been recently developed, providing an exact pre-defined sealant volume per click. Furthermore, the Vivostat® system (Vivostat, Allerod, Denmark), a device for the preparation of autologous fibrin sealant from patient blood samples, has been adapted for co-delivery of drugs or (stem) cells with the

fibrin preparation (Vivostat® Co-Delivery system). These and many more devices have contributed to the widespread clinical use of surgical sealants by improving the ease of handling, efficiency and safety of a variety of sealants, while allowing for specialized routes of sealant delivery depending on the type of surgical intervention.

3. RECENT ADVANCES AND EMERGING TECHNOLOGIES

The last decade has seen tremendous progress in the research directed to the development of novel surgical sealants as well as the refinement of existing ones to further increase sealant safety, mechanical properties and adhesive performance [1157]. In doing so, a great deal of research has focused on novel crosslinking strategies to minimize cytotoxicity while improving tissue adhesion of the sealant. The feasibility of mTG-mediated crosslinking of gelatin [1124] may provide a safe method to reduce the risks associated with GRF/GRFG glues. Lv et al. [1172] have recently evaluated a gelatin-mTG sealant in a rat liver hemostasis model and observed a similar hemostatic effect, but higher adhesive strength and elasticity, compared to a commercially available product. Although the safety of such sealants is not fully established yet, it is noteworthy to point out that mTG is approved for food use. Assmann et al. [1117] reported a highly adhesive sealant based on photo-crosslinked gelatin-methacryloyl (GelMA). By optimizing the sealant formulation, improved performance in a large animal lung sealing model compared to fibrin sealant (Evicel®), PEG-based sealants (ProGel™, CoSeal®) or sutures was observed. Photo-polymerization has earlier also been introduced to cross-link fibrin and the reported sealant showed a 5-fold increase in adhesive strength and higher tensile strength compared to a commercial fibrin sealant (Tisseel®) [1173]. In addition, optimizing sealant formulation and the degree of crosslinking has enabled control over the swelling behavior of natural [1125] and synthetic [1174] sealants. As an example, Henise at al. [1174] recently reported a sealant based on chemical crosslinking of novel PEG-derivatives, which allows for tunable swelling, burst pressures and biodegradation rates (ranging from hours to years).

At the same time, sealant formulations based on diverse natural and synthetic materials not yet broadly used in clinics are being constantly advanced and further developed. In this respect, various composite sealants, some combining the biocompatibility of natural polymers with the adhesive strength and elasticity of synthetic polymers, have been described. Recent examples include formulations based on chitosan-PEG [1175], chitosan-polylysine [1176], chondroitin sulfate-NHS-PEG [1177], dextran/chitosan [1178] or pollock-derived gelatin-PEG [1120], which were all demonstrated to have superior adhesive strength over commercially available fibrin sealants. Surgical sealants based on dendrimers, highly branched macromolecules with well-defined structures and numerous functional end groups, have also been extensively studied, especially in the context of corneal wound repair [1179, 1180]. An elastic sealant based on a poly(amidoamine) (PAMAM) dendrimer conjugated with a UV-sensitive crosslinker (diazirine) was recently reported by Feng et al. [1181], who demonstrated

the performance of this sealant on swine aortae *ex vivo*, emphasizing on reduced potential cytotoxicity since the presence of a photoinitiator is not required and low energy levels of UV light are sufficient for sealant curing. Another rapidly growing field is the development of surgical sealants that are inspired by nature. Specifically, bio-inspired adhesives based on mussel-, gecko- or slug-derived adhesive proteins have attracted widespread attention due to their ability to generate high adhesive strengths in wet environments [1182, 1183]. The mussel-derived amino acid dihydroxyphenylalanine (DOPA) has been identified as a strong mediator of adhesion, more precisely, its catechol side chain which can form water-resistant bonds through oxidation. Recombinant DNA technology now allows production of DOPA in large quantities [1184], which has driven the development of DOPA- or catechol-functionalized composite sealants with high adhesive strengths [1185-1187]. Inspired by geckos, Lang et al. [1118] recently reported a bio-inspired photo-crosslinkable elastic sealant based on poly(glycerol-co-sebacate acrylate) (PGSA). When applied to high-pressure large blood vessels and cardiac wall defects in pigs, PGSA patches remained attached and resisted supraphysiologic pressures for 24 hours, which is relevant to intracardiac interventions in humans. Among others, this study has led to the commercialization of a biocompatible, photo-curable PGSA-based sealant for vascular reconstruction, Setalum™ (Gecko Biomedical SAS, Paris, France), which has gained Conformité Européenne (CE) mark approval for commercialization in Europe in 2017.

4. EXPERT COMMENTARY

In the last decade, the increasing complexity of surgical interventions to control hemorrhage or wound leakage has further driven the evolution of novel surgical sealant devices for external and internal application. This has not only yielded a variety of newly approved liquid sealants, but also has expanded the surgical sealing toolbox with next-generation active hemostatic sealant patches. Importantly, the research endeavors of recent years have once more underscored that there is no "one size fits all" sealant that can be employed over multiple surgical applications. In fact, each sealant formulation has to be carefully evaluated for each clinical application [1119, 1163, 1165, 1188-1194]. In this respect, standardized definitions for the severity of wound leakage are crucial in two ways: first, the performance of different surgical sealant devices in preventing or stopping a leakage of distinct severity can be directly compared and, second, standardization allows clinicians to select the appropriate sealant for each leakage. New grading systems to quickly assess intraoperative bleeding intensities have recently been established. Lewis et al. [1195] proposed and validated an intraoperative bleeding severity (ViBe) scale which covers a full range of clinically relevant bleedings from ooze or intermittent flow (>1.0-5.0 mL/min) to continuous flow (>5.0-10.0 mL/min), controllable spurting and/or overwhelming flow (>10.0-50.0 mL/min) up to unidentified or inaccessible spurting or gushing (>50.0 mL/min). Alternatively, Spotnitz et al. [1196] recently reported the SPOT GRADE, a six level

severity scale that allows the quantification of surgical wound bleeding (none, minimal, mild, moderate, severe, and extreme). Zaraca et al. [1197] introduced a standardized ventilation mechanical test (VMT) for thoracoscopic surgery, classifying intraoperative alveolar air leaks in mild (<100 mL/min), moderate (100-400 mL/min) and severe (>400 mL/min). This test was shown to allow for accurate selection of patients needing treatment (sealing of moderate leakage with ProGel™ while mild leakage was left untreated) and therefore helped in reducing the length of hospitalization after treatment.

Apart from the development of novel sealants with the aim of increasing safety and performance, rigorous clinical testing and further refinement of existing sealant formulations has led to a rapid expansion of FDA and EMA approved products. Recent examples are ReSure© (Ocular Therapeutix Inc., Bedford, USA), a synthetic sealant indicated for intraoperative management of corneal incisions [1198], or Sylys© (Cohera Medical Inc., Raleigh, USA), a synthetic single-component sealant designed as adjunct to standard closure techniques in colectomy procedures [1199]. In addition, the emergence of novel crosslinking methods and advances in bio-inspired sealant concepts now enable researchers to design highly adhesive next-generation sealants that may solve the issue of suitable adhesive strength in wet environments such as mucosal surfaces [1115, 1117, 1118, 1124, 1178, 1181, 1182, 1200].

5. FIVE-YEAR VIEW

Recent advances in nanotechnology have been implemented into the development of active elastic surgical sealants to introduce new functionalities or to modulate sealant adhesion [1200]. In the near future, a more thorough implementation of such methodology into existing strategies is expected. This will include the development of nanoparticle-based sealants, and promising results with particle-induced nanobridging of tissues have already been reported [1201]. In addition, nanoparticles with antibacterial or hemostatic properties will increasingly be incorporated into sealants to further reduce the risk of infections or hemorrhage after surgeries. This may also be combined with sealant-based delivery of analgesic drugs [1202], which has already been implemented into bioresorbable sutures [1203]. At the same time, more stringent standardized clinical trials comparing different surgical sealant devices against each other over different applications, as opposed to the comparison of a novel product to the last-generation equivalent, will increase the clinical application fields of both novel liquid sealants and hemostatic sealant patches. This will also involve a more thorough analysis of the cost-effectiveness of both established and novel products, as the cost benefits of surgical sealant devices (as well as their overall performance) have been shown to be highly variable depending on the type of sealant used and the surgical intervention performed [1204-1207].

"Fibrin-based delivery strategies for acute and chronic wound healing"

Heher P.[1], Mühleder S.[1], Mittermar R., Redl H.[1,*], and Slezak P.[1]

[1] Ludwig Boltzmann Institute for Experimental and Clinical Traumatology/AUVA Research Center, Austrian Cluster for Tissue Regeneration, Vienna, Austria

* Corresponding Author: office@trauma.lbg.ac.at

ABSTRACT

Fibrin, a natural hydrogel, is the end product of the physiological blood coagulation cascade and naturally involved in wound healing. Beyond its role in hemostasis, it acts as a local reservoir for growth factors and as a provisional matrix for invading cells that drive the regenerative process. Its unique intrinsic features do not only promote wound healing directly via modulation of cell behavior but it can also be fine-tuned to evolve into a delivery system for sustained release of therapeutic biomolecules, cells and gene vectors. To further augment tissue regeneration potential, current strategies exploit and modify the chemical and physical characteristics of fibrin to employ combined incorporation of several factors and their timed release. In this work we show advanced therapeutic approaches employing fibrin matrices in wound healing and cover the many possibilities fibrin offers to the field of regenerative medicine.

1. INTRODUCTION

Chronic wounds represent a significant and often underestimated worldwide socio-economic burden to both patients and healthcare systems. In the United States only, approximately 6.5 million patients are affected by chronic wounds, with projected annual healthcare costs of more than US$25 billion [1208, 1209]. Often disguised as a co-morbidity, chronic wounds represent a silent epidemic and exact numbers on global prevalence and incidence are still missing [1210]. In Denmark, for example, it is estimated that 1% of the population in developed countries will suffer from a chronic wound [1211] and the direct and indirect socio-economic impacts are growing rapidly due to global population aging and the sharp rise in the incidence of diabetes and obesity. In general, every disruption of a previously normal anatomic tissue structure with consecutive loss of function can be classified as a wound. Normally, these wounds are repaired through a distinct timely and spatially orchestrated wound healing process. Chronic wounds, however, are defined as wounds that fail to proceed through this orderly and timely reparative process with full restoration of continuity within 3 months [526]. These full-thickness chronic wounds, also referred to as ulcers, often develop in patients with diabetes or vascular diseases and are attributed with slow or non-healing tendency, especially in the elderly [1212]. Some common features of these wounds include prolonged or excessive inflammation, persistent infections, formation of microbial biofilms and the inability of dermal or epidermal cells to respond to reparative stimuli, which altogether results in the failure of the wound to heal [1213]. In this respect, a high microbial load can severly impair acute and chronic wound healing, which is especially challenging in oral cavity wound care [1214].

Wound healing is a dynamic and highly conserved process that involves the complex and coordinated interplay of multiple cell types, growth factors, chemo-/cytokines and components of the extracellular matrix (ECM). Together, these elements drive the overlapping stages of wound healing: hemostasis, inflammation, reepithelialization, neovascularization, collagen deposition and matrix remodeling with scar formation. Today it is well known that fibrin, the end product of the physiological blood coagulation cascade, plays a pivotal role in many of these processes [524, 525]. During the final step of this cascade, circulating fibrinogen is cleaved by the action of the serine protease thrombin, resulting in the formation of an insoluble fibrin clot. In addition, thrombin activates the transglutaminase Factor XIII (FXIIIa) which further stabilizes the clot by cross-linking of fibrin polymers [528, 608]. While hemostasis is the primary function of fibrin in wound healing, the blood clot also serves as a provisional matrix for many cell types involved in later stages of tissue repair, making fibrin one of the most important ECM molecules in the wound bed. Under physiological conditions, the blood clot is not a permanent structure. To preserve the hemostatic balance, fibrinogenesis and blood coagulation are counteracted by the fibrinolytic system. In the course of fibroplasia and matrix remodeling, fibrinolysis occurs through the actions of plasminogen (PLG) which is activated by tissue-type plasminogen activator (tPA) or urokinase-type plasminogen activator

(uPA). These activators are secreted by several cells in the wound bed and convert PLG to plasmin, leading to fibrin degradation [663, 672, 676]. Maintenance of the hemostatic balance is of great significance for tissue repair, as both fibrin(ogen) and its degradation products exert multiple regulatory functions in wound healing such as immunomodulation [555], growth factor sequestration [565, 566] and modulation of cell phenotype, function and migration [534, 544, 552, 1215].

The necessity to effectively manage hemostasis and wound healing during surgical interventions has led to the development and commercialization of fibrin sealants (fibrin glues). These two-component plasma-derived products consist of fibrinogen/FXIII and thrombin concentrates which, when mixed, mimic the final stage of blood clotting, that is, the formation of a fibrin clot [1216]. Owing their efficiency, biocompatibility and -degradability, commercially available fibrin sealants have been granted clinical approval in a variety of surgical settings [304, 781, 783-786, 817, 819, 820, 883]. More recently, fibrin sealants have emerged as scaffold materials in the rapidly expanding field of tissue engineering and regenerative medicine. The vast amount of studies has demonstrated the feasibility of fibrin as a carrier for a variety of cell types [303, 919, 1217, 1218]. Furthermore, diverse fibrin formulations have been successfully utilized for the localized and controlled delivery of drugs and growth factors [302, 510, 833, 1219]. In addition, fibrin-based gene therapy approaches have attracted attention and the viral and non viral delivery of therapeutic gene vectors has been explored [302, 968, 970]. This review highlights the advantageous intrinsic qualities of fibrin for tissue engineering-based wound healing approaches, sustained delivery of therapeutic biomolecules and for efficient transplantation of cells. Furthermore, strategies to tailor and control growth factor release kinetics for optimized therapeutic outcome will be addressed. Since wound healing requires the spatiotemporal provision of several stimuli, recent advances in combinational delivery approaches such as dual/sequential growth factor release or release of cells and growth factors will also be discussed.

2. THE INTRINSIC FEATURES OF FIBRIN IN WOUND HEALING

Fibrin plays overlapping roles in wound healing through mediating both hemostasis and homeostasis. Initially, fibrin acts as a provisional matrix for several cell types. A stable blood clot is formed via interaction of the platelet integrin $\alpha_{IIb}\beta_3$ with fibrin [516, 1220]. Furthermore, fibrin contains Arg-Gly-Asp (RGD) sites that serve as recognition motifs for endothelial cells (ECs) and fibroblasts via integrin $\alpha_V\beta_3$ [537, 829]. Other ECM proteins like fibronectin [830], vitronectin [831] or thrombospondin [832] bind fibrin and effectively regulate cell adhesion, proliferation and migration - for example the influx of monocytes [535, 540] or fibroblasts [541, 543] during the formation of granulation tissue. Importantly, ECM binding of cells in the wound area also triggers integrin receptor-mediated signaling pathways which modulate cellular functions [544]. Monocytes bind the fibrin clot

via the integrin Mac-1 [593], which promotes phagocytosis/debridement and regulates the development of inflammatory (M1) and reparative (M2) macrophages [542, 545]. Macrophages play a crucial role in the transition between wound inflammation and repair and their adherence to fibrin(ogen) partially modulates their activity, thereby changing the rate of this transition [551]. At the same time, fibrin and fibronectin stimulate fibroblast proliferation and migration into the wound space [541, 543, 552], where they gradually remodel the matrix through fibrin degradation and collagen deposition [548, 549].

In combination with its function as a provisional matrix for cells, fibrin also serves as a local reservoir for the sequestration and spatiotemporal release of growth factors and cytokines in the wound area. Basic fibroblast growth factor (bFGF; FGF-2) [565, 568], vascular endothelial growth factor 165 ($VEGF_{165}$) [566], transforming growth factor-β1 (TGF-β1) [564], platelet-derived growth factor (PDGF) [563], insulin-like growth factor 1 (IGF-1) [563, 1221] and interleukin 1β (IL-1β) [567] can all be found within a natural fibrin clot. Moreover, circulating growth factors can be sequestered to fibrin via heparin [938, 1222] which has known affinity for epidermal growth factor (EGF) [912], bFGF [913], PDGF-A and -B [909, 911] and $VEGF_{165}$ [910]. The localized bioactivity and concerted actions of these growth factors in the clot drive neovascularization and subsequent remodeling of the wound bed, which is key to wound healing. It is well established that fibrin itself is angiogenic [569-571] and stimulates wound angiogenesis by two mechanisms: first, it provides a supportive matrix and, second, it displays selective chemotactic activity for the migration of endothelial cells (ECs) into the clot. In addition, fibrinolytic processes become increasingly important as wound remodeling progresses. Once the fibrin clot is present in the wound, invading cells gradually replace it with newly formed ECM. Enzymes and their regulators such as PLG [1223], tPA [1223], plasminogen activator inhibitor-1 (PAI-1) [1224] and thrombin [1225] are bound to fibrin and regulate the hemostatic balance. Controlling this equilibrium between fibrinogenesis and -lysis is a prerequisite to synergistically drive granulation tissue formation and neovascularization while allowing gradual degradation of the fibrin clot. In this respect, fragments of fibrin such as fibrinopeptides or fibrin degradation products (FDPs) have also been found to be important modulators of inflammation and angiogenesis during wound healing [555].

3. DELIVERY OF THERAPEUTIC BIOMOLECULES

The concept of fibrin-based drug or growth factor delivery is based on the incorporation of (one or several) pharmaceutically active substances into a fibrinogen/thrombin formulation which is subsequently applied to the site of injury (Fig. 48). Especially in chronic wounds which are characterized by excessive proteolytic activity, entrapment of growth factors can serve as a way to protect them from rapid degradation in this hostile environment. Owing to its structural and

mechanical properties as well as inherent biological features, fibrin presents an appealing delivery vector as it (i) can be injected and polymerizes *in situ*; (ii) can be functionalized by simply adding therapeutic molecules to the fibrinogen or thrombin component in the fibrin formulation; and (iii) as it can be tailored into diverse structures like microspheres or nanoparticles to control the release kinetics of the delivered molecule [1219]. Fibrinolysis and diffusion are the driving forces behind local delivery of substances from fibrin matrices. However, *in vivo*, rapid degradation may result in burst release and supra-physiological levels of the bioactive molecule which is then quickly metabolized. Thus, a variety of strategies to control drug and growth factor release kinetics from fibrin matrices have been introduced for sustained delivery at physiologically relevant doses [302, 510, 1226]. A list of key studies summarizing fibrin-based *in vivo* delivery of therapeutic biomolecules is shown in Table 9.

3.1. Factors affecting the release kinetics from fibrin matrices

The release profile of a bioactive molecule depends on its mode of interaction with fibrin (defining the diffusion rate) and the mechanical properties of the matrix in combination with the fibrinolytic activity in the area of application (defining the degradation rate). The main approaches to alter the release kinetics have thus focused on either modifying the biophysical properties of the fibrin matrix or modifying the substance of interest in a way to alter the interaction between the two (Fig. 49). Growth factors that weakly bind fibrin will quickly diffuse out of the matrix upon application to the injured site [864, 934, 935, 1227]. Growth factors with natural affinity for fibrin such as bFGF, VEGF$_{165}$ or IL-1β [565-567] will primarily be released upon cell infiltration and subsequent matrix degradation, allowing for sustained release. A feasible approach to circumvent the burst release kinetics of therapeutics that do not have natural affinity for fibrin is the incorporation of free heparin into the matrix. Heparin binds fibrin [938, 1228] as well as many growth factors [863, 933, 939, 940] and can thus be used to protect growth factors by sequestration in the matrix, which slows down diffusion and delays release. One of the benefits of this approach is that heparinized fibrin matrices will also sequester circulating growth factors *in situ*, thereby increasing the bioactivity of these endogenous factors [941]. Furthermore, adjusting the molar ratio between heparin and the incorporated growth factor allows modulation of its release kinetics. A popular approach for sustained delivery is the affinity-based incorporation of growth factors into fibrin via heparin-binding bi-domain peptides that are covalently linked to the matrix [942, 1229]. Alternatively, recombinant fusion proteins consisting of naturally occurring fibrin-anchors and growth factors have been introduced for covalent or affinity-based tethering to the fibrin matrix [951, 956, 957, 1230].

Alternatively, the structural and mechanical properties of the fibrin matrix itself can be modified through varying its composition, that is, the fibrinogen, thrombin and FXIIIa concentrations. These parameters, to some extent, define clot microstructure (pore size, density), stiffness and resistance to fibrinolysis [730, 742, 914, 1021] and have been shown to affect release kinetics in the context of

bFGF [940], nerve growth factor-β (NGF-β) [942], TGF-β1 [923] or epidermal growth factor (EGF) [926] delivery. The
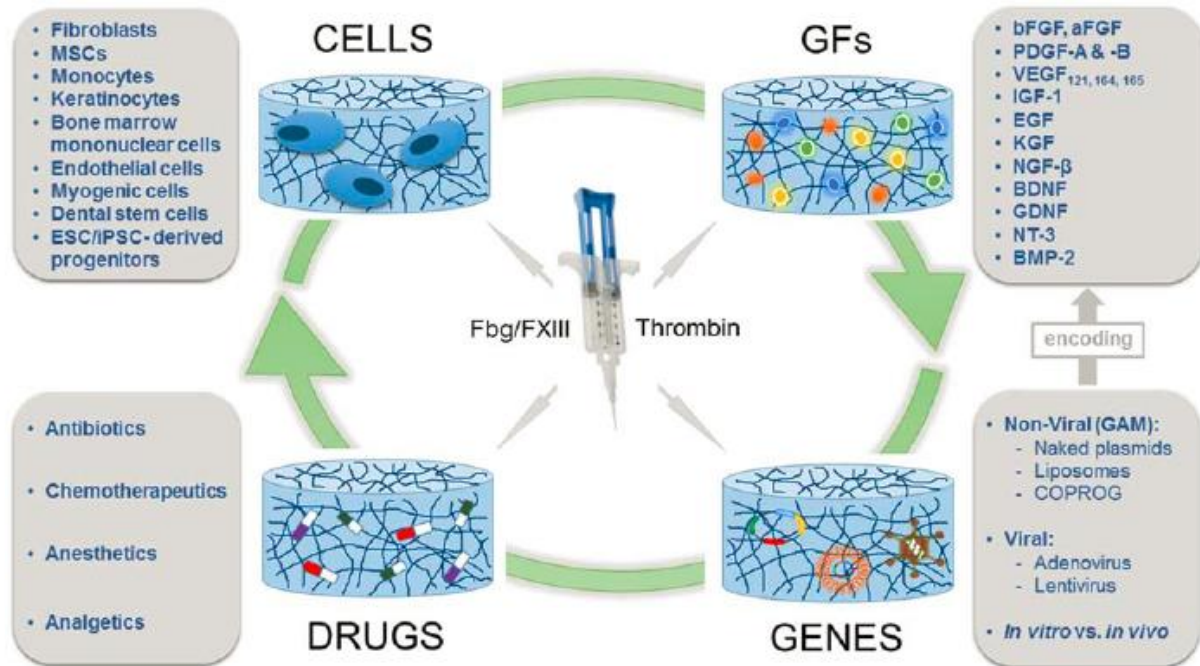

Fig. 48: *Experimental and clinical delivery applications of fibrin in wound healing.* Fibrin has been used to deliver cells, drugs, growth factors or gene vectors, and combinations thereof. GF: growth factor, Fbg: fibrinogen, FXIII: Factor XIII, MSCs: mesenchymal stem cells, ESC: embryonic stem cell, iPSC: induced pluripotent stem cell, FGF: fibroblast growth factor, PDGF: platelet-derived growth factor, VEGF: vascular endothelial growth factor, IGF: insulin-like growth factor, EGF: epidermal growth factor, KGF: keratinocyte growth factor, NGF: nerve growth factor, BDNF: brain-derived neurotrophic factor, GDNF: glial cell line-derived growth factor, NT: neurotrophin, BMP: bone morphogenetic protein, GAM: gene activated matrix, COPROG: copolymer protected gene vector (figure adapted from [302]).

growth factor release profile can further be altered by adjusting scaffold degradation rates. Anti-fibrinolytics like aprotinin [915, 917, 918] or tranexamic acid [916] can significantly prolong the time needed for fibrin degradation, however, they pose considerable safety issues when entering systemic circulation [1231]. To reduce these risks, a strategy to covalently cross-link aprotinin into fibrin has been developed by Sacchi et al. [1232]. This study reported a significant effect on matrix stability, allowing for sustained release of $VEGF_{164}$ for up to 4 weeks *in vivo*.

3.2. Release of growth factors

Initial studies on growth factor delivery for the treatment of acute and chronic wounds focused on finding adequate dosage of growth factors entrapped in fibrin. Pandit et al. investigated the fibrin-based delivery of acidic FGF (aFGF; FGF-1) in rabbit wound models and reported an increase in the fibroblastic and angiogenic response, resulting in improved wound healing [919, 934]. Other studies demonstrated the feasibility of fibrin to deliver neurotrophic factors such as glial cell line-derived neurotrophic factor (GDNF) [922, 935] or neurotrophin-3 (NT-3) [921] for nerve regeneration.

Furthermore, Cole et al. [1227] reported that macrophage activator lipoprotein peptide (MALP)-2 incorporated in fibrin stimulated human monocytes, modulating their cytokine secretion *in vitro*.

Field	Cargo	Mode of release	Outcome
Neovascularization/re-epithelialization			
Chronic ulcer	aFGF	Diffusion	Increased angiogenesis, re-epithelialization
Hindlimb ischemia	bFGF and heparin	Cell-mediated degradation	Increased angiogenesis
Hindlimb ischemia, ischemic and non-ischemic flap	VEGF$_{164}$ bi-domain peptide tethered *via* FXIIIa	Cell-mediated degradation	Increased angiogenesis/wound healing
Ischemic flap	PDGF-AB bi-domain peptide tethered *via* FXIIIa	Cell-mediated degradation	Increased angiogenesis/wound healing
Ischemic flap	VEGF$_{165}$	Cell-mediated degradation	Increased angiogenesis
Cell infiltration of subcutaneous fibrin clot	VEGF$_{121}$ bi-domain peptide tethered *via* FXIIIa	Cell-mediated degradation	Increased angiogenesis
Cell infiltration of subcutaneous fibrin clot	bFGF fused to Kringle 4	Cell-mediated degradation	Increased angiogenesis
Chick chorioallantoic membrane	Ephrin B2 bi-domain peptide tethered *via* FXIIIa	Cell-mediated degradation	Increased angiogenesis
Chick chorioallantoic membrane	VEGF$_{121}$/bFGF, VEGF$_{165}$/bFGF and heparin	Cell-mediated degradation	Increased angiogenesis
Cutaneous wound	VEGF$_{165}$ and PDGF-BB fused with PlGF2 peptide	Cell-mediated degradation	Increased angiogenesis/wound healing
Cutaneous wound	bFGF fused to Kringle1	Cell-mediated degradation	Improved wound healing/increased angiogenesis
Cutaneous wound	KGF bi-domain peptide tethered *via* FXIIIa	Cell-mediated degradation	Improved wound closure
Infection			
MDR *S. aureus* infection	Vancomycin	Diffusion	Suppression of local subcutaneous wound infection
MDR *S. aureus* infection	Streptomycin, tetracycline	Diffusion	Effective clearance of *S. aureus*-induced peritoneal sepsis
P. aeruginosa infection	Tobramycin	Diffusion	Bacterial growth reduction on corneal surface
Chemotherapy			
Glioblastoma	Microsphere-bound rhenium-188 and rhenium-186	Diffusion	Prevention of tumor reoccurrence after resection
Hepatoma	Doxorubicin (fibrin-alginate composite)	Diffusion	Improved localized delivery to tumor site
Retinoblastoma	Topotecan	Diffusion	Tumor regression
Retinoblastoma	Carboplatin	Diffusion	Tumor regression
Cells with growth factors			
Hindlimb ischemia	bFGF and bone marrow-derived mononuclear cells	Cell-mediated degradation	Increased angiogenesis
Hindlimb ischemia	G-CSF, bone marrow-derived mononuclear and endothelial progenitor cells	Diffusion/cell-mediated degradation	Increased angiogenesis
Cutaneous wound	Fibroblasts and PDGF-BB	Cell-mediated degradation	Increase of granulation tissue, epithelial migration
Epidermal regeneration	Keratinocytes and EGF	Cell-mediated degradation	Increased re-epithelialization
Odontogenesis	Dental bud MSCs and PRF	Diffusion/cell-mediated degradation	Improved dental regeneration (up to formation of a complete tooth)
Periodontal regeneration	MSCs and PRF	Diffusion/cell-mediated degradation	Enhanced alveolar augmentation after implant placement

Table 9: *Key in vivo studies on fibrin-based delivery of therapeutic biomolecules.*

However, early strategies did not allow for controllable and sustained release since these growth factors do not have natural affinity for fibrin. With the notion that locally sustained physiological dosage is required to induce the greatest therapeutic efficacy [932, 933], growth factors that naturally bind fibrin have been studied in a multitude of clinical settings. Incorporation of bFGF [920, 936] or VEGF [937, 1233] into fibrin has been shown to provide a delivery platform where the growth factor is released upon cellular infiltration and subsequent matrix degradation in a sustained manner. An interesting study by Wong et al. [937] evaluated the release profiles of bFGF, VEGF$_{165}$ and VEGF$_{121}$ from fibrin matrices and their therapeutic efficacy in a chicken embryonic chorioallantoic membrane (CAM) model. Notably, bFGF and VEGF$_{165}$ release was much slower than VEGF$_{121}$ release, leading to the finding that the C-terminal domain sequence of VEGF$_{165}$ (which is missing in VEGF$_{121}$) is

responsible for fibrin(ogen) binding [1234]. Mittermayr et al. [1233] reported that sustained release of VEGF$_{165}$ from a sprayed fibrin matrix induced angiogenesis and endogenous VEGF receptor 2 expression in a mouse ischemic flap model. This may also be a promising approach in the treatment of large area burns, as thin layers of fibrin have been shown to improve graft "take" in skin graft fixation procedures [883]. Notably, bFGF delivery has further been proposed as a promising regenerative strategy for periodontal and dental regeneration [1235], processes which are heavily challenged by the hostile microbial environment in the mouth. Fibrin alone promotes wound healing in the oral cavity [1236] and there are indications that fibrin-based delivery of bFGF improves healing of delayed-replanted teeth [1237]. This is supported by several studies reporting on the beneficial effects of platelet-rich fibrin (PRF), a formulation rich in growth factors, on bone and soft tissue regeneration in dentistry [1238-1240]. Furthermore, the incorporation of heparin into fibrin to enhance the retention of bFGF [863, 940], VEGF [937] or nerve growth factor (NGF) [939] has been feasible for sustained delivery. However, the fact that many other growth factors, especially neurotrophins [942], do not have high affinity for heparin led to the development of alternate strategies to control their release kinetics from fibrin.
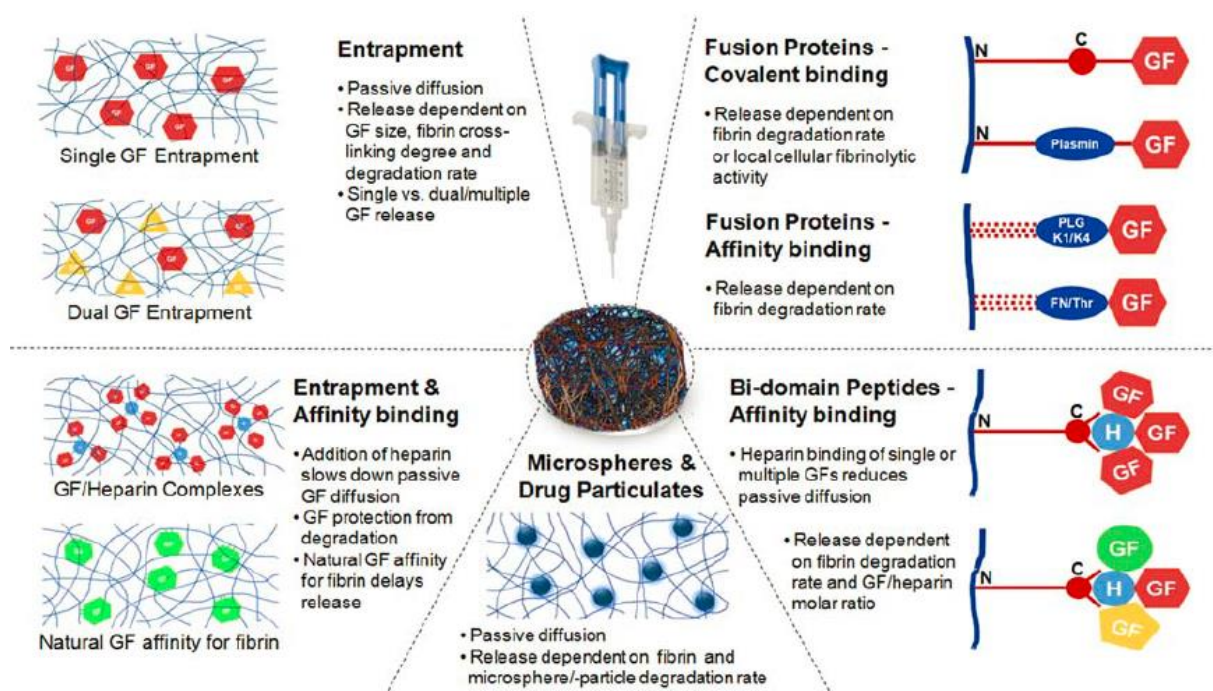

Fig. 49: *Modes of growth factor release from fibrin matrices.* Growth factors can be (i) entrapped into fibrin (burst release), (ii) bound via natural affinity or heparin complexation (slower release) or (iii) covalently bound via bi-domain peptide or fusion protein technologies (slowest release). Furthermore, microspheres carrying drugs or growth factors can be incorporated into the fibrin matrix for sustained release. GF: growth factor, H: heparin, PLG: Plasminogen, K1/4: kringle domain 1/4, FN: fibronectin, Thr: thrombin (figure adapted from [510]).

A significant advancement in the field of fibrin-based delivery systems was the covalent incorporation of growth factors into the fibrin matrix, which allows much longer retention than physical

encapsulation. Schense and Hubbell [943] designed a bi-domain peptide consisting of an N-terminal FXIIIa substrate (derived from α2-plasmin inhibitor; α2-PI) and a C-terminal bioactive domain of choice which can be a cell binding motif, a heparin binding site or a growth factor itself. Exploiting the ability of FXIIIa to cross-link such bi-domain peptides into fibrin during polymerization, covalent functionalization of fibrin with cell recognition motifs such as RGD and DGEA [943] or laminin and N-cadherin peptides [944] was achieved. Further use of this approach involved the sustained delivery of covalently bound $VEGF_{121}$ [924, 945, 1230], $VEGF_{164}$ [1232], PDGF-AB [1241] and ephrin B2 [946] to drive angiogenesis and improve the wound healing response *in vitro* and *in vivo*. Based on this methodology, Sakiyama-Elbert and Hubbell [942, 947] also developed a versatile affinity-based delivery system using bi-domain peptides with an N-terminal FXIIIa substrate and a C-terminal heparin binding domain (derived from antithrombin III). This system was extensively studied in the context of nerve regeneration and affinity-based delivery of bFGF [1229], NT-3 [852, 949], NGF-β [948], GDNF [950] or PDGF [852] yielded promising results in terms of peripheral or spinal cord regeneration.

Finally, Sakiyama-Elbert et al. [951] reported on an elegant refinement of the bi-domain peptide strategy, using a fusion protein consisting of a FXIIIa substrate, a plasmin α2 substrate sequence linker and a growth factor binding domain. This approach provides a variable growth factor release profile depending on the local cellular activity at the site of application, as the cells infiltrate the fibrin matrix and activate PLG. While this delivery system "on cellular demand" was initially developed and tested for sustained delivery of NGF-β [951], it was also shown to efficiently stimulate EC proliferation and maturation through $VEGF_{121}$ delivery in vitro [932]. Geer et al. [952] used plasmin sensitive bi-domain peptides for the sustained delivery of keratinocyte growth factor (KGF) and observed gradual KGF release for 7 days *in vivo*, with significantly enhanced wound closure compared to topical KGF delivery in a murine full-thickness hybrid wound model. Other studies reported on the delivery of parathyroid hormone (PTH) 1-34 [953] or bone morphogenetic protein (BMP)-2 [955] to improve bone formation through cell-mediated growth factor release. An alternative to the bi-functional peptide strategies are recombinant fusion proteins consisting of growth factors and other fibrin binding moieties. Zhao et al. [956, 957] introduced such an approach by fusing kringle domains 1 and 4 of human PLG to bFGF (K1bFGF and K4bFGF). These kringles mediate high affinity binding of PLG to fibrin and tethering of K1bFGF and K4bFGF to fibrin led to higher retention of the growth factor in the matrix compared to unmodified bFGF. Notably, the bioactivity of K1bFGF and K4bFGF was not affected and the recombinant bFGF fusion proteins were shown to improve neovascularization in a full-thickness rat wound model. Fragments of other naturally occurring fibrin anchors such as fibronectin [927] have also been investigated for tethering growth factors of the VEGF/PDGF and FGF families to fibrin [925]. In this respect, the fibrin binding moieties of thrombin may also serve as a potential target [983].

In vivo, multiple growth factors are spatiotemporally involved in the complex process of wound healing and tissue repair. Consequently, methods for the simultaneous or sequential release of two or more bioactive molecules have been explored to better replicate the physiological wound response. Dual- or multi-growth factor delivery from fibrin matrices without distinct release kinetics has been studied in the context of chronic wound healing [1242], nerve (NT-3, PDGF, sonic hedgehog) [852, 958] or tendon regeneration (PDGF, VEGF, bFGF, BMP-2) [928]. Sequential release can be achieved by either taking advantage of different binding affinities of growth factors for fibrin or by using fibrin composites, where growth factors interact with different matrix components (that have different degradation rates or growth factor binding affinities). The importance for sequential delivery approaches in angiogenesis has been shown by Wong et al. [937] who studied the effects of single and combined release of bFGF (highest fibrin affinity), $VEGF_{165}$ (high fibrin affinity) and $VEGF_{121}$ (low fibrin affinity) on neovascularization in a chicken embryo CAM model. Single delivery of each growth factor induced angiogenesis but resulted in the formation of leaky blood vessels, while hemorrhaging was not observed with combined sequential delivery. Similarly, controlled dual release of $VEGF_{165}$ and aFGF from fibrin loaded with heparin has also been reported [960]. Drinnan et al. [959] developed a multimodal delivery system, using PEGylated fibrin for the sequential release of PDGF-BB (entrapped in fibrin) and TGF-β (bound to a homobifunctional PEG linker). While PDGF-BB was rapidly released within 48 hours, TGF-β release could be sustained for over 10 days. Furthermore, Layman et al. [961, 962] reported on a sequential bFGF and granulocyte colony stimulating factor (G-CSF) delivery system using growth factor-loaded albumin microspheres embedded in fibrin. Combinational delivery of bFGF and G-CSF resulted in more robust hind limb reperfusion and capillary vessel formation in a mouse critical limb ischemia model after 8 weeks compared to either growth factor alone or bolus administration. These and many other studies demonstrate the feasibility of fibrin-based multi-growth factor delivery in supporting wound healing. However, the therapeutic outcome strongly relies on fine-tuned release kinetics to prevent adverse effects of the treatment [1243].

3.3. Release of drugs

Various clinical indications require localized, high-dose delivery of pharmaceuticals, which cannot be achieved via systemic administration. Severe trauma, large-area burns or chronic wounds which are characterized by persistent infections present such situations. Given the widespread use of fibrin sealants in the treatment of wounds, simultaneous delivery of antibiotics incorporated in fibrin augments the effectiveness of the sealant in post surgery wound healing through restricting infections. However, the main challenge has been to sustain drug delivery over adequate periods of time. Fibrin-based delivery of antibiotics, chemotherapeutic agents or anesthetics has been evaluated for many years and a comprehensive review has recently been provided by Ahmad et al. [833].

More than 30 years ago, a pioneering study [1004] evaluated the properties of fibrin sealants loaded with different antibiotics *in vitro*. Gentamycin, neomycin and polymyxin E were entrapped in fibrin and complete release within 3 days was observed. Notably, gentamycin incorporation reduced clot strength by affecting fibrinogen α-chain-cross-linking, which could be counteracted by increasing thrombin and FXIII concentration in the formulation. Similar results were reported by Greco et al. [1002] who compared release profiles of a multitude of antibiotics from fibrin. While some antibiotics (cefotaxime, mezlocillin) inhibited polymerization altogether, others displayed burst release profiles (ampicillin, carbenicillin, ceftazidine, clindamycin, gentamycin, tobramycin), with more than 50% of the entrapped antibiotic being released within 24 hours and the remaining within 48 to 96 hours. Tredwell et al. [929] reported that release of cefazolin from fibrin clots did not significantly alter drug stability (in contrast to erythromycin which degraded rapidly upon release), suggesting the potential of cafezolin-loaded fibrin sealants in postoperative antibiotic delivery. The release profiles and bacteriocidal activities of many other antibiotics have been investigated and vancomycin, ciprofloxacin and teicoplanin have been identified as potentially feasible targets for fibrin-based delivery [930, 931, 954, 1003, 1006, 1244, 1245]. Delivery of these antibiotics displayed effective bacteriocidal activity against clinical isolates of *Staphylococcus (S.) aureus* [954, 1003, 1244, 1245], *S. epidermidis* [1006] and *Escherichia (E.) coli* [1244]. One study even reported that ciprofloxacin was released from fibrin in pharmaceutically relevant doses over a surprisingly long period of several weeks [931]. In addition, Woolverton et al. [1005] reported that poorly soluble (lipophilic) antibiotics like tetracycline and streptomycin are retained longer in fibrin, demonstrating that sustained release correlates with drug hydrophobicity. More importantly, the study showed that intraperitoneal delivery of high doses of streptomycin in fibrin discs resulted in 100% survival of rats with multi-drug resistant (MDR) *S. aureus* peritonitis compared to controls receiving streptomycin in saline. A follow-up study by the same group further demonstrated the safety and long-term (5 weeks) efficacy of a single treatment with tetracycline-loaded fibrin discs to control *S. aureus*-induced peritoneal sepsis in mice [1007]. Strategies for the sustained release of hydrophilic drugs have also been reported and include fibrin microparticles [1011], freeze-dried fibrin discs [1008, 1009] or composite strategies such as fibrin coated drug particulates [1010, 1012, 1245].

Apart from antiobiotic delivery, fibrin has been studied as a delivery vector for chemotherapeutic agents. Investigating the release kinetics of mitomycin C, fluorouracil and enocitabine from fibrin sealant, Yoshida et al. [1013] reported that release rates correlated inversely with drug hydrophobicity. Similarly, Kitazawa et al. [1014] introduced a fibrin/alginate composite which was shown to safely deliver doxorubicin in a localized and sustained manner when implanted on the surface of AH60C tumors in the back of rats. Drug-loaded fibrin matrices have further been evaluated in the treatment of ophthalmic tumors and fibrin-based delivery of chemotherapeutics such as topotecan [1015] or carboplatin [1016, 1017, 1246] to the retina of mice and rabbits has been reported. In addition, the feasibility of fibrin to deliver microspheres of β-emitting radioisotopes has been shown in a 9L-

glioblastoma rat model, with decreased reoccurrence rates after tumor resection when the delivery system was applied [1018]. An alternative use of fibrin in drug delivery has been reported by Zhibo and Miaobo [1019], who used fibrin to locally deliver the anesthetic lidocaine to reduce pain after subpectoral breast augmentation in humans.

4. DELIVERY OF CELLS

Growth factor delivery as a strategy to improve wound healing generally holds great therapeutic promise, however, it relies on the capability of the cells *in situ* to respond to the delivered stimuli. In volumetric defects or dysfunctional tissues, the local cell population might not be sufficient to induce repair on their own and the presence of additional cells might be necessary to drive regeneration. Due to its natural role in wound healing and its exceptional biocompatibility, fibrin has been used in a variety of cell delivery approaches in the past. A vast amount of studies have reported the feasibility to culture cell types such as keratinocytes [838, 839], fibroblasts [548, 840], ECs [849, 870, 1247-1249], chondrocytes [862, 904, 1250], osteoblasts [842], dental stem cells [1251, 1252], adipocytes [844, 845], urothelial cells [846, 1253], hepatocytes [848] or myogenic cells [430, 836, 877] on/in fibrin. Furthermore, the cytocompatibility of fibrin with different stem cell types is now well established. Mesenchymal stem cells (MSCs) from different sources [841, 854-857] and, more recently, embryonic stem cell (ESC)- [858] or induced pluripotent stem cell (iPSC)-derived progenitor cells [859] have also been used in combination with fibrin. Am main advantage is that fibrin gels can attain high cell seeding densities and uniform cell distribution, while maintaining viability and effectively supporting cell proliferation, migration and differentiation. Consequently, a higher percentage of cells can engraft into the damaged tissue compared to local and systemic cell suspension injections [836, 1254].

4.1. Effects of fibrin matrix composition on the biological response of cells

Cell delivery approaches benefit strongly from fibrin matrix properties that provide an appropriate microenvironment for the respective cell type(s). As described earlier in the context of growth factor and drug delivery, the structural and mechanical properties of fibrin can be modulated by varying the concentrations of its principal constituents fibrinogen, FXIII and thrombin [730, 742, 914, 1021]. In this respect, fibrinogen concentration is the main factor and correlates directly with fibrin stiffness and clot density [578], and inversely with clot degradation rate [733]. A variety of studies have examined the effects of fibrin composition on the growth and proliferation of fibroblasts [840], keratinocytes [860, 861], monocytes [867] or MSCs [854, 865, 866]. Taken together, these studies have shown that fibrinogen has the strongest effect on cell proliferation, while the influence of thrombin is lower, but nevertheless considerable. Fibroblasts and MSCs were shown to favor fibrin matrices of low to intermediate stiffness (5-18 mg/mL fibrinogen) [840, 854], whereas keratinocytes grow well on very

soft matrices (1-3 mg/mL fibrinogen). In contrast, optimal monocyte proliferation was shown to require a stiffer fibrin matrix (26-50 mg/mL) [867]. Thrombin concentrations have direct effects on clot permeability and pore size and thus may affect cellular migration in fibrin matrices [862]. Furthermore, matrix stiffness has been shown to strongly affect cell differentiation, which has been exploited to drive maturation of cells on hydrogel matrices [355, 356, 855].

Summarizing, there is no universal fibrin composition for cell delivery. In fact, the matrix properties need to be carefully addressed for each cell delivery strategy to optimize the biological outcome and prevent detrimental effects on the cells [868, 869, 1255]. This is especially important in wound healing strategies that address angiogenesis, as increased fibrin matrix stiffness has been shown to inversely correlate with the formation of vascular networks within such matrices [1256, 1257]. Lower fibrin clot stiffness seems to be beneficial for vascularization and thus wound repair itself, however, such scaffolds may degrade rapidly and are therefore not suitable for sustained growth factor or drug delivery over long periods of time [1230]. Therefore, another way to promote scaffold stability while maintaining a certain degree of vascularization is by addressing scaffold degradation mechanisms. Several groups have published attempts to prolong fibrin stability by using antifibrinolytic agents that inhibit plasmin formation or activity [915-918, 988, 1232]. It has furthermore been reported that inhibition of plasmin-mediated fibrinolysis does not interfere with vascularization of fibrin scaffolds since matrix metalloproteinase (MMP) activity seems to be the key driver of vascular network formation [967, 1258]. It should be pointed out that these studies have exclusively used a fibrinogen formulation that was depleted of PLG in their experiments. Noteworthy, addition of antifibrinolytics to PLG-depleted fibrin clots had no effect on capillary formation of bFGF/tumor necrosis factor (TNF)-α-stimulated ECs, suggesting that these agents solely affect PLG-mediated mechanisms and not MMP activity [968]. However, it needs to be mentioned that vascular network formation in PLG-depleted fibrin scaffolds occurred to a sufficient degree although it might have been superior in scaffolds containing PLG. Unfortunately, there is no current *in vivo* comparison addressing the effect of PLG-containing fibrin on vascularization. Nevertheless, fine-tuning of fibrin degradation by using antifibrinolytic agents can result in prolonged scaffold stability even when lower stiffness is desired.

4.2. Cell delivery in wound healing applications

Many wound healing therapies have utilized fibrin-based cell delivery or tissue engineering strategies to promote neovascularization and regeneration of dermal and epidermal structures. In a vast majority of burns, acute or chronic wounds these two layers of the skin are affected the most. Therefore, this section will focus on recent approaches in cutaneous wound repair and strategies for vascularization of (epi)dermal tissues. The broader application of fibrin as a cell delivery and differentiation matrix in other tissue engineering fields has been reviewed elsewhere [303, 834, 896].

Skin grafting for cutaneous wound repair is one of the oldest surgical procedures in the clinical toolbox. While cultured epidermal autografts (CEAs) employing cultured keratinocytes [1259] have

been proven useful in clinics, their engraftment rates can vary greatly *in situ*. Furthermore, the limited availability of skin autografts (especially in patients with large-area burns) has driven the evolution of skin grafting techniques from initial auto- or allograft preparations to tissue-engineered skin replacements [1260]. More than 20 years ago, fibrin hydrogels and sealants have been identified as suitable matrices for the delivery of keratinocyte suspensions to wounds [885, 1261]. This led to the commercialization of BioSeed-S© (BioTissue Technologies AG, Freiburg, Germany), a fibrin-based autologous skin replacement product that has been shown to effectively promote closure and healing of burns, acute wounds and refractive chronic leg ulcers [839, 969, 970]. The versatility of this approach is further underscored by reports demonstrating that spraying of single cell keratinocyte suspensions alone [827] or in fibrin [838, 971] works well and is especially useful when large wound areas need to be covered. Given the widespread use of acellular dermal substitutes, Bannasch et al. [884] investigated the combination of cultured keratinocytes in fibrin with decellularised human dermis. Compared to plain epithelial grafts, the combinational treatment showed improved integration and wound contraction in a porcine full-thickness wound model and full wound closure was achieved. This is further supported by an earlier study by Geer et al. [882] who demonstrated the beneficial effects of fibrin on wound reepithelialization *in vitro* using human keratinocytes and acellular dermis. After incisional wounding, fibrin was found to promote keratinocyte growth and migration and significantly reduced the lag phase of keratinocyte activation. Autologous cultured epithelia grown from human keratinocytes on fibrin have been shown to provide long-term epidermal regeneration in burns [972]. However, keratinocytes alone seem to be unable to fully build up a new functioning basal membrane between the epidermis and dermis *in vitro* [971]. Therefore, co-cultures of keratinocytes and fibroblasts in fibrin have been addressed [886-888], demonstrating that the mutual interactions between these cells benefit skin regeneration. For example, Boehnke et al. [886] demonstrated a proliferative effect of keratinocytes on fibroblasts and found a strict dependence of epidermal tissue regeneration on the presence of fibroblasts *in vitro*. Furthermore, fibroblast/keratinocyte co-culture in split-thickness grafts has been shown to effectively support healing of full-thickness skin wounds in mice [888] and sheep [887]. A more recent study reported on a fibrin-based three-layered skin substitute consisting of a hypodermal (adipocytes, MSCs), dermal (fibroblasts) and epidermal layer (keratinocytes), however, the substitute was not evaluated *in vivo* [1262].

Even though a vast amount of skin regenerative strategies has utilized fibrin and keratinocytes, alone or in co-culture with fibroblasts, other cell types have also proven useful to recover cutaneous wounds. Falanga et al. [841] reported that spray application of autologous bone marrow-derived MSCs (BMMSCs) entrapped in fibrin into human full-thickness wounds resulted in full wound closure of acute (7 weeks) and chronic wounds (6 months). Parallel studies by the same group using GFP-labeled BMMSCs in diabetic mice (db/db) revealed full wound closure once more and, importantly, the cells were also found to contribute to neovascularization. Furthermore, human umbilical cord perivascular cells (HUCPVCs), an MSC population that can be harvested more easily than BMMSCs, were

reported to contribute to early stages of full-thickness wound repair when delivered with fibrin in mice [1263]. More recently, autologous BMMSCs, adipose tissue-derived MSCs (ASCs) or hair follicles have attracted clinical attention and have been or currently are subject to trials [973, 1264].

In the field of vascularization and angiogenesis, a great deal of research has focused on the formation of tissue-engineered vascular grafts for coronary bypasses or peripheral vascular anastomosis. However, these large caliber structures do not fit the needs of wound angiogenesis, where microvascular blood and lymphatic networks are required. As ECs are in contact with almost all tissues in the body, incorporating ECs in co-culture systems provides a feasible way to simulate tissue function *in vitro* [974]. Many fibrin co-cultures utilize ECs together with MSCs, ASCs, skeletal/smooth muscle cells or dermal fibroblasts that provide essential factors for the development of a vascular network, however, often without specific differentiation towards a certain target tissue other than skin [975, 1265]. Lesman et al. [1266] demonstrated that co-cultures of ECs, fibroblasts and skeletal myoblasts in fibrin form microvascular networks *in vitro* and *in vivo*. Furthermore, enhancing fibrin's mechanical strength by addition of poly(L-lactic acid)(PLLA)/polylactic-glycolic acid (PLGA) sponges enhanced neovascularization, vessel maturity and perfusion of vascular grafts *in vivo*. Interestingly, a recent study employed the use of both dermal lymphatic and blood vessel-derived ECs in co-culture with ASCs in fibrin which is important to accurately resemble the *in vivo* situation [1267]. Nevertheless, only a few reports demonstrate how differentiated tissues can be generated by using fibrin co-cultures. Recently, it was shown that vascularized adipose tissue could form when ECs and stromal vascular fraction (SVF) co-cultures were incubated in adipogenic media [978]. Vascular density peaked when using endothelial-growth media, however, adipogenesis was barely observable. The opposite effect occurred when using media supplemented with adipogenic factors. Correia et al. [1268] found that a consecutive induction of tissue differentiation is necessary to generate vascularized differentiated cell constructs. Specifically, after 2 weeks induction of vascular network formation osteogenic supplements were added to the EC/MSC fibrin construct for additional 4 weeks prior to subcutaneous implantation into nude mice. This led to significantly increased vessel density and bone mineralization compared to controls where only one effect (vessel density or mineralization) could be observed. Still, more studies need to be performed in order to determine how co-cultures can be used to generated differentiated tissues in fibrin gels.

In dentistry, the injectability of a scaffold biomaterial is a key prerequisite for the proper induction of dental and periodontal regeneration, which is mainly due to the comparably small and irregular shape of the defects [1217]. Fibrin has been reported a feasible carrier for the delivery of dental stem cells [1251, 1269, 1270], especially in combination with PRF [911, 1252]. Using a fully autologous approach, Yang et al. [1252] demonstrated that a combination of fibrin, PRF and dental bud cells could effectively trigger odontogenesis in porcine alveolar pockets. Furthermore, Ito et al. [911] showed the beneficial effects of MSC-loaded fibrin/PRF hydrogels on alveolar augmentation with simultaneous implant placement in dogs, reporting up to 53% bone-implant contact after 8 weeks.

4.3. Combined cell and growth factor delivery

Given the widespread use of both growth factor and cell delivery, synergistic approaches combining these two strategies to support tissue formation and functionality have been addressed. Gwak et al. [981] observed faster and more pronounced epidermal regeneration in mice when spraying a combination of keratinocytes and EGF in fibrin into full-thickness wounds compared to single controls, even though EGF was fully released from the matrix within 3 days. An interesting study in a rabbit ear cutaneous wound healing model by Mogford et al. [964] showed beneficial effects of dermal fibroblasts in fibrin gels loaded with PDGF-BB on wound healing, especially when diluted fibrin sealant formulations where used (17.3 mg/mL fibrinogen, 167 U/mL thrombin instead of 50 mg/mL fibrinogen, 250 U/mL thrombin). With the notion that bFGF stimulates dermal fibroblast proliferation in fibrin *in vitro* [963], Inoue et al. [1271] reported similar but bFGF concentration-dependent effects on fibroblast proliferation in cultured skin substrates composed of keratinocyte/fibroblast co-cultures *in vivo*. Furthermore, bFGF incorporation into the fibrin-based skin substrates also enhanced neovascularization after transplantation in nude mice. In addition, Jeon et al. [1272] showed a synergistic effect of combined bFGF and bone marrow mononuclear cell (BMMNC) delivery in fibrin on angiogenesis in mouse ischemic limbs. In a follow-up study, the same group also provided evidence that a combinational administration of BMMSCs, endothelial progenitor cells and G-CSF in fibrin potentiates the angiogenic efficacy of either single therapy in mouse limb ischemia [979].

5. GENE DELIVERY

The delivery of gene vectors encoding growth factors into target cells *ex vivo* or *in vivo* presents an alternative strategy to overcome the need for high and repeated doses in protein-based therapies [1273]. Although growth factor delivery has been successfully employed in a variety of tissues, the limited commercial availability, high costs as well as short half-life of growth factors *in vivo* (due to rapid proteolysis) prevent a more widespread use of this approach. The general principle in fibrin-based gene delivery is to transfect either endogenous target cells as they infiltrate the matrix during wound healing, or exogenous cells that are incorporated into fibrin prior to implantation. Fibrin matrices have been shown to be effective delivery systems for both viral [976, 977] and non-viral vectors [982, 1274, 1275] compared to injections in saline.

Concerning viral gene delivery, a combination of fibrin with recombinant adenoviruses presents an appealing delivery platform, which was confirmed in several proof-of-concept studies utilizing the lacZ transgene (β-galactosidase): two studies by Breen et al. [1276, 1277] showed that adenovirus release from fibrin depended on the scaffold formulation and could be attained for up to 8 days *in vitro*, while *in vivo* delivery did not elicit an inflammatory response or impaired chronic wound

healing compared to fibrin alone; moreover, adenoviral gene delivery of lacZ by fibrin spray application was reported a feasible strategy for gene transfer into mucosal surfaces [977]. In the context of cutaneous wound healing, fibrin-based delivery of adenovirus encoding endothelial nitric oxide synthase (AdeNOS) was evaluated in a rabbit ear ulcer model [984]. Compared to single treatment controls, AdeNOS delivery in fibrin induced local eNOS expression which enhanced reepithelialization of diabetic wound sites which are usually NO deficient. Similarly, adenoviral KGF delivery in fibrin promoted reepithelialization in a cutaneous humanized skin model in mice [986].

For non viral gene delivery, naked plasmids can be incorporated into fibrin, which allows retention of the vector DNA through ionic interaction with the matrix [983]. Such gene activated matrix (GAM) approaches provide a safe delivery method and sustained release of plasmid DNA for a period of at least 19 days has been reported [985]. Fibrin-based GAMs have been successfully used to enhance neovascularization of ischemic myocardium by delivery of pleiotrophin [1274] or angiogenesis in rodent hind limb or skin flap ischemia models through VEGF delivery [987, 1278]. To increase the relatively low transfection efficiencies observed in naked plasmid approaches, fibrin has been evaluated in several lipo-/polyplex approaches where complexes of DNA and transfection reagents are incorporated into the matrix [989, 1275, 1278, 1279]. Interestingly, entrapment of lipofectamine in fibrin was found to significantly decrease its cytotoxicity [989]. Furthermore, other modes of DNA condensation in fibrin such as copolymer protected gene vectors (COPROG) [982] or covalent cross-linking of plasmid DNA coupled to FXIII substrate peptides into fibrin have been described [990]. Addressing the problem of limited DNA loading capacity in fibrin, Kulkarni et al. [991] developed a method to release fibrin microspheres carrying DNA lipoplexes from fibrin matrices. A follow-up study by the same group [1280] used this system to deliver both Rab18 and eNOS into rabbit hyperglycemic ear ulcers, which enhanced wound closure by increasing functional angiogenesis and reducing local inflammation. Interestingly, this "fibrin-in-fibrin" approach could be used for sequential gene delivery, since fibrin microspheres and fibrin hydrogels have differential degradation profiles.

Finally, *in vitro* transfection of exogenous cells in fibrin and subsequent transplantation back to the site of injury presents an approach that does not rely on transfection efficiencies *in situ*, but rather uses the transfected cells as gene vector for localized growth factor production. For example, Andree et al. [1281] incorporated human keratinocytes transfected with an EGF expression plasmid into fibrin and found a 180-fold increase of local EGF concentration in murine full thickness wounds, which persisted over 7 days compared to controls. In a similar approach, PDGF-AA overexpressing human keratinocytes were shown to improve bioengineered skin graft performance in a mouse full-thickness wound model during the first week after transplantation [1282]. Adenoviral KGF transfer into human fibroblasts in fibrin and subsequent transplantation into cutaneous wounds was shown to provide wound reepithelialization in a more reliable way compared to fibrin-immobilized adenoviral KGF release [986]. Furthermore, transfection of VEGF$_{165}$ into human primary preadipocytes through electroporation prior to incorporation and delivery in fibrin was shown to increase vascularization in a

chicken embryonic CAM model [1000]. Table 10 provides a list of key studies summarizing fibrin-based viral and non viral *in vivo* delivery of gene vectors.

Field	Vector	Outcome
Viral delivery		
Safety/efficacy (ear ulcer)	Adenovirus encoding lacZ	Enhanced lacZ transgene expression without inflammatory response
Safety/efficacy (esophageal epithelium)	Adenovirus encoding lacZ	Endoscopic local delivery into epithelial cells in the mucosal surface through spraying
Re-epithelialization	Adenovirus encoding eNOS	Faster rate of re-epithelialization in chronic ulcers
Re-epithelialization	Human fibroblasts expressing KGF (adenovirus)	Enhanced re-epithelialization in a humanized skin model (human bioengineered skin grafting in mice)
Bone repair	Adenovirus encoding BMP7	Increased bone formation after intramuscular implantation
Non-viral delivery		
Safety/efficacy (ear ulcer)	Plasmids encoding lacZ or firefly luciferase, lipofectin	Significantly higher transgene expression by fibrin-lipoplex system compared to lipoplexes alone
Neovascularization	Plasmid encoding PTN	Increased neovasculature formation in ischemic myocardium
Neovascularization	Human preadipocytes expressing $VEGF_{165}$ (electroporation)	Increased vascularization in CAM model
Hindlimb ischemia	Plasmid encoding $VEGF_{165}$	Enhanced capillary density in hindlimb muscles
Ischemic flap	Plasmid encoding VEGF-A, lipofectamine	Improved wound angiogenesis (skin flap survival) with elevated tissue perfusion
Cutaneous wound	Human keratinocytes expressing EGF	180-fold increase in EGF concentration over 7 days in full-thickness wounds
Hyperglycemic wound	Plasmids encoding Rab18 and eNOS, lipoplexes ("fibrin-in-fibrin" approach)	Enhanced wound closure, increased wound angiogenesis, reduced inflammation

Table 10: *Key studies on fibrin-based delivery of viral and non-viral gene vectors to promote wound healing in vivo.*

6. FUTURE PERSPECTIVES - CAN FIBRIN BE A DESIGNER MATRIX?

Growth factor delivery has yielded promising clinical results, however, a commercially available product based on a PDGF-BB gel, becaplermin (Regranex®; Smith & Nephew plc, London, UK), has been withdrawn in Europe due to safety issues. This underlines the necessity for further fine-tuning of existing growth factor delivery strategies. While incorporation into hydrogels has partially solved the issue of spatial release, tailoring physiologically relevant temporal release profiles (especially in multi-growth factor release approaches) remains difficult [1283]. Simultaneous and sequential release of therapeutic stimuli from matrices mimicking the natural microenvironments of tissue formation and repair will be necessary to properly induce wound healing *in vivo*. In this respect, a careful re-evaluation of the matrix properties is indispensable, as it plays a dual role in delivering bioactive substances while simultaneously acting as a scaffold for incorporated or endogenous cells *in situ*. Given the critical role of the ECM in guiding tissue repair by coordinating cell adhesion and modulating growth factor signaling, an ideal delivery matrix is expected to support both these processes upon implantation. Fibrin matrices have been shown to provide such a versatile delivery system, however, the scaffold formulations used for sustained growth factor release are very different from those favoring cell infiltration and proliferation - and vice versa. The trade-off between control of degradation rate (through use of high fibrinogen content) and cytocompatibility (medium to low fibrinogen content) creates a need to find strategies to stabilize soft fibrin matrices without

compromising sustained growth factor release. In this respect, novel and safe anti-fibrinolytics may provide sufficient control over fibrinolysis of cell and growth factor-laden clots *in situ* [993]. Otherwise, the amount of incorporated growth factor(s) needed to elicit a suitable regenerative response might be drastically reduced by designing the microfeatures of fibrin in a way to cluster integrin and growth factor receptors [1284]. The formation of molecular complexes between growth factors and ECM proteins present in fibrin, such as fibronectin or vitronectin, has been shown enhance growth factor signaling [994, 1285-1287]. Therefore, clustering of cell adhesion motifs with bound growth factors could be exploited to enhance and prolong growth factor signaling in a synergistic way, even when low doses of growth factor are used [925, 1288, 1289]. Whether this can be precisely achieved in a natural hydrogel like fibrin remains elusive. Nevertheless, advances in fibrin/cell inkjet bioprinting techniques may offer a promising tool to gain more control over the microtopological features of fibrin [1290]. Such methods allow defined spatial deposition of growth factors onto fibrin matrices [1291, 1292], which may enable generation of instructive matrices with high-resolution control over growth factor arrangement and quantity for localized cell responses within the matrix [1293].

7. CONCLUSION

After more than a century of research, fibrin can more than ever be considered one of the most versatile delivery vehicles in the tissue engineering toolbox. Fibrin is an excellent carrier for a vast amount of cell types and has also been found very effective in delivering growth factors, drugs or genes. Although other natural hydrogels have also yielded promising results in the treatment of (chronic) wounds, fibrin has intrinsic properties that render it superior in wound healing applications. Due to its natural involvement in hemostasis and wound healing, fibrin can act as a reservoir for many growth factors and contains a variety of cell adhesion motifs. Furthermore, it has been shown to directly stimulate angiogenesis, which is key to efficient wound healing. The development of strategies to control the release kinetics of therapeutic molecules from fibrin, such as bi-domain peptides or recombinant growth factor fusion proteins, has led to the emergence of sophisticated fibrin-based therapeutic delivery systems. These approaches involve combined cell and growth factor or dual/sequential growth factor release and have been proven efficient to promote wound healing *in vivo*. More recently, fibrin-based gene delivery (viral or non viral) has been introduced, with the outcome that gene vectors delivered in fibrin give more consistent results than naked plasmid injections. Although the safety of this strategy will further need to be carefully evaluated, gene delivery holds great potential to replace growth factor delivery in the future. The main advantage of fibrin-based delivery is the possibility to covalently functionalize fibrin with growth factors or DNA under very mild conditions during polymerization, which preserves the stability of the incorporated

biomolecules. Moreover, fibrin provides a clinically approved delivery platform that can be injected into the site of injury by minimally invasive means. Owing to its intrinsic biological and structural features and the availability of tunable delivery methodology, one can expect the continuing widespread clinical use of fibrin in wound care management. However, future challenges will lie in finding controllable ways to spatiotemporally deliver the specific and appropriate therapeutic stimuli *in situ* to mimic the natural wound healing response.

6. REFERENCES

1. Weinstein, S.L., *2000-2010: the bone and joint decade.* J Bone Joint Surg Am, 2000. **82**(1): p. 1-3.
2. Woolf, A.D., *The bone and joint decade 2000-2010.* Ann Rheum Dis, 2000. **59**(2): p. 81-2.
3. *The burden of musculoskeletal conditions at the start of the new millennium.* World Health Organ Tech Rep Ser, 2003. **919**: p. i-x, 1-218, back cover.
4. Woolf, A.D., T. Vos, and L. March, *How to measure the impact of musculoskeletal conditions.* Best Pract Res Clin Rheumatol, 2010. **24**(6): p. 723-32.
5. United States Bone and Joint Initiative: The Burden of Musculoskeletal Diseases in the United States (BMUS), T.E., 2014. Rosemont, IL. Available at http://www.boneandjointburden.org. Accessed on Feb 8th 2018. ISBN: 978-0-9963091-0-3.
6. Bevan, S., *Economic impact of musculoskeletal disorders (MSDs) on work in Europe.* Best Pract Res Clin Rheumatol, 2015. **29**(3): p. 356-73.
7. Roberts, S.J., et al., *Clinical applications of musculoskeletal tissue engineering.* Br Med Bull, 2008. **86**: p. 7-22.
8. Langer, R. and J.P. Vacanti, *Tissue engineering.* Science, 1993. **260**(5110): p. 920-6.
9. Smith, B.D. and D.A. Grande, *The current state of scaffolds for musculoskeletal regenerative applications.* Nat Rev Rheumatol, 2015. **11**(4): p. 213-22.
10. Akpancar, S., et al., *The Current Perspectives of Stem Cell Therapy in Orthopedic Surgery.* Arch Trauma Res, 2016. **5**(4): p. e37976.
11. Noth, U., et al., *Cell delivery therapeutics for musculoskeletal regeneration.* Adv Drug Deliv Rev, 2010. **62**(7-8): p. 765-83.
12. Tuan, R.S., *Regenerative medicine in 2012: the coming of age of musculoskeletal tissue engineering.* Nat Rev Rheumatol, 2013. **9**(2): p. 74-6.
13. Stevanovic, M. and F. Sharpe, *Functional free muscle transfer for upper extremity reconstruction.* Plast Reconstr Surg, 2014. **134**(2): p. 257e-274e.
14. Cittadella Vigodarzere, G. and S. Mantero, *Skeletal muscle tissue engineering: strategies for volumetric constructs.* Front Physiol, 2014. **5**: p. 362.
15. Ostrovidov, S., et al., *Skeletal muscle tissue engineering: methods to form skeletal myotubes and their applications.* Tissue Eng Part B Rev, 2014. **20**(5): p. 403-36.
16. Qazi, T.H., et al., *Biomaterials based strategies for skeletal muscle tissue engineering: existing technologies and future trends.* Biomaterials, 2015. **53**: p. 502-21.
17. Rouwkema, J., et al., *In vitro platforms for tissue engineering: implications for basic research and clinical translation.* J Tissue Eng Regen Med, 2011. **5**(8): p. e164-7.
18. Janssen, I., et al., *Skeletal muscle mass and distribution in 468 men and women aged 18-88 yr.* J Appl Physiol (1985), 2000. **89**(1): p. 81-8.
19. Frontera, W.R. and J. Ochala, *Skeletal muscle: a brief review of structure and function.* Calcif Tissue Int, 2015. **96**(3): p. 183-95.
20. Tuomilehto, J., et al., *Prevention of type 2 diabetes mellitus by changes in lifestyle among subjects with impaired glucose tolerance.* N Engl J Med, 2001. **344**(18): p. 1343-50.
21. Nocon, M., et al., *Association of physical activity with all-cause and cardiovascular mortality: a systematic review and meta-analysis.* Eur J Cardiovasc Prev Rehabil, 2008. **15**(3): p. 239-46.
22. Monninkhof, E.M., et al., *Physical activity and breast cancer: a systematic review.* Epidemiology, 2007. **18**(1): p. 137-57.
23. Wolin, K.Y., et al., *Physical activity and colon cancer prevention: a meta-analysis.* Br J Cancer, 2009. **100**(4): p. 611-6.
24. Rovio, S., et al., *Leisure-time physical activity at midlife and the risk of dementia and Alzheimer's disease.* Lancet Neurol, 2005. **4**(11): p. 705-11.
25. Paffenbarger, R.S., Jr., I.M. Lee, and R. Leung, *Physical activity and personal characteristics associated with depression and suicide in American college men.* Acta Psychiatr Scand Suppl, 1994. **377**: p. 16-22.
26. Wolfe, R.R., *The underappreciated role of muscle in health and disease.* Am J Clin Nutr, 2006. **84**(3): p. 475-82.
27. Pedersen, B.K., *Muscles and their myokines.* J Exp Biol, 2011. **214**(Pt 2): p. 337-46.
28. Pedersen, B.K. and M.A. Febbraio, *Muscle as an endocrine organ: focus on muscle-derived interleukin-6.* Physiol Rev, 2008. **88**(4): p. 1379-406.
29. Mintz, B. and W.W. Baker, *Normal mammalian muscle differentiation and gene control of isocitrate dehydrogenase synthesis.* Proc Natl Acad Sci U S A, 1967. **58**(2): p. 592-8.
30. Greising, S.M., et al., *Systems biology of skeletal muscle: fiber type as an organizing principle.* Wiley Interdiscip Rev Syst Biol Med, 2012. **4**(5): p. 457-73.
31. Relaix, F. and P.S. Zammit, *Satellite cells are essential for skeletal muscle regeneration: the cell on the edge returns centre stage.* Development, 2012. **139**(16): p. 2845-56.
32. Huxley, A.F. and R. Niedergerke, *Measurement of muscle striations in stretch and contraction.* J Physiol, 1954. **124**(2): p. 46-7P.
33. Huxley, H. and J. Hanson, *Changes in the cross-striations of muscle during contraction and stretch and their structural interpretation.* Nature, 1954. **173**(4412): p. 973-6.
34. Bottinelli, R. and C. Reggiani, *Human skeletal muscle fibres: molecular and functional diversity.* Prog Biophys Mol Biol, 2000. **73**(2-4): p. 195-262.
35. Monroy, J.A., et al., *What is the role of titin in active muscle?* Exerc Sport Sci Rev, 2012. **40**(2): p. 73-8.

36. Ottenheijm, C.A. and H. Granzier, *Lifting the nebula: novel insights into skeletal muscle contractility.* Physiology (Bethesda), 2010. **25**(5): p. 304-10.

37. Gillies, A.R. and R.L. Lieber, *Structure and function of the skeletal muscle extracellular matrix.* Muscle Nerve, 2011. **44**(3): p. 318-31.

38. Jayasinghe, I.D. and B.S. Launikonis, *Three-dimensional reconstruction and analysis of the tubular system of vertebrate skeletal muscle.* J Cell Sci, 2013. **126**(Pt 17): p. 4048-58.

39. Kerr, J.P., C.W. Ward, and R.J. Bloch, *Dysferlin at transverse tubules regulates Ca(2+) homeostasis in skeletal muscle.* Front Physiol, 2014. **5**: p. 89.

40. Lek, A., et al., *Ferlins: regulators of vesicle fusion for auditory neurotransmission, receptor trafficking and membrane repair.* Traffic, 2012. **13**(2): p. 185-94.

41. Lamboley, C.R., et al., *Sarcoplasmic reticulum Ca2+ uptake and leak properties, and SERCA isoform expression, in type I and type II fibres of human skeletal muscle.* J Physiol, 2014. **592**(6): p. 1381-95.

42. Dahl, R., et al., *Three-dimensional reconstruction of the human skeletal muscle mitochondrial network as a tool to assess mitochondrial content and structural organization.* Acta Physiol (Oxf), 2015. **213**(1): p. 145-55.

43. Ogata, T. and Y. Yamasaki, *Ultra-high-resolution scanning electron microscopy of mitochondria and sarcoplasmic reticulum arrangement in human red, white, and intermediate muscle fibers.* Anat Rec, 1997. **248**(2): p. 214-23.

44. Sandow, A., *Excitation-contraction coupling in muscular response.* Yale J Biol Med, 1952. **25**(3): p. 176-201.

45. Rebbeck, R.T., et al., *Skeletal muscle excitation-contraction coupling: who are the dancing partners?* Int J Biochem Cell Biol, 2014. **48**: p. 28-38.

46. Lehman, W., et al., *Troponin organization on relaxed and activated thin filaments revealed by electron microscopy and three-dimensional reconstruction.* J Mol Biol, 2001. **307**(3): p. 739-44.

47. Zierath, J.R. and J.A. Hawley, *Skeletal muscle fiber type: influence on contractile and metabolic properties.* PLoS Biol, 2004. **2**(10): p. e348.

48. Schiaffino, S. and C. Reggiani, *Molecular diversity of myofibrillar proteins: gene regulation and functional significance.* Physiol Rev, 1996. **76**(2): p. 371-423.

49. Schiaffino, S. and C. Reggiani, *Fiber types in mammalian skeletal muscles.* Physiol Rev, 2011. **91**(4): p. 1447-531.

50. Galpin, A.J., et al., *Human skeletal muscle fiber type specific protein content.* Anal Biochem, 2012. **425**(2): p. 175-82.

51. Billeter, R., et al., *Analysis of myosin light and heavy chain types in single human skeletal muscle fibers.* Eur J Biochem, 1981. **116**(2): p. 389-95.

52. Smerdu, V., et al., *Type IIx myosin heavy chain transcripts are expressed in type IIb fibers of human skeletal muscle.* Am J Physiol, 1994. **267**(6 Pt 1): p. C1723-8.

53. Gallagher, P., et al., *Effects of 84-days of bedrest and resistance training on single muscle fibre myosin heavy chain distribution in human vastus lateralis and soleus muscles.* Acta Physiol Scand, 2005. **185**(1): p. 61-9.

54. Klitgaard, H., et al., *Ageing alters the myosin heavy chain composition of single fibres from human skeletal muscle.* Acta Physiol Scand, 1990. **140**(1): p. 55-62.

55. Trappe, S., et al., *Exercise in space: human skeletal muscle after 6 months aboard the International Space Station.* J Appl Physiol (1985), 2009. **106**(4): p. 1159-68.

56. Trappe, S., et al., *Single muscle fiber adaptations with marathon training.* J Appl Physiol (1985), 2006. **101**(3): p. 721-7.

57. Gayraud-Morel, B., F. Chretien, and S. Tajbakhsh, *Skeletal muscle as a paradigm for regenerative biology and medicine.* Regen Med, 2009. **4**(2): p. 293-319.

58. Tajbakhsh, S., *Skeletal muscle stem cells in developmental versus regenerative myogenesis.* J Intern Med, 2009. **266**(4): p. 372-89.

59. Gros, J., et al., *A common somitic origin for embryonic muscle progenitors and satellite cells.* Nature, 2005. **435**(7044): p. 954-8.

60. Bentzinger, C.F., Y.X. Wang, and M.A. Rudnicki, *Building muscle: molecular regulation of myogenesis.* Cold Spring Harb Perspect Biol, 2012. **4**(2).

61. Buckingham, M., et al., *The formation of skeletal muscle: from somite to limb.* J Anat, 2003. **202**(1): p. 59-68.

62. Charge, S.B. and M.A. Rudnicki, *Cellular and molecular regulation of muscle regeneration.* Physiol Rev, 2004. **84**(1): p. 209-38.

63. Pownall, M.E., M.K. Gustafsson, and C.P. Emerson, Jr., *Myogenic regulatory factors and the specification of muscle progenitors in vertebrate embryos.* Annu Rev Cell Dev Biol, 2002. **18**: p. 747-83.

64. Arnold, S.J. and E.J. Robertson, *Making a commitment: cell lineage allocation and axis patterning in the early mouse embryo.* Nat Rev Mol Cell Biol, 2009. **10**(2): p. 91-103.

65. Aulehla, A. and O. Pourquie, *On periodicity and directionality of somitogenesis.* Anat Embryol (Berl), 2006. **211 Suppl 1**: p. 3-8.

66. Cinnamon, Y., et al., *The sub-lip domain--a distinct pathway for myotome precursors that demonstrate rostral-caudal migration.* Development, 2001. **128**(3): p. 341-51.

67. Cinnamon, Y., N. Kahane, and C. Kalcheim, *Characterization of the early development of specific hypaxial muscles from the ventrolateral myotome.* Development, 1999. **126**(19): p. 4305-15.

68. Vasyutina, E. and C. Birchmeier, *The development of migrating muscle precursor cells.* Anat Embryol (Berl), 2006. **211 Suppl 1**: p. 37-41.

69. Weintraub, H., et al., *The myoD gene family: nodal point during specification of the muscle cell lineage.* Science, 1991. **251**(4995): p. 761-6.

70. Kassar-Duchossoy, L., et al., *Pax3/Pax7 mark a novel population of primitive myogenic cells during development.* Genes Dev, 2005. **19**(12): p. 1426-31.

71. Bober, E., et al., *Pax-3 is required for the development of limb muscles: a possible role for the migration of dermomyotomal muscle progenitor cells.* Development, 1994. **120**(3): p. 603-12.

72. Tajbakhsh, S., et al., *Redefining the genetic hierarchies controlling skeletal myogenesis: Pax-3 and Myf-5 act upstream of MyoD.* Cell, 1997. **89**(1): p. 127-38.

73. Hutcheson, D.A., et al., *Embryonic and fetal limb myogenic cells are derived from developmentally distinct progenitors and have different requirements for beta-catenin.* Genes Dev, 2009. **23**(8): p. 997-1013.

74. Seale, P., et al., *Pax7 is required for the specification of myogenic satellite cells.* Cell, 2000. **102**(6): p. 777-86.

75. Maqbool, T. and K. Jagla, *Genetic control of muscle development: learning from Drosophila.* J Muscle Res Cell Motil, 2007. **28**(7-8): p. 397-407.

76. Grifone, R., et al., *Six1 and Six4 homeoproteins are required for Pax3 and Mrf expression during myogenesis in the mouse embryo.* Development, 2005. **132**(9): p. 2235-49.

77. Grifone, R., et al., *Eya1 and Eya2 proteins are required for hypaxial somitic myogenesis in the mouse embryo.* Dev Biol, 2007. **302**(2): p. 602-16.

78. Buckingham, M., et al., *Expression of muscle genes in the mouse embryo.* Symp Soc Exp Biol, 1992. **46**: p. 203-17.

79. Ott, M.O., et al., *Early expression of the myogenic regulatory gene, myf-5, in precursor cells of skeletal muscle in the mouse embryo.* Development, 1991. **111**(4): p. 1097-107.

80. Parr, B.A., et al., *Mouse Wnt genes exhibit discrete domains of expression in the early embryonic CNS and limb buds.* Development, 1993. **119**(1): p. 247-61.

81. Ikeya, M. and S. Takada, *Wnt signaling from the dorsal neural tube is required for the formation of the medial dermomyotome.* Development, 1998. **125**(24): p. 4969-76.

82. Tajbakhsh, S., et al., *Differential activation of Myf5 and MyoD by different Wnts in explants of mouse paraxial mesoderm and the later activation of myogenesis in the absence of Myf5.* Development, 1998. **125**(21): p. 4155-62.

83. Lum, L. and P.A. Beachy, *The Hedgehog response network: sensors, switches, and routers.* Science, 2004. **304**(5678): p. 1755-9.

84. Chiang, C., et al., *Cyclopia and defective axial patterning in mice lacking Sonic hedgehog gene function.* Nature, 1996. **383**(6599): p. 407-13.

85. Zhang, X.M., M. Ramalho-Santos, and A.P. McMahon, *Smoothened mutants reveal redundant roles for Shh and Ihh signaling including regulation of L/R symmetry by the mouse node.* Cell, 2001. **106**(2): p. 781-92.

86. Borycki, A.G., L. Mendham, and C.P. Emerson, Jr., *Control of somite patterning by Sonic hedgehog and its downstream signal response genes.* Development, 1998. **125**(4): p. 777-90.

87. Johnson, R.L., et al., *Ectopic expression of Sonic hedgehog alters dorsal-ventral patterning of somites.* Cell, 1994. **79**(7): p. 1165-73.

88. Pourquie, O., et al., *Control of somite patterning by signals from the lateral plate.* Proc Natl Acad Sci U S A, 1995. **92**(8): p. 3219-23.

89. Hirsinger, E., et al., *Noggin acts downstream of Wnt and Sonic Hedgehog to antagonize BMP4 in avian somite patterning.* Development, 1997. **124**(22): p. 4605-14.

90. Marcelle, C., M.R. Stark, and M. Bronner-Fraser, *Coordinate actions of BMPs, Wnts, Shh and noggin mediate patterning of the dorsal somite.* Development, 1997. **124**(20): p. 3955-63.

91. Sambasivan, R. and S. Tajbakhsh, *Skeletal muscle stem cell birth and properties.* Semin Cell Dev Biol, 2007. **18**(6): p. 870-82.

92. Tajbakhsh, S. and M.E. Buckingham, *Mouse limb muscle is determined in the absence of the earliest myogenic factor myf-5.* Proc Natl Acad Sci U S A, 1994. **91**(2): p. 747-51.

93. Dietrich, S., et al., *The role of SF/HGF and c-Met in the development of skeletal muscle.* Development, 1999. **126**(8): p. 1621-9.

94. Bladt, F., et al., *Essential role for the c-met receptor in the migration of myogenic precursor cells into the limb bud.* Nature, 1995. **376**(6543): p. 768-71.

95. Schmidt, C., et al., *Scatter factor/hepatocyte growth factor is essential for liver development.* Nature, 1995. **373**(6516): p. 699-702.

96. Schafer, K. and T. Braun, *Early specification of limb muscle precursor cells by the homeobox gene Lbx1h.* Nat Genet, 1999. **23**(2): p. 213-6.

97. Houzelstein, D., et al., *The homeobox gene Msx1 is expressed in a subset of somites, and in muscle progenitor cells migrating into the forelimb.* Development, 1999. **126**(12): p. 2689-701.

98. Odelberg, S.J., A. Kollhoff, and M.T. Keating, *Dedifferentiation of mammalian myotubes induced by msx1.* Cell, 2000. **103**(7): p. 1099-109.

99. Edom-Vovard, F., M.A. Bonnin, and D. Duprez, *Misexpression of Fgf-4 in the chick limb inhibits myogenesis by down-regulating Frek expression.* Dev Biol, 2001. **233**(1): p. 56-71.

100. Webb, S.E., et al., *Fibroblast growth factors 2 and 4 stimulate migration of mouse embryonic limb myogenic cells.* Dev Dyn, 1997. **209**(2): p. 206-16.

101. Marics, I., et al., *FGFR4 signaling is a necessary step in limb muscle differentiation.* Development, 2002. **129**(19): p. 4559-69.

102. Potthoff, M.J. and E.N. Olson, *MEF2: a central regulator of diverse developmental programs.* Development, 2007. **134**(23): p. 4131-40.

103. Molkentin, J.D., et al., *Cooperative activation of muscle gene expression by MEF2 and myogenic bHLH proteins.* Cell, 1995. **83**(7): p. 1125-36.

104. Menko, A.S. and D. Boettiger, *Occupation of the extracellular matrix receptor, integrin, is a control point for myogenic differentiation.* Cell, 1987. **51**(1): p. 51-7.

105. Knudsen, K.A., S.A. McElwee, and L. Myers, *A role for the neural cell adhesion molecule, NCAM, in myoblast interaction during myogenesis.* Dev Biol, 1990. **138**(1): p. 159-68.

106. Mege, R.M., et al., *N-cadherin and N-CAM in myoblast fusion: compared localisation and effect of blockade by peptides and antibodies.* J Cell Sci, 1992. **103 (Pt 4)**: p. 897-906.

107. Doberstein, S.K., et al., *Genetic analysis of myoblast fusion: blown fuse is required for progression beyond the prefusion complex.* J Cell Biol, 1997. **136**(6): p. 1249-61.
108. Wakelam, M.J., *The fusion of myoblasts.* Biochem J, 1985. **228**(1): p. 1-12.
109. Ontell, M. and K. Kozeka, *The organogenesis of murine striated muscle: a cytoarchitectural study.* Am J Anat, 1984. **171**(2): p. 133-48.
110. Mauro, A., *Satellite cell of skeletal muscle fibers.* J Biophys Biochem Cytol, 1961. **9**: p. 493-5.
111. Katz, B., *The terminations of the afferent nerve fibre in the muscle spindle of the frog.* Trans Royal Soc Lond [Biol], 1961. **243**: p. 221-240.
112. Buckingham, M. and D. Montarras, *Skeletal muscle stem cells.* Curr Opin Genet Dev, 2008. **18**(4): p. 330-6.
113. Ten Broek, R.W., S. Grefte, and J.W. Von den Hoff, *Regulatory factors and cell populations involved in skeletal muscle regeneration.* J Cell Physiol, 2010. **224**(1): p. 7-16.
114. Yablonka-Reuveni, Z., *The skeletal muscle satellite cell: still young and fascinating at 50.* J Histochem Cytochem, 2011. **59**(12): p. 1041-59.
115. Zammit, P. and J. Beauchamp, *The skeletal muscle satellite cell: stem cell or son of stem cell?* Differentiation, 2001. **68**(4-5): p. 193-204.
116. Zammit, P.S., *All muscle satellite cells are equal, but are some more equal than others?* J Cell Sci, 2008. **121**(Pt 18): p. 2975-82.
117. Ciciliot, S. and S. Schiaffino, *Regeneration of mammalian skeletal muscle. Basic mechanisms and clinical implications.* Curr Pharm Des, 2010. **16**(8): p. 906-14.
118. Whalen, R.G., et al., *Expression of myosin isoforms during notexin-induced regeneration of rat soleus muscles.* Dev Biol, 1990. **141**(1): p. 24-40.
119. Zammit, P.S., et al., *Muscle satellite cells adopt divergent fates: a mechanism for self-renewal?* J Cell Biol, 2004. **166**(3): p. 347-57.
120. Zammit, P.S., et al., *Pax7 and myogenic progression in skeletal muscle satellite cells.* J Cell Sci, 2006. **119**(Pt 9): p. 1824-32.
121. Relaix, F., et al., *Pax3 and Pax7 have distinct and overlapping functions in adult muscle progenitor cells.* J Cell Biol, 2006. **172**(1): p. 91-102.
122. Beauchamp, J.R., et al., *Expression of CD34 and Myf5 defines the majority of quiescent adult skeletal muscle satellite cells.* J Cell Biol, 2000. **151**(6): p. 1221-34.
123. Wang, Y.X. and M.A. Rudnicki, *Satellite cells, the engines of muscle repair.* Nat Rev Mol Cell Biol, 2011. **13**(2): p. 127-33.
124. Tedesco, F.S., et al., *Repairing skeletal muscle: regenerative potential of skeletal muscle stem cells.* J Clin Invest, 2010. **120**(1): p. 11-9.
125. Kuang, S., et al., *Asymmetric self-renewal and commitment of satellite stem cells in muscle.* Cell, 2007. **129**(5): p. 999-1010.
126. Conboy, I.M. and T.A. Rando, *The regulation of Notch signaling controls satellite cell activation and cell fate determination in postnatal myogenesis.* Dev Cell, 2002. **3**(3): p. 397-409.
127. Le Grand, F., et al., *Wnt7a activates the planar cell polarity pathway to drive the symmetric expansion of satellite stem cells.* Cell Stem Cell, 2009. **4**(6): p. 535-47.
128. Shi, X. and D.J. Garry, *Muscle stem cells in development, regeneration, and disease.* Genes Dev, 2006. **20**(13): p. 1692-708.
129. Cheng, M., et al., *Endogenous interferon-gamma is required for efficient skeletal muscle regeneration.* Am J Physiol Cell Physiol, 2008. **294**(5): p. C1183-91.
130. Stratos, I., et al., *Granulocyte-colony stimulating factor enhances muscle proliferation and strength following skeletal muscle injury in rats.* J Appl Physiol (1985), 2007. **103**(5): p. 1857-63.
131. Gordon, K.J. and G.C. Blobe, *Role of transforming growth factor-beta superfamily signaling pathways in human disease.* Biochim Biophys Acta, 2008. **1782**(4): p. 197-228.
132. Kollias, H.D. and J.C. McDermott, *Transforming growth factor-beta and myostatin signaling in skeletal muscle.* J Appl Physiol (1985), 2008. **104**(3): p. 579-87.
133. Christov, C., et al., *Muscle satellite cells and endothelial cells: close neighbors and privileged partners.* Mol Biol Cell, 2007. **18**(4): p. 1397-409.
134. Boppart, M.D., D.J. Burkin, and S.J. Kaufman, *Alpha7beta1-integrin regulates mechanotransduction and prevents skeletal muscle injury.* Am J Physiol Cell Physiol, 2006. **290**(6): p. C1660-5.
135. Boonen, K.J. and M.J. Post, *The muscle stem cell niche: regulation of satellite cells during regeneration.* Tissue Eng Part B Rev, 2008. **14**(4): p. 419-31.
136. Timpl, R., *Proteoglycans of basement membranes.* EXS, 1994. **70**: p. 123-44.
137. Kresse, H. and E. Schonherr, *Proteoglycans of the extracellular matrix and growth control.* J Cell Physiol, 2001. **189**(3): p. 266-74.
138. Miura, T., et al., *Decorin binds myostatin and modulates its activity to muscle cells.* Biochem Biophys Res Commun, 2006. **340**(2): p. 675-80.
139. Cornelison, D.D., et al., *Syndecan-3 and syndecan-4 specifically mark skeletal muscle satellite cells and are implicated in satellite cell maintenance and muscle regeneration.* Dev Biol, 2001. **239**(1): p. 79-94.
140. Guerin, C.W. and P.C. Holland, *Synthesis and secretion of matrix-degrading metalloproteases by human skeletal muscle satellite cells.* Dev Dyn, 1995. **202**(1): p. 91-9.
141. Torrente, Y., et al., *Intramuscular migration of myoblasts transplanted after muscle pretreatment with metalloproteinases.* Cell Transplant, 2000. **9**(4): p. 539-49.
142. Miyagoe, Y., et al., *Laminin alpha2 chain-null mutant mice by targeted disruption of the Lama2 gene: a new model of merosin (laminin 2)-deficient congenital muscular dystrophy.* FEBS Lett, 1997. **415**(1): p. 33-9.

143. Girgenrath, M., C.A. Kostek, and J.B. Miller, *Diseased muscles that lack dystrophin or laminin-alpha2 have altered compositions and proliferation of mononuclear cell populations.* BMC Neurol, 2005. **5**(1): p. 7.

144. Turner, N.J. and S.F. Badylak, *Regeneration of skeletal muscle.* Cell Tissue Res, 2012. **347**(3): p. 759-74.

145. Belcastro, A.N., L.D. Shewchuk, and D.A. Raj, *Exercise-induced muscle injury: a calpain hypothesis.* Mol Cell Biochem, 1998. **179**(1-2): p. 135-45.

146. Fielding, R.A., et al., *Acute phase response in exercise. III. Neutrophil and IL-1 beta accumulation in skeletal muscle.* Am J Physiol, 1993. **265**(1 Pt 2): p. R166-72.

147. Tidball, J.G. and S.A. Villalta, *Regulatory interactions between muscle and the immune system during muscle regeneration.* Am J Physiol Regul Integr Comp Physiol, 2010. **298**(5): p. R1173-87.

148. Chazaud, B., et al., *Dual and beneficial roles of macrophages during skeletal muscle regeneration.* Exerc Sport Sci Rev, 2009. **37**(1): p. 18-22.

149. Cantini, M., et al., *Macrophage-secreted myogenic factors: a promising tool for greatly enhancing the proliferative capacity of myoblasts in vitro and in vivo.* Neurol Sci, 2002. **23**(4): p. 189-94.

150. Nagata, Y., et al., *Entry of muscle satellite cells into the cell cycle requires sphingolipid signaling.* J Cell Biol, 2006. **174**(2): p. 245-53.

151. Tatsumi, R., et al., *Satellite cell activation in stretched skeletal muscle and the role of nitric oxide and hepatocyte growth factor.* Am J Physiol Cell Physiol, 2006. **290**(6): p. C1487-94.

152. Brack, A.S., et al., *A temporal switch from notch to Wnt signaling in muscle stem cells is necessary for normal adult myogenesis.* Cell Stem Cell, 2008. **2**(1): p. 50-9.

153. Conboy, I.M., et al., *Notch-mediated restoration of regenerative potential to aged muscle.* Science, 2003. **302**(5650): p. 1575-7.

154. Grubb, B.D., J.B. Harris, and I.S. Schofield, *Neuromuscular transmission at newly formed neuromuscular junctions in the regenerating soleus muscle of the rat.* J Physiol, 1991. **441**: p. 405-21.

155. Jirmanova, I. and S. Thesleff, *Ultrastructural study of experimental muscle degeneration and regeneration in the adult rat.* Z Zellforsch Mikrosk Anat, 1972. **131**(1): p. 77-97.

156. Jerkovic, R., et al., *Early myosin switching induced by nerve activity in regenerating slow skeletal muscle.* Cell Struct Funct, 1997. **22**(1): p. 147-53.

157. Kalhovde, J.M., et al., *"Fast" and "slow" muscle fibres in hindlimb muscles of adult rats regenerate from intrinsically different satellite cells.* J Physiol, 2005. **562**(Pt 3): p. 847-57.

158. Ferrari, G., et al., *Muscle regeneration by bone marrow-derived myogenic progenitors.* Science, 1998. **279**(5356): p. 1528-30.

159. Torrente, Y., et al., *Human circulating AC133(+) stem cells restore dystrophin expression and ameliorate function in dystrophic skeletal muscle.* J Clin Invest, 2004. **114**(2): p. 182-95.

160. Benchaouir, R., et al., *Restoration of human dystrophin following transplantation of exon-skipping-engineered DMD patient stem cells into dystrophic mice.* Cell Stem Cell, 2007. **1**(6): p. 646-57.

161. Asakura, A., et al., *Myogenic specification of side population cells in skeletal muscle.* J Cell Biol, 2002. **159**(1): p. 123-34.

162. Gussoni, E., et al., *Dystrophin expression in the mdx mouse restored by stem cell transplantation.* Nature, 1999. **401**(6751): p. 390-4.

163. Qu-Petersen, Z., et al., *Identification of a novel population of muscle stem cells in mice: potential for muscle regeneration.* J Cell Biol, 2002. **157**(5): p. 851-64.

164. Minasi, M.G., et al., *The meso-angioblast: a multipotent, self-renewing cell that originates from the dorsal aorta and differentiates into most mesodermal tissues.* Development, 2002. **129**(11): p. 2773-83.

165. Dellavalle, A., et al., *Pericytes of human skeletal muscle are myogenic precursors distinct from satellite cells.* Nat Cell Biol, 2007. **9**(3): p. 255-67.

166. Sampaolesi, M., et al., *Mesoangioblast stem cells ameliorate muscle function in dystrophic dogs.* Nature, 2006. **444**(7119): p. 574-9.

167. Sampaolesi, M., et al., *Cell therapy of alpha-sarcoglycan null dystrophic mice through intra-arterial delivery of mesoangioblasts.* Science, 2003. **301**(5632): p. 487-92.

168. Zheng, B., et al., *Prospective identification of myogenic endothelial cells in human skeletal muscle.* Nat Biotechnol, 2007. **25**(9): p. 1025-34.

169. Goudenege, S., et al., *Enhancement of myogenic and muscle repair capacities of human adipose-derived stem cells with forced expression of MyoD.* Mol Ther, 2009. **17**(6): p. 1064-72.

170. Gang, E.J., et al., *Engraftment of mesenchymal stem cells into dystrophin-deficient mice is not accompanied by functional recovery.* Exp Cell Res, 2009. **315**(15): p. 2624-36.

171. Wakao, S., et al., *Muse cells, newly found non-tumorigenic pluripotent stem cells, reside in human mesenchymal tissues.* Pathol Int, 2014. **64**(1): p. 1-9.

172. Kuroda, Y., et al., *Unique multipotent cells in adult human mesenchymal cell populations.* Proc Natl Acad Sci U S A, 2010. **107**(19): p. 8639-43.

173. Lepper, C., T.A. Partridge, and C.M. Fan, *An absolute requirement for Pax7-positive satellite cells in acute injury-induced skeletal muscle regeneration.* Development, 2011. **138**(17): p. 3639-46.

174. Canale, S.T., et al., *A chronicle of injuries of an American intercollegiate football team.* Am J Sports Med, 1981. **9**(6): p. 384-9.

175. Garrett, W.E., Jr., *Muscle strain injuries: clinical and basic aspects.* Med Sci Sports Exerc, 1990. **22**(4): p. 436-43.

176. Lehto, M.U. and M.J. Jarvinen, *Muscle injuries, their healing process and treatment.* Ann Chir Gynaecol, 1991. **80**(2): p. 102-8.

177. Carlson, B.M. and E. Gutmann, *Development of contractile properties of minced muscle regenerates in the rat.* Exp Neurol, 1972. **36**(2): p. 239-49.

178. Aarimaa, V., et al., *Restoration of myofiber continuity after transection injury in the rat soleus.* Neuromuscul Disord, 2004. **14**(7): p. 421-8.

179. Garrett, W.E., Jr., et al., *Recovery of skeletal muscle after laceration and repair.* J Hand Surg Am, 1984. **9**(5): p. 683-92.

180. Menetrey, J., et al., *Suturing versus immobilization of a muscle laceration. A morphological and functional study in a mouse model.* Am J Sports Med, 1999. **27**(2): p. 222-9.

181. Garg, K., et al., *Volumetric muscle loss: persistent functional deficits beyond frank loss of tissue.* J Orthop Res, 2015. **33**(1): p. 40-6.

182. Grogan, B.F. and J.R. Hsu, *Volumetric muscle loss.* J Am Acad Orthop Surg, 2011. **19 Suppl 1**: p. S35-7.

183. Lin, C.H., et al., *Free functioning muscle transfer for lower extremity posttraumatic composite structure and functional defect.* Plast Reconstr Surg, 2007. **119**(7): p. 2118-26.

184. Tu, Y.K., et al., *Soft-tissue injury management and flap reconstruction for mangled lower extremities.* Injury, 2008. **39 Suppl 4**: p. 75-95.

185. Schmalbruch, H., *The morphology of regeneration of skeletal muscles in the rat.* Tissue Cell, 1976. **8**(4): p. 673-92.

186. Rosenberg, I.H., *Sarcopenia: origins and clinical relevance.* J Nutr, 1997. **127**(5 Suppl): p. 990S-991S.

187. McLean, R.R. and D.P. Kiel, *Developing consensus criteria for sarcopenia: an update.* J Bone Miner Res, 2015. **30**(4): p. 588-92.

188. Chodzko-Zajko, W.J., et al., *American College of Sports Medicine position stand. Exercise and physical activity for older adults.* Med Sci Sports Exerc, 2009. **41**(7): p. 1510-30.

189. Cosman, F., et al., *Clinician's Guide to Prevention and Treatment of Osteoporosis.* Osteoporos Int, 2014. **25**(10): p. 2359-81.

190. Papa, E.V., X. Dong, and M. Hassan, *Skeletal Muscle Function Deficits in the Elderly: Current Perspectives on Resistance Training.* J Nat Sci, 2017. **3**(1).

191. Blau, H.M., B.D. Cosgrove, and A.T. Ho, *The central role of muscle stem cells in regenerative failure with aging.* Nat Med, 2015. **21**(8): p. 854-62.

192. Hepple, R.T. and C.L. Rice, *Innervation and neuromuscular control in ageing skeletal muscle.* J Physiol, 2016. **594**(8): p. 1965-78.

193. Brack, A.S., et al., *Increased Wnt signaling during aging alters muscle stem cell fate and increases fibrosis.* Science, 2007. **317**(5839): p. 807-10.

194. Egerman, M.A., et al., *GDF11 Increases with Age and Inhibits Skeletal Muscle Regeneration.* Cell Metab, 2015. **22**(1): p. 164-74.

195. Sinha, M., et al., *Restoring systemic GDF11 levels reverses age-related dysfunction in mouse skeletal muscle.* Science, 2014. **344**(6184): p. 649-52.

196. Morley, J.E., *Hormones and Sarcopenia.* Curr Pharm Des, 2017. **23**(30): p. 4484-4492.

197. Budui, S.L., A.P. Rossi, and M. Zamboni, *The pathogenetic bases of sarcopenia.* Clin Cases Miner Bone Metab, 2015. **12**(1): p. 22-6.

198. Carlson, B.M., et al., *Skeletal muscle regeneration in very old rats.* J Gerontol A Biol Sci Med Sci, 2001. **56**(5): p. B224-33.

199. Carlson, B.M. and J.A. Faulkner, *Muscle transplantation between young and old rats: age of host determines recovery.* Am J Physiol, 1989. **256**(6 Pt 1): p. C1262-6.

200. Carlson, B.M. and J.A. Faulkner, *Muscle regeneration in young and old rats: effects of motor nerve transection with and without marcaine treatment.* J Gerontol A Biol Sci Med Sci, 1998. **53**(1): p. B52-7.

201. Cederna, P.S., et al., *Motor unit properties of nerve-intact extensor digitorum longus muscle grafts in young and old rats.* J Gerontol A Biol Sci Med Sci, 2001. **56**(6): p. B254-8.

202. Conboy, I.M., et al., *Rejuvenation of aged progenitor cells by exposure to a young systemic environment.* Nature, 2005. **433**(7027): p. 760-4.

203. Bernet, J.D., et al., *p38 MAPK signaling underlies a cell-autonomous loss of stem cell self-renewal in skeletal muscle of aged mice.* Nat Med, 2014. **20**(3): p. 265-71.

204. Cosgrove, B.D., et al., *Rejuvenation of the muscle stem cell population restores strength to injured aged muscles.* Nat Med, 2014. **20**(3): p. 255-64.

205. Price, F.D., et al., *Inhibition of JAK-STAT signaling stimulates adult satellite cell function.* Nat Med, 2014. **20**(10): p. 1174-81.

206. Tierney, M.T., et al., *STAT3 signaling controls satellite cell expansion and skeletal muscle repair.* Nat Med, 2014. **20**(10): p. 1182-6.

207. Palacios, D., et al., *TNF/p38alpha/polycomb signaling to Pax7 locus in satellite cells links inflammation to the epigenetic control of muscle regeneration.* Cell Stem Cell, 2010. **7**(4): p. 455-69.

208. Gao, Y., et al., *Age-related changes in the mechanical properties of the epimysium in skeletal muscles of rats.* J Biomech, 2008. **41**(2): p. 465-9.

209. Scime, A., et al., *Transcriptional profiling of skeletal muscle reveals factors that are necessary to maintain satellite cell integrity during ageing.* Mech Ageing Dev, 2010. **131**(1): p. 9-20.

210. Peterson, M.D., et al., *Resistance exercise for muscular strength in older adults: a meta-analysis.* Ageing Res Rev, 2010. **9**(3): p. 226-37.

211. Brioche, T. and S. Lemoine-Morel, *Oxidative Stress, Sarcopenia, Antioxidant Strategies and Exercise: Molecular Aspects.* Curr Pharm Des, 2016. **22**(18): p. 2664-78.

212. Emery, A.E., *The muscular dystrophies.* Lancet, 2002. **359**(9307): p. 687-95.

213. Mercuri, E. and F. Muntoni, *Muscular dystrophies.* Lancet, 2013. **381**(9869): p. 845-60.

214. Ervasti, J.M., et al., *Deficiency of a glycoprotein component of the dystrophin complex in dystrophic muscle.* Nature, 1990. **345**(6273): p. 315-9.

215. Yoshida, M. and E. Ozawa, *Glycoprotein complex anchoring dystrophin to sarcolemma.* J Biochem, 1990. **108**(5): p. 748-52.

216. Anderson, M.S. and L.M. Kunkel, *The molecular and biochemical basis of Duchenne muscular dystrophy.* Trends Biochem Sci, 1992. **17**(8): p. 289-92.

217. Serrano, A.L., et al., *Cellular and molecular mechanisms regulating fibrosis in skeletal muscle repair and disease.* Curr Top Dev Biol, 2011. **96**: p. 167-201.

218. Webster, C. and H.M. Blau, *Accelerated age-related decline in replicative life-span of Duchenne muscular dystrophy myoblasts: implications for cell and gene therapy.* Somat Cell Mol Genet, 1990. **16**(6): p. 557-65.

219. McDonald, C.M., et al., *Profiles of neuromuscular diseases. Becker's muscular dystrophy.* Am J Phys Med Rehabil, 1995. **74**(5 Suppl): p. S93-103.

220. Bertini, E., et al., *Congenital muscular dystrophies: a brief review.* Semin Pediatr Neurol, 2011. **18**(4): p. 277-88.

221. Flanigan, K.M., *The muscular dystrophies.* Semin Neurol, 2012. **32**(3): p. 255-63.

222. Cavazza, M., et al., *Social/economic costs and health-related quality of life in patients with Duchenne muscular dystrophy in Europe.* Eur J Health Econ, 2016. **17 Suppl 1**: p. 19-29.

223. Landfeldt, E., et al., *The burden of Duchenne muscular dystrophy: an international, cross-sectional study.* Neurology, 2014. **83**(6): p. 529-36.

224. Schreiber-Katz, O., et al., *Comparative cost of illness analysis and assessment of health care burden of Duchenne and Becker muscular dystrophies in Germany.* Orphanet J Rare Dis, 2014. **9**: p. 210.

225. McGreevy, J.W., et al., *Animal models of Duchenne muscular dystrophy: from basic mechanisms to gene therapy.* Dis Model Mech, 2015. **8**(3): p. 195-213.

226. Partridge, T.A., et al., *Conversion of mdx myofibres from dystrophin-negative to -positive by injection of normal myoblasts.* Nature, 1989. **337**(6203): p. 176-9.

227. Law, P.K., et al., *Myoblast transfer therapy for Duchenne muscular dystrophy.* Acta Paediatr Jpn, 1991. **33**(2): p. 206-15.

228. Neumeyer, A.M., et al., *Pilot study of myoblast transfer in the treatment of Becker muscular dystrophy.* Neurology, 1998. **51**(2): p. 589-92.

229. Partridge, T., *The current status of myoblast transfer.* Neurol Sci, 2000. **21**(5 Suppl): p. S939-42.

230. Huard, J., et al., *Human myoblast transplantation between immunohistocompatible donors and recipients produces immune reactions.* Transplant Proc, 1992. **24**(6): p. 3049-51.

231. Fan, Y., et al., *Rapid death of injected myoblasts in myoblast transfer therapy.* Muscle Nerve, 1996. **19**(7): p. 853-60.

232. Cossu, G. and M. Sampaolesi, *New therapies for Duchenne muscular dystrophy: challenges, prospects and clinical trials.* Trends Mol Med, 2007. **13**(12): p. 520-6.

233. Tennyson, C.N., H.J. Klamut, and R.G. Worton, *The human dystrophin gene requires 16 hours to be transcribed and is cotranscriptionally spliced.* Nat Genet, 1995. **9**(2): p. 184-90.

234. Deconinck, N., et al., *Expression of truncated utrophin leads to major functional improvements in dystrophin-deficient muscles of mice.* Nat Med, 1997. **3**(11): p. 1216-21.

235. Tidball, J.G. and M.J. Spencer, *Skipping to new gene therapies for muscular dystrophy.* Nat Med, 2003. **9**(8): p. 997-8.

236. Le Guiner, C., et al., *Long-term microdystrophin gene therapy is effective in a canine model of Duchenne muscular dystrophy.* Nat Commun, 2017. **8**: p. 16105.

237. Kwee, B.J. and D.J. Mooney, *Biomaterials for skeletal muscle tissue engineering.* Curr Opin Biotechnol, 2017. **47**: p. 16-22.

238. Badylak, S.F., et al., *Mechanisms by which acellular biologic scaffolds promote functional skeletal muscle restoration.* Biomaterials, 2016. **103**: p. 128-136.

239. Borselli, C., et al., *The role of multifunctional delivery scaffold in the ability of cultured myoblasts to promote muscle regeneration.* Biomaterials, 2011. **32**(34): p. 8905-14.

240. McCullen, S.D., A.G. Chow, and M.M. Stevens, *In vivo tissue engineering of musculoskeletal tissues.* Curr Opin Biotechnol, 2011. **22**(5): p. 715-20.

241. Bian, W. and N. Bursac, *Tissue engineering of functional skeletal muscle: challenges and recent advances.* IEEE Eng Med Biol Mag, 2008. **27**(5): p. 109-13.

242. Kannan, R.Y., et al., *The roles of tissue engineering and vascularisation in the development of micro-vascular networks: a review.* Biomaterials, 2005. **26**(14): p. 1857-75.

243. Fishman, J.M., et al., *Skeletal muscle tissue engineering: which cell to use?* Tissue Eng Part B Rev, 2013. **19**(6): p. 503-15.

244. Montarras, D., et al., *Direct isolation of satellite cells for skeletal muscle regeneration.* Science, 2005. **309**(5743): p. 2064-7.

245. Motohashi, N., Y. Asakura, and A. Asakura, *Isolation, culture, and transplantation of muscle satellite cells.* J Vis Exp, 2014(86).

246. Sacco, A., et al., *Self-renewal and expansion of single transplanted muscle stem cells.* Nature, 2008. **456**(7221): p. 502-6.

247. Yaffe, D., *Retention of differentiation potentialities during prolonged cultivation of myogenic cells.* Proc Natl Acad Sci U S A, 1968. **61**(2): p. 477-83.

248. Gilbert, P.M., et al., *Substrate elasticity regulates skeletal muscle stem cell self-renewal in culture.* Science, 2010. **329**(5995): p. 1078-81.

249. Quarta, M., et al., *An artificial niche preserves the quiescence of muscle stem cells and enhances their therapeutic efficacy.* Nat Biotechnol, 2016. **34**(7): p. 752-9.

250. Juhas, M., J. Ye, and N. Bursac, *Design, evaluation, and application of engineered skeletal muscle.* Methods, 2016. **99**: p. 81-90.

251. Rosenblatt, J.D., et al., *Culturing satellite cells from living single muscle fiber explants.* In Vitro Cell Dev Biol Anim, 1995. **31**(10): p. 773-9.

252. Shefer, G., et al., *Satellite-cell pool size does matter: defining the myogenic potency of aging skeletal muscle.* Dev Biol, 2006. **294**(1): p. 50-66.

253. Rossi, C.A., et al., *In vivo tissue engineering of functional skeletal muscle by freshly isolated satellite cells embedded in a photopolymerizable hydrogel.* FASEB J, 2011. **25**(7): p. 2296-304.

254. Meng, J., F. Muntoni, and J.E. Morgan, *Stem cells to treat muscular dystrophies - where are we?* Neuromuscul Disord, 2011. **21**(1): p. 4-12.

255. Gussoni, E., et al., *Normal dystrophin transcripts detected in Duchenne muscular dystrophy patients after myoblast transplantation.* Nature, 1992. **356**(6368): p. 435-8.

256. Huard, J., et al., *Myoblast transplantation produced dystrophin-positive muscle fibres in a 16-year-old patient with Duchenne muscular dystrophy.* Clin Sci (Lond), 1991. **81**(2): p. 287-8.

257. Mendell, J.R., et al., *Myoblast transfer in the treatment of Duchenne's muscular dystrophy.* N Engl J Med, 1995. **333**(13): p. 832-8.

258. Tremblay, J.P., et al., *Myoblast transplantation between monozygotic twin girl carriers of Duchenne muscular dystrophy.* Neuromuscul Disord, 1993. **3**(5-6): p. 583-92.

259. Borschel, G.H., R.G. Dennis, and W.M. Kuzon, Jr., *Contractile skeletal muscle tissue-engineered on an acellular scaffold.* Plast Reconstr Surg, 2004. **113**(2): p. 595-602; discussion 603-4.

260. Borschel, G.H., et al., *Tissue-engineered axially vascularized contractile skeletal muscle.* Plast Reconstr Surg, 2006. **117**(7): p. 2235-42.

261. Levenberg, S., et al., *Engineering vascularized skeletal muscle tissue.* Nat Biotechnol, 2005. **23**(7): p. 879-84.

262. Machingal, M.A., et al., *A tissue-engineered muscle repair construct for functional restoration of an irrecoverable muscle injury in a murine model.* Tissue Eng Part A, 2011. **17**(17-18): p. 2291-303.

263. Yaffe, D. and O. Saxel, *Serial passaging and differentiation of myogenic cells isolated from dystrophic mouse muscle.* Nature, 1977. **270**(5639): p. 725-7.

264. Mamchaoui, K., et al., *Immortalized pathological human myoblasts: towards a universal tool for the study of neuromuscular disorders.* Skelet Muscle, 2011. **1**: p. 34.

265. Thorley, M., et al., *Skeletal muscle characteristics are preserved in hTERT/cdk4 human myogenic cell lines.* Skelet Muscle, 2016. **6**(1): p. 43.

266. Tedesco, F.S. and G. Cossu, *Stem cell therapies for muscle disorders.* Curr Opin Neurol, 2012. **25**(5): p. 597-603.

267. Fuoco, C., et al., *Injectable polyethylene glycol-fibrinogen hydrogel adjuvant improves survival and differentiation of transplanted mesoangioblasts in acute and chronic skeletal-muscle degeneration.* Skelet Muscle, 2012. **2**(1): p. 24.

268. Tanaka, K.K., et al., *Syndecan-4-expressing muscle progenitor cells in the SP engraft as satellite cells during muscle regeneration.* Cell Stem Cell, 2009. **4**(3): p. 217-25.

269. Pavlath, G.K. and E. Gussoni, *Human myoblasts and muscle-derived SP cells.* Methods Mol Med, 2005. **107**: p. 97-110.

270. Negroni, E., et al., *In vivo myogenic potential of human CD133+ muscle-derived stem cells: a quantitative study.* Mol Ther, 2009. **17**(10): p. 1771-8.

271. Bianco, P., et al., *The meaning, the sense and the significance: translating the science of mesenchymal stem cells into medicine.* Nat Med, 2013. **19**(1): p. 35-42.

272. De Bari, C., et al., *Skeletal muscle repair by adult human mesenchymal stem cells from synovial membrane.* J Cell Biol, 2003. **160**(6): p. 909-18.

273. Sassoli, C., S. Zecchi-Orlandini, and L. Formigli, *Trophic actions of bone marrow-derived mesenchymal stromal cells for muscle repair/regeneration.* Cells, 2012. **1**(4): p. 832-50.

274. De Coppi, P., et al., *Isolation of amniotic stem cell lines with potential for therapy.* Nat Biotechnol, 2007. **25**(1): p. 100-6.

275. Piccoli, M., et al., *Amniotic fluid stem cells restore the muscle cell niche in a HSA-Cre, Smn(F7/F7) mouse model.* Stem Cells, 2012. **30**(8): p. 1675-84.

276. Barberi, T., et al., *Derivation of engraftable skeletal myoblasts from human embryonic stem cells.* Nat Med, 2007. **13**(5): p. 642-8.

277. Darabi, R., et al., *Functional skeletal muscle regeneration from differentiating embryonic stem cells.* Nat Med, 2008. **14**(2): p. 134-43.

278. Zheng, J.K., et al., *Skeletal myogenesis by human embryonic stem cells.* Cell Res, 2006. **16**(8): p. 713-22.

279. Tedesco, F.S., et al., *Transplantation of genetically corrected human iPSC-derived progenitors in mice with limb-girdle muscular dystrophy.* Sci Transl Med, 2012. **4**(140): p. 140ra89.

280. Karp, J.M. and R. Langer, *Development and therapeutic applications of advanced biomaterials.* Curr Opin Biotechnol, 2007. **18**(5): p. 454-9.

281. Lutolf, M.P. and J.A. Hubbell, *Synthetic biomaterials as instructive extracellular microenvironments for morphogenesis in tissue engineering.* Nat Biotechnol, 2005. **23**(1): p. 47-55.

282. Chan, B.P. and K.W. Leong, *Scaffolding in tissue engineering: general approaches and tissue-specific considerations.* Eur Spine J, 2008. **17 Suppl 4**: p. 467-79.

283. Han, W.M., Y.C. Jang, and A.J. Garcia, *Engineered matrices for skeletal muscle satellite cell engraftment and function.* Matrix Biol, 2017. **60-61**: p. 96-109.

284. Koning, M., et al., *Current opportunities and challenges in skeletal muscle tissue engineering.* J Tissue Eng Regen Med, 2009. **3**(6): p. 407-15.

285. Drury, J.L. and D.J. Mooney, *Hydrogels for tissue engineering: scaffold design variables and applications.* Biomaterials, 2003. **24**(24): p. 4337-51.

286. Cezar, C.A. and D.J. Mooney, *Biomaterial-based delivery for skeletal muscle repair.* Adv Drug Deliv Rev, 2015. **84**: p. 188-97.

287. Cheema, U., et al., *3-D in vitro model of early skeletal muscle development.* Cell Motil Cytoskeleton, 2003. **54**(3): p. 226-36.

288. Chen, S., et al., *Engineering multi-layered skeletal muscle tissue by using 3D microgrooved collagen scaffolds.* Biomaterials, 2015. **73**: p. 23-31.

289. Smith, A.S., et al., *Characterization and optimization of a simple, repeatable system for the long term in vitro culture of aligned myotubes in 3D.* J Cell Biochem, 2012. **113**(3): p. 1044-53.

290. Vandenburgh, H.H., P. Karlisch, and L. Farr, *Maintenance of highly contractile tissue-cultured avian skeletal myotubes in collagen gel.* In Vitro Cell Dev Biol, 1988. **24**(3): p. 166-74.

291. Yun, Y.R., et al., *Fibroblast growth factor 2-functionalized collagen matrices for skeletal muscle tissue engineering.* Biotechnol Lett, 2012. **34**(4): p. 771-8.

292. Beier, J.P., et al., *Tissue engineering of injectable muscle: three-dimensional myoblast-fibrin injection in the syngeneic rat animal model.* Plast Reconstr Surg, 2006. **118**(5): p. 1113-21; discussion 1122-4.

293. Huang, Y.C., et al., *Rapid formation of functional muscle in vitro using fibrin gels.* J Appl Physiol (1985), 2005. **98**(2): p. 706-13.

294. Juhas, M. and N. Bursac, *Roles of adherent myogenic cells and dynamic culture in engineered muscle function and maintenance of satellite cells.* Biomaterials, 2014. **35**(35): p. 9438-46.

295. Matsumoto, T., et al., *Three-dimensional cell and tissue patterning in a strained fibrin gel system.* PLoS One, 2007. **2**(11): p. e1211.

296. Page, R.L., et al., *Restoration of skeletal muscle defects with adult human cells delivered on fibrin microthreads.* Tissue Eng Part A, 2011. **17**(21-22): p. 2629-40.

297. Wang, W., et al., *Compatibility of hyaluronic acid hydrogel and skeletal muscle myoblasts.* Biomed Mater, 2009. **4**(2): p. 025011.

298. Hill, E., T. Boontheekul, and D.J. Mooney, *Designing scaffolds to enhance transplanted myoblast survival and migration.* Tissue Eng, 2006. **12**(5): p. 1295-304.

299. Rowley, J.A. and D.J. Mooney, *Alginate type and RGD density control myoblast phenotype.* J Biomed Mater Res, 2002. **60**(2): p. 217-23.

300. Lee, C.H., A. Singla, and Y. Lee, *Biomedical applications of collagen.* Int J Pharm, 2001. **221**(1-2): p. 1-22.

301. Hall, C.L. and E.A. Turley, *Hyaluronan: RHAMM mediated cell locomotion and signaling in tumorigenesis.* J Neurooncol, 1995. **26**(3): p. 221-9.

302. Breen, A., T. O'Brien, and A. Pandit, *Fibrin as a delivery system for therapeutic drugs and biomolecules.* Tissue Eng Part B Rev, 2009. **15**(2): p. 201-14.

303. de la Puente, P. and D. Ludena, *Cell culture in autologous fibrin scaffolds for applications in tissue engineering.* Exp Cell Res, 2014. **322**(1): p. 1-11.

304. Spotnitz, W.D., *Fibrin Sealant: The Only Approved Hemostat, Sealant, and Adhesive-a Laboratory and Clinical Perspective.* ISRN Surg, 2014. **2014**: p. 203943.

305. Ching, S.H., N. Bansal, and B. Bhandari, *Alginate gel particles-A review of production techniques and physical properties.* Crit Rev Food Sci Nutr, 2017. **57**(6): p. 1133-1152.

306. Jeon, O., et al., *Affinity-based growth factor delivery using biodegradable, photocrosslinked heparin-alginate hydrogels.* J Control Release, 2011. **154**(3): p. 258-66.

307. Oh, E.J., et al., *Target specific and long-acting delivery of protein, peptide, and nucleotide therapeutics using hyaluronic acid derivatives.* J Control Release, 2010. **141**(1): p. 2-12.

308. Wallace, D.G. and J. Rosenblatt, *Collagen gel systems for sustained delivery and tissue engineering.* Adv Drug Deliv Rev, 2003. **55**(12): p. 1631-49.

309. Gilmore, A.P., *Anoikis.* Cell Death Differ, 2005. **12 Suppl 2**: p. 1473-7.

310. Ma, J., et al., *The application of three-dimensional collagen-scaffolds seeded with myoblasts to repair skeletal muscle defects.* J Biomed Biotechnol, 2011. **2011**: p. 812135.

311. Fuoco, C., et al., *Matrix scaffolding for stem cell guidance toward skeletal muscle tissue engineering.* J Orthop Surg Res, 2016. **11**(1): p. 86.

312. Khademhosseini, A. and N.A. Peppas, *Micro- and nanoengineering of biomaterials for healthcare applications.* Adv Healthc Mater, 2013. **2**(1): p. 10-2.

313. Zhu, J. and R.E. Marchant, *Design properties of hydrogel tissue-engineering scaffolds.* Expert Rev Med Devices, 2011. **8**(5): p. 607-26.

314. Almany, L. and D. Seliktar, *Biosynthetic hydrogel scaffolds made from fibrinogen and polyethylene glycol for 3D cell cultures.* Biomaterials, 2005. **26**(15): p. 2467-77.

315. Liu, S.Q., et al., *Injectable Biodegradable Poly(ethylene glycol)/RGD Peptide Hybrid Hydrogels for in vitro Chondrogenesis of Human Mesenchymal Stem Cells.* Macromol Rapid Commun, 2010. **31**(13): p. 1148-54.

316. Fuoco, C., et al., *In vivo generation of a mature and functional artificial skeletal muscle.* EMBO Mol Med, 2015. **7**(4): p. 411-22.

317. Fuoco, C., et al., *3D hydrogel environment rejuvenates aged pericytes for skeletal muscle tissue engineering.* Front Physiol, 2014. **5**: p. 203.

318. Hammers, D.W., et al., *Controlled release of IGF-I from a biodegradable matrix improves functional recovery of skeletal muscle from ischemia/reperfusion.* Biotechnol Bioeng, 2012. **109**(4): p. 1051-9.

319. Rybalko, V.Y., et al., *Controlled delivery of SDF-1alpha and IGF-1: CXCR4(+) cell recruitment and functional skeletal muscle recovery.* Biomater Sci, 2015. **3**(11): p. 1475-86.

320. Wolf, M.T., et al., *Naturally derived and synthetic scaffolds for skeletal muscle reconstruction.* Adv Drug Deliv Rev, 2015. **84**: p. 208-21.

321. Zhu, H., J. Schulz, and H. Schliephake, *Human bone marrow stroma stem cell distribution in calcium carbonate scaffolds using two different seeding methods.* Clin Oral Implants Res, 2010. **21**(2): p. 182-8.

322. Lee, K., E.A. Silva, and D.J. Mooney, *Growth factor delivery-based tissue engineering: general approaches and a review of recent developments.* J R Soc Interface, 2011. **8**(55): p. 153-70.

323. Cronin, E.M., et al., *Protein-coated poly(L-lactic acid) fibers provide a substrate for differentiation of human skeletal muscle cells.* J Biomed Mater Res A, 2004. **69**(3): p. 373-81.

324. Ju, Y.M., et al., *In situ regeneration of skeletal muscle tissue through host cell recruitment.* Acta Biomater, 2014. **10**(10): p. 4332-9.

325. Kim, M., et al., *Muscle regeneration by adipose tissue-derived adult stem cells attached to injectable PLGA spheres.* Biochem Biophys Res Commun, 2006. **348**(2): p. 386-92.

326. Saxena, A.K., et al., *Skeletal muscle tissue engineering using isolated myoblasts on synthetic biodegradable polymers: preliminary studies.* Tissue Eng, 1999. **5**(6): p. 525-32.

327. Shandalov, Y., et al., *An engineered muscle flap for reconstruction of large soft tissue defects.* Proc Natl Acad Sci U S A, 2014. **111**(16): p. 6010-5.

328. Yang, H.S., et al., *Nanopatterned muscle cell patches for enhanced myogenesis and dystrophin expression in a mouse model of muscular dystrophy.* Biomaterials, 2014. **35**(5): p. 1478-86.

329. Davoudi, S. and P.M. Gilbert, *Optimization of Satellite Cell Culture Through Biomaterials.* Methods Mol Biol, 2017. **1556**: p. 329-341.

330. Huang, N.F., et al., *Myotube assembly on nanofibrous and micropatterned polymers.* Nano Lett, 2006. **6**(3): p. 537-42.

331. Shah, R., et al., *Development of a novel smart scaffold for human skeletal muscle regeneration.* J Tissue Eng Regen Med, 2016. **10**(2): p. 162-71.

332. Choi, J.S., et al., *The influence of electrospun aligned poly(epsilon-caprolactone)/collagen nanofiber meshes on the formation of self-aligned skeletal muscle myotubes.* Biomaterials, 2008. **29**(19): p. 2899-906.

333. Gilbert, T.W., T.L. Sellaro, and S.F. Badylak, *Decellularization of tissues and organs.* Biomaterials, 2006. **27**(19): p. 3675-83.

334. Perniconi, B., et al., *The pro-myogenic environment provided by whole organ scale acellular scaffolds from skeletal muscle.* Biomaterials, 2011. **32**(31): p. 7870-82.

335. Conconi, M.T., et al., *Homologous muscle acellular matrix seeded with autologous myoblasts as a tissue-engineering approach to abdominal wall-defect repair.* Biomaterials, 2005. **26**(15): p. 2567-74.

336. Merritt, E.K., et al., *Repair of traumatic skeletal muscle injury with bone-marrow-derived mesenchymal stem cells seeded on extracellular matrix.* Tissue Eng Part A, 2010. **16**(9): p. 2871-81.

337. Piccoli, M., et al., *Improvement of diaphragmatic performance through orthotopic application of decellularized extracellular matrix patch.* Biomaterials, 2016. **74**: p. 245-55.

338. Sicari, B.M., et al., *An acellular biologic scaffold promotes skeletal muscle formation in mice and humans with volumetric muscle loss.* Sci Transl Med, 2014. **6**(234): p. 234ra58.

339. Turner, N.J., et al., *Xenogeneic extracellular matrix as an inductive scaffold for regeneration of a functioning musculotendinous junction.* Tissue Eng Part A, 2010. **16**(11): p. 3309-17.

340. Valentin, J.E., et al., *Functional skeletal muscle formation with a biologic scaffold.* Biomaterials, 2010. **31**(29): p. 7475-84.

341. Badylak, S.F. and T.W. Gilbert, *Immune response to biologic scaffold materials.* Semin Immunol, 2008. **20**(2): p. 109-16.

342. DeQuach, J.A., et al., *Injectable skeletal muscle matrix hydrogel promotes neovascularization and muscle cell infiltration in a hindlimb ischemia model.* Eur Cell Mater, 2012. **23**: p. 400-12; discussion 412.

343. Mase, V.J., Jr., et al., *Clinical application of an acellular biologic scaffold for surgical repair of a large, traumatic quadriceps femoris muscle defect.* Orthopedics, 2010. **33**(7): p. 511.

344. Juhas, M. and N. Bursac, *Engineering skeletal muscle repair.* Curr Opin Biotechnol, 2013. **24**(5): p. 880-6.

345. Strohman, R.C., et al., *Myogenesis and histogenesis of skeletal muscle on flexible membranes in vitro.* In Vitro Cell Dev Biol, 1990. **26**(2): p. 201-8.

346. Carosio, S., et al., *Generation of eX vivo-vascularized Muscle Engineered Tissue (X-MET).* Sci Rep, 2013. **3**: p. 1420.

347. Dennis, R.G., et al., *Excitability and contractility of skeletal muscle engineered from primary cultures and cell lines.* Am J Physiol Cell Physiol, 2001. **280**(2): p. C288-95.

348. Kosnik, P.E., J.A. Faulkner, and R.G. Dennis, *Functional development of engineered skeletal muscle from adult and neonatal rats.* Tissue Eng, 2001. **7**(5): p. 573-84.

349. Shansky, J., et al., *A simplified method for tissue engineering skeletal muscle organoids in vitro.* In Vitro Cell Dev Biol Anim, 1997. **33**(9): p. 659-61.

350. Powell, C.A., et al., *Mechanical stimulation improves tissue-engineered human skeletal muscle.* Am J Physiol Cell Physiol, 2002. **283**(5): p. C1557-65.

351. Bian, W. and N. Bursac, *Engineered skeletal muscle tissue networks with controllable architecture.* Biomaterials, 2009. **30**(7): p. 1401-12.

352. Juhas, M., et al., *Biomimetic engineered muscle with capacity for vascular integration and functional maturation in vivo.* Proc Natl Acad Sci U S A, 2014. **111**(15): p. 5508-13.

353. Martin, N.R., et al., *Factors affecting the structure and maturation of human tissue engineered skeletal muscle.* Biomaterials, 2013. **34**(23): p. 5759-65.

354. Boontheekul, T., et al., *Quantifying the relation between bond number and myoblast proliferation.* Faraday Discuss, 2008. **139**: p. 53-70; discussion 105-28, 419-20.

355. Engler, A.J., et al., *Matrix elasticity directs stem cell lineage specification.* Cell, 2006. **126**(4): p. 677-89.

356. Engler, A.J., et al., *Myotubes differentiate optimally on substrates with tissue-like stiffness: pathological implications for soft or stiff microenvironments.* J Cell Biol, 2004. **166**(6): p. 877-87.

357. Boontheekul, T., et al., *Regulating myoblast phenotype through controlled gel stiffness and degradation.* Tissue Eng, 2007. **13**(7): p. 1431-42.

358. Kaully, T., et al., *Vascularization--the conduit to viable engineered tissues.* Tissue Eng Part B Rev, 2009. **15**(2): p. 159-69.

359. Ikada, Y., *Challenges in tissue engineering.* J R Soc Interface, 2006. **3**(10): p. 589-601.

360. Bian, W., et al., *Local tissue geometry determines contractile force generation of engineered muscle networks.* Tissue Eng Part A, 2012. **18**(9-10): p. 957-67.

361. Clark, P., et al., *Alignment of myoblasts on ultrafine gratings inhibits fusion in vitro.* Int J Biochem Cell Biol, 2002. **34**(7): p. 816-25.

362. Boudriot, U., et al., *Electrospinning approaches toward scaffold engineering--a brief overview.* Artif Organs, 2006. **30**(10): p. 785-92.

363. Murugan, R. and S. Ramakrishna, *Design strategies of tissue engineering scaffolds with controlled fiber orientation.* Tissue Eng, 2007. **13**(8): p. 1845-66.

364. Buttafoco, L., et al., *Electrospinning of collagen and elastin for tissue engineering applications.* Biomaterials, 2006. **27**(5): p. 724-34.

365. Lee, K.Y., et al., *Electrospinning of polysaccharides for regenerative medicine.* Adv Drug Deliv Rev, 2009. **61**(12): p. 1020-32.

366. Sell, S.A., et al., *Electrospinning of collagen/biopolymers for regenerative medicine and cardiovascular tissue engineering.* Adv Drug Deliv Rev, 2009. **61**(12): p. 1007-19.

367. Aviss, K.J., J.E. Gough, and S. Downes, *Aligned electrospun polymer fibres for skeletal muscle regeneration.* Eur Cell Mater, 2010. **19**: p. 193-204.

368. Bolgen, N., et al., *In vitro and in vivo degradation of non-woven materials made of poly(epsilon-caprolactone) nanofibers prepared by electrospinning under different conditions.* J Biomater Sci Polym Ed, 2005. **16**(12): p. 1537-55.

369. Huber, A., A. Pickett, and K.M. Shakesheff, *Reconstruction of spatially orientated myotubes in vitro using electrospun, parallel microfibre arrays.* Eur Cell Mater, 2007. **14**: p. 56-63.

370. Klumpp, D., et al., *Engineering skeletal muscle tissue--new perspectives in vitro and in vivo.* J Cell Mol Med, 2010. **14**(11): p. 2622-9.

371. Kim, M.S., et al., *The development of genipin-crosslinked poly(caprolactone) (PCL)/gelatin nanofibers for tissue engineering applications.* Macromol Biosci, 2010. **10**(1): p. 91-100.

372. Neumann, T., S.D. Hauschka, and J.E. Sanders, *Tissue engineering of skeletal muscle using polymer fiber arrays.* Tissue Eng, 2003. **9**(5): p. 995-1003.

373. Riboldi, S.A., et al., *Electrospun degradable polyesterurethane membranes: potential scaffolds for skeletal muscle tissue engineering.* Biomaterials, 2005. **26**(22): p. 4606-15.

374. Zhang, Y.Z., et al., *Characterization of the surface biocompatibility of the electrospun PCL-collagen nanofibers using fibroblasts.* Biomacromolecules, 2005. **6**(5): p. 2583-9.

375. Baker, B.M. and R.L. Mauck, *The effect of nanofiber alignment on the maturation of engineered meniscus constructs.* Biomaterials, 2007. **28**(11): p. 1967-77.

376. Telemeco, T.A., et al., *Regulation of cellular infiltration into tissue engineering scaffolds composed of submicron diameter fibrils produced by electrospinning.* Acta Biomater, 2005. **1**(4): p. 377-85.

377. Baker, B.M., et al., *The potential to improve cell infiltration in composite fiber-aligned electrospun scaffolds by the selective removal of sacrificial fibers.* Biomaterials, 2008. **29**(15): p. 2348-58.

378. Jana, S., et al., *Uniaxially aligned nanofibrous cylinders by electrospinning.* ACS Appl Mater Interfaces, 2012. **4**(9): p. 4817-24.

379. Tsang, V.L. and S.N. Bhatia, *Three-dimensional tissue fabrication.* Adv Drug Deliv Rev, 2004. **56**(11): p. 1635-47.

380. Shimizu, K., H. Fujita, and E. Nagamori, *Alignment of skeletal muscle myoblasts and myotubes using linear micropatterned surfaces ground with abrasives.* Biotechnol Bioeng, 2009. **103**(3): p. 631-8.

381. Evans, D.J., S. Britland, and P.M. Wigmore, *Differential response of fetal and neonatal myoblasts to topographical guidance cues in vitro.* Dev Genes Evol, 1999. **209**(7): p. 438-42.

382. Hahn, M.S., et al., *Photolithographic patterning of polyethylene glycol hydrogels.* Biomaterials, 2006. **27**(12): p. 2519-24.

383. Norman, J.J. and T.A. Desai, *Control of cellular organization in three dimensions using a microfabricated polydimethylsiloxane-collagen composite tissue scaffold.* Tissue Eng, 2005. **11**(3-4): p. 378-86.

384. Tang, M.D., A.P. Golden, and J. Tien, *Molding of three-dimensional microstructures of gels.* J Am Chem Soc, 2003. **125**(43): p. 12988-9.

385. Kroehne, V., et al., *Use of a novel collagen matrix with oriented pore structure for muscle cell differentiation in cell culture and in grafts.* J Cell Mol Med, 2008. **12**(5A): p. 1640-8.

386. Walboomers, X.F. and J.A. Jansen, *Cell and tissue behavior on micro-grooved surfaces.* Odontology, 2001. **89**(1): p. 2-11.

387. Huang, N.F., R.J. Lee, and S. Li, *Engineering of aligned skeletal muscle by micropatterning.* Am J Transl Res, 2010. **2**(1): p. 43-55.

388. Bryant, S.J., et al., *Photo-patterning of porous hydrogels for tissue engineering.* Biomaterials, 2007. **28**(19): p. 2978-86.

389. Bian, W., et al., *Mesoscopic hydrogel molding to control the 3D geometry of bioartificial muscle tissues.* Nat Protoc, 2009. **4**(10): p. 1522-34.

390. Fedorovich, N.E., et al., *Hydrogels as extracellular matrices for skeletal tissue engineering: state-of-the-art and novel application in organ printing.* Tissue Eng, 2007. **13**(8): p. 1905-25.

214

391.   Zhang, H., et al., *Aligned two- and three-dimensional structures by directional freezing of polymers and nanoparticles.* Nat Mater, 2005. **4**(10): p. 787-93.

392.   Madaghiele, M., et al., *Collagen-based matrices with axially oriented pores.* J Biomed Mater Res A, 2008. **85**(3): p. 757-67.

393.   Schoof, H., et al., *Control of pore structure and size in freeze-dried collagen sponges.* J Biomed Mater Res, 2001. **58**(4): p. 352-7.

394.   Girton, T.S., N. Dubey, and R.T. Tranquillo, *Magnetic-induced alignment of collagen fibrils in tissue equivalents.* Methods Mol Med, 1999. **18**: p. 67-73.

395.   Namani, R., et al., *Anisotropic mechanical properties of magnetically aligned fibrin gels measured by magnetic resonance elastography.* J Biomech, 2009. **42**(13): p. 2047-53.

396.   Gessmann, J., et al., *Alignment of the Fibrin Network Within an Autologous Plasma Clot.* Tissue Eng Part C Methods, 2016. **22**(1): p. 30-7.

397.   Kang, H.W., et al., *A 3D bioprinting system to produce human-scale tissue constructs with structural integrity.* Nat Biotechnol, 2016. **34**(3): p. 312-9.

398.   Leong, K.F., C.M. Cheah, and C.K. Chua, *Solid freeform fabrication of three-dimensional scaffolds for engineering replacement tissues and organs.* Biomaterials, 2003. **24**(13): p. 2363-78.

399.   Shansky, J., et al., *Paracrine release of insulin-like growth factor 1 from a bioengineered tissue stimulates skeletal muscle growth in vitro.* Tissue Eng, 2006. **12**(7): p. 1833-41.

400.   Silva, E.A. and D.J. Mooney, *Spatiotemporal control of vascular endothelial growth factor delivery from injectable hydrogels enhances angiogenesis.* J Thromb Haemost, 2007. **5**(3): p. 590-8.

401.   Sheehan, S.M. and R.E. Allen, *Skeletal muscle satellite cell proliferation in response to members of the fibroblast growth factor family and hepatocyte growth factor.* J Cell Physiol, 1999. **181**(3): p. 499-506.

402.   Borselli, C., et al., *Functional muscle regeneration with combined delivery of angiogenesis and myogenesis factors.* Proc Natl Acad Sci U S A, 2010. **107**(8): p. 3287-92.

403.   Wang, L., et al., *Minimally invasive approach to the repair of injured skeletal muscle with a shape-memory scaffold.* Mol Ther, 2014. **22**(8): p. 1441-1449.

404.   Parker, M.H., et al., *Activation of Notch signaling during ex vivo expansion maintains donor muscle cell engraftment.* Stem Cells, 2012. **30**(10): p. 2212-20.

405.   Chen, H.C. and Y.C. Hu, *Bioreactors for tissue engineering.* Biotechnol Lett, 2006. **28**(18): p. 1415-23.

406.   Martin, I., D. Wendt, and M. Heberer, *The role of bioreactors in tissue engineering.* Trends Biotechnol, 2004. **22**(2): p. 80-6.

407.   Rangarajan, S., L. Madden, and N. Bursac, *Use of flow, electrical, and mechanical stimulation to promote engineering of striated muscles.* Ann Biomed Eng, 2014. **42**(7): p. 1391-405.

408.   Bardouille, C., et al., *Growth and differentiation of permanent and secondary mouse myogenic cell lines on microcarriers.* Appl Microbiol Biotechnol, 2001. **55**(5): p. 556-62.

409.   Slentz, D.H., G.A. Truskey, and W.E. Kraus, *Effects of chronic exposure to simulated microgravity on skeletal muscle cell proliferation and differentiation.* In Vitro Cell Dev Biol Anim, 2001. **37**(3): p. 148-56.

410.   Flaibani, M., et al., *Flow cytometric cell cycle analysis of muscle precursor cells cultured within 3D scaffolds in a perfusion bioreactor.* Biotechnol Prog, 2009. **25**(1): p. 286-95.

411.   Shimizu, K., et al., *Microfluidic devices for construction of contractile skeletal muscle microtissues.* J Biosci Bioeng, 2015. **119**(2): p. 212-6.

412.   Chi, C.W., et al., *Microfluidic cell chips for high-throughput drug screening.* Bioanalysis, 2016. **8**(9): p. 921-37.

413.   Kasper, A.M., et al., *Mimicking exercise in three-dimensional bioengineered skeletal muscle to investigate cellular and molecular mechanisms of physiological adaptation.* J Cell Physiol, 2018. **233**(3): p. 1985-1998.

414.   Vandenburgh, H.H. and P. Karlisch, *Longitudinal growth of skeletal myotubes in vitro in a new horizontal mechanical cell stimulator.* In Vitro Cell Dev Biol, 1989. **25**(7): p. 607-16.

415.   Corona, B.T., et al., *Further development of a tissue engineered muscle repair construct in vitro for enhanced functional recovery following implantation in vivo in a murine model of volumetric muscle loss injury.* Tissue Eng Part A, 2012. **18**(11-12): p. 1213-28.

416.   Moon du, G., et al., *Cyclic mechanical preconditioning improves engineered muscle contraction.* Tissue Eng Part A, 2008. **14**(4): p. 473-82.

417.   Gaffney, P.J., et al., *Monoclonal antibodies to crosslinked fibrin degradation products (XL-FDP). I. Characterization and preliminary evaluation in plasma.* Br J Haematol, 1988. **68**(1): p. 83-90.

418.   Goldberg, A.L., *Work-induced growth of skeletal muscle in normal and hypophysectomized rats.* Am J Physiol, 1967. **213**(5): p. 1193-8.

419.   Goldberg, A.L. and H.M. Goodman, *Amino acid transport during work-induced growth of skeletal muscle.* Am J Physiol, 1969. **216**(5): p. 1111-5.

420.   Goldspink, D.F., *The influence of immobilization and stretch on protein turnover of rat skeletal muscle.* J Physiol, 1977. **264**(1): p. 267-82.

421.   Olwin, B.B., et al., *Role of FGFs in skeletal muscle and limb development.* Mol Reprod Dev, 1994. **39**(1): p. 90-100; discussion 100-1.

422.   Rosenblatt, J.D. and D.J. Parry, *Gamma irradiation prevents compensatory hypertrophy of overloaded mouse extensor digitorum longus muscle.* J Appl Physiol (1985), 1992. **73**(6): p. 2538-43.

423.   Schiaffino, S., S.P. Bormioli, and M. Aloisi, *Cell proliferation in rat skeletal muscle during early stages of compensatory hypertrophy.* Virchows Arch B Cell Pathol, 1972. **11**(3): p. 268-73.

424.   Vandenburgh, H. and S. Kaufman, *In vitro model for stretch-induced hypertrophy of skeletal muscle.* Science, 1979. **203**(4377): p. 265-8.

425.   Vandenburgh, H.H., et al., *Skeletal muscle growth is stimulated by intermittent stretch-relaxation in tissue culture.* Am J Physiol, 1989. **256**(3 Pt 1): p. C674-82.

426. Auluck, A., et al., *A three-dimensional in vitro model system to study the adaptation of craniofacial skeletal muscle following mechanostimulation.* Eur J Oral Sci, 2005. **113**(3): p. 218-24.

427. Candiani, G., et al., *Cyclic mechanical stimulation favors myosin heavy chain accumulation in engineered skeletal muscle constructs.* J Appl Biomater Biomech, 2010. **8**(2): p. 68-75.

428. Cheema, U., et al., *Mechanical signals and IGF-I gene splicing in vitro in relation to development of skeletal muscle.* J Cell Physiol, 2005. **202**(1): p. 67-75.

429. Okano, T. and T. Matsuda, *Tissue engineered skeletal muscle: preparation of highly dense, highly oriented hybrid muscular tissues.* Cell Transplant, 1998. **7**(1): p. 71-82.

430. Heher, P., et al., *A novel bioreactor for the generation of highly aligned 3D skeletal muscle-like constructs through orientation of fibrin via application of static strain.* Acta Biomater, 2015. **24**: p. 251-65.

431. Egusa, H., et al., *Application of cyclic strain for accelerated skeletal myogenic differentiation of mouse bone marrow-derived mesenchymal stromal cells with cell alignment.* Tissue Eng Part A, 2013. **19**(5-6): p. 770-82.

432. Yilgor Huri, P., et al., *Biophysical cues enhance myogenesis of human adipose derived stem/stromal cells.* Biochem Biophys Res Commun, 2013. **438**(1): p. 180-5.

433. Burkholder, T.J., *Mechanotransduction in skeletal muscle.* Front Biosci, 2007. **12**: p. 174-91.

434. Hornberger, T.A. and K.A. Esser, *Mechanotransduction and the regulation of protein synthesis in skeletal muscle.* Proc Nutr Soc, 2004. **63**(2): p. 331-5.

435. Perrone, C.E., D. Fenwick-Smith, and H.H. Vandenburgh, *Collagen and stretch modulate autocrine secretion of insulin-like growth factor-1 and insulin-like growth factor binding proteins from differentiated skeletal muscle cells.* J Biol Chem, 1995. **270**(5): p. 2099-106.

436. Tatsumi, R., et al., *Release of hepatocyte growth factor from mechanically stretched skeletal muscle satellite cells and role of pH and nitric oxide.* Mol Biol Cell, 2002. **13**(8): p. 2909-18.

437. Martineau, L.C. and P.F. Gardiner, *Insight into skeletal muscle mechanotransduction: MAPK activation is quantitatively related to tension.* J Appl Physiol (1985), 2001. **91**(2): p. 693-702.

438. Musi, N., H. Yu, and L.J. Goodyear, *AMP-activated protein kinase regulation and action in skeletal muscle during exercise.* Biochem Soc Trans, 2003. **31**(Pt 1): p. 191-5.

439. Ryder, J.W., et al., *Effect of contraction on mitogen-activated protein kinase signal transduction in skeletal muscle. Involvement Of the mitogen- and stress-activated protein kinase 1.* J Biol Chem, 2000. **275**(2): p. 1457-62.

440. Vandenburgh, H.H., et al., *Mechanical stimulation of skeletal muscle generates lipid-related second messengers by phospholipase activation.* J Cell Physiol, 1993. **155**(1): p. 63-71.

441. Liu, W.S. and C.A. Heckman, *The sevenfold way of PKC regulation.* Cell Signal, 1998. **10**(8): p. 529-42.

442. Tidball, J.G., *Mechanical signal transduction in skeletal muscle growth and adaptation.* J Appl Physiol (1985), 2005. **98**(5): p. 1900-8.

443. Yeung, E.W., et al., *Effects of stretch-activated channel blockers on [Ca2+]i and muscle damage in the mdx mouse.* J Physiol, 2005. **562**(Pt 2): p. 367-80.

444. Olson, E.N. and R.S. Williams, *Remodeling muscles with calcineurin.* Bioessays, 2000. **22**(6): p. 510-9.

445. Wu, H., et al., *Activation of MEF2 by muscle activity is mediated through a calcineurin-dependent pathway.* EMBO J, 2001. **20**(22): p. 6414-23.

446. Dunn, S.E., J.L. Burns, and R.N. Michel, *Calcineurin is required for skeletal muscle hypertrophy.* J Biol Chem, 1999. **274**(31): p. 21908-12.

447. Rauch, C. and P.T. Loughna, *Static stretch promotes MEF2A nuclear translocation and expression of neonatal myosin heavy chain in C2C12 myocytes in a calcineurin- and p38-dependent manner.* Am J Physiol Cell Physiol, 2005. **288**(3): p. C593-605.

448. Hornberger, T.A., *Mechanotransduction and the regulation of mTORC1 signaling in skeletal muscle.* Int J Biochem Cell Biol, 2011. **43**(9): p. 1267-76.

449. Reiling, J.H. and D.M. Sabatini, *Stress and mTORture signaling.* Oncogene, 2006. **25**(48): p. 6373-83.

450. Bodine, S.C., et al., *Akt/mTOR pathway is a crucial regulator of skeletal muscle hypertrophy and can prevent muscle atrophy in vivo.* Nat Cell Biol, 2001. **3**(11): p. 1014-9.

451. Fingar, D.C., et al., *Mammalian cell size is controlled by mTOR and its downstream targets S6K1 and 4EBP1/eIF4E.* Genes Dev, 2002. **16**(12): p. 1472-87.

452. Hornberger, T.A., et al., *Mechanical stimuli regulate rapamycin-sensitive signalling by a phosphoinositide 3-kinase-, protein kinase B- and growth factor-independent mechanism.* Biochem J, 2004. **380**(Pt 3): p. 795-804.

453. Baar, K. and K. Esser, *Phosphorylation of p70(S6k) correlates with increased skeletal muscle mass following resistance exercise.* Am J Physiol, 1999. **276**(1 Pt 1): p. C120-7.

454. Drummond, M.J., et al., *Rapamycin administration in humans blocks the contraction-induced increase in skeletal muscle protein synthesis.* J Physiol, 2009. **587**(Pt 7): p. 1535-46.

455. Akimoto, T., et al., *Mechanical stretch is a down-regulatory signal for differentiation of C2C12 myogenic cells.* Mater Sci Eng C, 2001. **17**: p. 75-78.

456. Kook, S.H., et al., *Cyclic mechanical stretch stimulates the proliferation of C2C12 myoblasts and inhibits their differentiation via prolonged activation of p38 MAPK.* Mol Cells, 2008. **25**(4): p. 479-86.

457. Hanke, N., et al., *Passive mechanical forces upregulate the fast myosin heavy chain IId/x via integrin and p38 MAP kinase activation in a primary muscle cell culture.* Am J Physiol Cell Physiol, 2010. **298**(4): p. C910-20.

458. Kumar, A., et al., *Cyclic mechanical strain inhibits skeletal myogenesis through activation of focal adhesion kinase, Rac-1 GTPase, and NF-kappaB transcription factor.* FASEB J, 2004. **18**(13): p. 1524-35.

459. Zhang, S.J., G.A. Truskey, and W.E. Kraus, *Effect of cyclic stretch on beta1D-integrin expression and activation of FAK and RhoA.* Am J Physiol Cell Physiol, 2007. **292**(6): p. C2057-69.

460. Otis, J.S., T.J. Burkholder, and G.K. Pavlath, *Stretch-induced myoblast proliferation is dependent on the COX2 pathway.* Exp Cell Res, 2005. **310**(2): p. 417-25.

461. Tatsumi, R., et al., *Mechanical stretch induces activation of skeletal muscle satellite cells in vitro.* Exp Cell Res, 2001. **267**(1): p. 107-14.

462. Corona, B.T., et al., *Implantation of in vitro tissue engineered muscle repair constructs and bladder acellular matrices partially restore in vivo skeletal muscle function in a rat model of volumetric muscle loss injury.* Tissue Eng Part A, 2014. **20**(3-4): p. 705-15.

463. Goldspink, G., et al., *Gene expression in skeletal muscle in response to stretch and force generation.* Am J Physiol, 1992. **262**(3 Pt 2): p. R356-63.

464. Loughna, P.T., et al., *Disuse and passive stretch cause rapid alterations in expression of developmental and adult contractile protein genes in skeletal muscle.* Development, 1990. **109**(1): p. 217-23.

465. Nikolic, N., et al., *Electrical pulse stimulation of cultured skeletal muscle cells as a model for in vitro exercise - possibilities and limitations.* Acta Physiol (Oxf), 2017. **220**(3): p. 310-331.

466. Khodabukus, A., et al., *Role of contraction duration in inducing fast-to-slow contractile and metabolic protein and functional changes in engineered muscle.* J Cell Physiol, 2015. **230**(10): p. 2489-97.

467. Langelaan, M.L., et al., *Advanced maturation by electrical stimulation: Differences in response between C2C12 and primary muscle progenitor cells.* J Tissue Eng Regen Med, 2011. **5**(7): p. 529-39.

468. Nagamine, K., et al., *Micropatterning contractile C2C12 myotubes embedded in a fibrin gel.* Biotechnol Bioeng, 2010. **105**(6): p. 1161-7.

469. Serena, E., et al., *Electrophysiologic stimulation improves myogenic potential of muscle precursor cells grown in a 3D collagen scaffold.* Neurol Res, 2008. **30**(2): p. 207-14.

470. van der Schaft, D.W., et al., *Engineering skeletal muscle tissues from murine myoblast progenitor cells and application of electrical stimulation.* J Vis Exp, 2013(73): p. e4267.

471. Brevet, A., et al., *Myosin synthesis increased by electrical stimulation of skeletal muscle cell cultures.* Science, 1976. **193**(4258): p. 1152-4.

472. Naumann, K. and D. Pette, *Effects of chronic stimulation with different impulse patterns on the expression of myosin isoforms in rat myotube cultures.* Differentiation, 1994. **55**(3): p. 203-11.

473. Wehrle, U., S. Dusterhoft, and D. Pette, *Effects of chronic electrical stimulation on myosin heavy chain expression in satellite cell cultures derived from rat muscles of different fiber-type composition.* Differentiation, 1994. **58**(1): p. 37-46.

474. Pette, D., et al., *Partial fast-to-slow conversion of regenerating rat fast-twitch muscle by chronic low-frequency stimulation.* J Muscle Res Cell Motil, 2002. **23**(3): p. 215-21.

475. Donnelly, K., et al., *A novel bioreactor for stimulating skeletal muscle in vitro.* Tissue Eng Part C Methods, 2010. **16**(4): p. 711-8.

476. Nedachi, T., H. Fujita, and M. Kanzaki, *Contractile C2C12 myotube model for studying exercise-inducible responses in skeletal muscle.* Am J Physiol Endocrinol Metab, 2008. **295**(5): p. E1191-204.

477. Dennis, R.G. and P.E. Kosnik, 2nd, *Excitability and isometric contractile properties of mammalian skeletal muscle constructs engineered in vitro.* In Vitro Cell Dev Biol Anim, 2000. **36**(5): p. 327-35.

478. Fujita, H., T. Nedachi, and M. Kanzaki, *Accelerated de novo sarcomere assembly by electric pulse stimulation in C2C12 myotubes.* Exp Cell Res, 2007. **313**(9): p. 1853-65.

479. Khodabukus, A. and K. Baar, *Defined electrical stimulation emphasizing excitability for the development and testing of engineered skeletal muscle.* Tissue Eng Part C Methods, 2012. **18**(5): p. 349-57.

480. Liao, I.C., et al., *Effect of Electromechanical Stimulation on the Maturation of Myotubes on Aligned Electrospun Fibers.* Cell Mol Bioeng, 2008. **1**(2-3): p. 133-145.

481. Huang, Y.C., R.G. Dennis, and K. Baar, *Cultured slow vs. fast skeletal muscle cells differ in physiology and responsiveness to stimulation.* Am J Physiol Cell Physiol, 2006. **291**(1): p. C11-7.

482. Flaibani, M., et al., *Muscle differentiation and myotubes alignment is influenced by micropatterned surfaces and exogenous electrical stimulation.* Tissue Eng Part A, 2009. **15**(9): p. 2447-57.

483. Chen, M.C., Y.C. Sun, and Y.H. Chen, *Electrically conductive nanofibers with highly oriented structures and their potential application in skeletal muscle tissue engineering.* Acta Biomater, 2013. **9**(3): p. 5562-72.

484. Khodabukus, A. and K. Baar, *Factors That Affect Tissue-Engineered Skeletal Muscle Function and Physiology.* Cells Tissues Organs, 2016. **202**(3-4): p. 159-168.

485. Sicari, B.M., et al., *A murine model of volumetric muscle loss and a regenerative medicine approach for tissue replacement.* Tissue Eng Part A, 2012. **18**(19-20): p. 1941-8.

486. Bursac, N., M. Juhas, and T.A. Rando, *Synergizing Engineering and Biology to Treat and Model Skeletal Muscle Injury and Disease.* Annu Rev Biomed Eng, 2015. **17**: p. 217-42.

487. Levenberg, S. and R. Langer, *Advances in tissue engineering.* Curr Top Dev Biol, 2004. **61**: p. 113-34.

488. van der Schaft, D.W., et al., *Mechanoregulation of vascularization in aligned tissue-engineered muscle: a role for vascular endothelial growth factor.* Tissue Eng Part A, 2011. **17**(21-22): p. 2857-65.

489. Koffler, J., et al., *Improved vascular organization enhances functional integration of engineered skeletal muscle grafts.* Proc Natl Acad Sci U S A, 2011. **108**(36): p. 14789-94.

490. Sasagawa, T., et al., *Design of prevascularized three-dimensional cell-dense tissues using a cell sheet stacking manipulation technology.* Biomaterials, 2010. **31**(7): p. 1646-54.

491. Shvartsman, D., et al., *Sustained delivery of VEGF maintains innervation and promotes reperfusion in ischemic skeletal muscles via NGF/GDNF signaling.* Mol Ther, 2014. **22**(7): p. 1243-1253.

492. Zhou, W., et al., *Angiogenic gene-modified myoblasts promote vascularization during repair of skeletal muscle defects.* J Tissue Eng Regen Med, 2015. **9**(12): p. 1404-16.

493. Messina, A., et al., *Generation of a vascularized organoid using skeletal muscle as the inductive source.* FASEB J, 2005. **19**(11): p. 1570-2.

494. Tilkorn, D.J., et al., *Implanted myoblast survival is dependent on the degree of vascularization in a novel delayed implantation/prevascularization tissue engineering model.* Tissue Eng Part A, 2010. **16**(1): p. 165-78.

495.   Jarvinen, T.A., et al., *Muscle injuries: biology and treatment.* Am J Sports Med, 2005. **33**(5): p. 745-64.
496.   Guo, X., et al., *Neuromuscular junction formation between human stem-cell-derived motoneurons and rat skeletal muscle in a defined system.* Tissue Eng Part C Methods, 2010. **16**(6): p. 1347-55.
497.   Larkin, L.M., et al., *Functional evaluation of nerve-skeletal muscle constructs engineered in vitro.* In Vitro Cell Dev Biol Anim, 2006. **42**(3-4): p. 75-82.
498.   Morimoto, Y., et al., *Three-dimensional neuron-muscle constructs with neuromuscular junctions.* Biomaterials, 2013. **34**(37): p. 9413-9.
499.   Wagner, S., et al., *Functional maturation of nicotinic acetylcholine receptors as an indicator of murine muscular differentiation in a new nerve-muscle co-culture system.* Pflugers Arch, 2003. **447**(1): p. 14-22.
500.   Wang, L., J. Shansky, and H. Vandenburgh, *Induced formation and maturation of acetylcholine receptor clusters in a defined 3D bio-artificial muscle.* Mol Neurobiol, 2013. **48**(3): p. 397-403.
501.   Dhawan, V., et al., *Neurotization improves contractile forces of tissue-engineered skeletal muscle.* Tissue Eng, 2007. **13**(11): p. 2813-21.
502.   Kang, S.B., et al., *Functional recovery of completely denervated muscle: implications for innervation of tissue-engineered muscle.* Tissue Eng Part A, 2012. **18**(17-18): p. 1912-20.
503.   Bezakova, G., et al., *Effects of purified recombinant neural and muscle agrin on skeletal muscle fibers in vivo.* J Cell Biol, 2001. **153**(7): p. 1441-52.
504.   Bian, W. and N. Bursac, *Soluble miniagrin enhances contractile function of engineered skeletal muscle.* FASEB J, 2012. **26**(2): p. 955-65.
505.   Ko, I.K., et al., *The effect of in vitro formation of acetylcholine receptor (AChR) clusters in engineered muscle fibers on subsequent innervation of constructs in vivo.* Biomaterials, 2013. **34**(13): p. 3246-55.
506.   Morawitz, P., *Die Chemie der Blutgerinnung.* Ergebnisse der Physiologie, 1905. **4**(1): p. 307-422.
507.   Davie, E.W., K. Fujikawa, and W. Kisiel, *The coagulation cascade: initiation, maintenance, and regulation.* Biochemistry, 1991. **30**(43): p. 10363-70.
508.   Davie, E.W. and O.D. Ratnoff, *Waterfall Sequence for Intrinsic Blood Clotting.* Science, 1964. **145**(3638): p. 1310-2.
509.   Macfarlane, R.G., *An Enzyme Cascade in the Blood Clotting Mechanism, and Its Function as a Biochemical Amplifier.* Nature, 1964. **202**: p. 498-9.
510.   Whelan, D., N.M. Caplice, and A.J. Clover, *Fibrin as a delivery system in wound healing tissue engineering applications.* J Control Release, 2014. **196**: p. 1-8.
511.   Doolittle, R.F., *The evolution of vertebrate fibrinogen.* Fed Proc, 1976. **35**(10): p. 2145-9.
512.   Doolittle, R.F., G. Spraggon, and S.J. Everse, *Evolution of vertebrate fibrin formation and the process of its dissolution.* Ciba Found Symp, 1997. **212**: p. 4-17; discussion 17-23.
513.   Clemetson, K.J., *Platelets and primary haemostasis.* Thromb Res, 2012. **129**(3): p. 220-4.
514.   Heemskerk, J.W., E.M. Bevers, and T. Lindhout, *Platelet activation and blood coagulation.* Thromb Haemost, 2002. **88**(2): p. 186-93.
515.   Bennett, J.S., *Structure and function of the platelet integrin alphaIIbbeta3.* J Clin Invest, 2005. **115**(12): p. 3363-9.
516.   Charo, I.F., L.S. Bekeart, and D.R. Phillips, *Platelet glycoprotein IIb-IIIa-like proteins mediate endothelial cell attachment to adhesive proteins and the extracellular matrix.* J Biol Chem, 1987. **262**(21): p. 9935-8.
517.   Mackman, N., R.E. Tilley, and N.S. Key, *Role of the extrinsic pathway of blood coagulation in hemostasis and thrombosis.* Arterioscler Thromb Vasc Biol, 2007. **27**(8): p. 1687-93.
518.   Lasne, D., B. Jude, and S. Susen, *From normal to pathological hemostasis.* Can J Anaesth, 2006. **53**(6 Suppl): p. S2-11.
519.   Veldman, A., M. Hoffman, and S. Ehrenforth, *New insights into the coagulation system and implications for new therapeutic options with recombinant factor VIIa.* Curr Med Chem, 2003. **10**(10): p. 797-811.
520.   Owens, A.P., 3rd and N. Mackman, *Tissue factor and thrombosis: The clot starts here.* Thromb Haemost, 2010. **104**(3): p. 432-9.
521.   Gailani, D. and T. Renne, *Intrinsic pathway of coagulation and arterial thrombosis.* Arterioscler Thromb Vasc Biol, 2007. **27**(12): p. 2507-13.
522.   Renne, T. and D. Gailani, *Role of Factor XII in hemostasis and thrombosis: clinical implications.* Expert Rev Cardiovasc Ther, 2007. **5**(4): p. 733-41.
523.   Kalafatis, M., et al., *The regulation of clotting factors.* Crit Rev Eukaryot Gene Expr, 1997. **7**(3): p. 241-80.
524.   Clark, R.A., *Fibrin and wound healing.* Ann N Y Acad Sci, 2001. **936**: p. 355-67.
525.   Laurens, N., P. Koolwijk, and M.P. de Maat, *Fibrin structure and wound healing.* J Thromb Haemost, 2006. **4**(5): p. 932-9.
526.   Lazarus, G.S., et al., *Definitions and guidelines for assessment of wounds and evaluation of healing.* Wound Repair Regen, 1994. **2**(3): p. 165-70.
527.   Reinke, J.M. and H. Sorg, *Wound repair and regeneration.* Eur Surg Res, 2012. **49**(1): p. 35-43.
528.   Clark, R.A., *Fibrin is a many splendored thing.* J Invest Dermatol, 2003. **121**(5): p. xxi-xxii.
529.   Fernandez, H.N., et al., *Chemotactic response to human C3a and C5a anaphylatoxins. I. Evaluation of C3a and C5a leukotaxis in vitro and under stimulated in vivo conditions.* J Immunol, 1978. **120**(1): p. 109-15.
530.   Ghebrehiwet, B., M. Silverberg, and A.P. Kaplan, *Activation of the classical pathway of complement by Hageman factor fragment.* J Exp Med, 1981. **153**(3): p. 665-76.
531.   Muller-Esterl, W., *Kininogens, kinins and kinships.* Thromb Haemost, 1989. **61**(1): p. 2-6.
532.   Blystone, S.D., et al., *Integrin alpha v beta 3 differentially regulates adhesive and phagocytic functions of the fibronectin receptor alpha 5 beta 1.* J Cell Biol, 1994. **127**(4): p. 1129-37.
533.   Brown, L.F., et al., *Fibroblast migration in fibrin gel matrices.* Am J Pathol, 1993. **142**(1): p. 273-83.
534.   Cheresh, D.A., et al., *Recognition of distinct adhesive sites on fibrinogen by related integrins on platelets and endothelial cells.* Cell, 1989. **58**(5): p. 945-53.

535.   Ciano, P.S., et al., *Macrophage migration in fibrin gel matrices.* Lab Invest, 1986. **54**(1): p. 62-70.
536.   Clark, R.A., et al., *Transient functional expression of alphaVbeta 3 on vascular cells during wound repair.* Am J Pathol, 1996. **148**(5): p. 1407-21.
537.   Gailit, J., et al., *Human fibroblasts bind directly to fibrinogen at RGD sites through integrin alpha(v)beta3.* Exp Cell Res, 1997. **232**(1): p. 118-26.
538.   Greiling, D. and R.A. Clark, *Fibronectin provides a conduit for fibroblast transmigration from collagenous stroma into fibrin clot provisional matrix.* J Cell Sci, 1997. **110 (Pt 7)**: p. 861-70.
539.   Knox, P., S. Crooks, and C.S. Rimmer, *Role of fibronectin in the migration of fibroblasts into plasma clots.* J Cell Biol, 1986. **102**(6): p. 2318-23.
540.   Lanir, N., et al., *Macrophage migration in fibrin gel matrices. II. Effects of clotting factor XIII, fibronectin, and glycosaminoglycan content on cell migration.* J Immunol, 1988. **140**(7): p. 2340-9.
541.   Gray, A.J., et al., *A alpha and B beta chains of fibrinogen stimulate proliferation of human fibroblasts.* J Cell Sci, 1993. **104 (Pt 2)**: p. 409-13.
542.   Juliano, R.L. and S. Haskill, *Signal transduction from the extracellular matrix.* J Cell Biol, 1993. **120**(3): p. 577-85.
543.   Postlethwaite, A.E., et al., *Induction of fibroblast chemotaxis by fibronectin. Localization of the chemotactic region to a 140,000-molecular weight non-gelatin-binding fragment.* J Exp Med, 1981. **153**(2): p. 494-9.
544.   Schwartz, M.A., M.D. Schaller, and M.H. Ginsberg, *Integrins: emerging paradigms of signal transduction.* Annu Rev Cell Dev Biol, 1995. **11**: p. 549-99.
545.   Shaw, R.J., et al., *Adherence-dependent increase in human monocyte PDGF(B) mRNA is associated with increases in c-fos, c-jun, and EGR2 mRNA.* J Cell Biol, 1990. **111**(5 Pt 1): p. 2139-48.
546.   Simon, D.I., et al., *Mac-1 (CD11b/CD18) and the urokinase receptor (CD87) form a functional unit on monocytic cells.* Blood, 1996. **88**(8): p. 3185-94.
547.   Trezzini, C., et al., *Evidence that exposure to fibrinogen or to antibodies directed against Mac-1 (CD11b/CD18; CR3) modulates human monocyte effector functions.* Br J Haematol, 1991. **77**(1): p. 16-24.
548.   Tuan, T.L., et al., *In vitro fibroplasia: matrix contraction, cell growth, and collagen production of fibroblasts cultured in fibrin gels.* Exp Cell Res, 1996. **223**(1): p. 127-34.
549.   Vaalamo, M., et al., *Distinct populations of stromal cells express collagenase-3 (MMP-13) and collagenase-1 (MMP-1) in chronic ulcers but not in normally healing wounds.* J Invest Dermatol, 1997. **109**(1): p. 96-101.
550.   Welch, M.P., G.F. Odland, and R.A. Clark, *Temporal relationships of F-actin bundle formation, collagen and fibronectin matrix assembly, and fibronectin receptor expression to wound contraction.* J Cell Biol, 1990. **110**(1): p. 133-45.
551.   Wynn, T.A. and K.M. Vannella, *Macrophages in Tissue Repair, Regeneration, and Fibrosis.* Immunity, 2016. **44**(3): p. 450-62.
552.   Xu, J. and R.A. Clark, *Extracellular matrix alters PDGF regulation of fibroblast integrins.* J Cell Biol, 1996. **132**(1-2): p. 239-49.
553.   Brown, N.J., et al., *Fibrinogen E fragment selectively disrupts the vasculature and inhibits the growth of tumours in a syngeneic murine model.* Br J Cancer, 2002. **86**(11): p. 1813-6.
554.   Groger, M., et al., *Peptide Bbeta(15-42) preserves endothelial barrier function in shock.* PLoS One, 2009. **4**(4): p. e5391.
555.   Jennewein, C., et al., *Novel aspects of fibrin(ogen) fragments during inflammation.* Mol Med, 2011. **17**(5-6): p. 568-73.
556.   Kazura, J.W., et al., *Modulation of polymorphonuclear leukocyte microbicidal activity and oxidative metabolism by fibrinogen degradation products D and E.* J Clin Invest, 1989. **83**(6): p. 1916-24.
557.   Lalla, R.V., M.L. Tanzer, and D.L. Kreutzer, *Identification of a region of the fibrin molecule involved in upregulation of interleukin-8 expression from human oral squamous cell carcinoma cells.* Arch Oral Biol, 2003. **48**(4): p. 263-71.
558.   Richardson, D.L., D.S. Pepper, and A.B. Kay, *Chemotaxis for human monocytes by fibrinogen-derived peptides.* Br J Haematol, 1976. **32**(4): p. 507-13.
559.   Roesner, J.P., et al., *Bbeta15-42 (FX06) reduces pulmonary, myocardial, liver, and small intestine damage in a pig model of hemorrhagic shock and reperfusion.* Crit Care Med, 2009. **37**(2): p. 598-605.
560.   Senior, R.M., et al., *Effects of fibrinogen derivatives upon the inflammatory response. Studies with human fibrinopeptide B.* J Clin Invest, 1986. **77**(3): p. 1014-9.
561.   Staton, C.A., et al., *Alphastatin, a 24-amino acid fragment of human fibrinogen, is a potent new inhibitor of activated endothelial cells in vitro and in vivo.* Blood, 2004. **103**(2): p. 601-6.
562.   Campbell, P.G., et al., *Insulin-like growth factor-binding protein-3 binds fibrinogen and fibrin.* J Biol Chem, 1999. **274**(42): p. 30215-21.
563.   Dohan, D.M., et al., *Platelet-rich fibrin (PRF): a second-generation platelet concentrate. Part II: platelet-related biologic features.* Oral Surg Oral Med Oral Pathol Oral Radiol Endod, 2006. **101**(3): p. e45-50.
564.   Grainger, D.J., et al., *Release and activation of platelet latent TGF-beta in blood clots during dissolution with plasmin.* Nat Med, 1995. **1**(9): p. 932-7.
565.   Sahni, A., O.D. Altland, and C.W. Francis, *FGF-2 but not FGF-1 binds fibrin and supports prolonged endothelial cell growth.* J Thromb Haemost, 2003. **1**(6): p. 1304-10.
566.   Sahni, A. and C.W. Francis, *Vascular endothelial growth factor binds to fibrinogen and fibrin and stimulates endothelial cell proliferation.* Blood, 2000. **96**(12): p. 3772-8.
567.   Sahni, A., et al., *Interleukin-1beta but not IL-1alpha binds to fibrinogen and fibrin and has enhanced activity in the bound form.* Blood, 2004. **104**(2): p. 409-14.
568.   Sahni, A., T. Odrljin, and C.W. Francis, *Binding of basic fibroblast growth factor to fibrinogen and fibrin.* J Biol Chem, 1998. **273**(13): p. 7554-9.

569. Dvorak, H.F., et al., *Fibrin containing gels induce angiogenesis. Implications for tumor stroma generation and wound healing.* Lab Invest, 1987. **57**(6): p. 673-86.
570. Jakob, W., J. Zipper, and E.D. Jentzsch, *Is the formation of fibrin a necessary event for the initiation of angiogenic responses in the chick chorioallantoic membrane?* Exp Pathol, 1982. **21**(4): p. 251-62.
571. Knighton, D.R., et al., *Role of platelets and fibrin in the healing sequence: an in vivo study of angiogenesis and collagen synthesis.* Ann Surg, 1982. **196**(4): p. 379-88.
572. Bugge, T.H., et al., *Loss of fibrinogen rescues mice from the pleiotropic effects of plasminogen deficiency.* Cell, 1996. **87**(4): p. 709-19.
573. Romer, J., et al., *Plasminogen and wound healing.* Nat Med, 1996. **2**(7): p. 725.
574. Astrup, T., *The biological significance of fibrinolysis.* Lancet, 1956. **271**(6942): p. 565-8.
575. Astrup, T., *The haemostatic balance.* Thromb Diath Haemorrh, 1958. **2**(3-4): p. 347-57.
576. Sidelmann, J.J., et al., *Fibrin clot formation and lysis: basic mechanisms.* Semin Thromb Hemost, 2000. **26**(6): p. 605-18.
577. Sierra, D.H., *Fibrin sealant adhesive systems: a review of their chemistry, material properties and clinical applications.* J Biomater Appl, 1993. **7**(4): p. 309-52.
578. Weisel, J.W., *Fibrinogen and fibrin.* Adv Protein Chem, 2005. **70**: p. 247-99.
579. Mosesson, M.W., *Fibrinogen and fibrin structure and functions.* J Thromb Haemost, 2005. **3**(8): p. 1894-904.
580. Undas, A. and R.A. Ariens, *Fibrin clot structure and function: a role in the pathophysiology of arterial and venous thromboembolic diseases.* Arterioscler Thromb Vasc Biol, 2011. **31**(12): p. e88-99.
581. Burton, R.A., et al., *Identification of an ordered compact structure within the recombinant bovine fibrinogen alphaC-domain fragment by NMR.* Biochemistry, 2006. **45**(7): p. 2257-66.
582. Tsurupa, G., et al., *Structure, stability, and interaction of fibrin alphaC-domain polymers.* Biochemistry, 2011. **50**(37): p. 8028-37.
583. Veklich, Y.I., et al., *Carboxyl-terminal portions of the alpha chains of fibrinogen and fibrin. Localization by electron microscopy and the effects of isolated alpha C fragments on polymerization.* J Biol Chem, 1993. **268**(18): p. 13577-85.
584. Blomback, B., B. Hessel, and D. Hogg, *Disulfide bridges in nh2 -terminal part of human fibrinogen.* Thromb Res, 1976. **8**(5): p. 639-58.
585. Henschen, A., et al., *Covalent structure of fibrinogen.* Ann N Y Acad Sci, 1983. **408**: p. 28-43.
586. Hoeprich, P.D., Jr. and R.F. Doolittle, *Dimeric half-molecules of human fibrinogen are joined through disulfide bonds in an antiparallel orientation.* Biochemistry, 1983. **22**(9): p. 2049-55.
587. Huang, S., Z. Cao, and E.W. Davie, *The role of amino-terminal disulfide bonds in the structure and assembly of human fibrinogen.* Biochem Biophys Res Commun, 1993. **190**(2): p. 488-95.
588. Zhang, J.Z. and C.M. Redman, *Identification of B beta chain domains involved in human fibrinogen assembly.* J Biol Chem, 1992. **267**(30): p. 21727-32.
589. Zhang, J.Z. and C.M. Redman, *Role of interchain disulfide bonds on the assembly and secretion of human fibrinogen.* J Biol Chem, 1994. **269**(1): p. 652-8.
590. Chung, D.W. and E.W. Davie, *gamma and gamma' chains of human fibrinogen are produced by alternative mRNA processing.* Biochemistry, 1984. **23**(18): p. 4232-6.
591. Mosesson, M.W., J.S. Finlayson, and R.A. Umfleet, *Human fibrinogen heterogeneities. 3. Identification of chain variants.* J Biol Chem, 1972. **247**(16): p. 5223-7.
592. Wolfenstein-Todel, C. and M.W. Mosesson, *Human plasma fibrinogen heterogeneity: evidence for an extended carboxyl-terminal sequence in a normal gamma chain variant (gamma').* Proc Natl Acad Sci U S A, 1980. **77**(9): p. 5069-73.
593. Altieri, D.C., et al., *A unique recognition site mediates the interaction of fibrinogen with the leukocyte integrin Mac-1 (CD11b/CD18).* J Biol Chem, 1990. **265**(21): p. 12119-22.
594. Hettasch, J.M., M.G. Bolyard, and S.T. Lord, *The residues AGDV of recombinant gamma chains of human fibrinogen must be carboxy-terminal to support human platelet aggregation.* Thromb Haemost, 1992. **68**(6): p. 701-6.
595. Lishko, V.K., et al., *Regulated unmasking of the cryptic binding site for integrin alpha M beta 2 in the gamma C-domain of fibrinogen.* Biochemistry, 2002. **41**(43): p. 12942-51.
596. Dyr, J.E., et al., *Conversion of fibrinogen to fibrin induced by preferential release of fibrinopeptide B.* Biochim Biophys Acta, 1989. **990**(1): p. 18-24.
597. Mihalyi, E., *Clotting of bovine fibrinogen. Calcium binding to fibrin during clotting and its dependence on release of fibrinopeptide B.* Biochemistry, 1988. **27**(3): p. 967-76.
598. Odrljin, T.M., et al., *Calcium modulates plasmin cleavage of the fibrinogen D fragment gamma chain N-terminus: mapping of monoclonal antibody J88B to a plasmin sensitive domain of the gamma chain.* Biochim Biophys Acta, 1996. **1298**(1): p. 69-77.
599. Blomback, B., et al., *A two-step fibrinogen--fibrin transition in blood coagulation.* Nature, 1978. **275**(5680): p. 501-5.
600. Weisel, J.W. and R.I. Litvinov, *Mechanisms of fibrin polymerization and clinical implications.* Blood, 2013. **121**(10): p. 1712-9.
601. Pohl, J., H.D. Bruhn, and E. Christophers, *Thrombin and fibrin-induced growth of fibroblasts: role in wound repair and thrombus organization.* Klin Wochenschr, 1979. **57**(6): p. 273-7.
602. Weiss, R.H. and M. Maduri, *The mitogenic effect of thrombin in vascular smooth muscle cells is largely due to basic fibroblast growth factor.* J Biol Chem, 1993. **268**(8): p. 5724-7.
603. Weiss, R.H. and R. Nuccitelli, *Inhibition of tyrosine phosphorylation prevents thrombin-induced mitogenesis, but not intracellular free calcium release, in vascular smooth muscle cells.* J Biol Chem, 1992. **267**(8): p. 5608-13.
604. Hermans, J. and J. McDonagh, *Fibrin: structure and interactions.* Semin Thromb Hemost, 1982. **8**(1): p. 11-24.

605. Schwartz, M.L., et al., *Human Factor XIII from plasma and platelets. Molecular weights, subunit structures, proteolytic activation, and cross-linking of fibrinogen and fibrin.* J Biol Chem, 1973. **248**(4): p. 1395-407.

606. Bagoly, Z., et al., *Factor XIII, clot structure, thrombosis.* Thromb Res, 2012. **129**(3): p. 382-7.

607. Muszbek, L., R.A. Ariens, and A. Ichinose, *Factor XIII: recommended terms and abbreviations.* J Thromb Haemost, 2007. **5**(1): p. 181-3.

608. Lorand, L., *Factor XIII: structure, activation, and interactions with fibrinogen and fibrin.* Ann N Y Acad Sci, 2001. **936**: p. 291-311.

609. Janus, T.J., et al., *Promotion of thrombin-catalyzed activation of factor XIII by fibrinogen.* Biochemistry, 1983. **22**(26): p. 6269-72.

610. Lewis, S.D., et al., *Regulation of formation of factor XIIIa by its fibrin substrates.* Biochemistry, 1985. **24**(24): p. 6772-7.

611. Credo, R.B., C.G. Curtis, and L. Lorand, *Ca2+-related regulatory function of fibrinogen.* Proc Natl Acad Sci U S A, 1978. **75**(9): p. 4234-7.

612. Hornyak, T.J. and J.A. Shafer, *Role of calcium ion in the generation of factor XIII activity.* Biochemistry, 1991. **30**(25): p. 6175-82.

613. Lorand, L. and K. Konishi, *Activation of the Fibrin Stabilizing Factor of Plasma by Thrombin.* Arch Biochem Biophys, 1964. **105**: p. 58-67.

614. Donnelly, T.H., et al., *The proteolytic action of thrombin on fibrinogen.* J Biol Chem, 1956. **222**(2): p. 815-21.

615. Everse, S.J., et al., *Crystal structure of fragment double-D from human fibrin with two different bound ligands.* Biochemistry, 1998. **37**(24): p. 8637-42.

616. Pratt, K.P., et al., *The primary fibrin polymerization pocket: three-dimensional structure of a 30-kDa C-terminal gamma chain fragment complexed with the peptide Gly-Pro-Arg-Pro.* Proc Natl Acad Sci U S A, 1997. **94**(14): p. 7176-81.

617. Shimizu, A., G.M. Nagel, and R.F. Doolittle, *Photoaffinity labeling of the primary fibrin polymerization site: isolation and characterization of a labeled cyanogen bromide fragment corresponding to gamma-chain residues 337-379.* Proc Natl Acad Sci U S A, 1992. **89**(7): p. 2888-92.

618. Medved, L.V., et al., *Localization of a fibrin polymerization site complementary to Gly-His-Arg sequence.* FEBS Lett, 1993. **320**(3): p. 239-42.

619. Ferry, J.D., *The Mechanism of Polymerization of Fibrinogen.* Proc Natl Acad Sci U S A, 1952. **38**(7): p. 566-9.

620. Fowler, W.E., et al., *Structure of the fibrin protofibril.* Proc Natl Acad Sci U S A, 1981. **78**(8): p. 4872-6.

621. Medved, L., et al., *Electron microscope investigation of the early stages of fibrin assembly. Twisted protofibrils and fibers.* J Mol Biol, 1990. **216**(3): p. 503-9.

622. Mosesson, M.W., et al., *The role of fibrinogen D domain intermolecular association sites in the polymerization of fibrin and fibrinogen Tokyo II (gamma 275 Arg-->Cys).* J Clin Invest, 1995. **96**(2): p. 1053-8.

623. Spraggon, G., S.J. Everse, and R.F. Doolittle, *Crystal structures of fragment D from human fibrinogen and its crosslinked counterpart from fibrin.* Nature, 1997. **389**(6650): p. 455-62.

624. Weisel, J.W., Y. Veklich, and O. Gorkun, *The sequence of cleavage of fibrinopeptides from fibrinogen is important for protofibril formation and enhancement of lateral aggregation in fibrin clots.* J Mol Biol, 1993. **232**(1): p. 285-97.

625. Riedel, T., et al., *Fibrinopeptides A and B release in the process of surface fibrin formation.* Blood, 2011. **117**(5): p. 1700-6.

626. Litvinov, R.I., et al., *Polymerization of fibrin: Direct observation and quantification of individual B:b knob-hole interactions.* Blood, 2007. **109**(1): p. 130-8.

627. Litvinov, R.I., et al., *Polymerization of fibrin: specificity, strength, and stability of knob-hole interactions studied at the single-molecule level.* Blood, 2005. **106**(9): p. 2944-51.

628. Mosesson, M.W., et al., *Studies on the ultrastructure of fibrin lacking fibrinopeptide B (beta-fibrin).* Blood, 1987. **69**(4): p. 1073-81.

629. Shainoff, J.R. and B.N. Dardik, *Fibrinopeptide B in fibrin assembly and metabolism: physiologic significance in delayed release of the peptide.* Ann N Y Acad Sci, 1983. **408**: p. 254-68.

630. Litvinov, R.I., et al., *Direct evidence for specific interactions of the fibrinogen alphaC-domains with the central E region and with each other.* Biochemistry, 2007. **46**(31): p. 9133-42.

631. Weisel, J.W. and L. Medved, *The structure and function of the alpha C domains of fibrinogen.* Ann N Y Acad Sci, 2001. **936**: p. 312-27.

632. Yang, Z., I. Mochalkin, and R.F. Doolittle, *A model of fibrin formation based on crystal structures of fibrinogen and fibrin fragments complexed with synthetic peptides.* Proc Natl Acad Sci U S A, 2000. **97**(26): p. 14156-61.

633. Okumura, N., et al., *A novel variant fibrinogen, deletion of Bbeta111Ser in coiled-coil region, affecting fibrin lateral aggregation.* Clin Chim Acta, 2006. **365**(1-2): p. 160-7.

634. Langer, B.G., et al., *Deglycosylation of fibrinogen accelerates polymerization and increases lateral aggregation of fibrin fibers.* J Biol Chem, 1988. **263**(29): p. 15056-63.

635. Mosesson, M.W., et al., *Identification and mass analysis of human fibrinogen molecules and their domains by scanning transmission electron microscopy.* J Mol Biol, 1981. **153**(3): p. 695-718.

636. Gorkun, O.V., et al., *Role of the alpha C domains of fibrin in clot formation.* Biochemistry, 1994. **33**(22): p. 6986-97.

637. Collet, J.P., et al., *The alphaC domains of fibrinogen affect the structure of the fibrin clot, its physical properties, and its susceptibility to fibrinolysis.* Blood, 2005. **106**(12): p. 3824-30.

638. Chernysh, I.N., C. Nagaswami, and J.W. Weisel, *Visualization and identification of the structures formed during early stages of fibrin polymerization.* Blood, 2011. **117**(17): p. 4609-14.

639. Hantgan, R., et al., *Fibrin assembly: a comparison of electron microscopic and light scattering results.* Thromb Haemost, 1980. **44**(3): p. 119-24.

640. Hantgan, R.R. and J. Hermans, *Assembly of fibrin. A light scattering study.* J Biol Chem, 1979. **254**(22): p. 11272-81.

641. Cohen, C., J.P. Revel, and J. Kucera, *Paracrystalline forms of fibrinogen.* Science, 1963. **141**(3579): p. 436-8.

642. Stryer, L., C. Cohen, and R. Langridge, *Axial period of fibrinogen and fibrin.* Nature, 1963. **197**: p. 793-4.

643. Levy, J.H. and C. Greenberg, *Biology of Factor XIII and clinical manifestations of Factor XIII deficiency.* Transfusion, 2013. **53**(5): p. 1120-31.

644. Ariens, R.A., et al., *Role of factor XIII in fibrin clot formation and effects of genetic polymorphisms.* Blood, 2002. **100**(3): p. 743-54.

645. Chen, R. and R.F. Doolittle, *- cross-linking sites in human and bovine fibrin.* Biochemistry, 1971. **10**(24): p. 4487-91.

646. Doolittle, R.F., R. Chen, and F. Lau, *Hybrid fibrin: proof of the intermolecular nature of - crosslinking units.* Biochem Biophys Res Commun, 1971. **44**(1): p. 94-100.

647. Purves, L., M. Purves, and W. Brandt, *Cleavage of fibrin-derived D-dimer into monomers by endopeptidase from puff adder venom (Bitis arietans) acting at cross-linked sites of the gamma-chain. Sequence of carboxy-terminal cyanogen bromide gamma-chain fragments.* Biochemistry, 1987. **26**(15): p. 4640-6.

648. Mosesson, M.W., *Cross-linked gamma-chains in fibrin fibrils bridge 'transversely' between strands: yes.* J Thromb Haemost, 2004. **2**(3): p. 388-93.

649. Weisel, J.W., *Cross-linked gamma-chains in fibrin fibrils bridge transversely between strands: no.* J Thromb Haemost, 2004. **2**(3): p. 394-9.

650. Roska, F.J. and J.D. Ferry, *Studies of fibrin film. I. Stress relaxation and birefringence.* Biopolymers, 1982. **21**(9): p. 1811-32.

651. Guthold, M. and C.R. Carlisle, *Single fibrin fiber experiments suggest longitudinal rather than transverse cross-linking: reply to a rebuttal.* J Thromb Haemost, 2010. **8**: p. 2090-2091.

652. Liu, W., et al., *The mechanical properties of single fibrin fibers.* J Thromb Haemost, 2010. **8**(5): p. 1030-6.

653. Matsuka, Y.V., et al., *Factor XIIIa-catalyzed cross-linking of recombinant alpha C fragments of human fibrinogen.* Biochemistry, 1996. **35**(18): p. 5810-6.

654. Sobel, J.H. and M.A. Gawinowicz, *Identification of the alpha chain lysine donor sites involved in factor XIIIa fibrin cross-linking.* J Biol Chem, 1996. **271**(32): p. 19288-97.

655. Mosesson, M.W., et al., *Identification of covalently linked trimeric and tetrameric D domains in crosslinked fibrin.* Proc Natl Acad Sci U S A, 1989. **86**(4): p. 1113-7.

656. Standeven, K.F., et al., *Functional analysis of fibrin {gamma}-chain cross-linking by activated factor XIII: determination of a cross-linking pattern that maximizes clot stiffness.* Blood, 2007. **110**(3): p. 902-7.

657. Siebenlist, K.R. and M.W. Mosesson, *Evidence of intramolecular cross-linked A alpha.gamma chain heterodimers in plasma fibrinogen.* Biochemistry, 1996. **35**(18): p. 5817-21.

658. Mosesson, M.W., et al., *Evidence for a second type of fibril branch point in fibrin polymer networks, the trimolecular junction.* Blood, 1993. **82**(5): p. 1517-21.

659. Weisel, J.W. and C. Nagaswami, *Computer modeling of fibrin polymerization kinetics correlated with electron microscope and turbidity observations: clot structure and assembly are kinetically controlled.* Biophys J, 1992. **63**(1): p. 111-28.

660. Fogelson, A.L. and J.P. Keener, *Toward an understanding of fibrin branching structure.* Phys Rev E Stat Nonlin Soft Matter Phys, 2010. **81**(5 Pt 1): p. 051922.

661. Blomback, B., et al., *Fibrin in human plasma: gel architectures governed by rate and nature of fibrinogen activation.* Thromb Res, 1994. **75**(5): p. 521-38.

662. Ryan, E.A., et al., *Structural origins of fibrin clot rheology.* Biophys J, 1999. **77**(5): p. 2813-26.

663. Cesarman-Maus, G. and K.A. Hajjar, *Molecular mechanisms of fibrinolysis.* Br J Haematol, 2005. **129**(3): p. 307-21.

664. Raum, D., et al., *Synthesis of human plasminogen by the liver.* Science, 1980. **208**(4447): p. 1036-7.

665. Forsgren, M., et al., *Molecular cloning and characterization of a full-length cDNA clone for human plasminogen.* FEBS Lett, 1987. **213**(2): p. 254-60.

666. Miles, L.A., C.M. Dahlberg, and E.F. Plow, *The cell-binding domains of plasminogen and their function in plasma.* J Biol Chem, 1988. **263**(24): p. 11928-34.

667. Plow, E.F., J. Felez, and L.A. Miles, *Cellular regulation of fibrinolysis.* Thromb Haemost, 1991. **66**(1): p. 32-6.

668. Holvoet, P., H.R. Lijnen, and D. Collen, *A monoclonal antibody specific for Lys-plasminogen. Application to the study of the activation pathways of plasminogen in vivo.* J Biol Chem, 1985. **260**(22): p. 12106-11.

669. Medved, L. and W. Nieuwenhuizen, *Molecular mechanisms of initiation of fibrinolysis by fibrin.* Thromb Haemost, 2003. **89**(3): p. 409-19.

670. Law, R.H., et al., *The X-ray crystal structure of full-length human plasminogen.* Cell Rep, 2012. **1**(3): p. 185-90.

671. Longstaff, C. and K. Kolev, *Basic mechanisms and regulation of fibrinolysis.* J Thromb Haemost, 2015. **13 Suppl 1**: p. S98-105.

672. Levin, E.G. and G.J. del Zoppo, *Localization of tissue plasminogen activator in the endothelium of a limited number of vessels.* Am J Pathol, 1994. **144**(5): p. 855-61.

673. Horrevoets, A.J., H. Pannekoek, and M.E. Nesheim, *A steady-state template model that describes the kinetics of fibrin-stimulated [Glu1]- and [Lys78]plasminogen activation by native tissue-type plasminogen activator and variants that lack either the finger or kringle-2 domain.* J Biol Chem, 1997. **272**(4): p. 2183-91.

674. Hoylaerts, M., et al., *Kinetics of the activation of plasminogen by human tissue plasminogen activator. Role of fibrin.* J Biol Chem, 1982. **257**(6): p. 2912-9.

675. Kasai, S., et al., *Primary structure of single-chain pro-urokinase.* J Biol Chem, 1985. **260**(22): p. 12382-9.

676. Andreasen, P.A., et al., *The urokinase-type plasminogen activator system in cancer metastasis: a review.* Int J Cancer, 1997. **72**(1): p. 1-22.

677. Gurewich, V., et al., *Effective and fibrin-specific clot lysis by a zymogen precursor form of urokinase (pro-urokinase). A study in vitro and in two animal species.* J Clin Invest, 1984. **73**(6): p. 1731-9.

678. Lijnen, H.R., et al., *Activation of plasminogen by pro-urokinase. I. Mechanism.* J Biol Chem, 1986. **261**(3): p. 1253-8.

679. Bugge, T.H., et al., *Urokinase-type plasminogen activator is effective in fibrin clearance in the absence of its receptor or tissue-type plasminogen activator.* Proc Natl Acad Sci U S A, 1996. **93**(12): p. 5899-904.

680. Myohanen, H. and A. Vaheri, *Regulation and interactions in the activation of cell-associated plasminogen.* Cell Mol Life Sci, 2004. **61**(22): p. 2840-58.

681. Pennica, D., et al., *Cloning and expression of human tissue-type plasminogen activator cDNA in E. coli.* Nature, 1983. **301**(5897): p. 214-21.

682. Tate, K.M., et al., *Functional role of proteolytic cleavage at arginine-275 of human tissue plasminogen activator as assessed by site-directed mutagenesis.* Biochemistry, 1987. **26**(2): p. 338-43.

683. Colman, R.W., *Activation of plasminogen by human plasma kallikrein.* Biochem Biophys Res Commun, 1969. **35**(2): p. 273-9.

684. Goldsmith, G.H., Jr., H. Saito, and O.S. Ratnoff, *The activation of plasminogen by Hageman factor (Factor XII) and Hageman factor fragments.* J Clin Invest, 1978. **62**(1): p. 54-60.

685. Mandle, R.J., Jr. and A.P. Kaplan, *Hageman-factor-dependent fibrinolysis: generation of fibrinolytic activity by the interaction of human activated factor XI and plasminogen.* Blood, 1979. **54**(4): p. 850-62.

686. Travis, J. and G.S. Salvesen, *Human plasma proteinase inhibitors.* Annu Rev Biochem, 1983. **52**: p. 655-709.

687. Hekman, C.M. and D.J. Loskutoff, *Endothelial cells produce a latent inhibitor of plasminogen activators that can be activated by denaturants.* J Biol Chem, 1985. **260**(21): p. 11581-7.

688. Samad, F., K. Yamamoto, and D.J. Loskutoff, *Distribution and regulation of plasminogen activator inhibitor-1 in murine adipose tissue in vivo. Induction by tumor necrosis factor-alpha and lipopolysaccharide.* J Clin Invest, 1996. **97**(1): p. 37-46.

689. Wiman, B., L. Boman, and D. Collen, *On the kinetics of the reaction between human antiplasmin and a low-molecular-weight form of plasmin.* Eur J Biochem, 1978. **87**(1): p. 143-6.

690. Ponting, C.P., J.M. Marshall, and S.A. Cederholm-Williams, *Plasminogen: a structural review.* Blood Coagul Fibrinolysis, 1992. **3**(5): p. 605-14.

691. Schneider, M. and M. Nesheim, *A study of the protection of plasmin from antiplasmin inhibition within an intact fibrin clot during the course of clot lysis.* J Biol Chem, 2004. **279**(14): p. 13333-9.

692. Chapin, J.C. and K.A. Hajjar, *Fibrinolysis and the control of blood coagulation.* Blood Rev, 2015. **29**(1): p. 17-24.

693. Andreasen, P.A., et al., *Plasminogen activator inhibitor from human fibrosarcoma cells binds urokinase-type plasminogen activator, but not its proenzyme.* J Biol Chem, 1986. **261**(17): p. 7644-51.

694. Manchanda, N. and B.S. Schwartz, *Interaction of single-chain urokinase and plasminogen activator inhibitor type 1.* J Biol Chem, 1995. **270**(34): p. 20032-5.

695. Belin, D., *Biology and facultative secretion of plasminogen activator inhibitor-2.* Thromb Haemost, 1993. **70**(1): p. 144-7.

696. Mikus, P. and T. Ny, *Intracellular polymerization of the serpin plasminogen activator inhibitor type 2.* J Biol Chem, 1996. **271**(17): p. 10048-53.

697. Andreasen, P.A., et al., *Plasminogen activator inhibitors: hormonally regulated serpins.* Mol Cell Endocrinol, 1990. **68**(1): p. 1-19.

698. Ellis, V., et al., *Inhibition of receptor-bound urokinase by plasminogen-activator inhibitors.* J Biol Chem, 1990. **265**(17): p. 9904-8.

699. Sottrup-Jensen, L., *Alpha-macroglobulins: structure, shape, and mechanism of proteinase complex formation.* J Biol Chem, 1989. **264**(20): p. 11539-42.

700. Aoki, N., M. Moroi, and K. Tachiya, *Effects of alpha2-plasmin inhibitor on fibrin clot lysis. Its comparison with alpha2-macroglobulin.* Thromb Haemost, 1978. **39**(1): p. 22-31.

701. Stephens, R.W., et al., *Alpha 2-macroglobulin restricts plasminogen activation to the surface of RC2A leukemia cells.* Cell Regul, 1991. **2**(12): p. 1057-65.

702. Huisman, L.G., J.M. van Griensven, and C. Kluft, *On the role of C1-inhibitor as inhibitor of tissue-type plasminogen activator in human plasma.* Thromb Haemost, 1995. **73**(3): p. 466-71.

703. Bouton, M.C., et al., *Emerging role of serpinE2/protease nexin-1 in hemostasis and vascular biology.* Blood, 2012. **119**(11): p. 2452-7.

704. Eaton, D.L., et al., *Isolation, molecular cloning, and partial characterization of a novel carboxypeptidase B from human plasma.* J Biol Chem, 1991. **266**(32): p. 21833-8.

705. Nesheim, M., *Thrombin and fibrinolysis.* Chest, 2003. **124**(3 Suppl): p. 33S-9S.

706. Mutch, N.J., et al., *Thrombus lysis by uPA, scuPA and tPA is regulated by plasma TAFI.* J Thromb Haemost, 2003. **1**(9): p. 2000-7.

707. Silva, M.M., et al., *Regulation of fibrinolysis by C-terminal lysines operates through plasminogen and plasmin but not tissue-type plasminogen activator.* J Thromb Haemost, 2012. **10**(11): p. 2354-60.

708. Slaughter, T.F. and C.S. Greenberg, *Antifibrinolytic drugs and perioperative hemostasis.* Am J Hematol, 1997. **56**(1): p. 32-6.

709. Mosesson, M.W., et al., *Human fibrinogen heterogeneities. I. Structural and related studies of plasma fibrinogens which are high solubility catabolic intermediates.* J Biol Chem, 1972. **247**(16): p. 5210-9.

710. Koehn, J.A., et al., *Sequence of plasmin proteolysis at the NH2-terminus of the b beta-chain of human fibrinogen.* Anal Biochem, 1983. **133**(2): p. 502-10.

711. Kirschbaum, N.E. and A.Z. Budzynski, *A unique proteolytic fragment of human fibrinogen containing the A alpha COOH-terminal domain of the native molecule.* J Biol Chem, 1990. **265**(23): p. 13669-76.

712. Marder, V.J., N.R. Shulman, and W.R. Carroll, *High molecular weight derivatives of human fibrinogen produced by plasmin. I. Physicochemical and immunological characterization.* J Biol Chem, 1969. **244**(8): p. 2111-9.

713. Fowler, W.E., et al., *Electron microsocpy of plasmic fragments of human fibrinogen as related to trinodular structure of the intact molecule.* J Clin Invest, 1980. **66**(1): p. 50-6.

714. Norton, P.A. and H.S. Slayter, *Immune labeling of the D and E regions of human fibrinogen by electron microscopy.* Proc Natl Acad Sci U S A, 1981. **78**(3): p. 1661-5.

715. Price, T.M., et al., *Shadow-cast electron microscopy of fibrinogen with antibody fragments bound to specific regions.* Proc Natl Acad Sci U S A, 1981. **78**(1): p. 200-4.

716. Graeff, H. and R. Hafter, *Detection and relevance of crosslinked fibrin derivatives in blood.* Semin Thromb Hemost, 1982. **8**(1): p. 57-68.

717. Walker, J.B. and M.E. Nesheim, *The molecular weights, mass distribution, chain composition, and structure of soluble fibrin degradation products released from a fibrin clot perfused with plasmin.* J Biol Chem, 1999. **274**(8): p. 5201-12.

718. Varju, I., et al., *Fractal kinetic behavior of plasmin on the surface of fibrin meshwork.* Biochemistry, 2014. **53**(40): p. 6348-56.

719. Omar, M.N. and K.G. Mann, *Inactivation of factor Va by plasmin.* J Biol Chem, 1987. **262**(20): p. 9750-5.

720. Pryzdial, E.L., et al., *Plasmin converts factor X from coagulation zymogen to fibrinolysis cofactor.* J Biol Chem, 1999. **274**(13): p. 8500-5.

721. Rick, M.E. and D.M. Krizek, *Platelets modulate the proteolysis of factor VIII:C protein by plasmin.* Blood, 1986. **67**(6): p. 1649-54.

722. Samis, J.A., et al., *Proteolytic processing of human coagulation factor IX by plasmin.* Blood, 2000. **95**(3): p. 943-51.

723. Hoover-Plow, J., *Does plasmin have anticoagulant activity?* Vasc Health Risk Manag, 2010. **6**: p. 199-205.

724. Kaptoge, S., et al., *Associations of plasma fibrinogen levels with established cardiovascular disease risk factors, inflammatory markers, and other characteristics: individual participant meta-analysis of 154,211 adults in 31 prospective studies: the fibrinogen studies collaboration.* Am J Epidemiol, 2007. **166**(8): p. 867-79.

725. Undas, A., et al., *Altered fibrin clot structure/function in patients with idiopathic venous thromboembolism and in their relatives.* Blood, 2009. **114**(19): p. 4272-8.

726. Brown, A.C. and T.H. Barker, *Fibrin-based biomaterials: modulation of macroscopic properties through rational design at the molecular level.* Acta Biomater, 2014. **10**(4): p. 1502-14.

727. Benkherourou, M., et al., *Quantification and macroscopic modeling of the nonlinear viscoelastic behavior of strained gels with varying fibrin concentrations.* IEEE Trans Biomed Eng, 2000. **47**(11): p. 1465-75.

728. Velada, J.L., et al., *Reproducibility of the mechanical properties of Vivostat system patient-derived fibrin sealant.* Biomaterials, 2002. **23**(10): p. 2249-54.

729. Sierra, D.H., A.W. Eberhardt, and J.E. Lemons, *Failure characteristics of multiple-component fibrin-based adhesives.* J Biomed Mater Res, 2002. **59**(1): p. 1-11.

730. Duong, H., B. Wu, and B. Tawil, *Modulation of 3D fibrin matrix stiffness by intrinsic fibrinogen-thrombin compositions and by extrinsic cellular activity.* Tissue Eng Part A, 2009. **15**(7): p. 1865-76.

731. Wolberg, A.S., *Thrombin generation and fibrin clot structure.* Blood Rev, 2007. **21**(3): p. 131-42.

732. Collet, J.P., et al., *Altered fibrin architecture is associated with hypofibrinolysis and premature coronary atherothrombosis.* Arterioscler Thromb Vasc Biol, 2006. **26**(11): p. 2567-73.

733. Collet, J.P., et al., *Influence of fibrin network conformation and fibrin fiber diameter on fibrinolysis speed: dynamic and structural approaches by confocal microscopy.* Arterioscler Thromb Vasc Biol, 2000. **20**(5): p. 1354-61.

734. Carr, M.E., Jr., D.A. Gabriel, and J. McDonagh, *Influence of Ca2+ on the structure of reptilase-derived and thrombin-derived fibrin gels.* Biochem J, 1986. **239**(3): p. 513-6.

735. Wang, M.-C., G.D. Pins, and F.H. Silver, *Preparation of fibrin glue: the effects of calcium chloride and sodium chloride.* Materials Science and Engineering: C, 1995. **3**(2): p. 131-135.

736. Hardy, J.J., N.A. Carrell, and J. McDonagh, *Calcium ion functions in fibrinogen conversion to fibrin.* Ann N Y Acad Sci, 1983. **408**: p. 279-87.

737. Brass, E.P., et al., *Fibrin formation: effect of calcium ions.* Blood, 1978. **52**(4): p. 654-8.

738. Kopper, P.H., *Role of Calcium in Fibrin Formation.* Nature, 1963. **198**(4879): p. 493-494.

739. Haverkate, F. and G. Timan, *Protective effect of calcium in the plasmin degradation of fibrinogen and fibrin fragments D.* Thromb Res, 1977. **10**(6): p. 803-12.

740. Ly, B. and H.C. Godal, *Denaturation of Fibrinogen, the Protective Effect of Calcium.* Pathophysiology of Haemostasis and Thrombosis, 1972. **1**(3-4): p. 204-209.

741. Okada, M. and B. Blomback, *Calcium and fibrin gel structure.* Thromb Res, 1983. **29**(3): p. 269-80.

742. Chiu, C.L., et al., *Permeability of three-dimensional fibrin constructs corresponds to fibrinogen and thrombin concentrations.* Biores Open Access, 2012. **1**(1): p. 34-40.

743. Lord, S.T., *Molecular mechanisms affecting fibrin structure and stability.* Arterioscler Thromb Vasc Biol, 2011. **31**(3): p. 494-9.

744. Weisel, J.W. and R.I. Litvinov, *The biochemical and physical process of fibrinolysis and effects of clot structure and stability on the lysis rate.* Cardiovasc Hematol Agents Med Chem, 2008. **6**(3): p. 161-80.

745. Ajjan, R.A., et al., *Effects of aspirin on clot structure and fibrinolysis using a novel in vitro cellular system.* Arterioscler Thromb Vasc Biol, 2009. **29**(5): p. 712-7.

746. He, S., et al., *Effects of acetylsalicylic acid on increase of fibrin network porosity and the consequent upregulation of fibrinolysis.* J Cardiovasc Pharmacol, 2009. **53**(1): p. 24-9.

747. Smith, S.A. and J.H. Morrissey, *Polyphosphate enhances fibrin clot structure.* Blood, 2008. **112**(7): p. 2810-6.

748. Scheule, A.M., et al., *Repeated anaphylactic reactions to aprotinin in fibrin sealant.* Gastrointest Endosc, 1998. **48**(1): p. 83-5.

749. Aminbhavi, T.M., et al., *Controlled release of therapeutics using interpenetrating polymeric networks.* Expert Opin Drug Deliv, 2015. **12**(4): p. 669-88.

750. Zoratto, N. and P. Matricardi, *Semi-IPN- and IPN-Based Hydrogels.* Adv Exp Med Biol, 2018. **1059**: p. 155-188.

751. Jenkins, A.D., et al., *Glossary of basic terms in polymer science (IUPAC recommendations 1996).* Pure Appl Chem, 1996. **68**: p. 2287-2311.

752. Rowe, S.L. and J.P. Stegemann, *Interpenetrating collagen-fibrin composite matrices with varying protein contents and ratios.* Biomacromolecules, 2006. **7**(11): p. 2942-8.

753. Lee, F. and M. Kurisawa, *Formation and stability of interpenetrating polymer network hydrogels consisting of fibrin and hyaluronic acid for tissue engineering.* Acta Biomater, 2013. **9**(2): p. 5143-52.

754. Shikanov, A., et al., *Interpenetrating fibrin-alginate matrices for in vitro ovarian follicle development.* Biomaterials, 2009. **30**(29): p. 5476-85.

755. Akpalo, E., et al., *Fibrin-polyethylene oxide interpenetrating polymer networks: new self-supported biomaterials combining the properties of both protein gel and synthetic polymer.* Acta Biomater, 2011. **7**(6): p. 2418-27.

756. Gsib, O., et al., *Evaluation of Fibrin-Based Interpenetrating Polymer Networks as Potential Biomaterials for Tissue Engineering.* Nanomaterials (Basel), 2017. **7**(12).

757. Bidault, L., et al., *Self-supported fibrin-polyvinyl alcohol interpenetrating polymer networks: an easily handled and rehydratable biomaterial.* Biomacromolecules, 2013. **14**(11): p. 3870-9.

758. Lohani, A., et al., *Interpenetrating polymer networks as innovative drug delivery systems.* J Drug Deliv, 2014. **2014**: p. 583612.

759. Matricardi, P., et al., *Interpenetrating Polymer Networks polysaccharide hydrogels for drug delivery and tissue engineering.* Adv Drug Deliv Rev, 2013. **65**(9): p. 1172-87.

760. MacGillivray, T.E., *Fibrin sealants and glues.* J Card Surg, 2003. **18**(6): p. 480-5.

761. Mintz, P.D., et al., *Fibrin sealant: clinical use and the development of the University of Virginia Tissue Adhesive Center.* Ann Clin Lab Sci, 2001. **31**(1): p. 108-18.

762. Janmey, P.A., J.P. Winer, and J.W. Weisel, *Fibrin gels and their clinical and bioengineering applications.* J R Soc Interface, 2009. **6**(30): p. 1-10.

763. Bergel, S., *Über Wirkungen des Fibrins.* Dtsch Med Wochenschr, 1909. **35**: p. 633-665.

764. Cronkite, E.P., E.L. Lozner, and J.M. Deaver, *Use of thrombin and fibrinogen in skin grafting.* Journal of the American Medical Association, 1944. **124**: p. 976-978.

765. Tidrick, R.T. and E.D. Warner, *Fibrin fixation of skin transplants.* Surgery, 1944. **15**: p. 90-95.

766. Matras, H., et al., *[Suture-free interfascicular nerve transplantation in animal experiments].* Wien Med Wochenschr, 1972. **122**(37): p. 517-23.

767. Kuderna, H. and H. Matras, *Die klinische Anwendung der Klebung von Nervenanastomosen mit Gerinnungssubstanzen bei der Rekonstruktion verletzter periphärer Nerven.* Wien Klin Wschr, 1975. **37**: p. 495.

768. Fuhge, P., et al., *Readily Dissolvable Lyophilized Fibrinogen Formulation.* United States Patent #4, 1987: p. 650, 678.

769. Heimburger, N., P. Fuhge, and H. Ronneberge, *Single-Component Tissue Adhesives Containing Fibrinogen, Factor XIII, Thrombin Inhibitor, Prothrombin Factors and Calcium Ions in Aqueous Solution.* European Patent #87109374, 1987.

770. Dorion, R.P., et al., *Risk and clinical significance of developing antibodies induced by topical thrombin preparations.* Arch Pathol Lab Med, 1998. **122**(10): p. 887-94.

771. Ortel, T.L., et al., *Topical thrombin and acquired coagulation factor inhibitors: clinical spectrum and laboratory diagnosis.* Am J Hematol, 1994. **45**(2): p. 128-35.

772. Hile, J.P., *Fibrinogen (human): revocation of licenses.* Fed Regist, 1978(43): p. 1131-1132.

773. Joch, C., *The safety of fibrin sealants.* Cardiovasc Surg, 2003. **11 Suppl 1**: p. 23-8.

774. Albala, D.M., *Fibrin sealants in clinical practice.* Cardiovasc Surg, 2003. **11 Suppl 1**: p. 5-11.

775. Jackson, M.R., *Fibrin sealants in surgical practice: An overview.* Am J Surg, 2001. **182**(2 Suppl): p. 1S-7S.

776. Pankov, R. and K.M. Yamada, *Fibronectin at a glance.* J Cell Sci, 2002. **115**(Pt 20): p. 3861-3.

777. Igisu, K., *The role of fibronectin in the process of wound healing.* Thromb Res, 1986. **44**(4): p. 455-65.

778. Spotnitz, W.D. and S. Burks, *Hemostats, sealants, and adhesives: components of the surgical toolbox.* Transfusion, 2008. **48**(7): p. 1502-16.

779. Gibble, J.W. and P.M. Ness, *Fibrin glue: the perfect operative sealant?* Transfusion, 1990. **30**(8): p. 741-7.

780. Herod, E.L., *Cyanoacrylates in dentistry: a review of the literature.* J Can Dent Assoc, 1990. **56**(4): p. 331-4.

781. Kjaergard, H.K. and J.E. Fairbrother, *Controlled clinical studies of fibrin sealant in cardiothoracic surgery--a review.* Eur J Cardiothorac Surg, 1996. **10**(9): p. 727-33.

782. Matthew, T.L., et al., *Four years' experience with fibrin sealant in thoracic and cardiovascular surgery.* Ann Thorac Surg, 1990. **50**(1): p. 40-3; discussion 43-4.

783. Rousou, J., et al., *Randomized clinical trial of fibrin sealant in patients undergoing resternotomy or reoperation after cardiac operations. A multicenter study.* J Thorac Cardiovasc Surg, 1989. **97**(2): p. 194-203.

784. Kram, H.B., et al., *Use of fibrin glue in hepatic trauma.* J Trauma, 1988. **28**(8): p. 1195-201.

785. Gasser, G., et al., *[Modification of suprapubic prostatectomy using a biological gluing technic].* Wien Klin Wochenschr, 1983. **95**(12): p. 399-403.

786. Rutgeerts, P., et al., *Randomised trial of single and repeated fibrin glue compared with injection of polidocanol in treatment of bleeding peptic ulcer.* Lancet, 1997. **350**(9079): p. 692-6.

787. Spotnitz, W.D., *Fibrin sealant: past, present, and future: a brief review.* World J Surg, 2010. **34**(4): p. 632-4.

788. Lowe, J., et al., *Evaluation of the topical hemostatic efficacy and safety of TISSEEL VH S/D fibrin sealant compared with currently licensed TISSEEL VH in patients undergoing cardiac surgery: a phase 3, randomized, double-blind clinical study.* J Cardiovasc Surg (Torino), 2007. **48**(3): p. 323-31.

789. Nervi, C., et al., *A multicenter clinical trial to evaluate the topical hemostatic efficacy of fibrin sealant in burn patients.* J Burn Care Rehabil, 2001. **22**(2): p. 99-103.

790. Atkinson, J.B., et al., *Prospective, randomized evaluation of the efficacy of fibrin sealant as a topical hemostatic agent at the cannulation site in neonates undergoing extracorporeal membrane oxygenation.* Am J Surg, 1997. **173**(6): p. 479-84.

791. Schwartz, M., et al., *Comparison of a new fibrin sealant with standard topical hemostatic agents.* Arch Surg, 2004. **139**(11): p. 1148-54.

792. Levy, O., et al., *The use of fibrin tissue adhesive to reduce blood loss and the need for blood transfusion after total knee arthroplasty. A prospective, randomized, multicenter study.* J Bone Joint Surg Am, 1999. **81**(11): p. 1580-8.

793. Wang, G.J., et al., *Fibrin sealant reduces perioperative blood loss in total hip replacement.* J Long Term Eff Med Implants, 2003. **13**(5): p. 399-411.

794. Wang, G.J., et al., *Use of fibrin sealant to reduce bloody drainage and hemoglobin loss after total knee arthroplasty: a brief note on a randomized prospective trial.* J Bone Joint Surg Am, 2001. **83-A**(10): p. 1503-5.

795. Martinowitz, U., et al., *Dental extraction for patients on oral anticoagulant therapy.* Oral Surg Oral Med Oral Pathol, 1990. **70**(3): p. 274-7.

796. Rakocz, M., et al., *Dental extractions in patients with bleeding disorders. The use of fibrin glue.* Oral Surg Oral Med Oral Pathol, 1993. **75**(3): p. 280-2.

797. Chalmers, R.T., et al., *Randomized clinical trial of tranexamic acid-free fibrin sealant during vascular surgical procedures.* Br J Surg, 2010. **97**(12): p. 1784-9.

798. Saha, S.P., et al., *Use of fibrin sealant as a hemostatic agent in expanded polytetrafluoroethylene graft placement surgery.* Ann Vasc Surg, 2011. **25**(6): p. 813-22.

799. Saha, S.P., et al., *A prospective randomized study comparing fibrin sealant to manual compression for the treatment of anastomotic suture-hole bleeding in expanded polytetrafluoroethylene grafts.* J Vasc Surg, 2012. **56**(1): p. 134-41.

800. Schenk, W.G., 3rd, et al., *Fibrin sealant improves hemostasis in peripheral vascular surgery: a randomized prospective trial.* Ann Surg, 2003. **237**(6): p. 871-6; discussion 876.

801. Taylor, L.M., Jr., et al., *Prospective randomized multicenter trial of fibrin sealant versus thrombin-soaked gelatin sponge for suture- or needle-hole bleeding from polytetrafluoroethylene femoral artery grafts.* J Vasc Surg, 2003. **38**(4): p. 766-71.

802. Maisano, F., et al., *TachoSil surgical patch versus conventional haemostatic fleece material for control of bleeding in cardiovascular surgery: a randomised controlled trial.* Eur J Cardiothorac Surg, 2009. **36**(4): p. 708-14.

803. Fischer, L., et al., *Hemostatic efficacy of TachoSil in liver resection compared with argon beam coagulator treatment: an open, randomized, prospective, multicenter, parallel-group trial.* Surgery, 2011. **149**(1): p. 48-55.

804. Frilling, A., et al., *Effectiveness of a new carrier-bound fibrin sealant versus argon beamer as haemostatic agent during liver resection: a randomised prospective trial.* Langenbecks Arch Surg, 2005. **390**(2): p. 114-20.

805. Siemer, S., et al., *Efficacy and safety of TachoSil as haemostatic treatment versus standard suturing in kidney tumour resection: a randomised prospective study.* Eur Urol, 2007. **52**(4): p. 1156-63.

806. Corral, M., et al., *Clinician reported ease of use for a novel fibrin sealant patch for hemostasis: results from four randomized controlled trials.* Curr Med Res Opin, 2016. **32**(2): p. 367-75.

807. Fischer, C.P., et al., *A prospective, randomized, controlled trial of the efficacy and safety of fibrin pad as an adjunct to control soft tissue bleeding during abdominal, retroperitoneal, pelvic, and thoracic surgery.* J Am Coll Surg, 2013. **217**(3): p. 385-93.

808. Koea, J., et al., *Safety and Hemostatic Effectiveness of the Fibrin Pad for Severe Soft-Tissue Bleeding During Abdominal, Retroperitoneal, Pelvic, and Thoracic (Non-cardiac) Surgery: A Randomized, Controlled, Superiority Trial.* World J Surg, 2015. **39**(11): p. 2663-9.

809. Koea, J.B., et al., *A phase III, randomized, controlled, superiority trial evaluating the fibrin pad versus standard of care in controlling parenchymal bleeding during elective hepatic surgery.* HPB (Oxford), 2013. **15**(1): p. 61-70.

810. Brown, D.M., et al., *Decreased wound contraction with fibrin glue--treated skin grafts.* Arch Surg, 1992. **127**(4): p. 404-6.

811. Frey, M., et al., *Die Vorteile der aufgeschobenen Spalthauttransplantation und die Erweiterung ihres Anwendungsbereiches durch die Verwendung des Fibrinklebers - Advantages of delayed split skin transplantation and widened usage due to use of fibrin sealant.* European Surgery, 1979. **11**(5): p. 97-100.

812. Jabs, A.D., Jr., et al., *The effect of fibrin glue on skin grafts in infected sites.* Plast Reconstr Surg, 1992. **89**(2): p. 268-71.

813. Rendl, K.H. and O. Staindl, *Hauttransplantation mit Fibrinkleber beim Ulcus cruris - Skin transplantation with fibrin sealant.* Aktuelle Dermatologie, 1980. **6**: p. 199-203.

814. Foster, K., et al., *Efficacy and safety of a fibrin sealant for adherence of autologous skin grafts to burn wounds: results of a phase 3 clinical study.* J Burn Care Res, 2008. **29**(2): p. 293-303.

815. Hester, T.R., Jr., et al., *Randomized, controlled, phase 3 study to evaluate the safety and efficacy of fibrin sealant VH S/D 4 s-apr (Artiss) to improve tissue adherence in subjects undergoing rhytidectomy.* Aesthet Surg J, 2013. **33**(4): p. 487-96.

816. Bayfield, M.S. and W.D. Spotnitz, *Fibrin sealant in thoracic surgery. Pulmonary applications, including management of bronchopleural fistula.* Chest Surg Clin N Am, 1996. **6**(3): p. 567-83.

817. Chung, W., et al., *Anal fistula plug and fibrin glue versus conventional treatment in repair of complex anal fistulas.* Am J Surg, 2009. **197**(5): p. 604-8.

818. Fortelny, R.H., et al., *Fibrin sealant (Tisseel) for hiatal mesh fixation in an experimental model in pigs.* J Surg Res, 2010. **162**(1): p. 68-74.

819. Fortelny, R.H., et al., *The assessment of quality of life in a trial on lightweight mesh fixation with fibrin sealant in transabdominal preperitoneal hernia repair.* Hernia, 2008. **12**(5): p. 499-505.

820.	Ruggiero, R., et al., *Fibrin glue to reduce seroma after axillary lymphadenectomy for breast cancer.* Minerva Chir, 2008. **63**(3): p. 249-54.

821.	Shaffrey, C.I., et al., *Neurosurgical applications of fibrin glue: augmentation of dural closure in 134 patients.* Neurosurgery, 1990. **26**(2): p. 207-10.

822.	Mouritzen, C., M. Dromer, and H.O. Keinecke, *The effect of fibrin glueing to seal bronchial and alveolar leakages after pulmonary resections and decortications.* Eur J Cardiothorac Surg, 1993. **7**(2): p. 75-80.

823.	Detweiler, M.B., J.G. Detweiler, and J. Fenton, *Sutureless and reduced suture anastomosis of hollow vessels with fibrin glue: a review.* J Invest Surg, 1999. **12**(5): p. 245-62.

824.	Suri, A., V.S. Mehta, and C. Sarkar, *Microneural anastomosis with fibrin glue: an experimental study.* Neurol India, 2002. **50**(1): p. 23-6.

825.	Garcia-Olmo, D., et al., *Expanded adipose-derived stem cells for the treatment of complex perianal fistula: a phase II clinical trial.* Dis Colon Rectum, 2009. **52**(1): p. 79-86.

826.	Kim, Y.S., et al., *Mesenchymal stem cell implantation in osteoarthritic knees: is fibrin glue effective as a scaffold?* Am J Sports Med, 2015. **43**(1): p. 176-85.

827.	Breen, A., et al., *Fibrin scaffold promotes adenoviral gene transfer and controlled vector delivery.* J Biomed Mater Res A, 2009. **89**(4): p. 876-84.

828.	Yang, S., et al., *The design of scaffolds for use in tissue engineering. Part I. Traditional factors.* Tissue Eng, 2001. **7**(6): p. 679-89.

829.	Cheresh, D.A., *Human endothelial cells synthesize and express an Arg-Gly-Asp-directed adhesion receptor involved in attachment to fibrinogen and von Willebrand factor.* Proc Natl Acad Sci U S A, 1987. **84**(18): p. 6471-5.

830.	Makogonenko, E., et al., *Interaction of fibrin(ogen) with fibronectin: further characterization and localization of the fibronectin-binding site.* Biochemistry, 2002. **41**(25): p. 7907-13.

831.	Podor, T.J., et al., *Incorporation of vitronectin into fibrin clots. Evidence for a binding interaction between vitronectin and gamma A/gamma' fibrinogen.* J Biol Chem, 2002. **277**(9): p. 7520-8.

832.	Bacon-Baguley, T., et al., *Thrombospondin binding to specific sequences within the A alpha- and B beta-chains of fibrinogen.* J Biol Chem, 1990. **265**(4): p. 2317-23.

833.	Ahmad, E., et al., *Fibrin matrices: The versatile therapeutic delivery systems.* Int J Biol Macromol, 2015. **81**: p. 121-36.

834.	Ahmed, T.A., E.V. Dare, and M. Hincke, *Fibrin: a versatile scaffold for tissue engineering applications.* Tissue Eng Part B Rev, 2008. **14**(2): p. 199-215.

835.	Spicer, P.P. and A.G. Mikos, *Fibrin glue as a drug delivery system.* J Control Release, 2010. **148**(1): p. 49-55.

836.	Christman, K.L., et al., *Fibrin glue alone and skeletal myoblasts in a fibrin scaffold preserve cardiac function after myocardial infarction.* Tissue Eng, 2004. **10**(3-4): p. 403-9.

837.	Hunyadi, J., et al., *Keratinocyte grafting: a new means of transplantation for full-thickness wounds.* J Dermatol Surg Oncol, 1988. **14**(1): p. 75-8.

838.	Horch, R.E., H. Bannasch, and G.B. Stark, *Transplantation of cultured autologous keratinocytes in fibrin sealant biomatrix to resurface chronic wounds.* Transplant Proc, 2001. **33**(1-2): p. 642-4.

839.	Kopp, J., et al., *Applied tissue engineering in the closure of severe burns and chronic wounds using cultured human autologous keratinocytes in a natural fibrin matrix.* Cell Tissue Bank, 2004. **5**(2): p. 89-96.

840.	Cox, S., M. Cole, and B. Tawil, *Behavior of human dermal fibroblasts in three-dimensional fibrin clots: dependence on fibrinogen and thrombin concentration.* Tissue Eng, 2004. **10**(5-6): p. 942-54.

841.	Falanga, V., et al., *Autologous bone marrow-derived cultured mesenchymal stem cells delivered in a fibrin spray accelerate healing in murine and human cutaneous wounds.* Tissue Eng, 2007. **13**(6): p. 1299-312.

842.	Kim, S.J., J.D. Jang, and S.K. Lee, *Treatment of long tubular bone defect of rabbit using autologous cultured osteoblasts mixed with fibrin.* Cytotechnology, 2007. **54**(2): p. 115-20.

843.	Eyrich, D., et al., *In vitro and in vivo cartilage engineering using a combination of chondrocyte-seeded long-term stable fibrin gels and polycaprolactone-based polyurethane scaffolds.* Tissue Eng, 2007. **13**(9): p. 2207-18.

844.	Torio-Padron, N., et al., *Engineering of adipose tissue by injection of human preadipocytes in fibrin.* Aesthetic Plast Surg, 2007. **31**(3): p. 285-93.

845.	Wechselberger, G., et al., *Successful transplantation of three tissue-engineered cell types using capsule induction technique and fibrin glue as a delivery vehicle.* Plast Reconstr Surg, 2002. **110**(1): p. 123-9.

846.	Wechselberger, G., et al., *Fibrin glue as a delivery vehicle for autologous urothelial cell transplantation onto a prefabricated pouch.* J Urol, 1998. **160**(2): p. 583-6.

847.	Hankemeier, S., et al., *Tissue engineering of tendons and ligaments by human bone marrow stromal cells in a liquid fibrin matrix in immunodeficient rats: results of a histologic study.* Arch Orthop Trauma Surg, 2007. **127**(9): p. 815-21.

848.	Gwak, S.J., et al., *Stable hepatocyte transplantation using fibrin matrix.* Biotechnol Lett, 2004. **26**(6): p. 505-8.

849.	Holnthoner, W., et al., *Adipose-derived stem cells induce vascular tube formation of outgrowth endothelial cells in a fibrin matrix.* J Tissue Eng Regen Med, 2015. **9**(2): p. 127-36.

850.	Koch, S., et al., *Fibrin-polylactide-based tissue-engineered vascular graft in the arterial circulation.* Biomaterials, 2010. **31**(17): p. 4731-9.

851.	Matthias, N., et al., *Volumetric muscle loss injury repair using in situ fibrin gel cast seeded with muscle-derived stem cells (MDSCs).* Stem Cell Res, 2018. **27**: p. 65-73.

852.	Johnson, P.J., et al., *Controlled release of neurotrophin-3 and platelet-derived growth factor from fibrin scaffolds containing neural progenitor cells enhances survival and differentiation into neurons in a subacute model of SCI.* Cell Transplant, 2010. **19**(1): p. 89-101.

853.	Baumgartner, L., et al., *Human mesenchymal stem cells: Influence of oxygen pressure on proliferation and chondrogenic differentiation in fibrin glue in vitro.* J Biomed Mater Res A, 2010. **93**(3): p. 930-40.

854. Bensaid, W., et al., *A biodegradable fibrin scaffold for mesenchymal stem cell transplantation.* Biomaterials, 2003. **24**(14): p. 2497-502.

855. Catelas, I., et al., *Human mesenchymal stem cell proliferation and osteogenic differentiation in fibrin gels in vitro.* Tissue Eng, 2006. **12**(8): p. 2385-96.

856. Ruger, B.M., et al., *Vascular morphogenesis by adult bone marrow progenitor cells in three-dimensional fibrin matrices.* Differentiation, 2008. **76**(7): p. 772-83.

857. Ryu, J.H., et al., *Implantation of bone marrow mononuclear cells using injectable fibrin matrix enhances neovascularization in infarcted myocardium.* Biomaterials, 2005. **26**(3): p. 319-26.

858. Bellamy, V., et al., *Long-term functional benefits of human embryonic stem cell-derived cardiac progenitors embedded into a fibrin scaffold.* J Heart Lung Transplant, 2015. **34**(9): p. 1198-207.

859. Montgomery, A., et al., *Engineering personalized neural tissue by combining induced pluripotent stem cells with fibrin scaffolds.* Biomater Sci, 2015. **3**(2): p. 401-13.

860. Harkin, D.G., R.A. Dawson, and Z. Upton, *Optimized delivery of skin keratinocytes by aerosolization and suspension in fibrin tissue adhesive.* Wound Repair Regen, 2006. **14**(3): p. 354-63.

861. Sese, N., M. Cole, and B. Tawil, *Proliferation of human keratinocytes and cocultured human keratinocytes and fibroblasts in three-dimensional fibrin constructs.* Tissue Eng Part A, 2011. **17**(3-4): p. 429-37.

862. Kirilak, Y., et al., *Fibrin sealant promotes migration and proliferation of human articular chondrocytes: possible involvement of thrombin and protease-activated receptors.* Int J Mol Med, 2006. **17**(4): p. 551-8.

863. Oh, J.H., et al., *The effects of the modulation of the fibronectin-binding capacity of fibrin by thrombin on osteoblast differentiation.* Biomaterials, 2012. **33**(16): p. 4089-99.

864. Oh, J.H., et al., *Comparative evaluation of the biological properties of fibrin for bone regeneration.* BMB Rep, 2014. **47**(2): p. 110-4.

865. Ho, W., et al., *The behavior of human mesenchymal stem cells in 3D fibrin clots: dependence on fibrinogen concentration and clot structure.* Tissue Eng, 2006. **12**(6): p. 1587-95.

866. Peterbauer-Scherb, A., et al., *In vitro adipogenesis of adipose-derived stem cells in 3D fibrin matrix of low component concentration.* J Tissue Eng Regen Med, 2012. **6**(6): p. 434-42.

867. Mana, M., et al., *Human U937 monocyte behavior and protein expression on various formulations of three-dimensional fibrin clots.* Wound Repair Regen, 2006. **14**(1): p. 72-80.

868. Furst, W., A. Banerjee, and H. Redl, *Comparison of structure, strength and cytocompatibility of a fibrin matrix supplemented either with tranexamic acid or aprotinin.* J Biomed Mater Res B Appl Biomater, 2007. **82**(1): p. 109-14.

869. Macasev, D., et al., *Cell compatibility of fibrin sealants: in vitro study with cells involved in soft tissue repair.* J Biomater Appl, 2011. **26**(2): p. 129-49.

870. Rohringer, S., et al., *Mechanisms of vasculogenesis in 3D fibrin matrices mediated by the interaction of adipose-derived stem cells and endothelial cells.* Angiogenesis, 2014. **17**(4): p. 921-33.

871. Stekelenburg, M., et al., *Dynamic straining combined with fibrin gel cell seeding improves strength of tissue-engineered small-diameter vascular grafts.* Tissue Eng Part A, 2009. **15**(5): p. 1081-9.

872. Tschoeke, B., et al., *Tissue-engineered small-caliber vascular graft based on a novel biodegradable composite fibrin-polylactide scaffold.* Tissue Eng Part A, 2009. **15**(8): p. 1909-18.

873. Maidhof, R., et al., *Biomimetic perfusion and electrical stimulation applied in concert improved the assembly of engineered cardiac tissue.* J Tissue Eng Regen Med, 2012. **6**(10): p. e12-23.

874. Radisic, M., et al., *Functional assembly of engineered myocardium by electrical stimulation of cardiac myocytes cultured on scaffolds.* Proc Natl Acad Sci U S A, 2004. **101**(52): p. 18129-34.

875. Zimmermann, W.H., et al., *Tissue engineering of a differentiated cardiac muscle construct.* Circ Res, 2002. **90**(2): p. 223-30.

876. Mol, A., et al., *Fibrin as a cell carrier in cardiovascular tissue engineering applications.* Biomaterials, 2005. **26**(16): p. 3113-21.

877. Li, Y.S. and B.R. Gao, *Transplantation of neonatal cardiomyocytes plus fibrin sealant restores myocardial function in a rat model of myocardial infarction.* Chin Med J (Engl), 2007. **120**(22): p. 2022-7.

878. Hansen, A., et al., *Development of a drug screening platform based on engineered heart tissue.* Circ Res, 2010. **107**(1): p. 35-44.

879. Weinberger, F., et al., *Cardiac repair in guinea pigs with human engineered heart tissue from induced pluripotent stem cells.* Sci Transl Med, 2016. **8**(363): p. 363ra148.

880. Menasche, P., et al., *Human embryonic stem cell-derived cardiac progenitors for severe heart failure treatment: first clinical case report.* Eur Heart J, 2015. **36**(30): p. 2011-7.

881. Hojo, M., et al., *Induction of vascular endothelial growth factor by fibrin as a dermal substrate for cultured skin substitute.* Plast Reconstr Surg, 2003. **111**(5): p. 1638-45.

882. Geer, D.J., D.D. Swartz, and S.T. Andreadis, *Fibrin promotes migration in a three-dimensional in vitro model of wound regeneration.* Tissue Eng, 2002. **8**(5): p. 787-98.

883. Mittermayr, R., et al., *Skin graft fixation by slow clotting fibrin sealant applied as a thin layer.* Burns, 2006. **32**(3): p. 305-11.

884. Bannasch, H., et al., *Cultured keratinocytes in fibrin with decellularised dermis close porcine full-thickness wounds in a single step.* Burns, 2008. **34**(7): p. 1015-21.

885. Kaiser, H.W., et al., *Cultured autologous keratinocytes in fibrin glue suspension, exclusively and combined with STS-allograft (preliminary clinical and histological report of a new technique).* Burns, 1994. **20**(1): p. 23-9.

886. Boehnke, K., et al., *Effects of fibroblasts and microenvironment on epidermal regeneration and tissue function in long-term skin equivalents.* Eur J Cell Biol, 2007. **86**(11-12): p. 731-46.

887. Idrus, R.B., et al., *Full-thickness skin wound healing using autologous keratinocytes and dermal fibroblasts with fibrin: bilayered versus single-layered substitute.* Adv Skin Wound Care, 2014. **27**(4): p. 171-80.

888. Mazlyzam, A.L., et al., *Reconstruction of living bilayer human skin equivalent utilizing human fibrin as a scaffold.* Burns, 2007. **33**(3): p. 355-63.

889. Itosaka, H., et al., *Fibrin matrix provides a suitable scaffold for bone marrow stromal cells transplanted into injured spinal cord: a novel material for CNS tissue engineering.* Neuropathology, 2009. **29**(3): p. 248-57.

890. Willerth, S.M., et al., *Optimization of fibrin scaffolds for differentiation of murine embryonic stem cells into neural lineage cells.* Biomaterials, 2006. **27**(36): p. 5990-6003.

891. Isaacs, J.E., et al., *Comparative analysis of biomechanical performance of available "nerve glues".* J Hand Surg Am, 2008. **33**(6): p. 893-9.

892. Kalbermatten, D.F., et al., *New fibrin conduit for peripheral nerve repair.* J Reconstr Microsurg, 2009. **25**(1): p. 27-33.

893. Pettersson, J., et al., *Biodegradable fibrin conduit promotes long-term regeneration after peripheral nerve injury in adult rats.* J Plast Reconstr Aesthet Surg, 2010. **63**(11): p. 1893-9.

894. Kalbermatten, D.F., et al., *Fibrin matrix for suspension of regenerative cells in an artificial nerve conduit.* J Plast Reconstr Aesthet Surg, 2008. **61**(6): p. 669-75.

895. Schuh, C.M., et al., *Activated Schwann Cell-Like Cells on Aligned Fibrin-Poly(Lactic-Co-Glycolic Acid) Structures: A Novel Construct for Application in Peripheral Nerve Regeneration.* Cells Tissues Organs, 2015. **200**(5): p. 287-99.

896. Ducheyne, P., et al., *Comprehensive Biomaterials*2015: Elsevier Science.

897. Hendrickson, D.A., et al., *Chondrocyte-fibrin matrix transplants for resurfacing extensive articular cartilage defects.* J Orthop Res, 1994. **12**(4): p. 485-97.

898. Munirah, S., et al., *Expansion of human articular chondrocytes and formation of tissue-engineered cartilage: a step towards exploring a potential use of matrix-induced cell therapy.* Tissue Cell, 2010. **42**(5): p. 282-92.

899. Peretti, G.M., et al., *Review of injectable cartilage engineering using fibrin gel in mice and swine models.* Tissue Eng, 2006. **12**(5): p. 1151-68.

900. Ruszymah, B.H., et al., *Pediatric auricular chondrocytes gene expression analysis in monolayer culture and engineered elastic cartilage.* Int J Pediatr Otorhinolaryngol, 2007. **71**(8): p. 1225-34.

901. Silverman, R.P., et al., *Adhesion of tissue-engineered cartilate to native cartilage.* Plast Reconstr Surg, 2000. **105**(4): p. 1393-8.

902. Dutton, A.Q., et al., *Enhancement of meniscal repair in the avascular zone using mesenchymal stem cells in a porcine model.* J Bone Joint Surg Br, 2010. **92**(1): p. 169-75.

903. Izuta, Y., et al., *Meniscal repair using bone marrow-derived mesenchymal stem cells: experimental study using green fluorescent protein transgenic rats.* Knee, 2005. **12**(3): p. 217-23.

904. Ameer, G.A., T.A. Mahmood, and R. Langer, *A biodegradable composite scaffold for cell transplantation.* J Orthop Res, 2002. **20**(1): p. 16-9.

905. Sha'ban, M., et al., *Fibrin and poly(lactic-co-glycolic acid) hybrid scaffold promotes early chondrogenesis of articular chondrocytes: an in vitro study.* J Orthop Surg Res, 2008. **3**: p. 17.

906. Park, S.H., et al., *Potential of fortified fibrin/hyaluronic acid composite gel as a cell delivery vehicle for chondrocytes.* Artif Organs, 2009. **33**(6): p. 439-47.

907. Perka, C., et al., *Joint cartilage repair with transplantation of embryonic chondrocytes embedded in collagen-fibrin matrices.* Clin Exp Rheumatol, 2000. **18**(1): p. 13-22.

908. Almqvist, K.F., et al., *Culture of chondrocytes in alginate surrounded by fibrin gel: characteristics of the cells over a period of eight weeks.* Ann Rheum Dis, 2001. **60**(8): p. 781-90.

909. Abiraman, S., et al., *Fibrin glue as an osteoinductive protein in a mouse model.* Biomaterials, 2002. **23**(14): p. 3023-31.

910. Isogai, N., et al., *Experimental use of fibrin glue to induce site-directed osteogenesis from cultured periosteal cells.* Plast Reconstr Surg, 2000. **105**(3): p. 953-63.

911. Ito, K., et al., *Simultaneous implant placement and bone regeneration around dental implants using tissue-engineered bone with fibrin glue, mesenchymal stem cells and platelet-rich plasma.* Clin Oral Implants Res, 2006. **17**(5): p. 579-86.

912. Schwarz, N., et al., *Early osteoinduction in rats is not altered by fibrin sealant.* Clin Orthop Relat Res, 1993(293): p. 353-9.

913. Zilch, H. and R. Wolff, *[Fibrin glue and bone regeneration].* Z Orthop Ihre Grenzgeb, 1987. **125**(2): p. 214-8.

914. Seebach, E., et al., *Mesenchymal stroma cells trigger early attraction of M1 macrophages and endothelial cells into fibrin hydrogels, stimulating long bone healing without long-term engraftment.* Acta Biomater, 2014. **10**(11): p. 4730-4741.

915. Gurevich, O., et al., *Fibrin microbeads for isolating and growing bone marrow-derived progenitor cells capable of forming bone tissue.* Tissue Eng, 2002. **8**(4): p. 661-72.

916. Zangi, L., et al., *High-yield isolation, expansion, and differentiation of rat bone marrow-derived mesenchymal stem cells with fibrin microbeads.* Tissue Eng, 2006. **12**(8): p. 2343-54.

917. Ben-Ari, A., et al., *Isolation and implantation of bone marrow-derived mesenchymal stem cells with fibrin micro beads to repair a critical-size bone defect in mice.* Tissue Eng Part A, 2009. **15**(9): p. 2537-46.

918. Perka, C., et al., *Segmental bone repair by tissue-engineered periosteal cell transplants with bioresorbable fleece and fibrin scaffolds in rabbits.* Biomaterials, 2000. **21**(11): p. 1145-53.

919. Noori, A., et al., *A review of fibrin and fibrin composites for bone tissue engineering.* Int J Nanomedicine, 2017. **12**: p. 4937-4961.

920. Giannini, G., et al., *Use of autologous fibrin-platelet glue and bone fragments in maxillofacial surgery.* Transfus Apher Sci, 2004. **30**(2): p. 139-44.

921. Kim, J.T. and S.H. Lee, *Reconstruction of Inferior Orbital Wall Fractures Using Bone Fragments.* J Craniofac Surg, 2015. **26**(8): p. 2412-4.

922. Tayapongsak, P., et al., *Autologous fibrin adhesive in mandibular reconstruction with particulate cancellous bone and marrow.* J Oral Maxillofac Surg, 1994. **52**(2): p. 161-5; discussion 166.

923. Segura-Castillo, J.L., et al., *Reduction of bone resorption by the application of fibrin glue in the reconstruction of the alveolar cleft.* J Craniofac Surg, 2005. **16**(1): p. 105-12.

924. Le Guehennec, L., P. Layrolle, and G. Daculsi, *A review of bioceramics and fibrin sealant.* Eur Cell Mater, 2004. **8**: p. 1-10; discussion 10-1.

925. Woo, K.M., et al., *Comparative evaluation of different crystal-structured calcium sulfates as bone-filling materials.* J Biomed Mater Res B Appl Biomater, 2009. **91**(2): p. 545-54.

926. Lohse, N., J. Schulz, and H. Schliephake, *Effect of fibrin on osteogenic differentiation and VEGF expression of bone marrow stromal cells in mineralised scaffolds: a three-dimensional analysis.* Eur Cell Mater, 2012. **23**: p. 413-23; discussion 424.

927. Nair, M.B., H.K. Varma, and A. John, *Platelet-rich plasma and fibrin glue-coated bioactive ceramics enhance growth and differentiation of goat bone marrow-derived stem cells.* Tissue Eng Part A, 2009. **15**(7): p. 1619-31.

928. Lopez-Heredia, M.A., et al., *Bulk physicochemical, interconnectivity, and mechanical properties of calcium phosphate cements-fibrin glue composites for bone substitute applications.* J Biomed Mater Res A, 2013. **101**(2): p. 478-90.

929. Xiu, J., et al., *Different angiogenic abilities of self-setting calcium phosphate cement scaffolds consisting of different proportions of fibrin glue.* Biomed Res Int, 2014. **2014**: p. 785146.

930. Kopf, B.S., et al., *Enhanced differentiation of human osteoblasts on Ti surfaces pre-treated with human whole blood.* Acta Biomater, 2015. **19**: p. 180-90.

931. Kalia, P., et al., *Do autologous mesenchymal stem cells augment bone growth and contact to massive bone tumor implants?* Tissue Eng, 2006. **12**(6): p. 1617-26.

932. Ehrbar, M., et al., *Endothelial cell proliferation and progenitor maturation by fibrin-bound VEGF variants with differential susceptibilities to local cellular activity.* J Control Release, 2005. **101**(1-3): p. 93-109.

933. Jeon, O., et al., *Long-term delivery enhances in vivo osteogenic efficacy of bone morphogenetic protein-2 compared to short-term delivery.* Biochem Biophys Res Commun, 2008. **369**(2): p. 774-80.

934. Pandit, A.S., et al., *Stimulation of angiogenesis by FGF-1 delivered through a modified fibrin scaffold.* Growth Factors, 1998. **15**(2): p. 113-23.

935. Iwakawa, M., et al., *Intraspinal implants of fibrin glue containing glial cell line-derived neurotrophic factor promote dorsal root regeneration into spinal cord.* Neurorehabil Neural Repair, 2001. **15**(3): p. 173-82.

936. Ishii, I., et al., *Healing of full-thickness defects of the articular cartilage in rabbits using fibroblast growth factor-2 and a fibrin sealant.* J Bone Joint Surg Br, 2007. **89**(5): p. 693-700.

937. Wong, C., et al., *Fibrin-based biomaterials to deliver human growth factors.* Thromb Haemost, 2003. **89**(3): p. 573-82.

938. Yakovlev, S., et al., *Interaction of fibrin(ogen) with heparin: further characterization and localization of the heparin-binding site.* Biochemistry, 2003. **42**(25): p. 7709-16.

939. Bhang, S.H., et al., *Controlled release of nerve growth factor from fibrin gel.* J Biomed Mater Res A, 2007. **80**(4): p. 998-1002.

940. Jeon, O., et al., *Control of basic fibroblast growth factor release from fibrin gel with heparin and concentrations of fibrinogen and thrombin.* J Control Release, 2005. **105**(3): p. 249-59.

941. Burgess, W.H., et al., *Possible dissociation of the heparin-binding and mitogenic activities of heparin-binding (acidic fibroblast) growth factor-1 from its receptor-binding activities by site-directed mutagenesis of a single lysine residue.* J Cell Biol, 1990. **111**(5 Pt 1): p. 2129-38.

942. Sakiyama-Elbert, S.E. and J.A. Hubbell, *Controlled release of nerve growth factor from a heparin-containing fibrin-based cell ingrowth matrix.* J Control Release, 2000. **69**(1): p. 149-58.

943. Schense, J.C. and J.A. Hubbell, *Cross-linking exogenous bifunctional peptides into fibrin gels with factor XIIIa.* Bioconjug Chem, 1999. **10**(1): p. 75-81.

944. Schense, J.C., et al., *Enzymatic incorporation of bioactive peptides into fibrin matrices enhances neurite extension.* Nat Biotechnol, 2000. **18**(4): p. 415-9.

945. Ehrbar, M., et al., *Cell-demanded liberation of VEGF121 from fibrin implants induces local and controlled blood vessel growth.* Circ Res, 2004. **94**(8): p. 1124-32.

946. Zisch, A.H., et al., *Engineered fibrin matrices for functional display of cell membrane-bound growth factor-like activities: study of angiogenic signaling by ephrin-B2.* Biomaterials, 2004. **25**(16): p. 3245-57.

947. Sakiyama, S.E., J.C. Schense, and J.A. Hubbell, *Incorporation of heparin-binding peptides into fibrin gels enhances neurite extension: an example of designer matrices in tissue engineering.* FASEB J, 1999. **13**(15): p. 2214-24.

948. Lee, A.C., et al., *Controlled release of nerve growth factor enhances sciatic nerve regeneration.* Exp Neurol, 2003. **184**(1): p. 295-303.

949. Taylor, S.J., J.W. McDonald, 3rd, and S.E. Sakiyama-Elbert, *Controlled release of neurotrophin-3 from fibrin gels for spinal cord injury.* J Control Release, 2004. **98**(2): p. 281-94.

950. Wood, M.D., G.H. Borschel, and S.E. Sakiyama-Elbert, *Controlled release of glial-derived neurotrophic factor from fibrin matrices containing an affinity-based delivery system.* J Biomed Mater Res A, 2009. **89**(4): p. 909-18.

951. Sakiyama-Elbert, S.E., A. Panitch, and J.A. Hubbell, *Development of growth factor fusion proteins for cell-triggered drug delivery.* FASEB J, 2001. **15**(7): p. 1300-2.

952. Geer, D.J., D.D. Swartz, and S.T. Andreadis, *Biomimetic delivery of keratinocyte growth factor upon cellular demand for accelerated wound healing in vitro and in vivo.* Am J Pathol, 2005. **167**(6): p. 1575-86.

953. Arrighi, I., et al., *Bone healing induced by local delivery of an engineered parathyroid hormone prodrug.* Biomaterials, 2009. **30**(9): p. 1763-71.

954.	Schmoekel, H.G., et al., *Enhancement of bone healing using non-glycosylated rhBMP-2 released from a fibrin matrix in dogs and cats.* J Small Anim Pract, 2005. **46**(1): p. 17-21.

955.	Schmoekel, H.G., et al., *Bone repair with a form of BMP-2 engineered for incorporation into fibrin cell ingrowth matrices.* Biotechnol Bioeng, 2005. **89**(3): p. 253-62.

956.	Zhao, W., et al., *Improved neovascularization and wound repair by targeting human basic fibroblast growth factor (bFGF) to fibrin.* J Mol Med (Berl), 2008. **86**(10): p. 1127-38.

957.	Zhao, W., et al., *Human basic fibroblast growth factor fused with Kringle4 peptide binds to a fibrin scaffold and enhances angiogenesis.* Tissue Eng Part A, 2009. **15**(5): p. 991-8.

958.	Willerth, S.M., A. Rader, and S.E. Sakiyama-Elbert, *The effect of controlled growth factor delivery on embryonic stem cell differentiation inside fibrin scaffolds.* Stem Cell Res, 2008. **1**(3): p. 205-18.

959.	Drinnan, C.T., et al., *Multimodal release of transforming growth factor-beta1 and the BB isoform of platelet derived growth factor from PEGylated fibrin gels.* J Control Release, 2010. **147**(2): p. 180-6.

960.	Briganti, E., et al., *A composite fibrin-based scaffold for controlled delivery of bioactive pro-angiogenetic growth factors.* J Control Release, 2010. **142**(1): p. 14-21.

961.	Layman, H., et al., *Enhanced angiogenic efficacy through controlled and sustained delivery of FGF-2 and G-CSF from fibrin hydrogels containing ionic-albumin microspheres.* J Biomater Sci Polym Ed, 2012. **23**(1-4): p. 185-206.

962.	Layman, H., et al., *Synergistic angiogenic effect of codelivering fibroblast growth factor 2 and granulocyte-colony stimulating factor from fibrin scaffolds and bone marrow transplantation in critical limb ischemia.* Tissue Eng Part A, 2011. **17**(1-2): p. 243-54.

963.	de la Puente, P., et al., *Autologous fibrin scaffolds cultured dermal fibroblasts and enriched with encapsulated bFGF for tissue engineering.* J Biomed Mater Res A, 2011. **99**(4): p. 648-54.

964.	Mogford, J.E., et al., *Fibrin sealant combined with fibroblasts and platelet-derived growth factor enhance wound healing in excisional wounds.* Wound Repair Regen, 2009. **17**(3): p. 405-10.

965.	Park, J.S., et al., *Chondrogenic potential of stem cells derived from amniotic fluid, adipose tissue, or bone marrow encapsulated in fibrin gels containing TGF-beta3.* Biomaterials, 2011. **32**(32): p. 8139-49.

966.	Park, M.S., et al., *Enhancement of the osteogenic efficacy of osteoblast transplantation by the sustained delivery of basic fibroblast growth factor.* J Biomed Mater Res B Appl Biomater, 2006. **79**(2): p. 353-9.

967.	Bonadio, J., *Tissue engineering via local gene delivery: update and future prospects for enhancing the technology.* Adv Drug Deliv Rev, 2000. **44**(2-3): p. 185-94.

968.	Madrigal, J.L., R. Stilhano, and E.A. Silva, *Biomaterial-Guided Gene Delivery for Musculoskeletal Tissue Repair.* Tissue Eng Part B Rev, 2017. **23**(4): p. 347-361.

969.	Mellott, A.J., M.L. Forrest, and M.S. Detamore, *Physical non-viral gene delivery methods for tissue engineering.* Ann Biomed Eng, 2013. **41**(3): p. 446-68.

970.	Seidlits, S.K., et al., *Hydrogels for lentiviral gene delivery.* Expert Opin Drug Deliv, 2013. **10**(4): p. 499-509.

971.	Breen, A., et al., *Optimization of a fibrin scaffold for sustained release of an adenoviral gene vector.* J Biomed Mater Res A, 2006. **78**(4): p. 702-8.

972.	Schek, R.M., S.J. Hollister, and P.H. Krebsbach, *Delivery and protection of adenoviruses using biocompatible hydrogels for localized gene therapy.* Mol Ther, 2004. **9**(1): p. 130-8.

973.	Lee, H.H., et al., *Release of bioactive adeno-associated virus from fibrin scaffolds: effects of fibrin glue concentrations.* Tissue Eng Part A, 2011. **17**(15-16): p. 1969-78.

974.	Aviles, M.O. and L.D. Shea, *Hydrogels to modulate lentivirus delivery in vivo from microporous tissue engineering scaffolds.* Drug Deliv Transl Res, 2011. **1**(1): p. 91-101.

975.	Teraishi, F., et al., *A novel method for gene delivery and expression in esophageal epithelium with fibrin glues containing replication-deficient adenovirus vector.* Surg Endosc, 2003. **17**(11): p. 1845-8.

976.	Padmashali, R.M. and S.T. Andreadis, *Engineering fibrinogen-binding VSV-G envelope for spatially- and cell-controlled lentivirus delivery through fibrin hydrogels.* Biomaterials, 2011. **32**(12): p. 3330-9.

977.	Shin, S., et al., *Phosphatidylserine immobilization of lentivirus for localized gene transfer.* Biomaterials, 2010. **31**(15): p. 4353-9.

978.	Schek, R.M., et al., *Combined use of designed scaffolds and adenoviral gene therapy for skeletal tissue engineering.* Biomaterials, 2006. **27**(7): p. 1160-6.

979.	Gelse, K., et al., *Articular cartilage repair by gene therapy using growth factor-producing mesenchymal cells.* Arthritis Rheum, 2003. **48**(2): p. 430-41.

980.	Bara, J.J., et al., *A doxycycline inducible, adenoviral bone morphogenetic protein-2 gene delivery system to bone.* J Tissue Eng Regen Med, 2016.

981.	Escamez, M.J., et al., *Assessment of optimal virus-mediated growth factor gene delivery for human cutaneous wound healing enhancement.* J Invest Dermatol, 2008. **128**(6): p. 1565-75.

982.	Breen, A.M., et al., *The use of therapeutic gene eNOS delivered via a fibrin scaffold enhances wound healing in a compromised wound model.* Biomaterials, 2008. **29**(21): p. 3143-51.

983.	Morton, T.J., et al., *Controlled release of substances bound to fibrin-anchors or of DNA.* Drug Deliv, 2009. **16**(2): p. 102-7.

984.	des Rieux, A., A. Shikanov, and L.D. Shea, *Fibrin hydrogels for non-viral vector delivery in vitro.* J Control Release, 2009. **136**(2): p. 148-54.

985.	Kulkarni, M., et al., *Fibrin-lipoplex system for controlled topical delivery of multiple genes.* Biomacromolecules, 2009. **10**(6): p. 1650-4.

986.	Lei, P., R.M. Padmashali, and S.T. Andreadis, *Cell-controlled and spatially arrayed gene delivery from fibrin hydrogels.* Biomaterials, 2009. **30**(22): p. 3790-9.

987.	Saul, J.M., et al., *Delivery of non-viral gene carriers from sphere-templated fibrin scaffolds for sustained transgene expression.* Biomaterials, 2007. **28**(31): p. 4705-16.

988.   Schillinger, U., et al., *A fibrin glue composition as carrier for nucleic acid vectors.* Pharm Res, 2008. **25**(12): p. 2946-62.

989.   Jozkowicz, A., et al., *Delivery of high dose VEGF plasmid using fibrin carrier does not influence its angiogenic potency.* Int J Artif Organs, 2003. **26**(2): p. 161-9.

990.   Michlits, W., et al., *Fibrin-embedded administration of VEGF plasmid enhances skin flap survival.* Wound Repair Regen, 2007. **15**(3): p. 360-7.

991.   Christman, K.L., et al., *Enhanced neovasculature formation in ischemic myocardium following delivery of pleiotrophin plasmid in a biopolymer.* Biomaterials, 2005. **26**(10): p. 1139-44.

992.   Balmayor, E.R. and M. van Griensven, *Gene therapy for bone engineering.* Front Bioeng Biotechnol, 2015. **3**: p. 9.

993.   Schwabe, P., et al., *Effect of a novel nonviral gene delivery of BMP-2 on bone healing.* ScientificWorldJournal, 2012. **2012**: p. 560142.

994.   Kaipel, M., et al., *Evaluation of fibrin-based gene-activated matrices for BMP2/7 plasmid codelivery in a rat nonunion model.* Int Orthop, 2014. **38**(12): p. 2607-13.

995.   Yang, J.C., et al., *Gene therapy for diabetic rats by electroporational transfer of naked plasmid with human pre-pro-insulin gene into skeletal muscle.* Biotechnology Letters, 2002. **24**(10): p. 851-855.

996.   Feichtinger, G.A., et al., *Sonoporation increases therapeutic efficacy of inducible and constitutive BMP2/7 in vivo gene delivery.* Hum Gene Ther Methods, 2014. **25**(1): p. 57-71.

997.   Nomikou, N., et al., *Ultrasound-mediated gene transfer (sonoporation) in fibrin-based matrices: potential for use in tissue regeneration.* J Tissue Eng Regen Med, 2016. **10**(1): p. 29-39.

998.   Nomikou, N., et al., *Ultrasound-responsive gene-activated matrices for osteogenic gene therapy using matrix-assisted sonoporation.* J Tissue Eng Regen Med, 2017.

999.   Andree, C., et al., *Plasmid gene delivery to human keratinocytes through a fibrin-mediated transfection system.* Tissue Eng, 2001. **7**(6): p. 757-66.

1000. Torio-Padron, N., et al., *Implantation of VEGF transfected preadipocytes improves vascularization of fibrin implants on the cylinder chorioallantoic membrane (CAM) model.* Minim Invasive Ther Allied Technol, 2007. **16**(3): p. 155-62.

1001. Wang, W., et al., *In vivo restoration of full-thickness cartilage defects by poly(lactide-co-glycolide) sponges filled with fibrin gel, bone marrow mesenchymal stem cells and DNA complexes.* Biomaterials, 2010. **31**(23): p. 5953-65.

1002. Greco, F., et al., *Fibrin-antibiotic mixtures: an in vitro study assessing the possibility of using a biologic carrier for local drug delivery.* J Biomed Mater Res, 1991. **25**(1): p. 39-51.

1003. Kram, H.B., et al., *Antibacterial effects of fibrin glue-antibiotic mixtures.* J Surg Res, 1991. **50**(2): p. 175-8.

1004. Redl, H., et al., *In vitro properties of mixtures of fibrin seal and antibiotics.* Biomaterials, 1983. **4**(1): p. 29-32.

1005. Woolverton, C.J., et al., *Subverting bacterial resistance using high dose, low solubility antibiotics in fibrin.* Infection, 1999. **27**(1): p. 28-33.

1006. Marone, P., et al., *Antibiotic-impregnated fibrin glue in ocular surgery: in vitro antibacterial activity.* Ophthalmologica, 1999. **213**(1): p. 12-5.

1007. Woolverton, C.J., et al., *Tetracycline delivery from fibrin controls peritoneal infection without measurable systemic antibiotic.* J Antimicrob Chemother, 2001. **48**(6): p. 861-7.

1008. Itokazu, M., et al., *The sustained release of antibiotic from freeze-dried fibrin-antibiotic compound and efficacies in a rat model of osteomyelitis.* Infection, 1997. **25**(6): p. 359-63.

1009. Kumar, T.R., M. Vasantha Bai, and L.K. Krishnan, *A freeze-dried fibrin disc as a biodegradable drug release matrix.* Biologicals, 2004. **32**(1): p. 49-55.

1010. Frucht-Perry, J., et al., *Fibrin-enmeshed tobramycin liposomes: single application topical therapy of Pseudomonas keratitis.* Cornea, 1992. **11**(5): p. 393-7.

1011. Senderoff, R.I., M.T. Sheu, and T.D. Sokoloski, *Fibrin based drug delivery systems.* J Parenter Sci Technol, 1991. **45**(1): p. 2-6.

1012. Wang, S.S., M.C. Yang, and T.W. Chung, *Liposomes/chitosan scaffold/human fibrin gel composite systems for delivering hydrophilic drugs--release behaviors of tirofiban in vitro.* Drug Deliv, 2008. **15**(3): p. 149-57.

1013. Yoshida, H., et al., *Novel drug delivery system using autologous fibrin glue--release properties of anti-cancer drugs.* Biol Pharm Bull, 2000. **23**(3): p. 371-4.

1014. Kitazawa, H., et al., *Microdialysis assessment of fibrin glue containing sodium alginate for local delivery of doxorubicin in tumor-bearing rats.* Biol Pharm Bull, 1997. **20**(3): p. 278-81.

1015. Tsui, J.Y., et al., *Subconjunctival topotecan in fibrin sealant in the treatment of transgenic murine retinoblastoma.* Invest Ophthalmol Vis Sci, 2008. **49**(2): p. 490-6.

1016. Pardue, M.T., et al., *Retinal function after subconjunctival injection of carboplatin in fibrin sealant.* Retina, 2004. **24**(5): p. 776-82.

1017. Simpson, A.E., et al., *Transscleral diffusion of carboplatin: an in vitro and in vivo study.* Arch Ophthalmol, 2002. **120**(8): p. 1069-74.

1018. Hafeli, U.O., et al., *Fibrin glue system for adjuvant brachytherapy of brain tumors with 188Re and 186Re-labeled microspheres.* Eur J Pharm Biopharm, 2007. **65**(3): p. 282-8.

1019. Zhibo, X. and Z. Miaobo, *Effect of sustained-release lidocaine on reduction of pain after subpectoral breast augmentation.* Aesthet Surg J, 2009. **29**(1): p. 32-4.

1020. Baoge, L., et al., *Treatment of skeletal muscle injury: a review.* ISRN Orthop, 2012. **2012**: p. 689012.

1021. Rowe, S.L., S. Lee, and J.P. Stegemann, *Influence of thrombin concentration on the mechanical and morphological properties of cell-seeded fibrin hydrogels.* Acta Biomater, 2007. **3**(1): p. 59-67.

1022. Lieber, R.L. and J. Friden, *Functional and clinical significance of skeletal muscle architecture.* Muscle Nerve, 2000. **23**(11): p. 1647-66.

1023. Taylor, N.A. and J.G. Wilkinson, *Exercise-induced skeletal muscle growth. Hypertrophy or hyperplasia?* Sports Med, 1986. **3**(3): p. 190-200.

1024.   Atherton, P.J., et al., *Cyclic stretch reduces myofibrillar protein synthesis despite increases in FAK and anabolic signalling in L6 cells.* J Physiol, 2009. **587**(Pt 14): p. 3719-27.

1025.   Hosseini, V., et al., *Engineered contractile skeletal muscle tissue on a microgrooved methacrylated gelatin substrate.* Tissue Eng Part A, 2012. **18**(23-24): p. 2453-65.

1026.   Lam, M.T., et al., *Microfeature guided skeletal muscle tissue engineering for highly organized 3-dimensional free-standing constructs.* Biomaterials, 2009. **30**(6): p. 1150-5.

1027.   Schindelin, J., et al., *Fiji: an open-source platform for biological-image analysis.* Nat Methods, 2012. **9**(7): p. 676-82.

1028.   Capetanaki, Y., D.J. Milner, and G. Weitzer, *Desmin in muscle formation and maintenance: knockouts and consequences.* Cell Struct Funct, 1997. **22**(1): p. 103-16.

1029.   Costa, M.L., et al., *Desmin: molecular interactions and putative functions of the muscle intermediate filament protein.* Braz J Med Biol Res, 2004. **37**(12): p. 1819-30.

1030.   Aubin, H., et al., *Directed 3D cell alignment and elongation in microengineered hydrogels.* Biomaterials, 2010. **31**(27): p. 6941-6951.

1031.   Hyatt, J.P., et al., *PAX3/7 expression coincides with MyoD during chronic skeletal muscle overload.* Muscle Nerve, 2008. **38**(1): p. 861-6.

1032.   Olguin, H.C. and B.B. Olwin, *Pax-7 up-regulation inhibits myogenesis and cell cycle progression in satellite cells: a potential mechanism for self-renewal.* Dev Biol, 2004. **275**(2): p. 375-88.

1033.   Rudnicki, M.A., et al., *MyoD or Myf-5 is required for the formation of skeletal muscle.* Cell, 1993. **75**(7): p. 1351-9.

1034.   Yokoyama, S. and H. Asahara, *The myogenic transcriptional network.* Cell Mol Life Sci, 2011. **68**(11): p. 1843-9.

1035.   Collins, C.A., et al., *Integrated functions of Pax3 and Pax7 in the regulation of proliferation, cell size and myogenic differentiation.* PLoS One, 2009. **4**(2): p. e4475.

1036.   Londhe, P. and J.K. Davie, *Sequential association of myogenic regulatory factors and E proteins at muscle-specific genes.* Skelet Muscle, 2011. **1**(1): p. 14.

1037.   Wang, X., et al., *Cellular fate of truncated slow skeletal muscle troponin T produced by Glu180 nonsense mutation in amish nemaline myopathy.* J Biol Chem, 2005. **280**(14): p. 13241-9.

1038.   Wei, B. and J.P. Jin, *Troponin T isoforms and posttranscriptional modifications: Evolution, regulation and function.* Arch Biochem Biophys, 2011. **505**(2): p. 144-54.

1039.   Khodabukus, A. and K. Baar, *Regulating fibrinolysis to engineer skeletal muscle from the C2C12 cell line.* Tissue Eng Part C Methods, 2009. **15**(3): p. 501-11.

1040.   Vandenburgh, H.H., *Cell shape and growth regulation in skeletal muscle: exogenous versus endogenous factors.* J Cell Physiol, 1983. **116**(3): p. 363-71.

1041.   Bajaj, P., et al., *Patterning the differentiation of C2C12 skeletal myoblasts.* Integr Biol (Camb), 2011. **3**(9): p. 897-909.

1042.   Hume, S.L., et al., *Alignment of multi-layered muscle cells within three-dimensional hydrogel macrochannels.* Acta Biomater, 2012. **8**(6): p. 2193-202.

1043.   Zhan, M., et al., *TACE release of TNF-alpha mediates mechanotransduction-induced activation of p38 MAPK and myogenesis.* J Cell Sci, 2007. **120**(Pt 4): p. 692-701.

1044.   Boonen, K.J., et al., *Effects of a combined mechanical stimulation protocol: Value for skeletal muscle tissue engineering.* J Biomech, 2010. **43**(8): p. 1514-21.

1045.   Vandenburgh, H.H., S. Swasdison, and P. Karlisch, *Computer-aided mechanogenesis of skeletal muscle organs from single cells in vitro.* FASEB J, 1991. **5**(13): p. 2860-7.

1046.   Liu, M., et al., *Bio-stretch, a computerized cell strain apparatus for three-dimensional organotypic cultures.* In Vitro Cell Dev Biol Anim, 1999. **35**(2): p. 87-93.

1047.   Collinsworth, A.M., et al., *Apparent elastic modulus and hysteresis of skeletal muscle cells throughout differentiation.* Am J Physiol Cell Physiol, 2002. **283**(4): p. C1219-27.

1048.   Gugerell, A., et al., *High thrombin concentrations in fibrin sealants induce apoptosis in human keratinocytes.* J Biomed Mater Res A, 2012. **100**(5): p. 1239-47.

1049.   Stewart, D., *The Role of Tension in Muscle Growth.* Academic Press, Inc., New York, 1972.

1050.   Morgan, J.E. and T.A. Partridge, *Muscle satellite cells.* Int J Biochem Cell Biol, 2003. **35**(8): p. 1151-6.

1051.   Figeac, N., et al., *ErbB3 binding protein-1 (Ebp1) controls proliferation and myogenic differentiation of muscle stem cells.* Dev Biol, 2014. **386**(1): p. 135-51.

1052.   Zhang, P., et al., *mTOR is necessary for proper satellite cell activity and skeletal muscle regeneration.* Biochem Biophys Res Commun, 2015. **463**(1-2): p. 102-8.

1053.   Vandromme, M., et al., *Binding of the retinoblastoma protein is not the determinant for stable repression of some E2F-regulated promoters in muscle cells.* Mol Cancer Res, 2008. **6**(3): p. 418-25.

1054.   Murata, N., et al., *Ca2+ influx and ATP release mediated by mechanical stretch in human lung fibroblasts.* Biochem Biophys Res Commun, 2014. **453**(1): p. 101-5.

1055.   Ito, S., et al., *Actin cytoskeleton regulates stretch-activated Ca2+ influx in human pulmonary microvascular endothelial cells.* Am J Respir Cell Mol Biol, 2010. **43**(1): p. 26-34.

1056.   Zobel, C., et al., *Mechanisms of Ca2+-dependent calcineurin activation in mechanical stretch-induced hypertrophy.* Cardiology, 2007. **107**(4): p. 281-90.

1057.   Takayama, Y., et al., *Simple micropatterning method for enhancing fusion efficiency and responsiveness to electrical stimulation of C2C12 myotubes.* Biotechnol Prog, 2015. **31**(1): p. 220-5.

1058.   Vandenburgh, H.H., *Motion into mass: how does tension stimulate muscle growth?* Med Sci Sports Exerc, 1987. **19**(5 Suppl): p. S142-9.

1059.   Hegarty, P.V. and A.C. Hooper, *Sarcomere length and fibre diameter distributions in four different mouse skeletal muscles.* J Anat, 1971. **110**(Pt 2): p. 249-57.

1060. An, Y. and D. Li, *Engineering skeletal muscle tissue in bioreactor systems.* Chin Med J (Engl), 2014. **127**(23): p. 4130-9.

1061. Burattini, S., et al., *C2C12 murine myoblasts as a model of skeletal muscle development: morpho-functional characterization.* Eur J Histochem, 2004. **48**(3): p. 223-33.

1062. Kislinger, T., et al., *Proteome dynamics during C2C12 myoblast differentiation.* Mol Cell Proteomics, 2005. **4**(7): p. 887-901.

1063. Wallimann, T., et al., *Intracellular compartmentation, structure and function of creatine kinase isoenzymes in tissues with high and fluctuating energy demands: the 'phosphocreatine circuit' for cellular energy homeostasis.* Biochem J, 1992. **281 (Pt 1)**: p. 21-40.

1064. Baird, M.F., et al., *Creatine-kinase- and exercise-related muscle damage implications for muscle performance and recovery.* J Nutr Metab, 2012. **2012**: p. 960363.

1065. Buskin, J.N. and S.D. Hauschka, *Identification of a myocyte nuclear factor that binds to the muscle-specific enhancer of the mouse muscle creatine kinase gene.* Mol Cell Biol, 1989. **9**(6): p. 2627-40.

1066. Chamberlain, J.S., J.B. Jaynes, and S.D. Hauschka, *Regulation of creatine kinase induction in differentiating mouse myoblasts.* Mol Cell Biol, 1985. **5**(3): p. 484-92.

1067. Jaynes, J.B., et al., *Transcriptional regulation of the muscle creatine kinase gene and regulated expression in transfected mouse myoblasts.* Mol Cell Biol, 1986. **6**(8): p. 2855-64.

1068. Nguyen, Q.G., et al., *Transgenic and tissue culture analyses of the muscle creatine kinase enhancer Trex control element in skeletal and cardiac muscle indicate differences in gene expression between muscle types.* Transgenic Res, 2003. **12**(3): p. 337-49.

1069. Ritchie, M.E., *Human B creatine kinase gene expression in C2C12 cells is regulated by protein interactions involving the first exon.* Biochem Biophys Res Commun, 1996. **223**(3): p. 762-9.

1070. Shield, M.A., et al., *E-box sites and a proximal regulatory region of the muscle creatine kinase gene differentially regulate expression in diverse skeletal muscles and cardiac muscle of transgenic mice.* Mol Cell Biol, 1996. **16**(9): p. 5058-68.

1071. Weeratna, R.D., et al., *Designing gene therapy vectors: avoiding immune responses by using tissue-specific promoters.* Gene Ther, 2001. **8**(24): p. 1872-8.

1072. Sternberg, E.A., et al., *Identification of upstream and intragenic regulatory elements that confer cell-type-restricted and differentiation-specific expression on the muscle creatine kinase gene.* Mol Cell Biol, 1988. **8**(7): p. 2896-909.

1073. Donoviel, D.B., et al., *Analysis of muscle creatine kinase gene regulatory elements in skeletal and cardiac muscles of transgenic mice.* Mol Cell Biol, 1996. **16**(4): p. 1649-58.

1074. Dmitriev, P., et al., *Simultaneous miRNA and mRNA transcriptome profiling of human myoblasts reveals a novel set of myogenic differentiation-associated miRNAs and their target genes.* BMC Genomics, 2013. **14**: p. 265.

1075. Cardinali, B., et al., *Microrna-221 and microrna-222 modulate differentiation and maturation of skeletal muscle cells.* PLoS One, 2009. **4**(10): p. e7607.

1076. Sun, Y., et al., *Mammalian target of rapamycin regulates miRNA-1 and follistatin in skeletal myogenesis.* J Cell Biol, 2010. **189**(7): p. 1157-69.

1077. Granjon, A., et al., *The microRNA signature in response to insulin reveals its implication in the transcriptional action of insulin in human skeletal muscle and the role of a sterol regulatory element-binding protein-1c/myocyte enhancer factor 2C pathway.* Diabetes, 2009. **58**(11): p. 2555-64.

1078. Hauser, M.A., et al., *Analysis of muscle creatine kinase regulatory elements in recombinant adenoviral vectors.* Mol Ther, 2000. **2**(1): p. 16-25.

1079. Lassar, A.B., et al., *MyoD is a sequence-specific DNA binding protein requiring a region of myc homology to bind to the muscle creatine kinase enhancer.* Cell, 1989. **58**(5): p. 823-31.

1080. Apone, S. and S.D. Hauschka, *Muscle gene E-box control elements. Evidence for quantitatively different transcriptional activities and the binding of distinct regulatory factors.* J Biol Chem, 1995. **270**(36): p. 21420-7.

1081. Wang, B., et al., *Construction and analysis of compact muscle-specific promoters for AAV vectors.* Gene Ther, 2008. **15**(22): p. 1489-99.

1082. Williams, T. and R. Tjian, *Analysis of the DNA-binding and activation properties of the human transcription factor AP-2.* Genes Dev, 1991. **5**(4): p. 670-82.

1083. Taylor, M., et al., *Muscle-specific (CArG) and serum-responsive (SRE) promoter elements are functionally interchangeable in Xenopus embryos and mouse fibroblasts.* Development, 1989. **106**(1): p. 67-78.

1084. Feichtinger, G.A., et al., *Enhanced reporter gene assay for the detection of osteogenic differentiation.* Tissue Eng Part C Methods, 2011. **17**(4): p. 401-10.

1085. Lupold, S.E., et al., *A real time Metridia luciferase based non-invasive reporter assay of mammalian cell viability and cytotoxicity via the beta-actin promoter and enhancer.* PLoS One, 2012. **7**(5): p. e36535.

1086. Johnson, J.E., B.J. Wold, and S.D. Hauschka, *Muscle creatine kinase sequence elements regulating skeletal and cardiac muscle expression in transgenic mice.* Mol Cell Biol, 1989. **9**(8): p. 3393-9.

1087. Li, S., et al., *Muscle-specific enhancement of gene expression by incorporation of SV40 enhancer in the expression plasmid.* Gene Ther, 2001. **8**(6): p. 494-7.

1088. Andersen, C.R., et al., *Efficient expression from one CMV enhancer controlling two core promoters.* Mol Biotechnol, 2011. **48**(2): p. 128-37.

1089. Haugwitz, M., et al., *Multiplexing bioluminescent and fluorescent reporters to monitor live cells.* Curr Chem Genomics, 2008. **1**: p. 11-9.

1090. Seliktar, D., *Designing cell-compatible hydrogels for biomedical applications.* Science, 2012. **336**(6085): p. 1124-8.

1091. Hutmacher, D.W., *Scaffolds in tissue engineering bone and cartilage.* Biomaterials, 2000. **21**(24): p. 2529-43.

1092. Reis, R.L., et al., *Natural-based polmyers for biomedical applications.* Woodhead Publishing Limited, 2008.

1093. Brown, E.E., et al., *Potential of nanocrystalline cellulose-fibrin nanocomposites for artificial vascular graft applications.* Biomacromolecules, 2013. **14**(4): p. 1063-71.

1094. Snyder, T.N., et al., *A fibrin/hyaluronic acid hydrogel for the delivery of mesenchymal stem cells and potential for articular cartilage repair.* J Biol Eng, 2014. **8**: p. 10.

1095. Goa, K.L. and P. Benfield, *Hyaluronic acid. A review of its pharmacology and use as a surgical aid in ophthalmology, and its therapeutic potential in joint disease and wound healing.* Drugs, 1994. **47**(3): p. 536-66.

1096. Burdick, J.A. and G.D. Prestwich, *Hyaluronic acid hydrogels for biomedical applications.* Adv Mater, 2011. **23**(12): p. H41-56.

1097. Lee, J.Y. and A.P. Spicer, *Hyaluronan: a multifunctional, megaDalton, stealth molecule.* Curr Opin Cell Biol, 2000. **12**(5): p. 581-6.

1098. Nejadnik, M.R., et al., *Self-healing hybrid nanocomposites consisting of bisphosphonated hyaluronan and calcium phosphate nanoparticles.* Biomaterials, 2014. **35**(25): p. 6918-29.

1099. Varghese, O.P., et al., *In situ cross-linkable high molecular weight hyaluronan-bisphosphonate conjugate for localized delivery and cell-specific targeting: a hydrogel linked prodrug approach.* J Am Chem Soc, 2009. **131**(25): p. 8781-3.

1100. Ossipov, D.A., et al., *Modular approach to functional hyaluronic acid hydrogels using orthogonal chemical reactions.* Chem Commun (Camb), 2010. **46**(44): p. 8368-70.

1101. Ossipov, D., et al., *Orthogonal Chemoselective Assembly of Hyaluronic Acid Networks and Nanogels for Drug Delivery.* Macromolecules, 2013. **46**(10): p. 4105-4113.

1102. Shu, X.Z., et al., *Disulfide cross-linked hyaluronan hydrogels.* Biomacromolecules, 2002. **3**(6): p. 1304-11.

1103. Ossipov, D.A., et al., *Functionalization of hyaluronic acid with chemoselective groups via a disulfide-based protection strategy for in situ formation of mechanically stable hydrogels.* Biomacromolecules, 2010. **11**(9): p. 2247-54.

1104. Kheirabadi, M., et al., *In situ forming interpenetrating hydrogels of hyaluronic acid hybridized with iron oxide nanoparticles.* Biomater Sci, 2015. **3**(11): p. 1466-74.

1105. Jockenhoevel, S., et al., *Fibrin gel -- advantages of a new scaffold in cardiovascular tissue engineering.* Eur J Cardiothorac Surg, 2001. **19**(4): p. 424-30.

1106. Pedersen, L.C., et al., *Transglutaminase factor XIII uses proteinase-like catalytic triad to crosslink macromolecules.* Protein Sci, 1994. **3**(7): p. 1131-5.

1107. Fujita, M., et al., *Purification and characterization of a strong fibrinolytic enzyme (nattokinase) in the vegetable cheese natto, a popular soybean fermented food in Japan.* Biochem Biophys Res Commun, 1993. **197**(3): p. 1340-7.

1108. Peach, R.J., et al., *Identification of hyaluronic acid binding sites in the extracellular domain of CD44.* J Cell Biol, 1993. **122**(1): p. 257-64.

1109. Ahrens, T., et al., *CD44 is the principal mediator of hyaluronic-acid-induced melanoma cell proliferation.* J Invest Dermatol, 2001. **116**(1): p. 93-101.

1110. Hui, Z., et al., *The role of the hyaluronan receptor CD44 in mesenchymal stem cell migration in the extracellular matrix.* Stem Cell, 2006. **24**: p. 928-35.

1111. Haynes, A.B., et al., *A surgical safety checklist to reduce morbidity and mortality in a global population.* N Engl J Med, 2009. **360**(5): p. 491-9.

1112. Zegers, M., et al., *The incidence, root-causes, and outcomes of adverse events in surgical units: implication for potential prevention strategies.* Patient Saf Surg, 2011. **5**: p. 13.

1113. Scognamiglio, F., et al., *Adhesive and sealant interfaces for general surgery applications.* J Biomed Mater Res B Appl Biomater, 2016. **104**(3): p. 626-39.

1114. Jarrett, P. and A. Coury, *Tissue adhesives and sealants for surgical applications*, in *Joining and Assembly of Medical Materials and Devices*2013, Woodhead Publishing. p. 449-490.

1115. Annabi, N., et al., *Elastic sealants for surgical applications.* Eur J Pharm Biopharm, 2015. **95**(Pt A): p. 27-39.

1116. MedMarket Diligence, L., *Worldwide Markets for Medical and Surgical Sealants, Glues, and Hemostats, 2015-2022: Established and Emerging Products, Technologies and Markets in the Americas, Europe, Asia/Pacific and Rest of World.* Report #S290, 2016.

1117. Assmann, A., et al., *A highly adhesive and naturally derived sealant.* Biomaterials, 2017. **140**: p. 115-127.

1118. Lang, N., et al., *A blood-resistant surgical glue for minimally invasive repair of vessels and heart defects.* Sci Transl Med, 2014. **6**(218): p. 218ra6.

1119. Lewis, K.M., et al., *Clinical effectiveness and versatility of a sealing hemostatic patch (HEMOPATCH) in multiple surgical specialties.* Expert Rev Med Devices, 2018: p. 1-10.

1120. Mizuta, R. and T. Taguchi, *Enhanced Sealing by Hydrophobic Modification of Alaska Pollock-Derived Gelatin-Based Surgical Sealants for the Treatment of Pulmonary Air Leaks.* Macromol Biosci, 2017. **17**(4).

1121. Prior, J.J., et al., *A sprayable hemostat containing fibrillar collagen, bovine thrombin, and autologous plasma.* Ann Thorac Surg, 1999. **68**(2): p. 479-85.

1122. Albes, J.M., et al., *Biophysical properties of the gelatin-resorcin-formaldehyde/glutaraldehyde adhesive.* Ann Thorac Surg, 1993. **56**(4): p. 910-5.

1123. Suzuki, S., M. Masuda, and K. Imoto, *The use of surgical glue in acute type A aortic dissection.* Gen Thorac Cardiovasc Surg, 2014. **62**(4): p. 207-13.

1124. Fuchs, S., et al., *Transglutaminase: new insights into gelatin nanoparticle cross-linking.* J Microencapsul, 2010. **27**(8): p. 747-54.

1125. Elvin, C.M., et al., *A highly elastic tissue sealant based on photopolymerised gelatin.* Biomaterials, 2010. **31**(32): p. 8323-31.

1126. Liu, Y., et al., *Biomimetic sealant based on gelatin and microbial transglutaminase: an initial in vivo investigation.* J Biomed Mater Res B Appl Biomater, 2009. **91**(1): p. 5-16.

1127. Vuocolo, T., et al., *A highly elastic and adhesive gelatin tissue sealant for gastrointestinal surgery and colon anastomosis.* J Gastrointest Surg, 2012. **16**(4): p. 744-52.

1128. Bhamidipati, C.M., J.S. Coselli, and S.A. LeMaire, *BioGlue in 2011: what is its role in cardiac surgery?* J Extra Corpor Technol, 2012. **44**(1): p. P6-12.

1129. Florek, H.J., et al., *Results from a First-in-Human Trial of a Novel Vascular Sealant.* Front Surg, 2015. **2**: p. 29.

1130. Skorpil, J., et al., *Effective and rapid sealing of coronary, aortic and atrial suture lines dagger.* Interact Cardiovasc Thorac Surg, 2015. **20**(6): p. 720-4; discussion 724.

1131. Kobayashi, H., et al., *In vivo evaluation of a new sealant material on a rat lung air leak model.* J Biomed Mater Res, 2001. **58**(6): p. 658-65.

1132. Fuller, C., *Reduction of intraoperative air leaks with Progel in pulmonary resection: a comprehensive review.* J Cardiothorac Surg, 2013. **8**: p. 90.

1133. Peng, H.T. and P.N. Shek, *Novel wound sealants: biomaterials and applications.* Expert Rev Med Devices, 2010. **7**(5): p. 639-59.

1134. Ahmad, M., et al., *Chitosan centered bionanocomposites for medical specialty and curative applications: A review.* Int J Pharm, 2017. **529**(1-2): p. 200-217.

1135. Rickett, T.A., et al., *Rapidly photo-cross-linkable chitosan hydrogel for peripheral neurosurgeries.* Biomacromolecules, 2011. **12**(1): p. 57-65.

1136. Foster, L.J. and E. Karsten, *A chitosan based, laser activated thin film surgical adhesive, 'SurgiLux': preparation and demonstration.* J Vis Exp, 2012(68).

1137. Pozza, M. and R.W. Millner, *Celox (chitosan) for haemostasis in massive traumatic bleeding: experience in Afghanistan.* Eur J Emerg Med, 2011. **18**(1): p. 31-3.

1138. Araki, M., et al., *Development of new biodegradable hydrogel glue for preventing alveolar air leakage.* J Thorac Cardiovasc Surg, 2007. **134**(5): p. 1241-8.

1139. Hiemstra, C., et al., *Rapidly in situ-forming degradable hydrogels from dextran thiols through Michael addition.* Biomacromolecules, 2007. **8**(5): p. 1548-56.

1140. Jin, R., et al., *Enzyme-mediated fast in situ formation of hydrogels from dextran-tyramine conjugates.* Biomaterials, 2007. **28**(18): p. 2791-800.

1141. Bhatia, S.K., et al., *Interactions of polysaccharide-based tissue adhesives with clinically relevant fibroblast and macrophage cell lines.* Biotechnol Lett, 2007. **29**(11): p. 1645-9.

1142. Trew, G.H., et al., *A first-in-human, randomized, controlled, subject- and reviewer-blinded multicenter study of Actamax Adhesion Barrier.* Arch Gynecol Obstet, 2017. **295**(2): p. 383-395.

1143. Leonardi, M., et al., *Glubran 2((r)):a new acrylic glue for neuroradiological endovascular use: a complementary histological study.* Interv Neuroradiol, 2003. **9**(3): p. 249-54.

1144. Mattamal, G.J., *US FDA perspective on the regulations of medical-grade polymers: cyanoacrylate polymer medical device tissue adhesives.* Expert Rev Med Devices, 2008. **5**(1): p. 41-9.

1145. Yag-Howard, C., *Sutures, needles, and tissue adhesives: a review for dermatologic surgery.* Dermatol Surg, 2014. **40 Suppl 9**: p. S3-S15.

1146. Singer, A.J., L.C. Perry, and R.L. Allen, Jr., *In vivo study of wound bursting strength and compliance of topical skin adhesives.* Acad Emerg Med, 2008. **15**(12): p. 1290-4.

1147. Leggat, P.A., D.R. Smith, and U. Kedjarune, *Surgical applications of cyanoacrylate adhesives: a review of toxicity.* ANZ J Surg, 2007. **77**(4): p. 209-13.

1148. Allen, M.S., et al., *Prospective randomized study evaluating a biodegradable polymeric sealant for sealing intraoperative air leaks that occur during pulmonary resection.* Ann Thorac Surg, 2004. **77**(5): p. 1792-801.

1149. Kim, K.D. and N.M. Wright, *Polyethylene glycol hydrogel spinal sealant (DuraSeal Spinal Sealant) as an adjunct to sutured dural repair in the spine: results of a prospective, multicenter, randomized controlled study.* Spine (Phila Pa 1976), 2011. **36**(23): p. 1906-12.

1150. Macchiarini, P., et al., *Experimental and clinical evaluation of a new synthetic, absorbable sealant to reduce air leaks in thoracic operations.* J Thorac Cardiovasc Surg, 1999. **117**(4): p. 751-8.

1151. Preul, M.C., W.D. Bichard, and R.F. Spetzler, *Toward optimal tissue sealants for neurosurgery: use of a novel hydrogel sealant in a canine durotomy repair model.* Neurosurgery, 2003. **53**(5): p. 1189-98; discussion 1198-9.

1152. Zoia, C., et al., *First impressions about Adherus, a new dural sealant.* J Appl Biomater Funct Mater, 2015. **13**(4): p. e372-5.

1153. Ferreira, P., et al., *Development of a biodegradable bioadhesive containing urethane groups.* J Mater Sci Mater Med, 2008. **19**(1): p. 111-20.

1154. Kreye, O., H. Mutlu, and M.A.R. Meier, *Sustainable routes to polyurethane precursors.* Green Chemistry, 2013. **15**(6): p. 1431-1455.

1155. Gilbert, T.W., et al., *Lysine-derived urethane surgical adhesive prevents seroma formation in a canine abdominoplasty model.* Plast Reconstr Surg, 2008. **122**(1): p. 95-102.

1156. Walgenbach, K.J., et al., *Randomized, prospective study of TissuGlu(R) surgical adhesive in the management of wound drainage following abdominoplasty.* Aesthetic Plast Surg, 2012. **36**(3): p. 491-6.

1157. Zhu, W., Y.J. Chuah, and D.A. Wang, *Bioadhesives for internal medical applications: A review.* Acta Biomater, 2018.

1158. Jenkins, H.P., R. Janda, and J. Clarke, *Clinical and experimental observations on the use of gelatin sponge or foam.* Surgery, 1946. **20**(1): p. 124-32.

1159. Frantz, V.K., H.T. Clarke, and R. Lattes, *Hemostasis With Absorbable Gauze (Oxidized Cellulose).* Ann Surg, 1944. **120**(2): p. 181-98.

1160. Rickenbacher, A., et al., *Efficacy of TachoSil a fibrin-based haemostat in different fields of surgery--a systematic review.* Expert Opin Biol Ther, 2009. **9**(7): p. 897-907.

1161. Corral, M., et al., *Health and economic outcomes associated with uncontrolled surgical bleeding: a retrospective analysis of the Premier Perspectives Database.* Clinicoecon Outcomes Res, 2015. **7**: p. 409-21.

1162. Koea, J.B., et al., *A multicentre, prospective, randomized, controlled trial comparing EVARREST fibrin sealant patch to standard of care in controlling bleeding following elective hepatectomy: anatomic versus non-anatomic resection.* HPB (Oxford), 2016. **18**(3): p. 221-8.

1163. Lewis, K.M., C.E. Kuntze, and H. Gulle, *Control of bleeding in surgical procedures: critical appraisal of HEMOPATCH (Sealing Hemostat).* Med Devices (Auckl), 2016. **9**: p. 1-10.

1164. Ollinger, R., et al., *A multicentre, randomized clinical trial comparing the Veriset haemostatic patch with fibrin sealant for the management of bleeding during hepatic surgery.* HPB (Oxford), 2013. **15**(7): p. 548-58.

1165. Lewis, K.M., et al., *Swelling, sealing, and hemostatic ability of a novel biomaterial: A polyethylene glycol-coated collagen pad.* J Biomater Appl, 2014. **29**(5): p. 780-8.

1166. Howk, K., J. Fortier, and R. Poston, *A Novel Hemostatic Patch That Stops Bleeding in Cardiovascular and Peripheral Vascular Procedures.* Ann Vasc Surg, 2016. **31**: p. 186-95.

1167. Cheng, L., C.K. Lau, and G. Parker, *Use of TissuePatch sealant film in the management of chyle leak in major neck surgery.* Br J Oral Maxillofac Surg, 2014. **52**(1): p. 87-9.

1168. Surda, P., et al., *A purely synthetic and biodegradable material for repair of cerebrospinal fluid rhinorrhoea.* Clin Otolaryngol, 2016. **41**(2): p. 179-82.

1169. Zhang, R., et al., *TissuePatch as a novel synthetic sealant for repair of superficial lung defect: in vitro tests results.* Ann Surg Innov Res, 2012. **6**(1): p. 12.

1170. Marx, G., *Evolution of fibrin glue applicators.* Transfus Med Rev, 2003. **17**(4): p. 287-98.

1171. Felema, G.G., et al., *Venous air embolism from Tisseel use during endoscopic cranial vault remodeling for craniosynostosis repair: a case report.* Paediatr Anaesth, 2013. **23**(8): p. 754-6.

1172. Lv, F., et al., *Novel hemostatic agents based on gelatin-microbial transglutaminase mix.* Sci China Life Sci, 2017. **60**(4): p. 397-403.

1173. Elvin, C.M., et al., *The development of photochemically crosslinked native fibrinogen as a rapidly formed and mechanically strong surgical tissue sealant.* Biomaterials, 2009. **30**(11): p. 2059-65.

1174. Henise, J., et al., *Surgical sealants with tunable swelling, burst pressures, and biodegradation rates.* J Biomed Mater Res B Appl Biomater, 2017. **105**(6): p. 1602-1611.

1175. Lih, E., et al., *Rapidly curable chitosan-PEG hydrogels as tissue adhesives for hemostasis and wound healing.* Acta Biomater, 2012. **8**(9): p. 3261-9.

1176. Nie, W., et al., *Rapidly in situ forming chitosan/epsilon-polylysine hydrogels for adhesive sealants and hemostatic materials.* Carbohydr Polym, 2013. **96**(1): p. 342-8.

1177. Strehin, I., et al., *A versatile pH sensitive chondroitin sulfate-PEG tissue adhesive and hydrogel.* Biomaterials, 2010. **31**(10): p. 2788-97.

1178. Balakrishnan, B., et al., *A novel injectable tissue adhesive based on oxidized dextran and chitosan.* Acta Biomater, 2017. **53**: p. 343-354.

1179. Grinstaff, M.W., *Designing hydrogel adhesives for corneal wound repair.* Biomaterials, 2007. **28**(35): p. 5205-14.

1180. Lancina, M.G., 3rd and H. Yang, *Dendrimers for Ocular Drug Delivery.* Can J Chem, 2017. **95**(9): p. 897-902.

1181. Feng, G., et al., *Elastic Light Tunable Tissue Adhesive Dendrimers.* Macromol Biosci, 2016. **16**(7): p. 1072-82.

1182. Kord Forooshani, P. and B.P. Lee, *Recent approaches in designing bioadhesive materials inspired by mussel adhesive protein.* J Polym Sci A Polym Chem, 2017. **55**(1): p. 9-33.

1183. Mehdizadeh, M. and J. Yang, *Design strategies and applications of tissue bioadhesives.* Macromol Biosci, 2013. **13**(3): p. 271-88.

1184. Hwang, D.S., et al., *Practical recombinant hybrid mussel bioadhesive fp-151.* Biomaterials, 2007. **28**(24): p. 3560-8.

1185. Barrett, D.G., G.G. Bushnell, and P.B. Messersmith, *Mechanically robust, negative-swelling, mussel-inspired tissue adhesives.* Adv Healthc Mater, 2013. **2**(5): p. 745-55.

1186. Ryu, J.H., S. Hong, and H. Lee, *Bio-inspired adhesive catechol-conjugated chitosan for biomedical applications: A mini review.* Acta Biomater, 2015. **27**: p. 101-115.

1187. Zhang, H., et al., *Mussel-inspired hyperbranched poly(amino ester) polymer as strong wet tissue adhesive.* Biomaterials, 2014. **35**(2): p. 711-9.

1188. Dumville, J.C., et al., *Tissue adhesives for closure of surgical incisions.* Cochrane Database Syst Rev, 2014(11): p. CD004287.

1189. Gruber-Blum, S., et al., *Liquid antiadhesive agents for intraperitoneal hernia repair procedures: Artiss((R)) compared to CoSeal((R)) and Adept((R)) in an IPOM rat model.* Surg Endosc, 2017. **31**(12): p. 4973-4980.

1190. Hedrich, H.C., et al., *Fibrin chain cross-linking, fibrinolysis, and in vivo sealing efficacy of differently structured fibrin sealants.* J Biomed Mater Res B Appl Biomater, 2012. **100**(6): p. 1507-12.

1191. Lin, H., et al., *A meta-analysis of randomized control trials assessing mesh fixation with glue versus suture in Lichtenstein inguinal hernia repair.* Medicine (Baltimore), 2018. **97**(14): p. e0227.

1192. Rogers, A.C., et al., *Meta-analysis of the use of surgical sealants for suture-hole bleeding in arterial anastomoses.* Br J Surg, 2016. **103**(13): p. 1758-1767.

1193. Slezak, P., et al., *Properties of collagen-based hemostatic patch compared to oxidized cellulose-based patch.* J Mater Sci Mater Med, 2018. **29**(6): p. 71.

1194. Stergios, K., et al., *The potential effect of biological sealants on colorectal anastomosis healing in experimental research involving severe diabetes.* Ann R Coll Surg Engl, 2017. **99**(3): p. 189-192.

1195. Lewis, K.M., et al., *Development and validation of an intraoperative bleeding severity scale for use in clinical studies of hemostatic agents.* Surgery, 2017. **161**(3): p. 771-781.

1196. Spotnitz, W.D., et al., *The SPOT GRADE: A New Method for Reproducibly Quantifying Surgical Wound Bleeding.* Spine (Phila Pa 1976), 2018. **43**(11): p. E664-E671.

1197. Zaraca, F., et al., *Can a standardised Ventilation Mechanical Test for quantitative intraoperative air leak grading reduce the length of hospital stay after video-assisted thoracoscopic surgery lobectomy?* J Vis Surg, 2017. **3**: p. 179.

1198. Masket, S., et al., *Hydrogel sealant versus sutures to prevent fluid egress after cataract surgery.* J Cataract Refract Surg, 2014. **40**(12): p. 2057-66.

1199. Stam, M.A.W., et al., *Sylys® surgical sealant: a safe adjunct to standard bowel anastomosis closure.* Ann Surg Innov Res, 2014. **8**(1): p. 6.

1200. Annabi, N., et al., *Surgical Materials: Current Challenges and Nano-enabled Solutions.* Nano Today, 2014. **9**(5): p. 574-589.

1201. Meddahi-Pelle, A., et al., *Organ repair, hemostasis, and in vivo bonding of medical devices by aqueous solutions of nanoparticles.* Angew Chem Int Ed Engl, 2014. **53**(25): p. 6369-73.

1202. Henise, J., et al., *Biodegradable tetra-PEG hydrogels as carriers for a releasable drug delivery system.* Bioconjug Chem, 2015. **26**(2): p. 270-8.

1203. Lee, J.E., et al., *Surgical suture assembled with polymeric drug-delivery sheet for sustained, local pain relief.* Acta Biomater, 2013. **9**(9): p. 8318-27.

1204. Droghetti, A., et al., *Cost analysis of pulmonary lobectomy procedure: comparison of stapler versus precision dissection and sealant.* Clinicoecon Outcomes Res, 2017. **9**: p. 201-206.

1205. Massin, P., et al., *Does fibrin sealant use in total knee replacement reduce transfusion rates? A non-randomised comparative study.* Orthop Traumatol Surg Res, 2012. **98**(2): p. 180-5.

1206. Pandanaboyana, S., et al., *A cost-effective analysis of fibrin sealants versus no sealant following open right hemihepatectomy for colorectal liver metastases.* ANZ J Surg, 2017. **87**(6): p. E11-E14.

1207. Zaraca, F., et al., *Cost-effectiveness analysis of sealant impact in management of moderate intraoperative alveolar air leaks during video-assisted thoracoscopic surgery lobectomy: a multicentre randomised controlled trial.* J Thorac Dis, 2017. **9**(12): p. 5230-5238.

1208. Sen, C.K., et al., *Human skin wounds: a major and snowballing threat to public health and the economy.* Wound Repair Regen, 2009. **17**(6): p. 763-71.

1209. Singer, A.J. and R.A. Clark, *Cutaneous wound healing.* N Engl J Med, 1999. **341**(10): p. 738-46.

1210. Jarbrink, K., et al., *Prevalence and incidence of chronic wounds and related complications: a protocol for a systematic review.* Syst Rev, 2016. **5**(1): p. 152.

1211. Gottrup, F., *A specialized wound-healing center concept: importance of a multidisciplinary department structure and surgical treatment facilities in the treatment of chronic wounds.* Am J Surg, 2004. **187**(5A): p. 38S-43S.

1212. Wicke, C., et al., *Aging influences wound healing in patients with chronic lower extremity wounds treated in a specialized Wound Care Center.* Wound Repair Regen, 2009. **17**(1): p. 25-33.

1213. Frykberg, R.G. and J. Banks, *Challenges in the Treatment of Chronic Wounds.* Adv Wound Care (New Rochelle), 2015. **4**(9): p. 560-582.

1214. Politis, C., et al., *Wound Healing Problems in the Mouth.* Front Physiol, 2016. **7**: p. 507.

1215. Feng, X., et al., *Fibrin and collagen differentially regulate human dermal microvascular endothelial cell integrins: stabilization of alphav/beta3 mRNA by fibrin1.* J Invest Dermatol, 1999. **113**(6): p. 913-9.

1216. Spotnitz, W.D., *Commercial fibrin sealants in surgical care.* Am J Surg, 2001. **182**(2 Suppl): p. 8S-14S.

1217. Chang, B., et al., *Injectable scaffolds: Preparation and application in dental and craniofacial regeneration.* Mater Sci Eng R Rep, 2017. **111**: p. 1-26.

1218. Li, Y., et al., *Fibrin gel as an injectable biodegradable scaffold and cell carrier for tissue engineering.* ScientificWorldJournal, 2015. **2015**: p. 685690.

1219. Rajangam, T. and S.S. An, *Fibrinogen and fibrin based micro and nano scaffolds incorporated with drugs, proteins, cells and genes for therapeutic biomedical applications.* Int J Nanomedicine, 2013. **8**: p. 3641-62.

1220. Blokhuis, T.J. and J.J. Arts, *Bioactive and osteoinductive bone graft substitutes: definitions, facts and myths.* Injury, 2011. **42 Suppl 2**: p. S26-9.

1221. Hench, L.L., *Biomaterials: a forecast for the future.* Biomaterials, 1998. **19**(16): p. 1419-23.

1222. Navarro, M., et al., *Biomaterials in orthopaedics.* J R Soc Interface, 2008. **5**(27): p. 1137-58.

1223. Tsurupa, G. and L. Medved, *Identification and characterization of novel tPA- and plasminogen-binding sites within fibrin(ogen) alpha C-domains.* Biochemistry, 2001. **40**(3): p. 801-8.

1224. Wagner, O.F., et al., *Interaction between plasminogen activator inhibitor type 1 (PAI-1) bound to fibrin and either tissue-type plasminogen activator (t-PA) or urokinase-type plasminogen activator (u-PA). Binding of t-PA/PAI-1 complexes to fibrin mediated by both the finger and the kringle-2 domain of t-PA.* J Clin Invest, 1989. **84**(2): p. 647-55.

1225. Hale, B.W., et al., *Effect of scaffold dilution on migration of mesenchymal stem cells from fibrin hydrogels.* Am J Vet Res, 2012. **73**(2): p. 313-8.

1226. Kim, B.S., et al., *Effects of fibrinogen concentration on fibrin glue and bone powder scaffolds in bone regeneration.* J Biosci Bioeng, 2014. **118**(4): p. 469-75.

1227. Cole, M., et al., *Fibrin as a delivery vehicle for active macrophage activator lipoprotein-2 peptide: in vitro studies.* Wound Repair Regen, 2007. **15**(4): p. 521-9.

1228. Odrljin, T.M., et al., *Heparin-binding domain of fibrin mediates its binding to endothelial cells.* Arterioscler Thromb Vasc Biol, 1996. **16**(12): p. 1544-51.

1229. Sakiyama-Elbert, S.E. and J.A. Hubbell, *Development of fibrin derivatives for controlled release of heparin-binding growth factors.* J Control Release, 2000. **65**(3): p. 389-402.

1230. Murphy, K.C., et al., *Engineered Fibrin Gels for Parallel Stimulation of Mesenchymal Stem Cell Proangiogenic and Osteogenic Potential.* Ann Biomed Eng, 2015. **43**(8): p. 2010-21.

1231. Ferraris, V.A., et al., *Perioperative blood transfusion and blood conservation in cardiac surgery: the Society of Thoracic Surgeons and The Society of Cardiovascular Anesthesiologists clinical practice guideline.* Ann Thorac Surg, 2007. **83**(5 Suppl): p. S27-86.

1232. Sacchi, V., et al., *Long-lasting fibrin matrices ensure stable and functional angiogenesis by highly tunable, sustained delivery of recombinant VEGF164.* Proc Natl Acad Sci U S A, 2014. **111**(19): p. 6952-7.

1233. Mittermayr, R., et al., *Sustained (rh)VEGF(165) release from a sprayed fibrin biomatrix induces angiogenesis, up-regulation of endogenous VEGF-R2, and reduces ischemic flap necrosis.* Wound Repair Regen, 2008. **16**(4): p. 542-50.

1234. Redl, H., et al., *Fibrin/fibrinogen-binding conjugate*, 2004, Google Patents.

1235. Sonmez, A.B. and J. Castelnuovo, *Applications of basic fibroblastic growth factor (FGF-2, bFGF) in dentistry.* Dent Traumatol, 2014. **30**(2): p. 107-11.

1236. Yucel, E.A., et al., *Effects of fibrin glue on wound healing in oral cavity.* J Dent, 2003. **31**(8): p. 569-75.

1237. Sae-Lim, V., et al., *The effect of basic fibroblast growth factor on delayed-replanted monkey teeth.* J Periodontol, 2004. **75**(12): p. 1570-8.

1238. Anitua, E., et al., *New insights into and novel applications for platelet-rich fibrin therapies.* Trends Biotechnol, 2006. **24**(5): p. 227-34.

1239. Borie, E., et al., *Platelet-rich fibrin application in dentistry: a literature review.* Int J Clin Exp Med, 2015. **8**(5): p. 7922-9.

1240. Cortese, A., et al., *Platelet-rich fibrin (PRF) in implant dentistry in combination with new bone regenerative technique in elderly patients.* Int J Surg Case Rep, 2016. **28**: p. 52-56.

1241. Mittermayr, R., et al., *Controlled release of fibrin matrix-conjugated platelet derived growth factor improves ischemic tissue regeneration by functional angiogenesis.* Acta Biomater, 2016. **29**: p. 11-20.

1242. Martino, M.M., et al., *Growth factors engineered for super-affinity to the extracellular matrix enhance tissue healing.* Science, 2014. **343**(6173): p. 885-8.

1243. Walpoth, B.H., et al., *Enhanced intimal thickening of expanded polytetrafluoroethylene grafts coated with fibrin or fibrin-releasing vascular endothelial growth factor in the pig carotid artery interposition model.* J Thorac Cardiovasc Surg, 2007. **133**(5): p. 1163-70.

1244. Kawamura, M. and M.R. Urist, *Human fibrin is a physiologic delivery system for bone morphogenetic protein.* Clin Orthop Relat Res, 1988(235): p. 302-10.

1245. Hou, T., et al., *In vitro evaluation of a fibrin gel antibiotic delivery system containing mesenchymal stem cells and vancomycin alginate beads for treating bone infections and facilitating bone formation.* Tissue Eng Part A, 2008. **14**(7): p. 1173-82.

1246. Schutzenberger, S., et al., *The optimal carrier for BMP-2: a comparison of collagen versus fibrin matrix.* Arch Orthop Trauma Surg, 2012. **132**(9): p. 1363-70.

1247. van der Stok, J., et al., *Full regeneration of segmental bone defects using porous titanium implants loaded with BMP-2 containing fibrin gels.* Eur Cell Mater, 2015. **29**: p. 141-53; discussion 153-4.

1248. Vila, O.F., et al., *Bioluminescent and micro-computed tomography imaging of bone repair induced by fibrin-binding growth factors.* Acta Biomater, 2014. **10**(10): p. 4377-89.

1249. Zhang, L., et al., *Improvement in angiogenesis and osteogenesis with modified cannulated screws combined with VEGF/PLGA/fibrin glue in femoral neck fractures.* J Mater Sci Mater Med, 2014. **25**(4): p. 1165-72.

1250. Eyrich, D., et al., *Long-term stable fibrin gels for cartilage engineering.* Biomaterials, 2007. **28**(1): p. 55-65.

1251. Galler, K.M., et al., *Bioengineering of dental stem cells in a PEGylated fibrin gel.* Regen Med, 2011. **6**(2): p. 191-200.

1252. Yang, K.C., et al., *Fibrin glue mixed with platelet-rich fibrin as a scaffold seeded with dental bud cells for tooth regeneration.* J Tissue Eng Regen Med, 2012. **6**(10): p. 777-85.

1253. Bach, A.D., et al., *Fibrin glue as matrix for cultured autologous urothelial cells in urethral reconstruction.* Tissue Eng, 2001. **7**(1): p. 45-53.

1254. Christman, K.L., et al., *Injectable fibrin scaffold improves cell transplant survival, reduces infarct expansion, and induces neovasculature formation in ischemic myocardium.* J Am Coll Cardiol, 2004. **44**(3): p. 654-60.

1255. Arkudas, A., et al., *Automatic quantitative micro-computed tomography evaluation of angiogenesis in an axially vascularized tissue-engineered bone construct.* Tissue Eng Part C Methods, 2010. **16**(6): p. 1503-14.

1256. Branski, L.K., et al., *A review of gene and stem cell therapy in cutaneous wound healing.* Burns, 2009. **35**(2): p. 171-80.

1257. Lv, J., et al., *Enhanced angiogenesis and osteogenesis in critical bone defects by the controlled release of BMP-2 and VEGF: implantation of electron beam melting-fabricated porous Ti6Al4V scaffolds incorporating growth factor-doped fibrin glue.* Biomed Mater, 2015. **10**(3): p. 035013.

1258. Hotary, K.B., et al., *Matrix metalloproteinases (MMPs) regulate fibrin-invasive activity via MT1-MMP-dependent and -independent processes.* J Exp Med, 2002. **195**(3): p. 295-308.

1259. Green, H., O. Kehinde, and J. Thomas, *Growth of cultured human epidermal cells into multiple epithelia suitable for grafting.* Proc Natl Acad Sci U S A, 1979. **76**(11): p. 5665-8.

1260. Horch, R.E., et al., *Tissue engineering of cultured skin substitutes.* J Cell Mol Med, 2005. **9**(3): p. 592-608.

1261. Hafemann, B., et al., *Treatment of skin defects using suspensions of in vitro cultured keratinocytes.* Burns, 1994. **20**(2): p. 168-72.

1262. Kidd, M.E., S. Shin, and L.D. Shea, *Fibrin hydrogels for lentiviral gene delivery in vitro and in vivo.* J Control Release, 2012. **157**(1): p. 80-5.

1263. Zebardast, N., D. Lickorish, and J.E. Davies, *Human umbilical cord perivascular cells (HUCPVC): A mesenchymal cell source for dermal wound healing.* Organogenesis, 2010. **6**(4): p. 197-203.

1264. Cerqueira, M.T., R.P. Pirraco, and A.P. Marques, *Stem Cells in Skin Wound Healing: Are We There Yet?* Adv Wound Care (New Rochelle), 2016. **5**(4): p. 164-175.

1265. Wan, L., D. Li, and Q. Wu, *Perivenous application of fibrin glue as external support enhanced adventitial adenovirus transfection in rabbit model.* J Surg Res, 2006. **135**(2): p. 312-6.

1266. Lesman, A., et al., *Engineering vessel-like networks within multicellular fibrin-based constructs.* Biomaterials, 2011. **32**(31): p. 7856-69.

1267. Xu, T., et al., *Inkjet-mediated gene transfection into living cells combined with targeted delivery.* Tissue Eng Part A, 2009. **15**(1): p. 95-101.

1268. Correia, C., et al., *In vitro model of vascularized bone: synergizing vascular development and osteogenesis.* PLoS One, 2011. **6**(12): p. e28352.

1269. Ohara, T., et al., *Evaluation of scaffold materials for tooth tissue engineering.* J Biomed Mater Res A, 2010. **94**(3): p. 800-5.

1270. Wang, Z.S., et al., *The use of platelet-rich fibrin combined with periodontal ligament and jaw bone mesenchymal stem cell sheets for periodontal tissue engineering.* Sci Rep, 2016. **6**: p. 28126.

1271. Inoue, S., et al., *The effectiveness of basic fibroblast growth factor in fibrin-based cultured skin substitute in vivo.* J Burn Care Res, 2009. **30**(3): p. 514-9.

1272. Jeon, O., et al., *Synergistic effect of sustained delivery of basic fibroblast growth factor and bone marrow mononuclear cell transplantation on angiogenesis in mouse ischemic limbs.* Biomaterials, 2006. **27**(8): p. 1617-25.

1273. Leen, A.M., et al., *Identification of hexon-specific CD4 and CD8 T-cell epitopes for vaccine and immunotherapy.* J Virol, 2008. **82**(1): p. 546-54.

1274. Sakuma, T., M.A. Barry, and Y. Ikeda, *Lentiviral vectors: basic to translational.* Biochem J, 2012. **443**(3): p. 603-18.

1275. Rey-Rico, A. and M. Cucchiarini, *Recent tissue engineering-based advances for effective rAAV-mediated gene transfer in the musculoskeletal system.* Bioengineered, 2016. **7**(3): p. 175-88.

1276. Fang, J., et al., *Stimulation of new bone formation by direct transfer of osteogenic plasmid genes.* Proc Natl Acad Sci U S A, 1996. **93**(12): p. 5753-8.

1277. Bertoni, C., et al., *Enhancement of plasmid-mediated gene therapy for muscular dystrophy by directed plasmid integration.* Proc Natl Acad Sci U S A, 2006. **103**(2): p. 419-24.

1278. Trentin, D., J. Hubbell, and H. Hall, *Non-viral gene delivery for local and controlled DNA release.* J Control Release, 2005. **102**(1): p. 263-75.

1279. Kulkarni, M.M., et al., *A temporal gene delivery system based on fibrin microspheres.* Mol Pharm, 2011. **8**(2): p. 439-46.

1280. Trentin, D., et al., *Peptide-matrix-mediated gene transfer of an oxygen-insensitive hypoxia-inducible factor-1alpha variant for local induction of angiogenesis.* Proc Natl Acad Sci U S A, 2006. **103**(8): p. 2506-11.

1281. Kulkarni, M., et al., *Use of a fibrin-based system for enhancing angiogenesis and modulating inflammation in the treatment of hyperglycemic wounds.* Biomaterials, 2014. **35**(6): p. 2001-10.

1282. Stilhano, R.S., et al., *Gene and cell therapy for muscle regeneration.* Curr Rev Musculoskelet Med, 2015. **8**(2): p. 182-187.

1283. Chen, F.M., M. Zhang, and Z.F. Wu, *Toward delivery of multiple growth factors in tissue engineering.* Biomaterials, 2010. **31**(24): p. 6279-308.

1284. Briquez, P.S., J.A. Hubbell, and M.M. Martino, *Extracellular Matrix-Inspired Growth Factor Delivery Systems for Skin Wound Healing.* Adv Wound Care (New Rochelle), 2015. **4**(8): p. 479-489.

1285. Faensen, B., et al., *Local application of BMP-2 specific plasmids in fibrin glue does not promote implant fixation.* BMC Musculoskelet Disord, 2011. **12**: p. 163.

1286. Upton, Z., et al., *Vitronectin: growth factor complexes hold potential as a wound therapy approach.* J Invest Dermatol, 2008. **128**(6): p. 1535-44.

1287. Upton, Z., et al., *Human pilot studies reveal the potential of a vitronectin: growth factor complex as a treatment for chronic wounds.* Int Wound J, 2011. **8**(5): p. 522-32.

1288. Comoglio, P.M., C. Boccaccio, and L. Trusolino, *Interactions between growth factor receptors and adhesion molecules: breaking the rules.* Curr Opin Cell Biol, 2003. **15**(5): p. 565-71.

1289. Yamada, K.M. and S. Even-Ram, *Integrin regulation of growth factor receptors.* Nat Cell Biol, 2002. **4**(4): p. E75-6.

1290. Cui, X. and T. Boland, *Human microvasculature fabrication using thermal inkjet printing technology.* Biomaterials, 2009. **30**(31): p. 6221-7.

1291. Campbell, P.G., et al., *Engineered spatial patterns of FGF-2 immobilized on fibrin direct cell organization.* Biomaterials, 2005. **26**(33): p. 6762-70.

1292. Miller, E.D., et al., *Dose-dependent cell growth in response to concentration modulated patterns of FGF-2 printed on fibrin.* Biomaterials, 2006. **27**(10): p. 2213-21.

1293. Miller, E.D., et al., *Inkjet printing of growth factor concentration gradients and combinatorial arrays immobilized on biologically-relevant substrates.* Comb Chem High Throughput Screen, 2009. **12**(6): p. 604-18.

7. LIST OF ABBREVIATIONS

α_2-macroglobulin	α_2-MG
α2-plasmin inhibitor (α2-antiplasmin)	α2-PI
ϵ-aminocaproic acid	EACA
1-Ethyl-3-(3-dimethylaminopropyl) carbodiimide	EDC
2,2′-dithiodiethanol DL-dithiothreitol	DTT
3 phosphoinositide-dependent protein kinase-1	PDK1
4',6-Diamidino-2-phenylindole	DAPI
4-acidobenzoic acid	Az
Acetylcholine receptor	AChR
Acetylcholine	ACh
Acrylic acid	AA
Adeno-associated virus	AAV
Adenosine diphosphate	ADP
Adenosine monophosphate activated kinase	AMPK
Adenosine monophosphate	AMP
Adenosine triphosphatase	ATPase
Adenosine triphosphate	ATP
Adenovirus	Ad
Adipose-derived mesenchymal stem cell	ADMSC
Amniotic fluid stem cell	AFSC
Analysis of variance	ANOVA
Angiotensin-coverting-enzyme	ACE
Arg-Gly-Asp	RGD
Basic helix-loop-helix	bHLH
Becker muscular dystrophy	BMD
Bone marrow mononuclear cell	BMMNC
Bone marrow-derived mesenchymal stem cell	BMMSC
Bone morphogenetic protein	BMP
Bovine serum albumin	BSA
Brain-derived neurotrophic factor	BDNF
Carboxypeptidase U	CPU
Cardiotoxin	CTX
Cardiovascular disease	CVD
Cell adhesion molecule	CAM
Chicken chorioallantoic membrane	CAM
China Food and Drug Administration	CFDA
Chronic low-frequency stimulation	CLFS
c-Jun NH2-terminal kinase	JNK
Clot formation time	CFT
Clotting time	CT
Cluster of differentiation	CD
Cluster of differentiation	CD
(active) Coagulation factor	$F_{(a)}$
Conformité Européenne	CE
Congenital muscular dystrophy	CMD
Copolymer protected	COPROG
Creatine phosphate	CP
Cultured epidermal autograft	CEA
Cycle threshold	C_T
Cytomegalovirus	CMV
Deoxyribonuclease	DNase
Deoxyribonucleic acid	DNA
Differentiation medium	DM

Dihydroxyphenylalanine	DOPA
Distal muscular dystrophy	DD
Dorsal medial lip	DML
Duchenne muscular dystrophy	DMD
Dulbeccos's modified Eagle's medium	DMEM
Dystrophin-glycoprotein complex	DGC
Elastic (Young's) modulus	E
Electrical pulse stimulation	EPS
Embryoid body	EB
Embryonic myosin heavy chain	eMHC
Embryonic stem cell	ESC
Emery-Dreifuss muscular dystrophy	EDMD
Endothelial cell	EC
Endothelial progenitor cell	EPC
Engineered heart tissue	EHT
Epidermal growth factor	EGF
Ethylenediaminetetraacetic acid	EDTA
European Medicines Agency	EMA
Excitation-contraction coupling	ECC
Extracellular matrix	ECM
Extracellular regulated kinase	ERK
Extracellular-signal regulated kinase	ERK
Eyes-absent homologue	Eya
Facioscapulohumoral muscular dystrophy	FSHD
Fetal calf serum	FCS
Fibrin degradation product	FDP
Fibrin microbead	FMB
Fibrinogen	Fbg
Fibrinopeptide (A/B)	FpA/B
Fibroblast growth factor receptor	FGFR
Fibroblast growth factor	FGF
Fibronectin	FN
Fluorescence-activated cell sorting	FACS
Food and Drug Administration	FDA
Free functional muscle transfer	FFMT
G protein-coupled receptor	GPCR
Gelatin-methacryloyl	GelMA
Gelatin-resorcinol-formaldehyde	GRF
Gelatin-resorcinol-formaldehyde-glutaraldehyde	GRFG
Gene activated matrix	GAM
Glial cell line-derived neurotrophic factor	GDNF
Glioma-associated oncogene	Gli
Glyceraldehyde 3-phosphate dehydrogenase	GAPDH
Granulocyte colony stimulating factor	G-CSF
Green fluorescent protein	GFP
Gross domestic product	GDP
Growth factor	GF
Growth medium	GM
Half relaxation time	1/2RT
Hematopoietic stem cell	HSC
Heparan sulfate proteoglycan	HSPG
Heparin	H
Hepatocyte growth factor	HGF
Human bioartificial muscle	HBAM
Human umbilical cord vein endothelial cell	HUVEC
Hyaluronic acid (hyaluronan)	HA

Hypoxanthine phosphoribosyl transferase	HPRT
Immunofluorescence	IF
Induced pluripotent stem cell	iPSC
Insulin-like growth factor	IGF
Interleukin	IL
Interpenetrating polymer network	IPN
Janus kinase/Signal Transducer and Activator of transcription	JAK/STAT
Kallikrein inhibiting unit	KIU
Keratinocyte growth factor	KGF
Lentivirus	LV
Limb-girdle muscular dystrophy	LGMD
Macrophage activator lipoprotein peptide	MALP
Magnetic-activated cell sorting	MACS
Mammalian target of rapamycin complex	mTORC
Mammalian target of rapamycin	mTOR
Matrix metalloproteinase	MMP
Matrix-assisted sonoporation	MAS
Maximum clot firmness	MCF
Mesenchymal stem cell	MSC
Mesoangioblast	MAP
Metridia luciferase	MetLuc
microRNA	miRNA
Minimally invasive surgery	MIS
miRNA complementary target seed sequence	miRT
Mitogen-activated protein kinase	MAPK
Mitogen-activated protein kinase	MAPK
Muscle creatine kinase	MCK
Muscle precursor cell	mpc
Muscle stem cell	MuSC
Muscle-derived stem cell	MDSC
Muscular Dystrophy	MD
Musculoskeletal disorder	MSD
Multilineage differentiating stress enduring	Muse
Myocyte enhancer factor	MEF
Myogenic differentiation 1	MyoD
Myogenic factor	Myf
Myogenic regulatory factor	MRF
Myogenin	MyoG/MYG
Myosin heavy chain	MHC
Myotonic muscular dystrophy	DM
National Health Interview Survey	NHIS
Nerve growth factor	NGF-β
Neuromuscular junction	NMJ
Neurotrophin	NT-3
N-hydroxybenzotriazole	HOBt
N-hydroxysuccinimide	NHS
Nitric oxide synthase	NOS
Nitric oxide	NO
Nuclear factor of activated T cells	NFAT
Nuclear magnetic resonance	NMR
Oculopharyngeal muscular dystrophy	OPMD
Osteocalcin	OC
Paired box	Pax
Paired-homeobox	Pax
Para-formaldehyde	PFA
Penicillin/streptomycin	P/S

Peripheral nervous system	PNS
Phosphate-buffered saline	PBS
Phosphoinositide 3-kinase	PI3K
Phospholipase C	PLC
Plasminogen activator inhibitor	PAI
Plasminogen	PLG
Platelet-derived growth factor	PDGF
Platelet-rich fibrin	PRF
Pleiotrophin	PTN
Poly(amidoamine)	PAMAM
Poly(ethylene glycol)	PEG
Poly(glycerol-co-sebacate acrylate)	PGSA
Poly(glycolic acid)	PGA
Poly(lactic acid)	PLA
Poly(lactic-co-glycolic acid)	PLGA
Poly(l-lactic acid)	PLLA
Poly(vinyl alcohol)	PVA
Poly(vinyl pyrrolidone)	PVP
Poly(ε-caprolactone)	PCL
Poly(ε-caprolactone-co-lactide)	PCLA
Polyadenylation signal	Poly A
Polydimethylsiloxane	PDMS
Polyurethane	PU
Propidium iodide	PI
Protein kinase B	AKT
Protein kinase B	PKB
Protein kinase C	PKC
P-value	p
Reactive oxygen species	ROS
Reverse transcription quantitative polymerase chain reaction	RT-qPCR
Ribonucleic acid	RNA
Ribosomal protein S6 kinase	(p70)S6K
Rotational thromboelastometry	ROTEM
Sarco(endo)plasmic reticulum Ca2+ ATPase	SERCA
Satellite cell	SC
Scanning electron microscopy	SEM
Side population	SP
Sine oculis-related homeobox	Six
Skeletal muscle tissue engineering	SMTE
Sonic hedgehog	Shh
Standard deviation	S.D.
Standard deviation	SD
Storage (shear) modulus	G'
Stretch-activated channel	SAC
Stromal cell-derived factor	SDF
Stromal vascular fraction	SVF
Tensile strength	TS
Three-dimensional	3D
Thrombin	Thr
Thrombin-activatable fibrinolysis inhibitor	TAFIa
Tibialis anterior	TA
Time to peak twitch tension	TPT
Tissue engineering and regenerative medicine	TERM
Tissue Engineering	TE
Tissue Factor	TF
Tissue-type plasminogen activator	tPA

Tranexamic acid	TEA
Transcription factor	TF
Transforming growth factor	TGF
Transglutaminase	TG
Transverse tubule	T tubule
Tris-buffered saline	TBS
Troponin T	TnnT
Tuberous sclerosis complex 1/2	TSC1/2
Tumor necrosis factor α	TNF-α
Two-dimensional	2D
Untranslated region	UTR
Urokinase-type plasminogen activator receptor	uPAR
Urokinase-type plasminogen activator	uPA
Vascular endothelial growth factor	VEGF
Vascular smooth muscle cell	VSMC
Ventilation mechanical test	VMT
Ventral lateral lip	VLL
Volumetric muscle loss	VML
von Willebrand Factor	vWF
Weight per volume	w/v
Wingless-Int	Wnt
Young's (elastic) modulus	E_{mod}

8. CURRICULUM VITAE

PHILIPP HEHER

Praterstrasse 30/2/17• Vienna, 1020, AUSTRIA • philipp.heher@kcl.ac.uk • +43 (0)680 2335821

EDUCATION

Vienna University of Technology   Vienna, Austria

Faculty of Technical Chemistry   **expected November 2018**

PhD **(Doctoral Program in Natural Sciences)**

• Specializations: Tissue Engineering, Biomaterials Science, Bioreactors, Natural Hydrogels

University of Vienna   Vienna, Austria

Center of Molecular Biology   **December, 2012**

Mag. **in Molecular Biology** (passed with distinction)

• Specializations: Cell Biology, Microbiology and Immunology, Molecular Medicine
• Study program includes practical courses and lectures in Genetics and Gene Expression, Biochemistry, Inorganic Chemistry, Organic Chemistry, Analytic Chemistry, Cell Biology, Biotechnology, Microbiology and Cellular Immunology, Molecular Medicine, Developmental Biology, Molecular Pathology, Neurobiology

PROFESSIONAL EXPERIENCE

Trauma Care Consult GmbH / LBI Trauma   Vienna, Austria

PhD fellow   **March, 2014 - present**

• Development of standard scaffolds for the rational design of bioactive materials for tissue regeneration within a collaborative EU wide research project (EU 7th Framework Programme - "Biodesign")
• Establishment and evaluation of bioreactor systems for *in vitro* generation of functional muscle, tendon and ligament tissue

UAS Technikum Wien   Vienna, Austria

Department of Biomedical Engineering   **September 2012 - February 2018**

Lecturer

• Teaching activities in two study programs: Biomedical Engineering (BSc program) and Tissue Engineering and Regenerative Medicine (MSc program)
• Lectures, seminars and practical courses in cell biology, tissue engineering and regenerative medicine, stem cell research, gene therapy, molecular biological methods
• Practical and theoretical supervision of Bachelor's and Master's theses

UAS Technikum Wien   Vienna, Austria

Department of Biomedical Engineering   **July 2012 - March 2014**

Technician

- Implementation of molecular cell biological working techniques into 3D cell culture tissue engineering applications in bioreactor systems
- Establishment of bioreactor systems for *in vitro* generation of functional tendons and ligaments

Max F. Perutz Laboratories / Vienna Biocenter   Vienna, Austria

Department of Medical Biochemistry   **October 2010 - April 2012**

Diploma Student (**Weitzer Lab**)

- Thesis: "A novel Strategy for the Isolation of Cardiovascular Progenitor Cells from murine Hearts"

PUBLICATIONS

An Overview of Surgical Sealant Devices: Current Approaches and Future Trends. **Heher P**, Ferguson J, Redl H, Slezak P. Expert Rev Med Dev 2018 (accepted for publication). doi: 10.1080/17434440.2018.1526672

The Importance of Biophysical and Biochemical Stimuli in Dynamic Skeletal Muscle Models. Maleiner B, Tomasch J, **Heher P**, Spadiut O, Rünzler D, Fuchs C. Front. Physiol. 2018 Aug;9:1130. doi: 10.3389/fphys.2018.01130

Efficacy of Topical Hemostatic Agents: A Comparative Evaluation of Two Gelatin/Thrombin-Based Hemostatic Matrices in a Porcine Kidney Surgical Model. Slezak P, **Heher P**, Monforte X, Keibl C, Redl H, Spazierer D, Gulle H. J Invest Surg. 2018 Mar 21:1-8. doi: 10.1080/08941939.2018.1447619.

Fibrin-based delivery strategies for acute and chronic wound healing. **Heher P**, Mühleder S, Mittermayr R, Redl H, Slezak P. Adv Drug Deliv Rev. 2018 Apr;129:134-47. doi: 10.1016/j.addr.2017.12.007.

A Noninvasive In Vitro Monitoring System Reporting Skeletal Muscle Differentiation. Öztürk-Kaloglu D, Hercher D, **Heher P**, Posa-Markaryan K, Sperger S, Zimmermann A, Wolbank S, Redl H, Hacobian A. Tissue Eng Part C Methods. 2017 Jan;23(1):1-11. doi: 10.1089/ten.TEC.2016.0366.

Hyaluronic acid-fibrin interpenetrating double network hydrogel prepared in situ by orthogonal disulfide cross-linking reaction for biomedical applications. Zhang Y, **Heher P**, Hilborn J, Redl H, Ossipov DA. Acta Biomater. 2016 Jul 1;38:23-32. doi: 10.1016/j.actbio.2016.04.041.

Desmin enters the nucleus of cardiac stem cells and modulates Nkx2.5 expression by participating in transcription factor complexes that interact with the nkx2.5 gene. Fuchs C, Gawlas S, **Heher P**, Nikouli S, Paar H, Ivankovic M, Schultheis M, Klammer J, Gottschamel T, Capetanaki Y, Weitzer G. Biol Open. 2016 Jan 19;5(2):140-53. doi: 10.1242/bio.014993.

A novel bioreactor for the generation of highly aligned 3D skeletal muscle-like constructs through orientation of fibrin via application of static strain. **Heher P**, Maleiner B, Prüller J, Teuschl AH, Kollmitzer J, Monforte X, Redl H, Rünzler D, and Fuchs C. Acta Biomater. 2015 Sept. 15; 24:251-265. doi: 10.1016/j.actbio.2015.06.033.

In vitro extracorporeal shock wave treatment enhances stemness and preserves multipotency of rat and human adipose-derived stem cells. Schuh CM, **Heher P**, Weihs AM, Banerjee A, Fuchs C, Gabriel C, Wolbank S, Mittermayr R, Redl H, Rünzler D, Teuschl AH. Cytotherapy. 2014 Dec;16(12):1666-78. doi: 10.1016/j.jcyt.2014.07.005. Epub 2014 Aug 28.

VUT-MK142: a new cardiomyogenic small molecule promoting the differentiation of pre-cardiac mesoderm into cardiomyocytes. Koley M, Mike AK, **Heher P**, Koenig X, Schön M, Schnürch M, Hilber K, Weitzer G, Mihovilovic MD. Medchemcomm. 2013 Aug 1;4(8):1189-1195. doi: 10.1039/C3MD00101F.

Small molecule cardiogenol C upregulates cardiac markers and induces cardiac functional properties in lineage-committed progenitor cells. Mike AK, Koenig X, Koley M, **Heher P**, Wahl G, Rubi L, Schnürch M, Mihovilovic MD, Weitzer G, Hilber K. Cell Physiol Biochem. 2014;33(1):205-21. doi: 10.1159/000356663.

Embryonic Stem Cells Facilitate the Isolation of Persistent Clonal Cardiovascular Progenitor Cell Lines and Leukemia Inhibitor Factor Maintains their Self-Renewal and Myocardial Differentiation Potential In Vitro. Hoebaus J, **Heher P**, Gottschamel T, Scheinast M, Auner H, Walder D, Wiedner M, Taubenschmid J, Miksch M, Sauer T, Schultheis M, Kuzmenkin A, Seiser C, Hescheler J, and Weitzer G. Cells Tissues Organs. 2013 Jan. 22; 197(4):249-268. doi: 10.1159/000345804.

BOOK CHAPTERS

From Hemostasis to Tissue Engineering - the manifold Applications of Fibrin Sealants in Regenerative Medicine. **Heher P**, Prüller J, Fuchs C, Redl H. Tissue Engineering and Regeneration (Springer Publishing), Ed. Redl H. (currently in revision)

Fibrin. Kerbl M, **Heher P**, Ferguson J, Redl H. Biomaterials from Nature for Advanced Devices and Therapies (John Wiley & Sons Publishing), Eds. Neves NM and Reis RL. 2016 Oct. 21. doi: 10.1002/9781119126218.ch10

AWARDS

Prize for best Short Talk (awarded at the 3rd annual meeting of the Austrian Association of Molecular Life Sciences and Biotechnology, Salzburg, Austria, 28th to 30th of September, 2011)

ADDITIONAL INFORMATION

Personal: born January 3rd, 1985; Austrian nationality

Languages: German (mother tongue), English (fluent), French (intermediate), Spanish (basic)